High energy nuclear physics and multiparticle dynamics

Michal Šumbera, CSc.

A Thesis presented for the degree of
Doctor of Sciences

Center for Physics of Ultra-Relativistic Nuclear Collisions

Nuclear Physics Institute
Academy of Sciences of the Czech Republic
Řež / Prague, Czech Republic

July 2009

High energy nuclear physics and multiparticle dynamics

Michal Šumbera, CSc.

Submitted for the degree of Doctor of Sciences
July 2009

Abstract

In this thesis selected results from four heavy ion experiments: TAPS at GSI SIS, WA98 and CERES at CERN SPS and STAR at BNL RHIC are reviewed. In addition to this physics capabilities of newly build ALICE experiment at CERN LHC and results of phenomenological analysis of multiparticle production in high-energy hadron-hadron collisions are presented. Enormous c.m.s. energy region covered – from 2.3 GeV to 5.4 TeV per nucleon-nucleon pair – allows me to discuss in a unified way several important phenomena characterizing novel trends in high energy nuclear physics: elliptic flow, sub-threshold particle production, thermalization, search for the disoriented chiral condensate and discovery of a new state of matter created in high-energy nuclear collisions.

Declaration

The work presented in this thesis is based in part on research carried out within large multi-national collaborations: ALICE, NA45/CERES and WA98 at CERN. STAR at BNL RHIC and TAPS at GSI SIS. Chapter 2 of the thesis is based on joint research with Imrich Zborovský from Nuclear Physics Institute ASCR and Miloš Pachr and Vláďa Šimák from Faculty of Nuclear Sciences and Physical Engineering of the Czech Technical University in Prague.

This means that with exception of the whole Chapter 2 and section 5.3 some parts of material in this thesis might have been submitted elsewhere for any other degree or qualification by member of the above mentioned collaborations. My own contribution to the Chapters 3-5 is the following one.

In 1991, together with three of my NPI colleagues (A. Kugler, M. Pachr and V. Wagner) I have proposed a small-scale experiment based on a simple BaF_2 crystal-based spectrometer to measure the neutron spectra in Bi+Pb collisions at 1 AGeV. The experiment was performed in summer 1991 at GSI SIS. I have also proposed to interpret the measured spectra within the scale-invariant approach to sub- and near-threshold particle production. The results of performed analysis (sections 3.4.2 and 3.4.3) were part of the PhD thesis of Miloš Pachr's which was accomplished under my supervision.

From 1991 till 1993 while working as a visiting scientist at the KVI Groningen, The Netherlands, I was involved in the **TAPS** experiment. In addition to work related to the preparation and conduction of experiments at GSI SIS and at MAMI-B I have analyzed azimuthal and transverse momentum spectra of neutral pions and performed microscopic transport models simulations. My scientific interest at that time has focused on the application of the scale-invariant approach to particle production at SIS energies.

In the lead ion beam CERN SPS experiments **WA98** and **CERES** my responsibility included among the other things activities related to the preparation, maintenance, operation and, in part, also to data analysis of the Silicon Drift Detectors. During 1994-1996 and 1998-2000 I was regularly involved in the data taking shifts of the **WA98** and **NA45/CERES** experiments at the SPS, respectively. Similarly to my previous activities in the **TAPS** collaboration, I have implemented several microscopical transport models of heavy ion collisions and suggested several analyses. In both experiments I

was a team leader of the NPI ASCR group.

At the RHIC experiment **STAR** in addition to the above mentioned activities I have also supervised several graduate and undergraduate students. Some of the results presented in Chapter 5 (section 5.2.2) were obtained by them under my supervision. In addition to this I was also actively involved in writing the summary article presented in section 5.1.1.

The material presented in section 5.3.2 on **ALICE** experiment at the LHC is in part based on some preliminary estimates done by J. Schukraft and P. Giubellino. The rest is my own contribution.

Acknowledgements

During the last twenty five years - a period covered by the material of this thesis - I had a nice opportunity to collaborate with many outstanding scientists and, what is even more important, to learn few important things about the physics from them. My first thanks go to my oldest collaborators Prof. Vláďa Šimák, who has already supervised my undergraduate thesis many years ago, and to dr. Imrich Zborovský.

I would like to thank Prof. Herbert Löhner for a nice hospitality and working conditions in his group at KVI. I also would like to thank the other **TAPS** collaborators, in particular Prof. Volker Mettag (that time the **TAPS** spokesperson), Prof. Rolf Siemssen, dr. Reinhard Simon, dr. Hans Wilschut and graduate students Lars Venema, Ansgaar Raschke, Olaf Schwalb and Frank-Dietter Berg. I have extremely enjoyed the collaboration with the authors of the microscopical transport codes: Prof. Steffan Bass, dr. Slava Toneev and dr. Gyuri Wolf. Last but not least my thanks go also to my NPI colleagues: dr. Andrej Kugler, dr. Miloš Pachr and dr. Vláďa Wagner, my collaborators at that time.

I am very grateful to Prof. Hans Gutbrod (that time the spokesperson of the **WA98** Collaboration) and to dr. Frank Plasil who have already in 1993 paved the way to the NPI team participation in the lead beam program at CERN SPS. I also would like to thank the other **WA98** colleagues: dr. Terry Awes (current WA98 spokesperson), Prof. Herbert Löhner, Prof. Thomas Peitzmann, Prof. Bolek Wysłouch, dr. Tapan Nayak, dr. Gerrit van Nieuwenhuizen, dr. Peter Steinberg (then the graduate student), and many others, last but not least also to Tony Przibylla (the technician of both the **WA98** and **NA45/CERES** experiments). I also appreciate the help from dr. Nikolai Amelin, dr. Heinz Sorge and Prof. Klaus Werner concerning the simulation of ultra-relativistic heavy ion collisions.

I have extremely profitted from the collaboration with my **NA45/CERES** colleagues: Prof. Johanna Stachel (the spokesperson), Prof. Hans Specht, Prof. Itzak Tserruya, Prof. Hannes Wessels and Prof. Peter Wurm. Since both the **WA98** and **CERES** experiments have used the same type of the Silicon Drift Detectors it was my great privilege to collaborate with dr. Pavel Rehak, the inventor and designer of these detectors. I also thank to dr. Chillo Garabatos, dr. Anna Marín and dr. Stepan Yurevich.

In thew **STAR** collaboration my gratitude goes first of all to Prof. Yuri Panebratsev

and dr. Richard Lednicý without whose insistence I would never find a courage to enter this beautiful experiment. I would like to thank dr. Tim Hallman and dr. Nu Xu (former and current **STAR** spokespersons, respectively). I also acknowledge the help of Prof. Tom Humanic and Prof. Tom Trainor in promoting the NPI group to a full membership in the STAR collaboration. Extremely nice and fruitful was a collaboration with some of the STAR femtoscopists: dr. Richard Lednický, Prof. Mike Lisa, dr. Fabrice Retière and, last but not least, with my graduate students - Petr Chaloupka and Michal Bysterský - working on the same subject.

In early days of the **ALICE** project preparation I have extremely profitted from discussions with dr. Jurgen Schukraft (the ALICE spokesperson) and dr. Paolo Giubellino (leader of the ALICE Silicon Drift Detector project).

In most of the above mentioned experimental activities at CERN SPS and LHC great deal of support came from my closest NPI colleagues: dr. Vojtěch Petráček and dr. Jan Rak who have started to work on this fascinating subject in my team but then has left to work on their own. I also thank dr. Dagmar Adamová, dr. Jana Bielčíková, dr. Ivana Hřivnáčová and dr. Svetlana Kushpil and dr. Vasily Kushpil (the graduate students at that time).

Finally, I would like to thank to my wife Věra without whose encouragement and support this thesis could not have been neither started nor finished.

Contents

Chapter 1

Introduction

1.1 Motivation

High-energy nuclear physics (HENP) studies nuclear matter in energy regimes delegated until recently to particle physics only (see Fig.1.1, left). Aim of this new field of science [R1] is to apply and extend the Standard Model (SM) of particle physics to complex and dynamically evolving systems of finite size. Its primary goal is to study and understand how collective phenomena and macroscopic properties, involving many degrees of freedom, emerge from the microscopic laws of elementary-particle physics [236]. The most striking case of a collective bulk phenomenon affecting crucially our current understanding of both the structure of the SM at low energy and of the evolution of the early Universe are the phase transitions in quantum fields at characteristic energy densities [R23–R25]. HENP thus fulfills part of the important mission of nuclear science – to explain the origin, evolution, and structure of the baryonic matter of the universe.

Since quarks discovery in the 1960s, the basic landscape of nuclear and particle physics has evolved dramatically. The nucleus – long viewed as a densely packed assembly of neutrons and protons bound together by a strong force carried by pions and other mesons – is not anymore in its centre. Protons, neutrons, pions, and the elaborate array of other hadrons discovered in the last half-century are now understood to be rather complicated systems which must be explained in terms of their fundamental pointlike constituents: quarks (and antiquarks) bound together through interactions mediated by gluons quarks and gluons. Quantum chromodynamics (QCD), the current theory of the strong interactions, is a field theory of quarks and gluons. It forbids the appearance of free quarks or gluons which otherwise play a fundamental role in the nature of matter.

The study of the fundamental theory of the strong interaction - QCD - under extreme conditions of temperature, density and parton momentum fraction (low-x) has attracted an increasing experimental and theoretical interest during the last 20 years

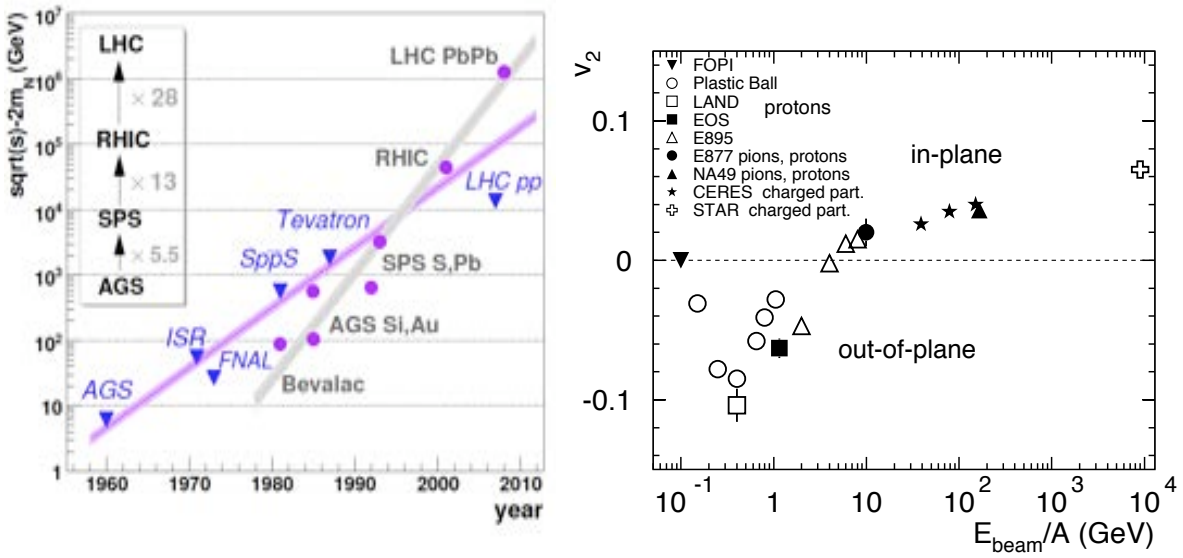

Figure 1.1: Left: 'Livingston plot' for (anti)proton and ion accelerators in the period 1960- 2008 [R2]. Right: Second harmonics of the azimuthal emission anisothropy v_2 (near midrapidity, integrated over p_T) as a function of the beam kinetic energy for semi-central collisions of Pb or Au nuclei [90].

[236,R1]. In addition to being a quantum field theory with an extremely rich dynamical content - such as asymptotic freedom, infrared slavery, (approximate) chiral symmetry, non-trivial vacuum topology, strong CP violation problem, UA(1) axial-vector anomaly, color superconductivity, ...- QCD is the only sector of the SM whose full collective behavior - phase diagram, phase transitions, thermalization of fundamental fields - is accessible to scrutiny in the laboratory [236,R1]. The study of the many-body dynamics of high-density QCD covers thus a vast range of fundamental physics problems.

Let us give one example [R74] of the bulk phenomena which has been driving physics of heavy ion collision for the last two decades [R1,R3,R4]. In non-zero impact parameter ($b > 0$) collisions of two nuclei the overlap region is not azimuthally symmetric. The circular symmetry breaking almond shape manifests itself via reaction plane defined by the direction of the impact parameter and the direction of the beam axis. It is customary to quantify particle emission with respect to this reaction plane via the Fourier coefficients v_n [R74]:

$$E\frac{d^3N}{dp^3} = \frac{1}{2\pi}\frac{d^3N}{p_T dp_T dy}\Big(1 + \sum 2v_n \cos(n\phi)\Big) \qquad (1.1)$$

where the reaction plane is approximated by the vector $\overrightarrow{Q}_n \equiv \sum_\nu w_\nu \overrightarrow{p_T}(\nu)$ where $p_T(\nu)$ is the transverse momentum and w_ν being an appropriately chosen weight for the individual particle in an event. The azimuthally symmetric coefficient v_0 is generally called transverse radial flow, v_1 is called directed or sidewards flow and v_2 is called elliptic flow.

The beam energy dependence of elliptic flow of charged particles is displayed on Fig.1.1. Its rich structure, including two changes of sign, has a simple meaning [R74].

At very low energies (not shown on this figure), due to the rotation of the compound system generated in the collision, the emission is in-plane ($v_2 > 0$). At around 100 MeV/nucleon, the preferred emission turns into out-of-plane and v_2 becomes negative [43, 46]. Since the slowly moving spectator matter prevents the in-plane emission of participating nucleons or produced pions they appear to be sqeezed-out of the reaction zone. As the spectators move faster at Lorentz $\gamma \geq 3$ ($E_{beam} \approx 6$ GeV/nucleon) this shadowing disappears changing the pattern back to the in-plane emission. Above this energy v_2 increases monotonically [90] up to the highest RHIC energies [171].

Let us note that while at the beam energies below few GeV/nucleon the matter flow is baryon-dominated above this energy it is dominated by the newly formed particles - mostly the mesons. Key ingredient of azimuthal asymmetry is thus an interesting interplay between the formation time of hadrons and the time it takes for colliding nuclei to pass through each other [R5].

Let us stress that only the interactions among the constituents of the matter formed in initially spatially deformed overlap can produce $v_2 > 0$ [R4]. Transfer of this spatial deformation into momentum space provides a unique signature for re-interactions in the fireball and proves that the matter has undergone significant nontrivial dynamics between creation and freeze-out [R6]. Moreover, the rapid degradation of initial spatial deformation due to rescattering causes the 'self-quenching' of elliptic flow: if elliptic flow does not develop early, when the collision fireball was still spatially deformed, it does not develops at all [R6]. v_2 thus reflects the pressure due to rescattering induced expansion and stiffness of the equation of state (EOS) during the earliest collision stages.

Let us note that elliptic flow affects all final state particles and so in contrast to many other early fireball signatures, it can be easily measured with high statistical accuracy (see Fig.1.1). Its continuous rise with the energy up to its highest value at RHIC indicates that the early pressure increases too. Since near to a phase transition the EOS becomes very soft preventing the generation of flow [R21] the anisotropic flow generation is concentrated to even earlier times, when the system is still entirely partonic and has not even begun to hadronize [R6]. At highest RHIC energy this means that almost all of the finally observed elliptic flow is created during the first 3-4 fm/c [171].

The second topic of this thesis is soft hadron production in hadron-hadron collisions [R9]. This field of strong interaction physics is historically older than HENP but has a substantial overlap with it [R73]. Its origin dates back to pioneering works of Heisenberg [R7], Fermi [R8] and Landau [R8]. Final states produced in collisions of two hadrons are highly complex multiparticle systems and theory only rarely provides experimentalist with a clear guidance [R9]. The main question in this field therefore is how can one usefully look at the data without being seduced by a model? One of the goal of this thesis is therefore to discuss simple phenomenological approach developed

by the author and his collaborators [30, 33, 40, 42] in order to extract a maximum amount of information from experimental data. This information can then be used to make some robust predictions about the properties of the multiparticle final states produced at higher energies.

With the start up of the Large Hadron Collider at CERN both topics discussed in this thesis – the heavy ion and hadron-hadron collisions – will, very likely, merge into a single one. At LHC energies both the incident protons and lead nuclei will be just a densely packed parton beams and that's where the HENP and multiparticle dynamics will find its climax!

1.2 History

The basic hopes and goals, associated with investigations of heavy ion collisions were first formulated in mid-seventies [R10–R12]. It was the experience with astrophysical objects like supernovae and neutron stars, and with thermonuclear ignition, which led the authors to an idea that nuclear matter shock compression of about five-fold normal nuclear density should be accomplished in violent head-on collisions of heavy nuclei [R1]. The goal was to find out the response of the nuclear medium under compression by pressure resisting that compression, i.e. to study the nuclear matter equation of state (EOS). The original question was: is such a bulk nuclear matter EOS accessible within the dynamics of relativistic heavy ion collisions? [R20]. The prospect to observe phase transition at highly compressed nuclear matter [R13] was lurking behind.

The interest in collisions of high-energy nuclei as a possible route to a new state of nuclear matter was substantially strengthened with the emergence of QCD. Shortly after the idea of asymptotic freedom was introduced by Gross, Wilczek [R14] and Politzer [R15], two groups [R16, R17] realized independently that it has a fascinating consequence. When temperatures or densities become very high [R72], strongly interacting quarks and gluons become free and transform themselves into a new, de-confined phase of matter [R70, R71, R77]. For the latter the term *quark gluon plasma* (QGP) was coined [R18]. The big theoretical problems concerning the early history of the universe and its composition at temperatures above 100 MeV [R19] were thus solved.

Since mid-seventies the particle physics community began to adapt existing high-energy accelerators to provide heavy-ion nuclear beams (see Fig.1.1). The Berkeley Bevalac and JINR Synchrophasotron started to accelerate nuclei to kinetic energies from few hundreds of MeV to several GeV per nucleon [R1,R20]. By the mid-1980s, the first ultra-relativistic nuclear beams became available. Silicon and gold ions were accelerated to 10 GeV/nucleon at Brookhaven's Alternating Gradient Synchrotron (AGS).

The first nuclear collisions took place at CERN in early eighties when alpha particles were accelerated to $\sqrt{s_{NN}} = 64$ GeV at ISR collider. The proposal by L. van Hove and few others to continue this programme using heavy nuclei was rejected, the experiments never went beyond the alpha-particles, and then this first hadronic collider was physically destroyed. As we know now, QGP could have been discovered and studied at ISR 20 years prior to RHIC [R21].

The new era of HENP begun at CERN in fall 1986 when oxygen and later on (in summer 1990) sulphur ions were injected into the SPS and accelerated to energy of 200 AGeV ($\sqrt{s_{NN}} = 19.6$ GeV [R1]. However, genuine heavy ion programme started only in 1994, after the CERN accelerator complex has been upgraded with a new lead ion source which was linked to pre-existing, interconnected accelerators, the Proton Synchrotron (PS) and the SPS. The seven large experiments involved (NA44, NA45/CERES, NA49, NA50, NA52, WA97/NA57 and WA98) have studied different

aspects of Pb+Pb and Pb+Au collisions at $\sqrt{s_{NN}} = 17.3$ GeV and $\sqrt{s_{NN}} = 8.6$ GeV.

In the meantime at the Brookhaven National Laboratory (BNL) Relativistic Heavy Ion Collider (RHIC) rose up from the ashes of ISABELLE/CBA $\bar{p}p$ collider project abandoned in 1983 by the particle physicist. In 1984 the first proposal for the dedicated nucleus-nucleus machine accelerating gold nuclei up to $\sqrt{s_{NN}} = 200$ GeV was submitted. Funding to proceed with the construction was received in 1991 and on June 12th, 2000 first Au+Au collisions at $\sqrt{s_{NN}} = 130$ GeV were recorded by the BRAHMS, PHENIX, PHOBOS and STAR experiments.

The idea of the Large Hadron Collider (LHC) dates even further back - to the early 1980s. Although CERNs Large Electron Positron Collider (LEP), which ran from 1989 to 2000, was not built yet, scientists considered re-using the 27-kilometer LEP ring for an even more powerful $p + p$ machine running at highest possible collision energies $\sqrt{s} = 14$ TeV and intensities. The ion option ($\sqrt{s_{NN}} = 5.4$ TeV per nucleon-nucleon pair for Pb+Pb collisions) was considered since the beginning [228]. The LHC was approved in December 1994, its official inauguration took place in October 2008 at CERN.

Moreover in 1990, SchwerIonenSynchrotron (SIS) was inaugurated at GSI Darmstadt. This dedicated heavy ion accelerator delivers nuclear beams up to uranium at energy of 1 AGeV. The goal of this nuclear research facility is to provide a continuation of the Bevalac programme.

1.3 Theoretical Basis

1.3.1 QCD phase transitions

The known matter appears in a variety of phases, which can be transformed into each other by modifying external conditions. Transitions between the phases are often accompanied by a dramatic change in their physical properties, such as density, heat conductivity, light transmission etc. A famous example is water where changes in external pressure and temperature result in a rich phase diagram (see left panel of Fig.1.2). Let us note that in addition to well understood liquid and gaseous phases plentiful spectrum of solid phases exists in which the H_20 molecules arrange themselves in spatial lattices of certain symmetries. Famous points in the phase diagram are the triple point where the solid, liquid and gas phases coexist and the critical point where no distinction between the liquid and gas phase can not be found.

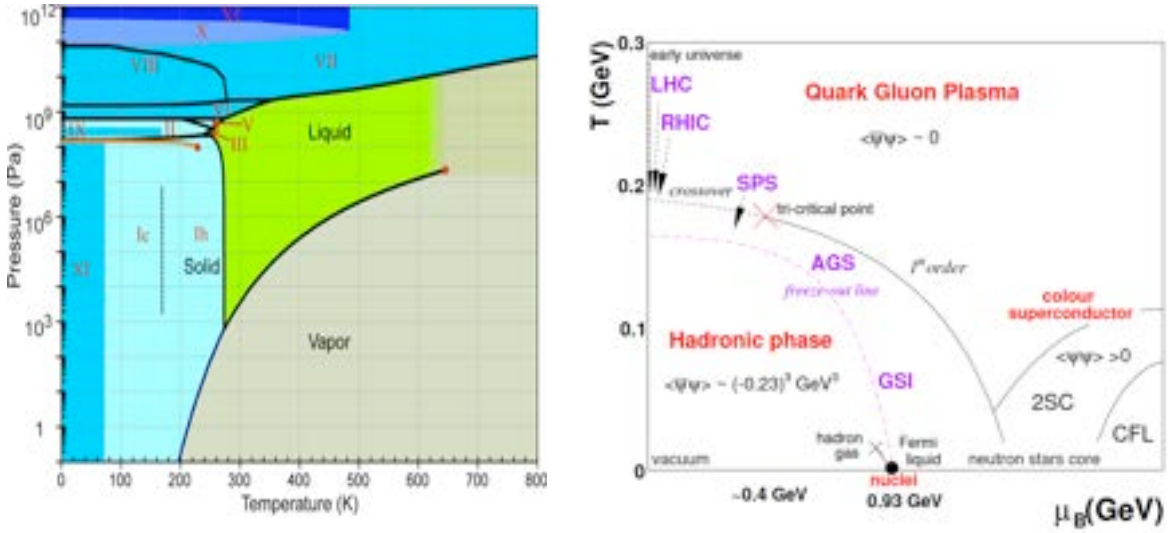

Figure 1.2: Left: The phase diagram of water [R22]. Right: The QCD phase diagram in the temperature vs. baryon chemical potential (T, μ_B) plane [R2]. The arrows indicate the expected crossing through the de-confinement transition during the expansion phase in heavy-ion collisions at different accelerators. The (dashed) freeze-out curve indicates where hadro-chemical equilibrium is attained in the final stage of the collision. The ground-state of nuclear matter at T = 0 and μ_B = 0.93 GeV and the approximate position of the QCD critical point at $\mu_B \approx 0.4$ GeV are also indicated.

During the evolution of the Universe several particle-physics related transitions took place [R23]. Although there are now strong indications of an inflationary period [R24], not much is known about its effect on possible transitions of our known physical model. To understand the consequences, clear picture of these cosmologically relevant transitions is needed first.

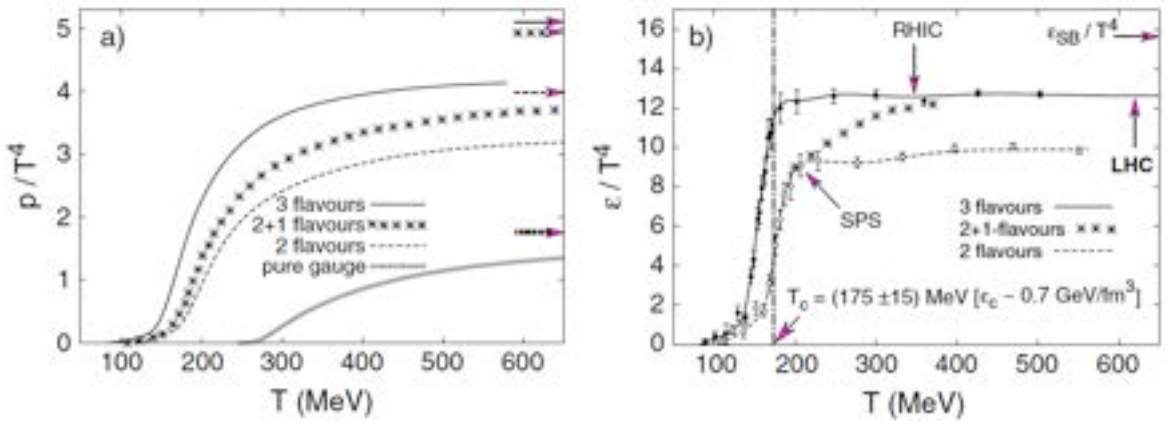

Figure 1.3: The pressure (a) and energy density (b), in QCD with 0, 2 and 3 degenerate quark flavors as well as with two light and a heavier (strange) quark [236]. The $n_f = 0$ calculations were performed on a $N_t = 4$ lattice using improved gauge and staggered fermion actions. In the case of the SU(3) pure-gauge theory the continuum extrapolated result is shown. The arrows on the right-side ordinates show the value of the SB limit (1.2) for an ideal quark-gluon gas.

The SM predicts two such transitions [R23]. One transition occurs at temperatures of a few hundred GeV. This transition is responsible for the spontaneous breaking of the electroweak (EW) symmetry giving the masses to elementary particles. This transition is also related to the EW baryon-number violating processes, which had a major influence on the observed baryon-asymmetry of the Universe. Lattice results have shown that the EW transition in the SM is an analytic crossover [R25].

The second transition happens at $T < 200$ MeV and is related to the spontaneous breaking of the chiral symmetry of QCD. The nature of this transition affects substantially our understanding of the Universes evolution [R23]. For instance in a strong first-order phase transition the QGP supercools before bubbles of hadron gas are formed. Since the hadronic phase is the initial condition for nucleosynthesis the inhomogeneities in this phase could have a strong effect on nucleosynthesis [R23]. Knowing that typical baryon chemical potentials are much smaller than the typical hadron masses ($\mu \approx 45$ MeV at RHIC [171] and negligible in the early Universe) we can use QCD lattice calculations performed at $\mu = 0$. The results [R26] provide a strong evidence that also the QCD transition is a crossover, and thus the above mentioned scenarios – and many others – are ruled out. Numerical simulations on the lattice also indicate that at $\mu \approx 0$ MeV the two phase transitions which are possible in the QCD – deconfining and chiral symmetry restoring – occur at essentially the same point [R27].

Situation at $\mu \gg 0$ MeV and $T \gg 0$ MeV is more complicated (see the right panel of Fig.1.2). Here the wealth of novel QCD phases is predicted to exist [R28] including so called quarkyonic phase [R29]. At $T \approx 0$ MeV and $\mu \geq 1$GeV a variety

of color superconducting phases occur [R28, R30]. Somewhere on the phase boundary at $\mu_B \approx 400$ MeV critical point separating first and second order phase transition is predicted [R28]. Let us note that Cabibbo and Parisi in their seminal 1975 paper [R17] predicting the QCD deconfinement phase transition argued that: *The true phase diagram may actually be more complex, due to other kinds of phase transitions....*

Thermodynamical properties of QCD plasma are shown on Fig.1.3 where pressure p and energy density ε normalized to T^4 are plotted as a function of temperature T. Hadron gas to QGP phase transition shows up as an order of magnitude change in ϵ in a narrow range of temperatures $\Delta T \approx 10 - 20$ MeV around $T \approx T_c \approx 160$ MeV. Let us note that if the deconfined phase would comply with original expectations [R16] and behave as a gas of weakly interacting quarks and gluons with $N_c = 3$ colors and $N_f = 3$ quark flavors, the Stefan-Boltzmann (SB) limit:

$$\frac{P}{T^4} = g\frac{\pi^2}{90}, \quad \frac{\varepsilon}{T^4} = g\frac{\pi^2}{30}, \quad g = 2(N_c^2 - 1) + \tfrac{7}{2}N_c N_f = 47.5 \qquad (1.2)$$

would be reached soon after the phase transition. This is at variance with the lattice QCD calculations shown on Fig.1.3. p/T^4 rises rapidly above T_c, then begins to saturate by about $2T_c$, but at values substantially below the SB limit indicating substantial remaining interactions among the quarks and gluons in the QGP phase. Let us note that it was not these theoretical calculations but the correct interpretation [R31] of experimental data [171] which led to the fall of 30 years old paradigm of weakly interacting QGP controlled by perturbative QCD (pQCD) and to the rise of a new one based on strongly coupled Quark–Gluon Plasma (sQGP) [R21, R31].

By definition, plasmas are states of matter in which charged particles interact via long range (massless) gauge fields. This distinguishes them from neutral gases, liquids or solids in which the inter-particle interaction is of short range. So plasmas themselves can be gases, liquids or solids depending on the value of plasma parameter Γ which is the ratio of interaction energy to kinetic energy [R32]. Strongly coupled classical electromagnetic plasmas $\Gamma > 1$, are not exotic objects at all. For example, table salt NaCl can be considered a crystalline plasma made of permanently charged ions Na^+ and Cl^- [R21]. At $T \approx 10^3$ K (still too small to ionize non-valence electrons) it transforms into a molten salt, which is liquid plasma with $\Gamma \approx 60$. Current estimate of this parameter for the sQGP at RHIC energies $\Gamma = 1.5 - 6$ [R33] corresponds also to the liquid plasma.

1.3.2 Transport models

One of the main tasks of the theory is to link experimental observables to the different phases and manifestations of the QCD matter. To achieve this goal, a detailed understanding of the dynamics of heavy ion reactions is essential. This is facilitated by transport theory which helps to interpret or predict the quantitative features of heavy ion reactions. It is particularly well suited for the non-equilibrium situation, finite

size effects, non-homogeneity, N-body phase space, particle/resonance production and freeze-out as well as for collective dynamics. Microscopic [R34–R36] and macroscopic (hydrodynamical) [R3,R6] transport models attempt to describe the full time-evolution from the initial state of the heavy ion reaction up to the freeze-out of all initial and produced particles after the reaction.

Hadronic cascade models, some with mean-field interactions, have succeeded in reproducing the gross and many detailed features of the nuclear reactions measured at Dubna Synchrophasotron [8] and GSI SIS [48, 49, R34, R35]. They have become indispensable for experimentalists who wish to identify interesting features in their data or to make predictions to plan new experiments (see Sec. 3 and 4 of this thesis). However, the general success of these models at lower energies can easily lead to misconceptions at higher energies. For instance all models based on the hadronic dynamics are fundamentally inconsistent at high particle densities. This makes their application to collisions of heavy systems at the SPS and above quite controversial. Asking the question, which fraction of the energy is contained in known hadrons and which fraction is temporarily stored in much less certain to exist objects, such as pre-hadronized strings, it was found [R35] that up to a time of 8 fm/c most of the energy density resides in strings and other high-mass continuum states that have not fully decayed. Physical properties of these objects are poorly known even when they occur in isolation, not to speak about their interactions (or even their existence) in a dense environment. The application of these models to the early phase of collision of two heavy nuclei at the SPS and above is therefore ill-founded.

The idea to use the laws of ideal hydrodynamics to describe the expansion of the strongly interacting matter formed in high energy hadronic collisions was first formulated by Landau in 1953 [R8]. The phenomenological success of his model of multiparticle production was for decades big challenge to high energy physics [R73]. First because hydrodynamics is a classical theory, second that it assumes local equilibrium. Both these assumptions imply a large number of degrees of freedom and it is by no means clear that the highly excited, but still small systems produced in violent nuclear collisions satisfy the criteria justifying treatment in terms of a macroscopic theory [R6]. Therefore the Landau model (and other statistical models of strong interactions [R72]) were considered up to the mid-seventies as exotic approaches, outside mainstream physics. Then the authors of [R11, R12, R37] realized that exploitation of hydrodynamics in the interpretation of data is their only chance of proving in the laboratory the existence of a new state of matter. This is a trivial corollary of the well known fact that a state of matter is defined by its EOS, and there is no other way to get information about the EOS than by using the hydrodynamics [R3, R6].

It is important to stress here the emergent nature of the hydrodynamics [R38]. The hydrodynamical laws are universal, exact mathematical relationships among measured quantities that develop at long length scales in liquids and gases and cannot be de-

duced from the underlying equations of motion of their constituents. It is a physical phenomenon - one we know to be exactly true because it is measured to be true. Indeed, the history of using hydrodynamics for high-energy phenomenology is checkered, with qualitative successes overshadowed by quantitative failures [R6]. Only recently, with data from the RHIC [171], came striking evidence for a strong collective expansion that is, for the first time, in good quantitative agreement with hydrodynamic predictions.

1.4 This thesis

In this work, HENP and multiparticle dynamics are studied extensively. Starting from a simple phenomenological description of the multiparticle production in high energy hadron-hadron collisions the author proceeds to the relativistic nuclear collisions at 1 AGeV studied in early 1990 at GSI SIS by experiment TAPS, continuing with the ultra-relativistic lead beam experiments WA98 and NA45/CERES at 158 and 40 AGeV which were performed between 1994-2001 at the CERN SPS, ending up with the collider experiments STAR at RHIC and ALICE at LHC, first running from 2000 till now, second at the time of writing this thesis still awaiting its first beams.

The thesis consists of 14 publications dealing with various aspects of HENP. The papers collected in the thesis cover the period since 1986 till 2007. Most of the papers were published in the well-known international physical journals, based on the experimental data measured and analyzed within large international collaborations. The complete list of authors publication can be found in section 7.1. The list other references is at section 7.2.

The general outline of this thesis consists of four topics.

The first theme – the study of multiparticle production in high energy hadron-hadron collisions 2.1.2, 2.2, 2.3 ([30, 33, 40]) – is discussed in Chapter 2.

The second theme, presented in Chapter 3, is devoted to the early heavy ion programme at GSI SIS. Its two main themes are the discovery of azimuthal anizothropy of neutral pions 3.1.2, 3.1.5 ([43, 46]) and the near threshold and subthreshold particle production 3.1.2, 3.2, 3.3, 3.4.2, 3.4.3 ([43, 48, 49, 52]). The major part of the material presented in this section was obtained by the author during his stay at KVI Groningen within the TAPS experiment. The results from [52] are due to a smaller Rez-GSI-Bratislava collaboration.

The third topic (Chapter 4) covers selected topics from the ultra-relativistic heavy ion programme at CERN SPS. Results on production of equilibrated system 4.1 ([63]), particle flow 4.3.2 ([90]) and search for the chiral phase transition 4.3.2, 4.2 ([59, 90]) are presented. In both international collaborations (WA98, NA45/CERES) the author was a team leader of the NPI ASCR group.

The last topic (Chapter 5) concentrates on HENP at the nuclear colliders - the RHIC and LHC. Results presented in sections 5.1.1 and 5.2.2 are based on the data collected

by thy STAR experiment during its first four years of operation at RHIC. They cover the discovery of ideal strongly interacting liquid at RHIC [171] and selected results from femtoscopy [200]. The chapter is closed with the section 5.3.2 devoted to original expectations for the heavy ion collisions at the LHC ([228]) and their confrontation with today's expectations for the QCD matter created in most central Pb+Pb collisions to be studied soon by the ALICE experiment.

Chapter 2

Multiparticle production in high-energy hadron-hadron collisions

Basic quantity characterizing high-energy inelastic collisions is multiplicty distribution (MD) of produced hadrons $P(N)$. Even though the information about multiparticle correlations is contained in MD in an integrated form it provides a general and sensitive means to probe the dynamics of the interaction [R9, R39]. In $e^+e^- \to \bar{q}q \to X$ despite uncertainties in the modeling of hadronization - the transition of quarks and gluons to hadrons at the final stage of the shower evolution - main characteristics of the MD can be understood quantitatively from the dynamics of the perturbative parton shower evolution [R39]. In contrast to this, hadronic collisions are dominated by processes involving non-perturbatively small momentum transfers. So there are many MD models [R9] but the first principles understanding is missing.

Lattice calculations imply that hadronization is an inherent property of QCD [R39]. Due to its confinement-induced character parton-hadron transition provides an example of highly non-perturpative phenomenon . Phenomenologically, the distributions of partons and hadrons are often found to be remarkably similar, implying that the properties of high-energy multihadronic events are primarily determined at the partonic level. This is supported by the simplified estimates suggesting [R9] that hadronization does not drastically alter the parton level results or that its effects can be estimated from the energy dependence of experimental observables. Hence in the process of hadronization the parton distributionsare simply renormalized without changing their shape [R39]. This property - called local parton-hadron duality (LPHD) - has its orogin in the idea of soft pre-confinement, when partons group into colorless clusters without disturbing the initial spectra [R9]. The LPHD is frequently used to make a contact between results of pQCD calculations and measured hadrons. Phenomenological models of hadronization (see e.g. [R36] and the models used in 2.3) are incorporated into Monte Carlo simulations of inelastic processes [R35] and in most cases they support the approximate property of LPHD [R39].

2.1 Energy Independent Number of Clusters and Multiplicity Distribution at Collider and Beyond

2.1.1 Introductory notes

In the analysis of various count distributions occurring in nature the so-called infinitely divisible distributions [R40] play a distinguished role. In multiparticle dynamics their importance was discovered independently by Giovannini and Van Hove [R41] and by Šimák and Šumbera [30]. A discrete distribution $P(N)$ is said to be infinitely divisible if $\forall$ integer $k > 0$ there exists k independent identically distributed random variables $N_1, \ldots, N_k$ whose sum is distributed as $P(N)$. In terms of its generating function (g.f.) $Q(w) \equiv \sum_N P(N) w^N$ this means that $\forall k > 0$ integer $\sqrt[k]{Q(w)}$ is again the g.f. of a certain distribution. Moreover, any infinitely divisible distribution can be written as a Compound Poisson Distribution (CPD) [R40]:

$$Q(w) = f\left[g(w)\right], \quad \text{where} \quad f(w) = e^{-\langle\nu\rangle(w-1)} \tag{2.1}$$

where $f(w)$ is g.f. of Poisson distribution and $g(w)$ is g.f. of some other discrete distribution.

To illustrate this property let us assume that we want to describe the ensemble of interacting particles occupying volume V at temperature T and chemical potential μ using grand canonical partition function $Z(T, V, \mu)$. Since the particles are in mutual interactions they have to be correlated. So we do not expect that their number distribution $P(N) = \partial \ln Z / \partial \ln \mu$ will correspond to an ideal gas. Nonetheless it may turn out that the $P(N)$ is with a good accuracy some infinitely divisible distribution. From (2.1) it then follows that the ensemble of interacting particles can be looked at as an ideal (i.e. non-interacting) gas of quasi-particles whose number distribution is Poissonian with g.f. $f(w)$. Number of particles n corresponding to the fixed number $\nu = 1$ of quasi-particles does not have a sharp value and is distributed according to some probability distribution $p(n)$ with g.f. $g(w)$.

Notwithstanding the fact that such quasi-particle/hierarchical clustering models are nowadays quite popular in the high-energy physics [R9, R39, R84, R85] as well as in the astrophysics [R44], they were not very common at mid-eighties when the UA5 Collaboration published their results on MD of charged particles from non-single diffractive $\bar{p}p$ events at $S\bar{p}pS$ collider at CERN [R45].

Article reprint

ENERGY INDEPENDENT NUMBER OF CLUSTERS AND MULTIPLICITY DISTRIBUTION AT COLLIDER AND BEYOND*)

V. Šimák

Institute of Physics, Czechosl. Acad. Sci., Na Slovance 2, 180 40 Praha 8, Czechoslovakia

M. Šumbera

Nuclear Physics Institute, Czechosl. Acad. Sci., 250 68 Řež near Prague, Czechoslovakia

Multiplicity distributions up to the Collider energies could be described by various two-parameter compounded distributions having in common Poisson distributed number of clusters. Among them the logarithmic distribution for hadronization via decaying clusters leads to energy-independent number of clusters above the ISR energies, replacing the previous KNO-scaling.

I. INTRODUCTION

Recent result from the study of non-single diffractive $\bar{p}p$ interactions at $\sqrt{(s)} = 540$ GeV [1] has shown the violation of KNO scaling. The experimental distributions of multiplicity of charged particles in $\bar{p}p$ and pp collisions at $\sqrt{(s)} > 10$ GeV was approximated by negative binomial distribution [2]

$$P_(N) = \binom{N + k - 1}{k - 1} q^N (1 - q)^k, \quad q = \frac{\langle N \rangle}{k + \langle N \rangle} \tag{1}$$

where $k^{-1} = (-0{\cdot}098 \pm 0{\cdot}008) + (0{\cdot}0282 \pm 0{\cdot}0009) \ln s$ is the parameter describing the KNO-scaling violation. The distribution (1) has been widely used for description of multiplicity distributions at high energies (see [3] and references cited therein). The interpretation of (1) as a result of k independently produced clusters decaying according to Bose-Einstein distribution (BE) has been naturally considered [4]. The experimental non integer value of $k = 3{\cdot}69 \pm 0{\cdot}09$ together with decrease of k with energy and its increase with the width of pseudorapidity interval [5] makes this interpretation discutable.

In this note a randomization in the number of particle sources inside of two parameter compound distributions are considered. Among them the compound Poisson and logarithmic distribution provides a new asymptotic regularity.

II. NEGATIVE BINOMIAL DISTRIBUTION WITH INCREASING NUMBER OF SOURCES

The generating function (g.f.) of the distribution (1) is

$$Q(w) = \sum_{N=0}^{\infty} P_(N)\, w^N = \left(\frac{1 - q}{1 - qw}\right)^k \tag{2}$$

*) Dedicated to the 30th anniversary of the Joint Institute for Nuclear Research.

where the expression in brackets is g.f. of BE distribution in accordance with the interpretation mentioned above. An alternative way of expressing (2) in the form of the compound distribution is [6]

$$f(w) = \exp\left[\langle \nu \rangle (w - 1)\right] \tag{3a}$$

$$Q(w) = f[g(w)]$$

$$g(w) = \frac{\ln(1 - qw)}{\ln(1 - q)} \tag{3b}$$

where f, g is the g.f. of the Poisson and logarithmic distribution, respectively. Therefore, the negative binomial distribution (1) can be also interpreted as the sum of Poisson distributed clusters [7, 8] with average number value

$$\langle \nu \rangle = k \cdot \ln\left(1 + \frac{\langle N \rangle}{k}\right) \tag{4}$$

each of them decaying according to the logarithmic distribution

$$P(n) = \frac{1}{-\ln(1 - q)} \cdot \frac{q^n}{n}, \quad n \geqq 1 . \tag{5}$$

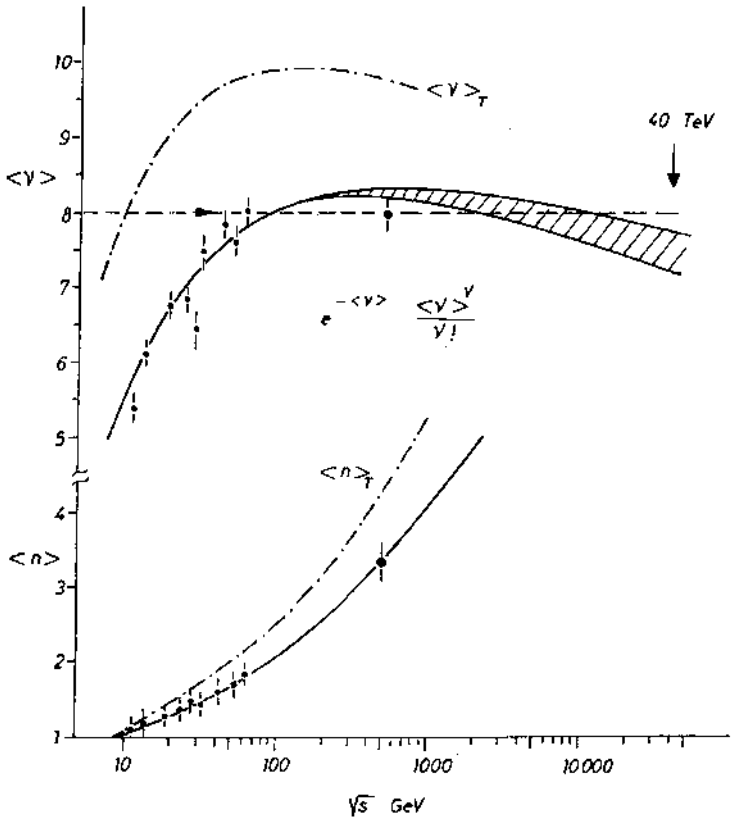

Fig. 1. Average number of clusters $\langle \nu \rangle$ and average number of decay particles in one cluster from compound Poisson-logarithmic distribution, eq. (4) and (6). Dashed lines represent the $\langle \nu \rangle_T$ corrected to the neutral particles.

Each cluster thus consists of at least one particle, with average number of particles in a cluster

$$\langle n \rangle = \frac{\langle N \rangle}{k \,.\, \ln\left(1 + \langle N \rangle / k\right)}. \tag{6}$$

The energy dependence of $\langle v \rangle$ and $\langle n \rangle$ is presented in fig. 1. In this interpretation average number of clusters is an increasing function of energy and moreover saturates at the ISR energies $\langle v \rangle \approx 8$. Curves correspond to the parametrizations of k and $\langle N \rangle$ [2]. The shaded region in extrapolation of the $\langle v \rangle$ reflects an uncertainty in two different parametrizations of $\langle N \rangle$.

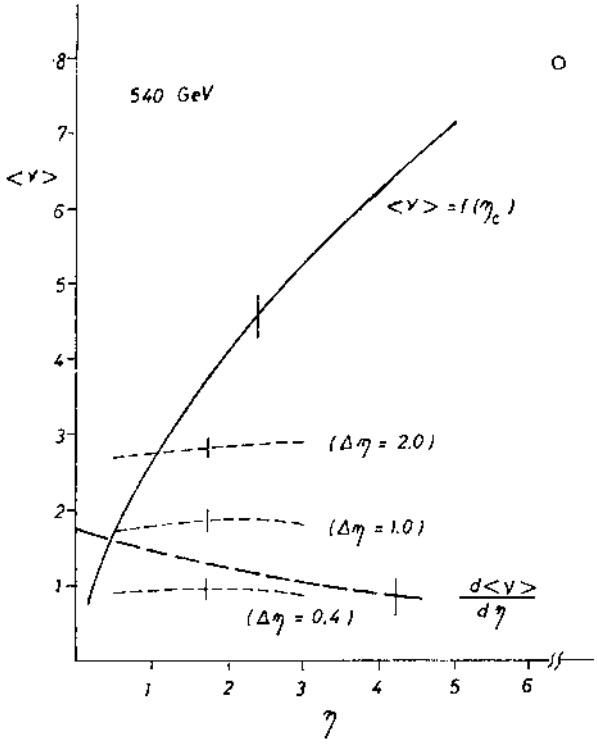

Fig. 2.

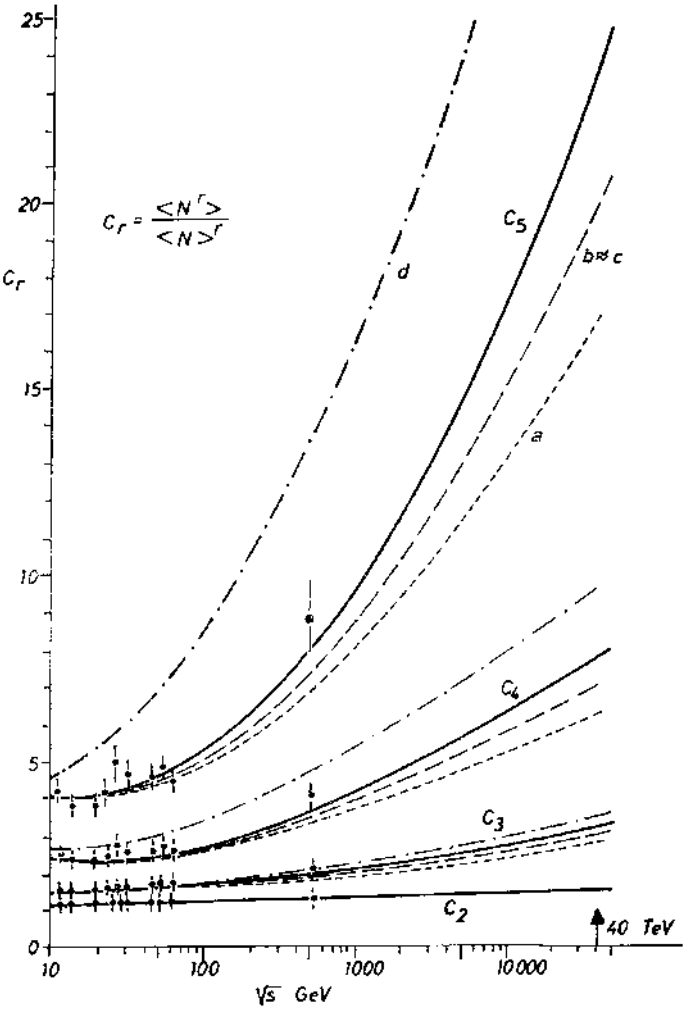

Fig. 3.

Fig. 2. Normalized statistical moments predicted for high energies under the assumption of constant number of clusters $\langle v \rangle = 8$. Full curves correspond to the compound Poisson-logarithmic distribution and curves a, b, c, d are calculated from distributions discussed in chapter III.

Fig. 3. Average number of clusters as a function of rapidity interval η_c centered at $\eta = 0$. Circle corresponds to the full phase space. Dashed line represents the change of the slope of $\langle v \rangle$ and dotted lines correspond to the moving window $\Delta\eta$ according to [3].

In terms of variables $\langle v\rangle$ and k the average number of charged particles and $\langle N\rangle/D$ ratio of distribution (1) are

$$\langle N\rangle = k[\exp(\langle v\rangle/k) - 1] \to k \,.\, \exp(8/k)\,, \tag{7}$$

$$\frac{\langle N\rangle}{D} = \{k[1 - \exp(-\langle v\rangle/k)]\}^{1/2} \to \sqrt{k}\,. \tag{8}$$

Corresponding energy dependence of normalized moments C_r for $r = 3, 4, 5$ is plotted in fig. 2.

The constant number of clusters at high energies actually means that the evolution of the shape of multiplicity distribution is governed by the logarithmic distribution which is also obtained as limit $k \to 0$ of distribution (1) (truncated in accordance with experimental condition $N > 0$).

At fixed energy $\sqrt{(s)} = 540$ GeV $\langle v\rangle$ is a rising function of the width of pseudorapidity window η_c (fig. 3). The increase is, however, not a linear one as in the case of k-dependence [5]. This possibly means that the distribution of number of the clusters is not uniform in pseudorapidity. The constant number of clusters is also a natural source of observed increase of long-range correlations of particles with the energy.

III. COMPOUND DISTRIBUTIONS – ALTERNATIVES

It was pointed out [5] that (1) may be only an approximation to the experimental data. To the check the information content of experimentally data we have considered several other two-parameter compound distributions:

a) Poisson distributed clusters decaying according to Poisson distribution (Neymann type A – contagious distribution)

$$P(N) = \frac{\langle n\rangle^N}{N!}\, e^{-\langle v\rangle} \sum_{j=0}^{\infty} \frac{j^N}{j!} (\langle v\rangle\, e^{-\langle n\rangle})^j\,, \tag{9}$$

b) Poisson distributed BE clusters,

c) Poisson distributed BE clusters with $n \geqq 1$ (TBE)

$$P(n) = \frac{1}{\langle n\rangle}\left(1 - \frac{1}{\langle n\rangle}\right)^{n-1} \tag{10}$$

with

$$P(N) = e^{-\langle v\rangle}\left(1 - \frac{1}{\langle n\rangle}\right)^N \sum_{j=1}^{N} \binom{N-1}{j-1} \frac{1}{j!} \left(\frac{\langle v\rangle}{\langle n\rangle - 1}\right)^j. \tag{11}$$

The average number of clusters $\langle v\rangle$ in a), b), c) equals to k, $2k$, $2k\langle N\rangle/(2k + \langle N\rangle)$ respectively. While in the a) and b) the $\langle v\rangle$ is entirely function of k, and thus falling with energy, distribution (11) has a nontrivial behaviour: after the initial rise it

reaches a maximum around the ISR energies ($\langle \nu \rangle \approx 7{\cdot}1$) and then it falls down to the value $\langle \nu \rangle \approx 6{\cdot}1$ at Collider energies.

Above distributions have in common with negative binomial distribution an assumption that the correlations between particles are entirely due to their grouping into clusters. Thus the clusters are produced independently according to the Poisson distribution [7, 8]. We have also considered an oposite scenario:

d) Clusters distributed according to the TBE distribution (10) and Poisson distribution of its decay products. In this case the particle correlations are due to the correlations between the clusters with average number of clusters $\langle \nu \rangle = k/(k-1)$.

Taking as an input experimental values of the first two moments of multiplicity distributions in the energy range $\sqrt{(s)} = (10{\cdot}5 - 540)$ GeV as compiled in [2] we have calculated C_3, C_4 and C_5 for the alternative compound distributions a)–d). The result of these calculations together with the extrapolarion based on k-parametrization and $\langle \nu \rangle = 8$ is presented on fig. 2. Only the distribution d) is excluded by the present experimental data – confirming the importance of independent cluster emission. On the other hand the mechanism of cluster decay is not determined by experiment and we have to wait for the data at higher energies. This leaves the space for other more parametric distribution [9], e.g. Glauber-Lachs-Peřina-McGill distribution, which can be also written into the form of Poisson distributed BE, clusters.

IV. DISCUSSION

Several models have bern proposed to explain the KNO-violation by different mechanism of particle production: e.g. DTU scheme [10], leading particle effect [11], preasymptotic behaviour [12], energy-statistics balance [13], additive quark model [14] etc. Some of their results are similar in spite of their physical assumption.

We have examined more modest approach to evaluate informational contents of experimental data. Comparing them with the two-parameter compound distributions we have found that the data prefer an independent cluster emission, suggested also by QCD in LLA calculations [8]. An attractive candidate describing the cluster decay we have found the logarithmic distribution which has no KNO limit. The compound Poisson and logarithmic distribution with constant average number of clusters is most economical way to incorporate both the observed KNO scaling violation and long-range correlations. It enables with single parameter k to predict multiplicity distributions above the ISR energies.

We should like to point out that the limiting value $\langle \nu \rangle = 8$ has been obtained only from charged particle data. Inclusion of neutral particles ($\langle N \rangle_T = 3\langle N \rangle/2$) leads to an increase in $\langle \nu \rangle$, and $\langle n \rangle$ (fig. 1).

After completion of this work we become aware that some our results have been recently obtained by A. Giovannini and L. Van Hove [15]. We are grateful to W.-Q. Chao for paying our attention to this paper.

Received 28. 1. 1986.

References

[1] Alner G. J. et al.: Phys. Lett. B *138* (1984) 304.
[2] Alner G. J. et al.: Phys. Lett. B *160* (1985) 199.
[3] Garetto M. et al.: Nuovo Cimento A *37* (1977) 38.
[4] Giovannini A.: Nuovo Cimento A *15* (1973) 543;
Carruthers P., Shih C. C.: Phys. Lett. B *127* (1983) 242;
Mrówczyński S.: Z. Phys. C — Particles and Fields *27* (1985) 131.
[5] Alner G. J. et al.: Preprint CERN-EP/85/61.
[6] Kendall M. G., Stuart A.: The Advanced Theory of Statistics, Vol. 1. Ch. Griffin & Co., London, 1963.
[7] Levy D.: Nucl. Phys. B *59* (1973) 583.
[8] Hayot F., Sterman G.: Phys. Lett. B *121* (1983) 419.
[9] Biyajima M., Suzuki N.: Prog. Theor. Phys. *73* (1985) 918;
Blažek M.: Z. Phys. C — Particles and Fields *26* (1984) 455.
[10] Capella A., Tran Van Y.: Phys. Lett. B *114* (1982) 450.
[11] Basile M. et al.: Lett. Nuovo Cimento *41* (1984) 298.
[12] Bialas A., Derado I., Stodolsky L.: Phys. Lett. B *156* (1985) 421.
[13] Cai Xu et al.: Univ. of West Berlin Preprint FUB/HEP-85-4.
[14] Rudaz S., Valin P.: Preprint CERN-Th/4240/85.
[15] Giovannini A., Van Hove L.: Preprint CERN-Th/4230/85.

2.1.3 Citations

1. Chia Chang Shih, *Superclusters and hadronic multiplicity distribution*, Physical Review **D** 34, 2710-2719 1986.

2. Ballestrero, A; Carazza, B, *A Simple Interpretation of Multiparticle Distributions in Different Pseudorapidity Intervals* Zeitschrift fur Physik **C**-Particles And Fields, **50** (1): 61-67 1991

3. Zborovksý, I; *Evolution of Clans in Multiparticle Production* Zeitschrift fur Physik **C**-Particles And Fields **63** (2): 257-261 1994

2.1.4 Conference presentations

1. M. Šumbera, *Poisson Distributed Clusters: an Alternative Interpretation of New UA5 Multiplicity Measurements*, presented at the International Seminar on High Energy Physics, Liblice Castle, June 24-28, 1985. Unpublished.

2. V. Šimák, M. Šumbera and I. Zborovský, *Superclusters in Multiplicity Distributions?*, SPIRES entry Proceedings of the IX Warsaw Symposium on Elementary Particle Physics, Kazimierz, Poland, May 25-31, 1986. Edited by Z. Ajduk, WARSZAWA 1986, p. 67-74.

Article reprint

Volume 206, number 1 PHYSICS LETTERS B 12 May 1988

ENTROPY IN MULTIPARTICLE PRODUCTION AND ULTIMATE MULTIPLICITY SCALING

V. ŠIMÁK
Institute of Physics, Czechoslovak Academy of Sciences CS-18040 Prague 8, Czechoslovakia

M. ŠUMBERA and I. ZBOROVSKÝ
Nuclear Physics Institute, Czechoslovak Academy of Sciences, CS-25068 Řež near Prague, Czechoslovakia

Received 9 March 1988

The entropy $S=-\sum P(n)\ln P(n)$ of multiplicity distributions of charged particles in hadron–hadron collisions is investigated. The observed linear increase of S with maximum possible CMS rapidity Y_m, $S=(0.417\pm0.009)Y_m$, may be a special case of a more general scaling $S/Y_m=F(y_c/Y_m)$, found in (pseudo) rapidity windows $|y|<y_c$. We predict an ultimate multiplicity scaling in the few TeV region.

Experimental results from the CERN SppS Collider have considerably changed our understanding of asymptotic behavior of multiparticle production [1]. Multiplicity distributions of particles in full phase space and also in different rapidity windows are usually analysed using the statistical moments [1–4], their energy dependence being interpreted in terms of KNO-scaling [5] and its possible violation [1,2,6,7].

In this note we would like to point out and exploit a different strategy [8]. We introduce a new quantity characterizing charged particle multiplicity distributions $P(n)$-entropy [9]:

$$S=-\sum P(N)\ln P(N),\quad \sum P(N)=1\,. \tag{1}$$

Let us mention some properties of S:

(i) The entropy describes a general pattern of independent particle emission. The total entropy produced from ν statistical independent phase regions (e.g. Poisson distribution clans or superclusters [6] is equal to the sum of entropies of individual sources:

$$S=S_1+S_2+S_3+\ldots+S_\nu\,. \tag{2}$$

(ii) The entropy is invariant under an arbitrary distorsion of multiplicity scale. Insertion of zeros between two points on the multiplicity scale, or mutual permutation of different bins can influence both the shape and statistical moments of $P(n)$, but not its entropy. In particular, the entropy calculated from charged particles and negative ones or produced pairs in full phase space give the same S.

(iii) The simple relation (4) between S, the average multiplicity $\langle n\rangle$ and the KNO function $\psi(z)$ follows from the identity

$$S-\ln\langle n\rangle=-\frac{1}{\langle n\rangle}\sum[\langle n\rangle P(n)]\ln[\langle n\rangle P(n)]\,. \tag{3}$$

For $\langle n\rangle$ large enough the RHS of (3) can be approximated by the entropy of the $\psi(z)$ function

$$S-\ln\langle n\rangle=\frac{1}{2}\int_0^\infty \psi(z)\ln[\psi(z)]\,\mathrm{d}z\,, \tag{4a}$$

with $\psi(z)$ for charged particles normalized as

$$\int\psi(z)\,\mathrm{d}z=\int z\psi(z)\,\mathrm{d}z=2\,.$$

The corresponding S for produced pairs reads

$$S=\ln\langle N\rangle-\int_0^\infty \psi(z)\ln[\psi(z)]\,\mathrm{d}z\,, \tag{4b}$$

with $\int\psi(z)\,\mathrm{d}z=\int z\psi(z)\,\mathrm{d}z=1$.

Volume 206, number 1 PHYSICS LETTERS B 12 May 1988

(iv) An upper bound on the entropy of the $\psi(z)$ function,

$$S-\ln\langle N\rangle = S-\ln\tfrac{1}{2}\langle n\rangle \leqslant 1\,. \qquad (5)$$

is reached for the KNO function of the geometrical distribution $\psi(z)=\exp(-z)$.

The experimental situation concerning the evolution of entropy with CMS energy $\sqrt{s}$ for pp, $p\bar{p}$, π^+p, π^-p, K^+p, and K^-p inelastic interactions [1–3,7] is presented in fig. 1. The increase of entropy with energy seems to be similar for all hadron–proton interactions. For $\sqrt{s}>20$ GeV this behaviour reveals a universal asymptotic linearity with maximum rapidity of the hadrons produced $Y_m=\ln(\sqrt{s}/m_\pi)$:

$$S=(0.417\pm0.009)Y_m\,,$$

$$\chi^2/\mathrm{ND}=6.6/13\,. \qquad (6)$$

This suggests that in hp collisions the entropy per unit of rapidity S/Y_m is an energy-independent quantitity.

The observed behavior of entropy together with the limiting property (5) puts severe restrictions on the energy dependence of both $\langle n\rangle$ and $\psi(z)$. We illustrate this statement in fig. 2. The approximate energy independence of $\psi(z)$ (early KNO scaling) is violated by Collider data. The experimental data up to $\sqrt{s}=900$ GeV are yet far from saturation of the bound (5). Nevertheless, the behavior of multiplicity distributions at still higher energies must be governed by (5): either the entropy S must slow down, or the average charged multiplicity $\langle n\rangle$ must grow faster with energy than the present parametrization of the data indicates [2]. In the latter case the extrapolation of (6) to the asymptotic region gives $\langle n\rangle \sim s^{(0.21\pm0.02)}$. Furthermore, the onset of ultimate multiplicity scaling is expected in the few TeV region (fig. 2), unless some new mechanism of particle production emerges, which would force the entropy to decrease.

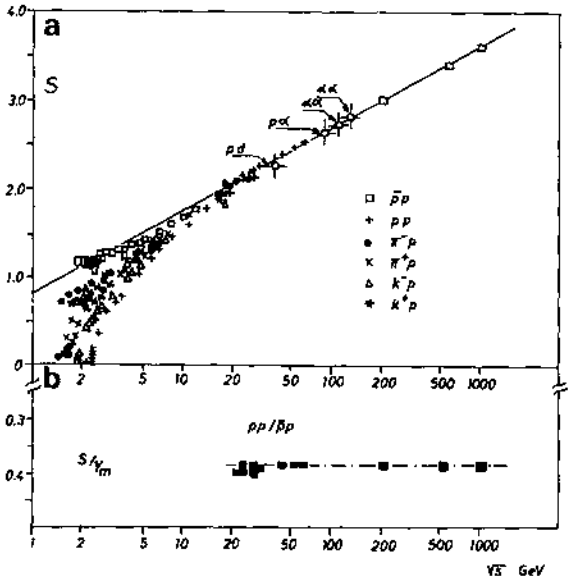

Fig. 1. The entropy of charged particle multiplicity distributions (1) for $\bar{p}p$, pp, π^+p, π^-p, K^+p, K^-p inelastic (compiled in ref. [7] and $\bar{p}p$ non-single-diffractive interactions [1,12] together with data on high energy nuclear collisions [10,11] (a). The ratio S/Y_m versus Y_m for pp and $\bar{p}p$ above $\sqrt{s}=20$ GeV (b). The lines correspond to the fit (6).

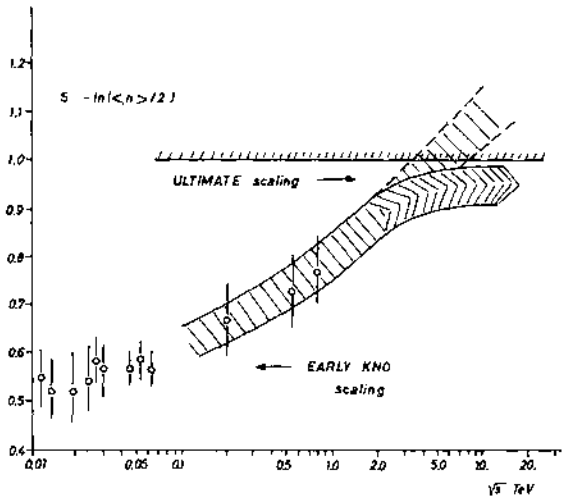

Fig. 2. Energy dependence of the entropy of the KNO function $\psi(z)$ (calculated from $S-\ln(\langle n\rangle/2)$. The shaded corridor corresponds to parametrizations of S and $\langle n\rangle$ given by (6) and of ref. [1], respectively. The bent part indicates our prediction of the onset of ultimate multiplicity scaling.

Using the FNAL [10] and ISR [11] data on multiplicities of charged or negative secondaries from pd, αp and αα inelastic interactions we try to extend the observed regularity to the case of high energy collisions of the lightest nuclei (fig. 1). The agreement with the universal hadron–nucleon curve is surprisingly good and helps to fill the gap between the pp ISR and $\bar{p}p$ Collider data (we have used the total CMS nucleus–nucleus energy for calculation of $\sqrt{s}$).

Data on multiplicity distributions in the central intervals of (pseudo) rapidity $|y|<y_c$ [3,4,12] allow

Volume 206, number 1 PHYSICS LETTERS B 12 May 1988

us to study the evolution of entropy with y_c starting from very small central windows up to Y_m. Let us first examine the following general condition:

$$S^-(y_c)+S^+(y_c)=S(y_c)=S^-(y_c)\,, \qquad (7)$$

relating the entropies S^-, S^+ and S of negative, positive and charged secondaries in the same window y_c. If no correlations between positive and negative particles are present we have $S=S^-+S^+$. On the opposite extreme, the charge conservation condition at $y_c=Y_m$ as a particular example, a lower bound saturation takes place. In addition to this $S^+(y_c)=S^-(y_c)$ is expected to hold in these phase space regions where the leading charge contribution can be neglected (e.g. at small y_c).

At present only one set of experimental data is available on multiplicity distributions of both negative and charged secondaries (at $\sqrt{s}=22$ GeV [3,4]). In terms of the reduced rapidity variable $\xi=y_c/Y_m$ these data show monotonous increase of both S^+, S^- and S up to $\xi=0.5$. While a further increase of S^+ and S^- seems to be negligible, S starts to decline to reach at last its final full phase space value $S(\xi=1)=S^-(\xi=1)$.

The non-monotonic behavior of the entropy of a charged particle is illustrated in fig. 3a, where also $\bar{p}p$ Collider data are included. The extension of the linear proportionality between S and Y_m as observed at $\xi=1$ (6) into smaller rapidity subintervals has been tested by plotting the quantity S/Y_m instead of S. Apart from the region of smal $\xi(<0.2)$ one observes a violation of the suggested scaling behaviour $S/Y_m=F(\xi)$. On the other hand, by supposing particles to be produced via neutral clusters each consisting of two oppositely charged hadrons [13,14], this scaling can be restored (fig. 3a).

The multiplicity distributions of pairs (clusters) $P(N)$ produced serving as an input for the evaluation of the corresponding entropies, were estimated from the multiplicity distributions of charged secondaries $P(n)$, either by assuming that the clusters are not affected by cuts in rapidity [8] or, what is more realistic, by taking into account the effect of finite extensions of clusters in rapidity space. Assuming that the form of $P(N)$ does not change when going from Y_m into smaller windows we were able, with the help of information from the first three moments of the charged multiplicity distribution $P(n)$, to extract

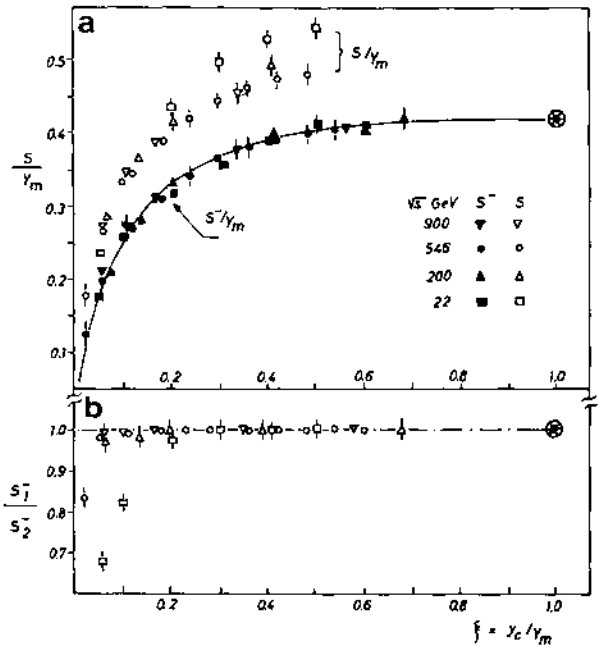

Fig. 3. The entropy of the multiplicity distribution of charged particles and clusters (rescaled by Y_m) as a function of ξ (S, S^-). The curve corresponds to the fit (8) (a). The ratio S_1^-/S_2^- ($S_2^-=S^-$) of entropies for two different assumptions concerning extensions of neutral clusters in rapidity (b).

$P(N)$ from the Collider data. Let us add that for the $p\bar{p}$ case the first approach suggests $P(n^-)=P(\frac{1}{2}n)$ independently of ξ, while the second one assumes only that $\langle n^-\rangle=\langle\frac{1}{2}n\rangle$. As follows from fig. 3b, both methods are equivalent for $\xi>0.2$. 22 GeV pp data were used to compare the entropy of negative particles with the entropy obtained by the second method for the clusters. In spite of large uncertainties due to the exclusion of leading (positive) charges, we have obtained within statistical errors the same value of the entropy for negatives and clusters.

From fig. 3 it follows that the entropy of pairs produced (negative particles) reaches its full phase space value quite early, for $\xi>0.5$. Thus entropy production in the fragmentation region seems to be negligible. This could be expressed by the following parametrization of the scaling function $F(\xi)$:

$$S(y_c)/Y_m=(0.407\pm0.009)$$
$$\times\{1-\exp[-(8.6\pm0.6)\xi]\}\,, \qquad (8)$$

fitting the data with $\chi^2/\mathrm{ND}=45/30$. Given the val-

Volume 206, number 1 PHYSICS LETTERS B 12 May 1988

ues of y_c and Y_m, one can use the scaling (8) to predict the energy evolution of the particle density in the central region [15,16].

For the semiinclusive distribution the scaling in reduced rapidity ξ has been proposed long ago [17]. Its connection with the observed violation of KNO scaling has been reviewed recently [18]. Original arguments in favour of this scaling law were based on Feynman's analogy between the statistical properties of a (one-dimensional) fluid contained inside a finite volume and the distribution of the produced particles in rapidity space. The longitudinal geometric scaling states [17] that this distribution of particles does not change with external volume Y_m provided we use instead of rapidity y its reduced value ξ to label the particle position inside the volume. Such a type of self-similarity need not be generally true for any fluid. Nevertheless, the extensive character of both the volume y_c and the entropy of the fluid guarantees that the entropy of the multiplicity distribution should be always a homogeneous function of its volume: $S(\lambda y_c)=\lambda S(y_c)$. Taking $\lambda=1/Y_m$ the scaling (8) and regularity (6) follow.

We thank J. Dias de Deus, G. Ekspong, K. Fialkowski, L. Van Hove and Meng Ta-Chung for valuable conversations.

References

[1] UA5 Collab., G.J. Alner et al., Phys. Lett. B 138 (1984) 304; B 167 (1986) 476.
[2] UA5 Collab., G.J. Alner et al., Phys. Lett. B 160 (1985) 199.
[3] NA2 Collab., M. Adamus et al., Phys. Lett. B 177 (1986) 239.
[4] F. Meijers, Ph.D. Thesis, Nijmegen (1987).
[5] Z. Koba, H.B. Nielsen and P. Olesen, Nucl. Phys. B 40 (1972) 317.
[6] A. Giovannini and L. Van Hove, Z. Phys. C 30 (1986) 391; V. Šimák and M. Šumbera, Czech. J. Phys. B 36 (1986) 1267.
[7] R. Szwed, G. Wrochna and A.K. Wroblewski, Warsaw preprint IFD/3/87.
[8] V. Šimák, M. Šumbera and I. Zborovský, Proc. Intern. Europhysics Conf. on High energy physics (Uppsala, Sweden, June 1987), p. 467.
[9] A. Wehrl, Rev. Mod. Phys. 50 (1978) 221.
[10] S. Dado et al., Phys. Rev. D 20 (1979) 1589.
[11] W. Bell et al., Phys. Lett. B 128 (1983) 349.
[12] UA5 Collab. G.J. Alner et al., Phys. Lett. B 160 (1985) 239; C. Fuglesang, Proc. XVIIth Intern. Symp. on Multiparticle dynamics (Seewinkel, Austria, 1986) (World Scientific, Singapore).
[13] K. Fialkowski and H.I. Mietinen, Phys. Lett. B 43 (1973) 61;
T.T. Chou and C.N. Yang, Phys. Lett. B 135 (1984) 175.
[14] P. Carruthers and C.C. Shih, Phys. Lett. B 165 (1985) 209.
[15] V. Šimák, M. Šumbera and I. Zborovský, Proc XVIII Intern. Symp. on Multiparticle dynamics (Tashkent, USSR, September 1987).
[16] M. Plümer, S. Raha and R.M. Weiner, preprint University of Marburg (October 1987).
[17] A.J. Buras and J. Dias de Deus, Nucl. Phys. B 78 (1974) 445.
[18] J. Dias de Deus, Phys. Lett. B 178 (1986) 301.

2.2.1 Citations

1. Ghosh D., Deb A., Biswas S., *et al.*, *Fractality of emission of compound multiplicity in C-12-AgBr interactions at 4.5A GeV.* Canadian Journal of Physics 85(4)385-392, 2007.
2. A. Bialas, *Summary of ISMD 2005.* 35th International Symposium on Multiparticle Dynamics (ISMD 05), Kromeriz, Czech Republic, 9-15 Aug 2005. Published in AIP Conf.Proc.828:409-418,2006.
3. Zhiming Li, *Entropy analysis in pi(+)p and K(+)p collisions at root s=22 GeV* . 35th International Symposium on Multiparticle Dynamics (ISMD 05), Kromeriz, Czech Republic, 9-15 Aug 2005. Published in AIP Conf.Proc.828:124-129,2006.
4. W. Kittel, E.A. De Wolf, *Soft multihadron dynamics.* Hackensack, USA: World Scientific (2005) 652 p.
5. Ghosh D., Deb A., Pal S. *Fractal analysis of pionisation process in hadron-nucleus interactions - evidence of multifractality in compound (proton plus pion) multiplicity distribution* Indian Journal of Physics and Proceedings of the Indian Association for the Cultivation of Science, 79(12) 1395-1402, 2005.
6. Ghosh D., Deb A., Pal S. *Evidence of fractal behavior of pions and protons in high energy interactions - An experimental investigation* Fractals-Complex Geometry Patterns and Scaling in Nature and Society, 13(4)325-339, 2005.
7. A. Giovannini, R. Ugoccioni, *Global event properties in proton proton physics with ALICE.* Contribution to the ALICE Physics Performance Report. e-Print: hep-ph/0203215.
8. B.Z. Belashev, M.K. Suleymanov, *The Maximum entropy techniques and the statistical description of systems.* e-Print: hep-ex/0110041.
9. W. Ochs, *New Developments In Strong Interaction Physics.* MPI-PAE/PTh-79/89, Nov 1989. Summary talk given at the 12th Warsaw Symposium in Elementary Particle Physics, Kazimierz, Poland, May 20 - Jun 2, 1989. Published in Warsaw Symp. 1989:0659-675 (QCD161:W3:1989).
10. Ghosh D., Deb A., Pal S., *Fractal analysis of pionisation process in hadron-nucleus interactions - evidence of multifractality in compound (proton plus pion) multiplicity distribution* .Indian Journal of Physics and Proceedings of the Indian Association for the Cultivation of Science, 79 (12): 1395-1402 DEC 2005.
11. Ghosh D., Deb A., Pal S., Haldar P.K., Bhattacharyya S., Mandal P., Biswas S., Mondal M, *Evidence of fractal behavior of pions and protons in high energy interactions - An experimental investigation* . Fractals-Complex Geometry Patterns and Scaling in Nature and Society, 13 (4): 325-339 DEC 2005.
12. Kittel W. *General characteristics of hadron-hadron collisions* Acta Physica Polonica **B**, 35 (12): 2817-2872 Dec 2004.
13. Ghosh, D; Deb, A; Sahoo, SR; Haldar, PK; Mondal, M *Proton emission in nucleus-nucleus interactions at 14.5 A GeV - evidence of monofractality* . Europhysics Letters, 65 (4): 472-477 Feb 2004.
14. Ghosh, D; Deb, A; Dutta, K; Sarkar, R; Dutta, I; Mondal, M *Multifractality and multifractal specific heat in fragmentation process in Mg-24-AgBr interaction at 4.5 AGeV.* Indian Journal of Physics and Proceedings of the Indian Association for the Cultivation of Science-Part A, **78A** (3): 359-362 May 2004.
15. Ghosh, D; Deb, A; Haldar, PK; Sahoo, SR; Maity, D *Validity of the negative binomial multiplicity distribution in case of ultra-relativistic nucleus-nucleus interaction in different azimuthal bins* Europhysics Letters, 65 (3): 311-315 Feb 2004.
16. Ghosh, D; Deb, A; Biswas, S; Mandal, P; Ghosh, J; Bhattacharyya, S; Patra, KK; Mondal, M *Evidence of multifractal structure of compound multiplicity distribution in Mg-24-AgBr interactions at 4.5AGeV* Czechoslovak Journal of Physics, 53 (12): 1173-1181 Dec 2003.
17. Ghosh, D; Deb, A; Mondal, M; Bhattacharyya, S; Ghosh, J Fractal *behavior of nuclear fragments in high energy interactions Source.* Fractals-Complex Geometry Patterns and Scaling in Nature and Society, 11 (4): 331-343 Dec 2003.

18. Andersen, E; Blaes, R; Brom, JM; Cherney, M; de la Cruz, B; Fernandez, C; Garabatos, C; Garzon, JA; Geist, WM; Greiner, DE; Gruhn, CR; Hafidouni, M; Hrubec, J; Jones, PG; Judd, EG; Kuipers, JPM; Ladrem, M; de Guevara, PL; Lovhoiden, G; MacNaughton, J; Mosquera, J; Natkaniec, Z; Nelson, JM; Neuhofer, G; de los Heros, CP; Plo, M; Porth, P; Powell, B; Ramil, A; Rohringer, H; Sakrejda, I; Thorsteinsen, TF; Traxler, J; Voltolini, C; Wozniak, K; Yanez, A; Zybert, R *Measurement of negative particle multiplicity in S-Pb collisions at 200 GeV/c per nucleon with the NA36 TPC* Physics Letters **B**, 516 (3-4): 249-256 Sep 20 2001.
19. Dremin, I M; Gary, J W *Hadron multiplicities* Physics Reports-Review Section of Physics Letters, 349 (4): 302-393 Aug 2001.
20. Bialas, A; Czyz, W *Renyi entropies in multiparticle production* . Acta Physica Polonica **B**, 31 (12): 2803-2817 Dec 2000.
21. Bialas, A; Czyz, W *Event by event analysis and entropy of multiparticle systems* .Physical Review **D**, 61 (7): Art. No. 074021 Apr 1 2000
22. Ghosh, D; Deb, A; Chattopadhyay, R; Jafry, AK; Lahiri, M; Biswas, B; Purkait, K; Das, S; Roychoudhury, J; Das, S; Roy, S *Multifractality and intermittency study of ultrarelativistic S-32-AgBr and O-16-AgBr interactions: Further evidence of a nonthermal phase transition* . International Journal of Modern Physics **A**, 14 (13): 2091-2101 MAY 20 1999
23. Ghosh, D; Purkait, K; Sengupta, R; Sarkar, S; Dev, A *Multifractality study in "hot" and "cold" events in C-12-AgBr interactions at 4.5A GeV/c . NUOVO CIMENTO DELLA SOCIETA ITALIANA DI FISICA A-NUCLEI PARTICLES AND FIELDS*, 110 (11): 1289-1295 Nov 1997.
24. Ghosh, D; Lahiri, M; Deb, A; Das, S; Purkait, K; Biswas, B; Choudhury, JR; Chatterjee, R; Jafry, AK *Fluctuation study of pionisation in ultrarelativistic nucleus-nucleus interaction* . Zeitschrift fur Physik **C**-Particles and Fields, 71 (2): 243-249 Jun 1996.
25. Brogueira, P; deDeus, JD; daSilva, IP *Information entropy and particle production in branching processes* . Physical Review **D**, 53 (9): 5283-5285 May 1 1996.
26. Golyak, I; Galayda, S *Negative binomial parameters and the two-mechanism model* .Zeitschrift fur Physik **C**-Particles and Fields, 70 (2): 227-231 Apr 1996.
27. Takagi, F Multifractal *Structure of Multiplicity Distributions in Particle Collisions at High-Energies* Physical Review Letters, 72 (1): 32-35 Jan 3 1994.
28. Sengupta, K; Cherry, M L; Jones, W V; Wefel, J P; Dabrowska, A; Holynski, R; Jurak, A; Olszewski, A; Szarska, M; Trzupek, A; Wilczynska, B; Wilczynski, H; Wolter, W; Wosiek, B; Wozniak, K; Freier, P S; Waddington, C J *Multifractal Analysis of Nucleus-Nucleus Interactions* . Physical Review **D**, 48 (7): 3174-3181 Oct 1 1993.
29. Mukhopadhyay, A; Jain, P L; Singh, G *Multiplicity Distributions in High-Energy Heavy-Ion Collisions* .Nuovo Cimento Della Societa Italiana di Fisica **A**-Nuclei Particles And Fields, 106 (7): 967-978 Jul 1993.
30. Mukhopadhyay, A; Jain, P L; Singh, G *Entropy and Fractal Characteristics of Multiparticle Production at Relativistic Heavy-Ion Interactions* . Physical Review **C**, 47 (1): 410-412 Jan 1993.
31. Adamovich, M I; Aggarwal, M M; Alexandrov, Y A; Andreeva, N P; Anson, Z V; Arora, R; Avetyan, F A; Badyal, S K; Basova, E; Bhalla, Kb; Bhasin, A; Bhatia, Vs; Bogdanov, Vg; Bubnov, VI; Burnett, TH; Cai, X; Chasnikov, IY; Chernova, LP; Chernyavsky, MM; Eligbaeva, GZ; Eremenko, LE; Gaitinov, AS; Ganssauge, ER; Garpman, S; Gerassimov, SG; Grote, J; Gulamov, KG; Gupta, SK; Gupta, VK; Heckman, HH; Huang, H; Jakobsson, B; Judek, B; Just, L; Kachroo, S; Kalyachkina, GS; Kanygina, EK; Karabova, M; Kaul, GL; Kitroo, S; Kharlamov, SP; Krasnov, SA; Kulikova, S; Kumar, V; Lal, P; Larionova, VG; Lepetan, VN; Liu, LS; Lokanathan, S; Lord, J; Lukicheva, NS; Luo, SB; Maksimkina, TN; Mangotra, LK; Marutyan, NA; Maslennikova, NV; Mittra, IS; Mookerjee, S; Nasrulaeva, H; Nasyrov, SH; Navotny, VS; Nystrand, J; Orlova, GI; Otterlund, I; Palsania, HS; Peresadko, NG; Petrov, NV; Plyushchev, VA; Qarshiev, DA; Qian, WY; Qin, YM; Raniwala, R; Raniwala, S; Rao, NK; Rappoport, VM; Rhee, JT; Saidkhanov, N; Salmanova, NA; Sarkisova, LG; Sarkisyan, VR; Shabratova, GS; Shakhova, TI; Shpilev, SN; Skelding, D; Soderstrom, K; Solovjeva, ZI; Stenlund, E; Surin, EL; Svechnikova, LN; Tolstov, KD; Tothova, M; Tretyakova, MI; Trofimova, TP; Tuleeva, U; Vokal, S; Wang, HQ; Weng, ZQ; Wilkes, RJ; Xia, YL; Xu, GF; Zhang, DH; Zheng, PY; Zhochova, SI; Zhou, DC *Local Particle Densities and Global Multiplicities in Central Heavy-Ion Interactions at 3.7, 14.6, 60 and 200 A-GeV*. Zeitschrift fur Physik **C**-Particles And Fields, 56 (4): 509-520 Dec 1992.

32. Ghosh, D; Roy, J; Sengupta, A G; Thakurata, Adtg; D E, A; Hossain, S A; Mukherjee, H; Halder, S; Naha, S; Halder, D; Lahiri, M; Sen, S; Basu, M T *The Study of Multiplicity Characteristics and Reduced Entropy of Particles Produced by Hadrons (70-400 GeV) and Heavy-Ions (2.1-4.5 GeV).* Canadian Journal of Physics, 70 (8): 667-669 Aug 1992.
33. Chaudhuri, A K *Energy-Dependence of Parameters of Negative-Binomial Distributions in NN Collisions.* Physical Review **D**, 45 (11): 4057-4063 Part 1 Jun 1 1992.
34. Majernik, V; Mamojka, B *On the Nonstandard Measures of Uncertainty and Organization* Physica Scripta, 44 (5): 412-417 Nov 1991.
35. Valin, P *Theoretical Unitarity Bounds, Theorems and Scalings for the Strong-Interactions at High-Energies* Physics Reports-Review Section of Physics Letters, 203 (4): 233-287 May 1991.
36. Bialas, A *Intermittency 90* Nuclear Physics **A**, 525: C345-C360 Apr 1 1991.
37. Nakada, T) *CP violation and K and B meson decays.* Preprint PSI-PR-91-02, Jan 1991. 66pp. SPIRES entry
38. Ghosh, D; Mukhopadhyay, A; Ghosh, A; Sarkar, S; Sengupta, R; Roy, J D *Multiplicity Characteristics of Symmetric and Asymmetric Heavy-Ion Interactions at 4.5 A GeV/c.* Europhysics Letters, 11 (6): 535-540 Mar 15 1990.
39. De Deus, J D *Leading Charges And Charged-Particle Distributions In Limited Rapidity Bins.* Zeitschrift fur Physik **C**-Particles And Fields, 46 (1): 125-128 1990.
40. Hegyi, S; Krasznovszky, S *Regular Features of Predicted Multiplicity Distributions for Very High-Energies* . Physics Letters **B**, 235 (1-2): 203-207 Jan 25 1990.
41. Takagi, F *Entropy and information dimension in multiparticle production at high-energies.* Preprint Tohoku University TU-90-354, Aug 1990. SPIRES entry
42. Xu Cai, Jing-chen Zhou, Dai-cui Zhou, Zhuo-wei Zhou *Relative Entropy Scaling In High-Energy Multi - Hadron Production.* Preprint Hua-Zhong Normal University, HZPP-90-03, Mar 1990.
43. Stern, I. *Entropy Scaling And The Generalized Information Dimensions Of The Multiplicity Distribution.* PRINT-90-0121 (RADIATION-MONITORING), Jan 1990. 30pp.
44. Zhou, Z W; Cai, X *Entropy and Redundancy Scaling in Multihadron Production.* Chinese Physics Letters, 6 (7): 317-320 1989.
45. R.E. Ansorge, B. Asman, L. Burow, P. Carlson, R.S. DeWolf, B. Eckart, G. Ekspong, I. Evangelou, C. Fuglesang, J. Gaudaen, C. Geich-Gimbel, B. Holl, Kerstin B. Jon-And, F. Lotse, N. Manthos, D.J. Munday, W. Pelzer, John G. Rushbrooke, F. Triantis, L. Van hamme, C. Walck, C.P. Ward, D.R. Ward, C.J.S. Webber, T.O. White, G. Wilquet, N. Yamdagni *Charged Particle Multiplicity Distributions at 200-GeV and 900-GeV Center-Of-Mass Energy.* Zeitschrift fur Physik **C** 43:357,1989.
46. Kanki, T; Kinoshita, K; Sumiyoshi, H; Takagi, F *Multiparticle Production in Particle and Nuclear Collisions.* Progress of Theoretical Physics Supplement, (97A): Ur1-213 1988.
47. Carruthers, P; Shih, C C *Mutual Information and Forward-Backward Correlations in Multihadron Production.*Physical Review Letters, 62 (18): 2073-2076 May 1 1989.
48. Lam, C S *Entropy Content of Multiplicity Distributions.* Physics Letters **B**, 217 (4): 530-534 Feb 2 1989.
49. Takagi, F; Tsukamoto, T *Semi-Inclusive Rapidity Distributions from Entropy Maximization.* Physical Review **D**, 38 (7): 2288-2290 Oct 1 1988.

2.2.2 Conference presentations

1. V. Šimák, M. Šumbera and I. Zborovský, *Entropy of the Multiplicity Distributions.* Proceedings of the International Europhysics Conference on High Energy Physics. Edited by O. Botner, Uppsala Univ. Press, Uppsala 1987, vol. 1, p.324. [35]

2. V. Šimák, M. Šumbera and I. Zborovský, *Entropy in the Multiparticle Production*, proceedings of the 18th International Symposium on Multiparticle Dynamics, Tashkent, USSR, Sep 8-12, 1987. Edited by I. Dremin and K. Gulamov. (World Scientific, Singapore, 1988) p.205. [32]

3. V. Šimák, M. Šumbera and I. Zborovský, *Entropy Scaling: Evolution of Parton Showers or (Thermo)Dynamics?*, SPIRES entry Proceedings of the International Symposium "Hadron Interactions - Theory and Phenomenology", Bechyě, Czechoslovakia, 26 June - 1 July 1988. Edited by J. Fischer, P. Kolář, V. Kundrát, Prague 1988, p.387-393. [34]

4. V. Šimák, M. Šumbera and I. Zborovský, *Entropy Scaling at High Energy $p\bar{p}$ Interactions*, SPIRES entry Proceedings of the IIIrd International Symposium "High Energy Experiments and Methods - HEXAM 89", Bechyě, Czechoslovakia, June 25 - 30, 1989. Edited by P. Reimer, M. Suk, V. Šimák, Prague 1989, p.201-206 [38].

2.2.3 Further developments

As already mentioned in the previous section the energy dependence of the entropy is strongly correlated with that of average multiplicity. As the bounding value

$$S - \ln <n> \leq (1+ <n>) \ln(1 + \frac{1}{<n>}) = 1 + O(<n>^{-1}) \tag{2.2}$$

tends to unity, the observed monotonous increase of the entropy $S \sim \ln(\sqrt{s}/m_\pi)$, if valid at higher energies, will also govern the energy dependence of $<n>$:

$$< n > \approx \exp(S) = (\sqrt{s}/m_\pi)^{D_1}. \tag{2.3}$$

where $D_1 \equiv S/Y_m$. Such asymptotic power-law behavior of the average multiplicity should be contrasted with other approaches to multiparticle production. In particular in [R79], $<n>$ was predicted to increase as a second order polynomial in $\ln s$. Difference between these two predictions will be substantial at the top energy of LHC, because according to Eq. (2.3) $<n> \approx 110$ at $\sqrt{s} = 14$ TeV, while according to the parametrization used in [R79] $<n> \approx 70$ at this energy.

Simple interpretation of the value of coefficient relating entropy with maximum rapidity of produced pions $S = (0.417 \pm .009)Y_m$ was given in **[38]** 2.2. Using Feynman-Wilson fluid approach to multiparticle production [R76] which is based on the analogy between statistical properties of a one dimensional fluid contained inside a finite volume and distribution of produced particles in rapidity space T.D. Lee has made the following remark [R43]:
Usually, a thermodynamical system has three extensive variables: the number of particles N, the length (or volume) L and energy E; corresponding to these are three intensive variables: the fugacity z, the pressure p, and the temperature T. In the present case there are only two extensive variables: N and $L \backsim ln(s/m^2)$; correspondingly, there are also only two intensive variables: z and p. Hence, kT can be chosen to be unity.
Under this assumption the entropy density S/L of a one dimensional massless Boltzmann or Bose-Einstein gas with one degree of freedom which is contained inside the volume $L = Y_m$ equals (see e.g. [R70]):

$$\frac{S_{Bol}}{Y_m} = \frac{4}{\pi^2}(kT)^3\Big|_{kT=1} = 0.405$$
$$\frac{S_{B-E}}{Y_m} = \frac{4\pi^2}{90}(kT)^3\Big|_{kT=1} = 0.438 \qquad (2.4)$$

It is quite amusing to note that both values are within 3σ-range from the experimental value $(0.417 \pm .009)$.

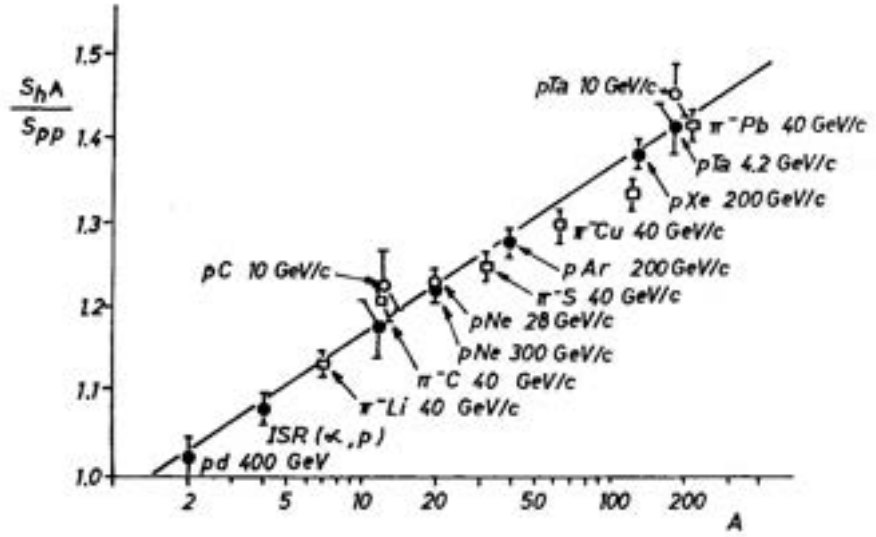

Figure 2.1: *Entropy production in hadron-nucleus collisions relative to pp-collisions* [**38**]

Finally, let us comment on the entropy production in hadron-nucleus collisions. In addition to the case of hadron-hadron inelastic interactions an extra contribution to the entropy of negative particle multiplicity distributions is expected to come from the fluctuating number of participating nucleons. Since the latter are supposed to be energy-independent, it is expected that the ratio S_{hA}/S_{pp} will be energy independent too [**38**]. This is illustrated on Fig.2.1. The proportionality $S_{hA} = S_{pp}[(0.97 \pm 0.030) + (0.085 \pm 0.005)lnA]$ holds over surprisingly large energy interval.

Recently CERN heavy ion experiment NA36 has measured entropy of the negative particle multiplicity distribution in S+Pb collisions at 200AGeV [R80]. The measured value of the entropy in full phase space was $S = (4.266 \pm .026)$. Generalizing the above equation to $S_{AB} \approx S_{pp}[(1. + (0.085 \pm 0.005)lnA][(1. + (0.085 \pm 0.005)lnB]$ we obtain $2.056 * [1 + (0.295 \pm 0.16)] * [1 + (0.454 \pm 0.23)] = 3.87 \pm 0.12$. This value is pnly by 10% smaller then the measured one. This may indicate some additional contribution to the total entropy not present neither in the proton-proton nor in hadron-nucleus collisions. Very likely candidate for this piece is the multiple nucleon-nucleon scattering.

Modern Physics Letters A, Vol. 7, No. 25 (1992) 2333–2339

Article reprint

ENTROPY, DIMENSIONS AND OTHER MULTIFRACTAL CHARACTERISTICS OF MULTIPLICITY DISTRIBUTIONS

M. PACHR, V. ŠIMÁK*, M. ŠUMBERA and I. ZBOROVSKÝ

Nuclear Physics Institute, Czechoslovak Academy of Sciences, CS 250 68 Řež near Prague, Czechoslovakia

**Institute of Physics, Czechoslovak Academy of Sciences, Na Slovance 2, CS 180 40 Prague, Czechoslovakia*

Received 15 November 1991
Revised 3 June 1992

Entropy scaling of multiplicity distributions is shown to be a special case of more general set of multifractal measures. We perform an analysis multiplicity distributions of data from hadron-hadron and electron-positron interactions.

1. Recently a large number of experimental data accumulated in hadron-hadron and electron-positron interactions has stimulated a new development in multiparticle dynamics. New methods introduced originally for description of chaotic dynamic systems, diffusion-limited growth of structures and other nonlinear phenomena[1] have also been applied to the spectra of particles created in high-energy collisions. Pioneer work in multiparticle dynamics in terms of multifractal variables have been carried out in Ref. 2. Several authors have studied intermittent behavior of particle distributions in a small rapidity bin. The exponential increase of a scaled factorial moments with decreasing window width was interpreted as a signal of multifractal property of (a chaotic) dynamics of multiparticle production.[3]

Our approach is different from the usual intermittency and multifractal analyzes in that our bin width is related not to the detector resolution but to the collision energy. We have suggested earlier to study the multiplicity distribution of particles in terms of its information entropy. The scaling properties of entropy in rapidity windows together with its linear increase in full phase with maximum rapidity of produced hadrons $Y_{\max} = \ln(\sqrt{s}/m_\pi)$ were found.[4] Using data on charged hadron multiplicity distributions P_n from hadron-hadron inelastic interactions it was demonstrated that for $\sqrt{s} > 20$ GeV the information entropy

$$S = -\sum P_n \ln P_n \tag{1}$$

stays constant when divided by $Y_{\max}$ ($S/Y_{\max} = 0.417 \pm 0.005$).

The Rennyi order-q information entropy[1]

$$I_q = \frac{1}{1-q} \ln \sum (P_n)^q \tag{2}$$

generalizes the information entropy S as follows from the relation $I_1 = S$. The experimental values of ratios $D_q = I_q/Y_{\max}$ for $q = 1, 3$ and ∞ are presented in Fig. 1a for pp and $p\bar{p}$ data.[5] For $q > 1$ they exhibit the same type of energy independent behavior as observed earlier for $q = 1$. Analogical plot (Fig. 1b) for data from e^+e^- collisions[6] generalizes observed regularity to lepton-lepton collisions. Energy averaged values of D_q's for both data samples are summarized in Table 1.

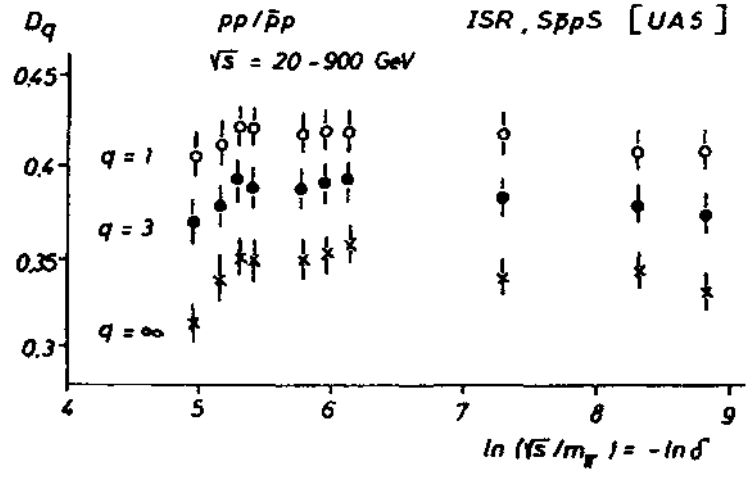

(a)

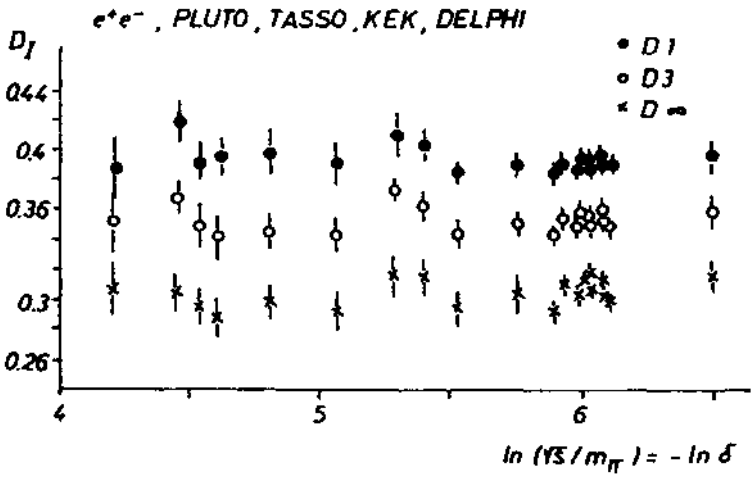

(b)

Fig. 1. Generalized fractal dimensions D_q as a function of $Y_{\max}$ for (a) $pp/p\bar{p}$ and (b) e^+e^- data.

Table 1.

D_q	$q=1$	$q=2$	$q=3$	$q=4$	$q=5$	$q=\infty$
$pp/p\bar{p}$	0.413	0.392	0.381	0.374	0.370	0.339
	±0.002	±0.002	±0.002	±0.003	±0.003	±0.004
e^+e^-	0.393	0.365	0.352	0.344	0.338	0.303
	±0.002	±0.002	±0.002	±0.002	±0.002	±0.002

2. Let us now translate these facts into the language of fractal geometry as used when studying the growth structures.[1] The fractal with overall extent $\sqrt{s}$ is composed of $N = \sqrt{s}/m_\pi$ discrete sites each of size m_π. To the nth site we assign the probability P_n (with normalization $\sum P_n = 1$), i.e., the probability that n charged particles were created. If the quantity $\sum(P_n)^q$ scales with improving relative resolution $\delta = 1/N$ like

$$G_q(\delta) = \sum(P_n)^q \sim \delta^{-\tau_q} \tag{3}$$

for δ small enough one usually speaks about multifractality of distribution P_n.[1] Since the major ambiguity in these types of analyzes is the determination of the slopes τ_q in the log-log plots, we present the $\ln G_q(\ln 1/\delta)$ in Fig. 2a for pp and $\bar{p}p$ data[5] and in Fig. 2b for e^+e^- data.[6] The linearity of $\ln G_q$ with $-\ln\delta$ is observed in a wide range of primary energies. The previously found energy and hence δ-independence of quantities D_q serves also as a direct sign of multifractality in multiplicity distributions. These quantities (sometimes called generalized dimensions[1]) can be related to the τ_q by

$$D_q = \frac{\tau_q}{1-q} \,. \tag{4}$$

The meaning of function τ_q is more obvious after performing the Legendre transformation from independent variables τ and q to the variables α and f:

$$\alpha_q = -\frac{d\tau_q}{dq} \tag{5}$$

$$f(\alpha_q) = q\alpha_q + \tau_q \,. \tag{6}$$

Then $f(\alpha)$ is a fractal dimension of a subset composed from bins whose occupancy probability lies in the interval $(P - dP, P + dP) = (\delta^{\alpha+d\alpha}, \delta^{\alpha-d\alpha})$ and is connected with frequency $N(\alpha,\delta)d\alpha$ of the occurrence of various probabilities at resolution δ by relation:

$$N(\alpha,\delta)d\alpha \sim \delta^{-f(\alpha)} \,. \tag{7}$$

As τ_1 is defined to be zero for normalized probability distributions, from (7) it follows that $f(\alpha)$ has a slope of unity where α and $f(\alpha)$ are equal to each other: $\alpha_1 = f(\alpha_1)$. From explicit dependence of $\alpha(q)$ on P_n and δ:

$$\alpha_q = \lim_{\delta\to 0} \frac{\sum P_n^q \ln P_n}{(\sum P_n^q)\ln\delta} \tag{8}$$

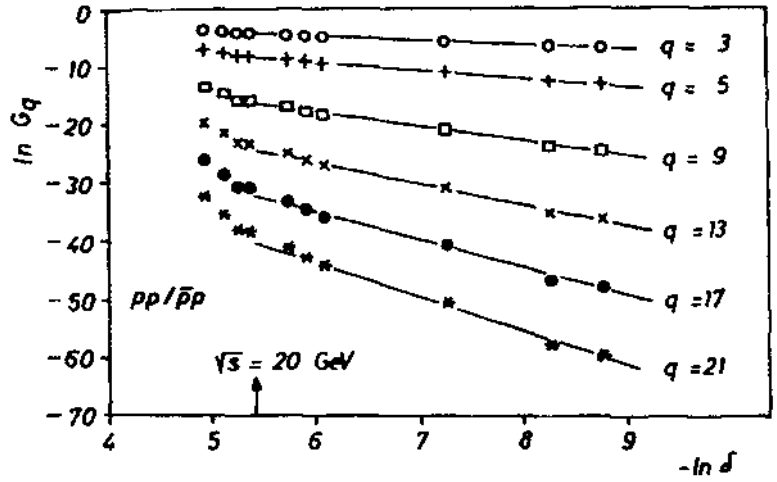

(a)

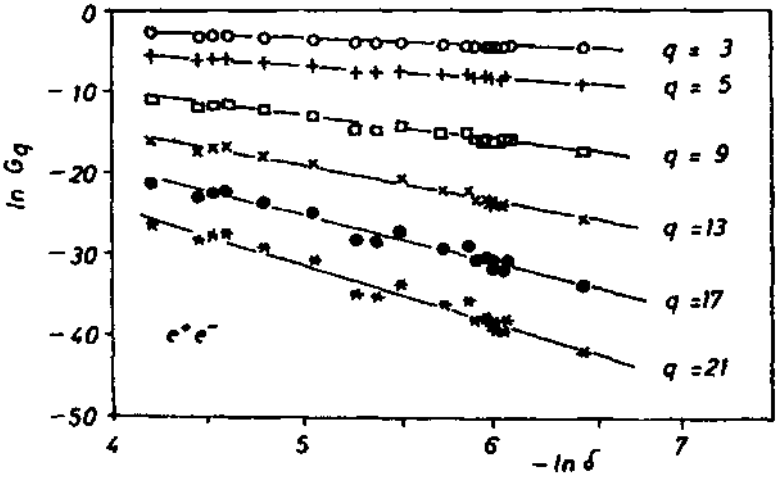

(b)

Fig. 2. $\ln(G_q)$ (see Eq. (3)) as a function of $-\ln\delta$ for (a) $pp/p\bar{p}$ and (b) e^+e^- data.

one obtains $\alpha_1 = D_1 = -S/\ln\delta$. For all other points $f(\alpha)$ is smaller than α. Hence the total probability $N(\alpha,\delta)d\alpha\ \delta^\alpha$ accumulated in bins with $P \approx \delta^\alpha$ is maximal for the subset with scaling exponent $\alpha_1 = D_1$. In other words with decreasing δ the total probability gradually concentrates on subsets with fractal dimension close to the entropy dimension $-S/\ln\delta$.

The $f(\alpha)$ curve for $pp/p\bar{p}$ data is presented in Fig. 3a, for e^+e^- in Fig. 3b. For both reactions the scaling is best around the region α_1.

3. In the intermittency studies multifractal behavior is frequently interpreted as manifestation of some self-similar particle production mechanism.[7] The D_q's are energy independent for such models which in the high energy limit exhibit both the KNO scaling of the multiplicity distribution and the power like behavior $\langle n\rangle \sim s^{\text{const}}$. To show this let us express the probability P_n that n charged particles were

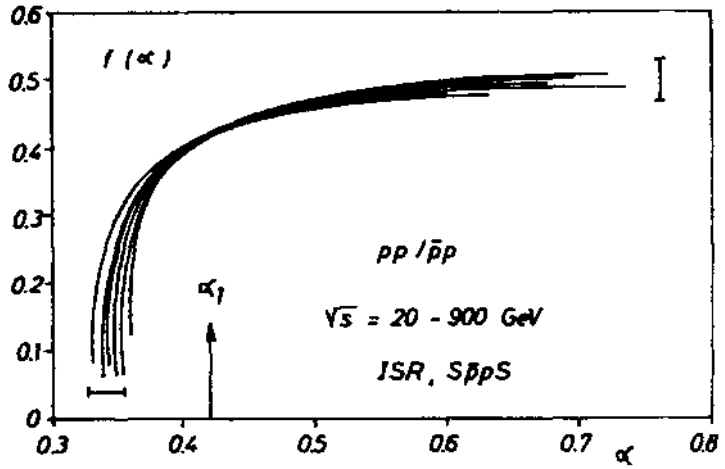

(a)

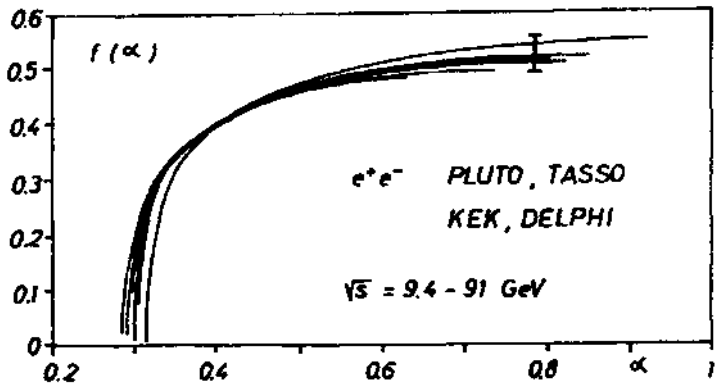

(b)

Fig. 3. $f(\alpha)$ curve for (a) $pp/p\bar{p}$ and (b) e^+e^- interactions. Statistical errors are indicated at the endpoints of the curves.

created in terms of a well known KNO function $\psi(z)$: $P_n = \frac{1}{\langle n \rangle}\psi(z = n/\langle n \rangle)$. After this substitution Eq. (3) gives

$$\tau_q = (q-1)\frac{\ln\langle n \rangle}{\ln \delta} - \frac{\ln \int \psi^q(z)/2 \; dz}{\ln \delta} \; . \tag{9}$$

For $Y_{\max} = -\ln \delta$ high enough the second term on the right-hand side of Eq. (9) vanishes and (from Eq. (4)) multifractality follows. However this multifractality is a trivial one because all D_q's degenerate to a single value. In the same limit (as follows from Eq. (6)) the $f(\alpha)$ curve shrinks into one point. Using language of the fractal geometry one may say that for such self-similar scale invariant branching models the underlying fractal is a homogeneous one.

Experimental data from both $pp/p\bar{p}$ and e^+e^- collisions provide much wider spectrum of generalized dimensions. Let us now show how such a non-trivial multifractal behavior restricts the energy evolution of the KNO function $\psi(z)$. From (8) we have:

$$P_{\max} \sim \delta^{-\alpha_\infty} \; , \tag{10}$$

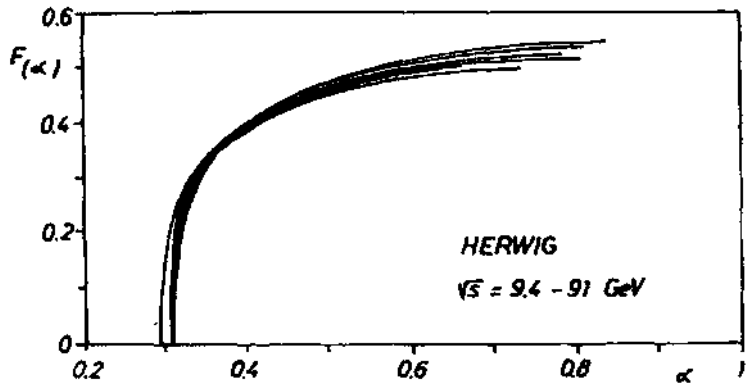

(a)

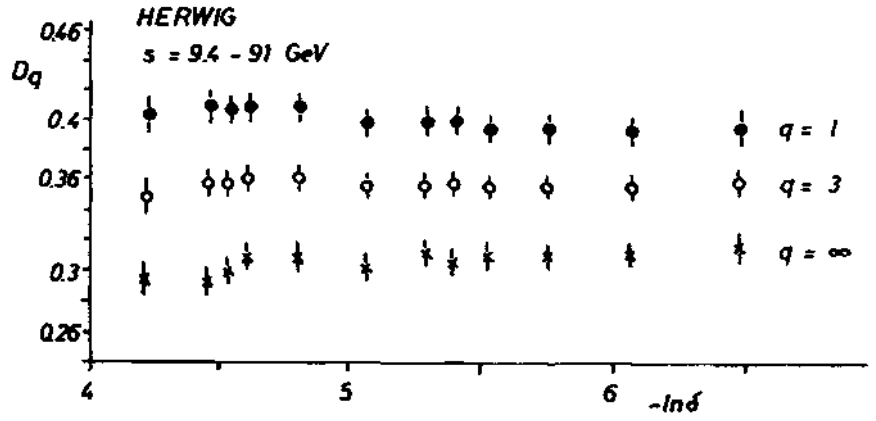

(b)

Fig. 4. HERWIG results for e^+e^- interactions: (a) $f(\alpha)$ curve and (b) D_1, D_3 and D_∞.

where $P_{\max} = \max\{P_n\}$. Using the entropy bound[4]:

$$\ln\langle n\rangle/2 + 1 \geq S = -\alpha_1 \ln \delta \tag{11}$$

one obtains:

$$\psi_{\max} = \langle n\rangle P_{\max} \sim \left(\frac{\sqrt{s}}{m_\pi}\right)^{\alpha_1 - \alpha_\infty} . \tag{12}$$

From unequality $\alpha_\infty \leq \alpha_q \leq \alpha_{-\infty}$ it follows that the multifractality with nondegenerate spectrum of α's must inevitably violate the KNO scaling. Qualitatively this means that in addition to the widening of function $\psi(z)$ with increasing energy (as unambiguously observed in $pp/p\bar{p}$ collisions) its shape will be determined by more and more pronounced peak. It is interesting whether such non-trivial behavior can be reproduced by other phenomenological approaches.

For e^+e^- collisions the situation is not clear. Available data do not yet allow us to distinguish between trivial and genuine multifractality. At finite energies an approximate KNO scaling may not be in disagreement with observed energy dependence of the negative binomial parameter k^{-1} (see the DELPHI paper[6]). However asymptotically both regularities cannot coexist.

We have used Monte-Carlo QCD-based generator HERWIG[8] to calculate $f(\alpha)$ curve (Fig. 4a) and D_1, D_3 and D_∞ (Fig. 4b) for the corresponding set of e^+e^- data. The model within the errors reproduces observed multifractal behavior in this energy region. We hope that the presented analysis could play a useful role also in future investigations for higher energies.

References

1. J. Feder, *Fractals* (Plenum Press, 1988).
2. R. C. Hwa, *Int. J. Mod. Phys.* **A4**, 481 (1989); *Phys. Rev.* **D41**, 1456 (1990).
3. A. Bialas and R. Peschanski, *Nucl. Phys.* **B273**, 703 (1986).
4. V. Šimák, M. Šumbera and I. Zborovský, *Phys. Lett.* **B206**, 159 (1988).
5. M. Adamus *et al.*, NA22 collab., *Phys. Lett.* **B177**, 239 (1986); K. Alpgard *et al.*, *Phys. Lett.* **B115**, 71 (1982); G. J. Alner *et al.*, UA5 collab., *Phys. Lett.* **B138**, 304 (1984); R. G. Ansorge *et al.*, UA5 collab., *Z. Phys.* **C43**, 357 (1989).
6. PLUTO collab., {9.4, 12.0, 13.0, 17.0, 22.0, 27.5, 30.6 GeV} private communication; W. Braunschweig *et al.*, TASSO collab., *Z. Phys.* **C45**, 193 (1989); {14.0, 22.0, 34.8, 43.6 GeV}; H. W. Zheng *et al.*, AMY collab., KEK preprint 90-005, submitted to *Phys. Rev. D* {50., 52.0, 55.0, 56.0, 57.0, 60.0, 60.8, 61.4 GeV}; *Z. Phys.* DELPHI collab., **C50**, 185 (1991) {91 GeV}.
7. W. Ochs and J. Wosiek, *Phys. Lett.* **B214**, 617 (1988); W. Ochs, *Z. Phys.* **C23**, 131 (1984).
8. G. Marchesini and B. R. Weber, *Nucl. Phys.* **B310**, 461 (1988); T. Sjstrand, QCD generators, in CERN yellow report, "Z physics at LEP1", Vol. 3, CERN 89-08.

2.3.1 Citations

1. Zhiming Li, *Entropy analysis in pi(+)p and K(+)p collisions at root s=22 GeV* . 35th International Symposium on Multiparticle Dynamics (ISMD 05), Kromeriz, Czech Republic, 9-15 Aug 2005. Published in AIP Conf.Proc.828:124-129,2006.

2. W. Kittel, E.A. De Wolf, *Soft multihadron dynamics*. Hackensack, USA: World Scientific (2005) 652 p.

3. Kittel, W, *General characteristics of hadron-hadron collisions* Acta Physica Polonica **B**, 35 (12): 2817-2872 DEC 2004.

4. Andersen, E; Blaes, R; Brom, JM; Cherney, M; de la Cruz, B; Fernandez, C; Garabatos, C; Garzon, JA; Geist, WM; Greiner, DE; Gruhn, CR; Hafidouni, M; Hrubec, J; Jones, PG; Judd, EG; Kuipers, JPM; Ladrem, M; de Guevara, PL; Lovhoiden, G; MacNaughton, J; Mosquera, J; Natkaniec, Z; Nelson, JM; Neuhofer, G; de los Heros, CP; Plo, M; Porth, P; Powell, B; Ramil, A; Rohringer, H; Sakrejda, I; Thorsteinsen, TF; Traxler, J; Voltolini, C; Wozniak, K; Yanez, A; Zybert, R, *Measurement of negative particle multiplicity in S-Pb collisions at 200 GeV/c per nucleon with the NA36 TPC* Physics Letters **B**, 516 (3-4): 249-256 SEP 20 2001.

5. Dremin, IM; Gary, JW,*Hadron multiplicities Source* Physics Reports-Review Section of Physics Letters, 349 (4): 302-393 AUG 2001.

6. Mukhopadhyay, A; Jain, PL; Singh, G, ENTROPY AND FRACTAL *Characteristics of Multiparticle Production at Relativistic Heavy-Ion Interactions*, Physical Review **C**, 47 (1): 410-412 JAN 1993.

2.3.2 Further developments

Recently published Tevatron data [R57] extend the validity of these findings up to $\sqrt{s} = 1.8$ TeV. The experimental situation is shown in Fig.2.2 where the published errors of multiplicity distributions have been taken into account. Value of D_1 is within $\pm 2\%$ error band consistent with the predicted one $D_1 \equiv S/Y_m = 0.417 \pm 0.009$ **[33]** shown by the full/dashed lines in Fig.2.2. On closer inspection, however, one can see that D_1 calculated form E735 data is systematically above the UA5 values. It is connected with higher tails of the E735 multiplicity distribution as compared to the UA5 data. The discrepancy might be due to the sizable systematic uncertainty in both E735 and UA5 measurements since in both experiments the full phase space distributions were obtained by computer simulation from data measured in a restricted range of rapidity.

Let us note that multifractality besides predicting D_q to be decreasing functions of q does not, in general, provide any further information about the q-dependence of the spectrum of the generalized dimensions D_q. In particular knowledge of say D_1 and

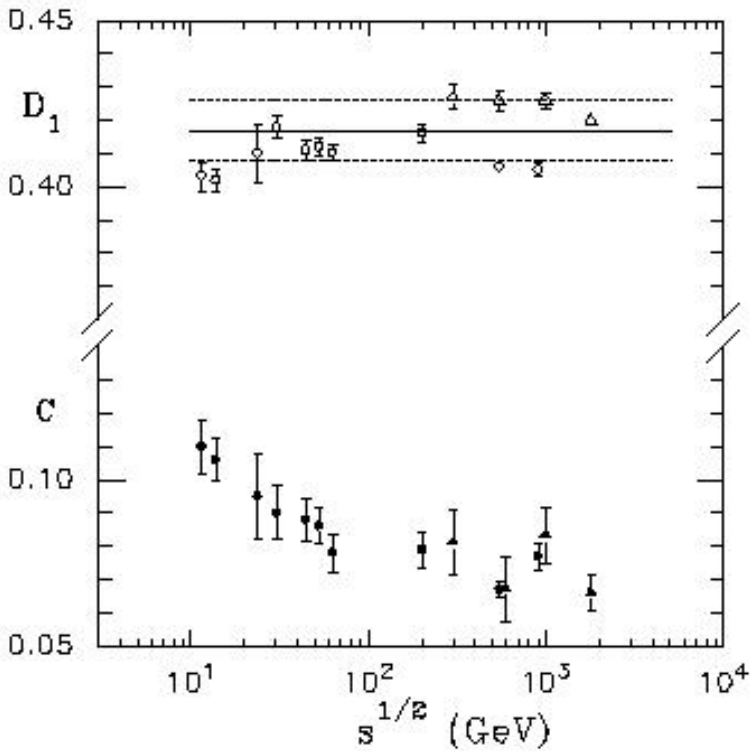

Figure 2.2: *The energy dependence of the entropy dimension D_1 and the multifractal specific heat c for charged particles. The triangles correspond to data form E735 experiment.* [**42**]

D_2 is insufficient to predict scaling behaviour of the higher q correlation integrals. It is thus gratifying to find out that this could be, at least in principle, achieved within interpretation of multifractality in thermodynamical terms [R86]. Latter is based on analogy between l.h.s. of Eq. (2.5)

$$\sum (P_n)^q \sim \delta^{-(1-q)D}. \tag{2.5}$$

and partition function

$$Z(q) \equiv \sum (P_n)^q \tag{2.6}$$

with q playing the rôle of inverse temperature $q \equiv T^{-1}$ and $V \equiv -\ln \delta$ representing volume. The thermodynamic limit of infinite volume $V \to \infty$ is then equivalent to the limit of increasing resolution $\delta \to 0$. In the constant specific heat approximation the q-dependence of the generalized dimensions D_q acquires particularly simple form [R86]

$$D_q \simeq (a - c) + c\frac{\ln q}{(q-1)}. \tag{2.7}$$

The coefficient c represents multifractal specific heat and $a = D_1$. Regular behaviour of this type is expected to occur for multifractals for which, in classical analogy with specific heat of gases and solids, the multifractal specific heat c is independent of temperature in a wide range of q.

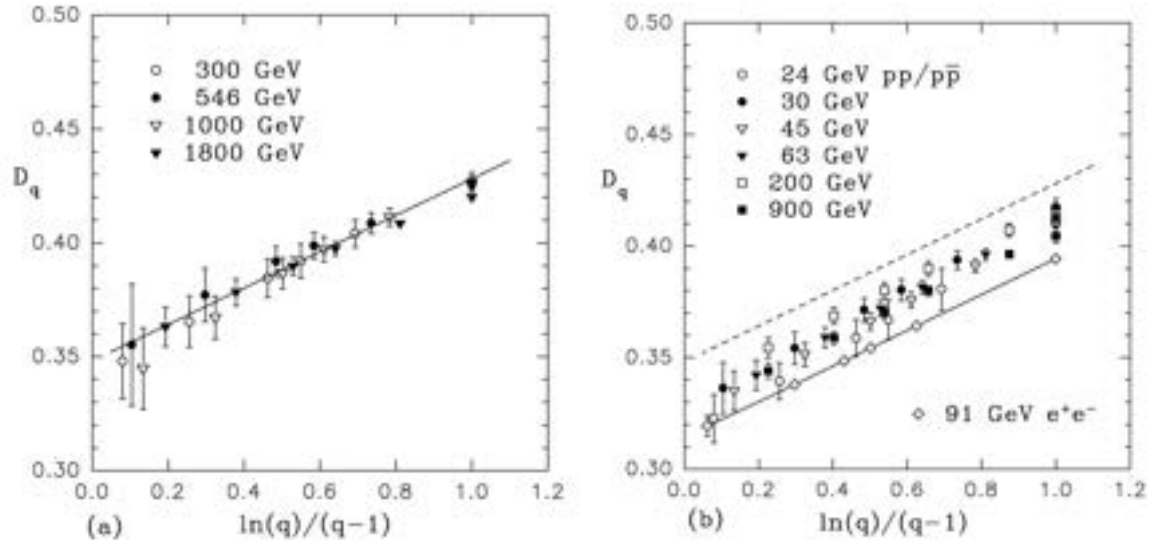

Figure 2.3: *The generalized dimensions D_q as function of ln(q)/(q-1) for charged particles. Data are taken (a) from E735 experiment [R57] and (b) from Refs. [R87–R90].* [42]

We have examined validity of the approximation given by Eq. (2.7). The q-dependence of generalized dimensions D_q calculated from the Tevatron data [R57] at $\sqrt{s} = 300$, 546, 1000, and 1800 GeV is presented in Fig.2.3a. One can see from the figure that the values of D_q reveal indeed linear increase as a function of $\ln(q)/(q-1)$. This behavior makes it possible to define the slope parameter c in the region $q \geq 1$. Similar D_q dependencies for data from CERN ISR and $Sp\bar{p}S$ Collider experiments [R87–R89] are shown in Fig.2.3b. The dashed line coincides with the full line in Fig.2.3a indicating position of D_q values calculated from E735 data. Both data sets obtained by Tevatron and CERN experiments reveal approximately the same slope while their intercepts are mutually shifted. The shift is due to larger values of D_1 for E735 data, as already shown in Fig. 2. As pointed in the previous section, the discrepancy in intercepts is connected with systematically larger high multiplicity tails of the data from Tevatron when compared to the data from the CERN $Sp\bar{p}S$ Collider. This might be connected with the mutual systematic uncertainties of the experimental procedures when extending measured data into the full phase space region.

Fitting the slope parameters for $q \geq 1$ at each separate energy, we have determined the values of multifractal specific heat c. The results are presented in the lower part of Fig.2.2. For $\sqrt{s} \geq 20$ GeV, the multifractal specific heat is within the estimated errors approximately energy independent and reaches the value $c \approx 0.08$ which is vert close to the slope obtained from the electron-positron multiplicity data [R90] what is indicated by the full line in Fig.2.3b. Since our study concerns the full phase space and it is performed in a different sense than the usual intermittency analysis, we obtain smaller value of c in comparison with the specific heat ($c \sim 0.26$) determined from

multifractal properties of the factorial moments [R91]. While the multifractal specific heat reported in Ref. [R92] reveals some kind of universality with respect to various interactions, energy dependence of D_q obtained with the same method [R93] seems to be significant. Contrary to this, our method gives smaller values of the generalized dimensions D_q which are approximately energy independent for $\sqrt{s} \geq 20$ GeV.

Chapter 3

Heavy ion collisions at GSI SIS

Meson production in heavy ion collisions has been extensively studied in 80. at LBL Bevalac [R20]. While these experiments concentrated on charged mesons a program to study neutral meson production has been initiated [43, 46, 48, 49] by Two Arm Photon Spectrometer (TAPS) Collaboration at the heavy ion synchrotron SIS which was inaugurated in early 90. at GSI Darmstadt.

TAPS detector system [51] is a modular electromagnetic calorimeter consisting of 4 (later on of 6) blocks of 64 modules. Each module represents one BaF_2 crystal - scintillator of hexagonal shape equipped with a separate NE102 plastic scintillator positioned in front of the crystal and serving as a Charged Particle Veto (CPV) detector. The blocks are mounted in two movable towers positioned symmetrically with respect to the beam direction allowing the simultaneous measurement of π^0's and η's over a small window at midrapidity ($|y - y_{c.m.}| \leq 0.1 - 0.2$) independent of the meson transverse momentum.

Particle identification is done in a two step process. First, neutral particles are separated from charged particles by requiring the absence of a signal in the CPV modules in front of the BaF_2 modules that have fired. Second, the time-of-flight information and the BaF_2 pulse shape analysis is used to separate photons from neutrons.

Forward Wall (FW) of the FOPI detector measuring charged particle multiplicity was used for event characterization. The FW comprising 512 plastic strips grouped into 8 sectors covers laboratory angles between 7° and 30°.

3.1 Neutral Pion Production in Heavy Ion Collisions at SIS-energies

3.1.1 Introductory notes

The theoretical analysis of the global event structure of heavy ion reactions was initiated by the hydrodynamical models [R3] at late seventies. Both macroscopic [R3]

and microscopic [R34, R35] approaches have indicated that the elliptic and directed flow observables are sensitive to the mean field and to the EOS. Soon after that effect of collective sideward emission (flow) of light charged baryons was established experimentally [R53], followed by observation of the out-of-plane emission *"squeeze-out"* of charged baryons [R54, R55].

The start up of GSI SIS heavy ion programme provided a good opportunity to test whether this novel behavior of high-density matter is unique to the baryons only or could be observed also for a newly created particles - the π-mesons.

In 1993 the pion squeeze-out was simultaneously discovered by the KAOS [R56] and TAPS [46] experiments. While the KAOS measurements covered the out-of-plane emission of charged pions, TAPS with rather poor azimuthal coverage and setup consisting of only 4 blocks (!) was able to prove existence of the squeeze-out effect for the neutral pions.

Article reprint

KVI-973

Neutral Pion Production
in Heavy Ion Collisions at SIS-energies

PREPRINT

M. Šumbera, H. Löhner, A.E. Raschke, L.B. Venema and H.W. Wilschut
for the TAPS collaboration

Talk presented at the XXI. International Workshop on Gross Properties of Nuclei and Nuclear Excitations, Hirschegg, Austria, January 18 - 22, 1993.

KVI
RIJKSUNIVERSITEIT GRONINGEN

KERNFYSISCH VERSNELLER INSTITUUT
ZERNIKELAAN 25 9747 AA GRONINGEN THE NETHERLANDS TELEFOON 050-633600

Neutral Pion Production in Heavy Ion Collisions at SIS-energies *

M. Šumbera[a], H. Löhner, A.E. Raschke, L.B. Venema and H.W. Wilschut
for the TAPS collaboration,
Kernfysisch Versneller Instituut, NL-9747 AA Groningen, The Netherlands

January 15, 1993

Abstract

The production of π^0 mesons has been studied in the reactions ^{40}Ar+Ca and ^{197}Au+Au at 1.0 GeV/u. While the pion transverse momentum spectrum from the reaction Ar+Ca is consistent with a simple thermal exponential slope a second component is seen for the system Au+Au. Both neutral pions, neutrons and charged particles exhibit an anisotropy in the reaction plane azimuth. At midrapidity the emission of pions perpendicular to the reaction plane increases with their energy.

1 Introduction

The modification of the nucleon-nucleon interaction in the dense nuclear medium can be studied with heavy ion reactions at sufficiently high energy. Central collisions of symmetric heavy ion systems at 1 GeV per nucleon incident energy are likely to yield about 3 times normal nuclear density. The complexity of the multi-nucleon dynamics requires exclusive experiments so that correlations among different observables reveal sufficient sensitivity to the various physical aspects of such a collision. Of special interest is the production of energetic particles near midrapidity. Such particles when emitted out of the reaction plane can provide an undistorted view of the hot and dense nuclear matter.

2 The experiment

The Two Arm Photon Spectrometer (TAPS) [1, 2, 3] was designed to identify neutral mesons by their 2-photon decay. During its operation at the heavy ion synchrotron SIS in 1990-91 the detector system consisted of 256 telescopes of plastic scintillator charged-particle-veto (CPV) detectors and BaF_2 crystals (hexagonal: face-to-face 59mm, depth 12 radiation lengths) arranged in 2 towers with 2 blocks each. The 2 towers were positioned at angles of $\theta=\pm 52^0$ with respect to the beam direction and the blocks, mounted at 1.20 m (Ar+Ca) and 2.0 m (Au+Au) from the target, were tilted by $\Phi = \pm 12^0$ (Ar+Ca) and $\Phi = \pm 7.3^0$ and $\pm 23^0$ (Au+Au) relative to the horizontal plane. The main trigger required two coincident neutral hits in TAPS (for Ar+Ca in two different blocks) and a signal from the in-beam start foil. For each event the BaF_2 time-of-flight, short gated (50ns width) and long-gated (2 μs width) pulse heights, together with the CPV signal were recorded.

For event characterization the Forward Wall (FW) of the FOPI-collaboration was employed. The hardware-derived charged particle multiplicity signal recorded in eight separate segments of the outer part of the FW covering laboratory angles between 7^0 and 30^0 has been used for the determination of the reaction plane and for impact parameter selection.

*Talk presented at the XXI. International Workshop on Gross Properties of Nuclei and Nuclear Excitations, Hirschegg, Austria, January 18 - 22, 1993. To appear in proceedings.

3 Data Analysis

Here we give only a brief account of the various subsequent steps in the data analysis. For more details see [2, 3]. First, neutral (charged particles) are separated by requiring an anticoincidence (coincidence) with the respective CPV in front of the BaF_2–module. In a second step, the time–of–flight information and the analysis of the BaF_2 pulse shape are used to separate photon candidates from neutrons. The response of the BaF_2–blocks to photons with energies from 50 to 750 MeV has been studied in a dedicated calibration experiment at the tagged photon beam facility at MAMI-B (Mainz) [4] and compared to Monte Carlo calculations using the code GEANT3 [5]. Invariant mass spectra have been calculated from pairs of photons using the expression

$$m_{\gamma\gamma} = \sqrt{2E_1E_2(1 - cos\Theta_{12})} \quad (1)$$

Here, E_1, E_2 are the energies of the reconstructed photon clusters and Θ_{12} is the relative angle between the cluster centers. The π^0 mass resolution of 11% FWHM has been achieved.

Though the TAPS angular position has been optimized to measure π^0 mesons at 90^0 in the center-of-mass system (i.e. at midrapidity) its arrangement in 4 blocks together with the 2–photon decay kinematics makes the geometrical acceptance a complicated function of the pion momentum. Hence, GEANT simulations have to be performed. The resulting π^0 efficiency is displayed in fig.1.

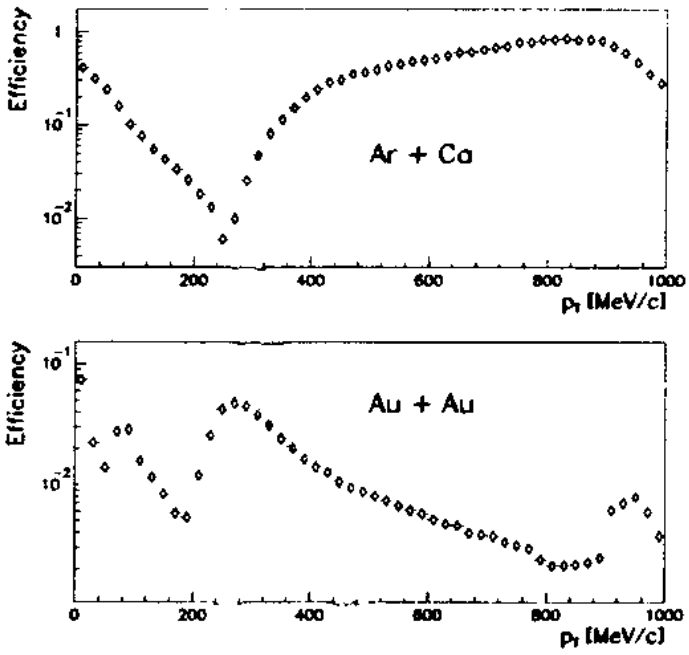

Figure 1: π^0 meson acceptance including the photon detection efficiency. The results were obtained in a Monte Carlo simulation for the TAPS geometry of the Ar+Ca (upper picture) and Au+Au (lower) run. The calculation assumes isotropic pion emission from the nucleon–nucleon center–of–mass system. A minimum energy of 20 MeV and at least 3 neighbouring detectors were required to surround the centroid of a photon cluster.

4 Experimental Results and Discussion

Efficiency corrected transverse momentum (p_T) distributions of π^0 mesons at midrapidity are shown in fig.2. A noticeable feature of the spectra is their large extension – up to $p_T \approx 1000$ MeV/c (Ar+Ca) and ≈1400 MeV/c (Au+Au), i.e. far beyond the free nucleon–nucleon kinematical limit (p_T^{max}=380 MeV/c at 1GeV/u). A fit to the p_T–spectrum in a narrow window at midrapidity with a thermal distribution

$$\frac{1}{p_T} \cdot \frac{d\sigma}{dp_T} \sim m_T \cdot e^{-\frac{m_T}{T}} \quad \text{with} \quad m_T = \sqrt{m_\pi^2 + p_T^2} \tag{2}$$

yields a value for the "temperature" parameter T = 66 ± 2 MeV (Ar+Ca) and T = 62 ± 2 MeV (Au+Au). While in the case of Ar+Ca the fit reproduces the full experimental spectrum up to the high momentum tail a significant departure from a one–temperature distribution is seen in the case of the heavier Au+Au system. In this case the spectrum is quantitatively described by a two-slope fit, formed as the sum of two thermal distributions (2) with temperatures T_1 = 53 ± 5 MeV and T_2 = 95 ± 5 MeV. For Au+Au T_1 and T_2 are within the errors the same for both semi–central and central FW–multiplicity–selected events. But with decreasing impact parameter the contribution of the second component seems to increase.

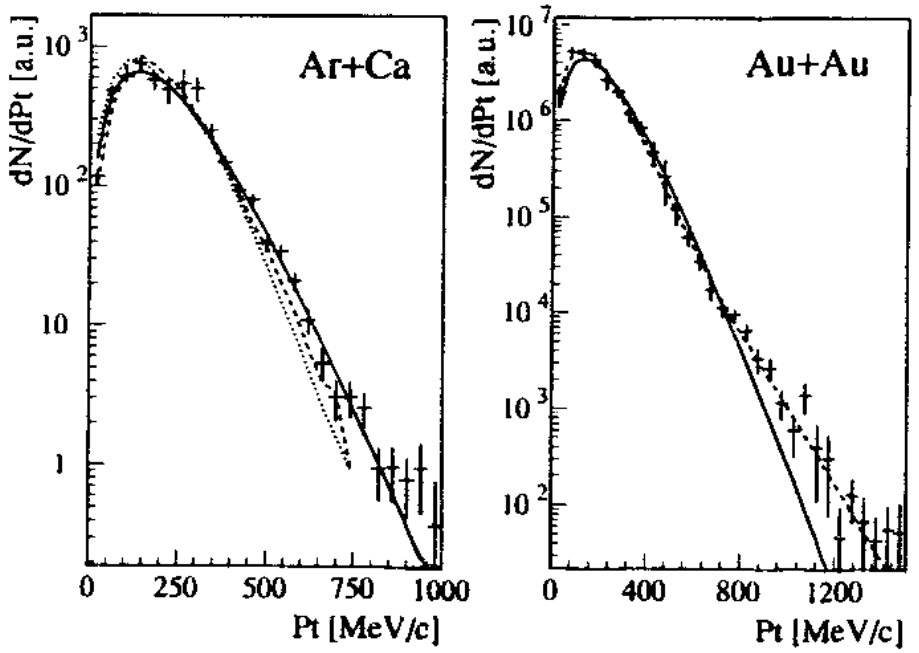

Figure 2: p_T–spectra of π^0 mesons from Ar+Ca in the rapidity window $|y - y_{c.m.}| \leq 0.2$ and from Au+Au collisions at 1GeV/u in the rapidity range $|y - y_{c.m.}| \leq 0.15$. Full line – a single–slope thermal fit. For Au+Au the dashed–line is a two–slope thermal fit. For Ar+Ca: RQMD – dashed line, QGSM – dotted line.

Let us note that indication of the second component was first observed for π^-–mesons at the BEVALAC [6, 7] and then confirmed also for π^0 [8] and π^+–mesons at SIS [9]. For the lighter

and/or non–equal mass reaction systems the two–temperature shape of CMS energy spectra of π^-–mesons has been reported for data from the Dubna Synchrophasotron [10, 11].

At energies around 1GeV/u the presence of two slopes T_1 and T_2 is explained as resulting either from two mechanisms of pion production: direct (T_2) and via Δ resonance decay (T_1) [6] or from a different contributions of Δ's produced at early and late stages of the reaction [12]. At Dubna energies (3.3 GeV/u) calculations performed in the framework of the intranuclear cascade model [13] were shown to reproduce the two–temperature shape of spectra qualitatively [11]. A quantitative discrepancy between experimental data and the model predictions was ascribed to uncertainties in the resonance–nucleon cross section.

Comparison of our experimental p_T–spectra with predictions of microscopic models (QGSM [13] and RQMD [14]) has shown that up to $p_T \approx 600$MeV/c they both qualitatively describe the data. In both models production of the baryon and meson resonances as well as their subsequent interactions have been implemented. This plays a vital role in the description of subthreshold particle production [8]. However, the description of the high–momentum part of the spectra is, besides being very CPU intensive also quite sensitive to the proper parameterization of the tail of the distribution functions describing different elementary processes.

A phenomenological approach to the subthreshold particle production based on the self-similarity hypothesis has been recently developed in [15]. It assumes that the invariant cross section of the inclusive nucleus-nucleus reaction:

$$A_1 + A_2 \rightarrow C + ... + X \tag{3}$$

has a scale–invariant dependence on the incoming and outcoming particle 4–momenta. Hence, only dimensionless Lorentz–invariant combinations are allowed. Quite generally, the threshold for production of particle C with a given 4–momentum p_C in reaction (3) can be related to the fractions x_1 and x_2 of the target and the projectile nucleus 4–momenta p_1 and p_2. This is expressed by the condition that the invariant mass squared

$$s = (x_1 p_1 + x_2 p_2)^2 \tag{4}$$

should be minimal. Its minimum value s_{min} and the fractions x_1, x_2 can be determined from the 4–momentum conservation law and the condition of minimum

$$(x_1 p_1 + x_2 p_2 - p_C)^2 = m_X^2, \qquad \frac{ds}{dx_{1,2}} = 0 \tag{5}$$

If x_1 and x_2 are expressed in units of the nucleon mass:

$$\xi_i = \frac{x_i m_i}{m_N}, \; i = 1, 2 \tag{6}$$

the new variables, when $\xi_1 > 1$ or $\xi_2 > 1$, formally define the subthreshold production. Using the dimensionless quantity $\Pi = \sqrt{s_{min}}/2m_N$ the invariant cross section has the form [15]:

$$E\frac{d^3\sigma}{d^3p} \sim A_1^{\alpha_1(\xi_1)} A_2^{\alpha_2(\xi_2)} f(\Pi) \quad \text{where} \quad \alpha_i = \frac{2}{3} + \frac{\xi_i}{3}, \; i = 1, 2 \tag{7}$$

Experimentally $f(\Pi) \sim exp(-\Pi/\Pi_0)$ with Π_0=0.13 for nucleus–nucleus subthreshold production in the projectile/target fragmentation region [15] and Π_0=0.16 for pp–data [16].

Let us now consider particle production at $\Theta_{CMS} = 90^0$. From symmetry it follows that $\xi_1 = \xi_2$ and the solution of the equation (5) is

$$\Pi = \xi\gamma \qquad \text{with} \quad \xi = \frac{E_C}{2m_N(\gamma - \gamma^{-1})}\left[1 + \sqrt{1 - \frac{m_C^2}{E_C^2}(1 - \gamma^{-2})}\right] \tag{8}$$

$$\text{where} \quad \gamma = \sqrt{(T_{lab} + 2m_N)/2m_N}$$

and T_{lab} is the projectile kinetic energy per nucleon. Using (7) we can relate the slope parameter T of the invariant cross section at midrapidity to the slope Π_0 of the universal function $f(\Pi)$:

$$T = \frac{T_{lab}}{T_{lab} + 2m_N} \cdot \frac{m_N}{\Pi_0^{-1} - \frac{\ln(A_1 A_2)}{3\gamma}} \tag{9}$$

The slope T is now dependent both on the incoming energy as well as on the masses of colliding nuclei (see fig.3). The value of Π_0 from pp–data was used. Moreover from $T_{lab} \approx 200$GeV the "temperature" T is quite close to its limiting value $T_o = \Pi_o m_N$.

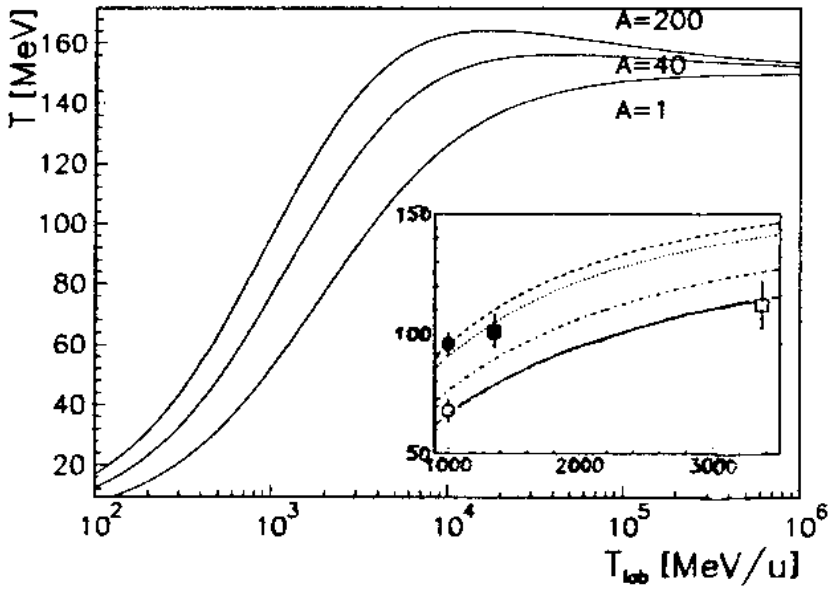

Figure 3: Energy dependence of the slope parameter T for symmetric systems. The inset shows a comparison with experimental data on T_2 at midrapidity. Dashed line and full circle – Au+Au (present experiment), dotted line and full square – La+La [7], dash-dotted line and empty circle – Ar+Ca (present experiment), full line and empty square – C+C [11]

Additional information on the collision dynamics can be obtained when studying particle emission with respect to the reaction plane. The azimuthal angular distributions of π^0 mesons for four p_T–bins (step 200MeV/c) are shown in fig.4. While for p_T <200MeV/c the distribution is approximately isotropic at higher p_T it peaks around 90^0 and 270^0. Moreover this anisotropy increases with pion energy. In the same picture the azimuthal distributions of neutrons and charged particles measured within the angular range $46^0 < \Theta_{lab} < 60^0$ are shown. Now the binning is in the particle velocity $\beta = v/c$ from $\beta = 0.5$ to $\beta = 0.8$ in steps of roughly 0.05. The corresponding rapidity interval is $0.42 < y_{c.m.} - y < 0.06$. In the target fragmentation region the the opposite–side emission of particles with respect to the projectile fragments can be observed. At midrapidity both the neutrons and the charged particles seem to be "squeezed–out" perpendicularly to the reaction plane [17] similarly to the pion case. More quantitative results can be extracted from the fits to the azimuthal distributions of particles with a function $f(\phi) = N_0(A\cos(\phi) + B\cos(2\phi) + 1)$. Values of the fit parameters A and B which measure the flow and squeeze–out, respectively, are summarized in table 1.

Table 1: Strength parameters for the distribution of emission angles with respect to the reaction plane for charged particles, neutrons and π^0.

β	charged part.		neutrons		p_T	π^0	
	A	B	A	B	(MeV/c)	A	B
0.49 – 0.53	-0.40	-0.04	-0.16	-0.03	0– 200	0.00	-0.03
0.53 – 0.58	-0.38	-0.05	-0.16	-0.07	200– 400	0.06	-0.37
0.58 – 0.63	-0.35	-0.07	-0.19	-0.03	400– 600	0.04	-0.66
0.63 – 0.69	-0.30	-0.09	-0.20	-0.08	600– 800	0.22	-0.72
0.69 – 0.78	-0.23	-0.10	-0.18	-0.07			
0.78 – 0.88	-0.11	-0.11	-0.10	-0.11			

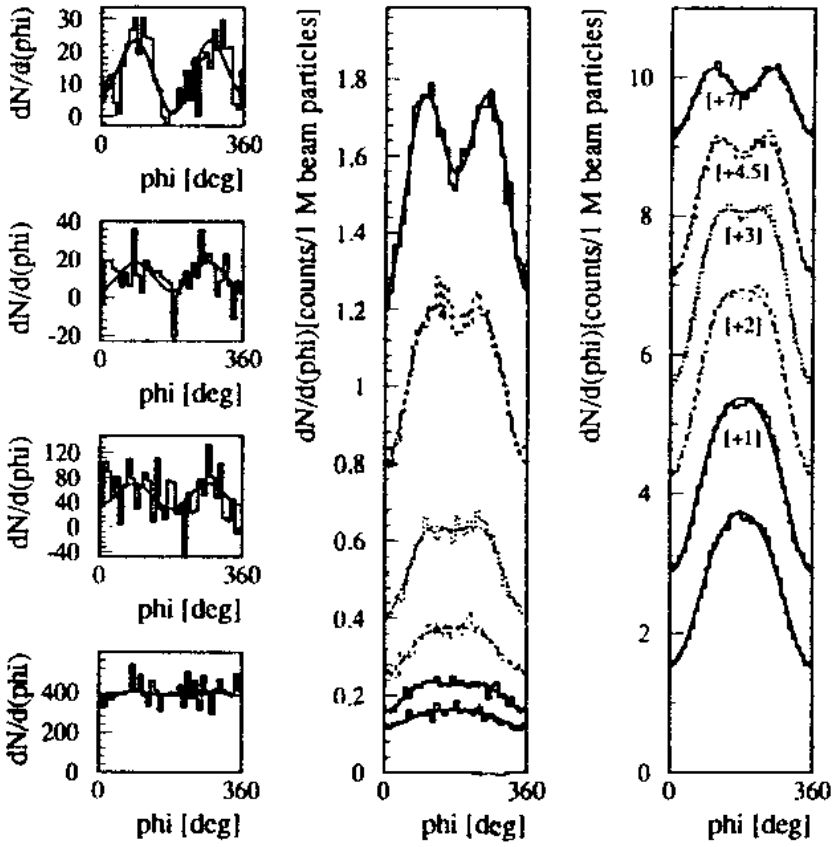

Figure 4: Azimuthal angle (ϕ) distributions of π^0 (left column), neutrons (middle) and charged particles (right) from Au+Au collisions at 1GeV/u as a function of increasing (from bottom to top) particle momentum/velocity. The results of fit $f(\phi) = N_0(A\cos(\phi) + B\cos(2\phi) + 1)$ are also shown.

a) on leave of absence from Nuclear Physics Institute of Czech Academy of Sciences,
Řež u Prahy, Czech Republic.

References

[1] R. Novotny, IEEE, Trans.Nucl.Sci. 38(1991)

[2] F. D. Berg et al., Z. Phys. A 337 (1990) 351

[3] F. D. Berg et al., Z. Phys. A 340 (1991) 297

[4] C. Molenaar, Diploma thesis, Univ. of Groningen 1992;
A.Gabler, Diploma thesis, Univ. of Gießen 1992

[5] R. Brun et al., GEANT3, CERN, /DD/EE/84-1, 1986

[6] R. Brockmann et al., Phys. Rev. Lett. 53 (1984) 2012

[7] G. Odyniec et al., Proc. 8th High Energy Heavy Ion Study,Berkely, 1987

[8] V. Metag, Proc. Int. Nucl.Phys. Conf., Wiesbaden 1992, to be published in Nucl.Phys. A, Special Issue

[9] P. Senger et al., ibid.

[10] L. Chkhaidze et al., Z. Phys. A 54 (1192) 179

[11] S. Backović et al., JINR Rapid Communications No.2(53) (1992) 58

[12] W. Bauer and B.Li, Phys. Rev. C 44 (1991) 450

[13] N. S. Amelin et al., Sov. J. Nucl. Phys. 52 (1990) 172

[14] H. Sorge, H. Stöcker and W. Greiner, Ann. Phys. 192 (1989) 266

[15] A. A. Baldin, JINR Rapid Communications No.3[54]-92

[16] V. S. Stavinsky, Proc. 9th Int. Seminar on High Energy Physics Problems , Vol.1.,JINR, D1, 2-88-6652, Dubna 1988, p.190

[17] H.H. Gutbrod et al. Phys. Rev. C 42 (1990) 640

3.1.3 Citations:

1. Li BA; *Nuclear Shadowing Effect in Relativistic Heavy-Ion Collisions* NUCLEAR PHYSICS **A 570** (3-4): 797-818 APR 4 1994.

3.1.4 Conference presentations

1. M. Šumbera, H. Lohner, A. E. Raschke, L. B. Venema and H. W. Wilschut
   Neutral pion production in heavy ion collisions at SIS energies
   Proc. 21st Int. Workshop on Gross Properties of Nuclei and Nuclear Excitations, Hirschegg, Austria, January 18-22, 1993. Ed. H. Feldmeier, Darmstadt, 1993. - S. 11 , 93.01.18-93.01.22 and preprint KVI-973(1993)

Article reprint

VOLUME 71, NUMBER 6 PHYSICAL REVIEW LETTERS 9 AUGUST 1993

Azimuthal Asymmetry of Neutral Pion Emission in Au+Au Reactions at 1 GeV/Nucleon

L. B. Venema,[1] H. Braak,[1] H. Löhner,[1] A. E. Raschke,[1] R. H. Siemssen,[1] M. Šumbera,[1,*] H. W. Wilschut,[1] F.-D. Berg,[2] W. Kühn,[2] V. Metag,[2] M. Notheisen,[2] R. Novotny,[2] M. Pfeiffer,[2] J. Ritman,[2] O. Schwalb,[2] A. Gobbi,[3] K. D. Hildenbrand,[3] S. Hlaváč,[3,†] R. Holzmann,[3] R. S. Simon,[3] U. Sodan,[3] K. Teh,[3] J. P. Wessels,[3] N. Herrmann,[4] T. Wienold,[4] R. Kotte,[5] J. Mösner,[5] W. Neubert,[5] D. Wohlfarth,[5] R. Ostendorf,[6] Y. Schutz,[6] N. Brummund,[7] and R. Santo[7]

[1]*Kernfysisch Versneller Instituut, Groningen, The Netherlands*
[2]*II. Physikalisches Institut, Universität Giessen, Giessen, Germany*
[3]*Gesellschaft für Schwerionenforschung, Darmstadt, Germany*
[4]*II. Physikalisches Institut, Universität Heidelberg, Heidelberg, Germany*
[5]*Forschungszentrum Rossendorf, Dresden, Germany*
[6]*GANIL, Caen, France*
[7]*Institut für Kernphysik, Universität Münster, Münster, Germany*

(Received 29 April 1993)

The azimuthal angle distributions of neutral pions at midrapidity from Au+Au reactions at 1 GeV/nucleon incident energy have been measured. An enhanced emission of π^0's perpendicular to the reaction plane is observed. The azimuthal asymmetry is dependent on the π^0 momentum: the π^0 spectrum perpendicular to the reaction plane is harder than in the reaction plane. The strength of the observed asymmetry appears to be more pronounced for π^0 than for charged particles and neutrons.

PACS numbers: 25.75.+r

Relativistic heavy ion collisions provide the dynamical conditions to study the properties of highly excited and compressed nuclear matter. The production probability of mesons in the course of the collision and their observed momentum distribution allow us to derive the degree of thermal excitation in the collision zone [1,2]. The collective motion of nucleons from the collision zone is influenced by repulsive forces among the interacting nucleons or, in a hydrodynamic model description, by the compressional energy [3,4].

The theoretical analysis of the global event structure of heavy ion reactions was initiated by hydrodynamic models. Microscopic dynamical models [Vlasov-Uehling-Uhlenbeck, quantum molecular dynamics (QMD)] [5–7] confirmed the effect of collective sideward emission (flow) of light charged baryons which was established experimentally [8]. Recently a new component of the collective flow, the out-of-reaction-plane *"squeezeout"* of charged baryons, was discovered experimentally [9]. QMD calculations [10] reproduce these observations and show a dependence of the collective emission pattern on the equation of state of nuclear matter.

We present here the first observation of enhanced π^0 emission perpendicular to the reaction plane in the Au+Au reaction at 1 GeV/nucleon. The enhancement increases for increasing transverse momentum of the π^0 mesons. At the same time the transverse momentum spectrum of π^0 mesons emitted perpendicularly to the reaction plane is seen to be harder than the spectrum of π^0 emitted in the reaction plane.

A Au target (0.188 g/cm^2) of 0.1 mm thickness was bombarded with a Au beam extracted from the SIS accelerator of GSI with a kinetic energy of 1 GeV/nucleon. The intensity was kept near 10^6 particles per spill, with a spill duration of 4 s, and a repetition rate of 9 s. Photons from the π^0 decay (branching ratio 98.8% for two-photon decay) were detected in the two-arm photon spectrometer (TAPS) [11]. Charged particles emitted in the forward direction were detected in the forward wall of the FoPi Collaboration [12] and used for the event characterization.

In this experiment the TAPS detector system consisted of 256 BaF_2 detectors arranged in 4 blocks with individual charged particle veto detectors (CPV) in front of each module. The blocks were mounted in two towers which were positioned at 52° with respect to the beam direction. The angle of the blocks with respect to the horizontal plane containing the beam line was changed during the experiment in order to provide different opening angles for the π^0 decay photons and thus to cover the full momentum range of the π^0. The trigger and the time zero signals were derived from a start detector consisting of an in-beam plastic scintillation foil of 200 μm thickness. It was mounted in the beam line with a tilt angle of 45°. A ring shaped plastic scintillator with a hole of 18 mm served as veto for the beam halo and reaction products from the start detector.

The forward wall is a plastic scintillator wall covering the polar angular range from 1° to 30°. It consists of two parts, the outer plastic wall (OPW) and a zero-degree detector. Only the OPW was used in the present analysis. The OPW, covering the angular range from 7° to 30°, is made of 512 plastic bars with photomultipliers at both ends. The 512 bars are grouped into 8 sectors, each

0031-9007/93/71(6)/835(4)$06.00

sector spanning 45° in azimuthal angle.

In the analysis the following steps were taken for particle identification. First, neutral particles were separated from charged particles by requiring the absence of a signal in the CPV modules in front of the BaF_2 modules that had fired. Second, the time-of-flight information and the BaF_2 pulse shape analysis were used to separate photons from neutrons. For the detection of charged particles a signal of the CPV was required in addition to the proper characteristic of the pulse shape in the BaF_2 scintillator. The present analysis does not separate the $\pi^{\pm}$ and light composite fragments from the dominating yield of protons.

The π^0 mesons are identified through the invariant mass analysis of all photon pairs detected by TAPS, using the relation $m_{\gamma\gamma} = \sqrt{2E_1E_2(1-\cos\Theta_{12})}$ where E_1 and E_2 are the photon energies and Θ_{12} is the opening angle of the photon pair. The resolution (FWHM / peak position) of the π^0 mass peak is 17%. The exact shape of the combinatorial background below the π^0 mass peak was determined by event mixing. In the mixing procedure special care was taken of the proper phase space occupation of the photons in mixed events.

The orientation of the reaction plane was determined by performing a modified transverse momentum analysis [13]. Usually [14] the transverse momenta of the particles are summed according to

$$\mathbf{Q} = \sum_{\nu=1}^{N} w_\nu \mathbf{p}_\nu^{\perp}(y > y_{\mathrm{c.m.}}) - w_\nu \mathbf{p}_\nu^{\perp}(y < y_{\mathrm{c.m.}}), \qquad (1)$$

where w_ν are weights for different kinds of particles, often taken equal to 1.0 [14,15]. In our case, each of the 8 sectors of the OPW was represented by its unit vector $\hat{\mathbf{u}}_i$ pointing to the center of a sector. The vectors $\hat{\mathbf{u}}_i$ were taken orthogonal to the beam axis. Since the coverage of the forward wall excludes the majority of particles with $y < y_{\mathrm{c.m.}}$, the *plane vector* $\mathbf{Q}$ can be approximated by

$$\mathbf{Q} \approx \sum_{\text{sectors}} \hat{\mathbf{u}}_i \mathcal{M}_i. \qquad (2)$$

$\mathcal{M}_i$ is the multiplicity measured in sector i of the OPW and $\sum_{\text{sectors}} \mathcal{M}_i \geq 30$ (25% of max. OPW multiplicity) was demanded in order to remove peripheral reactions. $\mathbf{Q}$ can only define the reaction plane if the flow is sufficiently pronounced. Therefore, a gate with $\|\mathbf{Q}\| \geq 5$ was applied. This removes only a fraction of 17% of all nonperipheral events, evenly distributed in multiplicity. In order to determine particle emission patterns, the reaction plane of each event was rotated so that the x axis coincided with $\mathbf{Q}$. Autocorrelations [14,16] are absent because the OPW determines the reaction plane independently of the measurement in TAPS. The angular coverages of the OPW and TAPS were mutually exclusive.

The accuracy of the reaction plane determination was estimated in two ways. First, each event was divided into two parts by randomly assigning each particle hit in the OPW to one of two subsets. From the difference between the reaction plane azimuths for these two subsets we deduce a resolution (σ) of 27° [14,17]. Second, the orientation of the reaction plane with respect to a single TAPS detector block was investigated. Since charged particles within the acceptance of TAPS are emitted at backward center of mass rapidity ($y < y_{\mathrm{c.m.}}$), we expect a 180° correlation with the preferred direction of particle emission in the acceptance of the OPW due to global momentum conservation. We found the relative azimuthal angles for the different TAPS blocks located at 180° up to an average deviation of 28°, consistent with the resolution determined earlier. The same studies were made for neutrons with similar results.

Azimuthal distributions of neutrons and charged particles relative to the reaction plane are shown in Fig. 1. The different histograms for neutrons and charged particles represent different cuts in time of flight and particle velocities range from $\beta = 0.5$ to $\beta = 0.9$ (see Table I). The angular acceptance from $50° < \Theta_{\mathrm{lab}} < 63°$ corresponds to a rapidity interval of $-0.45 < y - y_{\mathrm{c.m.}} < -0.04$. The curves which overlay the histograms in the figure are fits with

$$f(\phi) = N[1 + S_1\cos(\phi) + S_2\cos(2\phi)]. \qquad (3)$$

The $\cos(\phi)$ term is sensitive to the yield *within* the reaction plane. At backward rapidities it describes the collective sideward flow of particles in the backward hemisphere. The parameter S_1 is a measure of the strength

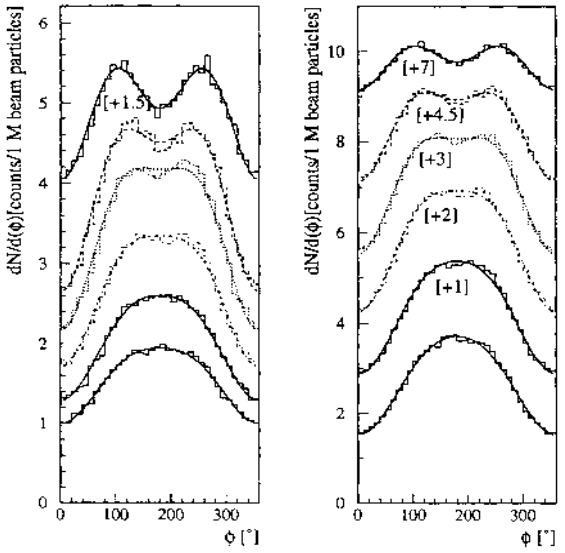

FIG. 1. Azimuthal angle (ϕ) distributions of neutrons (left) and charged particles (right) from Au+Au collisions at 1 GeV/nucleon as a function of increasing (from bottom to top) particle velocity from $\beta = 0.5$ to 0.9 (see Table I). Histograms are the experimental data and the curves represent fits according to Eq. (3). The spectra are separated in the plot by adding a constant value as given in the square brackets.

TABLE I. Strength parameters of Eq. (3) for the distribution of emission angles of charged particles and neutrons with respect to the reaction plane ($\|\mathbf{Q}\| \geq 5$). Results are presented for different particle velocity β. A systematic error of 0.03 has been estimated for S_1 and S_2.

	Charged particle			Neutrons		
β	S_1	S_2	R	S_1	S_2	R
0.49–0.53	−0.40	−0.04	1.08	−0.31	−0.05	1.10
0.53–0.58	−0.38	−0.05	1.10	−0.32	−0.05	1.10
0.58–0.63	−0.35	−0.07	1.15	−0.30	−0.07	1.14
0.63–0.69	−0.30	−0.09	1.20	−0.29	−0.09	1.19
0.69–0.78	−0.23	−0.10	1.23	−0.23	−0.10	1.23
0.78–0.88	−0.11	−0.11	1.25	−0.13	−0.13	1.30

of the flow. The parameter S_2 reflects the out-of-the-reaction-plane emission and is a measure of the strength of the so-called "squeezeout" effect. The values of these fit parameters are shown in Table I. The squeezeout ratio R is defined as

$$R = \frac{\frac{dN}{d\phi}(90°) + \frac{dN}{d\phi}(270°)}{\frac{dN}{d\phi}(0°) + \frac{dN}{d\phi}(180°)} = \frac{1 - S_2}{1 + S_2}. \quad (4)$$

Near midrapidity (the top histogram in Fig. 1) the baryons exhibit a clear effect of squeezeout and confirm earlier observations [9,15]. This squeezeout is superimposed on the backward particle flow. For slower particles, the rapidity window shifts to more backward rapidities and the squeezeout vanishes, whereas the backward flow increases in strength. The slightly stronger flow component for the charged particles, compared to the neutrons, may be attributed to the influence of composite particles [18], which are included in our charged particle selection.

Having verified the well established azimuthal asymmetry for baryons, we turn our attention to the new observable: the azimuthal distribution of neutral pions. The acceptance of TAPS covers a narrow window around midrapidity $|y_{\mathrm{c.m.}} - y| \leq 0.15$. This acceptance window is independent of the energy of the π^0. Figure 2 shows the azimuthal distribution of π^0 relative to the reaction plane for different cuts in transverse momentum. Again a parametrization according to Eq. (3) is shown with parameter values listed in Table II. From studies of the azimuthal symmetry of the forward wall response we conclude a residual systematic uncertainty in S_2 of 0.03. In the following, the azimuthally asymmetric emission of pions will be called squeezeout irrespective of its physical origin.

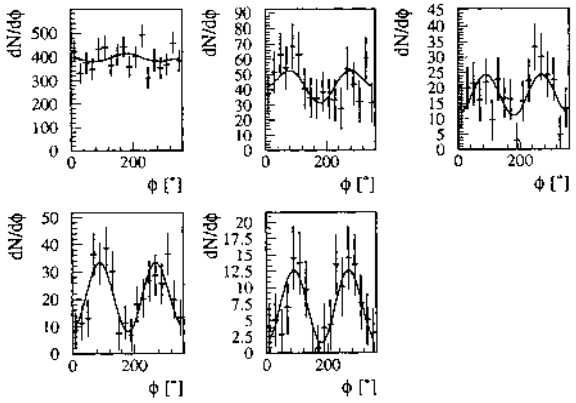

FIG. 2. Azimuthal angle (ϕ) distributions of π^0 from Au+Au collisions at 1 GeV/nucleon for increasing transverse momentum (from top left to bottom right) in equal bins of 200 MeV/c from 0 to 1000 MeV/c. The solid curves represent fits according to Eq. (3).

We observe a gradual increase in the squeezeout ratio R which has much larger values than the ratios for charged particles or neutrons. Clearly, the yield of high energy pions as compared to low energy pions is strongly reduced when emitted in the reaction plane. The magnitude of R at large p_T is remarkable. R decreases when we relax the condition $\|\mathbf{Q}\| \geq 5$ to $\|\mathbf{Q}\| \geq 0$ (see Table II). This effect is expected due to isotropic emission which is associated with small $\|\mathbf{Q}\|$. Recently the KaoS Collaboration reported [19] squeezeout for π^+ in the same reaction as studied here. They observe a dependence on transverse momentum which is not as strongly pronounced. This may indicate the importance of the rapidity window which is $y \approx y_{\mathrm{c.m.}}$ in our case versus $y \approx y_{\mathrm{c.m.}} + 0.2$ in [19].

Figure 3 shows the transverse momentum spectra of the π^0 mesons gated on two regions in azimuth: the first (I, in the reaction plane, open circles) given by

TABLE II. Strength parameters of Eq. (3) for the distribution of emission angles of π^0 with respect to the reaction plane for two gates on $\|\mathbf{Q}\|$. Results are presented for different π^0 transverse momenta near midrapidity ($|y_{\mathrm{c.m.}} - y| \leq 0.15$). The large error on R in the last p_T bin occurs due to the singularity in the definition of R at $S_2 = -1$.

p_T	$\|\mathbf{Q}\| \geq 5$			$\|\mathbf{Q}\| \geq 0$		
(MeV/c)	S_1	S_2	R	S_1	S_2	R
0–200	-0.03 ± 0.04	0.03 ± 0.03	0.9 ± 0.1	0.02 ± 0.03	0.03 ± 0.03	0.9 ± 0.1
200–400	0.12 ± 0.10	-0.18 ± 0.10	1.4 ± 0.3	0.07 ± 0.07	-0.19 ± 0.10	1.5 ± 0.3
400–600	0.04 ± 0.13	-0.38 ± 0.13	2.2 ± 0.7	0.02 ± 0.11	-0.41 ± 0.11	2.4 ± 0.6
600–800	0.03 ± 0.11	-0.64 ± 0.12	4.6 ± 1.9	0.08 ± 0.09	-0.49 ± 0.08	2.9 ± 0.6
800–1000	0.06 ± 0.20	-0.79 ± 0.24	9 ± 11	-0.12 ± 0.15	-0.54 ± 0.15	3.3 ± 1.4

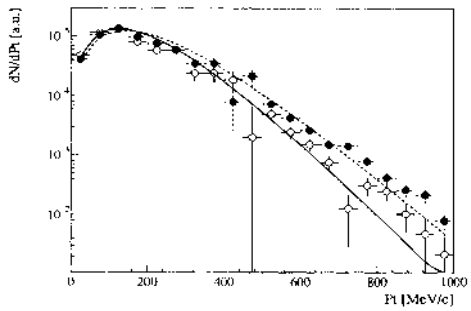

FIG. 3. Transverse momentum spectra of π^0 mesons emitted parallel to the reaction plane (I, open circles) and perpendicular to the reaction plane (II, closed circles), respectively. The curves represent a fit according to Eq. (5).

$\phi = 0° \pm 45°$ and $\phi = 180° \pm 45°$ and the other (II, out of the reaction plane, closed circles) by $\phi = 90° \pm 45°$ and $\phi = 270° \pm 45°$. The spectra were corrected for the acceptance of the detector system. The spectrum of the π^0 mesons emitted perpendicular to the reaction plane is much harder than the in-plane π^0 spectrum, as is indicated by the average transverse momentum: $\langle p_T \rangle_{\rm I} = 168 \pm 5$ MeV/c, and $\langle p_T \rangle_{\rm II} = 188 \pm 5$ MeV/c. These spectra have been compared to a thermal distribution at midrapidity

$$\frac{dN}{dp_T} \sim p_T m_T \exp\left(-\frac{m_T}{\mathcal{T}}\right), \tag{5}$$

where $m_T = \sqrt{m_{\pi^0}^2 + p_T^2}$. Resulting $\mathcal{T}$ parameters were $\mathcal{T}_{\rm I} = 58 \pm 2$ MeV and $\mathcal{T}_{\rm II} = 70 \pm 2$ MeV, respectively. Equation (5) can only provide a rough description of the momentum distributions since in general a concave shape of the spectra is observed.

The integrated yield of π^0 emission in the reaction plane is suppressed by 10% with respect to the out-of-plane yield. This fact suggests that the main reason for the observed azimuthal asymmetry is the enhanced absorption of fast pions in the reaction plane by the spectator matter. The importance of π absorption has already been suggested by results from the Diogene group [20]. Scattering would lead effectively to a similar result: Pion scattering on spectator nucleons will preferentially occur in the reaction plane while the subsequent reemission of pions is more isotropic. Thus π^0 yield is removed from the reaction plane. The absence of azimuthal asymmetry for low energy π^0 can be explained by a higher transparency of nuclear matter for low energy π^0 as well as an enhanced emission of low energy π^0 mesons by the colder spectator matter.

Recent calculations [21] using an extension of the QMD model show an enhanced out-of-plane emission of π^0 with $R \approx 1.4$ for minimum bias data and $p_T > 400$ MeV/c. In those calculations explicit tests are made to identify the cause of the azimuthal asymmetry in pion emission. The absorption ($\pi NN \to \Delta N \to NN$) channel and scattering channel ($\pi N \to \Delta \to \pi N$) were disabled independently of each other. The authors conclude that the absorption of pions is mainly responsible for the observed anisotropy.

We conclude that a squeezeout effect for neutral pions has been observed in Au + Au collisions at 1 GeV/nucleon. A determination of the reaction plane was achieved with a resolution of 27°. The strength of the π^0 squeezeout is an arresting feature of the data which show the most pronounced azimuthal asymmetry at large π^0 momentum. Therefore, the π^0 momentum spectrum observed perpendicular to the reaction plane appears to be harder than the spectrum in the reaction plane. The azimuthal angle distributions of charged particles and neutrons exhibit both squeezeout near midrapidity and collective particle flow near the target rapidity.

We thank the accelerator crew at GSI for providing excellent beam conditions and H. Folger and the GSI target laboratory staff for target preparations. Stimulating discussions with S.A. Bass, A. Kugler, and Gy. Wolf are gratefully acknowledged. This work was supported in part by GSI, by the German BMFT, the French IN2P3 and the Dutch FOM.

* On leave of absence from Nuclear Physics Institute of Czech Academy of Sciences, Řež u Prahy, Czech Rep.
† Permanent address: Institute of Physics of Slovak Academy of Sciences, Bratislava, Slovak Rep.

[1] R. Hagedorn and J. Rafelski, Phys. Lett. **97B**, 136 (1980).
[2] R. Stock, Phys. Rep. **135**, 259 (1986).
[3] W. Scheid, H. Müller, and W. Greiner, Phys. Rev. Lett. **32**, 741 (1974).
[4] M. Sano *et al.*, Phys. Lett. **156B**, 27 (1985).
[5] C. Hartnack *et al.*, Nucl. Phys. **A495**, 303 (1989).
[6] G. Peilert *et al.*, Phys. Rev. C **39**, 1402 (1989).
[7] W. Cassing and U. Mosel, Prog. Part. Nucl. Phys. **25**, 235 (1990).
[8] H.Å. Gustafsson *et al.*, Phys. Rev. Lett. **52**, 1590 (1984).
[9] H.H. Gutbrod *et al.*, Phys. Lett. B **216**, 267 (1989).
[10] Ch. Hartnack *et al.*, Nucl. Phys. **A538**, 53c (1992).
[11] R. Novotny *et al.*, IEEE Trans. Nucl. Sci. **38**, 379 (1991).
[12] A. Gobbi *et al.*, Nucl. Instrum. Methods Phys. Res., Sect. A **324**, 156 (1993).
[13] A. Kugler *et al.*, in *Proceedings of the XXI International Workshop on Gross Properties of Nuclei and Nuclear Excitations, Hirschegg, Austria, 1993*, edited by H. Feldmeier (GSI, Darmstadt, 1993), p. 23 (ISSN 0720-8715).
[14] P. Danielewicz and G. Odyniec, Phys. Lett. **157B**, 146 (1985).
[15] H.H. Gutbrod *et al.*, Phys. Rev. C **42**, 640 (1990).
[16] K.G.R. Doss *et al.*, Phys. Rev. Lett. **57**, 302 (1986).
[17] W.K. Wilson *et al.*, Phys. Rev. C **45**, 738 (1992).
[18] H.H. Gutbrod, A.M. Poskanzer, and H.G. Ritter, Rep. Prog. Phys. **52**, 1267 (1989).
[19] KaoS Collaboration, P. Senger *et al.*, Prog. Part. Nucl. Phys. **30**, 115 (1993); D. Brill *et al.*, Phys. Rev. Lett. **71**, 336 (1993).
[20] J. Gosset *et al.*, Phys. Rev. Lett. **62**, 1251 (1989).
[21] S.A. Bass, C. Hartnack, H. Stöcker, and W. Greiner, UFTP Report No. 328/1993 (to be published).

3.1.6 Citations

1. Linnyk, O (Linnyk, O.); Bratkovskaya, EL (Bratkovskaya, E. L.); Cassing, W (Cassing, W.) *Open and Hidden Charm in Proton-Nucleus and Heavy-Ion Collisions* International Journal of Modern Physics E-Nuclear Physics, 17 (8): 1367-1439 SEP 2008.
2. Li, BA (Li, Bao-An); Chen, LW (Chen, Lie-Wen); Ko, CM (Ko, Che Ming) *Recent progress and new challenges in isospin physics with heavy-ion reactions* Physics Reports-Review Section Of Physics Letters, 464 (4-6): 113-281 AUG 2008.
3. Yong, GC (Yong, Gao-Chan); Li, BA (Li, Bao-An); Chen, LW (Chen, Lie-Wen) *The neutron/proton ratio of squeezed-out nucleons and the high density behavior of the nuclear symmetry energy.* Physics Letters **B**, 650 (5-6): 344-347 JUL 12 2007.
4. Reisdorf, W; Stockmeier, M; Andronic, A; Benabderrahmane, ML; Hartmann, ON; Herrmann, N; Hildenbrand, KD; Kim, YJ; Kis, M; Koczon, P; Kress, T; Leifels, Y; Lopez, X; Merschmeyer, M; Schuttauf, A; Barret, V; Basrak, Z; Bastid, N; Caplar, R; Crochet, P; Dupieux, P; Dzelalija, M; Fodor, Z; Grishkin, Y; Hong, B; Kang, TI; Kecskemeti, J; Kirejczyk, M; Korolija, M; Kotte, R; Lebedev, A; Matulewicz, T; Neubert, W; Petrovici, M; Rami, F; Ryu, MS; Seres, Z; Sikora, B; Sim, KS; Simion, V; Siwek-Wilczynska, K; Smolyankin, V; Stoicea, G; Tyminski, Z; Wisniewski, K; Wohlfarth, D; Xiao, ZG; Xu, HS; Yushmanov, I; Zhilin, *Systematics of pion emission in heavy ion collisions in the 1 A GeV regime.* Nuclear Physics **A**, 781 (3-4): 459-508 Jan 15 2007.
5. Saeed-Uddin; Akhtar, N; Ali, M *Pion production and collective flow effects in intermediate energy nucleus-nucleus collisions* . International Journal of Modern Physics **A**, 21 (7): 1471-1491 Mar 20 2006.
6. Fuchs, C *Kaon production in heavy ion reactions at intermediate energies* .Progress in Particle and Nuclear Physics, Vol 56, No 1, 56 (1): 1-103 2006.
7. Stoicea, G; Petrovici, M; Andronic, A; Herrmann, N; Alard, JP; Basrak, Z; Barret, V; Bastid, N; Caplar, R; Crochet, P; Dupieux, P; Dzelalija, M; Fodor, Z; Hartmann, O; Hildenbrand, KD; Hong, B; Kecskemeti, J; Kim, YJ; Kirejczyk, M; Korolija, M; Kotte, R; Kress, T; Lebedev, A; Leifels, Y; Lopez, X; Merschmeier, M; Neubert, W; Pelte, D; Rami, F; Reisdorf, W; Schull, D; Seres, Z; Sikora, B; Sim, KS; Simion, V; Siwek-Wilczynska, K; Smolyankin, V; Stockmeier, M; Wisniewski, K; Wohlfarth, D; Yushmanov, I; Zhilin, A; Danielewicz, P (FOPI Collaboration) *Azimuthal dependence of collective expansion for symmetric heavy-ion collisions* . Physical Review Letters, 92 (7): Art. No. 072303 Feb 20 2004.
8. Klay, JL; Ajitanand, NN; Alexander, JM; Anderson, MG; Best, D; Brady, FP; Case, T; Caskey, W; Cebra, D; Chance, JL; Chung, P; Cole, B; Crowe, K; Das, AC; Draper, JE; Gilkes, ML; Gushue, S; Heffner, M; Hirsch, AS; Hjort, EL; Huo, L; Justice, M; Kaplan, M; Keane, D; Kintner, JC; Krofcheck, D; Lacey, RA; Lauret, J; Law, C; Lisa, MA; Liu, H; Liu, YM; McGrath, R; Milosevich, Z; Odyniec, G; Olson, DL; Panitkin, SY; Pinkenburg, C; Porile, NT; Rai, G; Ritter, HG; Romero, JL; Scharenberg, R; Srivastava, B; Stone, NTB; Symons, TJM; Wang, S; Wells, R; Whitfield, J; Wienold, T; Witt, R; Wood, L; Zhang, WN *Charged pion production in 2A to 8A GeV central Au + Au collisions* . Physical Review **C**, 68 (5): Art. No. 054905 Nov 2003.
9. Chkhaidze, LV; Djobava, TD; Kharkhelauri, LL *Experimental study of collective flow phenomena in high-energy nucleus-nucleus collisions* .Physics of Particles and Nuclei, 33 (2): 196-219 Mar-Apr 2002.
10. Andronic, A; Stoicea, G; Petrovici, M; Simion, V; Crochet, P; Alard, JP; Averbeck, R; Barret, V; Basrak, Z; Bastid, N; Bendarag, A; Berek, G; Caplar, R; Devismes, A; Dupieux, P; Dzelalija, M; Eskef, M; Finck, C; Fodor, Z; Gobbi, A; Grishkin, Y; Hartmann, ON; Herrmann, N; Hildenbrand, KD; Hong, B; Kecskemeti, J; Kim, YJ; Kirejczyk, M; Korolija, M; Kotte, R; Kress, T; Kutsche, R; Lebedev, A; Lee, KS; Leifels, Y; Manko, V; Merlitz, H; Neubert, W; Pelte, D; Plettner, C; Rami, F; Reisdorf, W; de Schauenburg, B; Schull, D; Seres, Z; Sikora, B; Sim, KS; Siwek-Wilczynska, K; Smolyankin, V; Stockmeier, MR; Vasiliev, M; Wagner, P; Wisniewski, K; Wohlfarth, D; Yushmanov, I; Zhilin, A (FOPI collaboration) *Transition from*

in-plane to out-of-plane azimuthal enhancement in Au + Au collisions . Nuclear Physics **A**, 679 (3-4): 765-792 Jan 1 2001.

11. Wagner, A; Muntz, C; Oeschler, H; Sturm, C; Barth, R; Cieslak, M; Debowski, M; Grosse, E; Koczon, P; Laue, F; Mang, M; Miskowiec, D; Schwab, E; Senger, P; Beckerle, P; Brill, D; Shin, Y; Strobele, H; Walus, W; Kohlmeyer, B; Puhlhofer, F; Speer, J; Yoo, IK *Emission pattern of high-energy pions: A new probe for the early phase of heavy-ion collisions.* Physical Review Letters, 85 (1): 18-21 Jul 3 2000.
12. Herrmann, N; Wessels, JP; Wienold, T *Collective flow in heavy-ion collisions* . Annual Review Of Nuclear And Particle Science, 49: 581-632 1999.
13. Huo, L; Zhang, WN; Chen, XJ; Zhang, JB; Liu, YM; Liu, DKH *Squeeze-out in Au + Au collisions at 600A MeV.* High Energy Physics And Nuclear Physics-Chinese Edition, 23 (12): 1177-1182 Dec 1999.
14. Adamovich, MI; Basova, ES; Chernyavsky, MM; Dirner, A; Gulamov, KG; Jakobsson, B; Just, L; Kharlamov, SP; Krasnov, SA; Kravcakova, A; Larionova, VG; Nasyrov, SZ; Navotny, VS; Ojha, ID; Orlova, GI; Peresadko, NG; Petrov, NV; Rusakova, VV; Salmanova, NA; Singh, BK; Singh, V; Soderstrom, K; Tothova, M; Tretyakova, MI; Trofimova, TP; Tuleeva, UI; Tuli, SK; Tursunov, BP; Vokal, S; Vrlakova, J; Yuldashev, BS *Flow effects in Kr-84 induced collisions in emulsion at 0.95 GeV per nucleon.* European Physical Journal **A**, 6 (4): 427-430 Dec 1999.
15. Wang, ZS; Fuchs, C; Faessler, A; Gross-Boelting, T Kaon squeeze-out in heavy ion reactions European Physical Journal **A**, 5 (3): 275-283 Jul 1999.
16. Ye, W; Shen, WQ; Ma, YG; Feng, J; Yoshida, K; Nakagawa, T; Yuasa-Nakagawa, K; Furutaka, K; Matsuda, K; Futami, Y; Lee, SM; Kasagi, J *Azimuthal distribution and azimuthal correlation of light particles emitted in 10.6MeV/u Kr-84+Al-27 collision* .High Energy Physics & Nuclear Physics-English Edition, 21 (1): 417-423 1997.
17. Senger, P; Strobele, H *Hadronic particle production in nucleus-nucleus collisions* .Journal of Physics G-Nuclear and Particle Physics, 25 (5): R59-R131 May 1999.
18. Ollitrault, J Y *Flow systematics from SIS to SPS energies* Nuclear Physics **A**, 638 (1-2): 195C-206C Aug 10 1998.
19. Shin, Y; Ahner, W; Barth, R; Beckerle, P; Brill, D; Cieslak, M; Debowski, M; Grosse, E; Koczon, P; Kohlmeyer, B; Mang, M; Miskowiec, D; Muntz, C; Oeschler, H; Puhlhofer, F; Schwab, E; Schicker, R; Senger, P; Speer, J; Strobele, H; Sturm, C; Volkel, K; Wagner, A; Walus, W *Enhanced out-of-plane emission of K+ mesons observed in Au+Au collisions at 1A GeV* .Physical Review Letters, 81 (8): 1576-1579 Aug 24 1998.
20. Wang, ZS; Faessler, A; Fuchs, C; Maheswari, VSU; Waindzoch, T *Radial flow of kaon mesons in heavy ion reactions* . Physical Review **C**, 57 (6): 3284-3291 Jun 1998.

    Reisdorf, W; Ritter, HG *Collective flow in heavy-ion collisions* .Annual Review of Nuclear And Particle Science, 47: 663-709 1997.
21. Maheswari, VSU; Fuchs, C; Faessler, A; Sehn, L; Kosov, DS; Wang, Z *In-medium dependence and Coulomb effects of the pion production in heavy ion collisions* .Nuclear Physics **A**, 628 (4): 669-685 Jan 26 1998.
22. Fuchs, C; Essler, P; Gaitanos, T; Wolter, HH *Temperature and thermodynamic instabilities in heavy-ion collisions* .Nuclear Physics A, 626 (4): 987-998 Dec 1 1997.
23. Bastid, N; Buta, A; Crochet, P; Dupieux, P; Petrovici, M; Rami, F; Alard, JP; Amouroux, V; Basrak, Z; Belyaev, I; Best, D; Biegansky, J; Blaich, T; Caplar, R; Cerruti, C; Cindro, N; Coffin, JP; Dona, R; Dzelalija, M; Ero, E; Fan, ZG; Fintz, P; Fodor, Z; Fraysse, L; Freifelder, RP; Gobbi, A; Guillaume, G; Herrmann, N; Hildenbrand, KD; Holbling, S; Hong, B; Jeong, SC; Jundt, F; Keczkemeti, J; Kirejczyk, M; Korchagin, Y; Kotte, R; Kramer, M; Kuhn, C; Legrand, I; Leifels, Y; Maazouzi, C; Manko, V; Mgebrishvili, G; Moisa, D; Mosner, J; Neubert, W; Pelte, D; Pinkenburg, C; Pras, P; Reisdorf, W; Ritman, JL; Roy, C; Sadchikov, AG; Schull, D; Seres, Z; Sikora, B; Simion, V; SiwekWilczynska, K; Smolyankin, V; Sodan, U; Teh, KM; Tizniti, L; Trzaska, M; Vasiliev, M; Wagner, P; Wang, GS; Wessels, JP; Wienold, T; Wisniewski, K; Wohlfarth, D; Zhilin, A *Out-of-plane emission of nuclear matter in Au+Au collisions between 100 and 800 A MeV* . Nuclear Physics **A**, 622 (4): 573-592 Sep 8 1997.
24. Badala, A; Barbera, R; Palmeri, A; Pappalardo, GS; Riggi, F; Russo, AC; Russo, G; Turrisi, R *Pion shadowing as a tool to study the topology of heavy-ion collisions at intermediate energies* .Physical Review **C**, 55 (5): 2506-2520 May 1997.

25. Brill, D; Beckerle, P; Bormann, C; Schwab, E; Shin, Y; Strobele, H; Baltes, P; Muntz, C; Oeschler, H; Sturm, C; Wagner, A; Barth, R; Cieslak, M; Debowski, M; Grosse, E; Koczon, P; Mang, M; Miskowiec, D; Schicker, R; Senger, P; Kohlmeyer, B; Puhlhofer, F; Speer, J; Volkel, K; Walus, W *Studies of the out-of-plane emission of pions in symmetric heavy-ion collisions* . Zeitschrift fur Physik **A**-Hadrons And Nuclei, 357 (2): 207-213 Mar 1997.
26. Pelte, D; Hafele, E; Best, D; Goebels, G; Herrmann, N; Pinkenburg, C; Reisdorf, W; Trzaska, M; Alard, JP; Amouroux, V; Andronic, A; Basrak, Z; Bastid, N; Belyaev, I; Biegansky, J; Buta, A; Caplar, R; Cindro, N; Coffin, JP; Crochet, P; Dupieux, P; Dzelalija, M; Ero, J; Eskel, M; Fintz, P; Fodor, Z; GenouxLubain, A; Gobbi, A; Guillaume, G; Hildenbrand, KD; Hong, B; Jundt, F; Kecskemeti, J; Kirejczyk, M; Koncz, P; Korolija, M; Korchagin, Y; Kotte, R; Kuhn, C; Lambrecht, D; Lebedev, A; Legrand, I; Leifels, Y; Manko, V; Merlitz, H; Mosner, J; Mohren, S; Moisa, D; Neubert, W; Petrovici, M; Pras, P; Rami, F; Ramillien, V; Ritman, JL; Roy, C; Schull, D; Seres, Z; Sikora, B; Simion, V; SiwekWilczynska, K; Smolyankin, V; Sodan, U; Vasiliev, MA; Wagner, P; Wang, GS; Wienold, T; Wohlfarth, D; Zhilin, A *Charged pion production in Au on Au collisions at 1 AGeV* .Zeitschrift fur Physik **A**-Hadrons And Nuclei, 357 (2): 215-234 Mar 1997.
27. Zipprich, J; Fuchs, C; Lehmann, E; Sehn, L; Huang, SW; Faessler, A *Influence of the pion-nucleon interaction on the collective pion flow in heavy ion reactions* .Journal of Physics **G**-Nuclear and Particle Physics, 23 (1): L1-L6 Jan 1997.
28. Fuchs, C; Sehn, L; Lehmann, E; Zipprich, J; Faessler, A *Influence of the in-medium pion dispersion relation in heavy ion collisions* .Physical Review **C**, 55 (1): 411-418 Jan 1997.
29. Hartnack, C; David, C; Aichelin, J *Studies on the rescattering of mesons in nuclear matter* .Acta Physica Polonica **B**, 27 (11): 3191-3202 Nov 1996.
30. Li, GQ; Ko, CM; Brown, GE *Kaon azimuthal distributions in heavy-ion collisions* .Physics Letters **B**, 381 (1-3): 17-22 Jul 18 1996.
31. Awes, TC; Bock, D; Bock, R; Clewing, G; Garpman, S; Glasow, R; Gustafsson, HA; Gutbrod, HH; Holker, G; Jacobs, P; Kampert, KH; Kolb, BW; Lister, T; Lohner, H; Lund, I; Obenshain, FE; Oskarsson, A; Otterlund, I; Peitzmann, T; Plasil, F; Poskanzer, AM; Purschke, M; Ritter, HG; Santo, R; Schmidt, HR; Siemiarczuk, T; Sorensen, SP; Steffens, K; Steinhaeuser, P; Stenlund, E; Stuken, D; Young, GR *Azimuthal correlations in the target fragmentation region of high energy nuclear collisions* .Physics Letters **B**, 381 (1-3): 29-34 Jul 18 1996.
32. Pinkenburg, CH; Hildenbrand, KD *Directed sideward flow of fragments and secondary particles in relativistic heavy ion collisions* . Acta Physica Polonica **B**, 27 (1-2): 243-252 Jan-Feb 1996.
33. Russkikh, VN; Ivanov, YB *Collective Flow of Pions in Relativistic Heavy-Ion Collisions.* Nuclear Physics **A**, 591 (4): 699-710 Sep 4 1995.
34. Justice, M; Albergo, S; Bieser, F; Brady, FP; Caccia, Z; Cebra, D; Chacon, AD; Chance, J; Choi, Y; Costa, S; Elliott, J; Gilkes, M; Hauger, J; Hirsch, A; Hjort, E; Insolia, A; Keane, D; Kintner, J; Lisa, M; Liu, H; Matis, HS; Mcgrath, R; Mcmahan, M; Mcparland, C; Olson, D; Partlan, M; Porile, N; Potenza, R; Rai, G; Rasmussen, J; Ritter, HG; Romanski, J; Romero, J; Russo, G; Scharenberg, R; Scott, A; Shao, Y; Srivastava, B; Symons, Tjm; Tincknell, M; Tuve, C; Wang, S; Warren, P; Weerasundara, D; Wieman, H; Wolf, K *Observation of Collective Effects in Lambda-Production at 2 GeV/Nucleon* .Nuclear Physics **A**, 590 (1-2): C549-C552 Jul 24 1995.
35. Bass, SA; Hartnack, C; Stocker, H; Greiner, W *Transverse Energy-Dependence of Neutron Squeeze-out in Relativistic Heavy-ion Collisions* .Zeitschrift fur Physik **A**-Hadrons and Nuclei, 352 (2): 171-174 Jul 1995.
36. Muntz, C; Baltes, P; Oeschler, H; Sartorius, A; Wagner, A; Ahner, W; Barth, R; Cieslak, M; Debowski, M; Grosse, E; Henning, W; Koczon, P; Miskowiec, D; Schicker, R; Senger, P; Bormann, C; Brill, D; Shin, Y; Stein, J; Stock, R; Strobele, H; Kohlmeyer, B; Poppl, H; Puhlhofer, F; Speer, J; Volkel, K; Walus, W *Properties Of High-Energy Pions Emitted from Heavy-ion Collisions at 1 GeV Nucleon.* Zeitschrift fur Physik **A**-Hadrons and Nuclei, 352 (2): 175-179 Jul 1995.
37. Ma, YG; Shen, WQ *Correlation-Functions and the Disappearance of Rotational Collective Motion in Nucleus-Nucleus Collisions below 100 MeV/Nucleon* . Physical Review **C**, 51 (6): 3256-3263 Jun 1995.
38. Bass, SA; Hartnack, C; Stocker, H; Greiner, W *Azimuthal Correlations of Pions in Relativistic Heavy-ion Collisions at 1 GeV/Nucleon* . Physical Review **C**, 51 (6): 3343-3356 Jun 1995.

39. Jain, PL; Singh, G; Mukhopadhyay, A *Nuclear Collective Flow in Au-197-Emulsion Interactions at 10.6A GeV* . Physical Review Letters, 74 (9): 1534-1537 Feb 27 1995.
40. Danielewicz, P *Effects of Compression and Collective Expansion on Particle-Emission from Central Heavy-ion Reactions.* Physical Review **C**, 51 (2): 716-750 Feb 1995.
41. Ma, YG; Shen, WQ; Zhu, ZY *Collective Motion of Reverse-Reaction System in the Intermediate-Energy Domain via the Quantum-Dynamics Molecular-Dynamics Approach* .Physical Review **C**, 51 (2): 1029-1032 Feb 1995.
42. Bass, SA; Hartnack, C; Stocker, H; Greiner, W *Pi-N Correlations Probe the Nuclear-Equation of State in Relativistic Heavy-ion Collisions* . Physical Review **C**, 51 (1): R12-R16 Jan 1995.
43. Kiselev, SM *Squeeze-out of Nuclear-Matter in High-Energy Heavy-ion Collisions in the Molecular-Dynamical Model.* Nuclear Physics **A**, 579 (3-4): 643-659 Oct 24 1994.
44. Bass, SA; Hartnack, C; Stocker, H; Greiner, W *High Pt Pions as Probes of the Dense Phase of Relativistic Heavy-ion Collisions.* Physical Review **C**, 50 (4): 2167-2172 Oct 1994.

Article reprint

VOLUME 72, NUMBER 7 PHYSICAL REVIEW LETTERS 14 FEBRUARY 1994

Transverse Momentum Distributions of η Mesons in Near-Threshold Relativistic Heavy Ion Reactions

F.-D. Berg,[1] M. Pfeiffer,[1] O. Schwalb,[1] M. Franke,[1] W. Kühn,[1] H. Löhner,[2] V. Metag,[1] M. Notheisen,[1] R. Novotny,[1] A. E. Raschke,[2] J. Ritman,[1] M. Röbig-Landau,[1] R. S. Simon,[3] M. Šumbera,[2] L. Venema,[2] and H. Wilschut [2]

[1]*II. Physikalisches Institut, D-35392 Universität Giessen, Germany*

[2]*Kernfysisch Versneller Institut, NL-9747 AA Groningen, The Netherlands*

[3]*Gesellschaft für Schwerionenforschung, D-64220 Darmstadt, Germany*

(Received 18 October 1993)

Transverse momentum spectra of η mesons have been measured near the free nucleon-nucleon production threshold in the heavy ion reactions ^{40}Ar+^{nat}Ca, ^{86}Kr+^{nat}Zr, and ^{197}Au+^{197}Au at 1.0A GeV and also in ^{40}Ar+^{nat}Ca at 1.5A GeV. The measured transverse momentum distributions are compared to model calculations. The relative abundance of $\Delta(1232)$ and $N(1535)$ resonances excited in the collision is deduced. A comparison to pion data reveals scaling with the transverse mass of the emitted meson.

PACS numbers: 25.75.+r

Relativistic heavy ion collisions are a unique tool to study highly excited and compressed nuclear matter. According to various theoretical predictions [1–3] baryon densities up to 3 times normal nuclear matter density ρ_0 are reached in the reaction volume. Furthermore, at bombarding energies of 1–2A GeV a gradual transition to *resonance matter* seems to occur, i.e., strongly interacting hadronic matter with about 30% of the baryons excited to Δ and N resonances corresponding to a density $\rho_\Delta \approx \rho_0$ [4–6]. To learn more about the properties of this form of matter it is important to determine its baryonic composition, i.e., the abundance of nucleons, Δ, and N resonances. Since these resonances decay by π and η emission a promising approach to investigate the population of excited baryonic states in the collision of two heavy nuclei is to measure meson yields. The rate of pions is in first approximation related to the excitation of the Δ resonance which decays into the π channel by 99%. η mesons almost exclusively originate from the decay of the $N(1535)$ resonance and are thus a very selective probe for the excitation of this resonance.

Although π^0 and η production in the 1A GeV energy regime proceeds through the excitation of different baryon resonances it is of interest to check to which extent η-production cross sections and transverse momentum spectra are governed by phase space and the average energy available per nucleon-nucleon collision. General scaling laws have been established for meson production in the 10A MeV to 14.0A GeV bombarding energy range [5,7,8]. At very high bombarding energies a scaling of meson abundancies with the transverse mass (m_t scaling) has been observed [9]. It is of importance to clarify whether such universal features of transverse momentum distributions also hold at bombarding energies as low as 1A GeV and whether there is a common underlying mechanism for the buildup of transverse mass.

Furthermore, the knowledge of η-meson production cross sections in heavy ion reactions is essential for the understanding of dilepton experiments [10], since the η Dalitz decay contributes substantially to the dilepton invariant mass spectra below masses of 500 MeV.

Meson production in heavy ion collisions has been extensively studied at the LBL Bevalac [11]. While these experiments concentrated on charged mesons a program studying neutral mesons has been initiated [12] at the heavy ion synchrotron SIS at GSI Darmstadt. In this Letter we report for the first time on transverse momentum spectra of η mesons produced in collision systems of different mass at energies below and above the threshold for η production in free nucleon-nucleon collisions.

We have investigated η production in the systems ^{40}Ar+^{nat}Ca at 1.0 and 1.5A GeV as well as in the systems ^{86}Kr+^{nat}Zr and ^{197}Au+^{197}Au at 1.0A GeV. Beams of up to 10^6 particles per spill provided by the heavy ion synchrotron SIS impinged on targets of ^{nat}Ca (1.02 g/cm^2), ^{nat}Zr (0.13 g/cm^2), and ^{197}Au (0.188 g/cm^2) corresponding to 1% (Ca) and 0.1% (Kr, Au) nuclear interaction length, respectively. The π^0 and η mesons have been measured via their two-photon decay channel (branching ratios: π^0, 98.8%; η, 38.9% [13]) using the Two Arm Photon Spectrometer (TAPS) [14]. This detector system consisted of 256 BaF_2 scintillators of hexagonal shape arranged in 4 blocks of 64 modules with individual charged particle veto detectors in front of each module. The geometry of the detector setups is summarized in Table I. The block configurations allowed the simultaneous measurement of pions and η's in a small window at midrapidity ($\mid y - y_{c.m.} \mid \leq 0.1 - 0.2$) independent of the meson transverse momentum.

An array of 16 plastic scintillation detectors covering a solid angle of 5% of 4π in the range $32° \leq \theta \leq 55°$ was mounted around the beam pipe at 6 cm distance from the beam axis to serve as a reaction trigger. In Kr+Zr and Ar+Ca at 1.5A GeV this device was used also as a time-zero detector whereas an in-beam start detector was available in the other experiments. For event characteri-

0031-9007/94/72(7)/977(4)$06.00

TABLE I. Geometrical setups of the TAPS detector system in the different experiments. In the Au+Au and 1.5A GeV Ar+Ca experiments two and three different detector setups have been used, respectively, in order to cover a larger kinematical range. Θ denotes the angle of a TAPS tower with respect to the beam direction and Φ the tilt angle of the block with respect to the horizontal plane containing the beam. d is the distance between the block front sides and the target.

Experiment	d (cm)	Θ (deg)	Φ (deg)
^{40}Ar+^{nat}Ca	120	±52.5	±12.1
^{86}Kr+^{nat}Zr	160	±52.2	±16/ ± 9.5
^{197}Au+^{197}Au	200	±52	±7.3/ ± 23
^{40}Ar+^{nat}Ca	220	±47.5	±7/ ± 15/ ± 23

zation the charged particle multiplicity was measured in the forward wall of the FOPI detector [15], comprising 512 plastic strips at laboratory angles between 7° and 30°. The main trigger required a signal in the time-zero detector together with two neutral hits in TAPS, which introduces no significant bias for π^0 and η detection. In addition, a signal was required in the forward wall in the case of Au+Au.

Photon-particle discrimination and η-meson identification via invariant mass analysis have been performed as described in [12]. η transverse momentum spectra have been derived by selecting events in the η mass region and by subtracting the combinatorial background deduced by event mixing. These spectra are corrected for the detector acceptance which has been obtained from Monte Carlo simulations with the GEANT3 [16] package.

Figure 1(a) presents the invariant mass distributions for all four experiments together with the combinatorial background which fits the spectra over the full mass range except for the π^0 and η signals. The mass range near the η meson is shown separately in Fig. 1(b) where a structure of FWHM $\approx$ 50 MeV can be identified at a peak/background level of (10–20)%. In the case of Kr+Zr and Au+Au a cut on the forward wall charged particle multiplicity M_{ch} of less than 85% and 60% of the maximum value has been applied, respectively, to reduce the combinatorial background due to the larger photon multiplicity in the heavier systems.

Combining the present results with π^0 data [17], η/π^0 ratios are deduced which are listed in Table II after correction for π^0 and η detection efficiencies. The η/π^0 ratio is found to vary by less than 40% as a function of M_{ch} in all collision systems. η/π^0 ratios obtained in the heavy systems for cuts in M_{ch} can thus be considered inclusive values within the errors quoted. The simultaneous measurement of both mesons reduces systematic errors in the η/π^0 ratio. These measured quantities are extrapolated to the full solid angle assuming a thermal and isotropic source in the nucleon-nucleon c.m. system as suggested by earlier π^- data [18]. The fraction of mesons observed in a given rapidity range depends on the temperature of

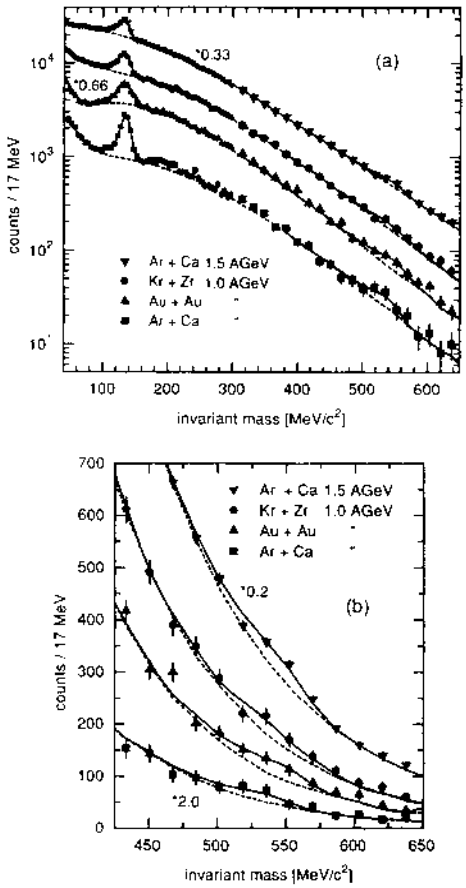

FIG. 1. (a) Invariant mass spectra for the systems Ar+Ca at 1.5A GeV, Kr+Zr, Au+Au, and Ar+Ca at 1.0A GeV (top to bottom) together with the mixed event background. Part (b) shows the same spectra in the η region. The spectra for the two heavier systems are accumulated under the condition of a forward wall charged particle multiplicity of less than 85% (Kr+Zr) and 60% (Au+Au) of the maximum value, respectively.

the source. Consequently, the uncertainty in the slope of the transverse momentum distribution in the case of Ar+Ca at 1.0A GeV gives rise to relatively large total errors. The high η/π^0 value of 1.9% for Ar+Ca at 1.0A GeV reduces to 1.3% assuming a slope parameter of only 64 MeV for the transverse momentum distribution which has been measured for pions in this reaction [17] and fits well into the systematics of the other systems. With this assumption a slight increase of the η/π^0 ratio with energy is found.

Table II lists the results of recent Boltzmann-Uehling-Uhlenbeck (BUU) calculations for the experimental rapidity range [19]. Using the code and parameters of [20], these microscopic transport-model calculations [2,6,20] describe heavy ion reactions as a sequence of nucleon-

VOLUME 72, NUMBER 7 PHYSICAL REVIEW LETTERS 14 FEBRUARY 1994

TABLE II. Summary of experimental results: The rapidity range (Δy) and the quantities measured within this interval are listed together with BUU results for this y range. In the case of Ar+Ca at 1.0A GeV the η/π^0 ratio and cross section are also listed for a temperature of 64 MeV which has been measured for pions. The last three columns show an extrapolation of the measured values to the full solid angle assuming a thermal and isotropic source in the c.m. system together with results from QGSM calculations [22].

	Expt. parameters			In rapidity range Δy				Extrapolation to full solid angle		
System	E_{beam}/A (GeV)	Δy	$y_{beam}/2$	T_η (MeV)	η/π^0 (%)	$\sigma_\eta^{\Delta y}$ (mb)	$(\eta/\pi^0)_{BUU}$ (%)	$\sigma_\eta^{4\pi}$ (mb)	η/π^0 (%)	$(\sigma_\eta^{4\pi})_{QGSM}$ (mb)
Ar+Ca	1.0	0.48 – 0.88	0.68	100^{+40}_{-20}	2.6 ± 1.6	11 ± 7		29 ± 18	1.9 ± 1.2	
				64 ± 1	2.1 ± 1.3	9 ± 6	2.3	19 ± 12	1.3 ± 0.8	12
Kr+Zr	1.0	0.52 – 0.84	0.68	70 ± 11	2.1 ± 0.9	50 ± 22	2.3	140 ± 60	1.3 ± 0.6	
Au+Au	1.0	0.52 – 0.84	0.68	63 ± 8	2.4 ± 0.9	150 ± 90	2.3	420 ± 250	1.4 ± 0.6	
Ar+Ca	1.5	0.68 – 0.84	0.80	79^{+11}_{-8}	4.0 ± 0.8	14 ± 3	5.6	72 ± 14	2.2 ± 0.4	44

nucleon collisions, taking mean field effects into account. They reproduce the η/π^0 ratios for all systems at 1A GeV within the errors of both experiment and simulation. At 1.5A GeV Ar+Ca the theoretical prediction is slightly too high. The total η cross sections are also in reasonable agreement with quark-gluon-string-model (QGSM) calculations [21,22] also listed in Table II.

From the η/π^0 ratio the relative abundance of the $\Delta(1232)$ and $N(1535)$ resonances at the respective freeze-out can be estimated, which can be related to the baryonic composition in the collision zone provided absorption is similar for both mesons [20]. Taking only the dominant $\Delta \rightarrow N\pi$ decay into account and applying the appropriate isospin factors together with a branching ratio

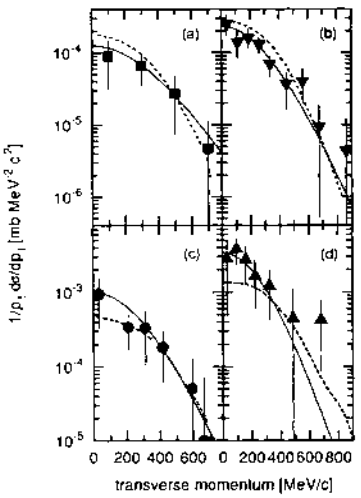

FIG. 2. Transverse momentum distributions at midrapidity for the systems Ar+Ca at 1.0 (a) and 1.5A GeV (b), Kr+Zr (c), and Au+Au (d) at 1.0A GeV. The solid curves represent fits with a thermal, isotropic source at midrapidity while the dashed curves show the BUU calculations by Ehehalt and Mosel [19]. The fit results and the rapidity range covered by TAPS are listed in Table II.

of 40% for the $N(1535)$ into the η channel [13], one gets a $N(1535)/\Delta(1232)$ ratio of $(1.1 \pm 0.6)\%$ and $(1.8 \pm 0.3)\%$ at 1.0 and 1.5A GeV, respectively. This result is similar to recent BUU simulations [6], which predict an excitation of the lowest lying nucleon resonances Δ, $N(1440)$, and $N(1535)$ with a fraction of 30%, 4%, and 1% of all baryons in the reaction volume at 2A GeV, respectively.

The transverse momentum distributions for η mesons are shown in Fig. 2 together with a fit with the expression $(1/p_t)d\sigma/dp_t \sim m_t e^{-m_t/T}$ with $m_t = \sqrt{p_t^2 + m_\eta^2}$, which corresponds to a thermal and isotropic η source observed in a small interval at midrapidity. At 1A GeV the temperatures obtained by this fit do not vary with the mass of the system within the errors, except for the Ar+Ca data which has poor statistics. Only a slight increase with the beam energy is observed. Figure 2 also shows BUU calculations [19], again based on the work of [20], which are in reasonable agreement with the experimental data. These calculations, however, do not yet use as input the recently measured elementary η-production cross sections [23,24].

More striking is the fact that the η transverse momenta show quantitatively the same behavior as the π^0 spectra. This is demonstrated in Fig. 3 where the transverse mass distribution $(1/m_t^2)d\sigma/dm_t \sim e^{-m_t/T}$ is plotted for the two Ar+Ca runs in the respective rapidity intervals. In this graph π^0- and η-meson data roughly fall on one line for $m_t \geq 550$ MeV, indicating that the energy required to produce a given transverse mass m_t is the important parameter determining the relative abundance of the two meson species. Hence, these spectra resemble the so-called m_t-scaling hypotheses [9] well known in high energy physics. There, however, the η/π^0 ratio asymptotically approaches ≈ 0.5 for high p_t, while in the SIS energy regime this ratio is closer to 1.0. This observation is nevertheless remarkable as in the energy regime of 1A GeV π^0 and η production proceeds through the excitation of different baryon resonances while other production mechanisms on the parton level prevail at higher energies. Transport model calculations address-

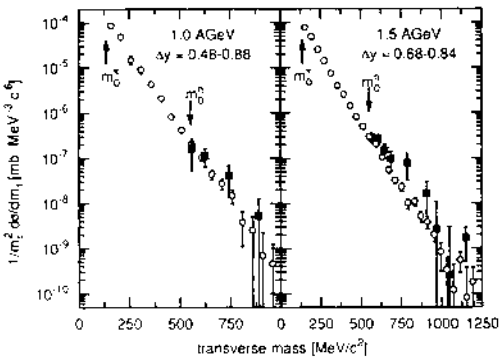

FIG. 3. Comparison of the transverse mass distributions of π^0 and η mesons in Ar+Ca at 1.0 and 1.5A GeV.

ing this universal feature of transverse mass production are highly needed.

In conclusion, η-meson production near the production threshold in free nucleon-nucleon collisions has been studied in heavy ion reactions in a first round of experiments with TAPS at the new heavy ion accelerator facility SIS at GSI. The measured η cross sections provide information on the baryonic composition of the resonance enriched matter formed in the collision zone. The experimental results are in resonable agreement with BUU and QGSM calculations. The transverse momentum spectra of pions and η's scale with the transverse mass.

We would like to thank the accelerator crew at GSI for the stable beams and the colleagues from the FOPI Collaboration for their support in performing the experiment. We are also grateful to U. Mosel and W. Cassing for many stimulating discussions and to W. Ehehalt who did the BUU calculations for all our collision systems. The strong technical support of our experiments by W. Döring, R. Engel, and W. Niebur is highly acknowledged. This work was supported in part by GSI under Contract No. GI Met K by BMFT under Contract No. 06 GI 174 I and by the Dutch Foundation FOM.

[1] J. Aichelin, Phys. Rep. **202**, 233 (1991).
[2] W. Cassing *et al.*, Phys. Rep. **188**, 363 (1990).
[3] H. Stöcker and W. Greiner, Phys. Rep. **137**, 277 (1986).
[4] U. Mosel and V. Metag, Phys. Bl. **5**, 426 (1993).
[5] V. Metag, Prog. Part. Nucl. Phys. **30**, 75 (1993).
[6] W. Ehehalt *et al.*, Phys. Rev. C **47**, 2467 (1993).
[7] A. Shor, Phys. Lett. B **274**, 11 (1992).
[8] A. A. Baldin, JINR Rapid Commun. **3**, 54 (1992).
[9] M. Bourquin and J. M. Gaillard, Nucl. Phys. **B114**, 334 (1976).
[10] G. Roche *et al.*, Phys. Lett. B **226**, 228 (1989).
[11] R. Stock, Phys. Rep. **135**, 259 (1986).
[12] F.-D. Berg *et al.*, Z. Phys. A **340**, 297 (1991).
[13] Particle Data Group, K. Hikasa *et al.*, Phys. Rev. D **45**, S1 (1992).
[14] R. Novotny, IEEE Trans. Nucl. Sci. **38**, 379 (1991).
[15] A. Gobbi *et al.*, Nucl. Instrum. Methods Phys. Res., Sect. A **324**, 156 (1993).
[16] R. Brun *et al.*, GEANT3 User's Guide, Report No. CERN-DD/EE/84-1, 1986 (unpublished).
[17] O. Schwalb *et al.*, Phys. Lett. B (to be published).
[18] R. Brockmann *et al.*, Phys. Rev. Lett. **53**, 2012 (1984).
[19] W. Ehehalt and U. Mosel (private communications).
[20] Gy. Wolf, Prog. Part. Nucl. Phys. **30**, 273 (1993).
[21] N. S. Amelin *et al.*, Yad. Fiz. **51**, 512 (1990) [Sov. J. Nucl. Phys. **51**, 327 (1990)].
[22] V. D. Toneev, in Proceedings of the 2nd TAPS Workshop (World Scientific, Singapore, to be published).
[23] A. M. Bergdolt *et al.*, Phys. Rev. D **48**, R2969 (1993).
[24] E. Chiavassa *et al.*, Nucl. Phys. **A519**, 413 (1990).

3.2.1 Citations

1. Fuchs, C *Kaon production in heavy ion reactions at intermediate energies* .Progress in Particle and Nuclear Physics, Vol 56, No 1, 56 (1): 1-103 2006.
2. D'yachenko, AT *Heavy meson production in nucleus-nucleus collisions in the fluid dynamic approach* . Izvestiya Akademii Nauk Seriya Fizicheskaya, 66 (3): 441-444 Mar 2002.
3. Senger, P; Strobele, H *Hadronic particle production in nucleus-nucleus collisions* . Journal of Physics **G**-Nuclear And Particle Physics, 25 (5): R59-R131 May 1999.
4. Cassing, W; Bratkovskaya, EL *Hadronic and electromagnetic probes of hot and dense nuclear matter* . Physics Reports-Review Section of Physics Letters, 308 (2-3): 65-233 Jan 1999.
5. Cassing, W *Meson production and meson properties at finite nuclear density* . Acta Physica Polonica **B**, 29 (11): 3175-3183 Nov 1998.
6. Eskef, M; Pelte, D; Goebels, G; Hafele, E; Herrmann, N; Korolija, M; Leifels, Y; Merlitz, H; Mohren, S; Stockmeier, MR; Trzaska, M; Alard, JP; Andronic, A; Averbeck, R; Basrak, Z; Bastid, N; Belyaev, I; Best, D; Buta, A; Caplar, R; Cindro, N; Coffin, JP; Crochet, P; Dupieux, P; Dzelalija, M; Fraysse, L; Fodor, Z; Genoux-Lubain, A; Gobbi, A; Hildenbrand, KD; Hong, B; Jundt, F; Kecskemeti, J; Kirejczyk, M; Kotte, R; Kutsche, R; Lebedev, A; Manko, V; Mosner, J; Moisa, D; Neubert, W; Petrovici, M; Pinkenburg, C; Plettner, C; Pras, P; Rami, F; Ramillien, V; Reisdorf, W; Ritman, JL; de Schauenburg, B; Schull, D; Seres, Z; Sikora, B; Simion, V; Siwek-Wilczynska, K; Smolyankin, V; Vasiliev, MA; Wagner, P; Wang, GS; Wisniewski, K; Wohlfarth, D; Zhilin, A *Identification of baryon resonances in central heavy-ion collisions at energies between 1 and 2 AGeV* . European Physical Journal **A**, 3 (4): 335-349 Dec 1998.
7. Porter, RJ; Beedoe, S; Bossingham, R; Bougteb, M; Christie, WB; Hallman, T; Huang, HZ; Igo, G; Kirk, P; Krebs, G; Letessier-Selvon, A; Madansky, L; Manso, F; Matis, HS; Miller, J; Naudet, C; Prunet, M; Roche, G; Schroeder, LS; Seidl, P; Wang, ZF; Welsh, RC; Wilson, WK; Yegneswaran, A *Dielectron production in A-A reactions at 1.0 A center dot GeV* .Nuclear Physics **A**, 638 (1-2): 499C-502C Aug 10 1998.
8. Ernst, C; Bass, SA; Belkacem, M; Stocker, H; Greiner, W *Intermediate mass excess of dilepton production in heavy ion collisions at relativistic energies* .Physical Review **C**, 58 (1): 447-456 Jul 1998.
9. Santra, AB; Jain, BK *Eta production in proton-proton collisions* . Nuclear Physics **A**, 634 (3): 309-324 May 11 1998.
10. Bratkovskaya, EL; Cassing, W; Rapp, R; Wambach, J *Dilepton production and m(T)-scaling at BEVALAC/SIS energies* . Nuclear Physics **A**, 634 (1-2): 168-189 May 4 1998.
11. Bratkovskaya, EL; Cassing, W; Mosel, U *Meson m(T)-scaling in heavy-ion collisions at SIS energies* . Physics Letters **B**, 424 (3-4): 244-252 Apr 9 1998
12. Hong, BS; Herrmann, N *Chemical equilibration and freeze-out in nucleus-nucleus collisions at incident beam energies from 1A to 2A GeV* . Journal of the Korean Physical Society, 32 (5): L631-L634 May 1998.
13. Mao, GJ; Neise, L; Stocker, H; Greiner, W; Li, ZX *Relativistic transport theory of N, Delta, and N*(1440) interacting through sigma, omega, and pi mesons* .Physical Review **C**, 57 (4): 1938-1961 Apr 1998.
14. Ko, CM; Koch, V; Li, GQ *Properties of hadrons in the nuclear medium* . Annual Review of Nuclear and Particle Science, 47: 505-539 1997.
15. Hong, B; Herrmann, N; Ritman, JL; Best, D; Gobbi, A; Hildenbrand, KD; Kirejczyk, M; Leifels, Y; Pinkenburg, C; Reisdorf, W; Schull, D; Sodan, U; Wang, GS; Wienold, T; Alard, JP; Amouroux, VJBA; Bastid, N; Belyaev, I; Berek, G; Biegansky, J; Buta, A; Coffin, JP; Crochet, P; de Schauenburg, B; Dona, R; Dupieux, P; Eskef, M; Fintz, P; Fodor, Z; Fraysse, L; Genoux-Lubain, A; Goebels, G; Guillaume, G; Hafele, E; Jundt, F; Kecskemeti, J; Korolija, M; Kotte, R; Kuhn, C; Lebedev, A; Legrand, I; Maazouzi, C; Manko, V; Mosner, J; Mohren, S; Neubert, W; Pelte, D; Petrovici, M; Pras, P; Rami, F; Roy, C; Seres, Z; Sikora, B; Simion, V; Siwek-Wilczynska, K; Somov, A; Tizniti, L; Trzaska, M; Vasiliev, MA; Wagner, P; Wohlfarth, D; Zhilin, A *Stopping and radial flow in central Ni-58+Ni-58 collisions between 1A and 2A GeV* .Physical Review **C**, 57 (1): 244-253 Jan 1998.

16. Best, D; Herrmann, N; Hong, B; Kirejczyk, M; Ritman, J; Wisniewski, K; Zhilin, A; Gobbi, A; Hildenbrand, KD; Leifels, Y; Pinkenburg, C; Reisdorf, W; Schull, D; Sodan, U; Wang, GS; Wienold, T; Alard, JP; Amouroux, V; Bastid, N; Belyaev, I; Berek, G; Biegansky, J; Cherbatchev, R; Coffin, JP; Crochet, P; Dupieux, P; Fodor, Z; GenouxLubain, A; Goebels, G; Guillaume, G; Hafele, E; Jundt, F; Kecskemeti, J; Korchagin, Y; Kotte, R; Kuhn, C; Lebedev, A; Lebedev, A; Legrand, I; Maazouzi, C; Manko, V; Mosner, J; Mohren, S; Moisa, D; Neubert, W; Pelte, D; Petrovici, M; Pras, P; Rami, F; Roy, C; Seres, Z; Sikora, B; Simion, V; SiwekWilczynska, K; Smolyankin, V; Somov, A; Tizniti, L; Trzaska, M; Vasiliev, MA; Wagner, P; Wohlfarth, D; Yushmanov, I *K+ production in the reaction Ni-58+Ni-58 at incident energies from 1 to 2 A GeV*. Nuclear Physics **A**, 625 (1-2): 307-324 Oct 27 1997.
17. Deutsch-Sauermann, C; Friman, B; Norenberg, W *Eta-meson photoproduction off protons and deuterons* . Physics Letters **B**, 409 (1-4): 51-57 Sep 18 1997.
18. Porter, RJ; Beedoe, S; Bossingham, R; Bougteb, M; Christie, WB; Carroll, J; Gong, WG; Hallman, T; Heilbronn, L; Huang, HZ; Igo, G; Kirk, P; Krebs, G; LetessierSelvon, A; Madansky, L; Manso, F; Matis, HS; Miller, J; Naudet, C; Prunet, M; Roche, G; Schroeder, LS; Seidl, P; Wang, ZF; Welsh, RC; Wilson, WK; Yegneswaran, A *Dielectron cross section measurements in nucleus-nucleus reactions at 1.0A GeV* . Physical Review Letters, 79 (7): 1229-1232 Aug 18 1997.
19. Hong, B; Herrmann, N; Ritman, JL; Best, D; Gobbi, A; Hildenbrand, KD; Kirejczyk, M; Leifels, Y; Pinkenburg, C; Reisdorf, W; Schull, D; Sodan, U; Wang, GS; Wienold, T; Alard, JP; Amouroux, V; Bastid, N; Belyaev, I; Berek, G; Biegansky, J; Buta, A; Coffin, JP; Crochet, P; Dona, R; Dupieux, P; Eskef, M; Fintz, P; Fodor, Z; Fraysse, L; GenouxLubain, A; Goebels, G; Guillaume, G; Hafele, E; Jundt, F; Kecskemeti, J; Korolija, M; Kotte, R; Kuhn, C; Lebedev, A; Legrand, I; Maazouzi, C; Manko, V; Mosner, J; Mohren, S; Neubert, W; Pelte, D; Petrovici, M; Pras, P; Rami, F; Roy, C; Seres, Z; Sikora, B; Simion, V; SiwekWilczynska, K; Somov, A; Tizniti, L; Trzaska, M; Vasiliev, MA; Wagner, P; Wohlfarth, D; Zhilin, A *Abundance of Delta resonances in Ni-58+Ni-58 collisions between 1 and 2 AGeV* . Physics Letters **B**, 407 (2): 115-120 Aug 28 1997.
20. Pelte, D; Hafele, E; Best, D; Goebels, G; Herrmann, N; Pinkenburg, C; Reisdorf, W; Trzaska, M; Alard, JP; Amouroux, V; Andronic, A; Basrak, Z; Bastid, N; Belyaev, I; Biegansky, J; Buta, A; Caplar, R; Cindro, N; Coffin, JP; Crochet, P; Dupieux, P; Dzelalija, M; Ero, J; Eskel, M; Fintz, P; Fodor, Z; GenouxLubain, A; Gobbi, A; Guillaume, G; Hildenbrand, KD; Hong, B; Jundt, F; Kecskemeti, J; Kirejczyk, M; Koncz, P; Korolija, M; Korchagin, Y; Kotte, R; Kuhn, C; Lambrecht, D; Lebedev, A; Legrand, I; Leifels, Y; Manko, V; Merlitz, H; Mosner, J; Mohren, S; Moisa, D; Neubert, W; Petrovici, M; Pras, P; Rami, F; Ramillien, V; Ritman, JL; Roy, C; Schull, D; Seres, Z; Sikora, B; Simion, V; SiwekWilczynska, K; Smolyankin, V; Sodan, U; Vasiliev, MA; Wagner, P; Wang, GS; Wienold, T; Wohlfarth, D; Zhilin, A *Charged pion production in Au on Au collisions at 1 AGeV* . Zeitschrift fur Physik **A**-Hadrons And Nuclei, 357 (2): 215-234 Mar 1997.
21. Ko, CM; Li, GQ *Medium effects in high energy heavy-ion collisions* . Journal Of Physics G-Nuclear And Particle Physics, 22 (12): 1673-1725 Dec 1996.
22. Ehehalt, W; Cassing, W *Relativistic transport approach for nucleus-nucleus collisions from SIS to SPS energies* . Nuclear Physics **A**, 602 (3-4): 449-486 Jun 3 1996.
23. Ko, CM; Li, GQ *Hadrons In Dense Matter*. Nuclear Physics **A**, 583: C591-C598 Feb 6 1995.
24. Bass, SA; Hartnack, C; Stocker, H; Greiner, W *Azimuthal Correlations of Pions in Relativistic Heavy-Ion Collisions at 1 GeV/Nucleon* . Physical Review **C**, 51 (6): 3343-3356 Jun 1995.
25. Sauermann, C; Friman, Bl; Norenberg, W *Resonance Model for pi-N Scattering and eta-Meson Production in the S-11 Channel* . Physics Letters **B**, 341 (3-4): 261-267 Jan 5 1995.
26. Li, BA; Ko, CM; Li, GQ *Effects of N-Asterisk(1440) Resonance on Particle-Production in Heavy-Ion Collisions at Subthreshold Energies* . Physical Review **C**, 50 (6): R2675-R2679 Dec 1994.

    Li, BA *Near-Threshold K+ Production In Heavy-Ion Collisions*. Physical Review **C**, 50 (4): 2144-2151 Oct 1994.

Article reprint

Physics Letters B 321 (1994) 20–25
North-Holland

PHYSICS LETTERS B

Mass dependence of π^0-production in heavy ion collisions at 1 A GeV

O. Schwalb [a], M. Pfeiffer [a], F.-D. Berg [a], M. Franke [a], W. Kühn [a], V. Metag [a], M. Notheisen [a], R. Novotny [a], J. Ritman [a,1], M.E. Röbig-Landau [a], J.P. Alard [e], N. Bastid [e], N. Brummund [d,3], P. Dupieux [e], A. Gobbi [c], N. Herrmann [f], K.D. Hildenbrand [c], S. Hlaváč [c,2], S.C. Jeong [c], H. Löhner [b], G. Montarou [e], W. Neubert [g], A.E. Raschke [b], R.S. Simon [c], U. Sodan [c], M. Šumbera [b,4], K. Teh [c,5], L.B. Venema [b], H.W. Wilschut [b], J.P. Wessels [c], T. Wienold [c] and D. Wohlfahrt [g]

[a] *II. Physikalisches Institut, Universität Gießen, D-35392 Gießen, Germany*
[b] *Kernfysisch Versneller Instituut, NL-9747 AA Groningen, The Netherlands*
[c] *Gesellschaft für Schwerionenforschung, D-64220 Darmstadt, Germany*
[d] *Institut für Kernphysik, Universität Münster, D-48149 Münster, Germany*
[e] *Laboratoire de Physique Corpusculaire, F-63177 Clermont-Ferrand, France*
[f] *Physikalisches Institut, Universität Heidelberg, D-69177 Heidelberg, Germany*
[g] *Forschungszentrum Rossendorf, D-01314 Dresden, Germany*

Received 22 October 1993; revised manuscript received 30 November 1993
Editor: R.H. Siemssen

The production of neutral pions has been studied in the reactions $^{40}Ar+^{nat}Ca$, $^{86}Kr+^{nat}Zr$ and $^{197}Au+^{197}Au$ at 1 A GeV. For high energy pions emitted from the heavier systems a steeper than linear rise of the pion multiplicity with the centrality of the reaction is observed, indicating a pion production process other than binary nucleon–nucleon collisions. At low transverse momenta an enhancement of the π^0-multiplicity increasing with the mass of the collision system is found. Systematic discrepancies between the experimental results and recent BUU, QMD and Cascade calculations are discussed.

Theoretical descriptions of relativistic heavy ion collisions [1–3] indicate that at bombarding energies of the order of 1 A GeV nuclear matter can be compressed as in stellar processes to 2–3 times the normal density. Simultaneously some 10% of the nucleons are excited to baryon resonances like $\Delta(1232)$ and higher states. Relativistic heavy ion collisions appear to provide the only access to the properties of such compressed and intrinsically excited hadronic matter under controlled conditions in the laboratory. Experimentally, two approaches have been pursued in these investigations. Emission patterns of nucleons and complex fragment formation in central heavy ion collisions have been measured and studied in a global analysis. Phenomena such as *sideward flow* [4], *squeeze-out* [5] of baryons and an explosion-like expansion of the collision zone [6] have been observed, providing information on the dynamics of the heavy ion reaction. A complementary approach is to investigate the production of particles [7] not present in the entrance channel, such as photons, mesons and antiprotons. These particles have been studied with respect to their abundancies, momentum spectra and their distribution relative to the reaction plane [8,9].

So far particle production in heavy ion reactions

[1] Present address: Gesellschaft für Schwerionenforschung, D-64220 Darmstadt, Germany.
[2] Permanent address: Institute of Physics, Slovak Academy of Sciences, Bratislava, Slovak Republic.
[3] Present address: Kernforschungsanlage, D-52428 Jülich, Germany.
[4] Present address: Nuclear Physics Institute, 25068 Řež near Prague, Czech Republic.
[5] Present address: Argonne National Laboratory, Argonne, Illinois, USA.

Elsevier Science B.V.
SSDI 0370-2693(93)E1532-3

Volume 321, number 1,2 PHYSICS LETTERS B 20 January 1994

has mainly focussed on charged pions [7,10–15]. Inclusive production cross sections show a linear rise with the number of participant nucleons which is explained by pion production via $\Delta(1232)$ excitation in binary nucleon–nucleon collisions [10,11]. Pion spectra exhibit a steep fall as a function of the transverse momentum p_t with an increasing concavity for higher bombarding energies and larger masses of the collision system [12,15]. Various possible explanations for the concave shape of pion spectra like collective flow, directly produced pions or higher resonance contributions have been suggested [15]. Presently there is no convincing proof for any of these interpretations. The excitation of higher baryon resonances in heavy ion collisions has, however, been demonstrated by the observation of η-mesons [16] which arise predominantly from the decay of the $S_{11}(1535)$ resonance. Consequently, low lying baryon resonances as N(1440) and N(1520) are very likely also excited. A more refined analysis is required to establish their contributions to the pion spectra. Recent BUU-simulations [17] suggest that higher baryon resonances are populated in multi-step processes which become more important in very heavy collision systems. A characteristic feature would be a deviation from a linear dependence of the π-multiplicity on the number of participant nucleons for high transverse momenta.

Contrary to charged pions which can only be detected above a certain p_t-threshold the measurement of neutral mesons offers the advantage that they can be detected via their two-photon decay down to transverse momentum $p_t = 0$ MeV/c, moreover their spectra are not distorted by Coulomb effects. A large body of π^0-data exists only at bombarding energies below the production threshold in free nucleon–nucleon collisions (280 MeV) [18,19]. This has motivated a series of experiments at higher energies performed at the new heavy ion synchrotron SIS at Gesellschaft für Schwerionenforschung in Darmstadt. Part of this work has recently been published [16,8].

In the present paper we report on a first systematic study of π^0-production in three approximately mass-symmetric systems of different total mass (^{40}Ar+$^{\text{nat}}$Ca, ^{86}Kr+$^{\text{nat}}$Zr and ^{197}Au+^{197}Au) at the same incident energy of 1 A GeV. Pion production cross sections and transverse momentum spectra were determined. In addition to earlier charged pion measurements the mass dependence of neutral pion production was studied for the first time for different bins in transverse momentum. Such an analysis offers the opportunity to distinguish between various production mechanisms for pions of different energy.

The beam intensity was 10^5–10^6 particles per spill with a duty factor of $\approx$ (30–40)%. The targets corresponded to reaction probabilities of 3.9% (Ar+Ca) and 0.45% for the two heavier systems, respectively. The π^0-decay photons were detected with the photon spectrometer TAPS (Two Arm Photon Spectrometer) [20]. Charged particles escaping from the reaction zone at laboratory angles between 1° and 30° with respect to the beam were observed in the Forward Wall (FOPI) of the 4π detector system [21]. Only the total charged particle multiplicity measured in the polar angle range from 7°–30° has been used in the present analysis.

Table 1
Geometrical setups and detection efficiencies of the TAPS detector system in the different experiments. In the Au+Au experiment two different detector setups have been used in order to cover a larger kinematical range. Φ denotes the angle of the TAPS blocks with respect to the horizontal plane. d is the distance between the blocks and the target. The angle of the TAPS towers with respect to the beamline (Θ) has been adjusted to $\pm 52.0°$ in all experiments. $\epsilon_{\pi^0}^{\text{geo}}$ is the geometrical efficiency for pions emitted from an isotropic thermal source with temperatures T (T_1 and T_2 for the heavier systems) from table 2 while ϵ_{π^0} includes photon and π^0-reconstruction efficiencies. The error in the detection efficiencies arising from an uncertainty in the temperature parameters amounts to less than 5%.

Experiment	d (cm)	Φ (deg.)	$\epsilon_{\pi^0}^{\text{geo}}$	ϵ_{π^0}
^{40}Ar+$^{\text{nat}}$Ca	120	± 12.1	1.8×10^{-3}	3.5×10^{-4}
^{86}Kr+$^{\text{nat}}$Zr	160	$\pm 16.0/\pm 9.5$	7.4×10^{-4}	2.9×10^{-4}
^{197}Au+^{197}Au (A)	200	± 23.0	4.4×10^{-4}	2.2×10^{-4}
^{197}Au+^{197}Au (B)	200	± 7.3	2.5×10^{-4}	1.2×10^{-4}

Volume 321, number 1,2 PHYSICS LETTERS B 20 January 1994

TAPS is a modular detector system consisting of 256 BaF_2 detectors arranged in 4 identical blocks with individual Charged Particle Veto detectors (CPV) mounted in front of each module. The blocks were arranged in two movable towers positioned symmetrically with respect to the beam direction to detect pions emitted in the mid-rapidity region (y_{lab} = 0.52–0.84). Within each tower the blocks were positioned symmetrically with respect to the horizontal plane containing the beam axis. All geometrical settings are listed in table 1. The main trigger required two coincident photon candidates in TAPS corresponding to a minimum bias condition for pion detection.

Charged particles were discriminated by requiring an anti-coincidence between a BaF_2- and the corresponding CPV-module. Photons and hadrons were separated via pulse-shape and time-of-flight analysis. A linear energy calibration of the BaF_2-modules was based on the energy-loss signals deposited by cosmic muons (≈38 MeV). Photon energies deposited in adjacent modules were summed in order to reconstruct the electromagnetic shower. The point of impact was determined from the shower distribution using logarithmic energy weights [22].

Neutral pions were identified via their invariant mass deduced from the measured photon energies and angles with a resolution in $\Delta m(\mathrm{FWHM})/m \approx 15\%$. The combinatorial background from uncorrelated photon pairs was obtained by event mixing. This background, which can be determined with high statistical accuracy, was subtracted from the invariant mass and pion momentum distributions. In order to correct the measured distributions the acceptance of TAPS was simulated as a function of the pion transverse momentum p_t and the lab rapidity y using the detector-response package GEANT3 [23]. The resulting efficiencies are listed in table 1. The experimental transverse momentum resolution amounts to $\Delta p_t(\mathrm{FWHM})/p_t \approx (7\text{–}16)\%$ depending on the value of p_t.

All measured cross sections and multiplicities for neutral pions emitted at mid-rapidity are listed in table 2. In addition the results of an extrapolation to the full solid angle assuming an isotropic thermal source with the measured slope parameters (see below) are given. The inclusive pion cross section (see table 2) can be factorized [2]

$$\sigma_{\pi^0} = \sigma_R M_{\pi^0} = \sigma_R \langle A_{\mathrm{part}} \rangle_b P_{\pi^0} \qquad (1)$$

where σ_R denotes the reaction cross section, M_{π^0} defines the measured pion multiplicity per reaction, P_{π^0} is the pion production probability per participant nucleon and $\langle A_{\mathrm{part}} \rangle_b$ is the number of participant nucleons averaged over the impact parameter b taken from a geometrical model [24]. The derived values for P_{π^0} are $(3.0 \pm 0.3)\%$ for Ar+Ca, $(4.6 \pm 0.7)\%$ for Kr+Zr and $(3.7 \pm 0.4)\%$ for Au+Au. Although an additional systematic error of 30% has to be taken into account in the direct comparison of the three target–projectile combinations the pion production probability seems to be somewhat higher in the heavier systems. Because of pion absorption one would naively expect the opposite trend, i.e. P_{π^0} to decrease with increasing mass. The experimental result indicates that pion absorption is compensated or even overcompensated in the heavy systems by additional production mechanisms discussed below in an analysis of the differential pion multiplicity. Harris et al. [10,11] observed a linear increase of the π^- multiplicity with the number of participant nucleons within a given collision system corresponding to a constant pion emission probability

Table 2
Cross section σ_{π^0} and multiplicity per reaction M_{π^0} for neutral pions emitted at mid-rapidity (y_{lab} = 0.52–0.84). $\langle p_t \rangle$ and the fitted temperature parameters (T for one and T_1,T_2 for two-component fits) refer to the pion transverse momentum spectra. The results of an extrapolation to the full solid angle taking the experimental temperatures into account are also given.

System	In rapidity range Δy						Extrapolation to 4π	
	$\sigma_{\pi^0}^{\Delta y}$ (b)	$M_{\pi^0}^{\Delta y}$	$\langle p_t \rangle$ (MeV/c)	T (MeV)	T_1 (MeV)	T_2 (MeV)	σ_{π^0} (b)	M_{π^0}
Ar+Ca	0.31 ± 0.03	0.12 ± 0.01	198 ± 9	64 ± 1	–	–	1.5 ± 0.2	0.6 ± 0.1
Kr+Zr	2.1 ± 0.3	0.43 ± 0.06	183 ± 7	60 ± 1	48 ± 8	76 ± 10	9.4 ± 1.3	1.9 ± 0.3
Au+Au	6.5 ± 0.7	0.83 ± 0.08	180 ± 7	60 ± 3	38 ± 4	78 ± 4	28.0 ± 3.0	3.7 ± 0.4

Volume 321, number 1,2 PHYSICS LETTERS B 20 January 1994

per participant nucleon. Stock [7] interpreted this observation as evidence for a chemical equilibrium between Δ's and nucleons established via the ΔN ⇔ NN channel. The present result on neutral pions obtained in a comparison of different systems is consistent with these earlier observations and interpretation.

Fig. 1 shows the measured π^0-transverse momentum p_t distributions for pions emitted at mid-rapidity. The average transverse momentum decreases systematically with the mass of the collision system (see table 2). In case of the lightest system (Ar+Ca) the measured shape can be well described (dashed curve) with the distribution

$$\frac{1}{p_t}\frac{d\sigma}{dp_t} \propto m_t \exp(-m_t/T), \qquad (2)$$

where $m_t = \sqrt{p_t^2 + m_{\pi^0}^2}$ and T is a fit parameter [25]. Only at high p_t a slight enhancement is noticeable. In contrast, the reproduction of the spectra of the heavier systems (Kr+Zr and Au+Au) requires the assumption of two components with temperature parameters T_1 and T_2 (solid curves). The

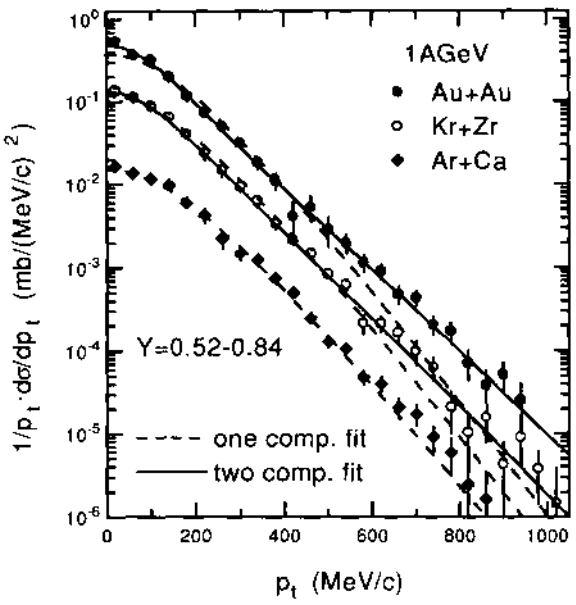

Fig. 1. Transverse momentum spectra for neutral pions at y = 0.52–0.84 measured for three systems with different total mass at a bombarding energy of 1 *A* GeV. The dashed and solid lines represent one- and two-component fits to the spectra, respectively, using eq. (2) (parameters see table 2).

difference in the temperature parameters increases with the total mass of the collision system, reflecting an increasing concavity of the spectral shape. All fit results are summarized in table 2.

In an attempt to identify possible contributions of higher baryon resonances to the spectra the differential pion multiplicity dM_π/dM_{cha} has been determined for different bins in p_t (a–d) as a function of the charged-particle multiplicity M_{cha} observed in the FW. This dependence has been parametrized as $dM_{\pi^0}/dM_{cha} \sim M_{cha}^{\alpha}$ (fig. 2). Hereby, M_{cha} is taken as proportional to the number of participant nucleons A_{part} determined by the centrality of the reaction [6]. If pion production occurs in independent binary nucleon–nucleon collisions a linear dependence on the number of participant nucleons is expected ($\alpha = 1$). In the lightest system (Ar+Ca) the exponent α does not depend on the pion momentum. In contrast to [10,11], we observe a steeper increase of the pion multiplicity for high energetic pions ($p_t >$ 600 MeV/c) in the heavier systems. This behaviour indicates a different production process and might be related to higher-order (=multi-step) processes such as multiple collisions leading to the population of heavier resonances. Such processes may involve the excitation of a Δ-resonance in a first nucleon–nucleon collision followed by a collision of the Δ with a third nucleon in which the Δ-mass is exploited for the excitation of a higher lying resonance. Thereby the energy of 3 nucleons can be pooled to populate a heavier baryon resonance which subsequently decays into pions of higher energy, leading to the observed enhancement in pion spectra at high momenta. BUU calculations [26] also indicate that the high p_t part of the pion momentum spectra is enhanced by an increasing contribution of pions from N(1440) decays. The probability for two-step processes is proportional to the third power of the baryon density. Their observation is thus a signature for the high compression reached in heavy ion collisions. The multi-step reaction mechanism is expected to be more favored in heavier systems where the high baryon density is maintained over a longer time period [17]

The overall change of the spectral shape for the investigated systems is also reflected by the ratio of the transverse momentum distributions of the two heavier systems divided by that of the system Ar+Ca (fig. 3). Here, an enhancement at low *and* high transverse mo-

Volume 321, number 1,2 PHYSICS LETTERS B 20 January 1994

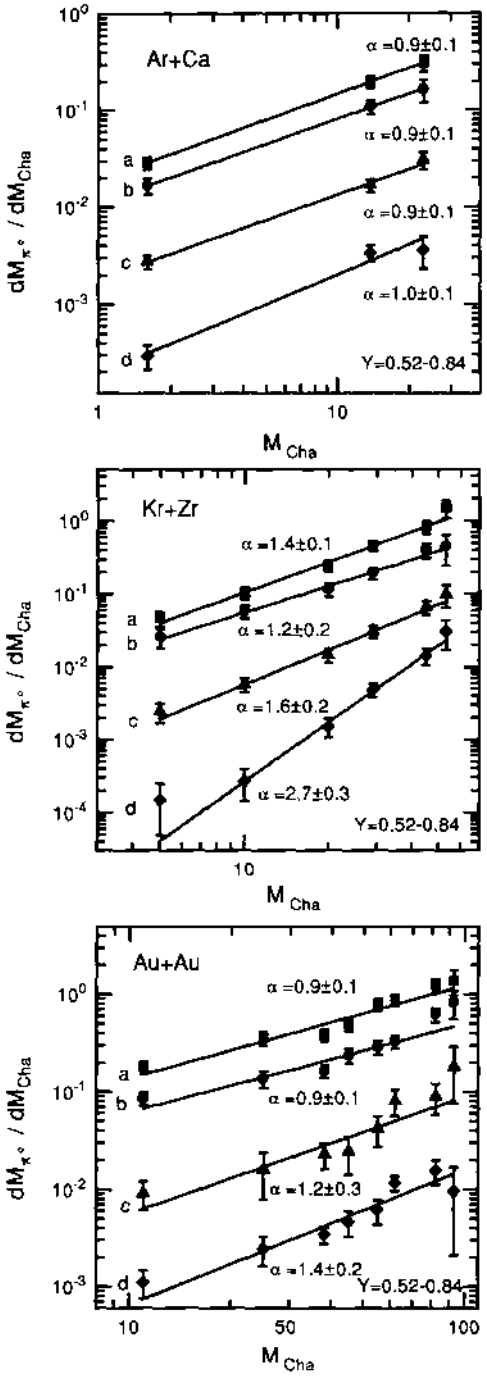

Fig. 2. Differential π^0 multiplicity per reaction for the three systems as a function of the charged particle multiplicity in the FW for different bins in p_t: 0–200 MeV/c (a), 200–400 MeV/c (b), 400–600 MeV/c (c) and 600–800 MeV/c (d).

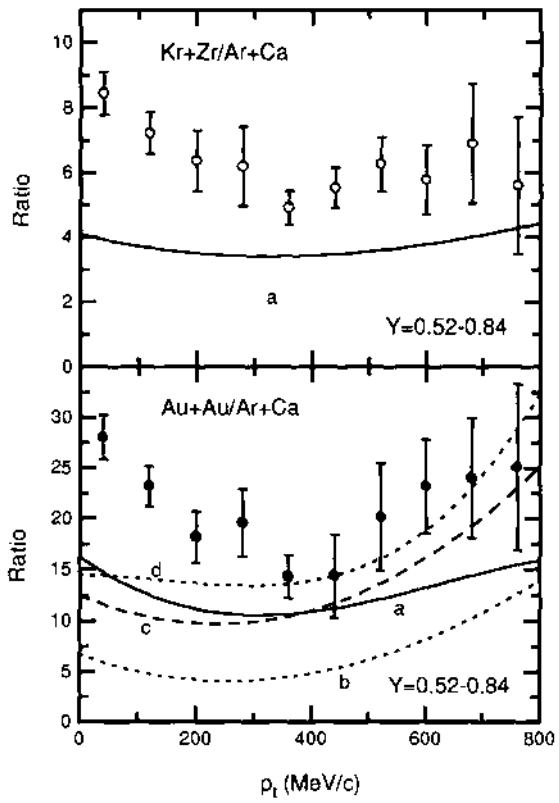

Fig. 3. Ratio of the measured transverse momentum spectra of the two heavy systems relative to the spectrum of the system Ar+Ca. For comparison the results of various theoretical calculations are shown (a: BUU [26], b: IQMD [27], c: RQMD [28], d: Cascade based on QGSM [29]).

menta is observed. For comparison, the results of various theoretical calculations are included, made available to us for the relevant rapidity ranges. Obviously, the mass dependence cannot be reproduced by any of these models. This is mainly caused by an overestimation of the cross section for light systems. Furthermore the spectral shape is not described quantitatively, in particular in the low p_t part which is underestimated for all systems. Models which include heavier baryon resonances but not the mean field (RQMD [28], QGSM [29]) predict an increase in the region above the free nucleon–nucleon kinematical limit where multiple collisions become important, in agreement with the observation. At low transverse momenta a large discrepancy between experiment and all models is found. This low-p_t enhancement of pion spectra, now established down to transverse momenta

$p_t = 0$, is still not quantitatively understood in current transport model calculations. At these pion energies a quantal description of meson propagation may be needed and/or medium effects may have to be included as proposed in [30]. It appears that current theoretical treatments are still lacking essential ingredients. Moreover, improved calculations will have to include a proper momentum dependence of pion-absorption and rescattering. Pion absorption requires at least two correlated nucleons and is thus very sensitive to the baryon density and its rapid variation in the expansion phase of the heavy ion collision. A satisfactory understanding of pion spectra will consequently require a simultaneous and consistent description of particle production data as well as nucleon and fragment emission patterns.

In conclusion, a first systematic study of the mass dependence of π^0 production at 1 A GeV projectile energy has been reported. The pion spectra exhibit an increasing concavity with the total mass of the colliding system. The mass dependence of high energy pions shows a deviation from a purely linear behaviour which is attributed to higher-order processes like multiple collisions leading to an increased population of higher baryon resonances. There is no generally accepted explanation for the enhanced π^0-yield at low transverse momenta. None of the presently available theoretical descriptions reproduces the mass dependence of pion production quantitatively, emphasizing the need for more refined calculations.

Acknowledgement

We would like to thank the accelerator crew at GSI for the stable beams. Excellent targets were provided by H. Folger and the GSI target laboratory staff. Illuminating discussions with W. Ehehalt, W. Cassing and U. Mosel are highly appreciated. We are grateful to S. Bass, C. Hartnack, and V. Toneev for communicating their calculations prior to publication. This work was in part supported by GSI under contract GI Met K, by BMFT under contract 06 GI 174 I, and by the Stichting voor Fundamental Onderzoek der Materie (FOM).

References

[1] J. Aichelin, Phys. Rep. 202 (1991) 233.
[2] W. Cassing, V. Metag, U. Mosel, K. Niita, Phys. Rep. 188 (1990) 363.
[3] U. Mosel, Ann. Rev. Nucl. Part. Sci. 41 (1991) 29.
[4] H.A. Gustafsson et al., Phys. Rev. Lett. 52 (1984) 1590.
[5] H.H. Gutbrod, Phys. Rev. C 42 (1990) 640.
[6] S.C. Jeong et al., submitted to Phys. Rev. Lett.
[7] R. Stock, Phys. Rep. 135 (1986) 259, and references therein.
[8] L. Venema et al., Phys. Rev. Lett. 71 (1993) 835.
[9] D. Brill et al., Phys. Rev. Lett. 71 (1993) 336.
[10] J.W. Harris et al., Phys. Lett. B 153 (1985) 377.
[11] J.W. Harris et al., Phys. Rev. Lett. 58 (1987) 463.
[12] G. Odyniec et al., in Proceedings of the 8th High Energy Heavy Ion Study (Berkeley, 1987).
[13] S. Hayashi et al., Phys. Rev. C 38 (1988) 1229.
[14] J. Gosset et al., Phys. Rev. Lett. 62 (1989) 1251.
[15] R. Brockmann et al., Phys. Rev. Lett. 53 (1984) 2012.
[16] F.D. Berg et al., Z. Phys. A 340 (1991) 297.
[17] W. Ehehalt et al., Phys. Rev. C 47 (1993) 2467.
[18] P. Braun-Munzinger and J. Stachel, Ann. Rev. Nucl. Part. Sci. 37 (1987) 1, and references therein.
[19] R.S. Mayer et al., Phys. Rev. Lett. 70 (1993) 904.
[20] R. Novotny, IEEE Trans. Nucl. Sci. 38 (1991) 379.
[21] A. Gobbi et al., Nucl. Instr. Methods A 324 (1993) 156.
[22] T.C. Awes et al., Nucl. Instr. Methods A 311 (1992) 130.
[23] R. Brun et al., GEANT3 User's Guide, CERN DD/EE/84-1 (1987).
[24] J. Cugnon et al., Nucl. Phys. A 360 (1981) 444.
[25] J. Stachel and G.R. Young, Ann. Rev. Nucl. Part. Sci. 42 (1992) 537.
[26] W. Ehehalt, private communication. The code is described in G. Wolf, W. Cassing and U. Mosel, Nucl. Phys. A 552 (1993) 549.
[27] S. Bass and C. Hartnack, contribution to the Workshop on Meson Production in Nuclear Collisions (GSI Darmstadt, 1993).
[28] H. Sorge, H. Stöcker, W. Greiner, Ann. Phys. 192 (1989) 266.
[29] N.S. Amelin et al., Sov. J. Nucl. Phys. 52 (1990) 172.
[30] L. Xiong, C.M. Ko and V. Koch, Phys. Rev. C 47 (1993) 788.

3.3.1 Citations

1. Knoll, J *Continuous decoupling of dynamically expanding systems* Nuclear Physics **A**, 821: 235-250 APR 15 2009
2. Norbury, JW *Pion cross section parametrizations for intermediate energy, nucleus-nucleus collisions* Physical Review C, 79 (3): Art. No. 037901 MAR 2009.
3. Norbury, JW; Townsend, LW *Parameterized total cross sections for pion production in nuclear collisions* . Nuclear Instruments & Methods in Physics Research Section **B**-Beam Interactions with Materials and Atoms, 254 (2): 187-192 Jan 2007.
4. Reisdorf, W; Stockmeier, M; Andronic, A; Benabderrahmane, ML; Hartmann, ON; Herrmann, N; Hildenbrand, KD; Kim, YJ; Kis, M; Koczon, P; Kress, T; Leifels, Y; Lopez, X; Merschmeyer, M; Schuttauf, A; Barret, V; Basrak, Z; Bastid, N; Caplar, R; Crochet, P; Dupieux, P; Dzelalija, M; Fodor, Z; Grishkin, Y; Hong, B; Kang, TI; Kecskemeti, J; Kirejczyk, M; Korolija, M; Kotte, R; Lebedev, A; Matulewicz, T; Neubert, W; Petrovici, M; Rami, F; Ryu, MS; Seres, Z; Sikora, B; Sim, KS; Simion, V; Siwek-Wilczynska, K; Smolyankin, V; Stoicea, G; Tyminski, Z; Wisniewski, K; Wohlfarth, D; Xiao, ZG; Xu, HS; Yushmanov, I; Zhilin, A *Systematics of pion emission in heavy ion collisions in the 1 A GeV regime* . Nuclear Physics **A**, 781 (3-4): 459-508 Jan 15 2007.
5. Saeed-Uddin; Akhtar, N; Ali, M *Pion production and collective flow effects in intermediate energy nucleus-nucleus collisions* . International Journal of Modern Physics **A**, 21 (7): 1471-1491 Mar 20 2006.
6. Liu, W; Ko, CM; Chen, LW *Eta absorption by mesons* . Nuclear Physics **A**, 765 (3-4): 401-425 Feb 6 2006.
7. Fuchs, C *Kaon production in heavy ion reactions at intermediate energies* .Progress in Particle and Nuclear Physics, Vol 56, No 1, 56 (1): 1-103 2006.
8. Hong, B; Kim, YJ; Herrmann, N; Stockmeier, MR; Andronic, A; Barret, V; Basrak, Z; Bastid, N; Benabderrahmane, ML; Caplar, R; Crochet, P; Dupieux, P; Dzelalija, M; Fodor, Z; Gobbi, A; Grishkin, Y; Hartmann, ON; Hildenbrand, KD; Kecskemeti, J; Kirejczyk, M; Koczon, P; Korolija, M; Kotte, R; Kress, T; Lebedev, A; Leifels, Y; Lopez, X; Mangiarotti, A; Merschmeyer, M; Neubert, W; Pelte, D; Petrovici, M; Rami, F; Reisdorf, W; Schuttauf, A; Seres, Z; Sikora, B; Sim, KS; Simion, V; Siwek-Wilczynska, K; Smolyankin, V; Stoicea, G; Tyminski, Z; Wagner, P; Wisniewski, K; Wohlfarth, D; Xiao, ZG; Yushmanov, I; Zhilin, A (FOPI Collaboration) *Charged pion production in Ru-96(44)+Ru-96(44) collisions at 400A and 1528A MeV* . Physical Review **C**, 71 (3): Art. No. 034902 Mar 2005.

   Klay, JL; Ajitanand, NN; Alexander, JM; Anderson, MG; Best, D; Brady, FP; Case, T; Caskey, W; Cebra, D; Chance, JL; Chung, P; Cole, B; Crowe, K; Das, AC; Draper, JE; Gilkes, ML; Gushue, S; Heffner, M; Hirsch, AS; Hjort, EL; Huo, L; Justice, M; Kaplan, M; Keane, D; Kintner, JC; Krofcheck, D; Lacey, RA; Lauret, J; Law, C; Lisa, MA; Liu, H; Liu, YM; McGrath, R; Milosevich, Z; Odyniec, G; Olson, DL; Panitkin, SY; Pinkenburg, C; Porile, NT; Rai, G; Ritter, HG; Romero, JL; Scharenberg, R; Srivastava, B; Stone, NTB; Symons, TJM; Wang, S; Wells, R; Whitfield, J; Wienold, T; Witt, R; Wood, L; Zhang, WN *Charged pion production in 2A to 8A GeV central Au plus Au collisions* . Physical Review **C**, 68 (5): Art. No. 054905 Nov 2003.
9. Larionov, AB; Mosel, U *Off-shell pions in Boltzmann-Uehling-Uhlenbeck transport theory* . Physical Review **C**, 66 (3): Art. No. 034902 Sep 2002.
10. Larionov, AB; Cassing, W; Leupold, S; Mosel, U *Quenching of resonance production in heavy-ion collisions at 1-2 A GeV* . Nuclear Physics **A**, 696 (3-4): 747-760 Dec 31 2001.
11. Senger, P; Strobele, H *Hadronic particle production in nucleus-nucleus collisions* Journal of Physics **G**-Nuclear and Particle Physics, 25 (5): R59-R131 May 1999.
12. Mao, GJ; Neise, L; Stocker, H; Greiner, W *Relativistic quantum transport theory of hadronic matter: The coupled nucleon, Delta, and pion system* . Physical Review **C**, 59 (3): 1674-1699 Mar 1999.

13. Cassing, W; Bratkovskaya, EL *Hadronic and electromagnetic probes of hot and dense nuclear matter* . Physics Reports-Review Section of Physics Letters, 308 (2-3): 65-233 Jan 1999.
14. Cassing, W *Meson production and meson properties at finite nuclear density* . Acta Physica Polonica **B**, 29 (11): 3175-3183 Nov 1998.
15. Helgesson, J; Randrup, J *Transport simulations with pi and Delta in-medium properties* . Physics Letters **B**, 439 (3-4): 243-250 Nov 5 1998.
16. Weinhold, W; Friman, B; Norenberg, W *Thermodynamics of Delta resonances* Physics Letters **B**, 433 (3-4): 236-242 Aug 13 1998.
17. Bass, SA; Belkacem, M; Bleicher, M; Brandstetter, M; Bravina, L; Ernst, C; Gerland, L; Hofmann, M; Hofmann, S; Konopka, J; Mao, G; Neise, L; Soff, S; Spieles, C; Weber, H; Winckelmann, LA; Stocker, H; Greiner, W; Hartnack, C; Aichelin, J; Amelin, N *Microscopic models for ultrarelativistic heavy ion collisions* . Progress in Particle and Nuclear Physics, Vol 41, 41: 255-369 1998.
18. Bratkovskaya, EL; Cassing, W; Rapp, R; Wambach, J *Dilepton production and m(T)-scaling at BEVALAC/SIS energies* . Nuclear Physics **A**, 634 (1-2): 168-189 May 4 1998.
19. Bratkovskaya, EL; Cassing, W; Mosel, U *Meson m(T)-scaling in heavy-ion collisions at SIS energies* . Physics Letters **B**, 424 (3-4): 244-252 Apr 9 1998.
20. Wagner, A; Muntz, C; Oeschler, H; Sturm, C; Barth, R; Cieslak, M; Dcebowski, M; Grosse, E; Koczon, P; Mang, M; Miskowiec, D; Schicker, R; Schwab, E; Senger, P; Beckerle, P; Brill, D; Shin, Y; Strobele, H; Walus, W; Kohlmeyer, B; Puhlhofer, F; Speer, J; Volkel, K *Evidence for different freeze-out radii of high-and low-energy pions emitted in Au+Au collisions at 1 A center dot GeV* . Physics Letters **B**, 420 (1-2): 20-24 Feb 19 1998.
21. Maheswari, VSU; Fuchs, C; Faessler, A; Sehn, L; Kosov, DS; Wang, Z *In-medium dependence and Coulomb effects of the pion production in heavy ion collisions* . Nuclear Physics **A**, 628 (4): 669-685 Jan 26 1998.
22. Senger, P *Meson production in dense nuclear matter* . Acta Physica Polonica **B**, 29 (1-2): 273-288 Jan-Feb 1998.
23. Fuchs, C; Essler, P; Gaitanos, T; Wolter, HH *Temperature and thermodynamic instabilities in heavy-ion collisions* Nuclear Physics **A**, 626 (4): 987-998 Dec 1 1997.
24. Pelte, D; Eskef, M; Goebels, G; Hafele, E; Herrmann, N; Korolija, M; Merlitz, H; Mohren, S; Trzaska, M; Alard, JP; Amouroux, V; Andronic, A; Basrak, Z; Bastid, N; Belyaev, I; Best, D; Biegansky, J; Buta, A; Claplar, R; Cindro, N; Coffin, JP; Crochet, P; Dupieux, P; Dzelalija, M; Ero, J; Fintz, P; Fodor, Z; GenouxLubain, A; Gobbi, A; Guillaume, G; Hildenbrand, KD; Hong, B; Jundt, F; Kecskemeti, J; Kirejczyk, M; Koncz, P; Korchagin, Y; Kotte, R; Kuhn, C; Lambrecht, D; Lebedev, A; Legrand, I; Leifels, Y; Manko, V; Mosner, J; Moisa, D; Neubert, W; Petrovici, M; Pinkenburg, C; Pras, P; Rami, F; Ramillien, V; Reisdorf, W; Ritman, JL; Roy, C; Schull, D; Seres, Z; Sikora, B; Simion, V; SiwekWilczynska, K; Smolyankin, V; Sodan, U; Vasiliev, MA; Wagner, P; Wang, GS; Wienold, T; Wohlfarth, D; Zhilin, A *Charged pions from Ni on Ni collisions between 1 and 2 AGeV* . Zeitschrift fur Physik **A**-Hadrons And Nuclei, 359 (1): 55-64 Sep 1997.
25. Porter, RJ; Beedoe, S; Bossingham, R; Bougteb, M; Christie, WB; Carroll, J; Gong, WG; Hallman, T; Heilbronn, L; Huang, HZ; Igo, G; Kirk, P; Krebs, G; LetessierSelvon, A; Madansky, L; Manso, F; Matis, HS; Miller, J; Naudet, C; Prunet, M; Roche, G; Schroeder, LS; Seidl, P; Wang, ZF; Welsh, RC; Wilson, WK; Yegneswaran, A *Dielectron cross section measurements in nucleus-nucleus reactions at 1.0A GeV* . Physical Review Letters, 79 (7): 1229-1232 Aug 18 1997.
26. Muntz, C; Baltes, P; Oeschler, H; Sartorius, C; Sturm, C; Wagner, A; Bormann, C; Brill, D; Shin, Y; Stein, J; Strobele, H; Ahner, W; Barth, R; Cieslak, M; Debowski, M; Grosse, E; Henning, W; Koczon, P; Mang, M; Miskowiec, D; Schicker, R; Senger, P; Kohlmeyer, B; Poppl, H; Puhlhofer, F; Speer, J; Volkel, K; Walus, W *Pion production in mass-symmetric heavy ion collisions at 0.8-1.8 AGeV* . Zeitschrift fur Physik **A**-Hadrons And Nuclei, 357 (4): 399-409 May 1997.
27. Pelte, D; Hafele, E; Best, D; Goebels, G; Herrmann, N; Pinkenburg, C; Reisdorf, W; Trzaska, M; Alard, JP; Amouroux, V; Andronic, A; Basrak, Z; Bastid, N; Belyaev, I; Biegansky, J; Buta, A; Caplar, R; Cindro, N; Coffin, JP; Crochet, P; Dupieux, P; Dzelalija, M; Ero, J; Eskel, M; Fintz, P; Fodor, Z; GenouxLubain, A; Gobbi, A; Guillaume, G; Hildenbrand, KD; Hong,

B; Jundt, F; Kecskemeti, J; Kirejczyk, M; Koncz, P; Korolija, M; Korchagin, Y; Kotte, R; Kuhn, C; Lambrecht, D; Lebedev, A; Legrand, I; Leifels, Y; Manko, V; Merlitz, H; Mosner, J; Mohren, S; Moisa, D; Neubert, W; Petrovici, M; Pras, P; Rami, F; Ramillien, V; Ritman, JL; Roy, C; Schull, D; Seres, Z; Sikora, B; Simion, V; SiwekWilczynska, K; Smolyankin, V; Sodan, U; Vasiliev, MA; Wagner, P; Wang, GS; Wienold, T; Wohlfarth, D; Zhilin, A *Charged pion production in Au on Au collisions at 1 AGeV* . Zeitschrift fur Physik **A**-Hadrons And Nuclei, 357 (2): 215-234 Mar 1997.

28. Teis, S; Cassing, W; Effenberger, M; Hombach, A; Mosel, U; Wolf, G *Pion-production in heavy-ion collisions at SIS energies.* Zeitschrift fur Physik **A**-Hadrons And Nuclei, 356 (4): 421-435 Jan 1997.
29. Zipprich, J; Fuchs, C; Lehmann, E; Sehn, L; Huang, SW; Faessler, A *Influence of the pion-nucleon interaction on the collective pion flow in heavy ion reactions* . Journal of Physics **G**-Nuclear and Particle Physics, 23 (1): L1-L6 Jan 1997.
30. Chu, ZL; Zheng, YM; Wang, F; Sa, BH; Lu, ZD *Unified dynamical simulation of kaon and pion production in heavy ion collisions* . High Energy Physics & Nuclear Physics-English Edition, 20 (2): 155-164 1996.
31. Fuchs, C; Sehn, L; Lehmann, E; Zipprich, J; Faessler, A *Influence of the in-medium pion dispersion relation in heavy ion collisions* . Physical Review **C**, 55 (1): 411-418 Jan 1997.
32. Wagner, A; Barth, R; Beckerle, P; Brill, D; Cieslak, M; Debowski, M; Grosse, E; Henning, W; Koczon, P; Kohlmeyer, B; Laue, F; Mang, M; Miskowiec, D; Muntz, C; Prokopowicz, W; Puhlhofer, F; Oeschler, H; Schwab, E; Senger, P; Shin, Y; Speer, J; Stock, R; Strobele, H; Sturm, C; Volkel, K; Walus, W; Yoo, IK *On the size of the pion emitting source in heavy ion collisions at 1 AGeV.* Acta Physica Polonica **B**, 27 (11): 3081-3086 Nov 1996.
33. Zheng, YM; Chu, ZL *Pion and kaon production in heavy-ion reactions at 1 GeV/nucleon* . Chinese Physics Letters, 13 (10): 730-733 1996.
34. Ko, CM; Li, GQ *Medium effects in high energy heavy-ion collisions* . Journal of Physics **G**-Nuclear and Particle Physics, 22 (12): 1673-1725 Dec 1996.
35. Russkikh, VN; Ivanov, YB *Collective Flow of Pions In Relativistic Heavy-Ion Collisions* . Nuclear Physics **A**, 591 (4): 699-710 Sep 4 1995.
36. Muntz, C; Baltes, P; Oeschler, H; Sartorius, A; Wagner, A; Ahner, W; Barth, R; Cieslak, M; Debowski, M; Grosse, E; Henning, W; Koczon, P; Miskowiec, D; Schicker, R; Senger, P; Bormann, C; Brill, D; Shin, Y; Stein, J; Stock, R; Strobele, H; Kohlmeyer, B; Poppl, H; Puhlhofer, F; Speer, J; Volkel, K; Walus, W *Properties of High-Energy Pions Emitted from Heavy-Ion Collisions at 1 GeV/Nucleon* . Zeitschrift fur Physik **A**-Hadrons And Nuclei, 352 (2): 175-179 Jul 1995.
37. Ko, CM; Li, GQ *Hadrons In Dense Matter* . Nuclear Physics **A**, 583: C591-C598 Feb 6 1995.
38. Bass, SA; Hartnack, C; Stocker, H; Greiner, W *Azimuthal Correlations of Pions in Relativistic Heavy-Ion Collisions at 1 Gev/Nucleon* . Physical Review **C**, 51 (6): 3343-3356 Jun 1995.
39. Li, GQ; Ko, CM *Enhancement of Low-M(T) Kaons in Heavy-Ion Collisions at AGS Energies* Physics Letters **B**, 351 (1-3): 37-42 May 25 1995.
40. Bass, SA; Hartnack, C; Stocker, H; Greiner, W *High Pt Pions as Probes of the Dense Phase of Relativistic Heavy-Ion Collisions* . Physical Review **C**, 50 (4): 2167-2172 Oct 1994.

3.4 Neutron Emission in Bi + Pb Collisions at 1GeV/u

3.4.1 Introductory notes

A novel phenomenological approach to subthreshold particle production was proposed in [R46]. Let us consider inclusive nuclear reaction $A+B \to C+X$, where X stands for all undetected particles. At high energies the invariant cross section for this reaction exhibits generally a smooth dependence on kinematical variables of particle C. This fact suggests that over a wide kinematical range, in particular near and beyond the free nucleon-nucleon kinematical limit, production of C can be interpreted as the scale-invariant threshold process when some part of the nucleus A interacts with other part of the nucleus B forming a cluster of minimal mass M. By introducing the fractions x_A and x_B of the colliding nuclei 4-momenta p_A and p_B the value of M can be found by minimizing $M^2 \equiv s = (x_A p_A + x_B p_B)^2$ under the additional energy-momentum conservation constraint:

$$(x_A p_A + x_B p_B - p_C)^2 = m_X^2. \tag{3.1}$$

Here $m_X^2 = (\sum_i p_i)^2$ is the invariant mass squared of the system X and p_C is the 4-momentum of particle C. Note that for M to be minimal m_X has to be minimal too. Hence the group X has to consist of the lightest particles compatible with the quantum number conservation needed to produce particle C which has to move with zero relative velocities.

$$min(m_C^2) = (x_a m_A + x_B m_B + M_{QN})^2 \tag{3.2}$$

where $m_{A,B}$ are the masses of colliding nuclei and M_{QN} is the total mass of particles needed for quantum number conservation. For example when particle C is nucleon $M_{QN} = -m_N$, when it is K^+ then $M_{QN} = m_{\Lambda^0} - m_N$ *etc.*

An explicit, though rather complicated, relation between x_A and x_B follows inserting (3.2) into (3.1). Equation $ds/dx_A = 0$ then leads to the 4-th order algebraic equation:

$$\begin{aligned} x_A(x_A-\mathcal{C})^3 m_A^2 \quad + \quad (x_A-\mathcal{C})^2(\mathcal{A}x_A-\mathcal{B})\mathcal{G} \quad + \\ x_A(x_A-\mathcal{C})(\mathcal{B}-\mathcal{A}\mathcal{C})\mathcal{G} \quad + \quad (\mathcal{A}x_A-\mathcal{B})(\mathcal{B}-\mathcal{A}\mathcal{C})m_B^2 \quad = \quad 0 \end{aligned} \tag{3.3}$$

Here $\mathcal{A}, \mathcal{B}, \mathcal{C}$ and $\mathcal{G}$ are known scalars constructed from p_A, p_B, p_C and M_{QN} [R46]. In particular $\mathcal{G} = p_A \cdot p_B$.

Solution of (3.3) can be used to construct $\sqrt{s_{min}} \equiv min\sqrt{s(x_A, x_B)}$ on which in addition to mass numbers A and B of colliding nuclei according to the self-similarity hypothesis [R46] the invariant spectrum for inclusive process $A+B \to C+X$ depends.

$$E\frac{d\sigma}{d^3p} \sim A_1^{\alpha_1(\xi_1)} A_2^{\alpha_2(\xi_2)} f(\Pi),\ \Pi \equiv \sqrt{s_{min}}/2m_N,\ \alpha_i = \frac{2}{3} + \frac{\xi_i}{3},\ \xi_i \equiv \frac{x_i m_i}{m_N},\ i = 1,2 \tag{3.4}$$

the new variables, when $\xi_1 > 1$ or $\xi_2 > 1$, formally define the subthreshold production. The fit to the experimental data at 9 GeV with function $f(\Pi) \sim exp(\Pi/\Pi_0)$ gave $\Pi_0 = 0.13$ for A+A subthreshold production in the projectile/target fragmentation region [R46] and $\Pi_0 = 0.16$ for p+p data [R47].

Numerical solution of (3.3) was used in [52] to interpret the neutron spectra from Bi+Pb collisions at 1 GeV/nucleon.

acta physica slovaca vol. 44 No. 1, 35 – 41 February 1994

NEUTRON EMISSION IN Bi + Pb COLLISIONS AT 1 GeV/u

M. Pachr, M. Šumbera, A. Kugler[1], V. Wagner

Nuclear Physics Institute, ASCR, 250 68 Řež, Czech Republic

S. Hlaváč[2,3], R.S. Simon

Gesellschaft für Schwerionenforschung, D-64220 Darmstadt, Germany

Received 26 November 1993, accepted 6. December 1993

We report energy spectra of neutrons originating from non-peripheral ^{209}Bi $+^{208}$Pb collisions at 1 GeV/u. A comparison of the spectra measured at three different polar laboratory angles (23.5°, 40° and 60°) shows that the observed emission pattern contradicts a picture where the neutrons are emitted from a single fireball. A unified description of all spectra (scaling) can be achieved under the assumption that the production cross section depends only on the minimum invariant mass necessary to emit the neutron.

I. Introduction

Subtreshold particle production in heavy ion collisions is generally accepted to provide important information about the collision dynamics. For nucleons which are already present in the collision system the equivalent process is the production of these particles with momenta beyond the free nucleon-nucleon kinematical limit. Since identification of minimum ionizing hydrogen isotopes is difficult experimentally, we investigate subtreshold neutron production where a time-of-flight (TOF) measurement is sufficient to determine both the particle type and its energy.

II. Experiment

The experiment was performed at the Heavy Ion Synchrotron SIS at GSI Darmstadt. A 1 GeV/u ^{209}Bi beam with an intensity of 3×10^6 particles per spill (spill duration 4s) was incident on a target tilted at 45° relative to the beam. A 420 mg/cm^2 isotopically enriched ^{208}Pb target was used. Neutrons were detected in a block of seven hexagonal BaF_2 scintillator modules (250 mm long, 59 mm diameter), equipped in front with

[1]e-mail address: KUGLER@VAX.UJF.CAS.CZ

[2]permanent address: Institute of Physics, Slovak Academy of Sciences, 842 28 Bratislava, Slovak Republic

[3]e-mail address: HLAVAC@V6000A.GSI.DE

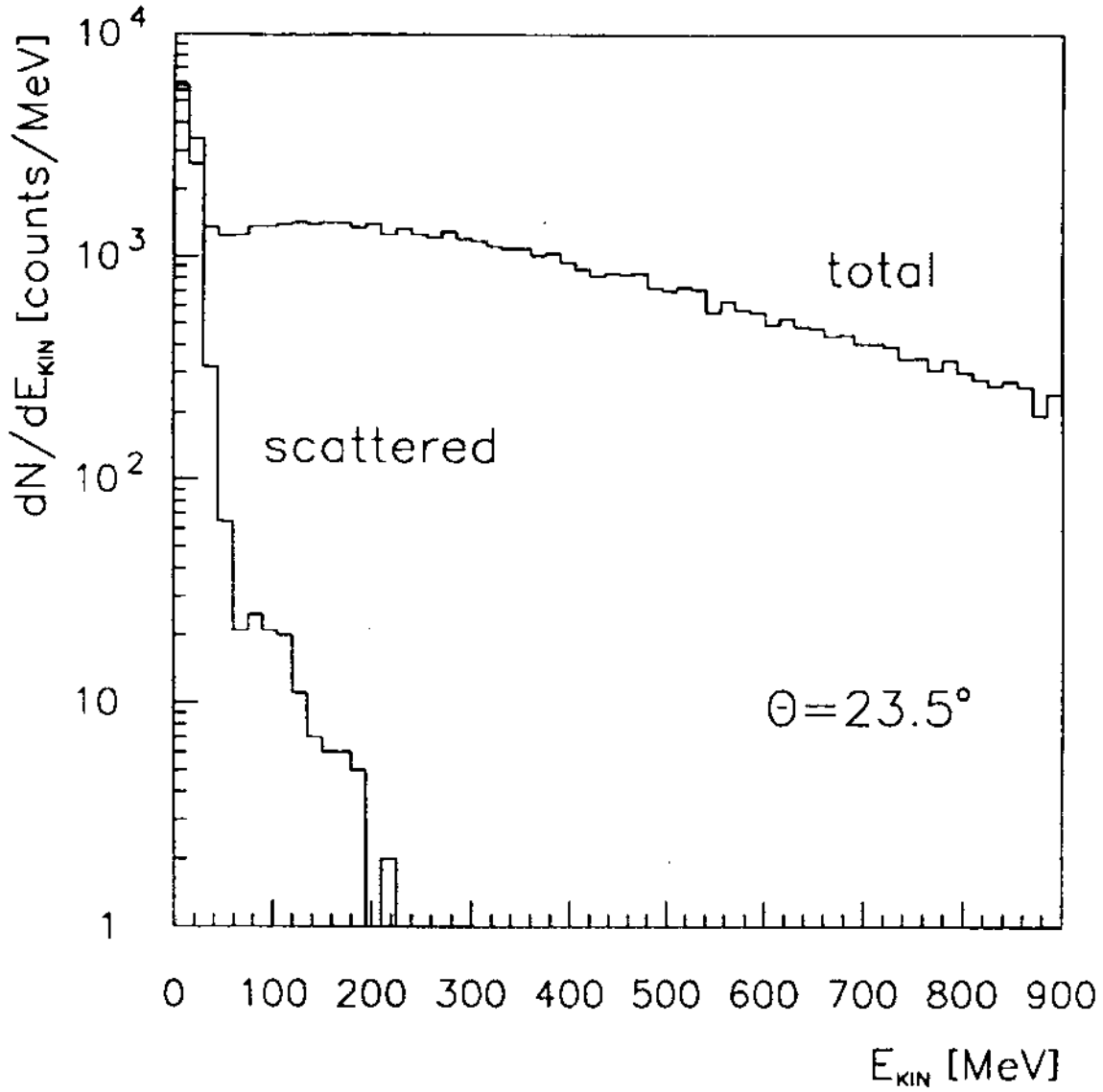

Fig. 1 Simulated kinetic energy spectra for direct and scattered neutrons. Input for the simulation is the neutron distribution of the Fig.2.

a common 10 mm thick plastic charged particle veto detector (CPV). The detector distance from the target was 4.3 m. The detector was placed at polar angles $\Theta = 23.5°$, $\Theta = 40°$ and $\Theta = 60°$, respectively.

The absence of a signal in the CPV allowed us to select neutral particles (neutrons and photons). The kinetic energy of the neutrons observed in the plastic-scintillator BaF_2 telescope was derived from their TOF. The achieved time resolution of photon peak of 360 ps allowed us to discriminate between the prompt photons and neutrons up to very high kinetic energies. For larger polar angles the photon intensity increases relative to the particle intensity. This restricts the maximum observable neutron energy to $E_{kin} < 2$ GeV, $E_{kin} < 1.5$ GeV and $E_{kin} < 1$ GeV for the detector positions at $\Theta = 23.5°$, $\Theta = 40°$ and $\Theta = 60°$, respectively.

Target and detector were positioned two meters above the floor of the experimen-

tal hall. At a target-detector distance of 4.3 m, the neutrons scattering off the floor therefore can still be discriminated against direct neutrons over a large range in neutron kinetic energy. Results of Monte Carlo simulations have shown that scattered neutrons have much longer flight paths and hence larger TOF values than direct ones of the same energy. Hence, scattered neutrons can only influence the low energy part of the data, see Fig.1. The shower of secondary particles generated by neutrons in BaF_2 depends on the neutron incident kinetic energy. Because the incident kinetic energy for scattered neutrons does not agree with the energy expected from their TOF, we can exploit the pulse shape information from BaF_2 to further discriminate against scattered neutrons. According to our simulations the background due to scattered neutrons is smaller than 1 % of the accepted events for neutron energies above 100 MeV.

The absolute efficiency of neutron detection in the BaF_2 modules was determined by comparison with that of a liquid NE213 scintillator. The NE213 efficiency is well described by the hadronic shower Monte Carlo program of Cecil et al. [1, 2]. The light-output threshold in BaF_2 was set to be equivalent to a photon energy of 7 MeV.

Events were recorded together with the charged particle multiplicity M_{ch} registered in the outer part of the forward wall (OFW) of the FOPI collaboration [3] which covers polar angles from 7° to 30°. The OFW multiplicity provides information on the centrality of the collision. The events were selected according to the condition that the total multiplicity of the charged fragments detected in the OFW was $M_{ch} \geq 60$. This multiplicity cut corresponds approximately to one half of the maximum measured M_{ch} and excludes peripheral events.

III. Results

Energy spectra of neutrons are shown on Figure 2. For all three angles the neutron spectra extend far beyond the phase space region which is kinematically accessible in free nucleon-nucleon scattering (E_{kin}^{NN} =775 MeV, 481 MeV and 179 MeV for Θ = 23.5°, 40° and 60°, respectively). Both Fermi motion and multiple scattering of the participants may be responsible for the production of neutrons with such high kinetic energies [4]. Especially the excitation of baryonic resonances and their subsequent decay seems to be an important process to achieve the highest particle momenta [4].

The relevance of these mechanisms could be tested within the framework of microscopic transport model calculations [5, 6]. Instead we perform a more phenomenological analysis of the spectra. First we assume that the observed particle originates from an equilibrated fireball. In a second scenario we weaken the assumption of equilibrium. In this picture the emission of the neutron proceeds in such a way that the number of participating nucleons needed to provide the neutron energy becomes minimal [7, 8].

3.1 Fireball

The data were fitted using the relativistic Boltzmann distribution [9]

$$E\frac{d^3\sigma}{d^3p} \sim m_t \cosh(y - y_{FB}) \exp\left\{-m_t \cosh(y - y_{FB})/T\right\}, \qquad (1)$$

where m_t and y are the neutron transverse mass and its rapidity, respectively, and y_{FB} is the rapidity of the fireball. T is the temperature parameter. The assumption that only one single fireball at mid-rapidity (i.e. $y_{FB} = y_{CMS}$) has been created leads to the following values of the temperature parameter: $T_{23.5°} = 97.5 \pm 0.3$ MeV, $T_{40°} = 80.2 \pm 1.0$ MeV, $T_{60°} = 81.5 \pm 0.5$ MeV. The large difference between the first and last two temperatures makes a unified description of all three data sets impossible. Furthermore, we see a deviation from a purely exponential shape for $\Theta = 40°$ and 60°, see Fig.2.

The hypothesis that the fireball rapidity may not coincide with y_{CMS} was also tested. The corresponding fits are shown by the dashed lines on Fig.2. The fireball rapidity y_{FB} is lower then y_{CMS} for all angles and decreases with increasing angle.

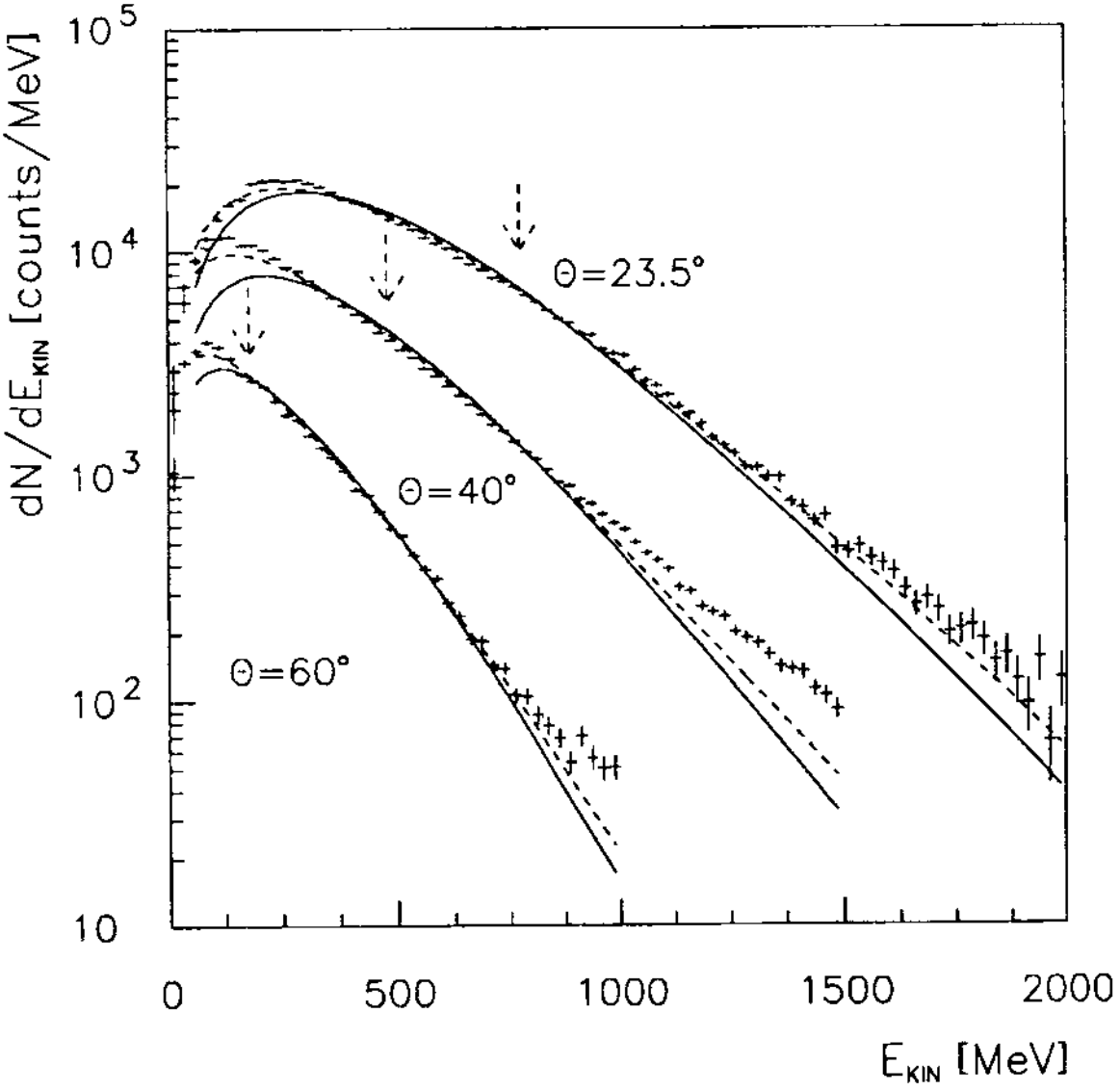

Fig. 2 The experimental energy neutron spectra (symbols) and their thermal fits for the rapidity of the fireball fixed at the value of CMS, $y_{FB} = y_{CMS}$ (full lines) and in the case if y_{FB} is treated as a free parameter (dashed lines).

3.2 Scaling

Consider the inclusive production of particle C in a nuclear reaction

$$A + B \longrightarrow C + X, \tag{2}$$

where X stands for the undetected particles. In this scenario the production of the particle C can be viewed as a process where a fraction of the nucleus A interacts with a fraction of the nucleus B forming a cluster with mass M. Provided the invariant cross section of the inclusive process (2), exhibits scale invariance the threshold for production of particle C with given 4-momentum p_C can be related to the fractions x_A and x_B of the target and the projectile nucleus 4-momenta P_A and P_B. Then the cluster invariant mass M can be written as

$$M = \sqrt{s} = \sqrt{(x_A P_A + x_B P_B)^2}. \tag{3}$$

The minimum value $\sqrt{s_{min}}$ can be determined from the 4-momentum conservation law

$$(x_A P_A + x_B P_B - p_C)^2 = M_{min}^2 \tag{4}$$

and the condition

$$\frac{ds}{dx_{A,B}} = 0. \tag{5}$$

The quantity M_{min} is the minimum value of the missing mass M_X of particle system X. Momentum conservation requires that the minimum of M_X is reached only when the relative velocities of all particles forming system X tend to zero. In this limit particle C is a product of a two-body decay. The value of $\sqrt{s_{min}}$ is a complex function of the 4-momentum p_C, see [7, 8].

By use of the dimensionless quantity $\Pi = \sqrt{s_{min}}/2m_N$ the invariant cross section for the inclusive reaction (2) acquires the scale invariant form:

$$E\frac{d^3\sigma}{d^3p} \sim f(\Pi) \tag{6}$$

Our data on $E\ d^3N/d^3p$ for the three polar angles as a function of the variable Π are plotted on Fig. 3. In the region of $0.8 \leq \Pi \leq 2.4$ the invariant cross section clearly exhibits scaling. The flow effect was observed by us in the same experiment [10]. Its magnitude is dependent on the rapidity of the neutron, therefore its influence on the data for the three polar angles is different. This fact can be the reason for the small scalling violation.

IV. Conclusions

We measured the inclusive neutron spectra in non-peripheral ^{209}Bi + ^{208}Pb collisions at 1 GeV/u close and above the free NN kinematical limit where multi-particle phenomena gain in importance. The simple picture of a single mid-rapidity Boltzmann source is not compatible with our data since it leads to an angle-dependent temperature.

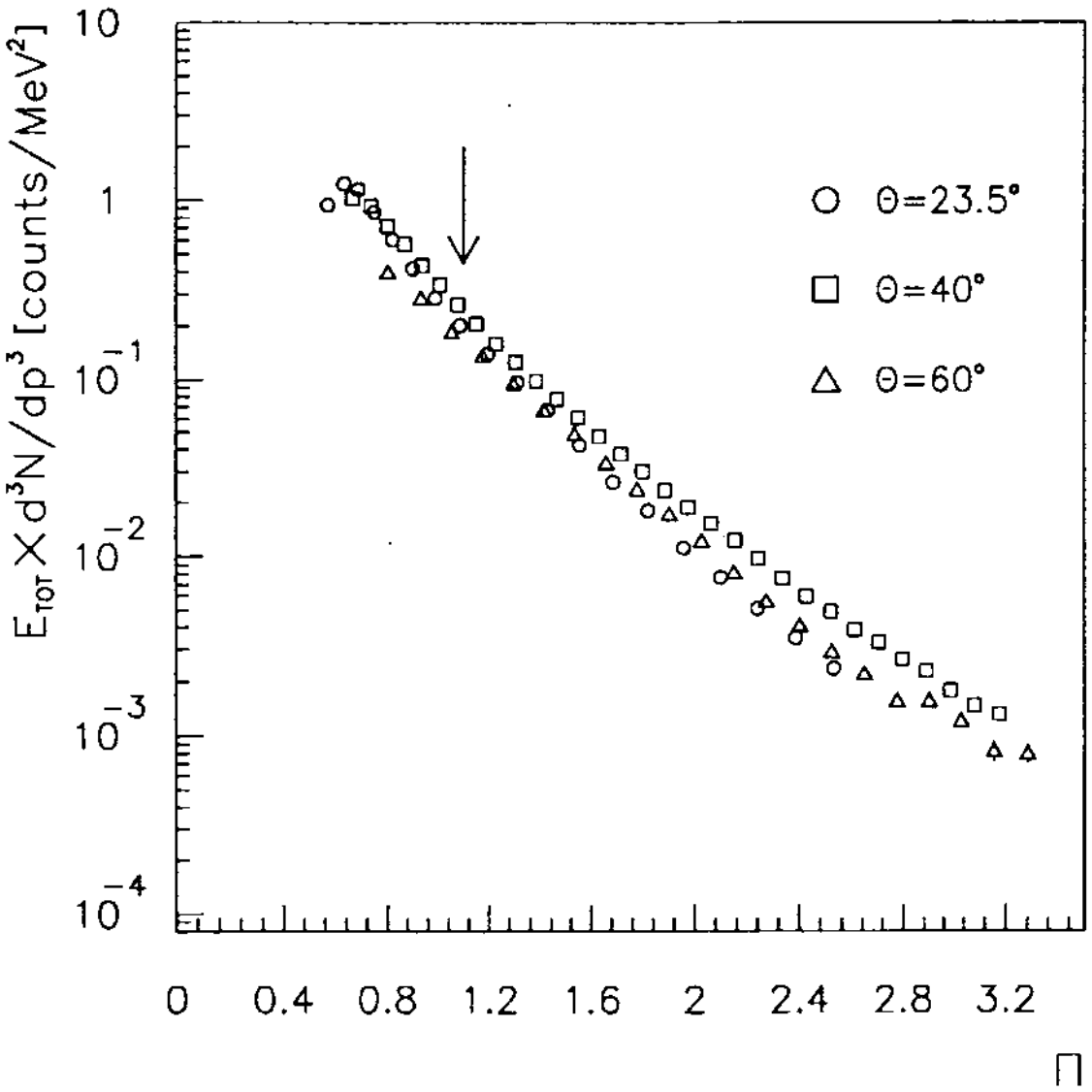

Fig. 3 The invariant cross section for neutron production in ^{209}Bi+^{208}Pb collisions at 1 GeV/u as a function of the scaling variable Π. The kinematical limit is indicated by the vertical arrow.

With the scale-invariant approach of Stavinsky [7] we achieve a good description of our data at all angles. An open question is whether the observed scaling also holds for more peripheral reactions and therefore would be true also for minimum bias data as originally suggested. Another question is how the scaling is related to the observed collective flow of nuclear matter.

Acknowledgement

We are grateful to the members of the FOPI and TAPS collaborations for their support during our experiment and for their permission to use the information from the forward wall for event characterization. This work was supported by the Academy of Sciences of the Czech Republic under contract No 14808.

References

[1] R.A. Cecil, et al.: *Nucl. Instr. and Meth.* **161** (1979), 439;

[2] A. Kugler, et al.: to be published in *Nucl. Instr. and Meth.*;

[3] A. Gobbi, et al.: *Nucl. Instr. and Meth.* **A324** (1993), 156;

[4] V.B. Kopeliovich: *Phys. Rep.* **139** (1986), 51;

[5] N.S. Amelin et al.: *Sov. J Nucl. Phys.* **51** (1990), 327;

[6] Aichelin, J.: *Phys. Rep.* **202** (191), 233;

[7] V.S. Stavinsky: *Proc. 9th Int. Seminar on High Energy Physics*, Vol. 1, JINR, D1, 2-88-6652, Dubna, p.190;

[8] A.A. Baldin: *Phys. At. Nucl.* **56** (1993), 385; Baldin, A.A.: *JINR Rapid Communications* No.3 [54]-92;

[9] E. Schnedermann, et al.: *NATO ASI Series B: Physics*, Vol. **303** Edited by H. H. Gutbrod and J. Rafelski p.175;

[10] A. Kugler, et al.: *Acta Physica Polonica* (1994), in press; A. Kugler, et al.: *GSI preprint* GSI-93-75 (1993);

NEUTRON EMISSION FROM Bi+Pb COLLISIONS AT 1 GeV/u *)

M. Pachr, A. Kugler, V. Wagner, M. Šumbera

Nuclear Physics Institute, Řež near Prague, Czech Republic

Yu. G. Sobolev

JINR, Dubna, Russia

R. S. Simon

GSI, Darmstadt, Germany

S. Hlaváč

Institute of Physics, Slovak Acad. Sci., Bratislava, Slovakia

Received 25 January 1995

The experimental study of the neutron emission from Bi+Pb collisions at 1 GeV/u was done using BaF_2 detector. The heavy-ion collision dynamics was investigated through genuine collective phenomena: nuclear flow effects and production of neutrons near and beyond free NN kinematical limit.

1 Experimental setup

The analyzed data were taken at experiments [1] performed on the Heavy Ion Synchrotron SIS at GSI Darmstadt during the TAPS runs in summer 1991. The 1 GeV/u ^{209}Bi beam and ^{208}Pb target were used. The main part of the used neutron detector (BAF) was formed by a block of seven hexagonal BaF_2 scintillator modules, each with the inscribed diameter of 59 mm and length of 250 mm. The BAF was equipped in front by a common charged particle veto (CPV) detector from 9 mm plastic scintillator. The data were recorded for polar angles (relative to the beam) $\theta = 23.5°$, $\theta = 40°$ and $\theta = 60°$. The individual positions were selected to cover projectile-like, center of mass and target like rapidity regions. The detector distance from the target was 4.3 m in all cases, the energy of neutrons was derived from their time of flight. The individual achieved energy resolution was $\sigma(E_n)/E_n \approx 2\%$ for neutrons with kinetic energy $E_n = 100$ MeV and increases up to 16% for neutrons with kinetic energy 2 GeV.

Hits in neutron detector were recorded together with the charged particle multiplicity M_{ch} in the outer part of the forward wall (OPW) of the FOPI collaboration [2]. The OPW covered polar angles from 7° to 30° and was divided into eight equal segments in azimuth. Thus OPW sector multiplicity provided information on the centrality of the collision and on the orientation of the reaction plane. Multiplicity values $M_{ch} = 3, 30, 60, 80$, which were chosen as points dividing the whole

*) Presented at the International School-Workshop "Relativistic Heavy-Ion Physics", Prague (Czech Republic), 19–23 September 1994.

multiplicity spectrum into several intervals, were using model predictions found as corresponding to average impact parameter values $\langle b \rangle \approx 12$, 10, 7, 5 fm, respectively. The accuracy of reaction plane determination method (described in Sect. 3) was tested according [12], i.e. dividing each event randomly into two subevents and then extracting corresponding azimuthal angles. The resolution of $\sigma = 314°$ was achieved in that way.

2 Energy spectra

Measured energy spectra of neutrons are illustrated for non-peripheral events in Figure 1.

Comparison with IQMD [3], QGSM [4,5] and BUU [6,7] model predictions shows that the data are described by all three models with the same quality. The shapes of neutron energy spectra are not sensitive enough to distinguish among various

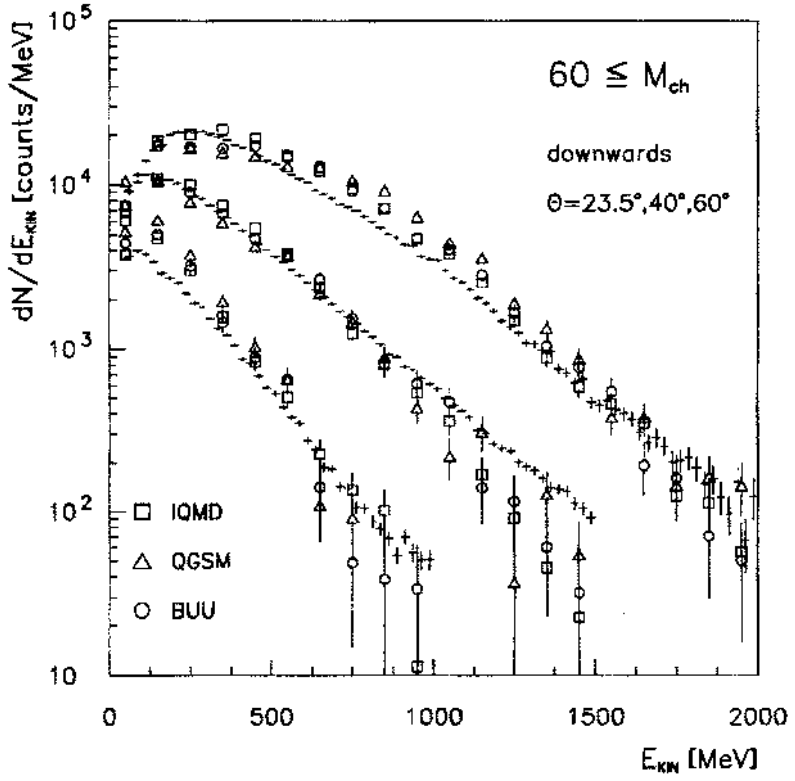

Fig. 1. The neutron energy spectra for non-peripheral events together with their model predictions. The theory results are normalized to the experimental data obtained at $\theta = 23.5°$ for each model independently.

reaction mechanisms implemented in tested models. To study simple principles roughly determining the shapes of spectra, two phenomenological approaches were applied.

In the first scenario it was assumed that observed particle comes from equilibrated fireball. The data plotted in Figure 2 were fitted using relativistic Boltzmann distribution [8] of the form

$$\frac{\mathrm{d}^3\sigma}{\mathrm{d}E\mathrm{d}\Omega} \sim pm_{\mathrm{T}}\cosh(y - y_{\mathrm{FB}})\mathrm{e}^{-m_{\mathrm{T}}\cosh(y-y_{\mathrm{FB}})/T}, \qquad (1)$$

where p, m_{T} and y are the particle momentum, transverse mass and rapidity, respectively, y_{FB} is rapidity of the fireball and T is its Boltzmann 'temperature' parameter.

To fit the data it is clearly necessary to use angle-dependent temperature parameter. This fact however contradicts the basic assumption of simple thermalized fireball. Furthermore, the spectra are well described in their middle parts only. The more parameters fit allowing fireball rapidity to be a free parameter was tested as

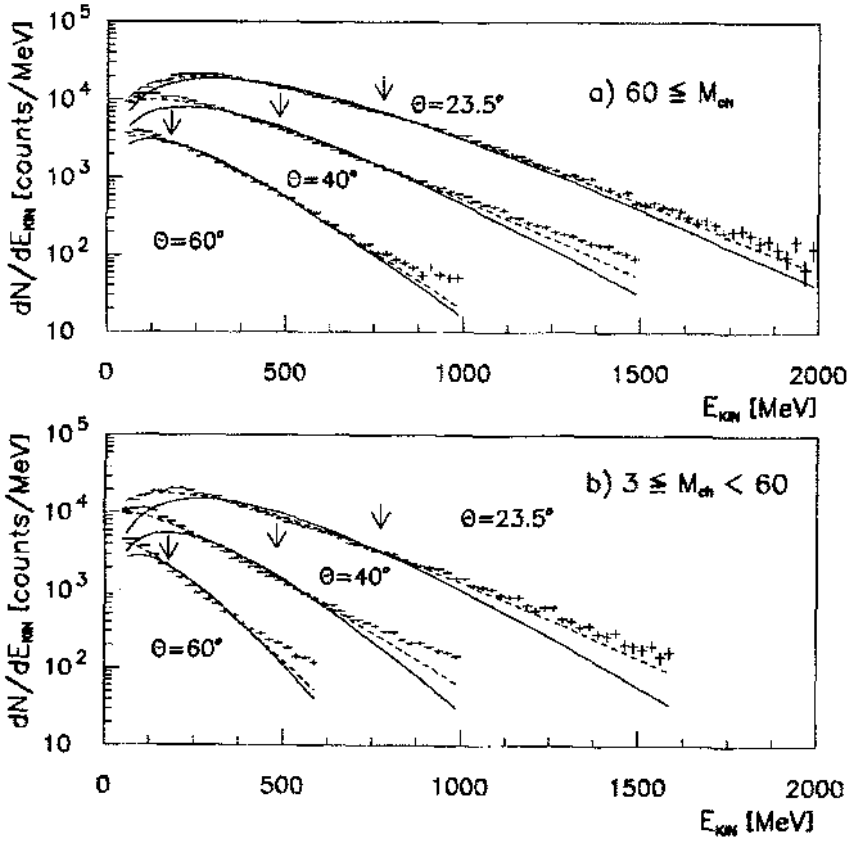

Fig. 2. The energy neutron spectra and their thermal fits for a) non-peripheral and b) peripheral events. The kinematical limits for N coming from the free NN collision are indicated by arrows for individual detector positions. The full lines correspond to a Boltzmann fireball fit with fixed fireball rapidity $y_{\mathrm{FB}} = y_{\mathrm{CMS}} = 0.68$ and fitted values of temperature parameter $T^{\mathrm{per}} = 75$, 61, 60 MeV and $T^{\mathrm{nonper}} = 98$, 97, 93 MeV for $\theta = 23.5$, 40, 60°, respectively. The averaged normalized χ^2 of the fit is 3.3 and 2.2 in the case of peripheral and non-peripheral spectra respectively. The dotted line correspond to the fit with y_{FB} being a free parameter.

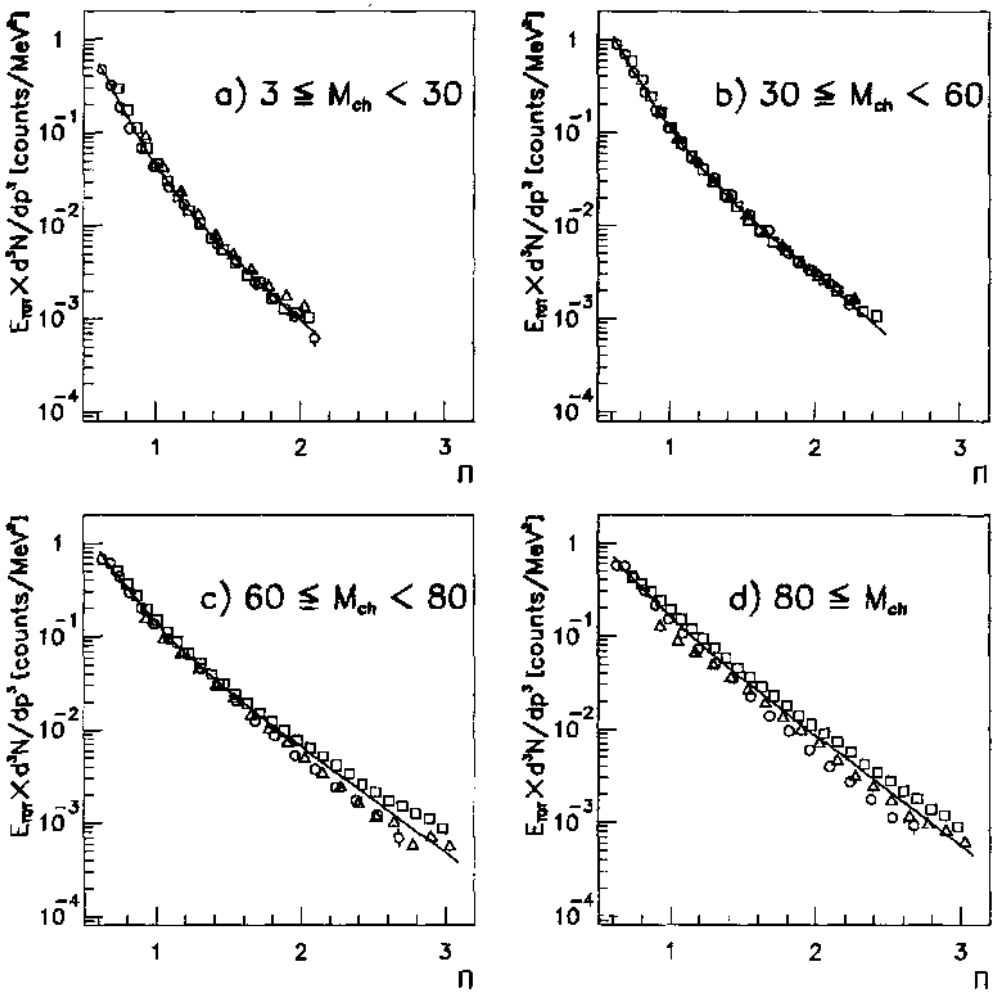

Fig. 3. The scaled form of neutron energy spectra for four $M_{\rm ch}$ multiplicity bins: a) $3 \leq M_{\rm ch} < 30$, b) $30 \leq M_{\rm ch} < 60$, c) $60 \leq M_{\rm ch} < 80$ and d) $80 \leq M_{\rm ch}$, where the polar angles $23.5°, 40°, 60°$ are labeled as: , □, △, respectively. The kinematical limits for N coming from the free NN collision corresponds to the value of $\Pi \approx 1.1$.

well, but the corresponding values of fitted parameters are more strongly dependent on polar angle.

In the second tested scenario it is assumed that emission of the neutron proceeds in such a way that the number of collaborating nucleons needed is the minimal one. Therefore a unified description of all spectra was searched under the assumption that the production invariant cross section depends only on the minimum invariant mass $s_{\rm min}$ necessary to produce the neutron with a given momentum. This relatively new method, so called minimum invariant mass (MIM) scaling [9], was applied to the multiplicity selected events separately. The data on $E{\rm d}N/{\rm d}p^3$ for various polar angles θ as a function of dimensionless variable $\Pi = \sqrt{s_{\rm min}}/2m_{\rm N}$ are plotted in Figure 3.

The MIM scaling especially for peripheral events is surprisingly good, generally it holds within an range given by a factor of 3.

3 Flow analysis

When discussing observables sensitive to the EOS, one may start with the so-called directivity $\mathcal{D}$ [10, 11]. In discussed experiment only the charged particle multiplicity information from the eight OPW sectors was available and therefore some approximation had to be used. First, the vector $\boldsymbol{Q}$ defined as

$$\boldsymbol{Q} = \sum_{i=1}^{8} M_i \boldsymbol{n}_i \tag{2}$$

was determined from the number of hits in each segment of the OPW. The sum in Eq. 2 runs over all eight OPW segments, $\boldsymbol{n}_i$ is a unit vector perpendicular to the beam direction pointing to the center of the i-th segment, M_i is the charged particle multiplicity registered in the i-th segment, i.e., $M_{\mathrm{ch}} = \sum_{i=1}^{8} M_i$. Using $\boldsymbol{Q}$ the directivity can be approximated as

$$\mathcal{D} \approx \frac{|\boldsymbol{Q}|}{M_{\mathrm{ch}}}. \tag{3}$$

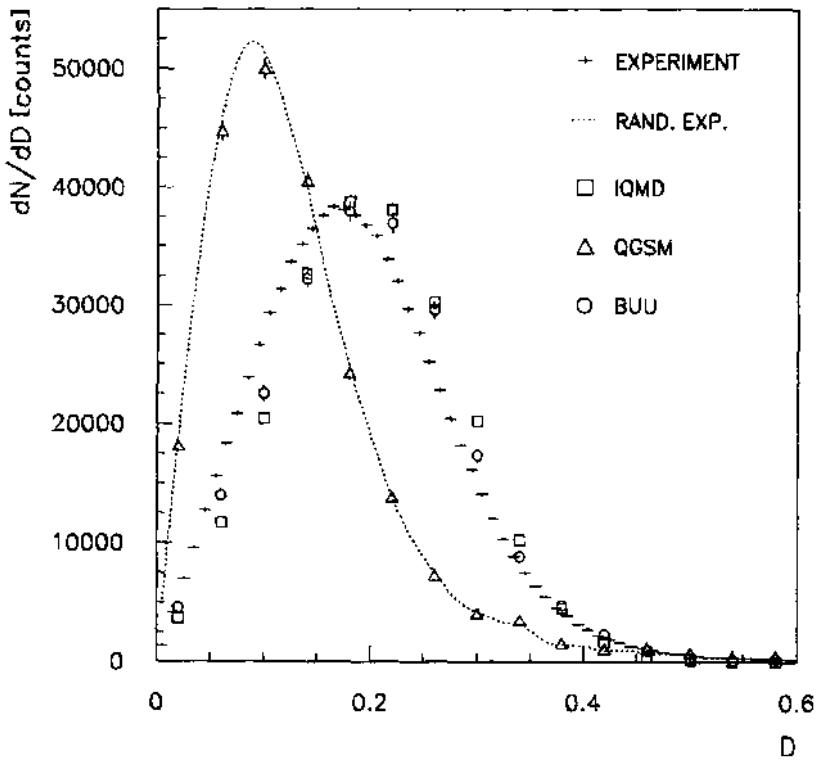

Fig. 4. The approximated directivity distribution in Bi+Pb 1 GeV/n collisions. The IQMD, QGSM and BUU calculation results are shown as well. The dotted line correspond to the modified experimental data, when the azimuthal angles of particles in the OPW sector were not taken from the experiment, but were chosen as random (all three models give in this case distributions which are very close to that one).

The non-trivial behaviour of directivity can indicate the collective nuclear flow effects. This is illustrated in Figure 4, where the distribution of approximated directivity is plotted together with that one obtained from experimental data, which were modified by randomizing hits uniformly over the whole OPW (i.e., the azimuthal angles of all particles in the OPW were chosen randomly) with the aim to destroy expected flow effects. Further analysis of the modified data was already the same as for the original ones. The figure shows that the experimental values and the predictions of IQMD and BUU models (with compressibility 380 MeV and 380 MeV respectively) behave similarly, while the QGSM predicts much narrower directivity distribution closely followed by the 'randomized' one, i.e., QGSM gives effectively too soft EOS, which is close to the EOS of ideal gas.

To study the flow effect for individual event in more detail, the reaction plane was defined by the beam direction and the vector $\boldsymbol{Q}$ (Eq. 2). Only events with $|\boldsymbol{Q}| > 5$ and $M_{ch} \geq 60$ were considered to ordinary reconstruct the reaction plane.

Azimuthal distributions $d^3N/d\theta dY_{rel} d\varphi$ of neutrons relative to the reaction plane at the detector positions $\theta = 23.5°$ and $40°$ are shown in Figure 5. There φ is the

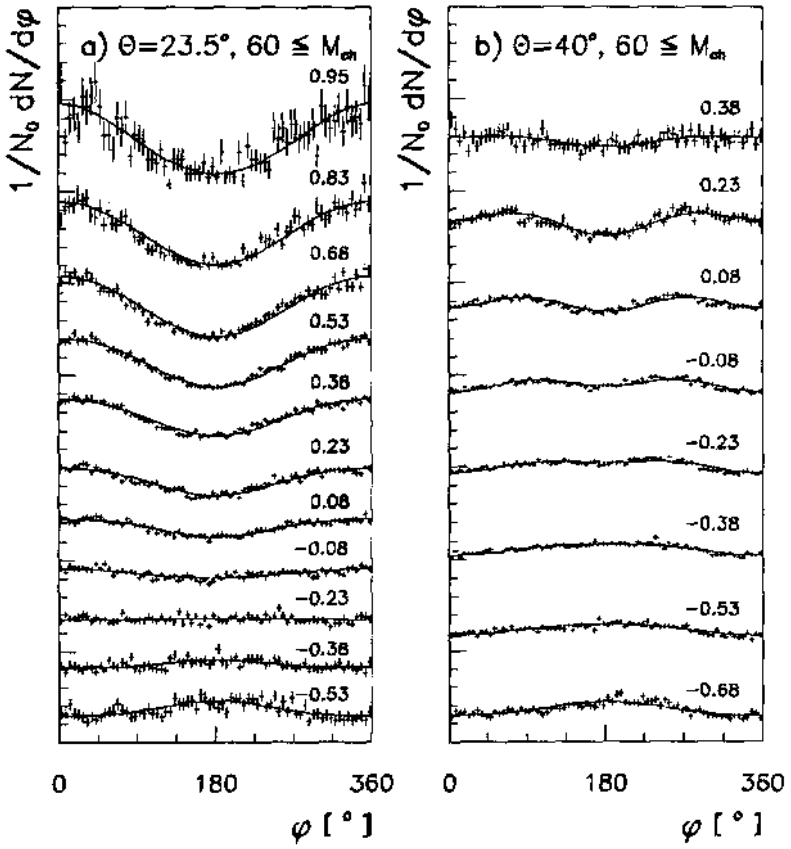

Fig. 5. Azimuthal distributions of neutrons from Bi+Pb 1 GeV/u collisions relatively to the reaction plane for different relative rapidities obtained for a) $\theta = 23.5°$ and b) $\theta = 40°$. The numbers above each of the experimental histograms are the relevant values of Y_{rel}. The histograms are fitted by the function 5.12 which is plotted as a smooth curve.

reaction plane azimuthal angle φ introduced as the angle between the horizontal plane containing beam and BAF detector and the reaction plane, θ is its polar angle and $Y_{\rm rel}$ is neutron relative rapidity defined by relation $Y_{\rm rel} = (Y - Y_{\rm CMS})/Y_{\rm CMS}$ ($Y_{\rm CMS}$ and Y are the rapidities of the CMS system and of the detected neutron, respectively).

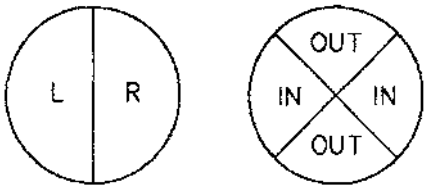

Fig. 6. Definition of the multiplicities $N_{\rm R}, N_{\rm L}, N_{\rm IN}, N_{\rm OUT}$.

The azimuthal distributions were fitted by second-order Fourier series. Only the even terms are allowed, since the odd ones correspond to the top-down asymmetry. Hence, obtained distributions were approximated with the function

$$F(\varphi) = \frac{N}{2\pi}(1 + S_1 \cos\varphi + S_2 \cos 2\varphi) \tag{4}$$

keeping N, S_1 and S_2 as free parameters.

Interpretation of coefficients S_1 and S_2 is straightforward. If $N_{\rm R}, N_{\rm L}, N_{\rm IN}, N_{\rm OUT}$ are the numbers of particles in azimuthal angle regions shown in Figure 6 and assuming that the corresponding probability distribution is of the form 4, then

$$S_1 = \frac{\pi}{2}\frac{N_{\rm L} - N_{\rm R}}{N_{\rm TOT}}, \tag{5}$$

$$S_2 = \frac{\pi}{2}\frac{N_{\rm IN} - N_{\rm OUT}}{N_{\rm TOT}}, \tag{6}$$

where $N_{\rm TOT}$ is the total number of particles, i.e. $M_{\rm ch}$ in studied case.

Hence, S_1 is sensitive to the collective sidewards flow only, while S_2 measures the particle emission perpendicular to the reaction plane.

Let us concentrate first on the projectile-like region case, i.e. spectra at $\theta = 23.5°$ (Fig. 5a). The single-humped structures visible for $Y_{\rm rel} < -0.3$ indicate the emission of particles opposite to the direction of the charged particles detected in the OPW. Since the polar angle is small, this corresponds to small transverse neutron momenta, $P_{\rm T} < 200\,{\rm MeV}/c$. The corresponding values of parameter S_1 are negative and the values of parameter S_2 are small. Similarly, positive values of the parameter S_1 with small values of the parameter S_2 correspond to the observation of particle flow for $Y_{\rm rel} > 0.1$, i.e., in the projectile fragmentation region, where the transverse neutron momenta are $P_{\rm T} > 300\,{\rm MeV}/c$.

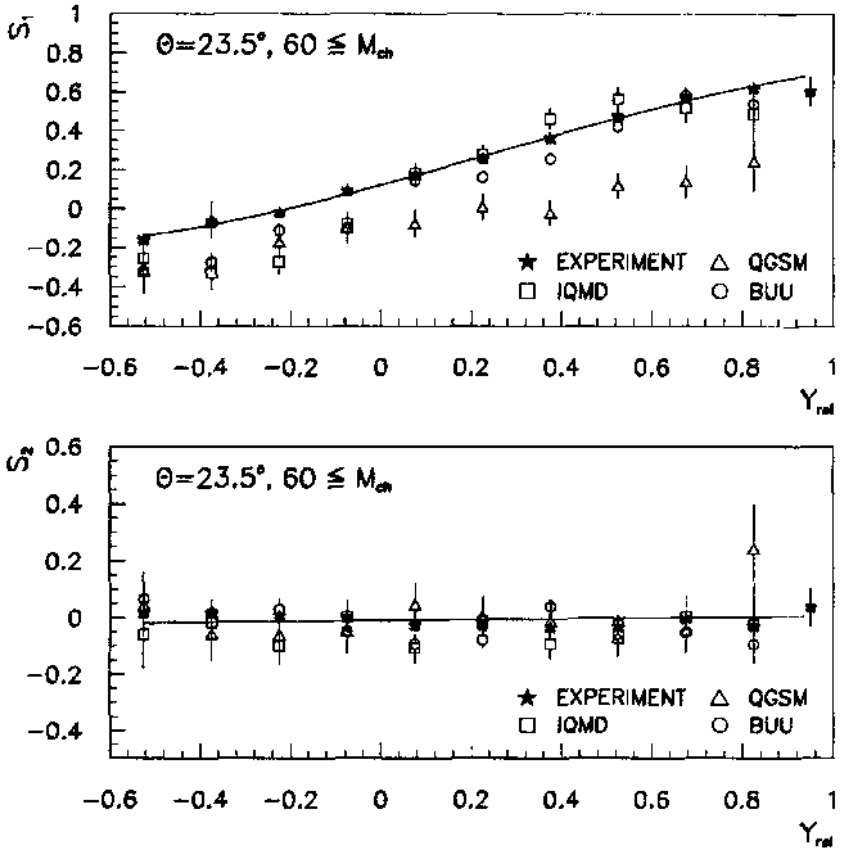

Fig. 7. Flow and squeeze-out parameters for $\theta = 23.5°$, Bi+Pb collisions 1 GeV/u. The full line is an eyeball fit.

The spectra at $\theta = 40°$ concern dominantly neutrons from the CMS mid-rapidity fireball. This position of the detector allowed to study the squeeze-out effect. The double-humped structures visible on figure 5b for $-0.2 < Y_{\mathrm{rel}} < 0.3$ indicate enhanced emission of high transverse momenta neutron near midrapidity ($P_{\mathrm{T}} > 400\,\mathrm{MeV}/c$). The emission occurs perpendicularly to the reaction plane. For rapidities $Y_{\mathrm{rel}} < -0.2$ the spectra are again dominated by a single-humped structure, what indicates the emission of particles opposite to the direction of the charged particles detected in the OPW, but now with up to two times higher neutron P_{T} than for the 23.5° case.

The experimental values and the model predictions of S_1 and S_2 parameters are plotted as functions of Y_{rel} in Figures 7 and 8. The predictions of S_1 parameter for 23.5° confirm already mentioned conclusion, that BUU and IQMD agree with the data substantially better then the QGSM with its very soft effective EOS.

In the case of 40° where the experiment does not exhibit substantial side flow effect this leads to apparent advantage of QGSM, while IQMD and BUU seem to be too hard at the low rapidity region. Nevertheless, according GEANT3 simulation the influence of neutrons rescattered off the floor is important in this case and can explain (at least partially) observed difference between data and IQMD or BUU

Neutron emission from Bi+Pb collisions at 1 GeV/u

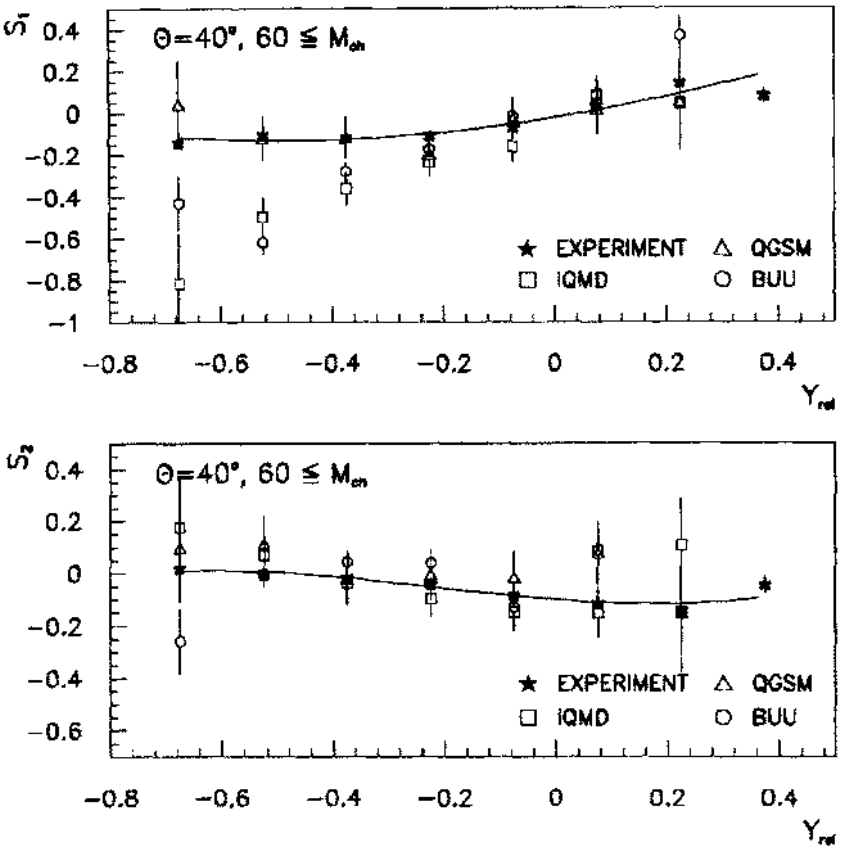

Fig. 8. Flow and squeeze-out parameters for $\theta = 40°$, Bi+Pb collisions 1 GeV/u. The full line is a eyeball fit.

prediction. Of course, the same effect will cause additional discrepancy of QGSM. In the case of S_2 parameter the predictions of all tested models agree within the error bars with the experimental data.

4 Conclusions

Inclusive energy distributions of neutrons at polar angle $\theta = 23.5°$, 40.0° and 60.0° were measured up to the region far beyond the free NN kinematical limit. The comparison of the shape of spectra with IQMD, QGSM and BUU models shows, that the data are approximately described by all models with the same accuracy. For the peripheral events all three models disagree with experiment for the 23.5° data. The simple picture of Boltzmann source without no implicit flow effects included is not compatible with data, nevertheless the unified description could be achieved on the base of MIM scaling.

Manifestation of the flow effects at directivity distribution was found. Reaction plane was determined with accuracy $\sigma \approx 31°$. Triple differential distributions of emitted neutrons exhibit neutron side-flow and squeeze-out effects. Significant

squeeze-out was found for the high P_T neutrons with rapidities close to the CMS region. Negative side-flow was observed for the neutrons with projectile-like rapidities and small and medium P_T. Strong positive flow was observed for the neutrons with projectile-like rapidities and middle and high P_T. The measured results agree with the predictions of BUU and IQMD models with non trivial EOS (compressibility $K = 308\,\mathrm{MeV}$ and $380\,\mathrm{MeV}$, respectively).

References

[1] Kugler A. et al.: Phys. Lett. B *335* (1994) 319.

[2] Gobbi A. et al.: Nucl. Instr. and Meth. A *324* (1993) 156.

[3] Hartnack Ch., Stöcker H., and Greiner W.: *in* The Nuclear Equation of State, Part A (Eds. W. Greiner and H. Stöcker), Plenum Press, New York, 1989, p. 239.

[4] Gudima K.K., Titov A.I., and Toncev V.D.: Phys. Lett. B *287* (1992) 302.

[5] Gudima K.K. and Toneev V.D.: Nucl Phys. A *400* (1983) 173.

[6] Wolf G. et al.: Nucl. Phys. A *517* (1990) 615.

[7] Wolf G. et al.: Nucl. Phys. A *545* (1992) 139.

[8] Schnedermann E. et al.: *in* Particle Production in Highly Excited Matter, NATO ASI Series, Series B: Physics, Vol. 303 (Eds. H. H. Gutbrod and J. Rafelski), p. 175.

[9] Baldin A.A.: Phys. At. Nucl. *56* (1993) 385.

[10] Beckmann P. et al.: Mod. Phys. Lett. A *2* (1987) 163.

[11] Alard J.P. et al.: Phys. Rev. Lett. *69* (1992) 889.

[12] Wilson W.K. et al.: Phys. Rev. C *45* (1992) 738.

3.4.4 Citations

1. Birgit Rotters; *Protonenemission in die rückwärtige Hemispäre bei ultrarelativistischen Schwerionenreaktionen*, Disertation, Fachbereich Physisk der J.W. Goethe Universität, Frankfurt am Main 1994.

3.4.5 Further developments

In 1996 the author used the formula (3.4) to analyze existing data on production of charged pions and kaons from Au+Au collisions at 1 AGeV [R56]. The results are presented in Fig.3.1. Note that with increasing transverse momenta of the particles data from Au+Au collisions closely approach the p+A data taken at 9× bigger energy per incident nucleon.

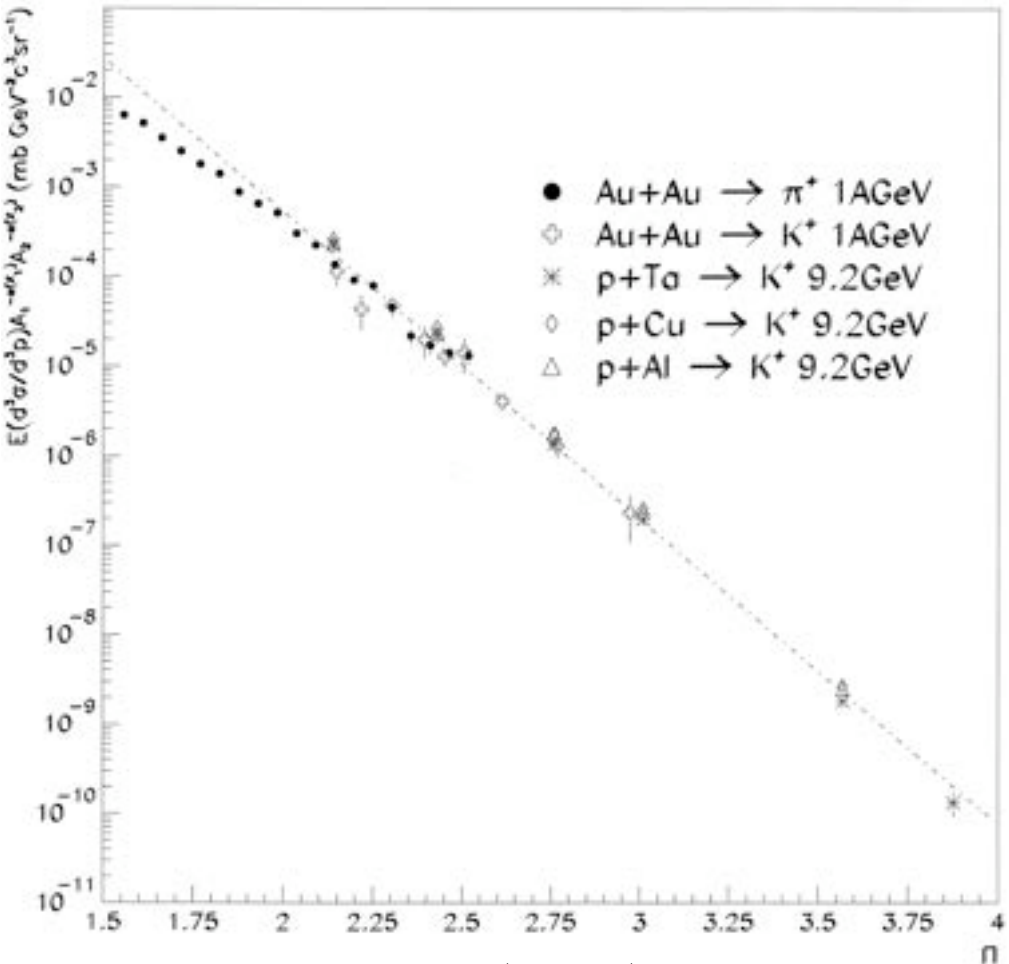

Figure 3.1: *Invariant cross section for π^+ and K^+ production in Au+Au (GSI SIS) and p+A (JINR Synchrophasontron) collisions as a function of dimensionless variable* $\Pi = \sqrt{s_{min}}/2m_N$. *Dash-dotted line represents the exponential* $exp(\Pi/\Pi_0)$, $\Pi_0 = 0.16$ *obtained in [R47] when fitting the p+A Dubna data only. [239]*

.

Chapter 4

Experiments with ultra-relativistic lead ion beams at CERN SPS

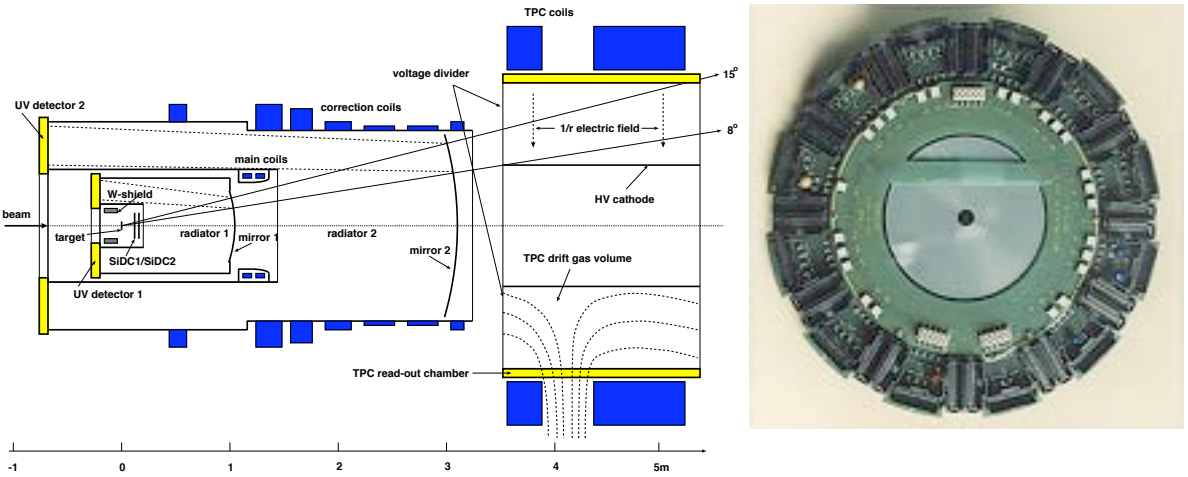

Figure 4.1: Left: schematic view of **C**herenkov **R**ing **E**lectron **S**pectrometer of NA45/CERES experiment at CERN SPS [90]. Right: cylindrical silicon drift detector(SDD). The detector, CD-like structure inside the motherboard, has 100 mm in diameter and 55 cm^2 active area. Horizontal structure going across it is a high-voltage bridge biasing the SDD. Achieved drift field of 700V/cm corresponds to the maximal drift time of 4 μs. Signal electrons created by ionization of charged particles drifted radially outward to an array of 360 anodes, at the periphery of the detector. Charged particles produced in the collision generate first signal in the two SDD (SDD1, SDD2), then cross the radiators of two ring imaging Cherenkov detectors (RICH1, RICH2) and in between them they are azimuthally deflected in the magnetic field produced by a superconducting magnet, and enter the TPC which is operated inside an inhomogeneous magnetic field generated by two opposite polarity coils. The electric field inside the TPC is radial, pointing from the readout chambers to the high voltage cylinder.

The author of this thesis and his team have joined the WA98 and NA45/CERES collaborations in 1993 and 1998, respectively. The experiments took data at the SPS in 1994-6 (WA98) and in 1999-2001 (NA45/CERES). The WA98 and NA45 detectors are shown in Fig.4.2 and Fig.4.1, respectively. In both experiments the main responsibility of the team revolved around preparation, maintenance and calibration of silicon drift detector(SDD) (Fig.4.1, right). In both experiments the SDDs was designated

to measure the charged particle multiplicity. In addition to this in NA45 experiment doublet of SDDs was used to reconstruct the interaction vertices originating from the thin distributed Au target.

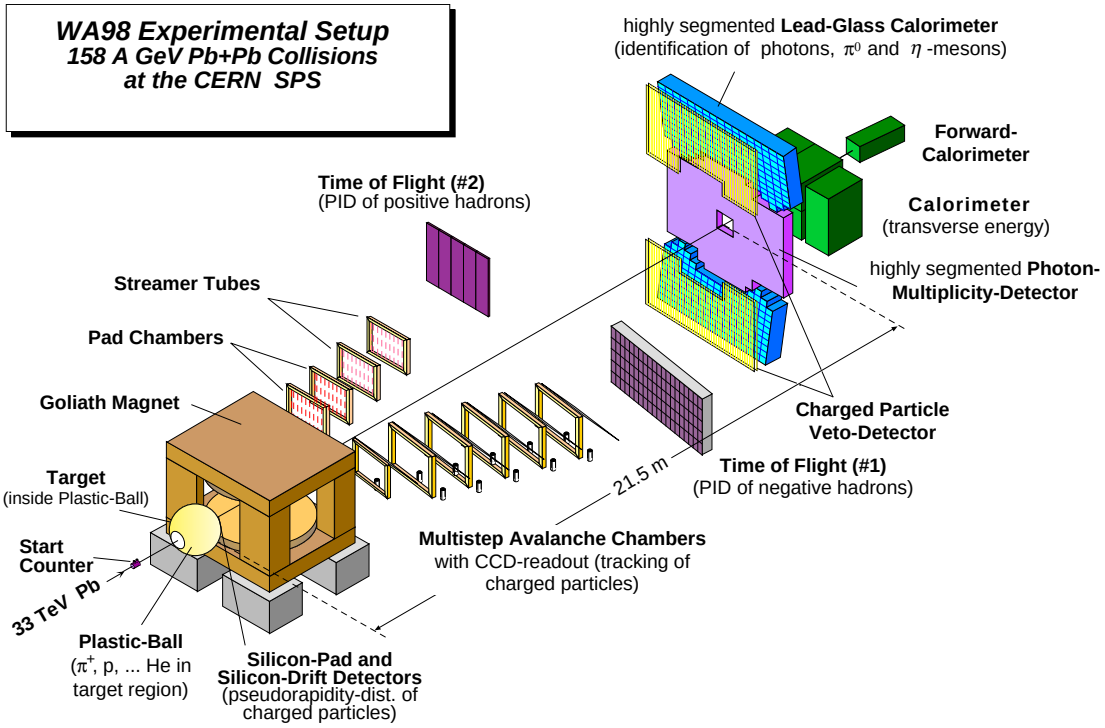

Figure 4.2: Schematic view of Large Acceptance Photon and Hadron Spectrometer of WA98 experiment at CERN SPS [59]. Charged particles produced in the target fragmentation region ($-1.7 < \eta < 0.5$) are detected via Plastic Ball. Charged particles at mid-rapidity ($2 < \eta < 3.75$) are measured by two types of silicon detectors, the Silicon Pad Multiplicity Detector (SPMD) and the Silicon Drift Detector (SDD). The Photon Multiplicity Detector (PMD) is a pre-shower detector which measures photon multiplicity from $2.8 < \eta < 4.4$. Photons produced in $2. < \eta < 3.$ are measured in the LEadglass Detector Array (LEDA). Charged Particle Veto (CPV) is positioned directly in front of LEDA. The produced transverse energy flow in $3.5 < \eta < 5.8$ is measured in the MIRAC calorimeter, located 24 meters downstream of the target. The Zero-Degree Calorimeter (ZDC) is positioned 30 meters downstream of the target. Tracking system is composed of two spectrometer arms and the large Goliath dipole magnet. Time-of-Flight (TOF) detector allows the calculation of the mass of the tracked particle.

Article reprint

VOLUME 81, NUMBER 19 PHYSICAL REVIEW LETTERS 9 NOVEMBER 1998

Centrality Dependence of Neutral Pion Production in 158A GeV ^{208}Pb + ^{208}Pb Collisions

M. M. Aggarwal,[1] A. Agnihotri,[2] Z. Ahammed,[3] A. L. S. Angelis,[4] V. Antonenko,[5] V. Arefiev,[6] V. Astakhov,[6] V. Avdeitchikov,[6] T. C. Awes,[7] P. V. K. S. Baba,[8] S. K. Badyal,[8] A. Baldine,[6] L. Barabach,[6] C. Barlag,[9] S. Bathe,[9] B. Batiounia,[6] T. Bernier,[10] K. B. Bhalla,[2] V. S. Bhatia,[1] C. Blume,[9] R. Bock,[11] E.-M. Bohne,[9] Z. K. Böröcz,[9] D. Bucher,[9] A. Buijs,[12] H. Büsching,[9] L. Carlen,[13] V. Chalyshev,[6] S. Chattopadhyay,[3] R. Cherbatchev,[5] T. Chujo,[14] A. Claussen,[9] A. C. Das,[3] M. P. Decowski,[18] V. Djordjadze,[6] P. Donni,[4] I. Doubovik,[5] M. R. Dutta Majumdar,[3] K. El Chenawi,[13] S. Eliseev,[15] K. Enosawa,[14] P. Foka,[4] S. Fokin,[5] V. Frolov,[6] M. S. Ganti,[3] S. Garpman,[13] O. Gavrishchuk,[6] F. J. M. Geurts,[12] T. K. Ghosh,[16] R. Glasow,[9] S. K. Gupta,[2] B. Guskov,[6] H. A. Gustafsson,[13] H. H. Gutbrod,[10] R. Higuchi,[14] I. Hrivnacova,[15] M. Ippolitov,[5] H. Kalechofsky,[4] R. Kamermans,[12] K.-H. Kampert,[9] K. Karadjev,[5] K. Karpio,[17] S. Kato,[14] S. Kees,[9] H. Kim,[7] B. W. Kolb,[11] I. Kosarev,[6] I. Koutcheryaev,[5] T. Krümpel,[9] A. Kugler,[15] P. Kulinich,[18] M. Kurata,[14] K. Kurita,[14] N. Kuzmin,[6] I. Langbein,[11] A. Lebedev,[5] Y. Y. Lee,[11] H. Löhner,[16] L. Luquin,[10] D. P. Mahapatra,[19] V. Manko,[5] M. Martin,[4] A. Maximov,[6] R. Mehdiyev,[6] G. Mgebrichvili,[5] Y. Miake,[14] D. Mikhalev,[6] G. C. Mishra,[19] Y. Miyamoto,[14] D. Morrison,[20] D. S. Mukhopadhyay,[3] V. Myalkovski,[6] H. Naef,[4] B. K. Nandi,[19] S. K. Nayak,[10] T. K. Nayak,[3] S. Neumaier,[11] A. Nianine,[5] V. Nikitine,[6] S. Nikolaev,[6] P. Nilsson,[13] S. Nishimura,[14] P. Nomokonov,[6] J. Nystrand,[13] F. E. Obenshain,[20] A. Oskarsson,[13] I. Otterlund,[13] M. Pachr,[15] A. Parfenov,[6] S. Pavliouk,[6] T. Pietzmann,[9] V. Patracek,[15] W. Pinanaud,[10] F. Plasil,[7] M. L. Purschke,[11] B. Raeven,[12] J. Rak,[15] R. Raniwala,[2] S. Raniwala,[2] V. S. Ramamurthy,[19] N. K. Rao,[8] F. Retiere,[10] K. Reygers,[9] G. Roland,[18] L. Rosselet,[4] I. Roufanov,[6] C. Roy,[10] J. M. Rubio,[4] H. Sako,[14] S. S. Sambyal,[8] R. Santo,[9] S. Sato,[14] H. Schlagheck,[9] H.-R. Schmidt,[11] G. Shabratova,[6] I. Sibiriak,[5] T. Siemiarczuk,[17] D. Silvermyr,[13] B. C. Sinha,[3] N. Slavine,[6] K. Söderström,[13] N. Solomey,[4] S. P. Sørensen,[20] P. Stankus,[7] G. Stefanek,[17] P. Steinberg,[18] E. Stenlund,[13] D. Stüken,[9] M. Sumbera,[15] T. Svensson,[13] M. D. Trivedi,[3] A. Tsvetkov,[5] C. Twenhöfel,[12] L. Tykarski,[17] J. Urbahn,[11] N. v. Eijndhoven,[12] G. J. v. Nieuwenhuizen,[18] A. Vinogradov,[5] Y. P. Viyogi,[3] A. Vodopianov,[6] S. Vörös,[4] B. Wysłouch,[18] K. Yagi,[14] Y. Yokota,[14] and G. R. Young[7]

(WA98 Collaboration)

[1]*University of Panjab, Chandigarh 160014, India*
[2]*University of Rajasthan, Jaipur 302004, India*
[3]*Variable Energy Cyclotron Centre, Calcutta 700 064, India*
[4]*University of Geneva, CH-1211 Geneva 4, Switzerland*
[5]*RRC (Kurchatov), RU-123182 Moscow, Russia*
[6]*Joint Institute for Nuclear Research, RU-141980 Dubna, Russia*
[7]*Oak Ridge National Laboratory, Oak Ridge, Tennessee 37831-6372*
[8]*University of Jammu, Jammu 180001, India*
[9]*University of Münster, D-48149 Münster, Germany*
[10]*SUBATECH, Ecole des Mines, Nantes, France*
[11]*Gesellschaft für Schwerionenforschung (GSI), D-64220 Darmstadt, Germany*
[12]*Universiteit Utrecht/NIKHEF, NL-3508 TA Utrecht, The Netherlands*
[13]*University of Lund, SE-221 00 Lund, Sweden*
[14]*University of Tsukuba, Ibaraki 305, Japan*
[15]*Nuclear Physics Institute, CZ-250 68 Rez, Czech Republic*
[16]*KVI, University of Groningen, NL-9747 AA Groningen, The Netherlands*
[17]*Institute for Nuclear Studies, 00-681 Warsaw, Poland*
[18]*MIT, Cambridge, Massachusetts 02139*
[19]*Institute of Physics, 751-005 Bhubaneswar, India*
[20]*University of Tennessee, Knoxville, Tennessee 37966*

(Received 26 June 1998)

The production of neutral pions in 158A GeV ^{208}Pb + ^{208}Pb collisions has been studied in the WA98 experiment at the CERN Super Proton Synchrotron (SPS). Transverse momentum spectra are studied for the range $0.3 \leq m_T - m_0 \leq 4.0$ GeV/c. The results for central collisions are compared to various models. The centrality dependence of the neutral pion spectral shape and yield is investigated. An invariance of the spectral shape and a simple scaling of the yield with the number of participating nucleons is observed for centralities with greater than about 30 participating nucleons. This is most naturally explained by assuming an equilibrated system. [S0031-9007(98)07532-2]

PACS numbers: 25.75.Dw

VOLUME 81, NUMBER 19 PHYSICAL REVIEW LETTERS 9 NOVEMBER 1998

Ultrarelativistic heavy-ion collisions produce dense matter which is expected to be in the form of a deconfined phase of quarks and gluons, or quark gluon plasma (QGP), at sufficiently high energy densities. The transverse momentum spectra of produced pions can provide information on both the initial and the final state properties of the hot hadronic matter. The low p_T pion production would dominantly reflect the temperature of the hadronic system at the freeze-out stage occurring late in the reaction. It is strongly influenced by rescattering among the final state hadrons. The high p_T pion production is expected to be dominated by hard scattering of the partons. In pA collisions the high p_T region is known to be enhanced (Cronin effect [1]) due to initial state scattering of the incident partons leading to a broadening of their incoming p_T. In AA collisions, many of the scattered partons must traverse the excited matter to escape and therefore may undergo additional rescatterings and energy loss [2]. In the case of significant parton rescattering, the parton distributions may approach thermal distributions with a temperature reflecting the initial state of the excited matter. The intermediate p_T region of the pion spectrum might then reflect this initial temperature. Indeed, one of the earliest signatures of QGP formation, proposed by Van Hove [3], was the observation of a saturation of the average transverse momentum with increasing energy (or entropy) density for systems excited just above the critical energy density. With increasing energy density, the initial temperature would not rise above the critical temperature until all of the latent heat of the QQP phase transition had been extracted.

For these reasons it is of interest to study the centrality dependence of the pion production. It is generally believed that the initial energy density increases with increasing centrality, due to the many overlapping interactions. Also, the volume of the excited matter increases with centrality, as well as the amount of rescattering. Since rescattering is the feature which distinguishes AA collisions nontrivially from pp collisions, and since significant rescattering is a prerequisite for thermalization, it is imperative to demonstrate an understanding of the centrality dependence of the AA results in order to understand the effects of rescattering. While those effects may be minor on extensive observables, like the particle multiplicity or transverse energy, they should be most evident on the momentum distribution of the produced particles. Recently it has been argued that a parton cascade description could successfully describe many of the features of central Pb + Pb collisions at the CERN Super Proton Synchrotron (SPS) energies [4]. Surprisingly, low momentum transfer soft parton collisions were found to have little influence on the final observables. Similarly, recent perturbative QCD calculations were able to reproduce the preliminary WA98 neutral pion result for central collisions [5,6] without need for the effects of parton energy loss or rescattering [7]. In this Letter we present neutral pion spectra for 158A GeV ^{208}Pb + ^{208}Pb collisions and investigate in detail the centrality dependence of the spectral shape and yield.

The CERN experiment WA98 [5,8] consists of large acceptance photon and hadron spectrometers together with several other large acceptance devices which allow one to measure various global variables on an event-by-event basis. The results presented here were obtained from an analysis of the data taken with Pb beams in 1995 and 1996. The minimum bias (min-bias) reactions ($\sigma_{\text{min-bias}} \approx 6300$ mb) are divided into eight centrality classes using the transverse energy E_T measured in the MIRAC calorimeter. In total, $\approx 9.6 \times 10^6$ reactions have been analyzed.

Neutral pions are reconstructed via their $\gamma\gamma$ decay branch using the WA98 lead-glass photon detector, LEDA, which consisted of 10 080 individual modules with photomultiplier readout. The detector was located at a distance of 21.5 m from the target and covered the pseudorapidity interval $2.35 < \eta < 2.95$. The measurement of neutral pions, though difficult at low transverse momenta, is superior to those of charged pions at high momenta because of the improving energy resolution of the calorimetric measurement.

The general analysis procedure is similar to that used in the WA80 experiment and described in [9]. Hits in the lead-glass detector are combined in pairs to provide distributions of pair mass vs pair transverse momentum (or transverse mass) for all possible combinations. Subtraction of the combinatorial background is performed using mixed event distributions. The resulting momentum distributions are corrected for geometrical acceptance and reconstruction efficiency. The efficiency depends on the particle occupancy in the detector and therefore has been calculated independently for each centrality bin. The systematic error of the pion yields is mainly due to errors in the reconstruction efficiency for central collisions and to corrections for nontarget interactions for peripheral collisions. The systematic error on the absolute yield is $\approx 10\%$ and increases sharply below $p_T = 0.4$ GeV/c. An additional systematic error originates from the uncertainty of the momentum scale of 1%. The influence of this rises slowly for higher p_T and leads to an error of 15% at $p_T = 4$ GeV/c. A detailed discussion of the analysis procedure and the error contributions will be given in a forthcoming publication.

The measured neutral pion spectrum from central Pb + Pb reactions (10% of min-bias cross section) as a function of $m_T - m_0$ is shown in Fig. 1. The data are compared to predictions of the string model Monte Carlo generators FRITIOF 7.02 [10] and VENUS 4.12 [11]. As already observed in S + Au reactions [9], both generators fail to describe the data well at large m_T. The FRITIOF prediction is more than an order of magnitude lower at high m_T while VENUS significantly overpredicts the data. Alternatively, it has recently been shown that

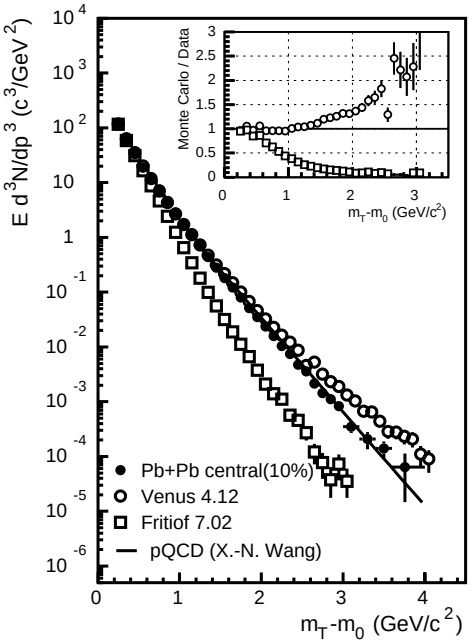

FIG. 1. Transverse mass spectra of neutral pions in central collisions of 158*A* GeV Pb + Pb. Invariant yields per event are compared to calculations using the FRITIOF 7.02 [10] and VENUS 4.12 [11] Monte Carlo programs. Predictions of a pQCD calculation [7] are included as a solid line. The inset shows the ratios of the results of the Monte Carlo codes to the experimental data.

perturbative QCD (pQCD) calculations, including initial state multiple scattering and intrinsic p_T [7], are able to describe the preliminary WA98 data at intermediate and high p_T. This prediction is included in Fig. 1 as a solid line. (The results shown have been corrected for a small numerical error by the author of [7] and have changed by $\approx 10\%-30\%$ compared to the publication.) The pQCD calculation shows a very good agreement in the high m_T region. This surprising agreement has been interpreted as an indication for unexpectedly small effects of parton energy loss [7]. On the other hand, the parton cascade Monte Carlo code, VNI, which provides a more detailed pQCD description, overpredicts the measured WA98 result by more than a factor of 10 at large p_T [4]. In an alternative picture, hydrodynamical descriptions (see, e.g., [12]) with properly adjusted parameters can describe the momentum spectra reasonably well.

In view of the above discussion and the difficulty to describe the details of the neutral pion spectrum, it is apparent that the theoretical description of ultrarelativistic nucleus-nucleus collisons remains uncertain. In order to demonstrate a consistent description of nuclear effects it is important to investigate the details of the pion production as a function of the system size. To study the centrality dependence of the spectral shape in a manner which is independent of model or fit function we have used the truncated mean transverse momentum $\langle p_T(p_T^{\min})\rangle$, where

$$\langle p_T(p_T^{\min})\rangle = \left(\int_{p_T^{\min}}^{\infty} p_T \frac{dN}{dp_T}\, dp_T \Big/ \int_{p_T^{\min}}^{\infty} \frac{dN}{dp_T}\, dp_T\right) - p_T^{\min}. \quad (1)$$

The lower cutoff $p_T^{\min} = 0.4$ GeV/c is introduced to avoid systematic errors from extrapolation to low p_T and has been chosen according to the lowest p_T of the present data where systematic uncertainties imposed by the necessary corrections are still small. In general, the value of $\langle p_T(p_T^{\min})\rangle$ differs from the true average p_T, except in the case of a purely exponential distribution $d\sigma/dp_T$. For a purely exponential invariant cross section, $d^2\sigma/dp_T^2$, $\langle p_T(p_T^{\min})\rangle$ decreases with increasing $p_T^{\min}$.

Figure 2 shows $\langle p_T(p_T^{\min})\rangle$ as a function of the average number of participants N_{part} for 158*A* GeV ^{208}Pb + Pb collisions. For comparison, $\langle p_T(p_T^{\min})\rangle$ values for 200*A* GeV S + Au [9] and from a parametrization of pp data [13] are also included. N_{part} is extracted by the assumption of a monotonic relation between impact parameter and transverse energy and using the resulting correspondence between measured cross section and impact parameter. The average number of participants is calculated from nuclear geometry using the extracted impact parameter. Together these data show the general trend of a rapid increase of $\langle p_T(p_T^{\min})\rangle$ compared to pp results for small system sizes. For N_{part} greater than about 30 the

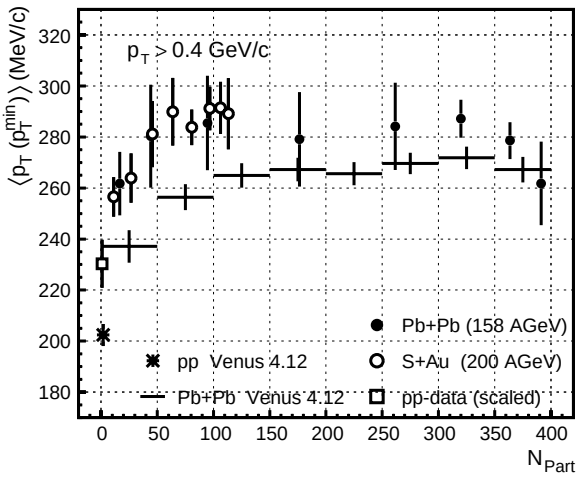

FIG. 2. Truncated mean transverse momentum $\langle p_T(p_T^{\min})\rangle$ of π^0 mesons as defined by Eq. (1) plotted as a function of the average number of participants N_{part}. The solid circles correspond to the 8 E_T based centrality selections for Pb + Pb. The open square shows $\langle p_T(p_T^{\min})\rangle$ extracted from a parametrization of pp data scaled to the same c.m. energy [13], the open circles the results for S + Au collisions at 200*A* GeV [9]. For comparison, results from VENUS 4.12 [11] are included as histograms for Pb + Pb collisions and as a star for pp. A cut parameter $p_T^{\min} = 0.4$ GeV/c was used.

mean transverse momentum appears to attain a limiting value of $\approx$280 MeV/c^2. [The variation of $\langle p_T(p_T^{\min})\rangle$ has been studied for values of $p_T^{\min} = 0.2$–1.0 GeV/c. The saturation is always observed; the statistical significance, however, decreases with increasing threshold.] VENUS 4.12 [11] calculations show a qualitatively similar behavior, but underpredict the present data, as well as the pp data. The simple implementation of rescattering which is used in this model seems to be strong enough to lead to a saturation for semiperipheral collisions as in the experimental data. One should, however, keep in mind that VENUS 4.12 does not correctly describe pion production at high p_T (see Fig. 1).

Earlier investigations of the dependence of $\langle p_T\rangle$ of pions on system size [9,14,15] at SPS energies have suggested such a saturation for large systems. The present study is the first investigation of the dependence with Pb ions at the SPS. Preliminary results from the AGS have indicated a weak increase in the average m_T of pions with the number of participants for Au + Au collisions [16].

It is important to note that the observed limiting behavior is very different from the observations in pp or $p\overline{p}$ collisions. For very high energies $\langle p_T\rangle$ rises with the pseudorapidity density of charged particles [17–20]. In that case, more violent parton scatterings presumably result in a harder spectrum of leading particles together with a greater multiplicity of fragmentation products. This would lead to the observed correlation between $\langle p_T\rangle$ and multiplicity. At lower $\sqrt{s}$, comparable to the data presented here, $\langle p_T\rangle$ decreases for increasing multiplicity [21], most likely due to energy conservation. In the case of nuclear reactions, this anticorrelation is lost due to the large number of binary collisions. Instead, the initial increase of $\langle p_T(p_T^{\min})\rangle$ with N_{part} is interpreted as a result of multiple scattering. Initial state multiple scattering, as suggested as an explanation for the Cronin effect [1], would imply a continuing increase of $\langle p_T(p_T^{\min})\rangle$ for more central collisions. Here, however, the surprising observation is that additional multiple scattering, implied by increasing N_{part}, does not alter the pion distributions. This is most easily understood as a consequence of final state rescattering and is, of course, the behavior expected for a thermalized system.

More detailed information about the centrality dependence of the pion spectral shape and yield is shown in Fig. 3 where the neutral pion yield per event has been parametrized as $Ed^3N/dp^3 \propto N_{\text{part}}^{\alpha(p_T)}\sigma_0(p_T)$. The results for $N_{\text{part}} > 30$ are well described by this scaling with an exponent $\alpha(p_T) \approx 1.3$, independent of p_T. Consistent with the previous discussion, the results indicate a constant spectral shape over the entire interval of measurement from $0.5 < p_T < 3$ GeV/c. The observed $N_{\text{part}}^{4/3}$ scaling for symmetric systems implies a scaling with the number of nucleon collisions, as confirmed by a similar analysis. However, this scaling does not extrapolate from the pp results. On the contrary, when comparing semiperipheral Pb + Pb collisions with pp the exponent

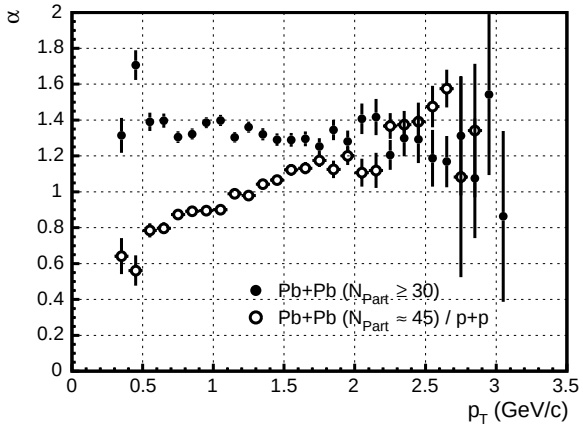

FIG. 3. The exponent $\alpha(p_T)$ of the dependence of the π^0 yield on the average number of participants N_{part} plotted as a function of the transverse momentum for 158A GeV Pb + Pb. The solid circles are calculated based on a fit to the centrality selections with $N_{\text{part}} \geq 30$. The open circles are calculated based on the ratio of the semiperipheral data ($N_{\text{part}} \approx 45$) to a parametrization of pp data.

α varies over the entire p_T interval, confirming the very different spectral shapes.

In summary, we have analyzed the centrality dependence of high precision transverse momentum spectra of neutral pions from 158A GeV Pb + Pb collisions. The neutral pion spectra are observed to show increasing deviation from pp results with increasing centrality, indicating the importance of multiple scattering effects. However, for centralities with more than about 30 participating nucleons, the shape of the transverse momentum spectrum becomes invariant over the interval $0.5 < p_T < 3$ GeV/c. In this interval the pion yield scales like $N_{\text{part}}^{1.3}$, or like the number of nucleon collisions, for this range of centralities. Since the amount of rescattering increases with centrality, the invariance of the spectral shape with respect to the number of rescatterings, most naturally suggests a dominantly thermal emission process. It will be important to determine whether cascade models which reproduce the observed invariant spectral shape will support the interpretation as an "effective" thermalization due to significant rescattering.

We wish to express our gratitude to the CERN accelerator division for excellent performance of the SPS accelerator complex. We acknowledge with appreciation the effort of all engineers, technicians, and support staff who have participated in the construction of the experiment. This work was supported jointly by the German BMBF and DFG, the U.S. DOE, the Swedish NFR and FRN, the Dutch Stichting FOM, the Stiftung für Deutsch-Polnische Zusammenarbeit, the Grant Agency of the Czech Republic under Contract No. 202/95/0217, the Department of Atomic Energy, the Department of Science and

Technology, the Council of Scientific and Industrial Research and the University Grants Commission of the Government of India, the Indo-FRG Exchange Program, the PPE division of CERN, the Swiss National Fund, the International Science Foundation under Contract No. N8Y000, the INTAS under Contract No. INTAS-93-2773, ORISE, Research-in-Aid for Scientific Research (Specially Promoted Research & International Scientific Research) of the Ministry of Education, Science and Culture, the University of Tsukuba Special Research Projects, and the JSPS Research Fellowships for Young Scientists. ORNL is managed by Lockheed Martin Energy Research Corporation under Contract No. DE-AC05-96OR22464 with the U.S. Department of Energy. The MIT group has been supported by the U.S. Department of Energy under the cooperative agreement DE-FC02-94ER40818.

[1] D. Antreasyan *et al.*, Phys. Rev. D **19**, 764 (1979).
[2] X.-N. Wang and M. Gyulassy, Phys. Rev. Lett. **68**, 1480 (1992).
[3] L. Van Hove, Phys. Lett. **118B**, 138 (1982).
[4] D. K. Srivastava and K. Geiger, Phys. Rev. C **56**, 2718 (1997).
[5] WA98 Collaboration, M. Aggarwal *et al.*, Nucl. Phys. **A610**, 200c (1996).
[6] WA98 Collaboration, T. Peitzmann *et al.*, in *Quark Matter '97, Proceedings of the 13th International Conference on Ultrarelativistic Nucleus-Nucleus Collisions, Tsukuba, Japan* (to be published).
[7] X.-N. Wang, e-print hep-ph/9804384, 1998; (private communication).
[8] WA98 Collaboration, Report No. CERN/SPSLC 91-17, SPSLC/P260, 1991.
[9] WA80 Collaboration, R. Albrecht *et al.*, Eur. Phys. J. C **5**, 255–267 (1998).
[10] B. Andersson, G. Gustafson, and H. Pi, Z. Phys. C **57**, 485 (1993).
[11] K. Werner, Phys. Rep. **232**, 87 (1993).
[12] U. A. Wiedemann and U. Heinz, Phys. Rev. C **56**, 3265 (1997).
[13] C. Blume, Doctoral thesis, University of Münster, Germany, 1998.
[14] WA80 Collaboration, R. Albrecht *et al.*, Phys. Lett. B **201**, 390 (1987).
[15] HELIOS Collaboration, T. Åkesson *et al.*, Z. Phys. C **46**, 361 (1990).
[16] E866 Collaboration, L. Ahle *et al.*, Nucl. Phys. **A610**, 139c (1996).
[17] SFM Collaboration, A. Breakstone *et al.*, Phys. Lett. B **183**, 227 (1987).
[18] UA1 Collaboration, G. Arnison *et al.*, Phys. Lett. **118B**, 167 (1982).
[19] CDF Collaboration, F. Abe *et al.*, Phys. Rev. Lett. **61**, 1819 (1988).
[20] E735 Collaboration, T. Alexopoulos *et al.*, Phys. Lett. B **336**, 599 (1987).
[21] T. Kafka *et al.*, Phys. Rev. D **16**, 1261 (1977).

VOLUME 84, NUMBER 3 PHYSICAL REVIEW LETTERS 17 JANUARY 2000

Erratum: Centrality Dependence of Neutral Pion Production in 158*A* GeV ^{208}Pb + ^{208}Pb Collisions [Phys. Rev. Lett. 81, 4087 (1998)]

M. M. Aggarwal, A. Agnihotri, Z. Ahammed, A. L. S. Angelis, V. Antonenko, V. Arefiev, V. Astakhov, V. Avdeitchikov, T. C. Awes, P. V. K. S. Baba, S. K. Badyal, A. Baldine, L. Barabach, C. Barlag, S. Bathe, B. Batiounia, T. Bernier, K. B. Bhalla, V. S. Bhatia, C. Blume, R. Bock, E.-M. Bohne, Z. K. Böröcz, D. Bucher, A. Buijs, H. Büsching, L. Carlen, V. Chalyshev, S. Chattopadhyay, R. Cherbatchev, T. Chujo, A. Claussen, A. C. Das, M. P. Decowski, V. Djordjadze, P. Donni, I. Doubovik, M. R. Dutta Majumdar, K. El Chenawi, S. Eliseev, K. Enosawa, P. Foka, S. Fokin, V. Frolov, M. S. Ganti, S. Garpman, O. Gavrishchuk, F. J. M. Geurts, T. K. Ghosh, R. Glasow, S. K. Gupta, B. Guskov, H. A. Gustafsson, H. H. Gutbrod, R. Higuchi, I. Hrivnacova, M. Ippolitov, H. Kalechofsky, R. Kamermans, K.-H. Kampert, K. Karadjev, K. Karpio, S. Kato, S. Kees, H. Kim, B. W. Kolb, I. Kosarev, I. Koutcheryaev, T. Krümpel, A. Kugler, P. Kulinich, M. Kurata, K. Kurita, N. Kuzmin, I. Langbein, A. Lebedev, Y. Y. Lee, H. Löhner, L. Luquin, D. P. Mahapatra, V. Manko, M. Martin, A. Maximov, R. Mehdiyev, G. Mgebrichvili, Y. Miake, D. Mikhalev, G. C. Mishra, Y. Miyamoto, D. Morrison, D. S. Mukhopadhyay, V. Myalkovski, H. Naef, B. K. Nandi, S. K. Nayak, T. K. Nayak, S. Neumaier, A. Nianine, V. Nikitine, S. Nikolaev, P. Nilsson, S. Nishimura, P. Nomokonov, J. Nystrand, F. E. Obenshain, A. Oskarsson, I. Otterlund, M. Pachr, A. Parfenov, S. Pavliouk, T. Peitzmann,* V. Petracek,* W. Pinanaud, F. Plasil, M. L. Purschke, B. Raeven, J. Rak, R. Raniwala, S. Raniwala, V. S. Ramamurthy, N. K. Rao, F. Retiere, K. Reygers, G. Roland, L. Rosselet, I. Roufanov, C. Roy, J. M. Rubio, H. Sako, S. S. Sambyal, R. Santo, S. Sato, H. Schlagheck, H.-R. Schmidt, G. Shabratova, I. Sibiriak, T. Siemiarczuk, D. Silvermyr, B. C. Sinha, N. Slavine, K. Söderström, N. Solomey, S. P. Sørensen, P. Stankus, G. Stefanek, P. Steinberg, E. Stenlund, D. Stüken, M. Sumbera, T. Svensson, M. D. Trivedi, A. Tsvetkov, C. Twenhöfel, L. Tykarski, J. Urbahn, N. v. Eijndhoven, G. J. v. Nieuwenhuizen, A. Vinogradov, Y. P. Viyogi, A. Vodopianov, S. Vörös, B. Wysłouch, K. Yagi, Y. Yokota, and G. R. Young

(WA98 Collaboration)

In this paper, the absolute cross section determination associated with the different centrality selections was made with a limited data set which was not representative of the full analysis. This resulted in a systematic overestimate of the number of participants N_{part} (or the number of collisions). The relative magnitude of this correction is significant for the most peripheral centrality class and nearly negligible for the most central event class. The neutral pion transverse momentum spectra are unchanged. As a result of this correction, the data points of Fig. 2 should be shifted by varying degrees towards the origin on the number of participants scale. However, the conclusion of a saturation of the average transverse momentum with increasing centrality drawn from this figure remains unchanged.

Similarly, the major conclusion of Fig. 3 remains unchanged: In the region of centralities where the saturation of the average transverse momentum is observed, the scaling of the pion yield is independent of the transverse momentum; i.e.,

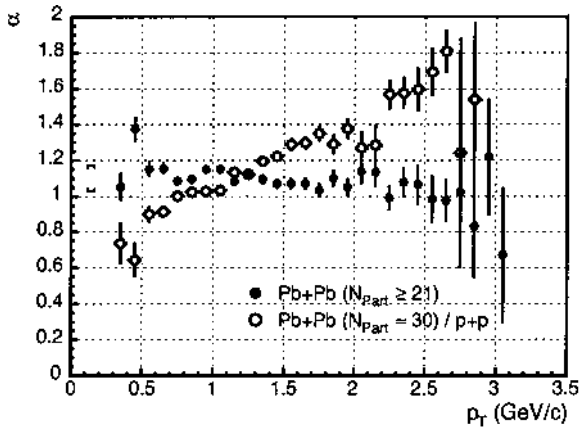

FIG. 1. The exponent $\alpha(p_T)$ of the dependence of the π^0 yield on the average number of participants N_{part} plotted as a function of the transverse momentum for 158*A* GeV Pb + Pb. The solid circles are calculated based on the centrality selections with $N_{\text{part}} \geq 21$. The open circles are calculated based on the ratio of the semiperipheral data ($N_{\text{part}} \approx 30$) to a parametrization of *pp* data. The brackets indicate the estimated systematic error on the exponent α.

 0031-9007/00/84(3)/578(2)$15.00

the spectral shape does not change. However, with the corrected assignment of the number of participants the scaling exponent is reduced to $\alpha \approx 1.1$ from the value of $\alpha \approx 1.3$ given previously. The corrected version of Fig. 3 is displayed in Fig. 1. In addition to the correction of the cross section determination, the event generator VENUS 4.12 [1] has been used to relate the measured cross section to the number of participants N_{part}. The differences in N_{part} from this calculation compared to various Glauber calculations are used to estimate the systematic error on the exponent α shown in Fig. 1. The values for the exponents α of the scaling from pp data compared to semiperipheral Pb + Pb data are slightly higher than before, while the fit using semiperipheral up to very central Pb + Pb data yields a significantly smaller value. A further conclusion can be drawn from this corrected analysis: At high transverse momentum the increase in pion production going from pp to peripheral heavy ion reactions is much stronger than in going from semiperipheral to central heavy ion reactions.

*The names of these authors were misspelled in the original publication.

[1] K. Werner, Phys. Rep. **232**, 87 (1993).

4.1.1 Citations

1. B. Sahlmueller, *Diagnosing energy loss: PHENIX results on high-p(T) hadron spectra*, Journal of Physics G-Nuclear and Particle Physics Volume: 34 Issue: 8 Special Issue: Sp. Iss. SI Pages: S969-S973 Published: AUG 2007.
2. I. Arsene *et al.*, *Rapidity dependence of high p_T suppression at $\sqrt{s_{NN}}$ = 62.4 GeV* arXiv:nucl-ex/0602018.
3. K. Zapp, *The soft scattering contribution to jet quenching in a quark-gluon plasma and general properties of partonic energy loss* arXiv:hep-ph/0511141.
4. Berdnikov, YA (Berdnikov, Ya. A.); Zavatsky, ME (Zavatsky, M. E.); Kim, VT (Kim, V. T.); Kosmach, VF (Kosmach, V. F.); Ryzhinskiy, MM (Ryzhinskiy, M. M.); Samsonov, VM (Samsonov, V. M.) *Nuclear effects in lepton-pair production in hadron-nucleus collisions* PHYSICS OF ATOMIC NUCLEI, 69 (3): 445-451 MAR 2006 ISSN: 1063-7788
5. Berdnikov, YA; Kim, VT; Kosmach, VF; Ryzhinskiy, MM; Samsonov, VM; Zavatsky, ME *Initial-state nuclear effects in proton-nucleus collisions* EUROPEAN PHYSICAL JOURNAL **A**, 26 (2): 179-184 NOV 2005 ISSN: 1434-6001
6. Agakichieva, G; Appelshauser, H; Bielcikova, J; Baur, R; Braun-Munzinger, P; Cherlin, A; Damjanovic, S; Drees, A; Esumi, S; Faschingbauer, U; Fraenkel, Z; Fuchs, C; Gatti, E; Glassel, P; Hering, G; Heros, CPD; Holl, P; Jung, C; Lenkeit, B; Marin, A; Messer, F; Messer, M; Miskowiec, D; Nix, O; Panebrattsev, Y; Pfeiffer, A; Rak, J; Ravinovich, I; Razin, S; Rehak, P; Richter, M; Sampietro, M; Sako, H; Saveljic, N; Schmitz, W; Schukraft, J; Seipp, W; Shimanskiy, S; Socol, E; Specht, HJ; Stachel, J; Tel-Zur, G; Tserruya, I; Ullrich, T; Voigt, C; Voloshin, S; Weber, C; Wessels, JP; Wienold, T; Wurm, JP; Yurevich, V Group (CERES Collaboration) *e(+)e(-) -pair production in Pb-Au collisions at 158 GeV per nucleon* EUROPEAN PHYSICAL JOURNAL **C**, 41 (4): 475-513 JUN 2005 ISSN: 1434-6044.
7. Roland, G; Back, BB; Baker, MD; Ballintijn, M; Barton, DS; Betts, RR; Bickley, AA; Bindel, R; Busza, W; Carroll, A; Chai, Z; Decowski, MP; Garcia, E; Gburek, T; George, N; Gulbrandsen, K; Halliwell, C; Hamblen, J; Hauer, M; Henderson, C; Hofman, DJ; Hollis, RS; Holynski, R; Holzman, B; Iordanova, A; Johnson, E; Kane, JL; Khan, N; Kulinich, P; Kuo, CM; Lin, WT; Manly, S; Mignerey, AC; Nouicer, R; Olszewski, A; Pak, R; Reed, C; Sagerer, J; Seals, H; Sedykh, I; Smith, CE; Stankiewicz, MA; Steinberg, P; Stephans, GSF; Sukhanov, A; Tonjes, MB; Trzupek, A; Vale, C; van Nieuwenhuizen, GJ; Vaurynovich, SS; Verdier, R; Veres, GI; Wenger, E; Wolfs, FLH; Wosiek, B; Wozniak, K; Wyslouch, B Group (PHOBOS Collaboration) *High-PT results from PHOBOS* EUROPEAN PHYSICAL JOURNAL **C**, 43 (1-4): 281-286 AUG 2005 ISSN: 1434-6044.
8. d'Enterria, D *High p(T) leading hadron suppression in nuclear collisions at root s(NN)approximate to 20-200 GeV: data versus parton energy loss models* EUROPEAN PHYSICAL JOURNAL **C**, 43 (1-4): 295-302 AUG 2005 ISSN: 1434-6044.
9. d'Enterria, D *Relevance of baseline hard proton-proton spectra for high-energy nucleus-nucleus physics* JOURNAL OF PHYSICS **G**-NUCLEAR AND PARTICLE PHYSICS, 31 (4): S491-S512 Sp. Iss. SI APR 2005 ISSN: 0954-3899.
10. Jacobs, P; Wang, X N *Matter in extremis: ultrarelativistic nuclear collisions at RHIC* PROGRESS IN PARTICLE AND NUCLEAR PHYSICS, VOL. 54, NO 2, 54 (2): 443-534 2004 Book series title: PROGRESS IN PARTICLE AND NUCLEAR PHYSICS ISSN: 0146-6410.
11. Back, BB; Baker, MD; Ballintijn, M; Barton, DS; Betts, RR; Bickley, AA; Bindel, R; Busza, W; Carroll, A; Chai, Z; Decowski, MP; Garcia, E; Gburek, T; George, N; Gulbrandsen, K; Halliwell, C; Hamblen, J; Hauer, M; Henderson, C; Hofman, DJ; Hollis, RS; Holynski, R; Holzman, B; Iordanova, A; Johnson, E; Kane, JL; Khan, N; Kulinich, P; Kuo, CM; Lin, WT; Manly, S; Mignerey, AC; Nouicer, R; Olszewski, A; Pak, R; Reed, C; Roland, C; Roland, G; Sagerer, J; Seals, H; Sedykh, I; Smith, CE; Stankiewicz, MA; Steinberg, P; Stephans, GSF; Sukhanov, A; Tonjes, MB; Trzupek, A; Vale, C; van Nieuwenhuizen, GJ; Vaurynovich, SS; Verdier, R; Veres, GI; Wenger, E; Wolfs, FLH; Wosiek, B; Wozniak, K; Wyslouch, B *Centrality dependence of charged hadron transverse momentum spectra in Au plus Au collisions from root*

s(NN)=62.4 to 200 GeV PHYSICAL REVIEW LETTERS, 94 (8): Art. No. 082304 MAR 4 2005 ISSN: 0031-9007.

12. Wang, XN *Discovery of jet quenching and beyond* NUCLEAR PHYSICS **A**, 750 (1): 98-120 MAR 21 2005 ISSN: 0375-9474.
13. Wang, XN Title: Energy dependence of jet quenching and lifetime of dense matter in high-energy heavy-ion collisions Source: PHYSICAL REVIEW C, 70 (3): Art. No. 031901 SEP 2004 ISSN: 0556-2813
14. Di Nezza, P (HERMES Collaboration) *Hadron suppression in DIS at HERMES* JOURNAL OF PHYSICS **G**-NUCLEAR AND PARTICLE PHYSICS, 30 (8): S783-S790 Sp. Iss. SI AUG 2004 ISSN: 0954-3899.
15. d'Enterria, D *Indications of suppressed high (pT) hadron production in nucleus-nucleus collisions at CERN-SPS* PHYSICS LETTERS **B**, 596 (1-2): 32-43 AUG 19 2004 ISSN: 0370-2693.
16. Rith, K Group (HERMES Collaboration) *Selected recent HERMES results* EUROPEAN PHYSICAL JOURNAL **A**, 19: 249-256 Suppl. 1 FEB 2004 ISSN: 1434-6001.
17. Muccifora, V (HERMES Collaboration)*Hadronization in deep inelastic scattering at HERMES* JOURNAL OF PHYSICS **G**-NUCLEAR AND PARTICLE PHYSICS, 30 (1): S103-S110 Sp. Iss. SI JAN 2004 ISSN: 0954-3899.
18. Wang, XN *Why the observed jet quenching at RHIC is due to parton energy loss* PHYSICS LETTERS **B**, 579 (3-4): 299-308 JAN 22 2004 ISSN: 0370-2693.
19. Airapetian, A; Akopov, N; Akopov, Z; Amarian, M; Ammosov, VV; Andrus, A; Aschenauer, EC; Augustyniak, W; Avakian, R; Avetissian, A; Avetissian, E; Bailey, P; Baturin, V; Baumgarten, C; Beckmann, M; Belostotski, S; Bernreuther, S; Bianchi, N; Blok, HP; Bottcher, H; Borissov, A; Borysenko, A; Bouwhuis, M; Brack, J; Brull, A; Bryzgalov, V; Capitani, GP; Chiang, HC; Ciullo, G; Contalbrigo, M; Dalpiaz, PF; De Leo, R; De Nardo, L; De Santis, E; Devitsin, E; Di Nezza, P; Duren, M; Ehrenfried, M; Elalaoui-Moulay, A; Elbakian, G; Ellinghaus, F; Elschenbroich, U; Ely, J; Fabbri, R; Fantoni, A; Fechtchenko, A; Felawka, L; Fox, B; Franz, J; Frullani, S; Gapienko, G; Gapienko, V; Garibaldi, F; Garrow, K; Garutti, E; Gaskell, D; Gavrilov, G; Gharibyan, V; Graw, G; Grebeniouk, O; Greeniaus, LG; Gregor, IM; Hafidi, K; Hartig, M; Hasch, D; Heesbeen, D; Henoch, M; Hertenberger, R; Hesselink, WHA; Hillenbrand, A; Hoek, M; Holler, Y; Hommez, B; Iarygin, G; Ivanilov, A; Izotov, A; Jackson, HE; Jgoun, A; Kaiser, R; Kinney, E; Kisselev, A; Konigsmann, K; Kopytin, M; Laziev, A; Lenisa, P; Liebing, P; Lindemann, T; Lipka, K; Lorenzon, W; Lu, J; Maiheu, B; Makins, NCR; Marianski, B; Marukyan, H; Masoli, F; Mexner, V; Meyners, N; Mikloukho, O; Miller, CA; Miyachi, Y; Muccifora, V; Nagaitsev, A; Nappi, E; Naryshkin, Y; Nass, A; Negodaev, M; Nowak, WD; Oganessyan, K; Ohsuga, H; Pickert, N; Potashov, S; Potterveld, DH; Raithel, M; Reggiani, D; Reimer, PE; Reischl, A; Reolon, AR; Riedl, C; Rith, K; Rosner, G; Rostomyan, A; Rubacek, L; Ryckbosch, D; Salomatin, Y; Sanjiev, I; Savin, I; Scarlett, C; Schafer, A; Schill, C; Schnell, G; Schuler, KP; Schwind, A; Seele, J; Seidl, R; Seitz, B; Shanidze, R; Shearer, C; Shibata, TA; Shutov, V; Simani, MC; Sinram, K; Stancari, M; Statera, M; Steffens, E; Steijger, JJM; Stenzel, H; Stewart, J; Stosslein, U; Tait, P; Tanaka, H; Taroian, S; Tchuiko, B; Terkulov, A; Tkabladze, A; Trzcinski, A; Tytgat, M; Vandenbroucke, A; van der Nat, P; van der Steenhoven, G; Vetterli, MC; Vikhrov, V; Vincter, M G; Vogel, C; Vogt, M; Volmer, J; Weiskopf, C; Wendland, J; Wilbert, J; Smit, GY; Yen, S; Zihlmann, B; Zohrabian, H; Zupranski, P (HERMES Collaboration) *Quark fragmentation to pi(+/-), pi(0), K-+/-, p and (p)over-bar in the nuclear environment* PHYSICS LETTERS **B**, 577 (1-2): 37-46 DEC 18 2003 ISSN: 0370-2693.
20. Yu. A. Tarasov, *The mesons and baryons production in nucleus nucleus collisions at SPS and RHIC energies and quark gluon plasma* arXiv:hep-ph/0307300.
21. Wang, XN *Rapidity asymmetry in high-energy d + A collisions* PHYSICS LETTERS **B**, 565 (1-4): 116-122 JUL 17 2003 ISSN: 0370-2693.
22. M. Gyulassy, I. Vitev, X. N. Wang and B. W. Zhang, *Jet quenching and radiative energy loss in dense nuclear matter* arXiv:nucl-th/0302077.
23. Majka, Z *Phases of nuclear matter observed in heavy ion collisions* ACTA PHYSICA POLONICA **B**, 34 (4): 2333-2341 APR 2003 ISSN: 0587-4254.
24. Kharzeev, D; Levin, E; McLerran, L *Parton saturation and N-part scaling of semi-hard processes in QCD* PHYSICS LETTERS **B**, 561 (1-2): 93-101 MAY 22 2003 ISSN: 0370-2693.

25. Rozental, I L; Snigirev, A M *Hydrodynamic interpretation of the interaction of high-energy particles and cosmic gamma-ray bursts* PHYSICS OF PARTICLES AND NUCLEI, 34 (1): 73-93 JAN-FEB 2003 ISSN: 1063-7796.
26. Bass, S A; Muller, B; Srivastava, DK S*emihard scattering of partons at root s=17 vs 200 GeV: A study in contrast* PHYSICAL REVIEW **C**, 66 (6): Art. No. 061902 DEC 2002 ISSN: 0556-2813.
27. Vitev, I; Gyulassy, M *High-p(T) tomography of d+Au and Au+Au at SPS, RHIC, and LHC* PHYSICAL REVIEW LETTERS, 89 (25): Art. No. 252301 DEC 16 2002 ISSN: 0031-9007.
28. Cai, X; Zhou, D M *Experimental status of ultra-high energy induced nuclear reactions* HIGH ENERGY PHYSICS AND NUCLEAR PHYSICS-CHINESE EDITION, 26 (9): 971-990 SEP 2002 ISSN: 0254-3052.
29. Kvasnikova, I; Gale, C; Srivastava, D K *Production of intermediate-mass dileptons in relativistic heavy ion collisions* PHYSICAL REVIEW **C**, 65 (6): Art. No. 064903 JUN 2002 ISSN: 0556-2813.
30. Drees, A *First hints of jet quenching at RHIC* NUCLEAR PHYSICS **A**, 698: 331C-340C FEB 11 2002 ISSN: 0375-9474.
31. Srivastava, DK; Sinha, B; Kvasnikova, I; Gale, C *Emission of single photons, hadrons, and dileptons in Pb plus Pb collisions at CERN SPS and quark hadron phase transition* NUCLEAR PHYSICS **A**, 698: 432C-435C FEB 11 2002 ISSN: 0375-9474.
32. Srivastava, D K *Scaling of hadronic transverse momenta in a hydrodynamic treatment of relativistic heavy ion collisions* PHYSICAL REVIEW **C**, 64 (6): Art. No. 064901 DEC 2001 ISSN: 0556-2813.
33. Dumitru, A; Frankfurt, L; Gerland, L; Stocker, H; Stikman, M *Nuclear broadening effects on hard prompt photons at relativistic energies* PHYSICAL REVIEW **C**, 64 (5): Art. No. 054909 NOV 2001 ISSN: 0556-2813.
34. M. V. Tokarev, *Asymptotic properties of high-p(T) particle production in hadron hadron, hadron nucleus and nucleus nucleus collisions at high energies* arXiv:hep-ph/0111202.
35. G. Hering [CERES Collaboration], *Dielectron production in heavy ion collisions at 158-GeV/c per nucleon* arXiv:nucl-ex/0203004.
36. Aphecetche, L; Bacelar, J; Delagrange, H; d'Enterria, D; Hoefman, M; Huisman, H; Kalantar-Nayestanaki, N; Lohner, H; Martinez, G; Matulewicz, T; Messchendorp, J; Mora, MJ; Ostendorf, R; Schadmand, S; Schutz, Y; Seip, M; Taranenko, A; Turrisi, R; Van Goethern, MJ; Volkerts, M; Wagner, V; Wischut, HW *Hard photon and neutral pion production in cold nuclear matter* PHYSICS LETTERS **B**, 519 (1-2): 8-14 OCT 25 2001 ISSN: 0370-2693.
37. Quercigh, E *Strangeness production in ultra relativistic heavy-ion collisions* NUCLEAR PHYSICS **A**, 691 (1-2): 407C-415C AUG 13 2001 ISSN: 0375-9474.
38. Srivastava, D K *Single photons, dileptons and hadrons from relativistic heavy ion collisions and quark-hadron phase transition* PRAMANA-JOURNAL OF PHYSICS, 57 (2-3): 235-249 AUG-SEP 2001 ISSN: 0304-4289.
39. Wang, E; Wang, X N *Interplay of soft and hard processes and hadron p(T) spectra in pA and AA collisions* PHYSICAL REVIEW **C**, 64 (3): Art. No. 034901 SEP 2001 ISSN: 0556-2813.
40. Srivastava, D K; Sinha, B *Radiation of single photons from Pb+Pb collisions at relativistic energies and the quark-hadron phase transition* PHYSICAL REVIEW **C**, 64 (3): Art. No. 034902 SEP 2001 ISSN: 0556-2813.
41. Wang, X N J*et quenching and azimuthal anisotropy of large p(T) spectra in noncentral high-energy heavy-ion collisions* PHYSICAL REVIEW **C**, 63 (5): Art. No. 054902 MAY 2001 ISSN: 0556-2813.
42. I. Vitev and M. Gyulassy, *Anomalous antiproton to negative pion ratio as revealed by jet quenching at RHIC* arXiv:hep-ph/0108045.
43. M. Gyulassy, *Lectures on the theory of high energy A + A at RHIC* Lect. Notes Phys. **583** (2002) 37. [arXiv:nucl-th/0106072].
44. Blaizot, J P; Dinh, P M; Ollitrault, J Y *Transverse energy fluctuations and the pattern of J/psi suppression in Pb-Pb collisions* PHYSICAL REVIEW LETTERS, 85 (19): 4012-4015 NOV 6 2000 ISSN: 0031-9007.
45. Borghini, N; Dinh, P M; Ollitrault, J Y *Is the analysis of flow at the CERN Super Proton Synchrotron reliable?* PHYSICAL REVIEW **C**, 62 (3): Art. No. 034902 SEP 2000 ISSN: 0556-2813.

46. Antinori, F; Bakke, H; Beusch, W; Bloodworth, IJ; Caliandro, R; Carrer, N; Di Bari, D; Di Liberto, S; Elia, D; Evans, D; Fanebust, K; Fini, RA; Ftacnik, J; Ghidini, B; Grella, G; Gulino, M; Helstrup, H; Holme, AK; Huss, D; Jacholkowski, A; Jones, GT; Kinson, JB; Knudson, K; Kralik, I; Lenti, V; Lietava, R; Loconsole, RA; Lovhoiden, G; Manzari, V; Mazzoni, MA; Meddi, F; Michalon, A; Michalon-Mentzer, ME; Morando, M; Norman, PI; Pastircak, B; Quercigh, E; Rohrich, D; Romano, G; Safarik, K; Sandor, L; Segato, G; Staroba, P; Thompson, M; Thorsteinsen, TF; Torrieri, GD; Tveter, TS; Urban, J; Baillie, OV; Virgili, T; Votruba, MF; Zavada, P (WA97 Collaboration) *Transverse mass spectra of strange and multi-strange particles in Pb-Pb collisions at 158 A GeV/c* EUROPEAN PHYSICAL JOURNAL **C**, 14 (4): 633-641 JUN 2000 ISSN: 1434-6044.
47. B. V. Jacak, *High energy heavy ion collisions: The physics of super-dense matter* arXiv:nucl-ex/0010018.
48. G. Agakishiev *et al.* [CERES Collaboration], *High-p(T) charged pion production in Pb Au collisions at 158-A-GeV/c* arXiv:hep-ex/0003012.
49. U. W. Heinz and M. Jacob, *Evidence for a new state of matter: An assessment of the results from the CERN lead beam programme* arXiv:nucl-th/0002042.
50. M. V. Tokarev, O. V. Rogachevsky and T. G. Dedovich, *A-dependence of pi0 meson production in proton nucleus and nucleus nucleus collisions at high energies* preprint JINR-E2-2000-90.
51. Kolb, P F; Sollfrank, J; Ruuskanen, P V; Heinz, U *Hydrodynamic simulation of elliptic flow* NUCLEAR PHYSICS **A**, 661: 349C-352C DEC 27 1999 ISSN: 0375-9474.
52. Sandor, L Group (WA97 Collaboration) *Transverse mass spectra of strange and multiply-strange particles in Pb-Pb collisions at 158 A GeV/c* NUCLEAR PHYSICS **A**, 661: 481C-484C DEC 27 1999 ISSN: 0375-9474.
53. Srivastava, DK; Geiger, K *Scaling of particle production with number of participants in high-energy A plus A collisions in the parton-cascade model* NUCLEAR PHYSICS **A**, 661: 592C-595C DEC 27 1999 ISSN: 0375-9474.
54. Spieles, C; Vogt, R; Gerland, L; Bass, SA; Bleicher, M; Stocker, H; Greiner, W *Modeling J/psi production and absorption in a microscopic nonequilibrium approach* PHYSICAL REVIEW **C**, 60 (5): Art. No. 054901 NOV 1999 ISSN: 0556-2813.
55. Kolb, P F; Sollfrank, J; Heinz, U *Anisotropic flow from AGS to LHC energies* PHYSICS LETTERS **B**, 459 (4): 667-673 JUL 29 1999 ISSN: 0370-2693.
56. Bass, SA; Gyulassy, M; Stocker, H; Greiner, W *Signatures of quark-gluon plasma formation in high energy heavy-ion collisions: a critical review* JOURNAL OF PHYSICS **G**-NUCLEAR AND PARTICLE PHYSICS, 25 (3): R1-R57 MAR 1999 ISSN: 0954-3899.
57. D. K. Srivastava and K. Geiger, *Scaling of particle production with number of participants in high-energy A + A collisions in the parton-cascade model* arXiv:nucl-th/9808042.
58. M. Gyulassy and P. Levai, *High p(T) phenomena in heavy ion collisions at s**(1/2) = 20-A-GeV and 200-A-GeV* arXiv:hep-ph/9809314.

4.1.2 Conference presentations

1. M. Šumbera, *Ultra-relativistic nucleus-nucleus collisions: past, present and future (from CERN to BNL and back)* . Czech-Taiwan workshop on the intermediate and high energy physics, Prague, March 3.-5. 2003. Czechoslovak Journal of Physics, Volume 53, Number 8 / August, 2003.

4.1.3 Further developments

In [81] we have studied transverse energy, charged particle pseudorapidity distributions and photon transverse momentum spectra of particles produced in 158·A GeV Pb+Pb collisions. The data covered a wide impact parameter range which allowed us to study the dependence of the above quantities on the number of participants (N_{part}) and the number of binary nucleon-nucleon collisions (N_{coll}). A scaling of the transverse

energy pseudorapidity density at midrapidity as $\sim N_{part}^{1.08\pm0.06}$ and $\sim N_{coll}^{0.83\pm0.05}$ was observed. We have also determined the average transverse energy per charged particle at midrapidity

$$\langle E_T\rangle/\langle N_{ch}\rangle|_{mid} \equiv \langle dE_T/d\eta|_{mid}\rangle/\langle dN_{ch}/d\eta|_{mid}\rangle, \tag{4.1}$$

a quantity that can be seen as a measure of the global mean transverse momentum averaged over all particle species. $\langle E_T\rangle/\langle N_{ch}\rangle|_{mid}$ appears to increase up to a system size of $N_{part} \approx 100$ which corresponds to an impact parameter of $b \approx 9$ fm. For more central collisions $\langle E_T\rangle/\langle N_{ch}\rangle|_{mid}$ levels off at a value of 0.80 GeV. Similarly to the analysis performed in 4.1 we conclude that the most natural explanation of such a behavior would be the assumption that thermalization is reached once the system exceeds a certain minimum size.

Article reprint

ELSEVIER

19 February 1998

PHYSICS LETTERS B

Physics Letters B 420 (1998) 169–179

Search for disoriented chiral condensates in 158 AGeV Pb + Pb collisions

WA98 Collaboration

M.M. Aggarwal [a], A. Agnihotri [b], Z. Ahammed [c], A.L.S. Angelis [d], V. Antonenko [e], V. Arefiev [f], V. Astakhov [f], V. Avdeitchikov [f], T.C. Awes [g], P.V.K.S. Baba [h], S.K. Badyal [b], A. Baldine [f], L. Barabach [f], C. Barlag [i], S. Bathe [i], B. Batiounia [f], T. Bernier [j], K.B. Bhalla [b], V.S. Bhatia [a], C. Blume [i], R. Bock [k], E.-M. Bohne [i], D. Bucher [i], A. Buijs [l], E.-J. Buis [l], H. Büsching [i], L. Carlen [m], V. Chalyshev [f], S. Chattopadhyay [c], R. Cherbatchev [e], T. Chujo [n], A. Claussen [i], A.C. Das [c], M.P. Decowski [r], V. Djordjadze [f], P. Donni [d], I. Doubovik [e], M.R. Dutta Majumdar [c], K. El Chenawi [m], S. Eliseev [o], K. Enosawa [n], P. Foka [d], S. Fokin [e], V. Frolov [f], M.S. Ganti [c], S. Garpman [m], O. Gavrishchuk [f], F.J.M. Geurts [l], T.K. Ghosh [p], R. Glasow [i], S.K. Gupta [b], B. Guskov [f], H.A. Gustafsson [m], H.H. Gutbrod [j], R. Higuchi [n], I. Hrivnacova [o], M. Ippolitov [e], H. Kalechofsky [d], R. Kamermans [l], K.-H. Kampert [i], K. Karadjev [e], K. Karpio [q], S. Kato [n], S. Kees [i], H. Kim [g], i B.W. Kolb [k], I. Kosarev [f], I. Koutcheryaev [e], A. Kugler [o], P. Kulinich [r], V. Kumar [b], M. Kurata [n], K. Kurita [n], N. Kuzmin [f], I. Langbein [k], A. Lebedev [e], Y.Y. Lee [k], H. Löhner [r], L. Luquin [j], D.P. Mahapatra [s], V. Manko [e], M. Martin [d], A. Maximov [f], R. Mehdiyev [f], G. Mgebrichvili [e], Y. Miake [n], D. Mikhalev [f], G.C. Mishra [s], Y. Miyamoto [n], D. Morrison [t], D.S. Mukhopadhyay [c], V. Myalkovski [f], H. Naef [d], B.K. Nandi [s], S.K. Nayak [t], T.K. Nayak [c], S. Neumaier [k], A. Nianine [e], V. Nikitine [f], S. Nikolaev [e], S. Nishimura [n], P. Nomokonov [f], J. Nystrand [m], F.E. Obenshain [t], A. Oskarsson [m], I Otterlund [m], M. Pachr [o], A. Parfenov [f], S. Pavliouk [f], T. Peitzmann [i], V. Petracek [o], F. Plasil [g], M.L. Purschke [k], B. Raeven [l], J. Rak [o], S. Raniwala [b], V.S. Ramamurthy [s], N.K. Rao [h], F. Retiere [j], K. Reygers [i], G. Roland [r], L. Rosselet [d], I. Roufanov [f], C. Roy [j], J.M. Rubio [d], H. Sako [n], S.S. Sambyal [b], R. Santo [i], S. Sato [n], H. Schlagheck [i], H.-R. Schmidt [k], G. Shabratova [f], I. Sibiriak [e], T. Siemiarczuk [q], B.C. Sinha [c], N. Slavine [f], K. Söderström [m], N. Solomey [d], S.P. Sørensen [t],

PII S0370-2693(97)01528-1

P. Stankus [g], G. Stefanek [q], P. Steinberg [r], E. Stenlund [m], D. Stüken [i], M. Sumbera [o], T. Svensson [m], M.D. Trivedi [c], A. Tsvetkov [e], C. Twenhöfel [l], L. Tykarski [q], J. Urbahn [k], N. v. Eijndhoven [l], W.H. v. Heeringen [l], G.J. v. Nieuwenhuizen [r], A. Vinogradov [e], Y.P. Viyogi [c], A. Vodopianov [f], S. Vörös [d], M.A. Vos [l], B. Wysłouch [r], K. Yagi [n], Y. Yokota [n], G.R. Young [g]

[a] *University of Panjab, Chandigarh 160014, India*
[b] *University of Rajasthan, Jaipur 302004, Rajasthan, India*
[c] *Variable Energy Cyclotron Centre, Calcutta 700 064, India*
[d] *University of Geneva, CH-1211 Geneva 4, Switzerland*
[e] *RRC (Kurchatov), RU-123182 Moscow, Russia*
[f] *Joint Institute for Nuclear Research, RU-141980 Dubna, Russia*
[g] *Oak Ridge National Laboratory, Oak Ridge, TN 37831-6372, USA*
[h] *University of Jammu, Jammu 180001, India*
University of Münster, D-48149 Münster, Germany
[j] *SUBATECH, Ecole des Mines, Nantes, France*
[k] *Gesellschaft für Schwerionenforschung (GSI), D-64220 Darmstadt, Germany*
[l] *Universiteit Utrecht / NIKHEF, NL-3508 TA Utrecht, The Netherlands*
[m] *University of Lund, SE-221 00 Lund, Sweden*
[n] *University of Tsukuba, Ibaraki 305, Japan*
[o] *Nuclear Physics Institute, CZ-250 68 Rez, Czech Republic*
[p] *KVI, University of Groningen, NL-9747 AA Groningen, The Netherlands*
[q] *Institute for Nuclear Studies, 00-681 Warsaw, Poland*
[r] *MIT Cambridge, MA 02139, USA*
[s] *Institute of Physics, 751 005 Bhubaneswar, India*
[t] *University of Tennessee, Knoxville, TN 37966, USA*

Received 1 October 1997; revised 23 November 1997
Editor: L. Montanet

Abstract

The restoration of chiral symmetry and its subsequent breaking through a phase transition has been predicted to create regions of Disoriented Chiral Condensates (DCC). This phenomenon has been predicted to cause anomalous fluctuations in the relative production of charged and neutral pions in high-energy hadronic and nuclear collisions. The WA98 experiment has been used to measure charged and photon multiplicities in the central region of 158 AGeV Pb + Pb collisions at the CERN SPS. In a sample of 212646 events, no clear DCC signal can be distinguished. Using a simple DCC model, we have set a 90% C.L. upper limit on the maximum DCC production allowed by the data. © 1998 Elsevier Science B.V.

1. Introduction

The approximate chiral symmetry of the QCD vacuum is believed to be spontaneously broken in nature by the formation of an isoscalar quark condensate. Disoriented Chiral Condensates (DCC) may form in large, hot regions of hadronic matter where this symmetry has been briefly restored [1]. A DCC has an equal probability to be in any state related to the normal vacuum by a chiral rotation. By projecting the space of these available states onto a basis of definite isospin, it has been found that the charge distribution of pions emitted from a single, large DCC domain has a characteristic form [2,3]:

$$P(f) = \frac{1}{2\sqrt{f}} \qquad (1)$$

where f is the neutral fraction,

$$f = \frac{N_{\pi^0}}{N_{\pi^0} + N_{\pi^+} + N_{\pi^-}} \tag{2}$$

where N_{π^0}, N_{π^+} and N_{π^-} are respectively the numbers of neutral, positive and negative pions produced. This allows the possibility of hadronic interactions with anomalous fluctuations between charged pions and neutral pions, as seen through their two-photon decay channel.

The phenomenology of DCCs was first introduced in the context of hadronic collisions by Bjorken et al., whose "Baked Alaska" model [4] postulated that a hot shell, expanding at the speed of light, could shield the cool interior from the influence of the normal vacuum outside, allowing a large region of DCC to form. Rajagopal and Wilczek [5,6] studied the production of DCCs in nuclear collisions by studying the chiral phase transition in QCD, via its similarity to the O(4) Heisenberg magnet [7]. Through numerical simulations, they found that as the system rapidly expands and cools through the phase transition, the equations of motion induce a non-equilibrium relaxation of the chiral fields which amplifies the production of soft pion modes in a well-defined chiral direction. This effectively creates clusters of low-p_t pions, with the cluster charge distribution following Eq. (1). It should be noted that, in both studies, the strongest influence on the final state composition is the symmetry itself rather than the exact physics scenario studied. Further work confirmed these initial results, even after accounting for quantum fluctuations, and proposed other mechanisms which might allow for large, long-lived DCCs [1].

By allowing the possibility of events with almost no electromagnetic energy, DCCs are an attractive hypothesis to explain the "Centauro" events seen in cosmic rays [8]. These events have already motivated searches for unusual charge fluctuations at the $S\bar{p}pS$ (by UA1 [9] and UA5 [10]) and at the Tevatron (by Minimax [11] and CDF [12]). And yet, there have been no systematic studies utilizing the simultaneous measurement of charged and neutral multiplicities in heavy ion collisions at any energy. It has been argued [1] that heavy ion collisions at SPS energies, the highest currently available, might create the large volumes which favor the development of long-wavelength oscillations within the reaction zone. It is true that large baryon number in the central region complicates theoretical calculations and may obscure the initial signal via the rescattering of secondaries. It is also possible that most of the pions measured in pp collisions at comparable energies are produced resonantly [13], leaving few "direct" pions which may be influenced by a DCC. We must keep in mind, however, that these are extrapolations from lower energies and smaller systems. Their cumulative effect is uncertain, especially at higher energies where the formation of a quark-gluon plasma would render previous measurements inapplicable. In any case, in the absence of any substantial experimental evidence for or against DCCs in heavy ion collisions at SPS energies, and a great deal of theoretical evidence in their favor, it is imperative to simultaneously measure charged and neutral particles at the SPS and analyze their fluctuations to perhaps isolate a DCC signal. Observing such a signal might be an indication of the chiral phase transition in hot nuclear matter.

2. Experimental setup

The WA98 experiment [14] is a general-purpose, large-acceptance photon and hadron spectrometer with the ability to measure several different global observables event-by-event. For this search, we use a subset of the full apparatus, shown schematically in Fig. 1. We measure charged particles with a Silicon Pad Multiplicity Detector (SPMD) and photons with a Photon Multiplicity Detector (PMD). Using these, we are able to count charged particles and photons in the central pseudorapidity region on an event-by-event basis. For a determination of the centrality of each collision, we use the transverse energy (E_T) measured in the Midrapidity Calorimeter (MIRAC [15]). For removal of background events, we also use the Zero-Degree Calorimeter (ZDC) and the Plastic Ball detector [16].

2.1. Charged particle multiplicity

We count charged particles using a circular Silicon Pad Multiplicity Detector (SPMD) [17] located

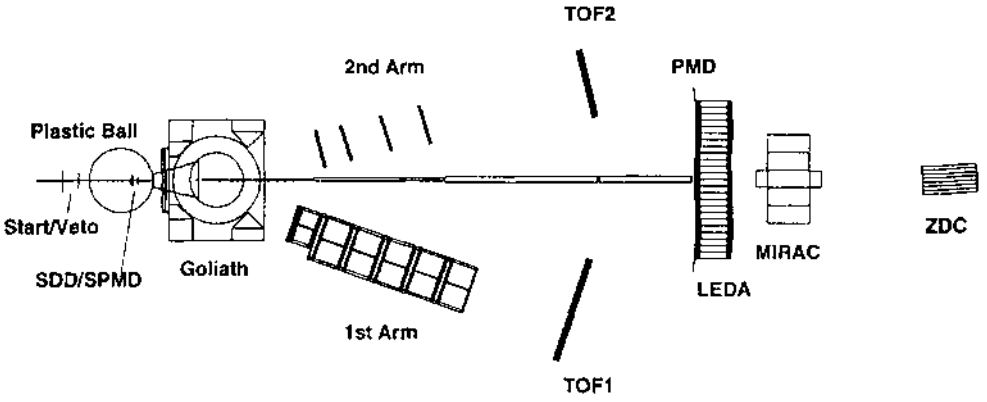

Fig. 1. The WA98 Experiment at the CERN SPS. This analysis uses the Silicon Pad Multiplicity Detector (SPMD) and the Photon Multiplicity Detector (PMD) to measure the charged and neutral multiplicity for each event, and the Mid-Rapidity Calorimeter (MIRAC) for the measurement of event centrality.

32.8 cm from the target covering $2.35 < \eta < 3.75$, the central rapidity region at SPS energies (where $\eta_{CMS} = 2.9$), and full azimuth. The detector consists of four overlapping quadrants, each fabricated from a single 300 μm thick silicon wafer. The active area of each quadrant is divided into 1012 pads forming 46 azimuthal wedges and 22 radial bins with a pad size increasing with radius to provide uniform pseudorapidity coverage. The efficiency of detecting a charged particle in the active area has been determined in a test beam to be better than 99%. Conversely, the detector is transparent to high energy photons, since only about 0.2% are expected to interact in the silicon. During the data taking, 95% of the pads worked properly and are used in this analysis.

In a central Pb + Pb collision, the occupancy can be as high as 20%, implying that $\approx 20\%$ of the hit pads contain two or more particles, a "hit" being defined as a pad with a deposited energy exceeding 1/2 of the most probable energy loss. An unbiased way to estimate the total number of charged particles in a given event under such conditions is to use the sum of the energy deposited in hit pads divided by the mean energy loss per particle as determined in low-multiplicity events:

$$N_{ch} = \sum_{i=\text{hits}} \frac{dE/dx_i}{\langle dE/dx \rangle}.$$

Because of the fluctuations in the energy loss, described by a Landau distribution, the uncertainty on N_{ch} can be estimated to be $\Delta N_{ch}/N_{ch} = 60\%/\sqrt{N_{ch}}$, the numerator being the width of the Landau distribution with the peak normalized to 1. For typical central events with a multiplicity of ≈ 600, this gives an uncertainty of about 2%. To check the overall scale, we compare the results with the multiplicity obtained by assuming that the particles are distributed uniformly so the multi-hit probability is given by Poisson statistics. A simple calculation gives $N'_{ch} = -N_{pads}\log(1 - N_{hits}/N_{pads})$, where N_{pads} is the total number of pads, and N_{hits} is the total number of hits. Using this as a check, we estimate the systematic error on N_{ch}, due to uncertainties in the gains and backgrounds, to be about 4%.

2.2. *Photon multiplicity*

We count photons in the preshower Photon Multiplicity Detector (PMD) situated 21.5 m from the target, covering the region $2.8 < \eta < 4.4$. The photons impinging on the detector are converted in 3.34 X_0 thick lead and iron and the secondaries are detected in 3mm-thick square plastic scintillator pads of varying sizes (15mm, 20mm and 23mm). A matrix of 50 × 38 pads is placed in one light-tight box module and read out individually via wavelength shifting optical fibers coupled to an image intensifier and CCD camera system similar to that described in [18]. The modules with smaller pads were mounted in the forward angle region to minimize cluster overlap at large multiplicities and to provide reason-

ably uniform occupancy. Out of a total of 28 box modules implemented in the PMD, the data presented here correspond to 19 box modules having 35524 pads. The average occupancy for the part of the detector considered in the present case is around 15% for central events.

The principle of photon identification makes use of the fact that photons are more likely to shower in the lead converter and produce a large signal in the scintillator pads, while non-showering hadrons will produce a signal corresponding to a single minimum ionizing particle (MIP). Signals from several neighbouring pads are combined to form clusters and those with energy deposition larger than that corresponding to 3 MIPs are considered to be "γ-like" clusters. We denote the number of γ-like clusters in each event as "$N_{\gamma\text{-like}}$". This selection criteria gives an average photon counting efficiency of about 70% which is almost uniform over the range of centrality and pseudorapidity considered. It also creates an effective lower p_T cutoff of 30 MeV/c, at which point the efficiency falls below 35%. About 15% of the produced hadrons impinging on the PMD interact in the converter, generating secondaries which also deposit large energy on the detector. This contamination constitutes a background to photon counting. In order to minimize effects due to variations in the angular distributions of charged particles, we only use data with the Goliath magnet turned off.

The lead target, the exit window of the vacuum chamber (extending to the edge of the magnet), and the air gap between the magnet and the PMD constitute about 10% X_0 of material upstream of the PMD. Although some low-energy photons tend to convert in the material and escape detection, higher-energy photons tend to be detected via a high-energy conversion electron or positron.

The photon counting efficiency, hadron contamination and the associated errors are derived using test beam data and GEANT simulation using a method similar to the ones described in [18,19]. The level of hadron contamination in the PMD was verified by comparing the azimuthal distribution of hits for magnet-on and magnet-off data [20]. The azimuthal distribution of charged tracks becomes very non-uniform in the presence of the magnetic field, the amount of non-uniformity indicating the magnitude of the hadron contamination.

It should be emphasized that in this analysis, we do not correct the data using the abovementioned parameters. Instead we account for all of the detector effects by fully simulating the conversion of particles in the detector, as described below.

2.3. Data and event selection

In this analysis, we study reactions induced by a 158 AGeV Pb beam incident upon a 213 μm thick ^{208}Pb target. The fundamental "beam" trigger condition consists of a signal in a gas Čerenkov start counter [21] located 3.5 meters upstream of the target and no coincident signal in a veto counter with a 3mm circular hole located 2.7 meters upstream from the target. A beam trigger is considered to be a minimum-bias interaction if the transverse energy sum in the full MIRAC acceptance exceeds a lower threshold.

Pileup events are eliminated by a combination of the start counter ADC, which measures the number of beam particles passing through the counter, and a system of TDCs each started by a particular trigger counter and stopped by a second trigger. Using these, we remove events where a second interaction trigger occurred within a $\pm$ 10μs window before and after the recorded event. After these cuts, we estimate that .02% of the remaining events are due to pileup. In addition pileup events are eliminated by requiring the sum of energy deposited in the MIRAC ($3.5 < \eta < 5.5$) and ZDC ($\eta > 6$) to be consistent with a single event. This leaves us with .01% of the event sample which may contain pileup events with less than 70 additional particles at mid-rapidity. After applying all cuts, 70% of the data sample remains.

3. General features of data and comparison with VENUS 4.12

To describe the bulk of the data, we use the VENUS 4.12 [22] event generator with its default settings. To compare VENUS with our data, we propagate the raw generator output through a full simulation of our experimental setup using the GEANT 3.21 [23] package from CERN. The simulation incorporates the detector physics effects and

folds them into the generated data, which is then analyzed using the same code used for the raw experimental data. In the rest of this paper, the term "VENUS" refers to the combination of VENUS 4.12 and the full GEANT 3.21 detector simulation, not to the raw generator output, unless otherwise specified.

The SPMD simulation includes the effect of Landau fluctuations in the energy loss of charged particles in the silicon and the pad geometry of the detector. In addition to the secondaries from the ion-ion collision itself, the SPMD is also sensitive to the beam halo as well as the δ-rays generated by the $^{82+}$Pb ion passing through the lead target. Since we have no means by which to distinguish the two components, we refer to all of the particles produced in beam events as "δ-rays". We can get a conservative estimate of the δ-ray multiplicity in physics events by studying events that satisfy the conditions for a beam trigger but not the interaction trigger. These "beam" events have a mean multiplicity in the SPMD of $11.4 \pm .5$ and a width of $5.9 + .3$. The angular distribution is consistent with a spatially uniform illumination of the detector surface. To include these ion-induced δ-rays in the simulation, we sample the measured charged multiplicity distribution for beam events and add it to the charged particle multiplicity for each simulated event. We estimate the uncertainty in the absolute scale of N_{ch} from the simulation to be less than 3% and the relative uncertainty between data and VENUS to be less than 2%.

The PMD simulation also incorporates the effects of additional fluctuations to the energy loss arising due to the statistical nature of the scintillation process; light transport through the wavelength shifting fibres and the image intensifier chains; and imperfections in the electro-optical imaging. The widths due to this extra fluctuation were obtained by a comparison of the GEANT and test beam results using single pions and electrons at various energies. As all of the readout chains were not used in the test beam experiment, a method of detailed intercomparison of the various features of data and simulation was used to obtain the gains of the individual readout units. We estimate the uncertainty on the absolute multiplicity scale of simulated γ-like clusters, due to uncertainties in various parameters of the simulation and data analysis, to be 15%, and that the relative uncertainty between data and VENUS is 5%.

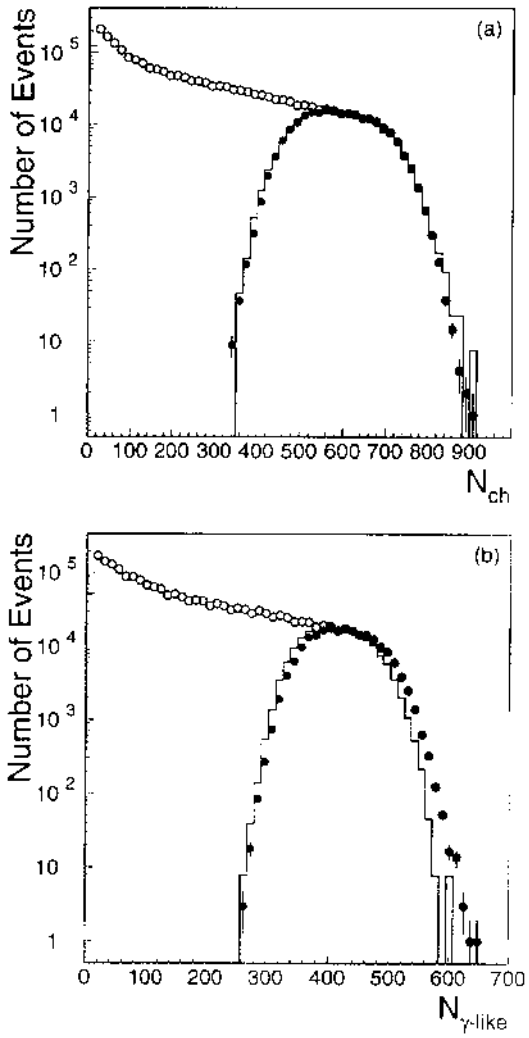

Fig. 2. The charged and neutral multiplicity distributions are shown in a) and b). The open circles represent the minimum-bias distribution. The "central" sample ($E_T > 300$ GeV) is represented by closed circles for the data and by histograms for VENUS.

In Figs. 2a and 2b we present the minimum-bias multiplicity distribution for charged particles and γ-like clusters. For the DCC search, we will concentrate on the most central events, defined by a measured transverse energy of at least 300 GeV in $3.5 < \eta < 5.5$. These correspond roughly to 10% of the measured Pb + Pb minimum bias cross section $\sigma_{\text{tot}} = 6200 \pm 620$ mb. After all cuts are applied,

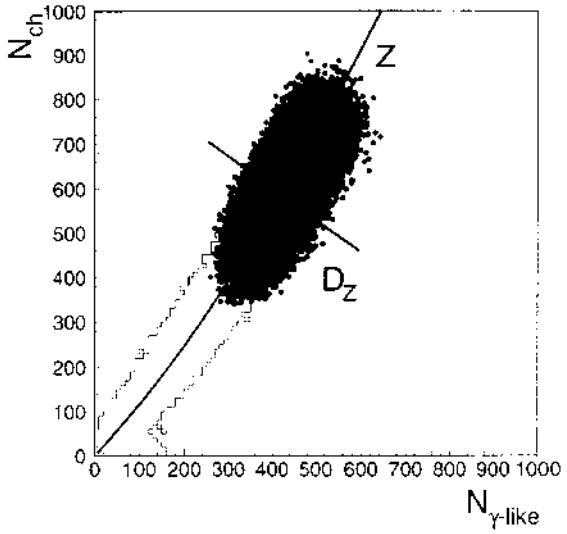

Fig. 3. The scatter plot showing the correlation between N_{ch} and $N_{\gamma\text{-like}}$. The solid outline shows the trend of the minimum bias data. The central sample (with $E_t > 300$ GeV) is shown as points for the data and as a hatched region for VENUS (with much lower statistics). Overlaid on the plot are the Z axis and the D_Z axis at a particular value of Z as explained in the text.

there are 212646 events in this sample, which we will refer to as the "central" sample in the rest of this paper. The central data sample is shown by closed circles in Figs. 2a and 2b and a comparison with VENUS events chosen by identical cuts is shown by the histogram. The correlation between the charged and neutral multiplicities is presented in Fig. 3 with the minimum bias distribution outlined, the central VENUS events hatched, and the central data events shown as scattered points, each point corresponding to a single event.

The most distinctive feature of the scatter plot is the strong correlation between the charged and neutral multiplicities. A reasonable explanation of this would be if most of the produced particles are pions with their charge states partitioned binomially, as measured in pp experiments at similar energies [24,25]. A binomial distribution leads to a correlation width $\sigma(N_{ch} - N_\gamma) \propto \sqrt{N_{ch} + N_\gamma}$, which would explain the very tight correlation, since the relative fluctuations are proportional to $1/\sqrt{N_{ch} + N_\gamma}$ and $N_\gamma \propto N_{\gamma\text{-like}}$. As this is seen in both data and VENUS, we can study the contributions to the different multiplicities to verify this hypothesis. In fact, about 80% of the charged particles produced in VENUS and detected in the SPMD are pions, the rest being protons and kaons. Most of the particles are produced at the interaction vertex, the rest being from η and strange decays, 12% coming from V_0's alone. About 85% of produced photons come from π^0 decays. Thus, by simply counting the charged particles and photons produced in a heavy ion collision, we have a reasonable estimate of the number of charged and neutral pions created.

We verify the binomial nature of the charge fluctuations in VENUS by studying its "binomiality":

$$B = \frac{N_{\pi_{ch}} - p_{ch} N_\pi}{\sqrt{p_{ch}(1 - p_{ch}) N_\pi}} \tag{3}$$

where $N_{\pi_{ch}}$ and N_π are number of charged pions and the total number of pions for each event, and $p_{ch} = N_{\pi_{ch}}/N_\pi$ is the probability that a pion is charged. For a pure binomial distribution, $p_{ch} = 2/3$ and B has a Gaussian distribution with a mean at zero and an RMS of one. For VENUS without GEANT, we find an RMS of approximately .95 for pions produced in the central rapidity region in events with an impact parameter less than 6 fm. This is consistent with the hypothesis that the correlation arises mainly from the binomial partition of N_π, the total pion multiplicity.

4. Event-by-event search for DCCs

DCCs should modify the binomial partitioning of N_π into charged and neutral pions. Events in which a DCC is produced (henceforth referred to as "DCC events") will show up as deviations from the binomial behavior and appear as outliers with respect to the bulk of the data. We have already discussed that the charged and neutral multiplicities are directly sensitive to the charged and neutral pion multiplicities in each event. Thus, DCC events should appear in the correlation of charged and neutral multiplicities, while the individual distributions will be mainly unaffected.

4.1. Data analysis

The strong correlation between charged and neutral multiplicities described above suggests a more

appropriate coordinate system with one axis being the measured correlation axis and the other perpendicular to it. If all detected particles were pions and the detectors were perfect and had identical pseudorapidity acceptance, then the correlation axis would be a straight line. Instead, we must account for the fact that at high multiplicities, the pseudorapidity distributions tend to narrow, changing the relative acceptance of charged and neutral particles due to the non-identical apertures of the SPMD and PMD. Moreover, the large occupancies in the PMD lead to a slight saturation effect. It is then useful to define a coordinate system consisting of a correlation axis (Z) described by a second-order polynomial, and the perpendicular distance (D_Z) from it, which is defined to be positive for points below this Z axis. These axes are shown superimposed on Fig. 3 and the projection along the Z-axis is shown in Fig. 4a. The full projection along the D_Z-axis is shown in Fig. 4b. To a very good approximation, the data are Gaussian distributed, which is consistent with binomial partition. The VENUS results, shown by the histogram, are also Gaussian, but with a slightly smaller width.

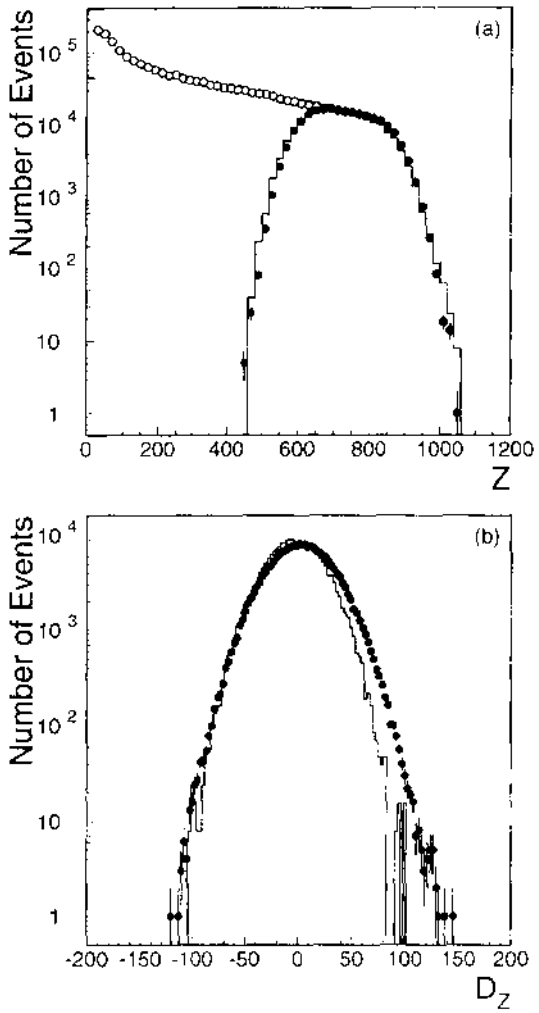

Fig. 4. a.) The distribution of Z, with the same conventions as in Fig. 2. b.) The distribution of D_Z in the "central" sample for the data (closed circles) and for VENUS (histogram). The difference in the mean between the two distributions arises due to the overall scale differences discussed in Section 3.

In both cases, σ_{D_Z}, the standard deviation of a gaussian fit in the D_Z direction, increases with increasing Z. We have chosen to work with the scaled variable $S_Z \equiv D_Z/\sigma_{D_Z}$ in order to compare relative fluctuations at different multiplicities. While binomial partition leads to fluctuations that grow as $\sqrt{N_\pi}$, the data as well as VENUS follow a slightly different power law, due to the presence of contaminating particles, like nucleons kaons, and etas. A reasonable parametrization of σ_{D_Z} for $Z > 200$ has been found to be $\sigma_{D_Z} = C + Z^\beta$ where $C = 7.5 \pm .1$ for the data, and $C = 4.8 \pm .1$ for the simulated events, the exponent being fixed to $\beta = .46$ in both cases. The discrepancy between VENUS and the data can be seen more clearly by measuring the width of the S_Z distribution with the σ_{D_Z} in the denominator taken from the simulation. The VENUS distribution is a gaussian of width $.998 \pm .002$ (fit error only) and the data is also gaussian, of width $1.13 \pm .07$ (error from relative scale uncertainties included). Henceforth, S_Z will refer to D_Z/σ_{D_Z}(VENUS) unless otherwise specified.

4.2. Model of DCC production

To estimate the effect of DCC production we have modified the VENUS events to include characteristic fluctuations in the relative production of charged and neutral pions. We assume that only a single domain of DCC is formed in each central collision. A certain fraction $\zeta = N_\pi^{\mathrm{DCC}}/N_\pi$ of the VENUS pions is associated with this domain (where N_π^{DCC} is the number of DCC pions) and a value of f

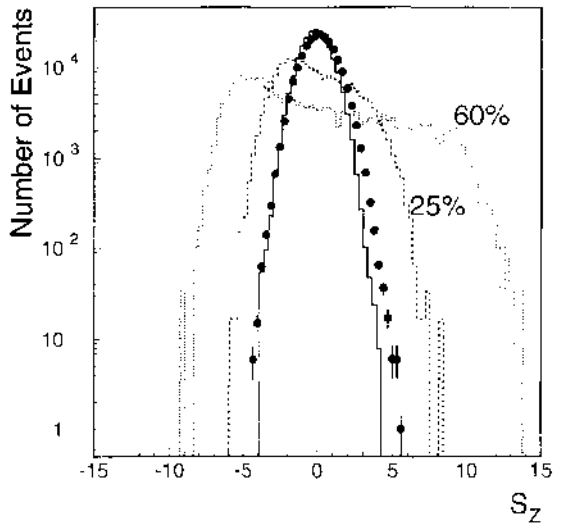

Fig. 5. S_Z distribution for the experimental data is shown, overlaid with VENUS simulations incorporating 0%, 25% and 60% DCC in every event. All of the distributions are normalized to the total number of real events.

is chosen randomly according to the distribution shown in Eq. (1). Then the charges of the pions are interchanged pairwise ($\pi^+\pi^-$ or $\pi^0\pi^0$) until the charge distribution matches the chosen value of f. We do not modify the momentum of the chosen pions, therefore the momentum spectrum of pions produced by a DCC is the same as for the non-DCC pions. This simulates a DCC accompanied by the normal hadronic background in a way that conserves energy, momentum, and charge. The S_Z distribution for the $\zeta = 0\%$, 25% and 60% DCC hypotheses are shown in Fig. 5 with the data overlaid as closed circles. It is clear that the distributions get wider as ζ is increased.

4.3. Upper limit calculation

As seen in the previous section, DCC events will show up as non-statistical tails on the D_Z axis. We see no such events in our data sample. Thus, we are faced with the possibilities that single-domain DCCs are very rare, very small, or both. To check which hypotheses are consistent with our data, we determine upper limits on the frequency of DCC production as a function of its size, as represented by ζ.

We have computed S_Z distributions for several values of ζ, ranging from 15% to 90%. To define an efficiency for detecting DCCs, we start from the observation that the distribution assuming the null hypothesis is Gaussian. With our statistics, we expect few events farther than 5 to 6 σ from the mean. An event containing a DCC, however, has an enhanced probability of being found in this region. The cut $|S_Z| > S_{\rm cut}$ then defines a two-dimensional region in the scatter plot in which all events are considered to be "DCC candidates". Once the cut is set, the DCC efficiency is defined, for $N_{\rm MC}$ VENUS events, as

$$\epsilon(S_{\rm cut},\zeta) = \frac{N(|S_Z| > S_{\rm cut},\zeta)}{N_{\rm MC}} \tag{4}$$

which is a function of both the DCC fraction and the cut position.

The expected non-DCC background is determined by a Gaussian fit to the VENUS distribution assuming $\zeta = 0$, in order to extrapolate beyond the Monte Carlo statistics. With the efficiency and background determined, we calculate the Poisson upper limit $N_{\rm C.L.}$ for a 90% confidence level, which is ≈ 2.3 if there are no measured events over the cut and no background events are expected. These three numbers are combined into an upper limit, for $N_{\rm Data}$ central events, via the formula:

$$\frac{N_{\rm DCC}}{N_{\rm Data}}(S_{\rm cut},\zeta) \le \frac{N_{\rm C.L.}}{\epsilon(S_{\rm cut},\zeta)}\frac{1}{N_{\rm Data}} \tag{5}$$

where $N_{\rm DCC}$ is the number of DCC events.

We have calculated limits for two scenarios. The first is based upon the conservative assumption that VENUS should describe the data perfectly in the absence of a DCC signal. Under these assumptions, $S_Z = D_Z/\sigma_{D_Z}$(VENUS) as obtained from VENUS (the default procedure) and $S_{\rm cut} = 6$., which is well away from the data point with the largest S_Z. The 90% C.L. limit is presented in Fig. 6 as a solid line. The other scenario assumes that the difference between the data and VENUS is due to detector effects and that the widths should be the same. In this case, $S_Z = D_Z/\sigma_{D_Z}$(data), with σ_{D_Z} taken from the data, and we choose a tighter cut $S_{\rm cut} = 5$. This limit is presented in the same figure as a dashed line. The two limits are quite different at $\zeta = 15\%$ but get closer at $\zeta > 30\%$. In both cases, the uncertainty in the absolute comparisons between the data and

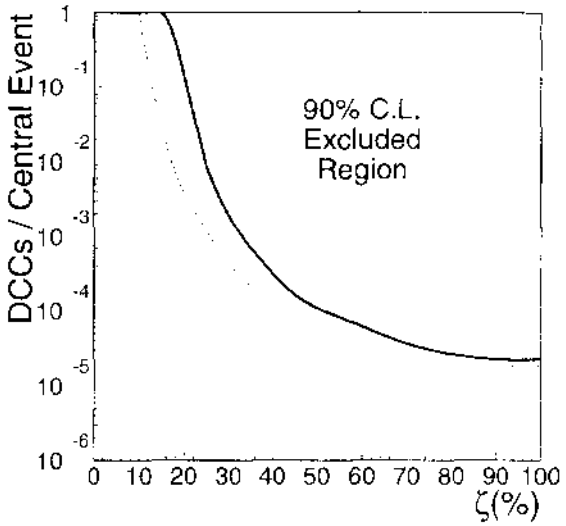

Fig. 6. 90% C.L. upper limit on DCC production per central event as a function of the fraction of DCC pions under two assumptions. The thick line gives the upper limit obtained by assuming the σ_{D_ζ} in S_ζ is completely given by the VENUS calculation requiring to make a cut at 6σ. The dashed line shows a less conservative limit obtained by using the σ_{D_ζ} measured in the data itself. This allows us to make a tighter cut at 5σ, increasing the DCC detection efficiency.

VENUS have not been included in the upper limit estimate.

5. Discussion

Earlier studies estimated the DCC radius to be around $R \approx 3$–4 fm. Coupled with a vacuum energy density u given by the chiral effective potential to be 60–120 MeV/fm^3, and an assumed Gaussian p_t distribution of width $\approx 1/R$, an average DCC was thought to generate $\frac{4}{3}\pi R^3(u/m_\pi) \approx 50$–230 pions [26]. The SPMD sees all of the charged particles produced in the central rapidity region, 80% of which are pions, letting us estimate the total number of centrally produced pions in an average event to be about 720. Thus, we would expect a DCC to correspond to $\zeta \approx$ 5–30%. Our analysis clearly rules out anything larger than about 25% within the scope of the assumed model, but cannot say much about anything smaller. However, if the pions tend to cluster in phase space, there are methods that should be able to find DCC events, and these are currently under study [27,28].

A small and frequent DCC might also appear as a slightly enhanced width, similar to what we observe in our data when compared to VENUS. However, this enhancement could also result from uncertainties in the detector modelling or the underlying physics model itself. For instance, theoretical uncertainties might arise because no model has ever been used to study charge correlations in heavy ion collisions. Rescattering phenomena, resonances, or Bose-Einstein effects may have predictable effects on the expected binomial distribution. These issues will be addressed in future studies.

6. Conclusions

We have used the WA98 apparatus to perform the first search for the production of Disoriented Chiral Condensates in 158 AGeV Pb + Pb collisions. No events with large charged-neutral fluctuations have been observed. By comparing the correlations of the charged and neutral multiplicity, measured on an event-by-event basis, to a simple model incorporating a DCC signal into VENUS 4.12 events, we have set a 90% CL upper limit on the frequency of DCC production as a function of its size.

Acknowledgements

We wish to express our gratitude to the CERN accelerator division for excellent performance of the SPS accelerator complex. We acknowledge with appreciation the effort of all engineers, technicians and support staff who have participated in the construction of the this experiment. This work was supported jointly by the German BMBF and DFG, the US DOE, ORISE, the Swedish NFR, the Dutch Stichting FOM, the Stiftung fuer Deutsch-Polnische Zusammenarbeit, the Grant Agency of the Czech Republic under contract No. 202/95/0217, the Department of Atomic Energy, the Department of Science and Technology, the Council of Scientific and Industrial Research and the University Grants Commission of the Government of India, the Indo-FRG Exchange Programme, the PPE division of CERN, the Swiss National Fund, the International Science Foundation under Contract N8Y000, the INTAS under Contract

INTAS-93-2773, Research-in-Aid for Scientific Research (Specially Promoted Research & International Scientific Research) of the Ministry of Education, Science and Culture, the University of Tsukuba Special Research Projects, and the JSPS Research Fellowships for Young Scientists. ORNL is managed by Lockheed Martin Energy Research Corporation under contract DE-AC05-96OR22464 with the US Department of Energy. The MIT group has been supported by the US Dept. of Energy under the cooperative agreement DE-FC02-94ER40818. In addition we would like to thank R. Birgeneau, H.Y. Chang, A.E. Chen, W.S. Edgerly, W.T. Lin, O. Runolfsson and B. Wadsworth.

References

[1] K. Rajagopal, in: Hwa (Ed.), Quark-Gluon Plasma 2, World Scientific, 1995.
[2] A. Anselm, M.G. Ryskin, Phys. Lett. B 266 (1991) 482.
[3] J.P. Blaizot, A. Krzywicki, Phys. Rev. D 46 (1992) 246.
[4] J.D. Bjorken, K.L. Kowalski, C.C. Taylor, SLAC-PUB-6109 1993.
[5] K. Rajagopal, F. Wilczek, Nucl. Phys. B 399 (1993) 395.
[6] K. Rajagopal, F. Wilczek, Nucl. Phys. B 404 (1993) 577.
[7] R.D. Pisarski, F. Wilczek, Phys. Rev. D 29 (1984) 338.
[8] Y. Fujimoto, S. Hasegawa, C.M.G. Lattes, Phys. Rep. 65 (1980) 151.
[9] G. Arnison et al., Phys. Lett. B 122 (1983) 189.
[10] G.J. Alner et al., Phys. Lett. B 180 (1986) 415.
[11] T.C. Brooks et al., Phys. Rev. D 55 (1997) 5667.
[12] P. Melese for the CDF Collaboration, in: Proceedings XI Topical Workshop on $\bar{p}p$ Collider Physics, Padova, Italy, May 27–June 1, 1996.
[13] F. Becattini, U. Heinz, Z. Phys. C 76 (1997) 269.
[14] P. Dönni et al., CERN/SPSLC 91-17 and CERN/SPSLC 95-35.
[15] T.C. Awes et al., Nucl. Instr. and Meth. A 279 (1989) 479.
[16] A. Baden et al., Nucl. Instr. and Meth. A 203 (1982) 189.
[17] W.T. Lin et al., Nucl. Inst. and Meth. A 389 (1997) 415.
[18] M.M. Aggarwal et al., Nucl. Inst. and Meth. A 372 (1996) 143.
[19] M.M. Aggarwal et al., submitted to Phys. Rev. C (1997).
[20] W.H. van Heeringen, Ph.D. thesis University of Utrecht, 1996.
[21] T. Chujo et al., Nucl. Instr. and Meth. A 383 (1996) 409.
[22] K. Werner, Phys. Rept. 232 (1993) 87.
[23] CERN, GEANT 3.21 Manual.
[24] P. Grassberger, H.I. Miettinen, Nucl. Phys. B 89 (1975) 109.
[25] J. Whitmore, Phys. Rep. C 10 (1974) 273.
[26] S. Gavin, Nucl. Phys. A 590 (1995) 163.
[27] Z. Huang, I. Sarcevic, R. Thews, X.N. Wang, Phys. Rev. D 54 (1996) 750.
[28] T.K. Nayak, in: B.C. Sinha, D.K. Srivastava, Y.P. Viyogi (Eds.), Proc. of International Conf. on Physics and Astrophysics of the Quark-Gluon Plasma (ICPA-QGP'97 New Delhi, 1997), Narosa Publishing House, in press.

4.2.1 Citations

1. d'Enterria D., Ballintijn M., Bedjidian M., Hofman D., Kodolova O., Loizides C., Lokthin I. P., Lourenco, Lourenco C., Mironov C., Petrushanko S. V., Roland, C., Roland, G., Sikler F., Veres G., *CMS physics technical design report: Addendum on high density QCD with heavy ions* Journal of Physics G-Nuclear and Particle Physics, 34 (11): 2307-2455 NOV 2007
2. Boyanovsky, D, de Vega, H J, Schwarz, D J *Phase transitions in the early and present universe*, ANNUAL REVIEW OF NUCLEAR AND PARTICLE SCIENCE, 56: 441-500 2006 ISSN: 0163-8998.
3. Mohanty, B; Serreau, J *Disoriented chiral condensate: Theory and experiment*, PHYSICS REPORTS-REVIEW SECTION OF PHYSICS LETTERS, 414 (6): 263-358 AUG 2005 ISSN: 0370-1573.
4. M. Martinis and V. Mikuta-Martinis, *Disoriented chiral condensate and charge-neutral particle fluctuations in heavy ion collisions*, Fizika B **13** (2004) 383 [arXiv:nucl-th/0309078].
5. Lednicky, R *Correlation femtoscopy of multiparticle processes* PHYSICS OF ATOMIC NUCLEI, 67 (1): 72-82 JAN 2004 ISSN: 1063-7788.
6. J. Serreau, *Disoriented chiral condensate formation in heavy ion collisions?*, arXiv:hep-ph/0304011.
7. Gladysz-Dziadus, E *Are centauros exotic signals of the quark-gluon plasma?*, PHYSICS OF PARTICLES AND NUCLEI, 34 (3): 285-347 MAY-JUN 2003 ISSN: 1063-7796.
8. Mohanty, B *Phi-measure and disoriented chiral condensates*, INTERNATIONAL JOURNAL OF MODERN PHYSICS **A**, 18 (7): 1067-1077 MAR 20 2003 ISSN: 0217-751X Record 12 of 45.
9. Charng, Y Y; Ng, K W; Lin, C Y; Lee, D S *Photon production from non-equilibrium disoriented chiral condensates in a spherical expansion*, PHYSICS LETTERS **B**, 548 (3-4): 175-188 NOV 21 2002 ISSN: 0370-2693.
10. Randrup, J *Charged-pion correlations caused by chiral relaxation dynamics in high-energy nuclear collisions* PHYSICAL REVIEW **C**, 65 (5): Art. No. 054906 MAY 2002 ISSN: 0556-2813.
11. S. M. H. Wong, *Equivalence of classical Skyrmions and coherent states of baryons. I: Constrained quantization on the SU(2) and SO(3) manifolds*, arXiv:hep-ph/0207194.
12. S. M. H. Wong, *Equivalence of classical Skyrmions and coherent states of baryons. II: Baryonic coherent state construction on compact manifolds*, arXiv:hep-ph/0207195.
13. Asakawa, M; Minakata, H; Muller, B *Experimental signatures of anomaly induced disoriented chiral condensate formation* PHYSICAL REVIEW **C**, 65 (5): Art. No. 057901 MAY 2002 ISSN: 0556-2813.
14. S. M. H. Wong, *What exactly is a Skyrmion?*, arXiv:hep-ph/0202250.
15. Ryskin, M G; Shuvaev, A G *Classical pion fields in the presence of a source* PHYSICS OF ATOMIC NUCLEI, 64 (8): 1508-1512 AUG 2001 ISSN: 1063-7788.
16. Bettencourt, L M A; Rajagopal, K; Steele, J V *Langevin evolution of disoriented chiral condensate* Source: NUCLEAR PHYSICS **A**, 693 (3-4): 825-843 OCT 22 2001 ISSN: 0375-9474.
17. Ko, C M *Medium effects on the flow of strange particles in heavy-ion collisions* JOURNAL OF PHYSICS **G**-NUCLEAR AND PARTICLE PHYSICS, 27 (3): 327-336 MAR 2001 ISSN: 0954-3899.
18. Rajagopal, K *Traversing the QCD phase transition: Quenching out of equilibrium vs. slowing out of equilibrium vs. bubbling out of equilibrium* NUCLEAR PHYSICS **A**, 680 (1-4): 211C-220C JAN 15 2001 ISSN: 0375-9474.
19. J. Serreau, *Out-of-equilibrium phenomena in high-energy nuclear collisions.* (In French), arXiv:hep-ph/0104023.
20. Asakawa, M *The novel world created by RHIC* PROGRESS OF THEORETICAL PHYSICS SUPPLEMENT, (140): 89-110 2000 ISSN: 0375-9687.
21. Nakamura, H; Seki, R *Effects of disoriented chiral condensates on two- and three-pion correlations of relativistic nuclear collisions* PHYSICAL REVIEW **C**, 62 (5): Art. No. 054903 NOV 2000 ISSN: 0556-2813.

22. Bleicher, M; Randrup, J; Snellings, R; Wang, X N *Enhanced event-by-event fluctuations in pion multiplicity as a signal of disoriented chiral condensates in relativistic heavy-ion collisions* PHYSICAL REVIEW **C**, 62 (4): Art. No. 041901 OCT 2000 ISSN: 0556-2813.
23. Srivastava, A M *Formation of disoriented chiral condensates in relativistic heavy-ion collisions* PRAMANA-JOURNAL OF PHYSICS, 55 (1-2): 53-62 Sp. Iss. SI JUL-AUG 2000 ISSN: 0304-4289.
24. Digal, S; Rajarshi, R; Sengupta, S; Srivastava, A M *Possibility of forming a large DCC in ultra-relativistic heavy-ion collisions* INTERNATIONAL JOURNAL OF MODERN PHYSICS **A**, 15 (15): 2269-2288 JUN 20 2000 ISSN: 0217-751X.
25. Asakawa, M *Relativistic heavy ion collisions - Where are we now? Where do we go?* NUCLEAR PHYSICS **A**, 670: 127C-134C MAY 8 2000 ISSN: 0375-9474.
26. Hiro-Oka, H; Minakata, H *Dynamical pion production via parametric resonance from disoriented chiral condensates* PHYSICAL REVIEW **C**, 61 (4): Art. No. 044903 APR 2000 ISSN: 0556-2813.
27. Z. Xu and C. Greiner, *Stochastic treatment of disoriented chiral condensates within a Langevin description*, Phys. Rev. D **62** (2000) 036012 [arXiv:hep-ph/9910562].
28. Kumar, S P; Boyanovsky, D; de Vega, H J; Holman, R *Anomalous pseudoscalar-photon vertex in and out of equilibrium* PHYSICAL REVIEW **D**, 61 (6): Art. No. 065002 MAR 15 2000 ISSN: 0556-2821.
29. Brooks, T C; Convery, M E; Davis, W L; Del Signore, K W; Jenkins, T L; Kangas, E; Knepley, M G; Kowalski, K L; Taylor, C C; Oh, SH; Walker, W D; Colestock, P L; Hanna, B; Martens, M; Streets, J; Ball, R C; Gustafson, H R; Jones, L W; Longo, M J; Bjorken, J D; Abashian, A; Morgan, N; Pruneau, CA *Search for disoriented chiral condensate at the Fermilab Tevatron* PHYSICAL REVIEW **D**, 61 (3): Art. No. 032003 FEB 1 2000 ISSN: 0556-2821.
30. Stephanov, M; Rajagopal, K; Shuryak, E *Event-by-event fluctuations in heavy ion collisions and the QCD critical point* PHYSICAL REVIEW **D**, 60 (11): Art. No. 114028 DEC 1 1999 ISSN: 0556-2821.
31. Chow, C K; Cohen, T D *Looking for disoriented chiral condensates from pion distributions* PHYSICAL REVIEW **C**, 60 (5): Art. No. 054902 NOV 1999 ISSN: 0556-2813.
32. Martinis, M; Mikuta-Martinis, V; Crnugelj, J *Disoriented chiral condensates and anomalous production of pions* ACTA PHYSICA SLOVACA, 49 (5): 875-888 OCT 1999 ISSN: 0323-0465.
33. Appelshauser, H; Bachler, J; Bailey, S J; Barna, D; Barnby, LS; Bartke, J; Barton, R A; Betev, L; Bialkowska, H; Billmeier, A; Blyth, C O; Bock, R; Boimska, B; Bormann, C; Brady, FP; Brockmann, R; Brun, R; Buncic, P; Caines, HL; Carr, L D; Cebra, D; Cooper, GE; Cramer, JG; Cristinziani, M; Csato, P; Dunn, J; Eckardt, V; Eckhardt, F; Ferguson, MI; Fischer, HG; Flierl, D; Fodor, Z; Foka, P; Freund, P; Friese, V; Fuchs, M; Gabler, F; Gal, J; Ganz, R; Gazdzicki, M; Geist, W; Gladysz, E; Grebieszkow, J; Gunther, J; Harris, JW; Hegyi, S; Henkel, T; Hill, L A; Hummler, H; Igo, G; Irmscher, D; Jacobs, P; Jones, P G; Kadija, K; Kolesnikov, VI; Kowalski, M; Lasiuk, B; Levai, P; Malakhov, A I; Margetis, S; Markert, C; Melkumov, GL; Mock, A; Molnar, J; Nelson, JM; Oldenburg, M; Odyniec, G; Palla, G; Panagiotou, A D; Petridis, A; Piper, A; Porter, R J; Poskanzer, A M; Prindle, D J; Puhlhofer, F; Reid, JG; Renfordt, R; Retyk, W; Ritter, HG; Rohrich, D; Roland, C; Roland, G; Rudolph, H; Rybicki, A; Sammer, T; Sandoval, A; Sann, H; Semenov, A Y; Schafer, E; Schmischke, D; Schmitz, N; Schonfelder, S; Seyboth, P; Seyerlein, J; Sikler, F; Skrzypczak, E; Snellings, R; Squier, GTA; Stock, R; Strobele, H; Struck, C; Susa, T; Szentpetery, I; Sziklai, J; Toy, M; Trainor, T A; Trentalange, S; Ullrich, T; Vassiliou, M; Veres, G; Vesztergombi, G; Voloshin, S; Vranic, D; Wang, F; Weerasundara, DD; Wenig, S; Whitten, C; Wienold, T; Wood, L; Xu, N; Yates, TA; Zimanyi, J; Zhu, XZ; Zybert, R (NA49 Collaboration) *Event-by-event fluctuations of average transverse momentum in central Pb plus Pb collisions at 158 GeV per nucleon* PHYSICS LETTERS **B**, 459 (4): 679-686 JUL 29 1999 ISSN: 0370-2693.
34. T. C. Petersen and J. Randrup, *Dynamical simulation of DCC formation in Bjorken rods*, Phys. Rev. C **61** (2000) 024906 [arXiv:nucl-th/9907051].
35. T. C. Brooks *et al.* [MiniMax Collaboration], *A search for disoriented chiral condensate at the Fermilab Tevatron*, Phys. Rev. D **61** (2000) 032003.
36. H. Hiro-Oka and H. Minakata, *Dynamical pion production via parametric resonance from disoriented chiral condensate*, Phys. Rev. C **61** (2000) 044903.
37. Asakawa, M; Minakata, H; Muller, B T *Anomaly induced domain formation of disoriented chiral condensates* PHYSICAL REVIEW **D**, 58 (9): Art. No. 094011 NOV 1 1998 ISSN: 0556-2821.

4.2.2 Conference presentations

1. M. Šumbera *Search for the chiral phase transition at CERN SPS*. Proceedings of the scientific conference of nuclear branch, Faculty of Nuclear Science and Physical Engineering, Prague,9.-10.9.1998. **Acta Polytechnica, 38 [3] 45-46 (1998)**.

4.2.3 Further developments

It is important to note that the above results concern fluctuations which extend over a large region of phase space. Logical follow-up was the DCC search in localized phase space regions [83]. Analyzing the charged versus neutral correlations in common phase space regions of varying azimuthal size the presence of non-statistical fluctuations in both charged particle and photon multiplicities in limited azimuthal regions were found. However, no correlated charge-neutral fluctuations were observed. Within the simple DCC model, upper limits on the presence of localized non-statistical DCC-like fluctuations of 10^{-2} for $\Delta\phi$ between $45-90^{\circ}$ and 3×10^{-3} for $\Delta\phi$ between $90-135^{\circ}$ were extracted.

Centrality dependence of localized fluctuations in the multiplicity of charged particles and photons produced 158A GeV/c Pb+Pb collisions was studied in [93]. For four different centrality classes the charged versus neutral particle multiplicity correlations in common phase space regions of varying azimuthal size were analyzed by two different methods. The first analysis method studied the magnitude of the N_{γ} -like versus $N_c h$ multiplicity fluctuations in decreasing phase space regions. The second analysis employed the discrete wavelet transformation technique to investigate the relative magnitude of the N_{γ} -like versus $N_c h$fluctuations in adjacent phase space regions. Using the results from the data, mixed events, and a simple model of DCC formation, an upper limit on DCC production in 158 AGeV Pb+Pb collisions has been set. The result is presented in Fig.4.3.

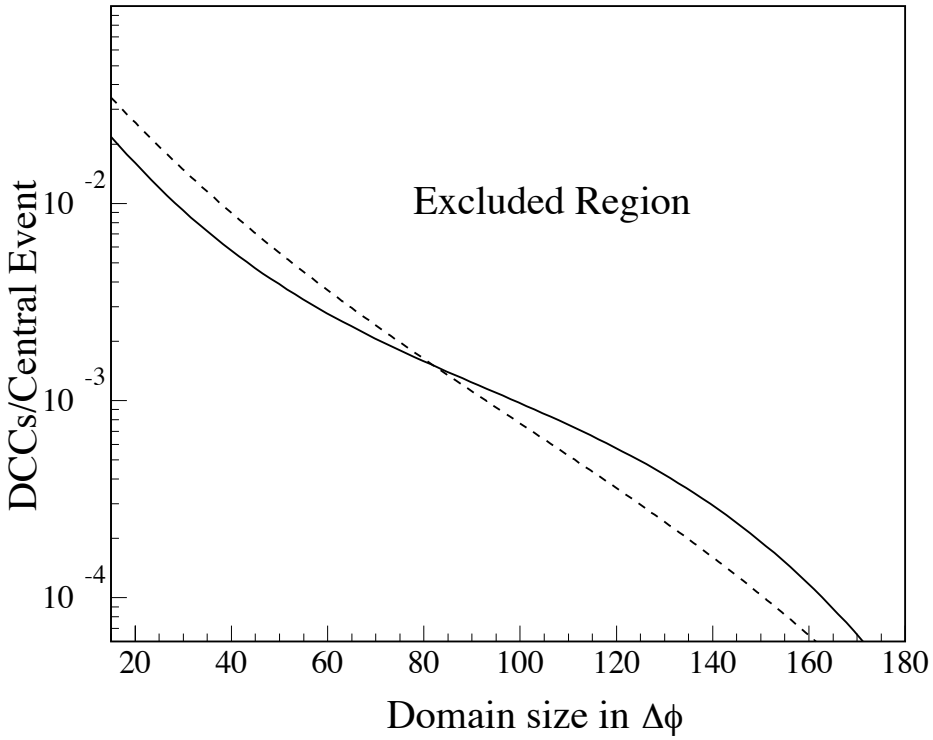

Figure 4.3: *The* 90% *confidence level upper limit on DCC production for central Pb+Pb collision at 158· A GeV/c, as a function of the DCC domain size in azimuthal angle [93]. The solid line corresponds to data from the top* 5% *and dashed line to top* $5-10\%$ *of the minimum bias cross section as determined by selection on the measured transverse energy distribution.*

4.3 Study of Pb+Au collisions at 40 AGeV

4.3.1 Introductory notes

The masses of hadrons are created dynamically by the strong interaction [R28], when confinement forces quarks and gluons to form color-neutral bound states. The generation of hadronic masses is connected to spontaneous chiral symmetry breaking, a basic feature of the vacuum structure of QCD [R52]. However, the quantitative understanding of the dynamics in this non-perturbative regime of QCD is still rather incomplete, and additional information from experiment is essential. In collisions of ultra-relativistic heavy nuclei energy densities far exceeding those needed for the deconfining phase transition are exceeded significantly and there is by now strong evidence for the formation of a QGP [171, R1]. Simultaneously with deconfinement transition, chiral symmetry is expected to be restored. On the way to chiral symmetry restoration in such matter, significant modifications of the properties of hadrons are expected, such as of their mass and width or more generally of the hadronic spectral function [R28].

The ρ meson is an ideal probe to investigate modifications of such in-medium properties. In a hot hadronic medium close to the phase boundary, ρ mesons are abundantly produced by annihilation of thermal pions. Due to its short lifetime ($c\tau$ = 1.3 fm), the decay of the ρ meson occurs inside the medium, and spectral modifications may be observable via the kinematic reconstruction of the decay products. Finally, its decay into lepton pairs provides essentially undisturbed information from the hot and dense phase, because leptons are not subject to final state rescattering in the strongly interacting medium.

ELSEVIER

Article reprint
NUCLEAR PHYSICS A

Nuclear Physics A698 (2002) 253c–260c

www.elsevier.com/locate/npe

New Results from CERES

H. Appelshäuser for the CERES Collaboration*:

D. Adamová[a], G. Agakichiev[b], H. Appelshäuser[c], V. Belaga[d], P. Braun-Munzinger[b], A. Cherlin[e], S. Damjanović[c], T. Dietel[c], L. Dietrich[c], A. Drees[f], S. I. Esumi[c], K. Filimonov[c], K. Fomenko[d], Z. Fraenkel[e], C. Garabatos[b], P. Glässel[c], G. Hering[b], J. Holeczek[b], V. Kushpil[a], B. Lenkeit[g], A. Maas[b], A. Marín[b], F. Messer[f], J. Milošević[c], A. Milov[e], D. Miśkowiec[b], Y. Panebrattsev[d], O. Petchenova[d], V. Petráček[c], A. Pfeiffer[g], J. Rak[b], I. Ravinovich[e], P. Rehak[h], H. Sako[b], W. Schmitz[c], J. Schukraft[g], S. Sedykh[b], W. Seipp[c], S. Shimansky[d], J. Slívová[c], H. J. Specht[c], J. Stachel[c], M. Šumbera[a], H. Tilsner[c], I. Tserruya[e], J. P. Wessels[c], T. Wienold[c], B. Windelband[c], J. P. Wurm[i], W. Xie[e], S. Yurevich[c], V. Yurevich[d]

[a]NPI/ASCR, Řež, Czech Republic
[b]GSI, Darmstadt, Germany
[c]Universität Heidelberg, Germany
[d]JINR, Dubna, Russia
[e]Weizmann Institute, Rehovot, Israel
[f]Department for Physics and Astronomy, SUNY Stony Brook, USA
[g]CERN, Geneva, Switzerland
[h]Brookhaven National Laboratory, Upton, USA
[i]Max-Planck-Institut für Kernphysik, Heidelberg, Germany

1. Introduction

The production of e^+e^--pairs in heavy ion collisions has raised great interest during the last years. Extensive theoretical discussions have been triggered in particular by the CERES measurements of the e^+e^--pair production in 158 AGeV Pb+Au collisions [1]. In the invariant mass region $0.25<m_{ee}<0.7$ GeV/c^2, a significant enhancement of the e^+e^--pair yield compared to the contribution of known hadronic sources was observed. Most of the enhancement is localized in the region of low transverse pair momentum $p_t^{ee}<500$ MeV/c. The threshold behavior of the excess at $\approx 2m_\pi$ together with the multiplicity dependence suggests pion annihilation to be a possible mechanism for additional e^+e^- production. However, the spectral shape of the e^+e^--yield cannot be explained without introducing modifications of the vector meson properties in medium, in particular of the ρ. It has been pointed out that medium modifications of this kind lead to an apparant shift of the hadron-parton duality 'threshold' towards lower masses [2]. The connection between in-medium modifications of meson properties and a possible restoration of chiral

*Supported by: U.S. DoE, German BMBF, the Israeli Science Foundation and the MINERVA Foundation

PII S0375-9474(01)01371-9

symmetry has been emphasized since the latter requires the degeneration of all hadronic parity doublets (as the $\rho(770)$ and the $a_1(1260)$) which exist in vacuum [2].

The limited mass resolution of the original CERES spectrometer did not allow for a systematic investigation of possible modifications in the mass region of the narrow resonances ω and ϕ. For that reason the CERES spectrometer has been upgraded by the addition of a new magnet system and a Time Projection Chamber (TPC), to provide a mass resolution on the level of the natural line widths ($\Delta m/m<2\%$) [3].

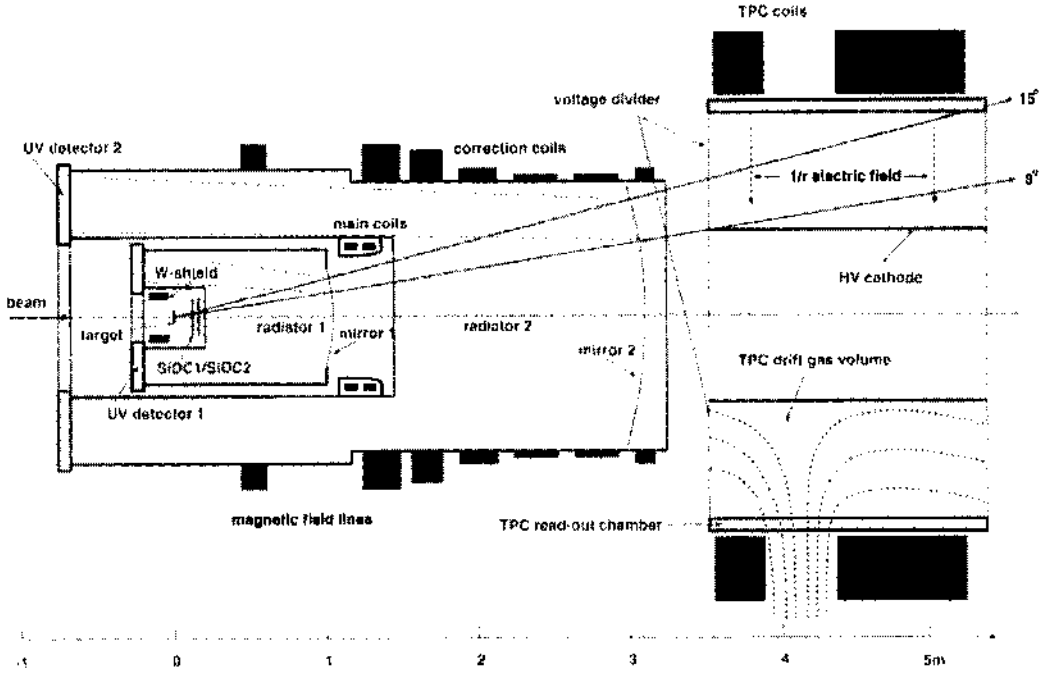

Figure 1. The upgraded CERES spectrometer at the CERN-SPS.

In the fall of 2000 the upgraded CERES spectrometer was operated with a very good overall performance. A sample of 33 M central 158 AGeV Pb+Au events and a smaller set of 0.7 M events at 80 AGeV were recorded. A few preliminary results of this data sample will be presented in this contribution.

We will focus here on results from the 1999 data taking period, where 8 M Pb+Au events at 40 AGeV were recorded. Since the new readout system of the TPC was not yet properly working, this data set is limited in terms of statistics and momentum resolution. Nevertheless, this data sample at lower beam energy allows to study initial conditions different from the ones at top SPS energy. This can be very useful to disentangle temperature and baryon density driven modifications of the dilepton spectrum.

2. Experimental Setup

The CERES spectrometer is dedicated to the measurement of low-mass e^+e^--pairs around midrapidity, providing full azimuthal acceptance in the polar angle region between 8° and 14.5° ($2.1<\eta<2.6$) (Fig.1). The discrimination of rare leptonic signals from the huge hadronic background requires a high electron identification capability. This is provided by two RICH detectors (each consisting of a radiator, a mirror and wire chambers for UV detection) which are operated at high Cherenkov threshold ($\gamma_{th}=32$) and are thus

insensitive to 95% of the charged hadrons. A precise angle measurement of charged particles and vertex reconstruction is provided by two silicon drift detectors (SiDC1,2) located 10 cm and 11.5 cm behind a segmented Au target. The radial drift TPC has an active length of 2 m and an outer diameter of 2.6 m. It is operated inside a magnetic field with a maximal radial component of 0.5 T and provides the measurement of up to 20 space points for each charged particle track. This allows for a precise determination of the momentum and additional electron ID via dE/dx. The magnet system between the two RICHes was not operated in the upgraded configuration.

3. e^+e^--Pair Analysis

Electrons are identified via their ring signature in the RICH detectors. The absence of magnetic deflection between RICH1 and RICH2 led to an improvement of the ring finding efficiency from 70% to 94%, since ring recognition could now be performed simultaneously in both RICHes. After matching to the SiDC and the TPC, electron tracks are combined to pairs. Only single electron tracks with p_t>200 MeV/c and fully reconstructed pairs with opening angle Θ_{ee}>35 mrad were accepted. The dilepton signal is derived from the number of unlike-sign pairs, subtracting the number of like-sign pairs to account for the combinatorial background. To reduce the combinatorial background arising mainly from unrecognized Dalitz pairs and conversions, further rejection steps have to be taken. The impact of these rejection steps on various subsamples is demonstrated in Fig.2.

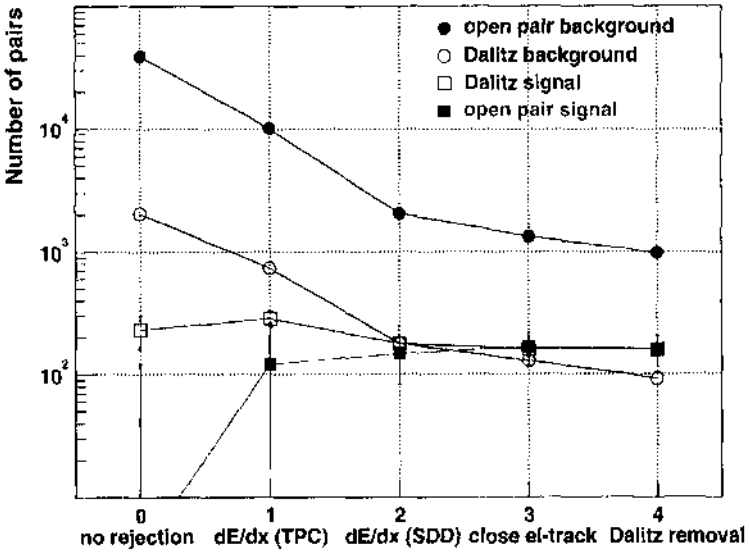

Figure 2. Evolution of the total number of pairs after various rejection steps, shown for the open pair signal (m_{ee}>0.2 GeV/c^2), open pair background (m_{ee}>0.2 GeV/c^2), Dalitz signal (m_{ee}<0.1 GeV/c^2) and Dalitz background (m_{ee}<0.1 GeV/c^2).

First, the electron sample is cleaned from remaining hadronic contaminations, mainly caused by incorrect matches between RICH and TPC. This is done using dE/dx information from the TPC. Conversions and Dalitz pairs which typically have small opening angles leave a clean signature in the SiDC's, because they produce a double energy loss within a small angular region. This allows to reject close pairs (Θ_{ee}<10 mrad) even if they are not recognized as two individual rings in the RICHes. Due to the incomplete azimuthal readout of the TPC in the 1999 data, an additional close track cut (Θ_{ee}<70 mrad) solely based on SiDC-RICH electron candidates was applied. Finally, tracks which combine to a Dalitz pair (m_{ee}<0.2 GeV/c^2) were removed from further combinatorics. By these cuts, the open pair background is reduced by roughly a factor of 40, while the open pair signal

remains unchanged, demonstrating that the signal behaves qualitatively different than the background. The total number of open pairs (m_{ee}>0.2 GeV/c^2) is 159$\pm$46 (stat.) at a signal to background ratio of S/B=1/6.

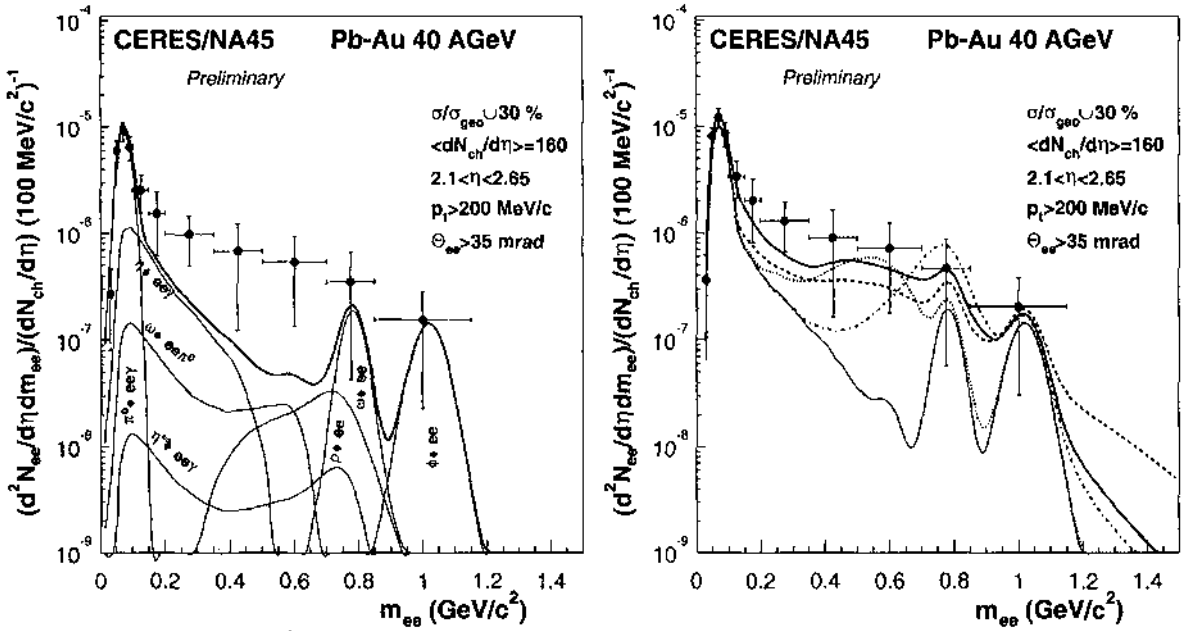

Figure 3. Inclusive e^+e^- invariant mass spectrum at 40 AGeV in comparison to expectations from known hadronic sources in heavy ion collisions ('hadronic cocktail') (left) and in comparison to model calculations (right) assuming the vacuum ρ spectral function (dash-dotted), a dropping ρ mass (dotted) and including medium modifications of the ρ spectral function (thick solid line). Also shown is the hadronic cocktail without ρ (thin solid line). The dashed line refers to a lowest order pQCD rate calculation. All calculations are from [4].

The resulting e^+e^- invariant mass spectrum was normalized to the hadronic cocktail in the π^0-Dalitz region (Fig.3). Compared to the expectation from known hadronic sources in heavy ion collisions, we observe an enhancement of the e^+e^--pair yield by a factor of 4.7$\pm$1.6 (stat.) in the mass range m_{ee}>0.2 GeV/c^2. Most of the enhancement is localized at low transverse pair momentum. This was also observed at 158 AGeV, where, in the same mass range, an enhancement factor of 2.5$\pm$0.4 (stat.) was found. In Fig.3 (right) we compare our result to different model calculations [4]. Clearly the measurement disfavors a purely hadronic scenario assuming the vacuum ρ spectral function, similar to our previous observations at top SPS energy.

4. Hadronic Observables

The addition of the TPC improves substantially the hadron capability of the CERES spectrometer. This allowed for a systematic investigation of hadronic observables around midrapidity. The momentum vector of charged particles is determined from their curvature in the TPC and the emission angle measured in the SiDC. The matching requirement to the SiDC system also leads to a very efficient suppression of non-vertex tracks. The

momentum scale of the TPC system has been checked by the width and position of the invariant mass peaks of reconstructed Λ and K^0_s hadrons. With the use of the UrQMD model, the multiplicity measurement in the SiDC was related to the corresponding number of participants N_{part}.

4.1. Charged Particle Production and Spectra

The transverse mass distributions of negatively charged hadrons h^- and proton-like positive net charges '(+) − (−)' have been measured in different bins of rapidity and centrality. The inverse slope parameters T have been obtained by fitting an exponential $1/m_t\ \mathrm{d}n/\mathrm{d}m_t \propto \exp(-m_t/T)$. In Fig.4 (left) the rapidity averaged results are shown as function of N_{part}. The slopes are similar to those observed at top AGS and SPS energies, with only a weak dependence on centrality. The large difference between h^- and (+)−(−) slopes ($T_{h^-} = 176 \pm 5$ MeV and $T_{(+)-(-)} = 278 \pm 12$ MeV) indicates the presence of strong radial flow also at 40 AGeV. This is only qualitatively reproduced by UrQMD.

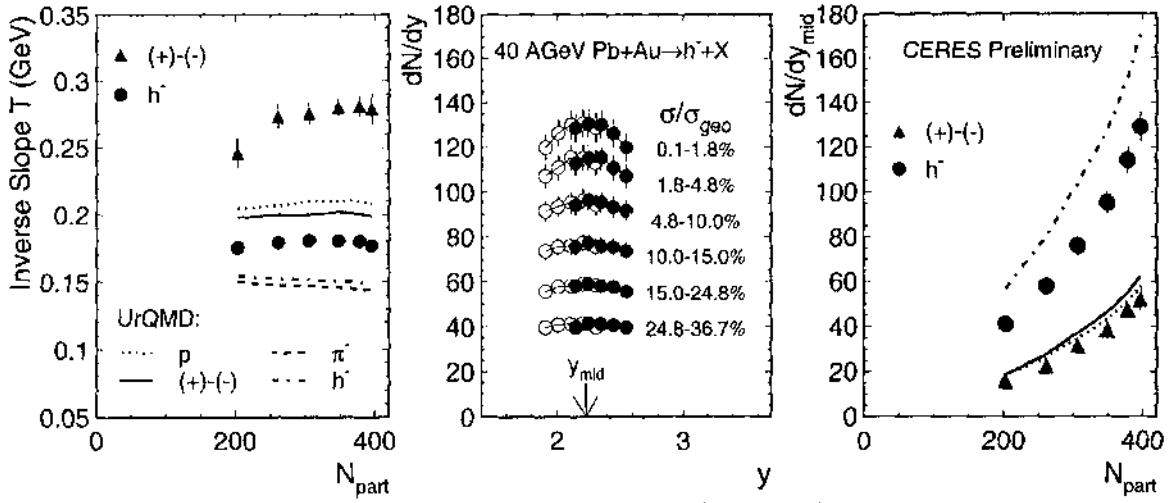

Figure 4. Left: Inverse slope parameters of h^- and (+) − (−) as function of N_{part}. The fit range is $0.1<(m_t-m_\pi)<0.8$ GeV/c^2, $2.2<y_\pi<2.5$ (h^-) and $0.3<(m_t-m_p)<1.5$ GeV/c^2, $2.1<y_p<2.4$ ((+) − (−)). Middle: Rapidity density $\mathrm{d}N/\mathrm{d}y$ of h^- in different centrality bins; open symbols are reflected around midrapidity. Right: The midrapidity yields of h^- and (+) − (−) as function of N_{part}. Also shown are results from UrQMD.

The rapidity densities $\mathrm{d}N/\mathrm{d}y$ (Fig.4, middle) have been obtained by extrapolating the transverse momentum spectra to p_t=0. The midrapidity yield of h^- as function of N_{part} (Fig.4, right) rises significantly stronger than linear, while a close-to-linear rise at top SPS energy has been reported recently [5]. This points to a change in the particle production mechanism going from 40 AGeV to 158 AGeV. In fact, a non-linear behaviour has also been observed at the AGS [6]. The trend is well described by UrQMD; however, the overall particle production is significantly overestimated. The non-linear rise of the midrapidity (+) − (−)-yield with N_{part} is caused by an increasing amount of stopping, in agreement with the UrQMD prediction.

4.2. Two Pion Bose-Einstein Interferometry

The investigation of two-pion Bose-Einstein correlations (HBT) allows a systematic study of the space-time evolution of the hadronic source. We apply a three-dimensional Gaussian parametrization of the correlation function C_2, splitting the three-momentum

difference vector into a longitudinal and two transverse components $\vec{q} = (q_{\rm long}, q_{\rm side}, q_{\rm out})$ [7]. Fitting this parametrization to the data yields the correlation strength λ, the homogeneity length parameters $R_{\rm long}$, $R_{\rm side}$, $R_{\rm out}$ and the $R^2_{\rm ol}$ cross-term, the latter being small or consistent with zero in our midrapidity data set. The lack of pion identification leads to a reduction of the correlation strength. However, we expect the shape of the correlation peak to remain unchanged. To account for the finite two-track resolution, only pairs with opening angles $\Theta_{\pi\pi}$>10 mrad were used. All correlation functions have been analyzed in the longitudinal rest frame of the pairs and were corrected for mutual Coulomb repulsion, assuming a finite source size. The relative momentum resolution $\delta q_{\rm long}$ and $\delta q_{\rm side}$ is below 10 MeV/c, leading to only small (<5%) corrections of the fitted source parameters. However, the strong momentum dependence of $\delta q_{\rm out}$ restricts the analysis of $R_{\rm out}$ to small p_t.

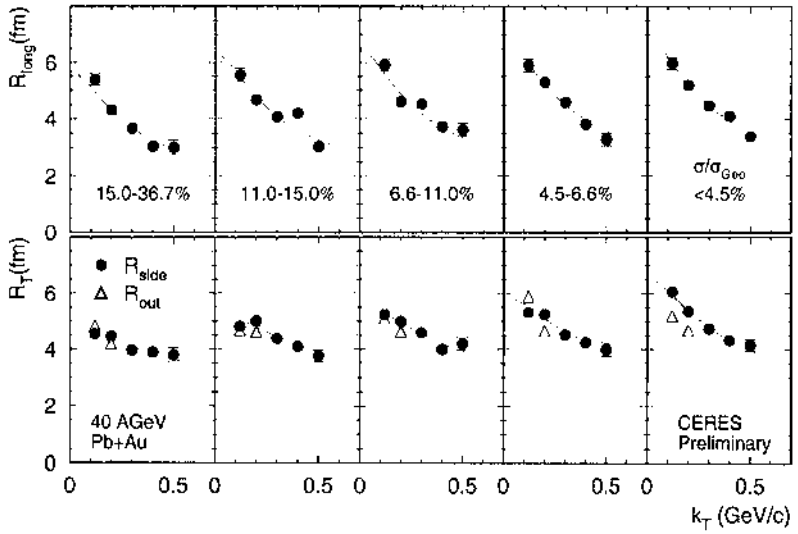

Figure 5. Radius parameters as function of the pair transverse momentum $k_T = \frac{1}{2}|\vec{p_{t,1}} + \vec{p_{t,2}}|$. The range in pair rapidity is $|y_{\pi\pi} - y_{mid}| < 0.25$. Also shown are the fits (see text).

Consistent with the picture of a boost-invariant longitudinal expansion, $R_{\rm long}$ shows a strong k_T dependence in all centrality bins (Fig.5, upper panels). The duration of expansion can be derived [8] by fitting $R_{\rm long} = \tau_0 (T_f/m_T)^{\frac{1}{2}}$, with $m_T = (m_\pi^2 + k_T^2)^{\frac{1}{2}}$. We obtain $\tau_0 = 6 - 7$ fm/c for $T_f = 120$ MeV.

The k_T dependence of $R_{\rm side}$ becomes more pronounced for more central collisions (Fig.5, lower panels), suggesting an increase with centrality of radial flow. We apply a model-dependent parametrization [9] of $R_{\rm side}(k_T)$ which allows to extract the 'true' geometrical source radius $R_{\rm geo}$ and the transverse flow rapidity η_f: $R^2_{\rm side} = R^2_{\rm geo}/(1 + m_T \cdot \eta_f^2/T_f)$. Assuming a Gaussian density profile and a thermal freeze-out temperature of T_f=120 MeV, we obtain from η_f an average transverse flow velocity $\langle \beta_t \rangle = 0.57^{+0.06}_{-0.09}$. A similar result has been obtained from a preliminary HBT analysis of the 80 AGeV data. These numbers are close to the velocity of sound in nuclear medium and similar to findings at top AGS and top SPS energies (Fig.6).

$R_{\rm geo}$ scales with $({\rm d}N/{\rm d}y)^{\frac{1}{3}}$ and is about 7.5 fm for the most central collisions. The freeze-out density can be estimated by $\rho_f = (3 \cdot {\rm d}N^-/{\rm d}y)/(2\pi \cdot R^2_{\rm geo} \cdot \tau_0) \approx 0.12$ pions/fm^3, independent of centrality and identical to results at top SPS and AGS energy [10].

The measured one- and two-particle distributions allow to estimate the spatially averaged phase-space density $\langle f \rangle$ of pions at freeze-out [11]. We observe that $\langle f \rangle$ is consistent with a thermal Bose-Einstein distribution at T=120 MeV independent of centrality (Fig.7). Small deviations from this behaviour at larger p_t can be attributed to the presence

of radial flow. Our results support the picture of a universal pion freeze-out phase-space density in heavy-ion reactions at SPS, as already pointed out in [12].

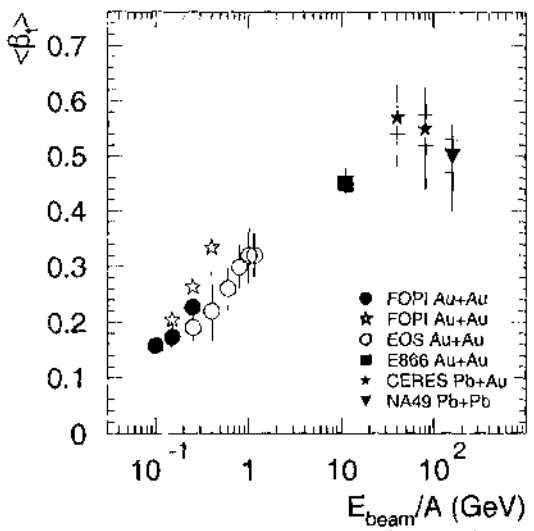

Figure 6. Average transverse flow velocity $\langle\beta_t\rangle$ as function of beam kinetic energy. SPS points are derived from HBT alone, assuming T_f=120 MeV (horizontal marks indicate ±20 MeV uncertainty in T_f).

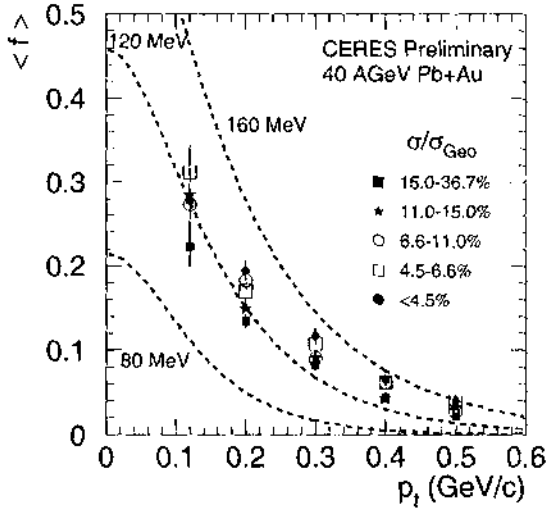

Figure 7. Pion freeze-out phase-space density $\langle f \rangle$ as function of p_t. Also shown are the expectations for static thermal Bose-Einstein distributions at various temperatures.

4.3. Azimuthal Correlations

The investigation of azimuthal correlations ('flow') of charged particles in non-central collisions has been proposed to provide information about the initial pressure in the collision region and the degree of thermalization during the expansion stage.

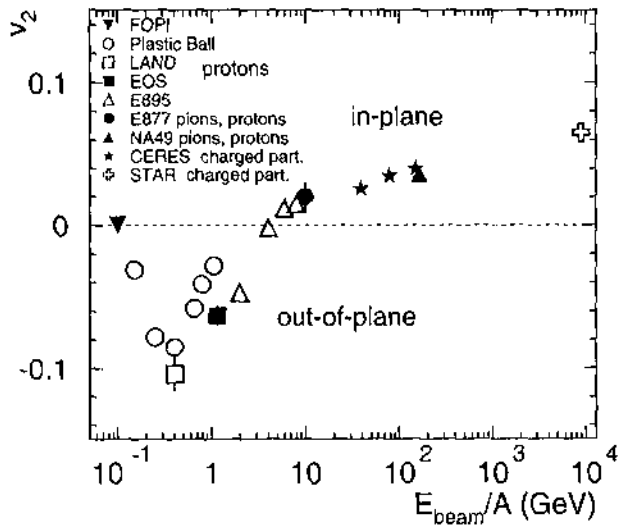

Figure 8. The strength of elliptic flow v_2 as function of the beam kinetic energy for semi-central collisions of Pb or Au nuclei.

A flow analysis of Pb+Au events at 40, 80 and 158 AGeV over a wide range of impact parameters has been performed. This analysis was based on the azimuthal hit distributions in the SiDC1,2. The two coefficients v_1 and v_2, respectively the strength of directed and elliptic flow, are obtained from a second order Fourier decomposition of the relative azimuthal charged particle distribution $dN/d(\phi-\Phi)$ (Φ is the orientation of the reaction plane) [13]. The v_1 and v_2 values have been corrected for the finite reaction plane resolution, determined by the subevent method. While v_1 exhibits the characteristic zero-crossing at midrapidity, v_2 is positive and independent of rapidity within our acceptance. It increases with beam energy and fits smoothly into the measured systematics at different beam energies (Fig.8).

4.4. Mean Transverse Momentum Fluctuations

Fluctuations of the event-wise average transverse momentum $\langle p_t \rangle$ have been predicted as a possible observable for critical phenomena close to the QCD phase boundary [14]. The $\langle p_t \rangle$ distributions of central Pb+Au events at 40, 80, and 158 AGeV are shown in Fig.9 and compared to the corresponding mixed-event distributions. The similarity of real and mixed events suggests that $\langle p_t \rangle$ fluctuations are mainly driven by finite number statistics. A more detailed investigation, however, indicates small additional contributions of order 5 MeV/c to the width of the $\langle p_t \rangle$ distribution, better visualized by the ratio of the real and mixed event distributions (Fig.9, lower panels). Similar results are obtained from an analysis of subevent correlations, as proposed in [15]. The influence of HBT, flow, impact parameter fluctuations and detector efficiency on $\langle p_t \rangle$ are under investigation.

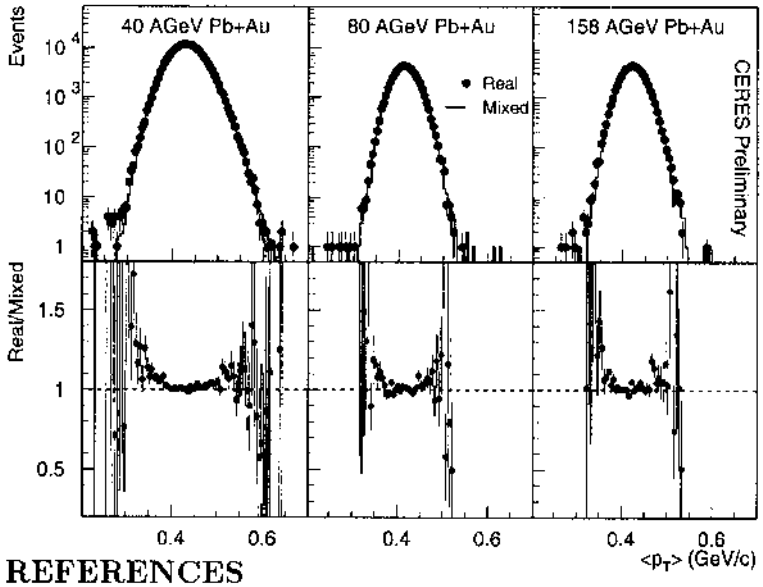

Figure 9. Upper panels: Event-by-event $\langle p_t \rangle$ distributions at three different beam energies. The solid line is obtained by event mixing. Lower panels: Ratio between real and mixed-event distributions. The centrality selection corresponds to σ/σ_{geo}<6.5%. For the calculation of $\langle p_t \rangle$ tracks with $0.05<p_t<1.5$ GeV/c were used.

REFERENCES

1. G. Agakichiev et al. (CERES Collaboration), Nucl. Phys. **A661** (1999) 23c.
2. R. Rapp and J. Wambach, Eur. Phys. J. **A6** (1999) 415; R. Rapp, Nucl. Phys. **A661** (1999) 33c; R. Rapp and J. Wambach, hep-ph/9909229.
3. G. Agakichiev et al. (CERES Collaboration), Nucl. Phys. **A661** (1999) 673c.
4. R. Rapp, private communication.
5. M.M. Aggarwal et al. (WA98 Collaboration), Eur. Phys. J. **C18** (2001) 651.
6. L. Ahle et al. (E802 Collaboration), Phys. Rev. **C59** (1999) 2173.
7. G. Bertsch, Nucl. Phys. **A498** (1989) 173c; S. Pratt, Phys. Rev. **D33**, (1986) 1314.
8. Y. Sinyukov, Nucl. Phys. **A498** (1989) 151c.
9. U. Wiedemann, Nucl. Phys. **A661** (1999) 65c.
10. J. Stachel, Nucl. Phys. **A654** (1999) 119c.
11. G. Bertsch, Phys. Rev. Lett. **72** (1996) 2349.
12. D. Ferenc, U. Heinz, B. Tomasik, U. Wiedemann and J.G. Cramer, Phys. Lett. **B457** (1999) 347.
13. S. Voloshin and Y. Zhang, Z. Phys. **C70** (1996) 665.
14. M. Stephanov, K. Rajagopal, E. Shuryak, Phys. Rev. Lett. **81** (1998) 4816.
15. S. Voloshin, NA49 Note number 178 (1999).

4.3.3 Citations

1. Q. Li, M. Bleicher and H. Stoecker, *Transport model analysis of particle correlations in relativistic heavy ion collisions at femtometer scales* Phys. Rev. C **73** (2006) 064908.
2. Andronic, A; Barret, V; Basrak, Z; Bastid, N; Benabderrahmane, L; Berek, G; Caplar, R; Cordier, E; Crochet, P; Dupieux, P; Dzelalija, M; Fodor, Z; Gasparic, I; Grishkin, Y; Hartmann, ON; Herrmann, N; Hildenbrand, KD; Hong, B; Kecskemeti, J; Kim, YJ; Kirejczyk, M; Koczon, P; Korolija, M; Kotte, R; Kress, T; Lebedev, A; Leifels, Y; Lopez, X; Mangiarotti, A; Merschmeyer, M; Neubert, W; Pelte, D; Petrovici, M; Rami, F; Reisdorf, W; de Schauenburg, B; Schuttauf, A; Seres, Z; Sikora, B; Sim, KS; Simion, V; Siwek-Wilczynska, K; Smolyankin, V; Stockmeier, MR; Stoicea, G; Tyminski, Z; Wagner, P; Wisniewski, K; Wohlfarth, D; Xiao, ZG; Yushmanov, I; Zhilin, A (FOPI Collaboration) *Excitation function of elliptic flow in Au plus Au collisions and the nuclear matter equation of state* , PHYSICS LETTERS B, 612 (3-4): 173-180 APR 21 2005 ISSN: 0370-2693.
3. Stephen Scott Adler, S. Afanasiev, C. Aidala, N.N. Ajitanand, Y. Akiba, J. Alexander, R. Amirikas, L. Aphecetche, S.H. Aronson, R. Averbeck, T.C. Awes, R. Azmoun, V. Babintsev, A. Baldisseri, K.N. Barish, P.D. Barnes, B. Bassalleck, S. Bathe, S. Batsouli, V. Baublis, A. Bazilevsky, S. Belikov, Y. Berdnikov, S. Bhagavatula, J.G. Boissevain, H. Borel, S. Borenstein, M.L. Brooks, D.S. Brown, N. Bruner, D. Bucher, H. Buesching, V. Bumazhnov, G. Bunce, J.M. Burward-Hoy, S. Butsyk, X. Camard, J.-S. Chai, P. Chand, W.C. Chang, S. Chernichenko, C.Y. Chi, J. Chiba, M. Chiu, I.J. Choi, J. Choi, R.K. Choudhury, T. Chujo, V. Cianciolo, Y. Cobigo, B.A. Cole, P. Constantin, David G. d'Enterria, G. David, H. Delagrange, A. Denisov, A. Deshpande, E.J. Desmond, O. Dietzsch, O. Drapier, A. Drees, R. du Rietz, A. Durum, D. Dutta, Y.V. Efremenko, K. El Chenawi, A. Enokizono, H. Enyo, S. Esumi, L. Ewell, D.E. Fields, F. Fleuret, S.L. Fokin, B.D. Fox, Z. Fraenkel, J.E. Frantz, A. Franz, A.D. Frawley, S.-Y. Fung, S. Garpman, T.K. Ghosh, A. Glenn, G. Gogiberidze, M. Gonin, J. Gosset, Y. Goto, R. Granier de Cassagnac, N. Grau, S.V. Greene, M. Grosse Perdekamp, W. Guryn, H.-A. Gustafsson, T. Hachiya, J.S. Haggerty, H. Hamagaki, A.G. Hansen, E.P. Hartouni, M. Harvey, R. Hayano, X. He, M. Heffner, T.K. Hemmick, J.M. Heuser, M. Hibino, J.C. Hill, W. Holzmann, K. Homma, B. Hong, A. Hoover, T. Ichihara, V.V. Ikonnikov, K. Imai, D. Isenhower, M. Ishihara, M. Issah, A. Isupov, B.V. Jacak, W.Y. Jang, Y. Jeong, J. Jia, O. Jinnouchi, B.M. Johnson, S.C. Johnson, K.S. Joo, D. Jouan, S. Kametani, N. Kamihara, J.H. Kang, S.S. Kapoor, K. Katou, S. Kelly, B. Khachaturov, A. Khanzadeev, J. Kikuchi, D.H. Kim, D.J. Kim, D.W. Kim, E. Kim, G.-B. Kim, H.J. Kim, E. Kistenev, A. Kiyomichi, K. Kiyoyama, Christian Klein-Boesing, H. Kobayashi, L. Kochenda, V. Kochetkov, D. Koehler, T. Kohama, M. Kopytine, D. Kotchetkov, A. Kozlov, P.J. Kroon, C.H. Kuberg, K. Kurita, Y. Kuroki, M.J. Kweon, Y. Kwon, G.S. Kyle, R. Lacey, V. Ladygin, J.G. Lajoie, A. Lebedev, S. Leckey, D.M. Lee, S. Lee, M.J. Leitch, X.H. Li, H. Lim, A. Litvinenko, M.X. Liu, Y. Liu, C.F. Maguire, Y.I. Makdisi, A. Malakhov, V.I. Manko, Y. Mao, G. Martinez, M.D. Marx, H. Masui, F. Matathias, T. Matsumoto, P.L. McGaughey, E. Melnikov, M. Mendenhall, F. Messer, Y. Miake, J. Milan, T.E. Miller, A. Milov, S. Mioduszewski, R.E. Mischke, G.C. Mishra, J.T. Mitchell, A.K. Mohanty, D.P. Morrison, J.M. Moss, F. Muhlbacher, D. Mukhopadhyay, M. Muniruzzaman, J. Murata, S. Nagamiya, J.L. Nagle, T. Nakamura, B.K. Nandi, M. Nara, J. Newby, P. Nilsson, A.S. Nyanin, J. Nystrand, E. O'Brien, C.A. Ogilvie, H. Ohnishi, I.D. Ojha, K. Okada, M. Ono, V. Onuchin, A. Oskarsson, I. Otterlund, K. Oyama, Kyoichiro Ozawa, D. Pal, A.P.T. Palounek, V.S. Pantuev, V. Papavassiliou, J. Park, A. Parmar, S.F. Pate, T. Peitzmann, J.-C. Peng, V. Peresedov, C. Pinkenburg, R.P. Pisani, F. Plasil, M.L. Purschke, A.K. Purwar, J. Rak, I. Ravinovich, K.F. Read, M. Reuter, K. Reygers, V. Riabov, Y. Riabov, G. Roche, A. Romana, M. Rosati, P. Rosnet, S.S. Ryu, M.E. Sadler, N. Saito, T. Sakaguchi, M. Sakai, S. Sakai, V. Samsonov, L. Sanfratello, R. Santo, H.D. Sato, S. Sato, S. Sawada, Y. Schutz, V. Semenov, R. Seto, M.R. Shaw, T.K. Shea, T.-A. Shibata, K. Shigaki, T. Shiina, C.L. Silva, D. Silvermyr, K.S. Sim, C.P. Singh, V. Singh, M. Sivertz, A. Soldatov, R.A. Soltz, W.E. Sondheim, S.P. Sorensen, I.V. Sourikova, F. Staley, P.W. Stankus, E. Stenlund, M. Stepanov, Andras Ster, S.P. Stoll, T. Sugitate, J.P. Sullivan, E.M. Takagui, A. Taketani, M. Tamai, K.H. Tanaka, Y. Tanaka, K. Tanida, M.J. Tannenbaum, P. Tarjan, J.D. Tepe, T.L. Thomas, J.

Tojo, H. Torii, R.S. Towell, Itzhak Tserruya, H. Tsuruoka, S.K. Tuli, H. Tydesjo, N. Tyurin, H.W. van Hecke, J. Velkovska, M. Velkovsky, L. Villatte, A.A. Vinogradov, M.A. Volkov, E. Vznuzdaev, X.R. Wang, Y. Watanabe, Sebastian N. White, F.K. Wohn, C.L. Woody, W. Xie, Y. Yang, A. Yanovich, S. Yokkaichi, G.R. Young, I.E. Yushmanov, W.A. Zajc, C. Zhang, S. Zhou, S.J. Zhou, L. Zolin, *Systematic studies of the centrality and s(NN)**(1/2) dependence of dE(T)/d mu and d N(ch)/d mu in heavy ion collisions at mid-rapidity*, Phys. Rev. C **71** (2005) 034908.

4. A. Milov [PHENIX Collaboration], *Centrality and s(NN)**(1/2) dependence of the dE(T)/d eta and dN(ch)/d eta in heavy ion collisions at mid-rapidity*, J. Phys. Conf. Ser. **5** (2005) 17.
5. Kugler, A; Agakishiev, H; Agodi, C; Alvarez-Pol, H; Balanda, A; Bellia, G; Bielcik, J; Bohmer, M; Boyard, J; Braun-Munzinger, P; Chernenko, S; Christ, T; Coniglione, R; Djeridi, R; Dohrmann, F; Duran, I; Eberl, T; Fabbietti, L; Fateev, O; Finocchiaro, P; Friese, J; Frohlich, I; Garzon, J; Gernhauser, R; Golubeva, M; Gonzales-Dias, D; Grosse, E; Guber, F; Hennino, T; Hlavac, S; Holzmann, R; Ierusalimov, A; Iori, I; Jaskula, M; Jurkovi, M; Kampfer, B; Kanaki, K; Karavicheva, T; Koenig, I; Koenig, W; Kolb, B; Kotte, R; Kotulic-Bunta, J; Krucken, R; Kuhn, W; Kulessa, R; Kurepin, A; Lang, S; Lehnert, J; Maiolino, C; Markert, J; Metag, V; Mousa, J; Munch, M; Muntz, C; Naumann, L; Novotny, R; Novotny, J; Otwinowski, J; Pachmayer, Y; Pechenov, V; Perez, T; Pietraszko, J; Pleskac, R; Pospisil, V; Przygoda, W; Rabin, N; Ramstein, B; Reshetin, A; Ritman, J; Roy-Stephan, M; Rustamov, A; Sadovski, A; Sailer, B; Salabura, P; Sanchez, M; Sapienza, P; Schmah, A; Simon, R; Smoliankin, V; Smykov, L; Spataro, S; Spruck, B; Strobele, H; Stroth, J; Sturm, C; Sudol, M; Tlusty, P; Toia, A; Traxler, M; Tsertos, H; Wagner, V; Wisniowski, M; Wojcik, T; Wustenfeld, J; Zanevsky, Y; Zovinec, D; Zumbruch, P Title: Charged hadrons and leptons identification at HADES Source: ACTA PHYSICA SLOVACA, 54 (4): 375-384 AUG 2004 ISSN: 0323-0465.
6. Kugler, A; Agakichiev, H; Agodi, C; Alvarez-Pardo, M; Alvarez-Pol, H; Badura, E; Balanda, A; Ballester, F; Bassi, A; Bassini, R; Bellia, G; Bertini, D; Bielcik, J; Bohmer, M; Boiano, C; Bokemeyer, H; Boyard, JL; Brambilla, S; Braun-Munzinger, P; Chernenko, S; Coniglione, R; Dahlinger, M; Daues, H; Diaz, R; Dohrmann, F; Duran, I; Eberl, T; Fabietti, L; Fateev, O; Fernandez, C; Finocchiaro, P; Friese, J; Frohlich, I; Fuentes, B; Garzon, JA; Genolini, B; Gernhauser, R; Golubeva, M; Gonzales, D; Goringer, H; Grosse, E; Guber, F; Hehner, J; Hennino, T; Hlavac, S; Hoffmann, J; Holzmann, R; Homolka, J; Ierusalimov, A; Iori, I; Jaksula, M; Kampfer, B; Kanaki, K; Karavichieva, T; Kirschner, D; Kidon, L; Kienle, P; Koenig, I; Koenig, W; Korner, HJ; Kolb, BW; Kopf, U; Kotte, R; Kuhn, W; Kurtukian, T; Krucken, R; Kulessa, R; Kurepin, A; Lehnert, J; Lins, E; Magestro, D; Maier-Komor, P; Maiolino, C; Markert, J; Metag, V; Mousa, J; Munch, M; Muntz, C; Naumann, L; Nekhaev, A; Niebur, W; Ott, W; Novotny, R; Otwinowski, J; Panebratsev, Y; Pechenov, V; Petri, M; Piattelli, P; Pietraszko, J; Pleskac, R; Ploskon, M; Przygoda, W; Rabin, N; Ramstein, B; Reshetin, A; Ritman, J; Rosier, P; Roy-Stephan, M; Rustamov, A; Sabin, J; Sadovski, A; Sailer, B; Salabura, P; Sanchez, M; Sapienza, P; Senger, P; Schroeder, C; Shileev, K; Shishov, P; Simon, R; Smoliankin, V; Smykov, L; Spataro, S; Stelzer, H; Strobele, H; Stroth, J; Sturm, C; Sudol, M; Taranenko, A; Tlusty, P; Toia, A; Traxler, M; Tsertos, H; Turzo, I; Vassiliev, D; Vazquez, A; Wagner, V; Walus, W; Winkler, S; Wisniowski, M; Wojcik, T; Wustenfeld, J; Yahlali, N; Zanevsky, Y; Zeitelhack, K; Zovinec, D; Zumbruch, P *Particle identification at HADES*, NUCLEAR PHYSICS A, 734: 78-81 APR 5 2004 ISSN: 0375-9474.
7. Ferreiro, EG; del Moral, F; Pajares, C *Transverse momentum fluctuations and percolation of strings* , PHYSICAL REVIEW C, 69 (3): Art. No. 034901 MAR 2004 ISSN: 0556-2813.
8. Liu, QJ; Trainor, TA *Jet quenching and event-wise mean-p(t) fluctuations in central Au-Au collisions at root s(NN)=200 GeV in Hijing-1.37* PHYSICS LETTERS B, 567 (3-4): 184-188 AUG 14 2003 ISSN: 0370-2693.
9. Xu, N *Collective dynamics at RHIC* , ACTA PHYSICA HUNGARICA NEW SERIES-HEAVY ION PHYSICS, 17 (2-4): 229-235 2003 ISSN: 1219-7580.
10. Ray, RL (STAR Collaboration) *Correlations, fluctuations, and flow measurements from the STAR experiment* , NUCLEAR PHYSICS A, 715: 45C-54C Sp. Iss. SI MAR 10 2003 ISSN: 0375-9474.
11. K. Kanaya, *Recent lattice results relevant for heavy ion collisions*, Nucl. Phys. A **715** (2003) 233.

12. P. Crochet, *Charm and leptons*, Nucl. Phys. A **715** (2003) 359
13. H. Satz, *Limits of confinement: The first 15 years of ultra-relativistic heavy ion studies*, Nucl. Phys. A **715** (2003) 3.
14. D. K. Srivastava, C. Gale and R. J. Fries, *Large mass dileptons from the passage of jets through quark gluon plasma*, Phys. Rev. C **67** (2003) 034903.
15. R. Rapp, Pramana **60** (2003) 675
16. Kvasnikova, I; Gale, C; Srivastava, DK *Production of intermediate-mass dileptons in relativistic heavy ion collisions*, Source: PHYSICAL REVIEW C, 65 (6): Art. No. 064903 JUN 2002 ISSN: 0556-2813.
17. Abreu, MC; Alessandro, B; Alexa, C; Arnaldi, R; Atayan, M; Baglin, C; Baldit, A; Bedjidian, M; Beole, S; Boldea, V; Bordalo, P; Borges, G; Bussiere, A; Capelli, L; Castanier, C; Castor, J; Chaurand, B; Chevrot, I; Cheynis, B; Chiavassa, E; Cicalo, C; Claudino, T; Comets, MP; Constans, N; Constantinescu, S; Cortese, P; De Falco, A; De Marco, N; Dellacasa, G; Devaux, A; Dita, S; Drapier, O; Ducroux, L; Espagnon, B; Fargeix, J; Force, P; Gallio, M; Gavrilov, YK; Gerschel, C; Giubellino, P; Golubeva, MB; Gonin, M; Grigorian, AA; Grigorian, S; Grossiord, JY; Guber, FF; Guichard, A; Gulkanyan, H; Hakobyan, R; Haroutunian, R; Idzik, M; Jouan, D; Karavitcheva, TL; Kluberg, L; Kurepin, AB; Le Bornec, Y; Lourenco, C; Macciotta, P; Mac Cormick, M; Marzari-Chiesa, A; Masera, M; Masoni, A; Monteno, M; Musso, A; Petiau, P; Piccotti, A; Pizzi, JR; da Silva, WLP; Prino, F; Puddu, G; Quintans, C; Ramello, L; Ramos, S; Mendes, PR; Riccati, L; Romana, A; Santos, H; Saturnini, P; Scalas, E; Scomparin, E; Serci, S; Shahoyan, R; Sigaudo, F; Silva, S; Sitta, M; Sonderegger, P; Tarrago, X; Topilskaya, NS; Usai, GL; Vercellin, E; Villatte, L; Willis, N (NA50 Collaboration) *Scaling of charged particle multiplicity in Pb-Pb collisions at SPS energies* PHYSICS LETTERS B, 530 (1-4): 43-55 MAR 28 2002 ISSN: 0370-2693.

4.3.4 Conference presentations

1. M. Šumbera, *Ultra-relativistic nucleus-nucleus collisions: past, present and future (from CERN to BNL and back)* Czech-Taiwan workshop on the intermediate and high energy physics, Prague, Czech Republic, 3.-5.3.2003. Czechoslovak Journal of Physics, Volume 53, Number 8 / August, 2003.

4.3.5 Further developments

Enhanced production of dileptons

Final results on enhanced production of low-mass e^-e^+ pairs in 40-AGeV Pb+Au collisions were published in [97]. The observed pair yield integrated over the range of invariant masses $0.2 < m \leq 1$ GeV/c^2 is enhanced over the expectation from neutral meson decays by a factor of $5.9 \pm 1.5(\text{stat}) \pm 1.2(\text{systdata}) \pm 1.8(\text{systmesondecays})$.

In [110] we have present a measurement of e^+e^- pair production in central Pb+Au collisions at 158A GeV/c. The improved mass resolution of the data set, recorded with the upgraded CERES experiment, allowed for a comparison of the data with different theoretical approaches. The data clearly favor a substantial in-medium broadening of the ρ spectral function over a density-dependent shift of the ρ pole mass. The in-medium broadening model implies that baryon induced interactions are the key mechanism to in-medium modifications of the ρ-meson in the hot fireball at SPS energy.

In 2002 we have submitted proposal to continue the study of electron pair and hadron production with In and Pb beams at the CERN SPS [99]. The proposal was rejected because the new NA60 experiment with much better dilepton mass resolution was already approved. The NA60 has studied low-mass dimuon production in 158

AGeV In-In collisions. The unprecedented sample size of 360 000 dimuons and the good mass resolution of about 2% allow them to isolate the excess by subtraction of the decay sources [R94]. The shape of the resulting mass spectrum was found to be consistent with a dominant contribution from $\pi^+\pi^- \rightarrow \rho \rightarrow \mu^+\mu^-$ annihilation. The associated space-time averaged ρ spectral function showed a strong broadening, but essentially no shift in mass. The results on the associated transverse momentum spectra [R95] have shown that the slope parameter T_{eff} rises with dimuon mass up to the mass of ρ meson, followed by a sudden decline above. While the initial rise is consistent with the expectations for radial flow of a hadronic decay source, the decline signals a transition to an emission source with much smaller flow. This may well represent the first direct evidence for thermal radiation of partonic origin in nuclear collisions. This result was confirmed in [R96]. Using the Collins-Soper reference frame, the NA60 has found that the structure function parameters λ, μ and ν are zero. The projected distributions in polar and azimuth angles were found to be uniform. The absence of any polarization was interpreted as consistent with the interpretation of the excess dimuons as thermal radiation from a randomized system. All these results are compatible with our previous findings.

Elliptic flow

Let us note that even at the SPS energies the v_2 of identified particles needs not to be necessarily a positive number. The WA98 measurement of semi-central Pb+Pb collisions at the top SPS energy [67], [68] have shown that while π^+ mesons, as expected, are emitted in the reaction plane, K^+ mesons are found to be preferentially emitted out of the reaction plane. The results suggest that even at such high energies the kaon emission is influenced by in-medium potential effects in addition to collective flow effects. This interpretation is supported by a simple model calculation in which K^+ mesons propagate through a static anisotropic distribution of nucleons with a repulsive K^+N potential. The final out-of-plane elliptic emission pattern emerges from an initially isotropic azimuthal distribution of K^+.

Fluctuations

Comparison between the event-by-event fluctuations of the mean transverse momentum in Pb + Au collisions at three different energies 40 AGeV, 80 AGeV and 158 A-GeV was studied in [103]. Significant excess of mean p_T fluctuations at mid-rapidity over the expectation from statistically independent particle emission was observed. The results are somewhat smaller than observed at $\sqrt{s_{NN}} = 130$ GeV at RHIC [147]. A possible non-monotonic behavior of the mean p_T fluctuations as function of collision energy, which may have indicated that the system has passed the critical point of the QCD phase diagram in the range of μ_B under investigation, has not been observed. A comparison to results from the RQMD and URQMD models [R35] indicates that secondary rescattering, if enabled, tends to decrease the fluctuation strength, while calculations without rescattering show reasonable agreement with the data. Such a scenario is supported by the observation of high densities and a short mean free path at thermal freeze-out, as derived from a recent analysis of pion interferometry data [95], which point to a short lifetime of the hadronic phase. Further result on this topic were published in [105] and [115].

Chapter 5

Heavy ion collider physics at BNL RHIC and CERN LHC

5.1 Experiment STAR at RHIC

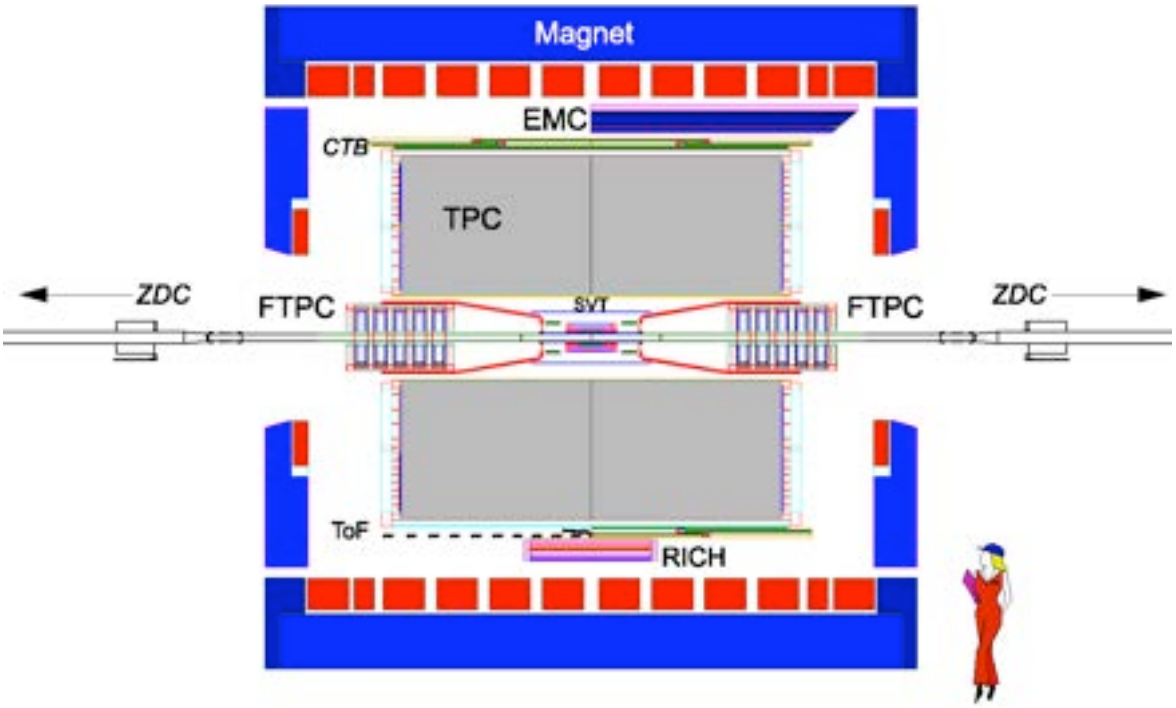

Figure 5.1: Cutaway side view of the **S**olenoidal **T**racker **a**t **R**HIC (STAR) detector as configured in 2001 [126]. Embeded into solenoidal magnet (outer diameter 7m) with a uniform magnetic field of maximum value 0.5 T are Silicon Vertex Tracker (SVT), a large volume Time Projection Chamber (TPC), central trigger barrel (CTB) detector, radial-drift TPC (FTPC), a ring imaging Cherenkov detector (RICH), a time-offlight (TOF) patch, barrel electromagnetic calorimeter (EMC) and an endcap electromagnetic calorimeter (EEMC). The fast detectors that provide input to the trigger system are CTB and zero-degree calorimeters (ZDC) located in the forward direction at $\theta < 2$ mrad. SVT, TPC, FTPC and CTB provide a full azimuthal acceptance.

Article reprint

Available online at www.sciencedirect.com
SCIENCE DIRECT®

ELSEVIER

Nuclear Physics A 757 (2005) 102–183

NUCLEAR PHYSICS A

Experimental and theoretical challenges in the search for the quark–gluon plasma: The STAR Collaboration's critical assessment of the evidence from RHIC collisions

STAR Collaboration

J. Adams [c], M.M. Aggarwal [ac], Z. Ahammed [aq], J. Amonett [t], B.D. Anderson [t], D. Arkhipkin [m], G.S. Averichev [l], S.K. Badyal [s], Y. Bai [aa], J. Balewski [q], O. Barannikova [af], L.S. Barnby [c], J. Baudot [r], S. Bekele [ab], V.V. Belaga [l], A. Bellingeri-Laurikainen [al], R. Bellwied [at], J. Berger [n], B.I. Bezverkhny [av], S. Bharadwaj [ag], A. Bhasin [s], A.K. Bhati [ac], V.S. Bhatia [ac], H. Bichsel [as], J. Bielcik [av], J. Bielcikova [av], A. Billmeier [at], L.C. Bland [d], C.O. Blyth [c], B.E. Bonner [ah], M. Botje [aa], A. Boucham [al], J. Bouchet [al], A.V. Brandin [y], A. Bravar [d], M. Bystersky [k], R.V. Cadman [a], X.Z. Cai [ak], H. Caines [av], M. Calderón de la Barca Sánchez [q], J. Castillo [u], O. Catu [av], D. Cebra [g], Z. Chajecki [ab], P. Chaloupka [k], S. Chattopadhyay [aq], H.F. Chen [aj], Y. Chen [h], J. Cheng [ao], M. Cherney [j], A. Chikanian [av], W. Christie [d], J.P. Coffin [r], T.M. Cormier [at], J.G. Cramer [as], H.J. Crawford [f], D. Das [aq], S. Das [aq], M.M. de Moura [ai], T.G. Dedovich [l], A.A. Derevschikov [ae], L. Didenko [d], T. Dietel [n], S.M. Dogra [s], W.J. Dong [h], X. Dong [aj], J.E. Draper [g], F. Du [av], A.K. Dubey [o], V.B. Dunin [l], J.C. Dunlop [d], M.R. Dutta Mazumdar [aq], V. Eckardt [w], W.R. Edwards [u], L.G. Efimov [l], V. Emelianov [y], J. Engelage [f], G. Eppley [ah], B. Erazmus [al], M. Estienne [al], P. Fachini [d], J. Faivre [r], R. Fatemi [q], J. Fedorisin [l], K. Filimonov [u], P. Filip [k], E. Finch [av], V. Fine [d],

0375-9474/$ – see front matter
doi:10.1016/j.nuclphysa.2005.03.085

Y. Fisyak [d], J. Fu [ao], C.A. Gagliardi [am], L. Gaillard [c], J. Gans [av], M.S. Ganti [aq], F. Geurts [ah], V. Ghazikhanian [h], P. Ghosh [aq], J.E. Gonzalez [h], H. Gos [ar], O. Grachov [at], O. Grebenyuk [aa], D. Grosnick [ap], S.M. Guertin [h], Y. Guo [at], A. Gupta [s], T.D. Gutierrez [g], T.J. Hallman [d,*], A. Hamed [at], D. Hardtke [u], J.W. Harris [av], M. Heinz [b], T.W. Henry [am], S. Hepplemann [ad], B. Hippolyte [r], A. Hirsch [af], E. Hjort [u], G.W. Hoffmann [an], H.Z. Huang [h], S.L. Huang [aj], E.W. Hughes [e], T.J. Humanic [ab], G. Igo [h], A. Ishihara [an], P. Jacobs [u], W.W. Jacobs [q], M. Jedynak [ar], H. Jiang [h], P.G. Jones [c], E.G. Judd [f], S. Kabana [b], K. Kang [ao], M. Kaplan [i], D. Keane [t], A. Kechechyan [l], V.Yu. Khodyrev [ae], J. Kiryluk [v], A. Kisiel [ar], E.M. Kislov [l], J. Klay [u], S.R. Klein [u], D.D. Koetke [ap], T. Kollegger [n], M. Kopytine [t], L. Kotchenda [y], M. Kramer [z], P. Kravtsov [y], V.I. Kravtsov [ae], K. Krueger [a], C. Kuhn [r], A.I. Kulikov [l], A. Kumar [ac], R.Kh. Kutuev [m], A.A. Kuznetsov [l], M.A.C. Lamont [av], J.M. Landgraf [d], S. Lange [n], F. Laue [d], J. Lauret [d], A. Lebedev [d], R. Lednicky [l], S. Lehocka [l], M.J. LeVine [d], C. Li [aj], Q. Li [at], Y. Li [ao], G. Lin [av], S.J. Lindenbaum [z], M.A. Lisa [ab], F. Liu [au], H. Liu [aj], L. Liu [au], Q.J. Liu [as], Z. Liu [au], T. Ljubicic [d], W.J. Llope [ah], H. Long [h], R.S. Longacre [d], M. Lopez-Noriega [ab], W.A. Love [d], Y. Lu [au], T. Ludlam [d], D. Lynn [d], G.L. Ma [ak], J.G. Ma [h], Y.G. Ma [ak], D. Magestro [ab], S. Mahajan [s], D.P. Mahapatra [o], R. Majka [av], L.K. Mangotra [s], R. Manweiler [ap], S. Margetis [t], C. Markert [t], L. Martin [al], J.N. Marx [u], H.S. Matis [u], Yu.A. Matulenko [ae], C.J. McClain [a], T.S. McShane [j], F. Meissner [u], Yu. Melnick [ae], A. Meschanin [ae], M.L. Miller [v], N.G. Minaev [ae], C. Mironov [t], A. Mischke [aa], D.K. Mishra [o], J. Mitchell [ah], B. Mohanty [aq], L. Molnar [af], C.F. Moore [an], D.A. Morozov [ae], M.G. Munhoz [ai], B.K. Nandi [aq], S.K. Nayak [s], T.K. Nayak [aq], J.M. Nelson [c], P.K. Netrakanti [aq], V.A. Nikitin [m], L.V. Nogach [ae], S.B. Nurushev [ae], G. Odyniec [u], A. Ogawa [d], V. Okorokov [y], M. Oldenburg [u], D. Olson [u], S.K. Pal [aq], Y. Panebratsev [l], S.Y. Panitkin [d], A.I. Pavlinov [at], T. Pawlak [ar], T. Peitzmann [aa], V. Perevoztchikov [d], C. Perkins [f], W. Peryt [ar], V.A. Petrov [at], S.C. Phatak [o], R. Picha [g], M. Planinic [aw], J. Pluta [ar], N. Porile [af], J. Porter [as], A.M. Poskanzer [u], M. Potekhin [d], E. Potrebenikova [l], B.V.K.S. Potukuchi [s], D. Prindle [as], C. Pruneau [at], J. Putschke [w],

G. Rakness [ad], R. Raniwala [ag], S. Raniwala [ag], O. Ravel [al], R.L. Ray [an], S.V. Razin [l], D. Reichhold [af], J.G. Reid [as], J. Reinnarth [al], G. Renault [al], F. Retiere [u], A. Ridiger [y], H.G. Ritter [u], J.B. Roberts [ah], O.V. Rogachevskiy [l], J.L. Romero [g], A. Rose [u], C. Roy [al], L. Ruan [aj], M. Russcher [aa], R. Sahoo [o], I. Sakrejda [u], S. Salur [av], J. Sandweiss [av], M. Sarsour [q], I. Savin [m], P.S. Sazhin [l], J. Schambach [an], R.P. Scharenberg [af], N. Schmitz [w], J. Seger [j], P. Seyboth [w], E. Shahaliev [l], M. Shao [aj], W. Shao [e], M. Sharma [ac], W.Q. Shen [ak], K.E. Shestermanov [ae], S.S. Shimanskiy [l], E. Sichtermann [u], F. Simon [w], R.N. Singaraju [aq], N. Smirnov [av], R. Snellings [aa], G. Sood [ap], P. Sorensen [u], J. Sowinski [q], J. Speltz [r], H.M. Spinka [a], B. Srivastava [af], A. Stadnik [l], T.D.S. Stanislaus [ap], R. Stock [n], A. Stolpovsky [at], M. Strikhanov [y], B. Stringfellow [af], A.A.P. Suaide [ai], E. Sugarbaker [ab], C. Suire [d], M. Sumbera [k], B. Surrow [v], M. Swanger [j], T.J.M. Symons [u], A. Szanto de Toledo [ai], A. Tai [h], J. Takahashi [ai], A.H. Tang [aa], T. Tarnowsky [af], D. Thein [h], J.H. Thomas [u], S. Timoshenko [y], M. Tokarev [l], S. Trentalange [h], R.E. Tribble [am], O.D. Tsai [h], J. Ulery [af], T. Ullrich [d], D.G. Underwood [a], G. Van Buren [d], M. van Leeuwen [u], A.M. Vander Molen [x], R. Varma [p], I.M. Vasilevski [m], A.N. Vasiliev [ae], R. Vernet [r], S.E. Vigdor [q], Y.P. Viyogi [aq], S. Vokal [l], S.A. Voloshin [at], W.T. Waggoner [j], F. Wang [af], G. Wang [t], G. Wang [e], X.L. Wang [aj], Y. Wang [an], Y. Wang [ao], Z.M. Wang [aj], H. Ward [an], J.W. Watson [t], J.C. Webb [q], G.D. Westfall [x], A. Wetzler [u], C. Whitten Jr. [h], H. Wieman [u], S.W. Wissink [q], R. Witt [b], J. Wood [h], J. Wu [aj], N. Xu [u], Z. Xu [d], Z.Z. Xu [aj], E. Yamamoto [u], P. Yepes [ah], V.I. Yurevich [l], I. Zborovsky [k], H. Zhang [d], W.M. Zhang [t], Y. Zhang [aj], Z.P. Zhang [aj], R. Zoulkarneev [m], Y. Zoulkarneeva [m], A.N. Zubarev [l]

[a] *Argonne National Laboratory, Argonne, IL 60439, USA*
[b] *University of Bern, 3012 Bern, Switzerland*
[c] *University of Birmingham, Birmingham, United Kingdom*
[d] *Brookhaven National Laboratory, Upton, NY 11973, USA*
[e] *California Institute of Technology, Pasadena, CA 91125, USA*
[f] *University of California, Berkeley, CA 94720, USA*
[g] *University of California, Davis, CA 95616, USA*
[h] *University of California, Los Angeles, CA 90095, USA*
[i] *Carnegie Mellon University, Pittsburgh, PA 15213, USA*
[j] *Creighton University, Omaha, NE 68178, USA*

[k] *Nuclear Physics Institute AS CR, 250 68 Řež/Prague, Czech Republic*
[l] *Laboratory for High Energy (JINR), Dubna, Russia*
[m] *Particle Physics Laboratory (JINR), Dubna, Russia*
[n] *University of Frankfurt, Frankfurt, Germany*
[o] *Institute of Physics, Bhubaneswar 751005, India*
[p] *Indian Institute of Technology, Mumbai, India*
[q] *Indiana University, Bloomington, IN 47408, USA*
[r] *Institut de Recherches Subatomiques, Strasbourg, France*
[s] *University of Jammu, Jammu 180001, India*
[t] *Kent State University, Kent, OH 44242, USA*
[u] *Lawrence Berkeley National Laboratory, Berkeley, CA 94720, USA*
[v] *Massachusetts Institute of Technology, Cambridge, MA 02139-4307, USA*
[w] *Max-Planck-Institut für Physik, Munich, Germany*
[x] *Michigan State University, East Lansing, MI 48824, USA*
[y] *Moscow Engineering Physics Institute, Moscow, Russia*
[z] *City College of New York, New York City, NY 10031, USA*
[aa] *NIKHEF and Utrecht University, Amsterdam, The Netherlands*
[ab] *Ohio State University, Columbus, OH 43210, USA*
[ac] *Panjab University, Chandigarh 160014, India*
[ad] *Pennsylvania State University, University Park, PA 16802, USA*
[ae] *Institute of High Energy Physics, Protvino, Russia*
[af] *Purdue University, West Lafayette, IN 47907, USA*
[ag] *University of Rajasthan, Jaipur 302004, India*
[ah] *Rice University, Houston, TX 77251, USA*
[ai] *Universidade de Sao Paulo, Sao Paulo, Brazil*
[aj] *University of Science & Technology of China, Anhui 230027, China*
[ak] *Shanghai Institute of Applied Physics, Shanghai 201800, China*
[al] *SUBATECH, Nantes, France*
[am] *Texas A&M University, College Station, TX 77843, USA*
[an] *University of Texas, Austin, TX 78712, USA*
[ao] *Tsinghua University, Beijing 100084, China*
[ap] *Valparaiso University, Valparaiso, IN 46383, USA*
[aq] *Variable Energy Cyclotron Centre, Kolkata 700064, India*
[ar] *Warsaw University of Technology, Warsaw, Poland*
[as] *University of Washington, Seattle, WA 98195, USA*
[at] *Wayne State University, Detroit, MI 48201, USA*
[au] *Institute of Particle Physics, CCNU (HZNU), Wuhan 430079, China*
[av] *Yale University, New Haven, CT 06520, USA*
[aw] *University of Zagreb, Zagreb, HR-10002, Croatia*

Received 15 October 2004; received in revised form 29 March 2005; accepted 9 May 2005

Available online 17 May 2005

Abstract

We review the most important experimental results from the first three years of nucleus–nucleus collision studies at RHIC, with emphasis on results from the STAR experiment, and we assess their interpretation and comparison to theory. The theory-experiment comparison suggests that central

* Corresponding author.
E-mail address: hallman@bnl.gov (T.J. Hallman).

Au + Au collisions at RHIC produce dense, rapidly thermalizing matter characterized by: (1) initial energy densities above the critical values predicted by lattice QCD for establishment of a quark–gluon plasma (QGP); (2) nearly ideal fluid flow, marked by constituent interactions of very short mean free path, established most probably at a stage preceding hadron formation; and (3) opacity to jets. Many of the observations are consistent with models incorporating QGP formation in the early collision stages, and have not found ready explanation in a hadronic framework. However, the measurements themselves do not yet establish unequivocal evidence for a transition to this new form of matter. The theoretical treatment of the collision evolution, despite impressive successes, invokes a suite of distinct models, degrees of freedom and assumptions of as yet unknown quantitative consequence. We pose a set of important open questions, and suggest additional measurements, at least some of which should be addressed in order to establish a compelling basis to conclude definitively that thermalized, deconfined quark–gluon matter has been produced at RHIC.

PACS: 25.75.-q

1. Introduction

The relativistic heavy ion collider was built to create and investigate strongly interacting matter at energy densities unprecedented in a laboratory setting—matter so hot that neutrons, protons and other hadrons are expected to "melt". Results from the four RHIC experiments already demonstrate that the facility has fulfilled its promise to reach such extreme conditions during the early stages of nucleus–nucleus collisions, forming matter that exhibits heretofore unobserved behavior. These results are summarized in this work and in a number of excellent recent reviews [1–5]. They afford RHIC the exciting scientific opportunity to discover the properties of matter under conditions believed to pertain during a critical, though fleeting, stage of the universe's earliest development following the big bang. The properties of such matter test fundamental predictions of quantum chromodynamics (QCD) in the non-perturbative regime.

In this document we review the results to date from RHIC experiments, with emphasis on those from STAR, in the context of a narrower, more pointed question. The specific prediction of QCD most often highlighted in discussions of RHIC since its conception is that of a transition from hadronic matter to a quark–gluon plasma (QGP) phase, defined below. Recent theoretical claims [6–8] that a type of QGP has indeed been revealed by RHIC experiments and interest in this subject by the popular press [9,10] make it especially timely to evaluate where we are with respect to this particular goal. The present paper has been written in response to a charge (see Appendix A) from the STAR Collaboration to itself, to assess whether RHIC results yet support a compelling discovery claim for the QGP, applying the high standards of scientific proof merited by the importance of this issue. We began this assessment before the end of the fourth successful RHIC running period, and we have based our evaluation on results from the first three RHIC runs, which are often dramatic, sometimes unexpected, and generally in excellent agreement among the four RHIC experiments (and we utilize results from all of the experiments here). Since we began, some analyses of data from run 4 have progressed to yield publicly presented

results that amplify or quantify some of our conclusions in this work, but do not contradict any of them.

In addressing our charge, it is critical to begin by defining clearly what we mean by the QGP, since theoretical expectations of its properties have evolved significantly over the 20 years since the case for RHIC was first made. For our purposes here, we take the QGP to be *a (locally) thermally equilibrated state of matter in which quarks and gluons are deconfined from hadrons, so that color degrees of freedom become manifest over* ***nuclear****, rather than merely nucleonic, volumes*. In concentrating on thermalization and deconfinement, we believe our definition to be consistent with what has been understood by the physics community at large since RHIC was first proposed, as summarized by planning documents quoted in Appendix B. In particular, thermalization is viewed as a necessary condition to be dealing with a state of matter, whose properties can be meaningfully compared to QCD predictions or applied to the evolution of the early universe. Observation of a deconfinement transition has always been a primary goal for RHIC, in the hope of illuminating the detailed mechanism of the normal color confinement in QCD. For reasons presented below, we do significantly omit from our list of necessary conditions some other features discussed as potentially relevant over the years since RHIC's conception.

- We do not demand that the quarks and gluons in the produced matter be non-interacting, as has been considered in some conceptions of the QGP. Lattice QCD calculations suggest that such an ideal state may be approached in static bulk QGP matter only at temperatures very much higher than that required for the deconfinement transition. Furthermore, attainment of thermalization on the ultra-short timescale of a RHIC collision must rely on frequent interactions among the constituents during the earliest stages of the collision—a requirement that is not easily reconcilable with production of an ideal gas. While the absence of interaction would allow considerable simplifications in the calculation of thermodynamic properties of the matter, we do not regard this as an essential feature of color-deconfined matter. In this light, some have suggested [6–8] that we label the matter we seek as the sQGP, for strongly-interacting quark–gluon plasma. Since we regard this as the form of QGP that should be normally anticipated, we consider the 's' qualifier to be superfluous.
- We do not require evidence of a first- or second-order phase transition, even though early theoretical conjecture [11] often focused on possible QGP signatures involving sharp changes in experimental observables with collision energy density. In fact, the nature of the predicted transition from hadron gas to QGP has only been significantly constrained by quite recent theory. Our definition allows for a QGP discovery in a thermodynamic regime beyond a possible critical point. Most modern lattice QCD calculations indeed suggest the existence of such a critical point at baryon densities well above those where RHIC collisions appear to first form the matter. Nonetheless, such calculations still predict a rapid (but unaccompanied by discontinuities in thermodynamic observables) crossover transition in the bulk properties of strongly interacting matter at zero baryon density.
- We consider that evidence for chiral symmetry restoration would be sufficient to demonstrate a new form of matter, but is not *necessary* for a compelling QGP discovery. Most lattice QCD calculations do predict that this transition will accompany

deconfinement, but the question is certainly not definitively decided theoretically. If clear evidence for deconfinement can be provided by the experiments, then the search for manifestations of chiral symmetry restoration will be one of the most profound goals of further investigation of the matter's properties, as they would provide the clearest evidence for fundamental modifications to the QCD vacuum, with potentially far-reaching consequences.

The above "relaxation" of demands, in comparison to initial expectations before initiation of the RHIC program, makes a daunting task even more challenging. The possible absence of a first- or second-order phase transition reduces hopes to observe some well-marked changes in behavior that might serve as an experimental "smoking gun" for a transition to a new form of matter. Indeed, even if there were a sharp transition as a function of bulk matter temperature, it would be unlikely to observe non-smooth behavior in heavy-ion collisions, which form finite-size systems spanning some range of local temperatures even at fixed collision energy or centrality. We thus have to rely more heavily for evidence of QGP formation on the comparison of experimental results with theory. But theoretical calculations of the properties of this matter become subject to all the complexities of strong QCD interactions, and hence to the technical limitations of lattice gauge calculations. Even more significantly, these QCD calculations must be supplemented by other models to describe the complex dynamical passage of heavy-ion collision matter into and out of the QGP state. Heavy ion collisions represent our best opportunity to make this unique matter in the laboratory, but we place exceptional demands on these collisions: they must not only produce the matter, but then must serve "pump and probe" functions somewhat analogous to the modern generation of condensed matter instruments—and they must do it all on distance scales of femtometers and a time scale of 10^{-23} seconds!

There are two basic classes of probes at our disposal in heavy ion collisions. In studying electroweak collision products, we exploit the *absence* of final-state interactions (FSI) with the evolving strongly interacting matter, hoping to isolate those produced during the early collision stages and bearing the imprints of the bulk properties characterizing those stages. But we have to deal with the relative scarcity of such products, and competing origins from hadron decay and interactions during later collision stages. Most of the RHIC results to date utilize instead the far more abundant produced hadrons, where one exploits (but then must understand) the FSI. It becomes critical to distinguish *partonic* FSI from *hadronic* FSI, and to distinguish both from initial-state interactions and the effects of (so far) poorly understood parton densities at very low momentum fraction in the entrance-channel nuclei. Furthermore, the formation of hadrons from a QGP involves soft processes (parton fragmentation and recombination) that cannot be calculated from perturbative QCD and are a priori not well characterized (nor even cleanly separable) inside hot strongly interacting matter.

In light of all these complicating features, it is remarkable that the RHIC experiments have already produced results that appear to confirm some of the more striking, and at least semi-quantitative, predictions made on the basis of QGP formation! Other, unexpected, RHIC results have stimulated new models that explain them within a QGP-based framework. The most exciting results reveal phenomena not previously observed or explored at lower center-of-mass energies, and indeed are distinct from the observations on

which a circumstantial case for QGP formation was previously argued at CERN [12]. In order to assess whether a discovery claim is now justified, we must judge the robustness of both the new experimental results and the theoretical predictions they seem to bear out. Do the RHIC data *demand* a QGP explanation? Can they alternatively be accounted for in a hadronic framework? Are the theories and models used for the predictions mutually compatible? Are those other experimental results that currently appear to deviate from theoretical expectations indicative of details yet to be worked out, or rather of fundamental problems with the QGP explanation?

We organize our discussion as follows. In Section 2 we briefly summarize the most relevant theoretical calculations and models, their underlying assumptions, limitations and most robust predictions. We thereby identify the *crucial* QGP features we feel must be demonstrated experimentally to justify a compelling discovery claim. We divide the experimental evidence into two broad areas in Sections 3–4, focusing first on what we have learned about the bulk thermodynamic properties of the early stage collision matter from such measures as hadron spectra, collective flow and correlations among the soft hadrons that constitute the vast majority of outgoing particles. We discuss the consistency of these results with thermalization and the exposure of new (color) degrees of freedom. Next we provide an overview of the observations of hadron production yields and angular correlations at high transverse momentum (p_T 4 GeV/c), and what they have taught us about the nature of FSI in the collision matter and their bearing on deconfinement.

In Section 5 we focus on open questions for experiment and theory, on important crosschecks and quantifications, on predictions not yet borne out by experiment and experimental results not yet accommodated by theory. Finally, we provide in Section 6 an extended summary, conclusions and outlook, with emphasis on additional measurements and theoretical improvements that we feel are needed to strengthen the case for QGP formation. The summary of results in Section 6 is extended so that readers already familiar with most of the theoretical and experimental background material covered in Sections 2–5 can skip to the concluding section without missing the arguments central to our assessment of the evidence.

The STAR detector and its capabilities have been described in detail elsewhere [13], and will not be discussed.

2. Predicted signatures of the QGP

The promise, and then the delivery, of experimental results from the AGS, SPS and RHIC have stimulated impressive and important advances over the past decade in the theoretical treatment of the thermodynamic and hydrodynamic properties of hot strongly interacting matter and of the propagation of partons through such matter. However, the complexities of heavy-ion collisions and of hadron formation still lead to a patchwork of theories and models to treat the entire collision evolution, and the difficulties of the strong interaction introduce significant quantitative ambiguities in all aspects of this treatment. In support of a possible compelling QGP discovery claim, we must then identify the most striking qualitative predictions of theory, which survive the quantitative ambiguities, and we must look for a congruence of various observations that confirm such robust predic-

tions. In this section, we provide a brief summary of the most important pieces of the theoretical framework, their underlying assumptions and quantitative limitations, and what we view as their most robust predictions. Some of these predictions will then be compared with RHIC experimental results in later sections.

2.1. Features of the phase transition in lattice QCD

The phase diagram of bulk thermally equilibrated strongly interacting matter should be described by QCD. At sufficiently high temperature one must expect hadrons to "melt", deconfining quarks and gluons. The exposure of new (color) degrees of freedom would then be manifested by a rapid increase in entropy density, hence in pressure, with increasing temperature, and by a consequent change in the equation of state (EOS). In the limit where the deconfined quarks and gluons are non-interacting, and the quarks are massless, the (Stefan–Boltzmann) pressure P_{SB} of this partonic state, as a function of temperature T at zero chemical potential (i.e., zero net quark density), would be simply determined by the number of degrees of freedom [2]:

$$\frac{P_{\mathrm{SB}}}{T^4} = \left[2\left(N_c^2 - 1\right) + \frac{7}{2} N_c N_f\right] \frac{\pi^2}{90}, \tag{1}$$

where N_c is the number of colors, N_f the number of quark flavors, the temperature is measured in energy units (throughout this paper), and we have taken $\hbar = c = 1$. The two terms on the right in Eq. (1) represent the gluon and quark contributions, respectively. Refinements to this basic expectation, to incorporate effects of color interactions among the constituents, as well as of non-vanishing quark masses and chemical potential, and to predict the location and nature of the transition from hadronic to partonic degrees of freedom, are best made via QCD calculations on a space–time lattice (LQCD).

In order to extract physically relevant predictions from LQCD calculations, these need to be extrapolated to the continuum (lattice spacing $\to 0$), chiral (actual current quark mass) and thermodynamic (large volume) limits. While computing power limitations have restricted the calculations to date to numbers of lattice points that are still considered somewhat marginal from the viewpoint of these extrapolations [2], enormous progress has been made in recent years. Within the constraints of computing cost, there have been important initial explorations of sensitivity to details of the calculations [2]: e.g., the number and masses of active quark flavors included; the technical treatment of quarks on the lattice; the presence or absence of the $U_A(1)$ anomaly in the QGP state. Additional numerical difficulties have been partially overcome to allow first calculations at non-zero chemical potential and to improve the determination of physical quark mass scales for a given lattice spacing [2].

Despite the technical complications, LQCD calculations have converged on the following predictions:

- There is indeed a predicted transition of some form between a hadronic and a QGP phase, occurring at a temperature in the vicinity of $T_c \simeq 160$ MeV for zero chemical potential. The precise value of the transition temperature depends on the treatment of quarks in the calculation.

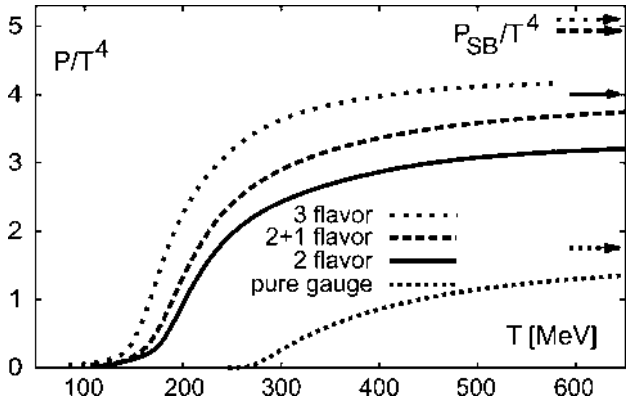

Fig. 1. LQCD calculation results from Ref. [14] for the pressure divided by T^4 of strongly interacting matter as a function of temperature, and for several different choices of the number of dynamical quark flavors. The arrows near the right axis indicate the corresponding Stefan–Boltzmann pressures for the same quark flavor assumptions.

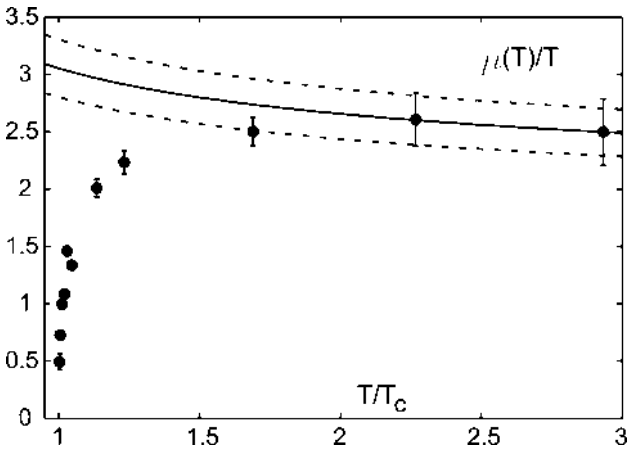

Fig. 2. Temperature-dependence of the heavy-quark screening mass (divided by temperature) as a function of temperature (in units of the phase transition temperature), from LQCD calculations in Ref. [15]. The curves represent perturbative expectations of the temperature-dependence.

- The pressure divided by T^4 rises rapidly above T_c, then begins to saturate by about $2T_c$, but at values substantially below the Stefan–Boltzmann limit (see Fig. 1) [14]. The deviation from the SB limit indicates substantial remaining interactions among the quarks and gluons in the QGP phase.
- Above T_c, the effective potential between a heavy quark–antiquark pair takes the form of a screened Coulomb potential, with screening mass (or inverse screening length) rising rapidly as temperature increases above T_c (see Fig. 2) [15]. As seen in the figure, the screening mass deviates strongly from perturbative QCD expectations in the vicinity of T_c, indicating large non-perturbative effects. The increased screening mass leads to a shortening of the range of the $q\bar{q}$ interaction, and to an anticipated suppression of charmonium production, in relation to open charm [16]. The predicted suppression appears to set in at substantially different temperatures for J/ψ (1.5–2.0T_c) and ψ' ($\sim 1.0T_c$) [17].

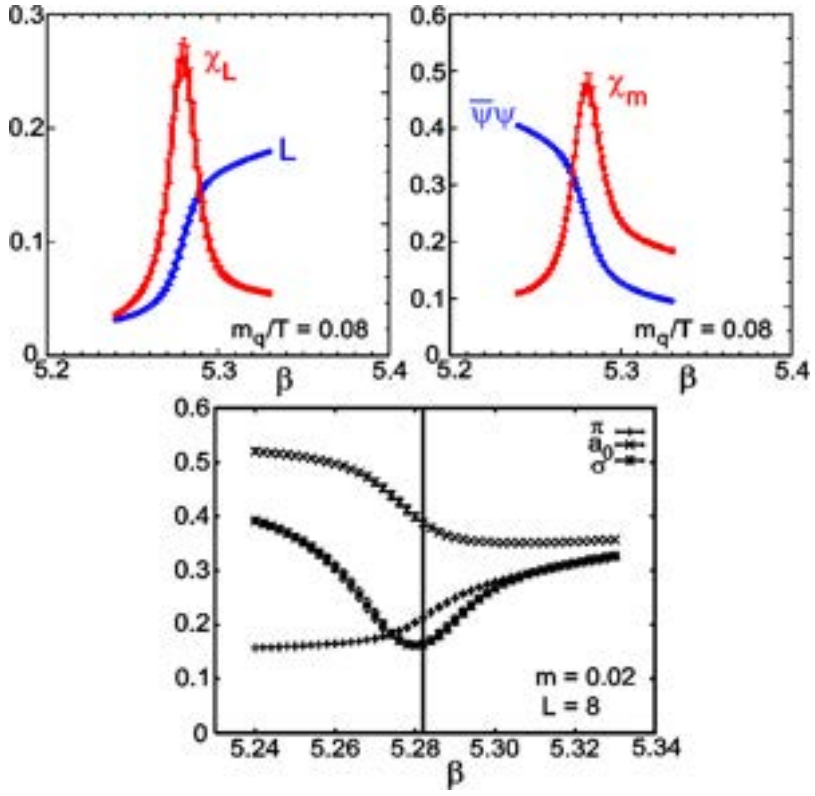

Fig. 3. LQCD calculations for two dynamical quark flavors [14] showing the coincidence of the chiral symmetry restoration (marked by the rapid decrease of chiral condensate $\langle\bar{\psi}\psi\rangle$ in the upper right-hand frame) and deconfinement (upper left frame) phase transitions. The lower plot shows that the chiral transition leads toward a mass degeneracy of the pion with scalar meson masses. All plots are as a function of the bare coupling strength β used in the calculations; increasing β corresponds to decreasing lattice spacing and to increasing temperature.

- In most calculations, the deconfinement transition is also accompanied by a chiral symmetry restoration transition, as seen in Fig. 3 [14]. The reduction in the chiral condensate leads to significant predicted variations in in-medium meson masses. These are also affected by the restoration of $U_A(1)$ symmetry, which occurs at higher temperature than chiral symmetry restoration in the calculation of Fig. 3.
- The nature of the transition from hadronic to QGP phase is highly sensitive to the number of dynamical quark flavors included in the calculation and to the quark masses [18]. For the most realistic calculations, incorporating two light (u, d) and one heavier (s) quark flavor relevant on the scale of T_c, the transition is most likely of the crossover type (with no discontinuities in thermodynamic observables—as opposed to first- or second-order phase transitions) at zero chemical potential, although the ambiguities in tying down the precise values of quark masses corresponding to given lattice spacings still permit some doubt.
- Calculations at non-zero chemical potential (μ_B), though not yet mature, suggest the existence of a critical point such as that illustrated in Fig. 4 [19]. The numerical challenges in such calculations leave considerable ambiguity about the value of μ_B at which the critical point occurs (e.g., it changes from $\mu_B \approx 700$ to 350 MeV between Refs. [20] and [19]), but it is most likely above the value at which RHIC collision

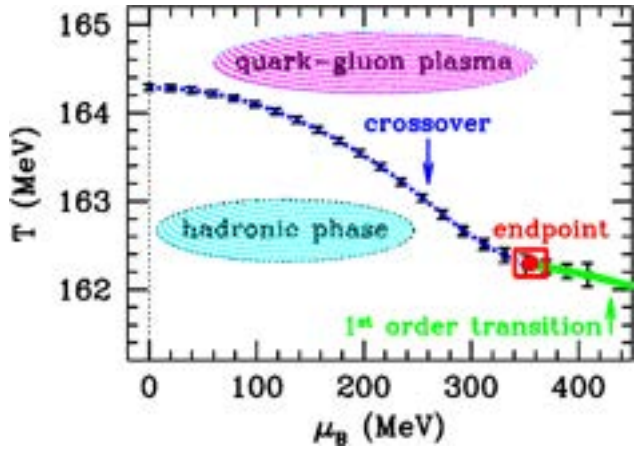

Fig. 4. LQCD calculation results for non-zero chemical potential [19], suggesting the existence of a critical point well above RHIC chemical potential values. The solid line indicates the locus of first-order phase transitions, while the dotted curve marks crossover transitions between the hadronic and QGP phases.

matter is formed, consistent with the crossover nature of the transition anticipated at RHIC.

- Even for crossover transitions, the LQCD calculations still predict a rapid temperature-dependence of the thermodynamic properties, as revealed in all of the figures considered above. However, in basing experimental expectations on this feature, it must be kept in mind that the early collision temperature varies slowly with collision energy and is not directly measured by any of the probes studied most extensively to date.

2.2. Hydrodynamic signatures

In order to determine how the properties of bulk QGP matter, as determined in LQCD calculations, may influence observable particle production spectra from RHIC collisions, one needs to model the time evolution of the collision "fireball". To the extent that the initial interactions among the constituents are sufficiently strong to establish local thermal equilibrium rapidly, and then to maintain it over a significant evolution time, the resulting matter may be treated as a relativistic fluid undergoing collective, hydrodynamic flow [3]. The application of hydrodynamics for the description of hadronic fireballs has a long history [21,22]. Relativistic hydrodynamics has been extensively applied to heavy ion collisions from BEVALAC to RHIC [3,22,23], but with the most striking successes at RHIC. The applicability of hydrodynamics at RHIC may provide the clearest evidence for the attainment of local thermal equilibrium at an early stage in these collisions. (On the other hand, there are alternative, non-equilibrium treatments of the fireball evolution that have also been compared to RHIC data [24].) The details of the hydrodynamic evolution are clearly sensitive to the EOS of the flowing matter, and hence to the possible crossing of a phase or crossover transition during the system expansion and cooling. It is critical to understand the relative sensitivity to the EOS as compared with that to other assumptions and parameters of the hydrodynamic treatment.

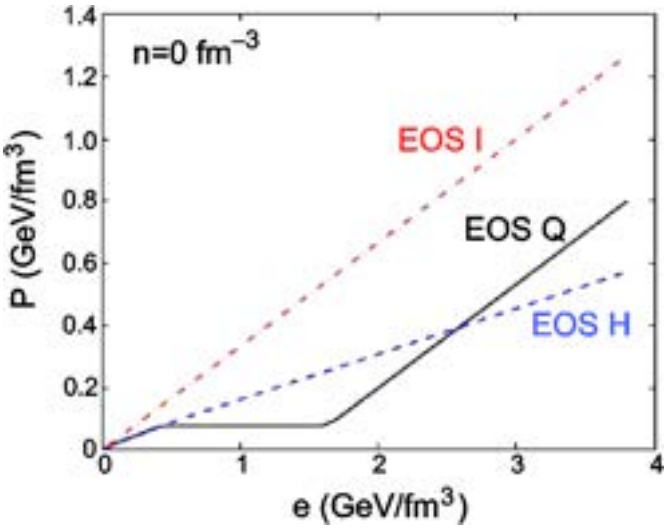

Fig. 5. Pressure as a function of energy density at vanishing net baryon density for three different equations of state of strongly interacting matter: a Hagedorn resonance gas (EOS H), an ideal gas of massless partons (EOS I) and a connection of the two via a first-order phase transition at $T_c = 164$ MeV (EOS Q). These EOS are used in hydrodynamics calculations in Ref. [3], from which the figure is taken.

Traditional hydrodynamics calculations cannot be applied to matter not in local thermal equilibrium, hence they must be supplemented by more phenomenological treatments of the early and late stages of the system evolution. These parameterize the initial conditions for the hydrodynamic flow and the transition to freezeout, where the structureless matter flow is converted into final hadron spectra. Since longitudinal flow is especially sensitive to initial conditions beyond the scope of the theory, most calculations to date have concentrated on *transverse* flow, and have assumed longitudinal boost-invariance of the predictions [3]. Furthermore, it is anticipated that hadrons produced at sufficiently high transverse momentum in initial partonic collisions will not have undergone sufficient rescatterings to come to thermal equilibrium with the surrounding matter, so that hydrodynamics will be applicable at best only for the softer features of observed spectra. Within the time range and momentum range of its applicability, most hydrodynamics calculations to date have treated the matter as an *ideal*, non-viscous fluid. The motion of this fluid is completely determined given the three components of the fluid velocity $\vec{v}$, the pressure (P) and the energy and baryon densities (e and n_B). The hydrodynamic equations of motion for an ideal fluid are derived from the exact local conservation laws for energy, momentum, and baryon number by assuming an ideal-fluid form for the energy–momentum tensor and baryon number current; they are closed by an equation of state $P(e, n_B)$ [21].

The EOS in hydrodynamics calculations for RHIC has been implemented using simplified models inspired by LQCD results, though not reproducing their details. One example is illustrated by the solid curve in Fig. 5, connecting an ideal gas of massless partons at high temperature to a Hagedorn hadron resonance gas [25] at low temperatures, via a first-order phase transition chosen to ensure consistency with ($\mu_B = 0$) LQCD results for critical temperature and net increase in entropy density across the transition [3]. In this implementation, the slope $\partial P/\partial e$ (giving the square of the velocity of sound in the matter) exhibits high values for the hadron gas and, especially, the QGP phases, but has a soft point at the

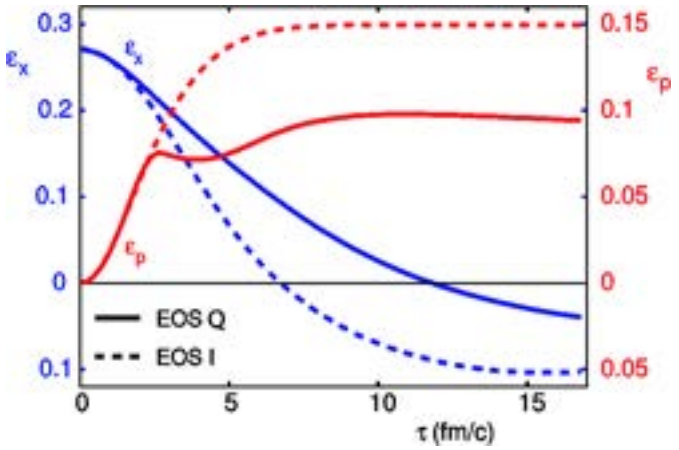

Fig. 6. Hydrodynamics calculations for the time evolution of the spatial eccentricity ϵ_x and the momentum anisotropy ϵ_p for non-central (7 fm impact parameter) Au + Au collisions at RHIC [3]. The solid and dashed curves result, respectively, from use of EOS Q and EOS I from Fig. 5. The gradual removal of the initial spatial eccentricity by the pressure gradients that lead to the buildup of ϵ_p reflects the self-quenching aspect of elliptic flow. The time scale runs from initial attainment of local thermal equilibrium through freezeout in this calculation.

mixed phase [3,22]. This generic softness of the EOS during the assumed phase transition has predictable consequences for the system evolution.

In heavy ion collisions, the measurable quantities are the momenta of the produced particles at the final state and their correlations. Transverse flow measures are key observables to compare quantitatively with model predictions in studying the EOS of the hot, dense matter. In non-central collisions, the reaction zone has an almond shape, resulting in azimuthally anisotropic pressure gradients, and therefore a non-trivial elliptic flow pattern. Experimentally, this elliptic flow pattern is usually measured using a Fourier decomposition of momentum spectra relative to the event-by-event reaction plane, in which the second Fourier component v_2 is the dominant contribution. The important feature of elliptic flow is that it is "self-quenching" [26,27], because the pressure-driven expansion tends to reduce the spatial anisotropy that causes the azimuthally anisotropic pressure gradient in the first place. This robust feature is illustrated in Fig. 6, which compares predictions for the spatial and resulting momentum eccentricities as a function of time during the system's hydrodynamic evolution, for two different choices of EOS [3]. The self-quenching makes the elliptic flow particularly sensitive to earlier collision stages, when the spatial anisotropy and pressure gradient are the greatest. In contrast, hadronic interactions at later stages may contribute significantly to the radial flow [28,29].

The solid momentum anisotropy curve in Fig. 6 also illustrates that entry into the soft EOS mixed phase during a transition from QGP to hadronic matter stalls the buildup of momentum anisotropy in the flowing matter. An even more dramatic predicted manifestation of this stall is shown by the dependence of p_T-integrated elliptic flow on produced hadron multiplicity in Fig. 7, where a dip is seen under conditions where the phase transition occupies most of the early collision stage. Since the calculations are carried out for a fixed impact parameter, measurements to confirm such a dip would have to be performed as a function of collision energy. In contrast to early (non-hydrodynamic) projections of particle multiplicities at RHIC (represented by horizontal arrows in Fig. 7), we now know

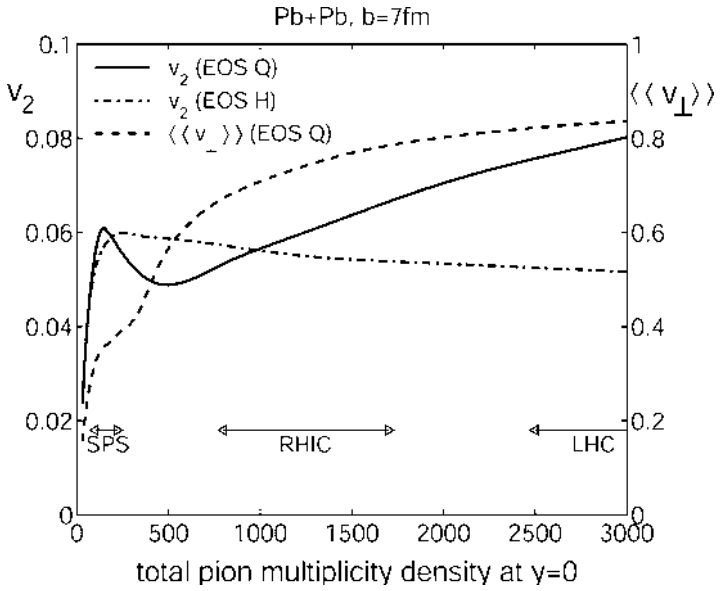

Fig. 7. Predicted hydrodynamic excitation function of p_T-integrated elliptic (v_2, solid curve, left axis) and radial ($\langle\langle v_\perp \rangle\rangle$, dashed, right axis) flow for non-central Pb + Pb collisions [30]. The calculations assume a sharp onset for freezeout along a surface of constant energy density corresponding to temperature ≈ 120 MeV. The soft phase transition stage in EOS Q gives rise to a dip in the elliptic flow. The horizontal arrows at the bottom reflect early projections of particle multiplicity for different facilities, but we now know that RHIC collisions produce multiplicities in the vicinity of the predicted dip.

that the multiplicity at the predicted dip is approximately achieved for appropriate centrality in RHIC Au + Au collisions at full energy. However, comparisons of predicted with measured excitation functions for elliptic flow are subject to an overriding ambiguity concerning where and when appropriate conditions of initial local thermal equilibrium for hydrodynamic applicability are actually achieved. Hydrodynamics itself has nothing to say concerning this issue.

One can alternatively attain sensitivity to the EOS in measurements for given collision energy and centrality by comparing to the predicted dependence of elliptic flow strength on hadron p_T and mass (see Fig. 8). The mass-dependence is of simple kinematic origin [3], and is thus a robust feature of hydrodynamics, but its quantitative extent, along with the magnitude of the flow itself, depends on the EOS [3].

Of course, the energy- and mass-dependence of v_2 can also be affected by species-specific hadronic FSI at and close to the freezeout where the particles decouple from the system, and hydrodynamics is no longer applicable [28,29]. A combination of macroscopic and microscopic models, with hydrodynamics applied at the early partonic and mixed-phase stages and a hadronic transport model such as RQMD [31] at the later hadronic stage, may offer a more realistic description of the whole evolution than that achieved with a simplified sharp freezeout treatment in Figs. 6, 7, 8. The combination of hydrodynamics with RQMD [29] has, for example, led to predictions of a substantially different, and monotonic, energy-dependence of elliptic flow, as can be seen by comparing Fig. 9 to Fig. 7. The difference between the two calculations may result primarily [6] from the elimination in [29] of the assumption of ideal fluid expansion even in the hadronic phase.

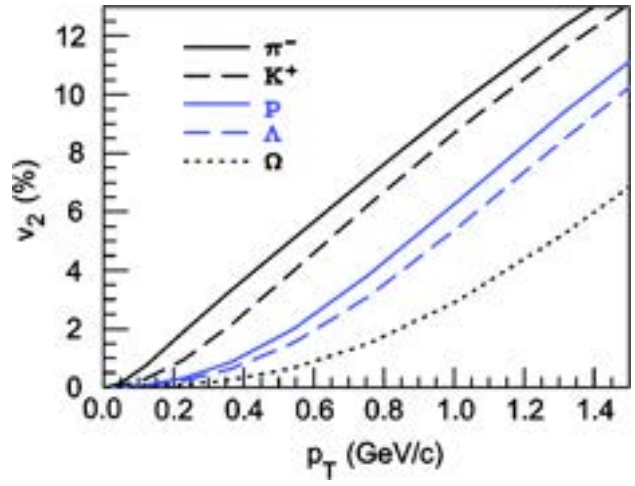

Fig. 8. Hydrodynamics predictions [32] of the p_T and mass-dependences of the elliptic flow parameter v_2 for identified final hadrons from Au + Au collisions at $\sqrt{s_{NN}} = 130$ GeV. The calculations employ EOS Q (see Fig. 5) and freezeout near 120 MeV.

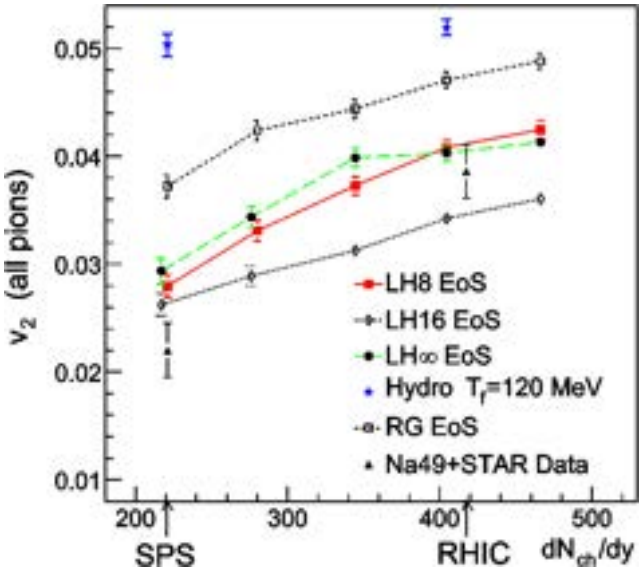

Fig. 9. Predictions [29] from a hybrid hydrodynamics-RQMD approach for the elliptic flow as a function of charged particle multiplicity in Pb + Pb collisions at an impact parameter $b = 6$ fm. Curves for different choices of EOS (LH8 is most similar to EOS Q in Fig. 7) are compared to experimental results derived [29] from SPS and RHIC measurements. The replacement of a simplified freezeout model for all hadron species and of the assumption of ideal hadronic fluid flow with the RQMD hadron cascade appears to remove any dip in v_2 values, such as seen in Fig. 7.

In any case, this comparison suggests that the energy dependence of elliptic flow in the quark–hadron transition region is at least as sensitive to the late hadronic interaction details as to the softening of the EOS in the mixed-phase region. Flow for multi-strange and charmed particles with small hadronic interaction cross sections may provide more selective sensitivity to the properties of the partonic and mixed phases [29,33,34]. There may be non-negligible sensitivity as well to the addition of such other complicating features

as viscosity [35] and deviations from longitudinal boost-invariance, studies of the latter effect requiring computationally challenging $(3+1)$-dimensional hydrodynamics calculations [36]. Certainly, the relative sensitivities to EOS variations vs. treatments of viscosity, boost-invariance, and the evolution of the hadronic stage must be clearly understood in order to interpret agreement between hydrodynamics calculations and measured flow.

In addition to predicting one-body hadron momentum spectra as a function of many kinematic variables, hydrodynamic evolution of the matter is also relevant for understanding two-hadron Hanbury-Brown-Twiss (HBT) quantum correlation functions [5]. From these correlation measurements one can extract information concerning the size and shape of the emitting surface at freezeout, i.e., at the end of the space–time evolution stage treated by hydrodynamics. While the detailed comparison certainly depends on improving models of the freezeout stage, it is reasonable to demand that hydrodynamics calculations consistent with the one-body hadron measurements be also at least roughly consistent with HBT results.

2.3. Statistical models

The aim of statistical models is to derive the equilibrium properties of a macroscopic system from the measured yields of the constituent particles [37,38]. Statistical models, however, do not describe how a system approaches equilibrium [38]. Hagedorn [25] and Fermi [39] pioneered their application to computing particle production yield ratios in high energy collisions, where conserved quantities such as baryon number and strangeness play important roles [40]. Statistical methods have become an important tool to study the properties of the fireball created in high energy heavy ion collisions [37,41], where they succeed admirably in reproducing measured yield ratios. Can this success be taken as evidence that the matter produced in these collisions has reached thermal and chemical equilibrium before hadronization? Can the temperature and chemical potential values extracted from such statistical model fits be interpreted as the equilibrium properties of the collision matter?

The answer to both of the above questions is "not on the basis of fits to integrated yields alone". The essential condition for applicability of statistical models is phase-space dominance in determining the distribution of a system with many degrees of freedom among relatively few observables [39,42], and this does not necessarily reflect a process of thermodynamic equilibration via interactions of the constituents. Indeed, statistical model fits can describe the observed hadron abundances well (albeit, only by including a strangeness undersaturation factor, $\gamma_s < 1$) in $p+p$, $e^+ + e^-$ and $p+A$ collisions, where thermal and chemical equilibrium are thought not to be achieved [37]. It is thus desirable to distinguish a system driven towards thermodynamic equilibrium from one born at hadronization with statistical phase space distributions, where "temperature" and "chemical potential" are simply Lagrange multipliers [43]. In order to make this distinction, it is necessary and sufficient to measure the extensive interactions among particles and to observe the change from canonical ensemble in a small system with the size of a nucleon ($p+p$, $e^+ + e^-$) and tens of produced particles, to grand canonical ensemble in a large system with extended volume and thousands of produced particles (central Au + Au) [37,40].

The evolution of the system from canonical to grand canonical ensemble can be observed, for example, via multi-particle correlations (especially of particles constrained by

conservation laws [42]) or by the centrality dependence of the strangeness suppression factor γ_s. The interactions among constituent particles, necessary to attainment of *thermal* equilibrium, can be measured by collective flow of many identified particles [29,44] and by resonance yields [45] that follow their hadronic rescattering cross sections. (Collective flow and resonance formation could, in principle, proceed via the dominant hadronic interactions that do not change hadron species, and hence are not strictly sufficient to establish *chemical* equilibration among hadrons, which would have to rely on relatively weak *inelastic* processes [43].)

If other measurements confirm the applicability of a grand canonical ensemble, then the hadron yield ratios can be used to extract the temperature and chemical potential of the system [37] at chemical freezeout. The latter is defined as the stage where hadrons have been created and the net numbers of stable particles of each type no longer change in further system evolution. These values place constraints on, but do not directly determine, the properties of the matter when thermal equilibrium was first attained in the wake of the collision. Direct measurement of the temperature at this early stage requires characterization of the yields of particles such as photons that are produced early but do not significantly interact on their way out of the collision zone.

2.4. Jet quenching and parton energy loss

Partons from the colliding nuclei that undergo a hard scattering in the initial stage of the collision provide colored probes for the colored bulk matter that may be formed in the collision's wake. It was Bjorken [46] who first suggested that partons traversing bulk partonic matter might undergo significant energy loss, with observable consequences on the parton's subsequent fragmentation into hadrons. More recent theoretical studies have demonstrated that the elastic parton scattering contribution to energy loss first contemplated by Bjorken is likely to be quite small, but that gluon radiation induced by passage through the matter may be quite sizable [4]. Such induced gluon radiation would be manifested by a significant softening and broadening of the jets resulting from the fragmentation of partons that traverse substantial lengths of matter containing a high density of partons—a phenomenon called "jet quenching". As will be documented in later sections, some of the most exciting of the RHIC results reveal jet quenching features quite strikingly. It is thus important to understand what features of this phenomenon may distinguish parton energy loss through a QGP from other possible sources of jet softening and broadening.

Several different theoretical evaluations of the non-Abelian radiative energy loss of partons in dense, but finite, QCD matter have been developed [47–50]. They give essentially consistent results, including the non-intuitive prediction that the energy loss varies with the square (L^2) of the thickness traversed through static matter, as a consequence of destructive interference effects in the coherent system of the leading quark and its first radiated gluon as they propagate through the matter. The overall energy loss is reduced, and the L-dependence shifted toward linearity, by the expansion of the matter resulting from heavy ion collisions. The significant deformation of the collision zone for non-central collisions, responsible for the observed elliptic flow (hence also for an azimuthal dependence of the rate of matter expansion), should give rise to a significant variation of the energy loss with angle with respect to the impact parameter plane. The scale of the net energy loss depends

on factors that can all be related to the rapidity density of gluons (dN_g/dy) in the matter traversed.

The energy loss calculated via any of these approaches is then embedded in a perturbative QCD (pQCD) treatment of the hard parton scattering. The latter treatment makes the standard factorization assumption (untested in the many-nucleon environment) that the cross section for producing a given final-state high-p_T hadron can be written as the product of suitable initial-state parton densities, pQCD hard-scattering cross section, and final-state fragmentation functions for the scattered partons. Nuclear modifications must be expected for the initial parton densities as well as for the fragmentation functions. Entrance-channel modifications—including both nuclear shadowing of parton densities and the introduction by multiple scattering of additional transverse momentum to the colliding partons—are capable of producing some broadening and softening of the final-state jets. But these effects can, in principle, be calibrated by complementing RHIC $A + A$ collision studies with $p + A$ or $d + A$, where QGP formation is not anticipated.

The existing theoretical treatments of the final-state modifications attribute the changes in effective fragmentation functions to the parton energy loss. That is, they assume vacuum fragmentation (as characterized phenomenologically from jet studies in more elementary systems) of the degraded parton and its spawned gluons [4]. This assumption may be valid in the high-energy limit, when the dilated fragmentation time should exceed the traversal time of the leading parton through the surrounding matter. However, its justification seems questionable for the soft radiated gluons and over the leading-parton momentum ranges to which it has been applied so far for RHIC collisions. In these cases, one might expect hadronization to be aided by the pickup of other partons from the surrounding QGP, and not to rely solely on the production of $q\bar{q}$ pairs from the vacuum. Indeed, RHIC experimental results to be described later in this document hint that the distinction between such recombination processes and parton fragmentation in the nuclear environment may not be clean. Furthermore, one of the developed models of parton energy loss [48] explicitly includes energy *gain* via absorption of gluons from the surrounding thermal QGP bath.

The assumption of vacuum fragmentation also implies a neglect of FSI effects for the hadronic fragmentation products, which might further contribute to jet broadening and softening. Models that attempt to account for *all* of the observed jet quenching via the alternative description of hadron energy loss in a hadronic gas environment are at this time still incomplete [51]. They must contend with the initial expectation of *color transparency* [52], i.e., that high momentum hadrons formed in strongly interacting matter begin their existence as point-like color-neutral particles with very small color dipole moments, hence weak interactions with surrounding nuclear matter. In order to produce energy loss consistent with RHIC measurements, these models must then introduce ad hoc assumptions about the rate of growth of these "pre-hadron" interaction cross sections during traversal of the surrounding matter [51].

The above caveats concerning assumptions of the parton energy loss models may call into question some of their quantitative conclusions, but are unlikely to alter the basic qualitative prediction that substantial jet quenching is a *necessary* result of QGP formation. The more difficult question is whether the observation of jet quenching can also be taken as a *sufficient* condition for a QGP discovery claim? Partonic traversal of matter can, in principle, be distinguished from effects of *hadronic* traversal by detailed dependences

of the energy loss, e.g., on azimuthal angle and system size (reflecting the nearly quadratic length-dependence characteristic of gluon radiation), on p_T (since hadron formation times should increase with increasing partonic momentum [53]), or on type of detected hadron (since hadronic energy losses should depend on particle type and size, while partonic energy loss should be considerably reduced for heavy quarks [53,54]). However, the energy loss calculations do not (with the exception of the small quantitative effect of *absorption* of thermal gluons [48]) distinguish confined from deconfined quarks and gluons in the surrounding matter. Indeed, the same approaches have been applied to experimental results from semi-inclusive deep inelastic scattering [55] or Drell–Yan dilepton production [56] experiments on nuclear targets to infer quark energy losses in *cold*, confined nuclear matter [57]. Baier et al. [58] have shown that the energy loss is expected to vary smoothly with energy density from cold hadronic to hot QGP matter, casting doubt on optimistic speculations [53] that the QGP transition might be accompanied by a rapid change in the extent of jet quenching with collision energy. Thus, the relevance of the QGP can only be inferred indirectly, from the magnitude of the gluon density dN_g/dy needed to reproduce jet quenching in RHIC collision matter, vis-à-vis that needed to explain the energy loss in cold nuclei. Is the extracted gluon density consistent with what one might expect for a QGP formed from RHIC collisions? To address this critical question, one must introduce new theoretical considerations of the initial state for RHIC collisions.

2.5. Saturation of gluon densities

In a partonic view, the initial conditions for the expanding matter formed in a RHIC collision are dominated by the scattering of gluons carrying small momentum fractions (Bjorken x) in the nucleons of the colliding nuclei. Gluon densities in the proton have been mapped down to quite small values of $x \sim 10^{-4}$ in deep inelastic scattering experiments at HERA [59]. When the measurements are made with high resolving power (i.e., with large 4-momentum transfer Q^2), the extracted gluon density $xg(x, Q^2)$ continues to grow rapidly down to the lowest x values measured. However, at moderate $Q^2 \sim$ few (GeV)^2, there are indications from the HERA data that $xg(x, Q^2)$ begins to saturate, as might be expected from the competition between gluon fusion ($g + g \to g$) and gluon splitting ($g \to g + g$) processes. It has been conjectured [60–63] that the onset of this saturation moves to considerably higher x values (for given Q^2) in a nuclear target, compared to a proton, and that a QGP state formed in RHIC collisions may begin with a saturated density of gluons. Indeed, birth within this saturated state might provide a natural mechanism for the rapid achievement of thermal equilibrium in such collisions [60].

The onset of saturation occurs when the product of the cross section for a QCD process (such as gluon fusion) of interest ($\sigma \sim \pi\alpha_s(Q^2)/Q^2$) and the areal density of partons (ρ) available to participate exceeds unity [66]. In this so-called color glass condensate region (see Fig. 10), QCD becomes highly non-linear, but amenable to classical field treatments, because the coupling strength remains weak ($\alpha_s \ll 1$) while the field strength is large [60–63]. The borderline of the CGC region is denoted by the "saturation scale" $Q_s^2(x, A)$. It depends on both x and target mass number A, because the target gluon density depends on both factors. In particular, at sufficiently low x and moderate Q^2, ρ is enhanced for a nucleus compared to a nucleon by a factor $\sim A^{1/3}$: the target sees the probe as hav-

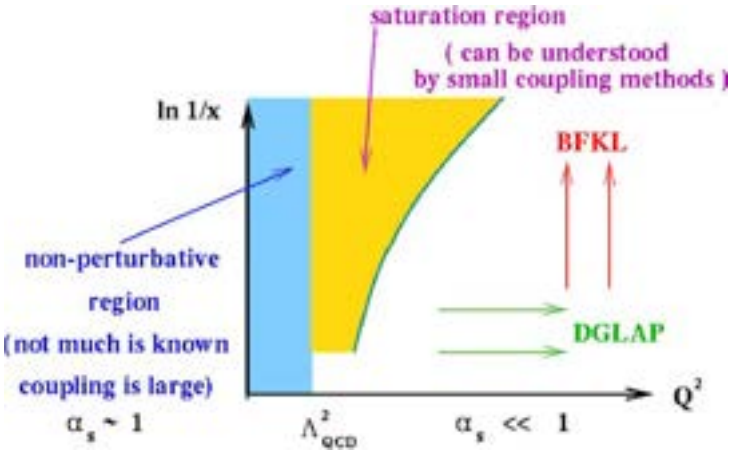

Fig. 10. Schematic layout of the QCD landscape in $x - Q^2$ space. The region at the right is the perturbative region, marked by applicability of the linear DGLAP [64] and BFKL [65] evolution equations for the Q^2- and x-dependence, respectively, of the parton distribution functions. At $Q^2 < \Lambda^2_{\mathrm{QCD}}$, the coupling constant is large and non-perturbative methods must be used to treat strongly interacting systems. The matter in RHIC collisions may be formed in the intermediate region, where gluon densities saturate, the coupling is still weak, but very strong color fields lead to non-linear behavior describable by classical field methods. The curve separating the saturation and perturbative regimes sets the saturation scale. Figure courtesy of Y. Kovchegov.

ing a longitudinal coherence length ($\ell_c \sim 1/m_N x$) much greater, but a transverse size ($\sim 1/Q^2$) much smaller, than the nuclear diameter. The probe thus interacts coherently with all the target gluons within a small diameter cylindrical "core" of the nucleus. The HERA data [59] suggest a rather slow variation—$xg(x) \propto x^{-\lambda}$, with $\lambda \sim 0.3$ at $Q^2 \sim$ few $(\mathrm{GeV})^2$—of gluon densities with x at low x. Consequently, one would have to probe a proton at roughly two orders of magnitude lower x than a Au nucleus to gain the same factor growth in gluon densities as is provided by $A^{1/3}$.

Under the assumption that QGP formation in a RHIC collision is dominated by gluon–gluon interactions below the saturation scale, saturation models predict the density of gluons produced per unit area and unit rapidity [60]:

$$\frac{d^2N}{d^2b\,dy} = C\frac{N_c^2 - 1}{4\pi^2\alpha_s(Q_s^2)N_c}Q_s^2(x, N_{\mathrm{part}}), \tag{2}$$

where A has been replaced by N_{part}, the number of nucleons participating in an $A + A$ collision at given impact parameter b, and $\hbar = c = 1$. The x-dependence of the saturation scale is taken from the HERA data

$$Q_s^2(x) = Q_0^2\left(\frac{x_0}{x}\right)^{\lambda}, \tag{3}$$

and the same values of $\lambda \sim 0.2$–0.3 are generally assumed to be valid inside the nucleus as well. However, the multiplicative factor C above, parameterizing the number of outgoing hadrons per initially present gluon, is typically adjusted to fit observed outgoing hadron multiplicities from RHIC collisions. (Variations in C are clearly not distinguishable, in the

context of Eq. (2), from changes to the overall saturation scale Q_0^2.) Once this parameter is fixed, gluon saturation models should be capable of predicting the dependence of hadron multiplicity on collision energy, rapidity, centrality and mass number. Furthermore, the initial QGP gluon densities extracted can be compared with the independent values obtained from parton energy loss model fits to jet quenching observations or from hydrodynamics calculations of elliptic flow.

While it is predictable within the QCD framework that gluon saturation should occur under appropriate conditions, and the theoretical treatment of the CGC state is highly evolved [60–63], the dependences of the saturation scale are not yet fully exposed by supporting data. Eventual confirmation of the existence of such a scale must come from comparing results for a wide range of high energy experiments from deep inelastic scattering in ep and eA (HERA, eRHIC) to pA and AA (RHIC, LHC) collisions.

2.6. Manifestations of quark recombination

The concept of quark recombination was introduced to describe hadron production in the forward region in $p + p$ collisions [67]. At forward rapidity, this mechanism allows a fast quark resulting from a hard parton scattering to recombine with a slow antiquark, which could be one in the original sea of the incident hadron, or one excited by a gluon [67]. If a QGP is formed in relativistic heavy ion collisions, then one might expect recombination of a different sort, namely, coalescence of the abundant thermal partons, to provide another important hadron production mechanism, active over a wide range of rapidity and transverse momentum [68]. In particular, at moderate p_T values (above the realm of hydrodynamics applicability), this hadron production "from below" (recombination of lower p_T partons from the thermal bath) has been predicted [69] to be competitive with production "from above" (fragmentation of higher p_T scattered partons). It has been suggested [70] that the need for substantial recombination to explain observed hadron yields and flow may be taken as a signature of QGP formation.

In order to explain observed features of RHIC collisions, the recombination models [68, 69] make the central assumption that coalescence proceeds via *constituent* quarks, whose number in a given hadron determines its production rate. The constituent quarks are presumed to follow a thermal (exponential) momentum spectrum and to carry a collective transverse velocity distribution. This picture leads to clear predicted effects on baryon and meson production rates, with the former depending on the spectrum of thermal constituent quarks and antiquarks at roughly one-third the baryon p_T, and the latter determined by the spectrum at one-half the meson p_T. Indeed, the recombination model was recently reintroduced in the RHIC context, precisely to explain an anomalous abundance of baryons vs. mesons observed at moderate p_T values [69]. If the observed (saturated) hadronic elliptic flow values in this momentum range result from coalescence of collectively flowing constituent quarks, then one can expect a similarly simple baryon vs. meson relationship [69]: the baryon (meson) flow would be 3 (2) times the quark flow at roughly one-third (one-half) the baryon p_T.

As will be discussed in later sections, RHIC experimental results showing just such simple predicted baryon vs. meson features would appear to provide strong evidence for QGP formation. However, the models do not spell out the connection between the inferred spec-

trum and flow of constituent quarks and the properties of the essentially massless partons (predominantly gluons) in a chirally restored QGP, where the chiral condensate (hence most of the constituent quark mass) has vanished. One may guess that the constituent quarks themselves arise from an earlier coalescence of gluons and *current* quarks during the chiral symmetry breaking transition back to hadronic matter, and that the constituent quark flow is carried over from the partonic phase.

However, alternative guesses concerning the relation of partons to the recombination degrees of freedom are also conceivable. Perhaps it is valence current, rather than constituent, quarks that recombine to determine hadron flow and momentum in this moderate-p_T range. In that case, hadronization might proceed through the formation of "pre-hadrons" (e.g., the pointlike color singlet objects discussed in connection with color transparency [52]) from the leading Fock (valence quark only) configurations, giving rise to the same 3-to-2 baryon-to-meson ratios as for constituent quarks. The internal pre-hadron wave functions would then subsequently evolve toward those of ordinary hadrons on their way out of the collision zone, so that the little-modified hadron momentum would in the end be shared substantially among sea quarks and gluons, as well as the progenitor valence quarks. Either of the above speculative (and quite possibly not orthogonal) interpretations of recombination would suggest that the hadron flow originates in, but is two steps removed from, *partonic* collectivity. But it is difficult to draw firm conclusions in light of the present ambiguity in connecting the effective degrees of freedom in coalescence models to the quarks and gluons treated by LQCD.

In addition, it is yet to be demonstrated that the coexistence of coalescence and fragmentation processes is quantitatively consistent with hadron angular correlations observed over p_T ranges where coalescence is predicted to dominate. These correlations exhibit prominent (near-side) peaks with angular widths (at least in azimuthal difference between two moderate-p_T hadrons) and charge sign ordering characteristic of jets from vacuum fragmentation of hard partons [71]. The coalescence yield might simply contribute to the background underlying these peaks, but one should also expect contributions from the "fast-slow" recombination (hard scattered parton with QGP bath partons) [72] for which the model was first introduced, and these could produce charge sign ordering. The latter effects—part of in-medium, as opposed to vacuum, fragmentation—complicate the interpretation of the baryon/meson comparisons and, indeed, muddy the distinction between fragmentation and recombination processes.

Finally, the picture provided by recombination is distinctly different from ideal hydrodynamics at a hadronic level, where velocity (mass) of a hadron is the crucial factor determining flow, rather than the number of constituent (or valence) quarks. At low momentum, energy and entropy conservations become a serious problem for quark coalescence, placing an effective lower limit on the p_T range over which the models can be credibly applied. The solution of this problem would require a dynamical, rather than purely kinematic treatment of the recombination process [69]. Such parton dynamics at low momentum might account for the thermodynamic properties of the macroscopic system discussed earlier, but we do not yet have a unified partonic theoretical framework.

3. Bulk properties

The multiplicities, yields, momentum spectra and correlations of hadrons emerging from heavy-ion collisions, especially in the soft sector comprising particles at transverse momenta p_T 1.5 GeV/c, reflect the properties of the bulk of the matter produced in the collision. In particular, we hope to infer constraints on its initial conditions, its degree of thermalization and its equation of state from measurements of soft hadrons.

The measured hadron spectra reflect the properties of the bulk of the matter at kinetic freezeout, after elastic collisions among the hadrons have ceased. At this stage the system is already relatively dilute and "cold". However, from the detailed properties of the hadron spectra at kinetic freezeout, information about the earlier hotter and denser stage can be obtained. Somewhat more direct information on an earlier stage can be deduced from the integrated yields of the different hadron species, which change only via *inelastic* collisions. These inelastic collisions cease already (at so-called chemical freezeout) before kinetic freezeout.

The transverse momentum distributions of the different particles reflect a random and a collective component. The random component can be identified with the temperature of the system at kinetic freezeout. The collective component arises from the matter density gradient from the center to the boundary of the fireball created in high-energy nuclear collisions. Interactions among constituents push matter outwards; frequent interactions lead to a common constituent velocity distribution. This so-called *collective flow* is therefore sensitive to the strength of the interactions. The collective flow is additive and thus accumulated over the whole system evolution, making it potentially sensitive to the equation of state of the expanding matter. At lower energies the collective flow reflects the properties of dense hadronic matter [73], while at RHIC energies a contribution from a pre-hadronic phase is anticipated.

In non-central heavy-ion collisions the initial transverse density gradient has an azimuthal anisotropy that leads to an azimuthal variation of the collective transverse flow velocity with respect to the impact parameter plane for the event. This azimuthal variation of flow is expected to be self-quenching (see Section 2.2), hence, especially sensitive to the interactions among constituents in the *early* stage of the collision [26,74], when the system at RHIC energies is anticipated to be well above the critical temperature for QGP formation.

Study of quantum (boson) correlations among pairs of emerging hadrons utilizes the Hanbury-Brown-Twiss effect to complement measurements of momentum spectra with information on the spatial size and shape of the emitting system. The measurement of more general two-particle correlations and of event-wise fluctuations can illuminate the degree of equilibration attained in the final hadronic system, as well as the dynamical origin of any observed non-equilibrium structures. Such dynamical correlations are prevalent in high-energy collisions of more elementary particles—where even relatively soft hadrons originate in large part from the fragmentation of partons—but are expected to be washed out by thermalization processes that produce phase space dominance of the final distribution probabilities.

In this section, we review the most important implications and questions arising from RHIC's vast body of data on soft hadrons. We also discuss some features of the transition

region (1.5 p_T 6 GeV/c), where the spectra gradually evolve toward the characteristic behavior of the hard parton fragmentation regime. In the process of going through the measured features of hadron spectra in the logical sequence outlined above, we devote special attention to a few critical features observed *for the first time* for central and near-central Au + Au collisions at STAR, that bear directly on the case for the QGP:

- hadron yields suggestive of chemical equilibration across the u, d and s quark sectors;
- elliptic flow of soft hadrons attaining the strength expected for an ideal relativistic fluid thermalized very shortly after the collision;
- elliptic flow results at intermediate p_T that appear to arise from the flow of quarks in a pre-hadronic stage of the matter.

3.1. Rapidity densities

Much has been made of the fact that predictions of hadron multiplicities in RHIC collisions before the year 2000 spanned a wide range of values, so that even the earliest RHIC measurements had significant discriminating power [7,75]. Mid-rapidity charged hadron densities measured in PHOBOS [76] and in STAR [77] are plotted in Fig. 11 as a function of collision centrality, as characterized by the number of participating nucleons, N_{part}, inferred from the fraction of the total geometric cross section accounted for in each analyzed bin. The solid curves in the figure represent calculations within a gluon saturation model [66], while the dashed curves in frames (a) and (b) represent two-component fits to the data [76] and in frames (c) and (d) represent an alternative model [78] assuming saturation of final-state mini-jet production. The apparent logarithmic dependence of the measured pseudorapidity densities on $\langle N_{\text{part}} \rangle$ is a characteristic feature of the gluon saturation model [66]. Consequently, the model's ability to reproduce the measured centrality and energy dependences have been presented as evidence for the relevance of the color glass condensate to the initial state for RHIC collisions, and used to constrain the saturation scale for initial gluon densities. This scale is in fair agreement with the scale extrapolated from HERA $e-p$ measurements at low Bjorken x [7].

However, these arguments are compromised because the particle multiplicity appears not to have strong discriminating power once one allows for adjustment of theoretical parameters. Furthermore, $\langle N_{\text{part}} \rangle$, which affects the scale on both axes in Fig. 11, is not a direct experimental observable. Glauber model calculations to associate values of $\langle N_{\text{part}} \rangle$ with given slices of the geometric cross section distribution have been carried out in two different ways, leading to an inconclusive theory vs. experiment comparison in Fig. 11(a) and (b). The preferred method for evaluating Glauber model cross sections in nucleus–nucleus collisions [79] invokes a Monte Carlo approach for integrating over all nucleon configurations, and has been used for the experimental results in frames (a), (b) and (d). However, the gluon saturation model calculations in *all* frames of Fig. 11 have employed the optical approximation, which ignores non-negligible correlation effects [79]. Comparison of the *experimental* results in frames (c) and (d), where the same STAR data have been plotted using these two Glauber prescriptions, illustrates the significant sensitivity to the use of the optical approximation. The "apples-to-apples" comparison of experiment and theory in frame (c) does not argue strongly in favor of initial-state gluon saturation, although an

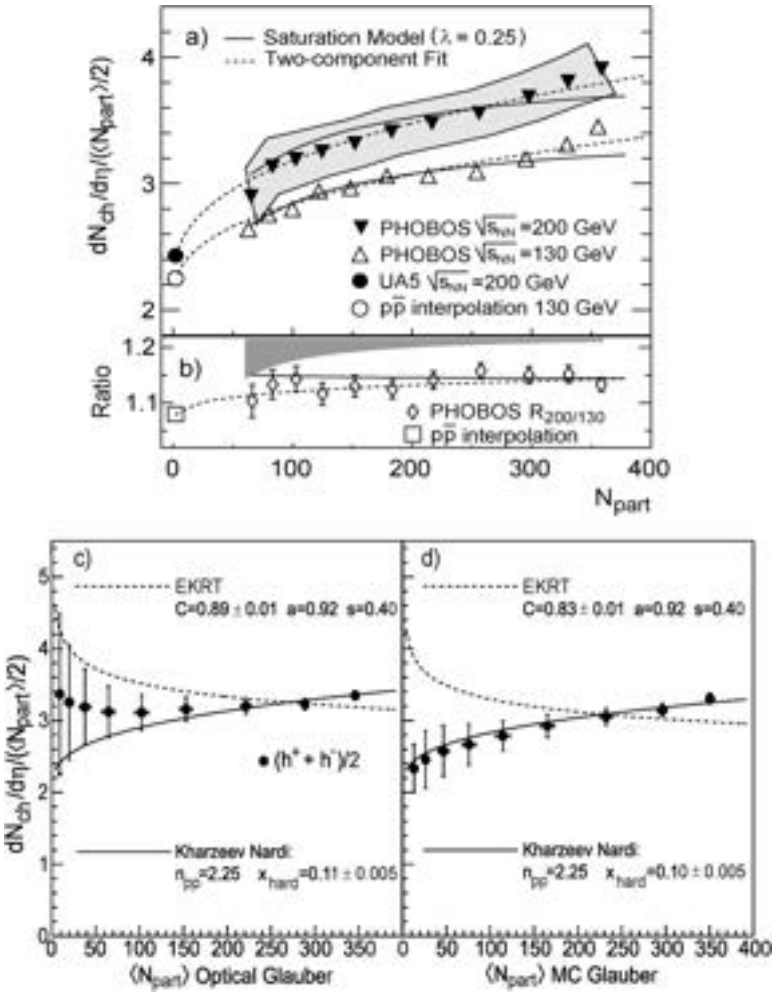

Fig. 11. Measured and calculated pseudorapidity densities $dN_{\rm ch}/d\eta_{|\eta|\ 1}/(\langle N_{\rm part}\rangle/2)$ of charged particles from RHIC Au + Au collisions as a function of $N_{\rm part}$. PHOBOS data [76] at $\sqrt{s_{NN}} = 130$ GeV (open triangles) and 200 GeV (closed triangles) are shown in frame (a), and their ratio is plotted in (b). The open and solid circles in (a) are $\bar{p}p$ collision results. STAR data for 130 GeV [77] are shown in frames (c) and (d), plotted with two different Glauber model treatments to deduce $\langle N_{\rm part}\rangle$. The data plotted in frames (a), (b) and (d) utilize the preferred Monte Carlo Glauber approach. However, the initial-state gluon saturation model calculations [66] shown as solid curves in all frames have been carried out utilizing the questionable optical approximation to the Glauber treatment, which is applied as well to the experimental results only in frame (c). The dashed curves in frames (a) and (b) represent two-component fits to the data [76] and in frames (c) and (d) represent an alternative model [78] assuming saturation of final-state mini-jet production.

analogous "apples-to-apples" comparison within the Monte Carlo Glauber framework is clearly desirable.

Furthermore, over a much broader energy range, the charged particle multiplicity is found to vary quite smoothly from AGS energies ($\sqrt{s_{NN}} \approx$ few GeV) to the top RHIC energy ($\sqrt{s_{NN}} = 200$ GeV) [80] (see Fig. 35). One would not expect CGC conditions to be dominant in collisions over this entire range [7], so the apparent success of CGC arguments for RHIC hadron multiplicities is less than compelling. Other evidence more directly relevant to CGC predictions will be discussed in Section 4.

Whatever physics ultimately governs the smooth increase in produced particle multiplicity with increasing collision energy and centrality seems also to govern the growth in total transverse energy per unit pseudorapidity ($dE_T/d\eta$). PHENIX measurements at $\sqrt{s_{NN}} = 130$ GeV [81] first revealed that RHIC collisions generate ≈ 0.8 GeV of transverse energy per-produced charged particle near mid-rapidity, independent of centrality—essentially the same value that is observed also in SPS collisions at an order of magnitude lower center-of-mass energy [82]. This trend persists to $\sqrt{s_{NN}} = 200$ GeV [83]. For RHIC central Au + Au collisions, this translates to the conversion of nearly 700 GeV per unit rapidity (dE_T/dy) from initial-state longitudinal to final-state transverse energy [81]. Under simplifying assumptions (longitudinal boost-invariance, free-streaming expansion in which the matter does no work) first suggested by Bjorken [84], one can extract from this observation a crude estimate of the initial spatial energy density of the bulk matter at the start of its transverse expansion:

$$e_{Bj} = \frac{dE_T}{dy}\frac{1}{\tau_0 \pi R^2}, \tag{4}$$

where τ_0 is the formation time and R the initial radius of the expanding system. With reasonable guesses for these parameter values ($\tau_0 \approx 1$ fm/c, $R \approx 1.2A^{1/3}$ fm), the PHENIX $dE_T/d\eta$ measurements suggest an initial energy density ~ 5 GeV/fm^3 for central Au + Au collisions at RHIC, well above the critical energy density ~ 1 GeV/fm^3 expected from LQCD for the transition to the QGP phase. This estimate of the initial energy density is larger than that in SPS collisions, since the particle multiplicity grows at RHIC, but by a modest factor (≈ 1.6 [81] at $\sqrt{s_{NN}} = 130$ GeV).

3.2. Hadron yields and spectra

Fig. 12 compares STAR measurements of integrated hadron yield ratios for central Au + Au collisions to statistical model fits. In comparison to results from $p + p$ collisions at similar energies, the relative yield of multi-strange baryons Ξ and Ω is considerably enhanced in RHIC Au + Au collisions [85,86]. The measured ratios are used to constrain the values of system temperature and baryon chemical potential at chemical freezeout, under the statistical model assumption that the system is in thermal and chemical equilibrium at that stage. The excellent fit obtained to the ratios in the figure, including stable and long-lived hadrons through multi-strange baryons, is consistent with the light flavors, u, d, and s, having reached chemical equilibrium (for central and near-central collisions only) at $T_{\rm ch} = 163 \pm 5$ MeV [37,85–87]. (The deviations of the short-lived resonance yields, such as those for Λ^* and K^* collected near the right side of Fig. 12, from the statistical model fits, presumably result from hadronic rescattering after the chemical freezeout.)

Although the success of the statistical model in Fig. 12 might, in isolation, indicate hadron production mechanisms dominated by kinematic phase space in elementary collisions (see Section 2.3), other measurements to be discussed below suggest that true thermal and chemical equilibration is at least approximately achieved in heavy-ion collisions at RHIC by interactions among the system's constituents. The saturation of the strange sector yields, attained for the first time in near-central RHIC collisions, is particularly significant. The saturation is indicated quantitatively by the value obtained for the non-equilibrium

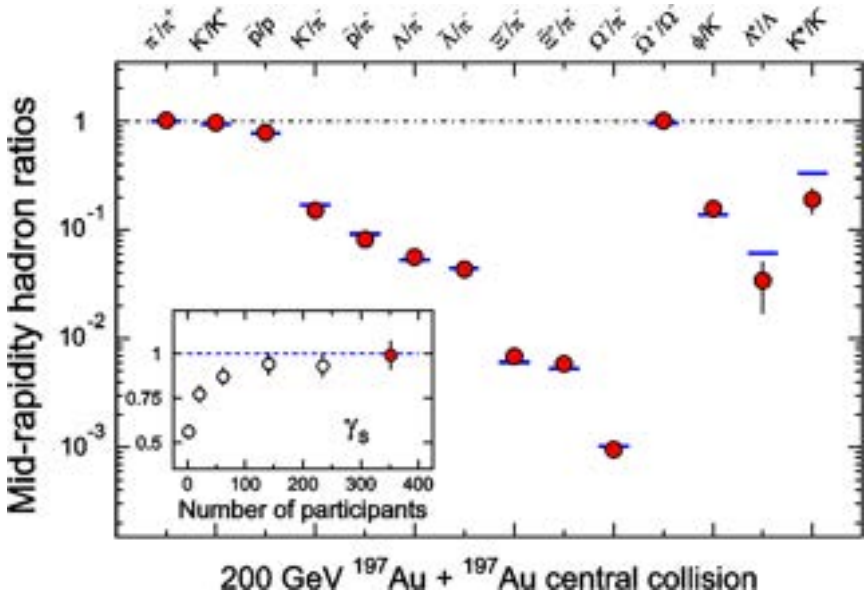

Fig. 12. Ratios of p_T-integrated mid-rapidity yields for different hadron species measured in STAR for central Au + Au collisions at $\sqrt{s_{NN}} = 200$ GeV. The horizontal bars represent statistical model fits to the measured yield ratios for stable and long-lived hadrons. The fit parameters are $T_{\rm ch} = 163 \pm 4$ MeV, $\mu_B = 24 \pm 4$ MeV, $\gamma_s = 0.99 \pm 0.07$ [86]. The variation of γ_s with centrality is shown in the inset, including the value (leftmost point) from fits to yield ratios measured by STAR for 200 GeV $p + p$ collisions.

parameter γ_s for the strange sector [88], included as a free parameter in the statistical model fits. As seen in the inset of Fig. 12, γ_s rises from ≈ 0.7 in peripheral Au + Au collisions to values statistically consistent with unity [85,86] for central collisions. The temperature deduced from the fits is essentially equal to the critical value for a QGP-to-hadron-gas transition predicted by LQCD [2,14], but is also close to the Hagedorn limit for a hadron resonance gas, predicted without any consideration of quark and gluon degrees of freedom [25].[1] If thermalization is indeed achieved by the bulk matter *prior* to chemical freezeout, then the deduced value of $T_{\rm ch}$ represents a lower limit on that thermalization temperature.

The characteristics of the system at *kinetic* freezeout can be explored by analysis of the transverse momentum distributions for various hadron species, some of which are shown in Fig. 13. In order to characterize the transverse motion, hydrodynamics-motivated fits [90] have been made to the measured spectra, permitting extraction of model parameters characterizing the random (generally interpreted as a kinetic freezeout temperature $T_{\rm fo}$) and collective (radial flow velocity $\langle \beta_T \rangle$) aspects. Results for these parameters are shown for different centrality bins and different hadron species in Fig. 14. (While theoretical studies [90] suggest caution in interpreting spectrum fits made without correction for resonance feed-down, as is the case in Fig. 14, auxiliary STAR analyses show little quantitative effect of the feed-down within the STAR p_T coverage.)

[1] Note that Hagedorn himself considered the Hagedorn temperature and the LQCD critical temperature to be identical [89].

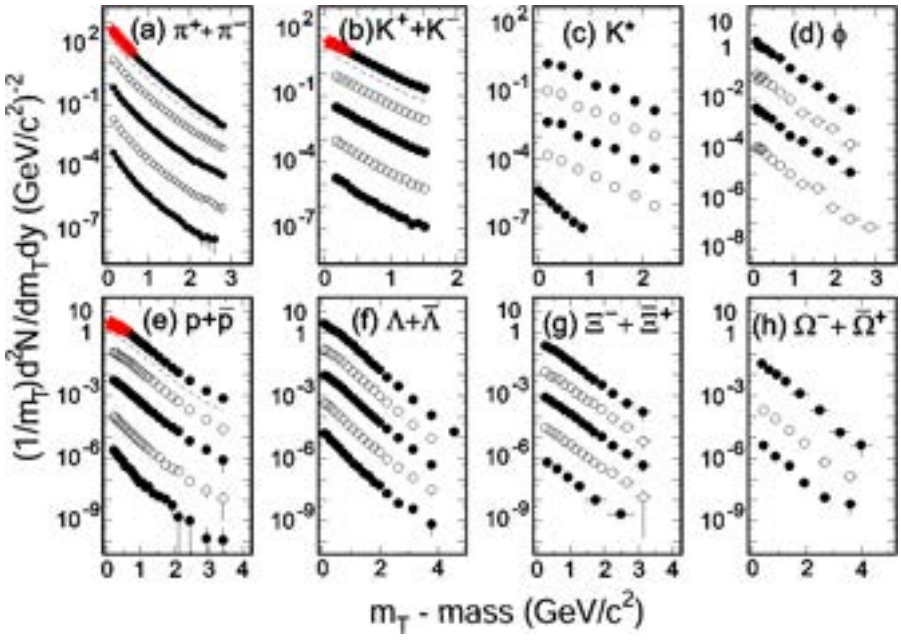

Fig. 13. Mid-rapidity hadron spectra from $\sqrt{s_{NN}} = 200$ GeV Au + Au collisions, as reported in Refs. [87, 94–96]. The spectra are displayed for steadily decreasing centrality from the top downwards within each frame, with appropriate scaling factors applied to aid visual comparison of the results for different centralities. For K^* only, the lowest spectrum shown is for 200 GeV $p + p$ collisions. The dashed curves in frames (a), (b) and (e) represent spectra from minimum-bias collisions. The invariant spectra are plotted as a function of $m_T - \text{mass} \equiv \sqrt{p_T^2/c^2 + \text{mass}^2} - \text{mass}$.

As the collisions become more and more central, the bulk of the system, dominated by the yields of π, K, p, appears from Fig. 14 to grow cooler at kinetic freezeout and to develop stronger collective flow. These results may indicate a more rapid expansion after chemical freezeout with increasing collision centrality. On the other hand, even for the most central collisions, the spectra for multi-strange particles ϕ and Ω appear, albeit with still large uncertainties, to reflect a higher temperature [86]. The ϕ and Ω results suggest diminished hadronic interactions with the expanding bulk matter after chemical freezeout [85,86,91,92], as predicted [28,33,93] for hadrons containing no valence u or d quarks. If this interpretation is correct, the substantial radial flow velocity inferred for ϕ and Ω would have to be accumulated prior to chemical freezeout, giving the multi-strange hadrons perhaps greater sensitivity to collective behavior during earlier partonic stages of the system evolution.

As one moves beyond the soft sector, the p_T and centrality dependences of the observed hadron spectra develop a systematic difference between mesons and baryons, distinct from the mass-dependence observed at lower p_T. This difference is illustrated in Fig. 15 by the binary-scaled ratio $R_{\rm CP}$ of hadron yields for the most central vs. a peripheral bin, corrected by the expected ratio of contributing binary nucleon–nucleon collisions in the two centrality bins [96]. The results are plotted as a function of p_T for mesons and baryons separately in panels (a) and (b), respectively, with the ratio of binary collision-scaled yields of all charged hadrons indicated in both panels by a dot-dashed curve to aid comparison. If the centrality-dependence simply followed the number of binary collisions, one would

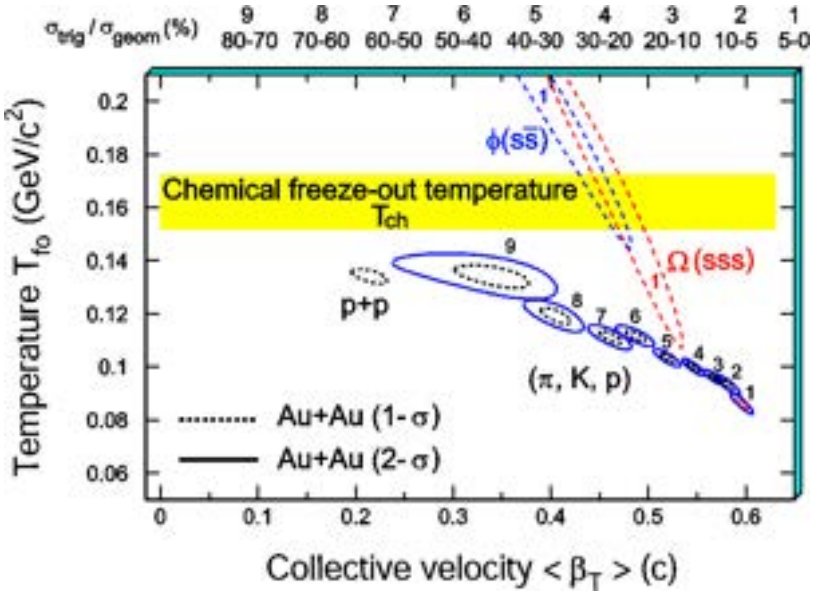

Fig. 14. The χ^2 contours, extracted from thermal + radial flow fits (without allowance for resonance feed-down), for copiously produced hadrons π, K and p and multi-strange hadrons ϕ and Ω. On the top of the plot, the numerical labels indicate the centrality selection. For π, K and p, 9 centrality bins (from top 5% to 70–80%) were used for $\sqrt{s_{NN}} = 200$ GeV Au + Au collisions [87]. The results from $p + p$ collisions are also shown. For ϕ and Ω, only the most central results [86] are presented. Dashed and solid lines are the 1-σ and 2-σ contours, respectively.

expect $R_{\mathrm{CP}} = 1$. This condition is nearly achieved for baryons near $p_T \approx 2.5$ GeV/c, but is never reached for mesons. The initial results for ϕ-mesons and Ω-baryons included in Fig. 15 suggest that the difference is not very sensitive to the mass of the hadron, but rather depends primarily on the number of valence quarks contained within it. The meson and baryon values appear to merge by $p_T \approx 5$ GeV/c, by which point $R_{\mathrm{CP}} \approx 0.3$.

The origin of this significant shortfall in central high-p_T hadron production will be discussed at length in Section 4. Here, we want simply to note that the clear difference seen in the centrality dependence of baryon vs. meson production is one of the defining features of the intermediate p_T range from ~ 1.5 to ~ 6 GeV/c in RHIC heavy-ion collisions, and it cannot be understood from $p + p$ collision results [97]. Another defining feature of this medium p_T range, to be discussed further below, is a similar meson–baryon difference in elliptic flow. Both facets of the meson–baryon differences can be explained naturally in quark recombination models for hadron formation [69].

3.3. Hadron yields versus the reaction plane

In non-central heavy-ion collisions, the beam direction and the impact parameter define a reaction plane for each event, and hence a preferred azimuthal orientation. The orientation of this plane can be estimated experimentally by various methods, e.g., using 2- or 4-particle correlations [98,99], with different sensitivities to azimuthal anisotropies not associated with collective flow. The observed particle yield versus azimuthal angle with respect to the event-by-event reaction plane promises information on the early collision

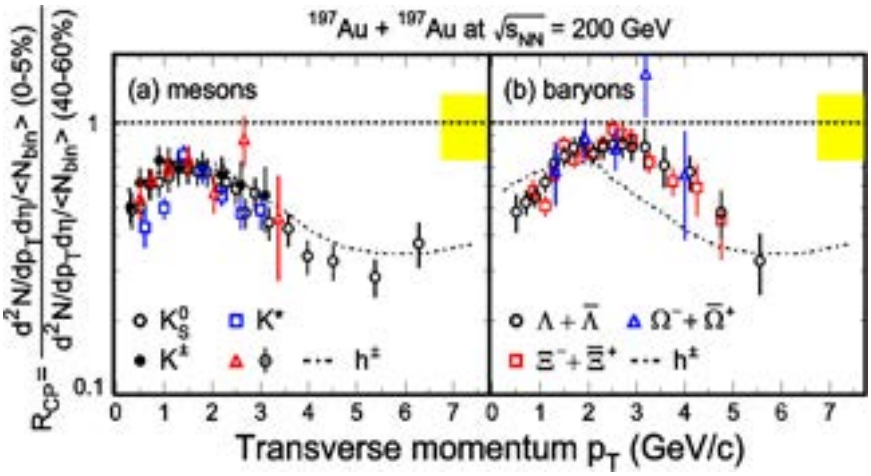

Fig. 15. STAR results [96] from $\sqrt{s_{NN}} = 200$ GeV Au + Au collisions for the ratio of mid-rapidity hadron yields R_{CP} in a central (0–5%) over a peripheral (40–60%) bin, plotted vs. p_T for mesons (a) and baryons (b). The yields are scaled in each centrality region by the calculated mean number $\langle N_{\mathrm{bin}} \rangle$ of binary contributing nucleon–nucleon collisions, calculated within a Monte Carlo Glauber model framework. The width of the shaded band around the line at unity represents the systematic uncertainty in model calculations of the centrality dependence of $\langle N_{\mathrm{bin}} \rangle$. R_{CP} for the sample of all charged hadrons is also shown by dot-dashed curves in both plots. The error bars on the measured ratios include both statistical and systematic uncertainties.

dynamics [27,74]. The anisotropy of the particle yield versus the reaction plane can be characterized in a Fourier expansion. Due to the geometry of the collision overlap region the second coefficient of this Fourier series—v_2, often referred to as the elliptic flow—is expected to be the dominant contribution.

Fig. 16 shows the mid-rapidity elliptic flow measurements, integrated over transverse momentum, as a function of collision centrality for one SPS [100] and two RHIC [101, 102] energies. One clearly observes a characteristic centrality dependence that reflects the increase of the initial spatial eccentricity of the collision overlap geometry with increasing impact parameter. The integrated elliptic flow value for produced particles increases about 70% from the top SPS energy to the top RHIC energy, and it appears to do so smoothly as a function of energy (see Fig. 34), so far exhibiting no obvious “dip” of the sort predicted [30] by ideal hydrodynamics in Fig. 7.

The origin of the energy dependence can be discerned by examining the differential $v_2(p_T)$, shown for the centrality selection 10–30% in Fig. 17. The comparison of the results for pions at $\sqrt{s_{NN}} = 200$ GeV and at the top SPS energy clearly reveals an increase in slope vs. p_T that accounts for part of the increase in p_T-integrated v_2 from SPS to RHIC. The remaining part of the change is due to the increase in $\langle p_T \rangle$. As measurements become available at more collision energies, it will be important to remove kinematic effects, such as the increase in $\langle p_T \rangle$, from comparisons of results, as they might mask finer, but still significant, deviations from smooth energy dependence.

Collective motion leads to predictable behavior of the shape of the momentum spectra as a function of particle mass, as reflected in the single inclusive spectra in Fig. 13. It is even more obvious in the dependence of $v_2(p_T)$ for the different mass particles. Fig. 18 shows the measured low-p_T v_2 distributions from 200 and 130 GeV Au + Au minimum bias collisions. Shown are the measurements for charged pions, K^0_S, antiprotons and Λ

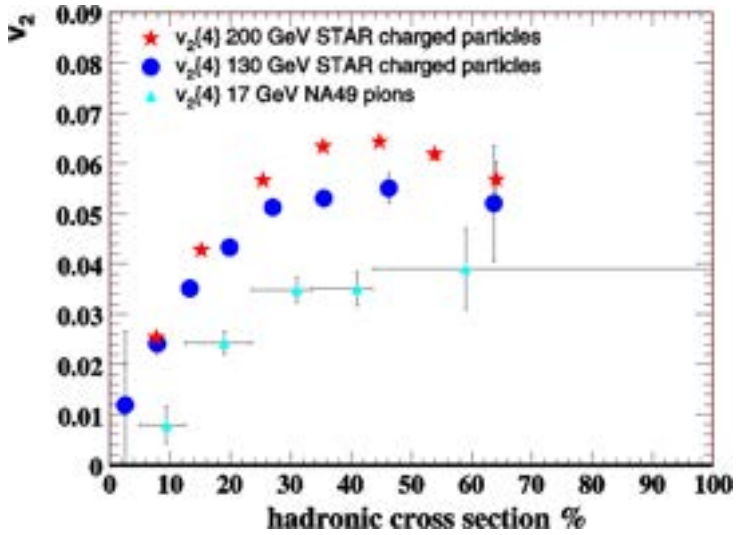

Fig. 16. Centrality dependence of v_2, integrated over p_T. The triangles are the NA49 measurements for pions at $\sqrt{s_{NN}} = 17$ GeV [100]. The circles and crosses are STAR measurements for charged particles at $\sqrt{s_{NN}} = 130$ GeV [101] and 200 GeV [102], respectively. The 4-particle cumulant method has been used to determine v_2 in each case.

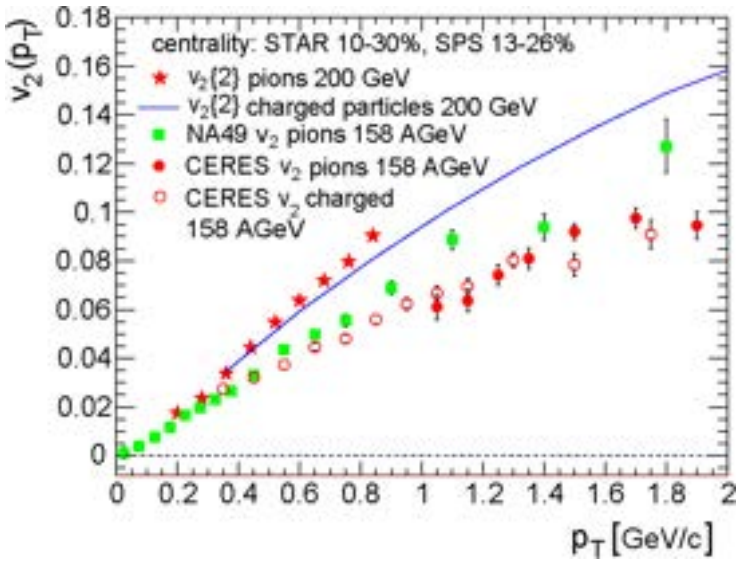

Fig. 17. $v_2(p_T)$ for one centrality (10–30%) range. The circles and squares are the CERES [103] and NA49 [100] measurements, respectively, at $\sqrt{s_{NN}} = 17$ GeV. The stars and the solid line are STAR measurements [102] for pions and for all charged particles, respectively, at $\sqrt{s_{NN}} = 200$ GeV (evaluated here by the 2-particle correlation method).

[104,105]. The clear, systematic mass-dependence of v_2 shown by the data is a strong indicator that a common transverse velocity field underlies the observations. This mass-dependence, as well as the absolute magnitude of v_2, is reproduced reasonably well (i.e., at the $\pm 30\%$ level) by the hydrodynamics calculations shown in Fig. 18. Parameters of these calculations have been tuned to achieve good agreement with the measured spectra for different particles, implying that they account for the observed radial flow and elliptic flow

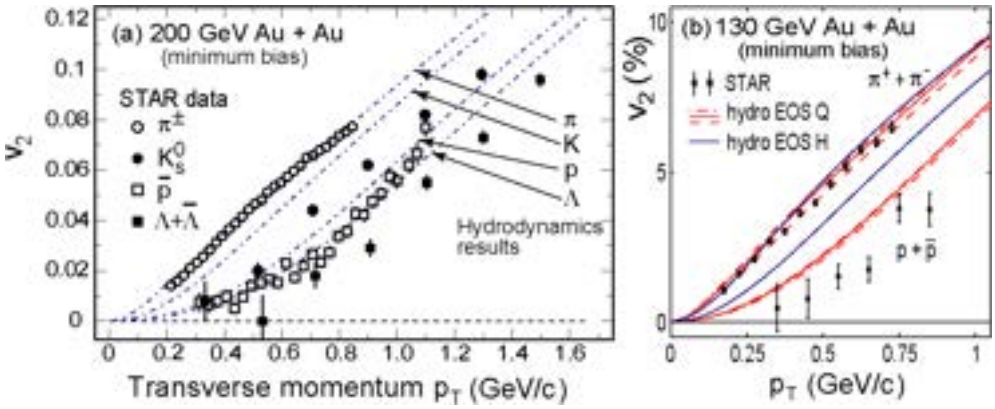

Fig. 18. (a) STAR experimental results of the transverse momentum dependence of the elliptic flow parameter in 200 GeV Au + Au collisions for charged $\pi^+ + \pi^-$, K^0_s, $\bar{p}$, and Λ [104]. Hydrodynamics calculations [32,106] assuming early thermalization, ideal fluid expansion, an equation of state consistent with LQCD calculations including a phase transition at $T_c = 165$ MeV (EOS Q in [32] and Fig. 5), and a sharp kinetic freezeout at a temperature of 130 MeV, are shown as dot-dashed lines. Only the lower p_T portion (p_T 1.5 GeV/c) of the distributions is shown. (b) Hydrodynamics calculations of the same sort as in (a), now for a hadron gas (EOS H) vs. QGP (EOS Q) equation of state (both defined in Fig. 5) [3,32], compared to STAR v_2 measurements for pions and protons in minimum bias 130 GeV Au + Au collisions [105]. Predictions with EOS Q are shown for a wider variety of hadron species in Fig. 8.

simultaneously. In particular, since the parameters are tuned for zero impact parameter, the theory-experiment comparison for v_2 as a function of centrality represents a significant test of these hydrodynamics calculations.

The agreement of these hydrodynamics calculations, which assume *ideal* relativistic fluid flow, with RHIC spectra and v_2 results is one of the centerpieces of recent QGP discovery claims [6–8]. The agreement appears to be optimized (though still with some quantitative differences, see Fig. 18) when it is assumed that local thermal equilibrium is attained very early ($\tau < 1$ fm/c) during the collision, and that the hydrodynamic expansion is characterized by an EOS (labeled Q in Fig. 18) containing a soft point roughly consistent with the LQCD-predicted phase transition from QGP to hadron gas [3,29,32]. When the expanding matter is treated as a pure hadron gas (EOS H in Fig. 18(b)), the mass-dependence of v_2 is significantly underpredicted. The inferred early thermalization suggests that the collision's early stages are dominated by very strongly interacting matter with very short constituent mean free paths—essentially a "perfect liquid" [107], free of viscosity. Similar QGP-based calculations that invoke ideal hydrodynamics up to freezeout overpredict the elliptic flow for more peripheral RHIC collisions and for lower energies. One possible interpretation of this observation is that thermalized, strongly interacting QGP matter dominates near-central Au + Au collisions at or near the full RHIC energy.

In assessing these claims, it is critical to ask how unique and robust the hydrodynamics account is in detail for the near-central RHIC collision flow measurements (radial and elliptic). Might the observed v_2 result alternatively from a harder EOS (such as EOS H) combined with later achievement of thermalization or with higher viscosity [35] (both conditions impeding the development of collective flow)? How does the sensitivity to the EOS in the calculations compare quantitatively with the sensitivity to other ambiguities or questionable assumptions in the hydrodynamics treatments? For example, the particular

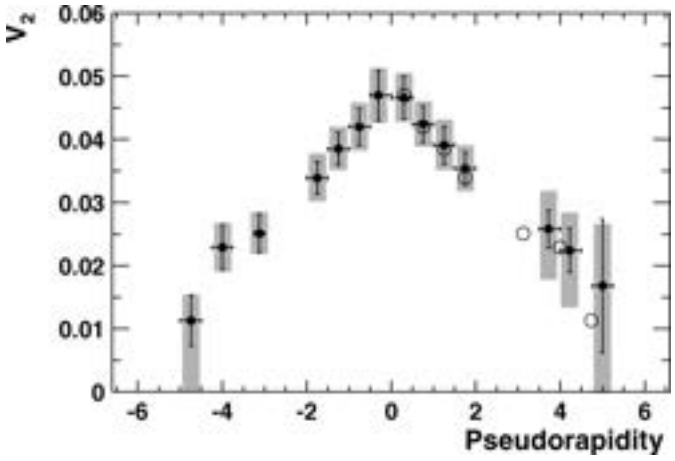

Fig. 19. Azimuthal anisotropies v_2 measured by the PHOBOS Collaboration [108] for Au + Au collisions at $\sqrt{s_{NN}} = 130$ GeV, as a function of pseudorapidity. Within each pseudorapidity bin, the results are averaged over all charged particles, over all centralities and over all p_T. The black error bars are statistical and the grey bands systematic uncertainties. The points on the negative side are reflected about $\eta = 0$ and plotted as open circles on the positive side, for comparison. Figure taken from Ref. [108].

calculations in Fig. 18 [32,106] invoke a simplified treatment with a sharp onset of kinetic freezeout along a surface of constant energy density corresponding to $T_{\rm fo} \approx 130$ MeV. The sensitivity to the assumed value of $T_{\rm fo}$, if it is kept within the range spanned by the measurements in Fig. 14, is relatively weak [32]. However, alternative approaches combining ideal hydrodynamics for the partonic stage with a hadron transport (RQMD) treatment of the presumably viscous hadronic stage [29] yield similar success in accounting for RHIC results, but certainly predict a dependence of v_2 on collision energy differing significantly from the sharp-freezeout predictions (compare Fig. 7 and Fig. 9). While the combination of partonic hydrodynamics and hadron transport offers the promise of a reasonable QGP-based account for the observed smooth energy dependence of p_T-integrated v_2 (see Figs. 9, 34), it also serves to emphasize that quantitative ambiguities of scale comparable to the EOS sensitivity remain to be understood.

In addition to questions about the thermalization time, viscosity and freezeout treatment, one also needs to address the robustness of the standard assumption of longitudinal boost-invariance in hydrodynamics calculations [3]. There is growing evidence at RHIC for significant deviations from boost-invariance. This is illustrated by PHOBOS results for v_2 as a function of pseudorapidity in Fig. 19, where one sees no evidence for a mid-rapidity plateau in elliptic flow strength [108]. Thus, while the successes of QGP-based hydrodynamics calculations at RHIC are tantalizing, substantially greater systematic investigation of their sensitivities—including computationally challenging full three-dimensional treatments—would be needed to make a compelling QGP claim on their basis alone.

At higher p_T values, as shown by experimental results from 200 GeV Au + Au minimum bias collisions in Fig. 20, the observed values of v_2 saturate and the level of the saturation differs substantially between mesons and baryons. Hydrodynamics calculations overpredict the flow in this region. The dot-dashed curves in Fig. 20(a)–(c) represent simple analytical function fits to the measured K^0_S and $\Lambda + \bar{\Lambda}$ v_2 distributions [104,109]. It is seen

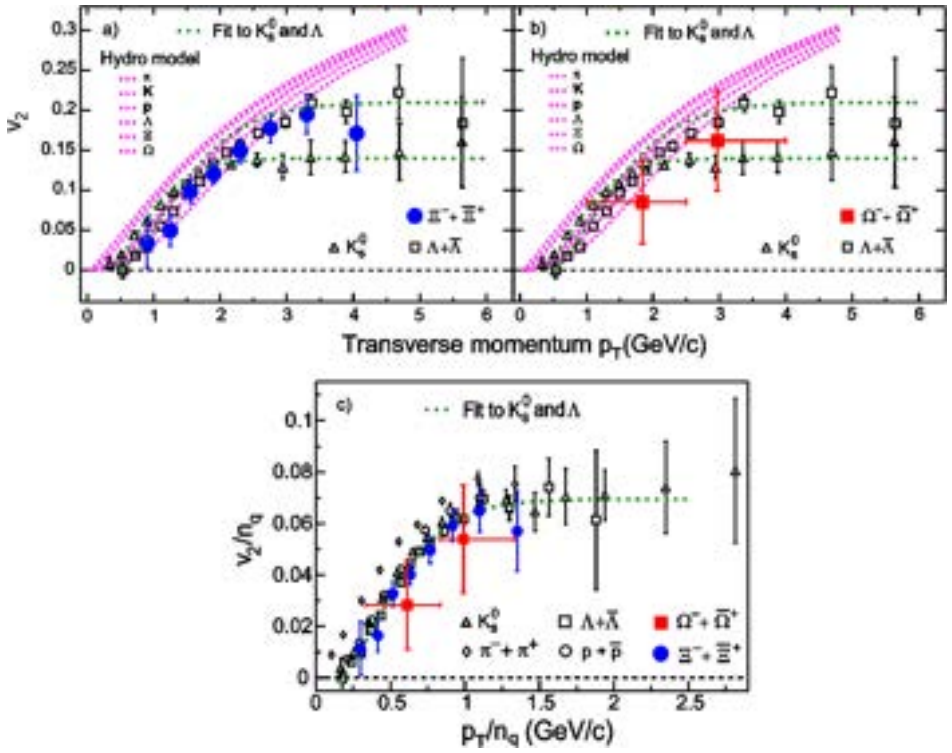

Fig. 20. Experimental results on the transverse momentum dependence of the event elliptic anisotropy parameter for various hadron species produced in minimum-bias Au + Au collisions at $\sqrt{s_{NN}} = 200$ GeV. STAR results [104] for K^0_S and $\Lambda + \bar{\Lambda}$ are shown in all frames, together with simple analytic function fits (dashed lines) to these data. Additional data shown are STAR multi-strange baryon elliptic flow [110] for Ξ (in frames (a) and (c)) and Ω ((b) and (c)), and PHENIX results [111] for π and $p + \bar{p}$ (frame (c)). Hydrodynamic calculations are indicated by dotted curves in frames (a) and (b). In (c), the flow results for all of the above hadrons are combined by scaling both v_2 and p_T by the number of valence quarks (n_q) in each hadron. The figure is an update of one in [109].

in Fig. 20(a) and (b) that STAR's most recent v_2 results for the multi-strange baryons Ξ and Ω [110] are consistent with that of Λ's but within still sizable statistical uncertainties.

In Fig. 20(c), particle-identified elliptic flow measurements for the 200 GeV Au + Au minimum-bias sample are combined by dividing both v_2 and p_T by the number of valence quarks (n_q) in the hadron of interest. The apparent scaling behavior seen in this figure for $p_T/n_q > 1$ GeV/c is intriguing, as the data themselves seem to be pointing to constituent quarks (or at least to valence quarks sharing the full hadron momentum, see Section 2.6) as the most effective degree of freedom in determining hadron flow at intermediate p_T values. The data need to be improved in statistical precision and p_T extent for more identified mesons and baryons in order to establish this scaling more definitively. Within error bars the size of those for $p_T/n_q > 1$ GeV/c, the low p_T data would also look as though they scale with the number of constituent quarks, whereas we already have seen in Fig. 18 that there is rather a clear hydrodynamic mass-dependence in the low p_T region. (Note that the pion data barely extend into the scaling region at $p_T/n_q > 1$ GeV/c.)

If the scaling behavior at intermediate p_T is confirmed with improved data, it will provide a very important clue to the origin of the meson–baryon differences (see also Fig. 15) that characterize this p_T range. In particular, both the v_2 scaling and the meson–baryon

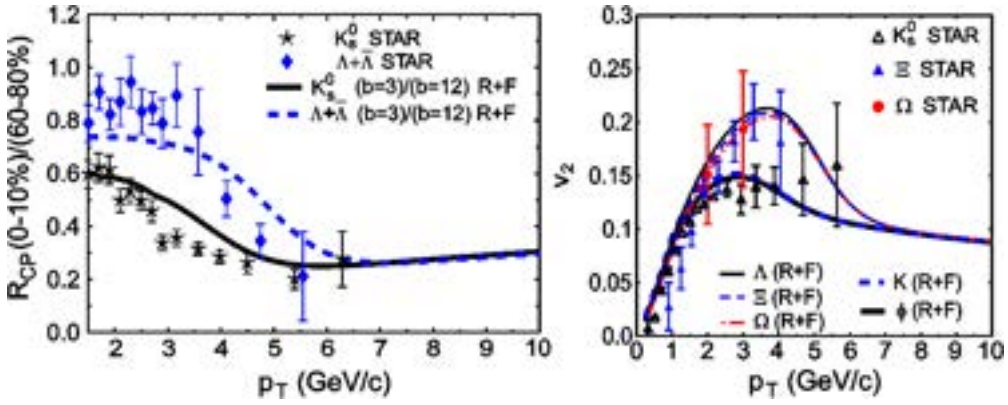

Fig. 21. Comparisons of calculations in the Duke quark recombination model [69,112] with STAR measurements [104,110] of (a) R_{CP} and (b) v_2 for strange mesons and baryons. "R + F" denotes the sum of recombination and fragmentation contributions. Comparison of the solid and broken curves in (b) reveals a weak mass-dependence in the calculations, superimposed on the predominant meson–baryon differences. The figures are taken from Ref. [70], and they include preliminary STAR data for multi-strange baryons that differ slightly from the values shown in Fig. 20.

R_{CP} differences can be explained [69,112] (see Fig. 21) by assuming that hadron formation at moderate p_T proceeds via two competing mechanisms: the coalescence of n_q constituent quarks at transverse momenta $\sim p_T/n_q$, drawn from a thermal (exponential) spectrum [69], plus more traditional fragmentation of hard-scattered partons giving rise to a power-law component of the spectrum. Note that, as discussed in Section 2.6, these models are not expected to apply at low p_T. It is not yet clear that the same models could simultaneously account as well for another observed feature characteristic of this intermediate p_T range, namely, a jet-like azimuthal correlation of hadron pairs that will be discussed further in Section 4.

In these coalescence models, the constituent quarks carry their own substantial azimuthal anisotropy, which is then summed to give the hadron v_2. The establishment of clearer evidence for such pre-hadronic collective flow would be an important milestone in elucidating the nature of the matter produced in RHIC collisions. In interpreting such evidence, it must be kept in mind that constituent quarks are not partons: they are effective degrees of freedom normally associated with chiral symmetry breaking and confinement, rather than with the deconfinement of a QGP. Until the mechanism for the emergence of these effective degrees of freedom from a QCD plasma of current quarks and gluons is clarified (see Section 2.6), collectively flowing constituent quarks should not be taken as definitive proof of a QGP stage, as we have defined it in Section 1. It is unclear, for example, whether the characteristic time scale for constituent quarks to coalesce from current quarks and gluons might not be shorter than that for the establishment of thermalization in the collision (leading to a sort of "constituent quark plasma", as opposed to a QGP). Furthermore, the constituent quark v_2 values needed to account for the observed hadron v_2 saturation might arise in part from differential energy loss of their progenitor partons in traversing the spatially anisotropic matter of non-central collisions [47], rather than strictly from the partonic hydrodynamic flow assumed in [112]. The unanticipated RHIC results in this intermediate p_T range thus raise a number of important and fasci-

nating questions that should be addressed further by future measurements and theoretical calculations.

In summary, the measured yields with respect to the reaction plane are among the most important results to date from RHIC: they provide critical hints of the properties of the bulk matter at early stages. They indicate that it behaves collectively, and is consistent with rapid (i.e., very short mean free path) attainment of at least approximate local thermal equilibrium in a QGP phase. Hydrodynamic accounts for the mass- and p_T-dependence of v_2 for soft hadrons appear to favor system evolution through a soft, mixed-phase EOS. The saturated v_2 values observed for identified mesons and baryons in the range 1.5 p_T 6 GeV/c suggest that hadronization in this region occurs largely via coalescence of collectively flowing constituent quarks. What has yet to be demonstrated is that these interpretations are unique and robust against improvements to both the measurements and the theory. In particular, it must be demonstrated more clearly that the sensitivity to the role of the QGP outweighs that to other, more mundane, ambiguities in the theoretical treatment.

3.4. Quantum correlation analyses

Two-hadron correlation measurements in principle should provide valuable information on the phase structure of the system at freezeout. From the experimentally measured momentum–space two-particle correlation functions, a Fourier transformation is then performed in order to extract information on the space–time structure [113]. Bertsch–Pratt parameterization [114] is often used to decompose total momentum in such measurements into components parallel to the beam (*long*), parallel to the pair transverse component (*out*) and along the remaining third direction (*side*). In this Cartesian system, information on the source duration time is mixed into the *out* components. Hence, the ratio of inferred emitting source radii $R_{\rm out}/R_{\rm side}$ is sensitive to the time duration of the source emission. For example, if a QGP is formed in collisions at RHIC, a long duration time and consequently large value of $R_{\rm out}/R_{\rm side}$ are anticipated [115].

Measured results for Hanbury-Brown-Twiss (HBT) pion interferometry, exploiting the boson symmetry of the two detected particles at low relative momenta, are shown in Figs. 22 and 23. A clear dependence of the 'size' parameters on the pair transverse momentum k_T is characteristic of collective expansion of the source [116,117], so the results are plotted vs. k_T in Fig. 22. As indicated by the set of curves in the figure, hydrodynamics calculations that can account for hadron spectra and elliptic flow at RHIC systematically over-predict $R_{\rm out}/R_{\rm side}$ [116,118]. One possible implication of this discrepancy is that the collective expansion does not last as long in reality as in the hydrodynamics accounts. However, shorter expansion times are difficult to reconcile with the observed magnitude of $R_{\rm side}$, and are not supported by a recent systematic study of HBT correlations relative to the event-by-event reaction plane [117]. The source eccentricity at freezeout inferred from these azimuthally sensitive measurements is shown in Fig. 23 to retain a significant fraction of the initial spatial eccentricity characteristic of the impact parameter for each centrality bin. The observed eccentricity retention is, in fact, quantitatively consistent with hydrodynamics expectations for the *time-integrated* pion emission surface to which HBT is sensitive [119]. Thus, the deformations in Fig. 23 tend to support the hydrodynamics

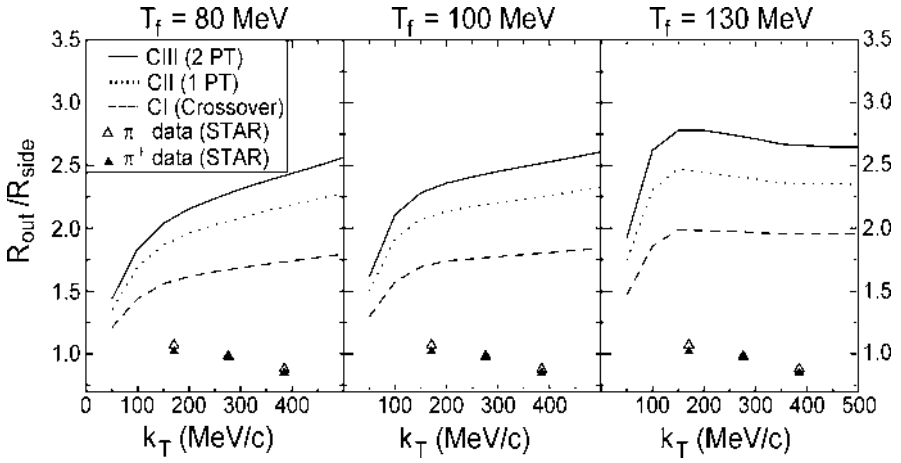

Fig. 22. STAR measurements [116] of $R_{\mathrm{out}}/R_{\mathrm{side}}$ from pion HBT correlations for central Au + Au collisions, plotted as a function of the pion pair transverse momentum k_T. The experimental results are identical in the three frames, but are compared to hydrodynamics calculations [118] performed for a variety of parameter values.

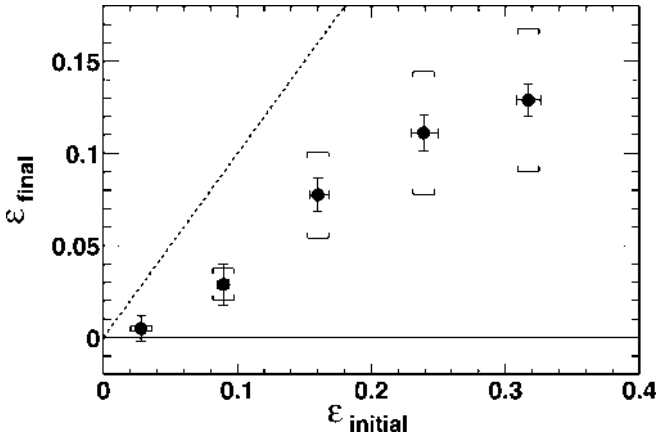

Fig. 23. The eccentricity $\epsilon_{\mathrm{final}}$ of the time-integrated emitting source of soft pions, inferred from STAR HBT correlations measured with respect to the reaction plane, plotted versus the initial spatial eccentricity $\epsilon_{\mathrm{initial}}$ deduced from a Glauber calculation for five different Au + Au centrality bins. The dotted line represents $\epsilon_{\mathrm{final}} = \epsilon_{\mathrm{initial}}$. See [117] for details.

view of the expansion pressure and timeline (see Fig. 6), which lead to an eventual complete quenching of the initial configuration-space anisotropy by the end of the freezeout process.

The failure of the hydrodynamics calculations to account for the HBT results in Fig. 22 raises another significant issue regarding the robustness of the hydrodynamics success in reproducing v_2 and radial flow data. Although the HBT interference only emerges after the freezeout of the strong interaction, whose treatment is beyond the scope of hydrodynamics, the measured correlation functions receive contributions from all times during the collision process. Furthermore, these HBT results are extracted from the low p_T region, where soft bulk production dominates. It is thus reasonable to expect the correct hydrodynamics account of the collective expansion to be consistent with the HBT source sizes. If improved treatment of the hadronic stage and/or the introduction of finite viscosity during the hydro-

dynamic expansion [35] are necessary to attain this consistency, then it is important to see how those improvements affect the agreement with elliptic flow and spectra.

STAR has also measured two-hadron momentum–space correlation functions for *non*-identical particles [120]. These are sensitive to differences in the average emission time and position for the different particle species. Such differences are very clearly revealed by the measured correlations between pions and kaons [120], and provide additional strong evidence for a collective transverse flow of the produced hadrons.

3.5. Correlations and fluctuations

A system evolving near a phase boundary should develop significant dynamical fluctuations away from the mean thermodynamic properties of the matter. For high-energy heavy ion collisions, it has been predicted that the general study of two-particle correlations and event-wise fluctuations might provide evidence for the formation of matter with partonic degrees of freedom [121–126]. In addition, non-statistical correlations and fluctuations may be introduced by incomplete equilibrium [127]. With its large acceptance and complete event-by-event reconstruction capabilities, the STAR detector holds great potential for fluctuation analyses of RHIC collisions.

An approach that has been used previously [128,129] to search for the presence of dynamical correlations involves extraction of measures of the excess variance of some observable above the statistical fluctuations that show up even in mixed-event samples. An example shown in Fig. 24 utilizes the square root of the covariance in p_T for charged-particle pairs from collisions at SPS (CERES [128]) and at STAR [130]. The presence of dynamical 2-particle correlations is revealed by non-zero values of this quantity, whose gross features exhibit a magnitude and a smooth centrality-dependence that are essentially independent of collision energy, once the variations of the inclusive mean p_T values ($\langle\langle p_T \rangle\rangle$) with centrality and energy have been divided out. However, the detailed nature of the dynamical correlations is best probed by fully exploiting the impressive statistical precision at STAR to investigate finer, multi-dimensional aspects of the correlation densities themselves, rather than of the integrals of correlation densities represented by excess variance measures.

For example, emerging STAR angular correlation results are already suggesting that there is appreciable soft hadron emission before the attainment of local thermal equilibrium, even in the most central RHIC collisions. The evidence resides in remnants of jet-like behavior observed [131] even in soft (0.15 p_T 2.0 GeV/c) hadron pair correlations on the angular difference variables $\Delta\eta \equiv \eta_1 - \eta_2$ (pseudorapidity) and $\Delta\phi \equiv \phi_1 - \phi_2$ (azimuthal angle), presented for peripheral and central Au + Au collisions in Fig. 25. The equivalent correlations for $p + p$ collisions at RHIC [131] emphasize the central role of parton fragmentation even down to hadron transverse momenta of 0.5 GeV/c, resulting in a prominent near-side jet peak symmetric about $\Delta\eta = \Delta\phi = 0$ and a broad $\Delta\eta$-independent away-side ($\Delta\phi = \pi$) jet ridge. One certainly anticipates some remnants of these correlations to survive in heavy-ion collisions at sufficiently high hadron p_T, and these correlations will be discussed in the next section. In the soft sector, however, attainment of a fully equilibrated state of all emerging hadrons at freezeout would wash out such initial hard-scattering dynamical correlations.

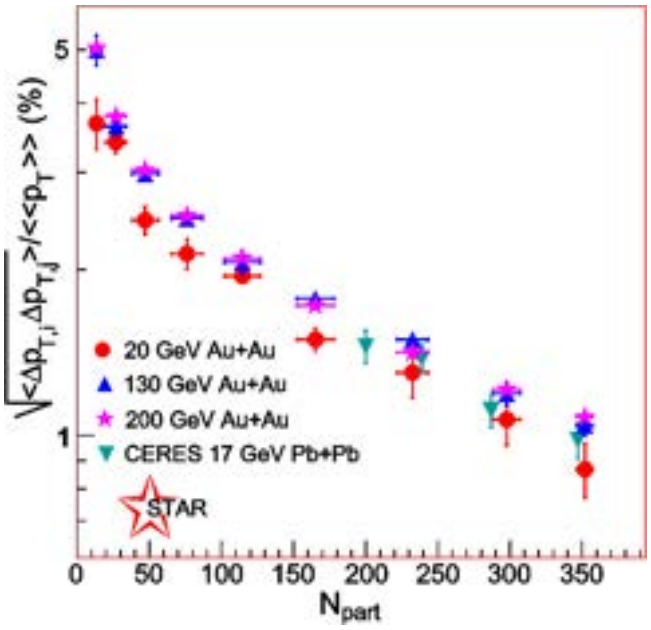

Fig. 24. The square root of the transverse momentum covariance for charged particle pairs, scaled by the inclusive mean p_T value for each centrality and collision energy, plotted vs. centrality for SPS [128] and RHIC [130] data at several energies. Both the centrality-dependence (nearly $\propto 1/N_{\text{part}}$) and magnitude of this quantity are essentially unchanged from SPS to RHIC energies, but its implicit integration of correlation densities over the full detector acceptance masks other interesting correlation features.

Instead, the observed soft-hadron-pair correlation for central Au + Au collisions shown in the upper right-hand frame of Fig. 25, after removal of multipole components representing elliptic flow (v_2) and momentum conservation (v_1) [131], exhibits a substantially modified remnant of the jet correlation on the near side, affecting typically 10–30% of the detected hadrons. Contributions to this near-side peak from HBT correlations and Coulomb final-state interactions between hadrons have been suppressed by cuts to remove pairs at very low relative momentum, reducing the overall strength of the correlation near $\Delta\eta = \Delta\phi = 0$ by ∼10% [131]. Simulations demonstrate that resonance decays make no more than a few percent contribution to the remaining near-side correlation strength. (The lack of evidence for any remaining away-side correlation in central collisions will be discussed further in the high-p_T context in Section 4. Its absence even for more peripheral collisions in the upper left frame of Fig. 25 can be attributed to the broad centrality bin used here to compensate for limited statistics in the 130 GeV Au + Au data sample, and to the v_1 subtraction that removes thermalized soft hadrons balancing the near-side jet's momentum.)

The observed near-side correlation in central Au + Au is clearly much broader in $\Delta\eta$ than that in $p + p$ or peripheral Au + Au collisions. The pseudorapidity spread, as characterized by the $\Delta\eta$ width of a two-dimensional Gaussian function fitted to the structure (ignoring the $\Delta\eta = \Delta\phi = 0$ bin, where conversion electron pairs contribute), grows rapidly with increasing collision centrality, as revealed in the lower frames of Fig. 25. This trend suggests that while some parton fragments are not yet fully equilibrated in the soft sector, they are nonetheless rather strongly coupled to the longitudinally expanding bulk medium.

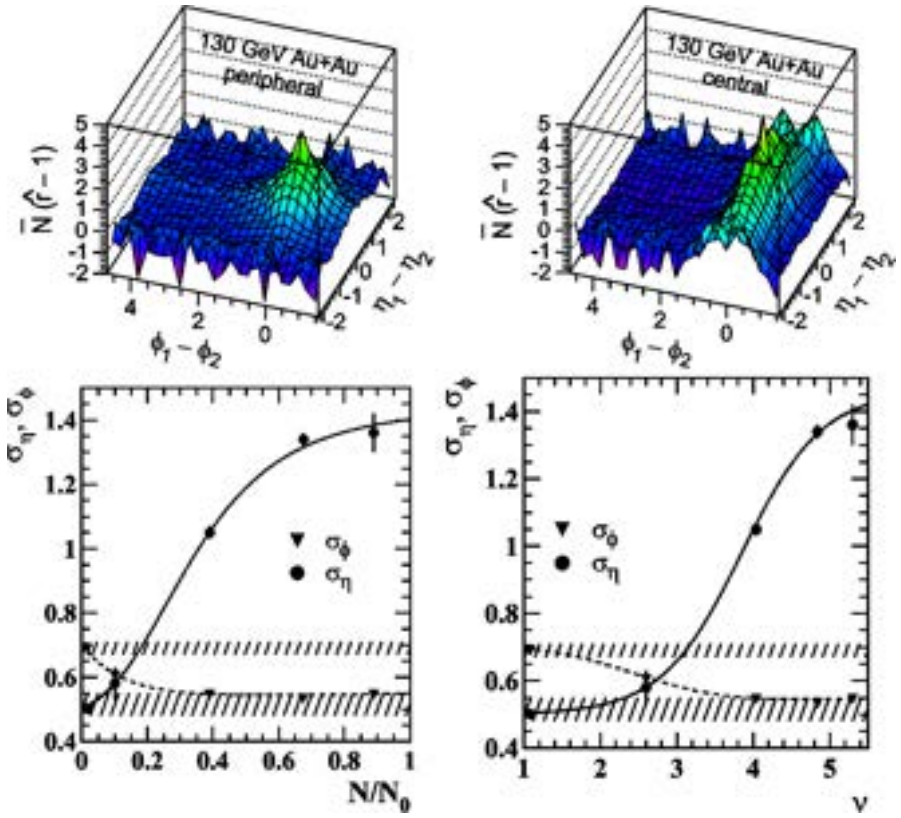

Fig. 25. Upper frames: joint autocorrelations measured by STAR, as a function of the hadron pair angle differences $\eta_1-\eta_2$ and $\phi_1-\phi_2$, for 0.15 p_T 2.0 GeV/c charged hadrons detected in 130 GeV Au + Au collisions [131]. The right frame contains data for central collisions, while the left frame spans a broad range of centralities for more peripheral collisions. The quantity $\bar{N}(\hat{r}-1)$ plotted on the vertical axes represents the average multiplicity for the selected centrality bin multiplied by the relative difference in charged particle pair yields between same events and mixed events. Elliptic flow and momentum conservation long-range correlations have been subtracted, as explained in [131]. Lower frames: centrality-dependence of the Au + Au pseudorapidity and azimuthal widths from two-dimensional Gaussian fits to the near-side correlation structure seen for two centrality bins in the upper frames. The same extracted widths for Au + Au collisions are plotted vs. two different measures of centrality: the observed charged-particle multiplicity divided by its maximum value (on the left), and the mean number ν of nucleons encountered by a typical participant nucleon (right). The hatched bands indicate the widths observed for $p+p$ collisions, and the curves guide the eye.

The onset of this coupling appears especially dramatic when the results are plotted (lower right-hand frame) vs. the alternative centrality measure $\nu \equiv (N_{\rm part}/2)^{1/3}$ (estimating the mean number of nucleons encountered by a typical participant nucleon along its path through the other nucleus), rather than the more traditional charged-particle multiplicity (lower left frame). The latter comparison serves as a reminder that, as we seek evidence for a transition in the nature of the matter produced in RHIC collisions, it is important to consider carefully the optimal variables to use to characterize the system.

The coupling to the longitudinal expansion can be seen more clearly as an equilibration mechanism from measurements of the power spectra P^λ of local fluctuations in the density of charged hadrons with respect to a mixed-event counterpart $P^\lambda_{\rm mix}$. The λ superscript distinguishes different directions (modes) of density variation, orthogonal in the wavelet

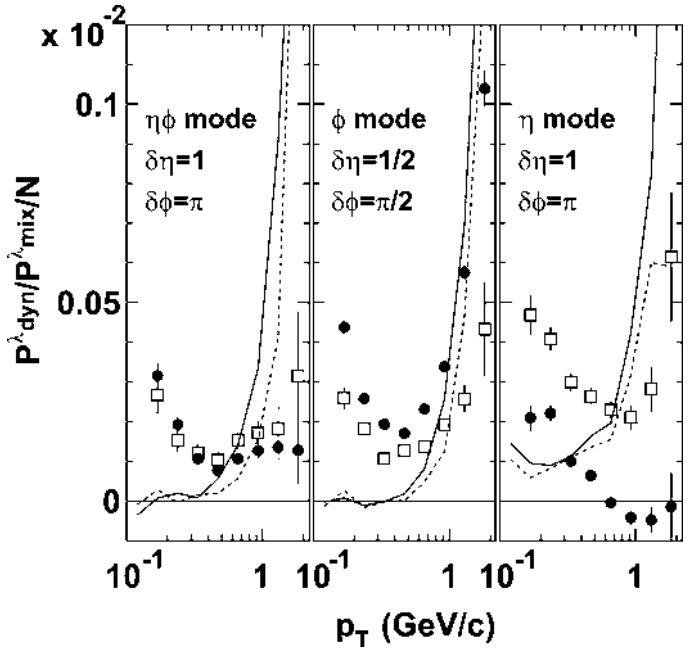

Fig. 26. STAR measurements (filled circles) of dynamic texture for the 4% most central Au + Au collisions at $\sqrt{s_{NN}} = 200$ GeV, compared to STAR peripheral (60–84%) collision data (boxes) renormalized for direct comparison, and to HIJING calculations with (dashed curves) and without (solid curves) inclusion of jet quenching. The dynamic texture measures the non-statistical excess in point-to-point fluctuations in the local density of charged hadrons in an event, averaged over the event ensemble. Figure taken from Ref. [133].

decomposition used [133] for the analysis: along η, along ϕ, and along the diagonal $\eta\phi$. The so-called "dynamic texture" [132] of the event, used to characterize the non-statistical excess in density fluctuations, is defined as $P^{\lambda}_{\rm dyn}/P^{\lambda}_{\rm mix}/N$, where $P^{\lambda}_{\rm dyn} = P^{\lambda} - P^{\lambda}_{\rm mix}$ and N is the average number of tracks in a given p_T interval per event. The dynamic texture is shown as a function of p_T for three different modes and for both central and peripheral collisions in Fig. 26 [133]. HIJING simulations [135] shown in the figure cannot account for the observed fluctuations, even when jet quenching is included, although they do suggest qualitatively that the rising trends in the data with increasing p_T are signals of "clumpiness" in the particle density caused by jets. In the absence of a successful model for these fluctuations, we can at least search for interesting centrality dependences. The box symbols in the figure represent what we would expect for the dynamic texture in central collisions, based on what STAR measures for peripheral collisions, if the correlation structure were independent of centrality. The strong suppression observed with respect to this expectation for the central collision η-mode fluctuations is interpreted as another manifestation of the coupling of parton fragments to the longitudinally expanding bulk medium [133].

The results in Figs. 25 and 26 are averaged over all charged hadrons without consideration of the sign of the charge. Detailed information on the hadronization of the medium can be obtained from the study of charge-*dependent* (CD) correlations, e.g., by examining the difference between angle-dependent correlations of like- vs. unlike-sign pairs. One method focuses on the "balance function", constructed [125,134] to measure the excess of unlike- over like-sign pairs as a function of their (pseudo)rapidity difference $\Delta\eta$. The results in Fig. 27 show that the width of this function in $\Delta\eta$ steadily decreases with increasing

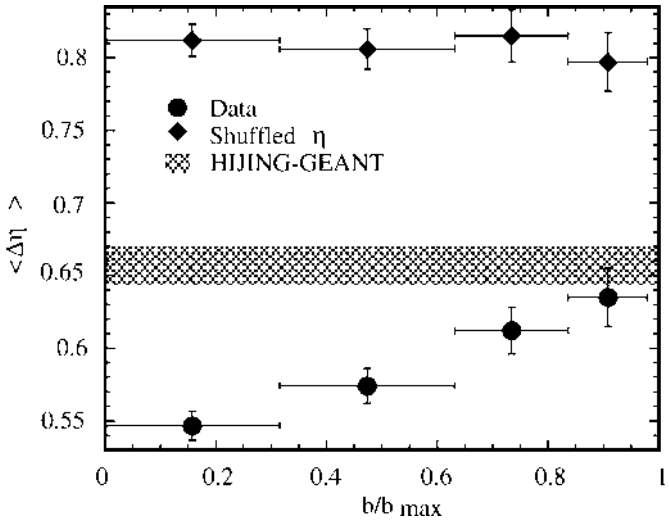

Fig. 27. Width $\langle\Delta\eta\rangle$ of the measured charged hadron balance function from Au + Au (filled circles) collisions at $\sqrt{s_{NN}} = 130$ GeV, plotted as a function of the relative impact parameter deduced from the charged particle multiplicities for each analyzed centrality bin. The cross-hatched band represents the centrality-independent results of HIJING simulations [135] of the balance function width measured within STAR for 130 GeV Au + Au collisions. The diamond-shaped points illustrate constraints imposed on the balance function by global charge conservation and the STAR detector acceptance, when dynamical correlations are removed by randomly shuffling the association of pseudorapidities with detected particles within each analyzed event. The figure is from Ref. [134].

Au + Au centrality [130,134], in contrast to HIJING simulations [135]. A related trend is observed in the CD two-dimensional autocorrelation [131] (not plotted) analogous in format to the charge-independent results shown in Fig. 25. The CD peak amplitude increases, and its width decreases, dramatically with increasing centrality. These trends indicate a marked change in the formation mechanism of charged hadron pairs in central Au + Au, relative to $p + p$, collisions. The implications of that change for the nature of the medium produced are now under intensive study with a growing array of correlation techniques.

3.6. Summary

In this section, we have presented important results on the bulk matter properties attained in Au + Au collisions at RHIC. The measured hadron spectra, yield ratios, and low p_T v_2, are all consistent from all experiments at RHIC. STAR, in particular, has made pioneering measurements of elliptic flow, of multi-strange baryons, and of dynamical hadron correlations that bear directly on the matter properties critical to establishing QGP formation. The yield ratios are consistent with chemical equilibration across the u, d and s sectors. The spectra and v_2 clearly reveal a collective velocity field in such collisions. The combined evidence for near-central Au + Au collisions at RHIC suggests that thermal equilibrium is largely, though not quite completely, attained, and that collective flow is established, at an early collision stage when sub-hadronic degrees of freedom dominate the matter. However, the quality of some of the data, and the constraints on ambiguities in some of the theoretical models used for interpretation, are not yet sufficient to demonstrate convincingly that thermalized, deconfined matter has been produced.

In particular, the unprecedented success of hydrodynamics in providing a reasonable quantitative account for collective flow at RHIC, and of the statistical model in reproducing hadron yields through the strange sector, together argue for an early approach toward thermalization spanning the u, d and s sectors. On the other hand, measurements of angle difference distributions for soft hadron pairs reveal that some (admittedly heavily modified) remnants of jet-like dynamical correlations survive the thermalization process, and indicate its incompleteness. The fitted parameters of the statistical model analyses, combined with inferences from the produced transverse energy per unit rapidity, suggest attainment of temperatures and energy densities at least comparable to the critical values for QGP formation in LQCD calculations of bulk, static strongly interacting matter.

The data in this section provide two hints of deconfinement that need to be sharpened in future work. One is the improvement in hydrodynamics accounts for measured low-p_T flow when the calculations include a soft point in the EOS, suggestive of a transition from partonic to hadronic matter. It needs to be better demonstrated that comparable improvement could not be obtained alternatively by addressing other ambiguities in the hydrodynamics treatment. One indication of such other ambiguities is the failure of hydrodynamics calculations to explain the emitting source sizes inferred from pion interferometry. The second hint is the apparent relevance of (constituent or valence) quark degrees of freedom in determining the observed meson–baryon differences in flow and yield in the intermediate-p_T region. Here the data need improved precision to establish more clearly the quark scaling behavior expected from coalescence models, while the theory needs to establish a clearer connection between the effective quarks that seem to coalesce and the current quarks and gluons of QCD.

4. Hard probes

Due to the transient nature of the matter created in high energy nuclear collisions, external probes cannot be used to study its properties. However, the dynamical processes that produce the bulk medium also produce energetic particles through hard scattering processes. The interaction of these energetic particles with the medium provides a class of unique, penetrating probes that are analogous to the method of computed tomography (CT) in medical science.

For p_T 5 GeV/c the observed hadron spectra in Au + Au collisions at RHIC exhibit the power-law falloff in cross section with increasing p_T that is characteristic of perturbative QCD hard-scattering processes [136]. The parameters of this power-law behavior vary systematically with collision centrality, in ways that reveal important properties of the matter traversed by these penetrating probes [136]. While we focus for the most part in this section on hadrons of p_T above 5 GeV/c, we do also consider data in the intermediate p_T range down to 2 GeV/c, when those data allow more statistically robust measurements of effects we associate with hard scattering.

4.1. Inclusive hadron yields at high p_T

There are several results to date from RHIC exhibiting large and striking effects of the traversed matter on hard probes in central collisions. Figs. 28 and 29 show the most significant high p_T measurements made at RHIC thus far. Both figures incorporate measurements of $\sqrt{s_{NN}} = 200$ GeV $p + p$, $d + \mathrm{Au}$ and centrality-selected $\mathrm{Au} + \mathrm{Au}$ collisions at RHIC, with the simpler $p + p$ and $d + \mathrm{Au}$ systems providing benchmarks for phenomena seen in the more complex $\mathrm{Au} + \mathrm{Au}$ collisions.

Fig. 28 shows $R_{AB}(p_T)$, the ratio of inclusive charged hadron yields in $A + B$ (either $\mathrm{Au} + \mathrm{Au}$ or $d + \mathrm{Au}$) collisions to $p + p$, corrected for trivial geometric effects via scaling by $\langle N_{\mathrm{bin}} \rangle$, the calculated mean number of binary nucleon–nucleon collisions contributing to each $A + B$ centrality bin:

$$R_{AB}(p_T) = \frac{dN_{AB}/d\eta\, d^2p_T}{T_{AB}\, d\sigma_{NN}/d\eta\, d^2p_T}, \tag{5}$$

where the overlap integral $T_{AB} = \langle N_{\mathrm{bin}} \rangle / \sigma^{pp}_{\mathrm{inelastic}}$. A striking phenomenon is seen: large p_T hadrons in central $\mathrm{Au} + \mathrm{Au}$ collisions are suppressed by a factor ≈ 5 relative to naive (binary scaling) expectations. Conventional nuclear effects, such as nuclear shadowing of the parton distribution functions and initial state multiple scattering, cannot account for the suppression. Furthermore, the suppression is not seen in $d + \mathrm{Au}$ but is unique to $\mathrm{Au} + \mathrm{Au}$ collisions, proving experimentally that it results not from nuclear effects in the initial state (such as gluon saturation), but rather from the final state interaction (FSI) of hard scattered partons or their fragmentation products in the dense medium generated in $\mathrm{Au} + \mathrm{Au}$ collisions [137–140].

These dominant FSI in $\mathrm{Au} + \mathrm{Au}$ are presumably superimposed on a variety of interesting initial-state effects revealed by the $d + \mathrm{Au}$ results. The enhancement seen in Fig. 28 in $R_{d\mathrm{Au}}$ for moderate p_T and mid-rapidity, known as the Cronin effect [141], is generally attributed [142] to the influence of multiple parton scattering through cold nuclear matter *prior to* the hard scattering that produces the observed high-p_T hadron. Other effects, revealed by the strong *rapidity*-dependence of $R_{d\mathrm{Au}}$, will be discussed in Section 4.4.

4.2. Dihadron azimuthal correlations

Fig. 29 shows seminal STAR measurements of correlations between high-p_T hadrons. The left panel shows the azimuthal distribution of hadrons with $p_T > 2$ GeV/c relative to a trigger hadron with $p_T^{\mathrm{trig}} > 4$ GeV/c. A hadron pair drawn from a single jet will generate an enhanced correlation at $\Delta\phi \approx 0$, as observed for $p + p$, $d + \mathrm{Au}$ and $\mathrm{Au} + \mathrm{Au}$, with similar correlation strengths, widths and (not shown) charge-sign ordering (the correlation is stronger for oppositely charged hadron pairs [71]). A hadron pair drawn from back-to-back dijets will generate an enhanced correlation at $\Delta\phi \approx \pi$, as observed for $p + p$ and for $d + \mathrm{Au}$ with somewhat broader width than the near-side correlation peak. However, the back-to-back dihadron correlation is strikingly, and uniquely, absent in central $\mathrm{Au} + \mathrm{Au}$ collisions, while for peripheral $\mathrm{Au} + \mathrm{Au}$ collisions the correlation appears quite similar to that seen in $p + p$ and $d + \mathrm{Au}$. If the correlation is indeed the result of jet fragmentation, the suppression is again due to the FSI of hard-scattered partons or their fragmentation

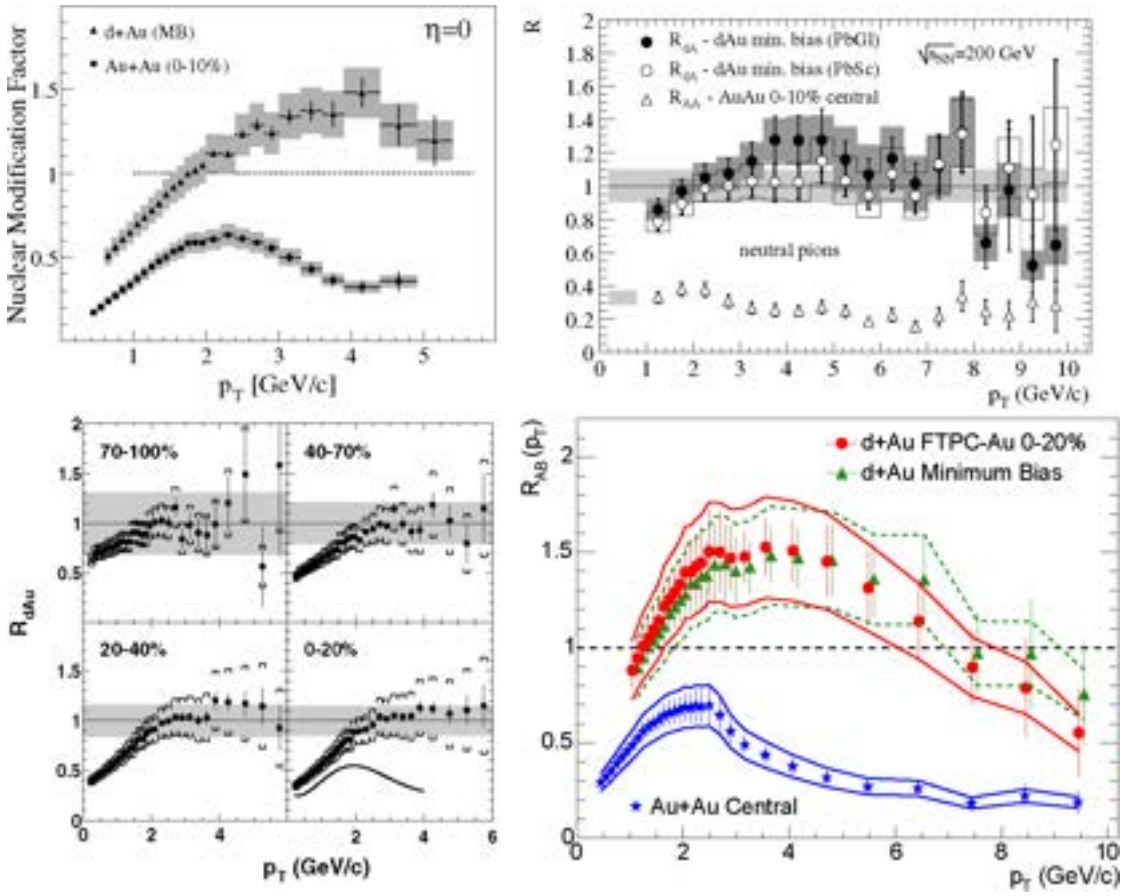

Fig. 28. Binary-scaled ratio $R_{AB}(p_T)$ (Eq. (5)) of charged hadron and π^0 inclusive yields from 200 GeV Au + Au and d + Au relative to that from $p + p$ collisions, from BRAHMS [137] (upper left), PHENIX [138] (upper right), PHOBOS [139] (lower left) and STAR [140] (lower right). The PHOBOS data points in the lower left frame are for d + Au, while the solid curve represents PHOBOS central (0–6%) Au + Au data. The shaded horizontal bands around unity represent the systematic uncertainties in the binary scaling corrections.

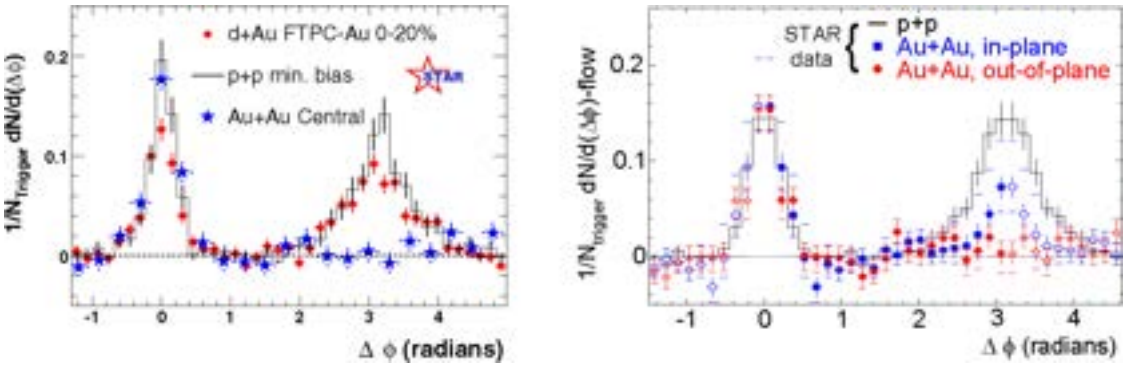

Fig. 29. Dihadron azimuthal correlations at high p_T. Left panel shows correlations for $p + p$, central d + Au and central Au + Au collisions (background subtracted) from STAR [71,140]. Right panel shows the background-subtracted high p_T dihadron correlation for different orientations of the trigger hadron relative to the Au + Au reaction plane [143].

products in the dense medium generated in Au + Au collisions [140]. In this environment, the hard hadrons we do see (and hence, the near-side correlation peak) would arise preferentially from partons scattered outward from the surface region of the collision zone, while the away-side partons must burrow through significant lengths of dense matter.

The qualification concerning the dominance of jet fragmentation is needed in this case, because the correlations have been measured to date primarily for hadrons in that intermediate p_T range (2–6 GeV/c) where sizable differences in meson vs. baryon yields have been observed (see Fig. 15), in contrast to expectations for jets fragmenting in vacuum. The systematics of the meson–baryon differences in this region suggest sizable contributions from softer mechanisms, such as quark coalescence [69]. Where the azimuthal correlation measurements have been extended to trigger particles above 6 GeV/c, they show a similar pattern to the results in Fig. 29, but with larger statistical uncertainties [144]. This suggests that the peak structures in the correlations do, indeed, reflect dijet production, and that the back-to-back suppression is indeed due to jet quenching. Coalescence processes in the intermediate p_T range may contribute predominantly to the smooth background, with only long-range (e.g., elliptic flow) correlations, that has already been subtracted from the data in Fig. 29.

It remains an open challenge for the quark coalescence models to account for the observed $\Delta\phi$ distributions at moderate p_T at the same time as the meson vs. baryon yield and elliptic flow differences discussed in Section 3 (see Fig. 21 and associated discussion). Can the size of the jet peaks seen in Fig. 29 be reconciled with the modest fragmentation contributions implied by the coalescence fits near $p_T \approx 4$ GeV/c (Fig. 21)? Do the jet $\Delta\phi$ peaks rather require substantial contributions also from recombination of a hard-scattered parton with thermal partons from the bulk matter [72]? Are models of the latter type of contributions, of constituent quark coalescence in a thermal ensemble [112] and of vacuum fragmentation [4] mutually compatible? They would appear to contain non-orthogonal contributions and to employ incompatible degrees of freedom. Until these questions are successfully addressed, some ambiguity remains in physics conclusions drawn from the intermediate-p_T region, including the dihadron correlations in Fig. 29.

A more differential probe of partonic energy loss is the measurement of high p_T dihadron correlations relative to the reaction plane orientation. The right panel of Fig. 29 shows a study from STAR of the high p_T dihadron correlation from 20–60% centrality Au + Au collisions, with the trigger hadron situated in the azimuthal quadrants centered either in the reaction plane ("in-plane") or orthogonal to it ("out-of-plane") [143]. The same-side dihadron correlation in both cases is similar to that in $p + p$ collisions. In contrast, the suppression of the back-to-back correlation depends strongly on the relative angle between the trigger hadron and the reaction plane. This systematic dependence is consistent with the picture of partonic energy loss: the path length in medium for a dijet oriented out of the reaction plane is longer than in the reaction plane, leading to correspondingly larger energy loss. The dependence of parton energy loss on path length is predicted [4] to be substantially stronger than linear. The orientation-dependence of the energy loss should be further affected by different rates of matter expansion in-plane vs. out-of-plane.

The energy lost by away-side partons traversing the collision matter must appear, in order to conserve transverse momentum, in the form of an excess of softer emerging hadrons.

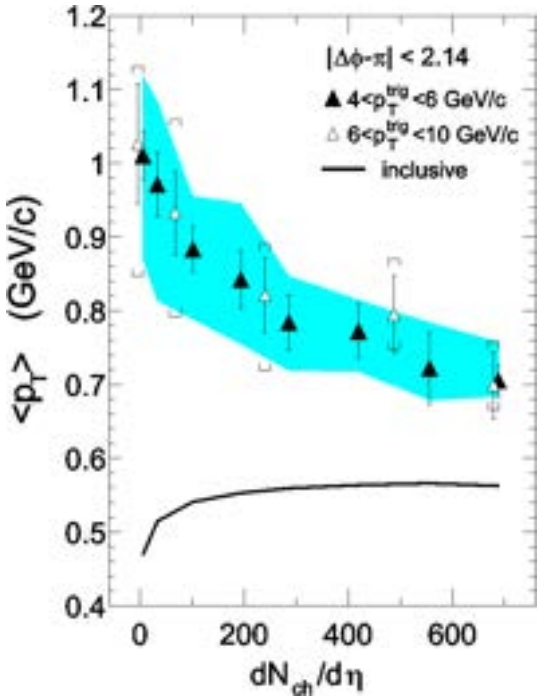

Fig. 30. Associated charged hadron $\langle p_T \rangle$ from the away-side in 200 GeV $p+p$ (two leftmost points) and Au + Au collisions at various centralities, in each case opposite a trigger hadron with p_T in the 4–6 GeV/c (filled triangles) or 6–10 GeV/c (open triangles) range [145]. The shaded band and the horizontal caps represent the systematic uncertainties for the filled and open symbols, respectively. $\langle p_T \rangle$ for inclusive hadron production in the Au + Au collisions is indicated by the solid curve.

An analysis of azimuthal correlations between hard and *soft* hadrons has thus been carried out for both 200 GeV $p + p$ and Au + Au collisions [145] in STAR, as a first attempt to trace the degree of degradation on the away side. With trigger hadrons still in the range $4 < p_T^{\text{trig}} < 6$ GeV/c, but the associated hadrons now sought over $0.15 < p_T < 4$ GeV/c, combinatorial coincidences dominate these correlations, and they must be removed statistically by a careful mixed-event subtraction, with an elliptic flow correlation correction added by hand [145]. The results demonstrate that, in comparison with $p + p$ and peripheral Au + Au collisions, the momentum-balancing hadrons opposite a high-p_T trigger in central Au + Au are greater in number, much more widely dispersed in azimuthal angle, and significantly softer. The latter point is illustrated in Fig. 30, showing the centrality dependence of $\langle p_T \rangle$ of the associated away-side charged hadrons in comparison to that of the bulk inclusive hadrons. While in peripheral collisions the values of $\langle p_T \rangle$ for the away-side hadrons are significantly larger than that of inclusive hadrons, the two values approach each other with increasing centrality. These results are again subject to the ambiguity arising from possible soft (e.g., coalescence) contributions to the observed correlations, as the away-side strength shows little remnant of jet-like behavior [145]. But again, preliminary results for higher trigger-hadron p_T values, shown in Fig. 30, appear to be consistent within larger uncertainties. If a hard-scattering interpretation framework turns out to be valid, the results suggest that even a moderately hard parton traversing a significant path length through the collision matter makes substantial progress toward

equilibration with the bulk. The rapid attainment of thermalization via the multitude of softer parton–parton interactions in the earliest collision stages would then not be surprising.

4.3. Theoretical interpretation of hadron suppression

Fig. 31 shows $R_{\mathrm{CP}}(p_T)$, the binary scaled ratio of yields from central relative to peripheral collisions for charged hadrons from 200 GeV Au + Au interactions. $R_{\mathrm{CP}}(p_T)$ is closely related to $R_{AB}(p_T)$, using as reference the binary-scaled spectrum from peripheral Au + Au collisions rather than $p+p$ collisions. The substitution of the reference set allows a slight extension in the p_T range for which useful ratios can be extracted. The error bars at the highest p_T are dominated by statistics and are therefore, to a large extent, uncorrelated from point to point. The suppression for central collisions is again seen to be a factor ≈ 5 relative to the most peripheral collisions, and for p_T 6 GeV/c it is independent of p_T within experimental uncertainties. Also shown in Fig. 31 are results from theoretical calculations based on pQCD incorporating partonic energy loss in dense matter (pQCD-I [146], pQCD-II [147]) and on suppression at high p_T due to gluon saturation effects (saturation [149], with implications discussed further in the following subsection). The negligible p_T-dependence of the suppression at high p_T is a prediction of the pQCD models [146, 147], resulting from the subtle interplay of partonic energy loss, Cronin (initial-state multiple scattering) enhancement, and nuclear shadowing. The variation in the suppression for p_T 5 GeV/c is related to differences in suppression in this region for mesons and baryons (see Fig. 15). It is accounted for in the pQCD-I calculation by the introduction of an additional non-fragmentation production mechanism for kaons and protons [146]. The magnitude of the hadron suppression in the pQCD calculations is adjusted to fit the measurements for central collisions, as discussed further below.

In order to deduce the magnitude of *partonic* energy loss in the medium it is essential to establish the degree to which *hadronic* interactions, specifically the interaction of hadronic jet fragments with the medium, can at least in part generate the observed high p_T phenomena and contribute substantially to the jet quenching [51,151,152]. Simple considerations already argue against this scenario. The dilated formation time of hadrons with energy E_h and mass m_h is $t_f = (E_h/m_h)\tau_f$, where the rest frame formation time $\tau_f \sim 0.5$–0.8 fm/c. Thus, a 10 GeV/c pion has formation time ~ 50 fm/c and is unlikely to interact as a fully formed pion in the medium. Since the formation time depends on the boost, the suppression due to hadronic absorption with constant or slowly varying cross section should turn off with rising p_T, at variance with observations (Fig. 31). A detailed hadronic transport calculation [51] leads to a similar conclusion: the absorption of formed hadrons in the medium fails by a large factor to account for the observed suppression. Rather, this calculation attributes the suppression to ad hoc medium interactions of "pre-hadrons" with short formation time and constant cross section. The properties of these "pre-hadrons" are thus similar to those of colored partons [51], and not to the expected color transparency of hadronic matter to small color singlet particles that might evolve into normal hadrons [52].

Additional considerations of the available high p_T data [53] also support the conclusion that jet quenching in heavy ion collisions at RHIC is the consequence of partonic energy loss. In particular, large v_2 values observed at high p_T and the systematics of the small-

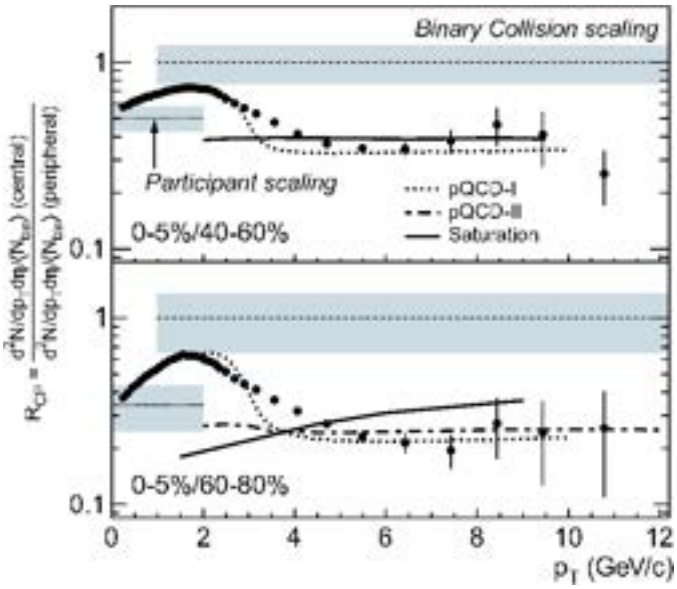

Fig. 31. Binary-scaled yield ratio $R_{\mathrm{CP}}(p_T)$ for central (0–5%) relative to peripheral (40–60%, 60–80%) collisions for charged hadrons from 200 GeV Au + Au collisions [150]. The shaded bands show the multiplicative uncertainty of the normalization of $R_{\mathrm{CP}}(p_T)$ relative to binary collision and participant number scaling.

angle dihadron correlations are difficult to reconcile with the hadronic absorption scenario. While further theoretical investigation of this question is certainly warranted, we conclude that there is no support in the data for *hadronic* absorption as the dominant mechanism underlying the observed suppression phenomena at high p_T, and we consider *partonic* energy loss to be well established as its primary origin. It is conceivable that there may be minor hadronic contributions from the fragments of soft gluons radiated by the primary hard partons during their traversal of the collision matter. In any case, we emphasize that while the jet quenching results seem to favor partons over hadrons *losing* energy, they do not allow any direct conclusion regarding whether the energy is lost *to* partonic or hadronic matter.

The magnitude of the suppression at high-p_T in central collisions is fit to the data in the pQCD-based models with partonic energy loss, by adjusting the initial gluon density of the medium. The agreement of the calculations with the measurements at $p_T > 5$ GeV/c is seen in Fig. 31 to be good. In order to describe the observed suppression, these models require an initial gluon density about a factor 50 greater than that of cold nuclear matter [146–148]. This is the main physics result of the high p_T studies carried out at RHIC to date. It should be kept in mind that the actual energy loss inferred for the rapidly expanding Au + Au collision matter is not very much larger than that inferred for static, cold nuclear matter from semi-inclusive deep inelastic scattering data [57]. But in order to account for this slightly larger energy loss *despite* the rapid expansion, one infers the much larger *initial* gluon density at the start of the expansion [146,147]. Certainly, then, the quantitative extraction of gluon density is subject to uncertainties from the theoretical treatment of the expansion and of the energy loss of partons in the entrance-channel cold nuclear matter before they initially collide.

The gluon density derived from energy loss calculations is consistent with estimates from the measured rapidity density of charged hadrons [153] using the Bjorken scenario [84], assuming isentropic expansion and duality between the number of initial gluons and final charged hadrons. Similar values are also deduced under the assumption that the initial state properties in central Au + Au RHIC collisions, and hence the measured particle multiplicities, are determined by gluon–gluon interactions below the gluon density saturation scale in the initial-state nuclei [66]. Additionally, the energy density is estimated from global measurements of transverse energy (see Section 3.1) to be of order 50–100 times that in cold nuclear matter, consistent with the values inferred from hydrodynamics accounts of measured hadron spectra and flow. The consistency among all these estimates, though only semi-quantitative at present, is quite significant. These inferred densities fall well into the regime where LQCD calculations predict equilibrated matter to reside in the QGP phase.

4.4. Rapidity-dependence of high p_T hadron yields in d + Au collisions

It had been proposed recently [149] that gluon saturation effects can extend well beyond the saturation momentum scale Q_s, resulting in hadron suppression relative to binary scaling ($R_{AB}(p_T) < 1$) for $p_T \sim 5$–10 GeV/c mid-rapidity hadron production at RHIC energies, in apparent agreement with the data in Fig. 31. However, since this predicted suppression originates in the properties of the incoming nuclear wave function, hadron production in d + Au collisions should also be suppressed by this mechanism [149]. Experimentally, an *enhancement* in mid-rapidity hadron production in d + Au is seen instead (Fig. 28 [137–140]), even in central d + Au collisions [140] where saturation effects should be most pronounced. The observed enhancement is at variance with saturation model expectations at high p_T [149].

However, at large rapidities in the deuteron direction, a suppression of the highest p_T hadrons studied is indeed observed in d + Au collisions, as revealed by the results from the Brahms experiment in Fig. 32 [154]. This is not true of large rapidities in the Au direction [157,158]. This distinct behavior is consistent with gluon saturation models, as seen by the fits [156] to these results in Fig. 32. High-p_T hadrons produced at small angles with respect to the deuteron beam arise preferentially from asymmetric partonic collisions involving gluons at low Bjorken x in the Au nucleus. (For example, in a next-to-leading order leading-twist perturbative QCD calculation, the mean x-value of partons probed in the Au nucleus has been found to be 0.03–0.05 when selecting on hadrons at $\eta = 3.2$ and $p_T = 1.5$ GeV/c [155]. Note, however, that such a calculation may have limited validity in the regime of strong gluonic fields.) It is precisely at low x in heavy nuclei that gluon saturation, and the resultant suppression in high-p_T hadron production, should set in. Thus, gluon saturation models predicted the qualitative behavior of increasing suppression with increasing rapidity in the deuteron direction before the experimental results became available [159], although parameter values had to be tuned after the fact [156] to adjust the saturation scale to obtain the fits shown in Fig. 32.

At the moderate p_T values kinematically accessible at large pseudorapidity, one may worry legitimately that softer hadron production mechanisms (e.g., quark recombination) and initial-state multiple scattering of partons before hard collisions complicate the inter-

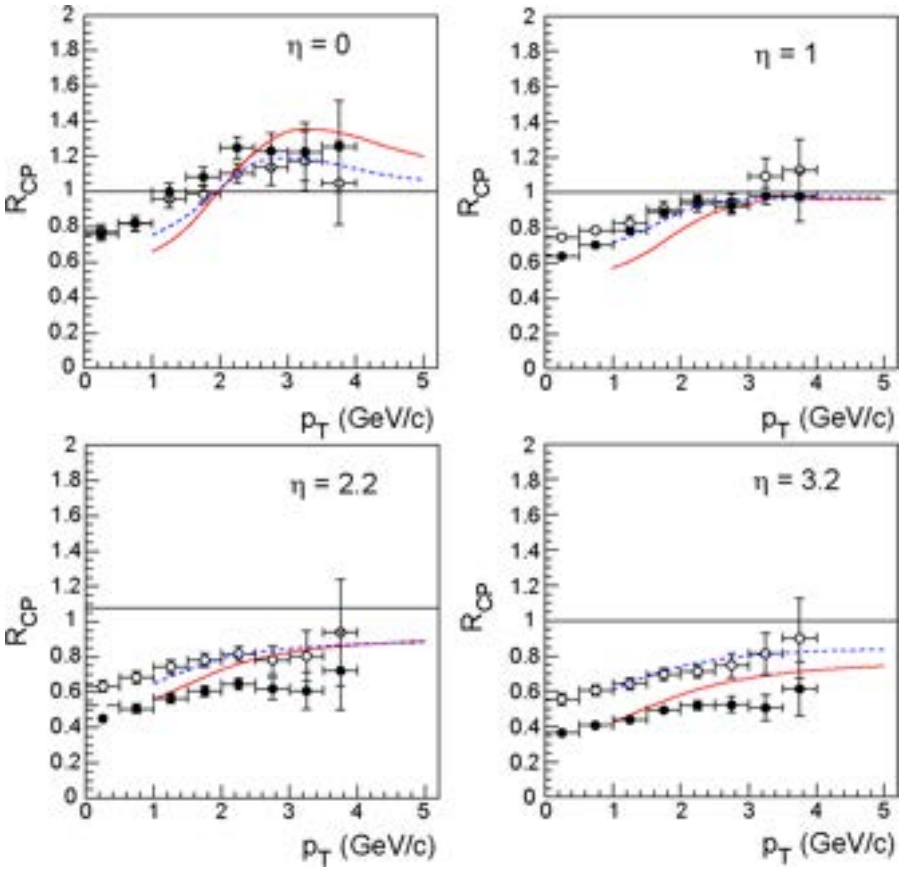

Fig. 32. The ratio R_{CP} of binary-scaled central to peripheral hadron yields for d + Au collisions at $\sqrt{s_{NN}} = 200$ GeV, plotted as a function of p_T for four different pseudorapidity bins, centered at $\eta = 0$, $\eta = 1$, $\eta = 2.2$ and $\eta = 3.2$. The measurements are from the Brahms Collaboration [154], for all charged hadrons (negative hadrons only) in the case of the former (latter) two η bins. The curves represent gluon saturation model fits from [156]. The filled circles and solid curves compare yields in the 0–20% to 60–80% centrality bins, while the open circles and dashed curves compare 30–50% to 60–80% . The figure is taken from Ref. [156].

pretation of the d + Au results. The same basic suppression of hadrons in the deuteron, relative to the Au, direction can be seen extending to higher p_T in the mid-rapidity backward/forward yield ratios from STAR [158], shown in Fig. 33. The same gluon saturation model calculations [156] shown in Fig. 32 are seen in Fig. 33 to be qualitatively, but not quantitatively, consistent with the observed dependences of the hadron yields on pseudorapidity, p_T and centrality. In particular, both measurements and calculations suggest that the mid-rapidity suppression fades away at transverse momenta above 5–6 GeV/c, as one probes higher-x partons in the Au nucleus.

The results in Figs. 32 and 33 represent the strongest evidence yet available for the applicability of color glass condensate concepts within the kinematic range spanned by RHIC collisions. Nonetheless, more mundane origins of this forward hadron suppression in d + Au have not been ruled out. Di-hadron correlation measurements involving these forward hadrons in d + Au collisions may help to distinguish between CGC and other explanations [160]. A critical characteristic of the CGC is that it can be treated as a classical gluon field. Forward hadrons that result from the interaction of a quark from the deuteron

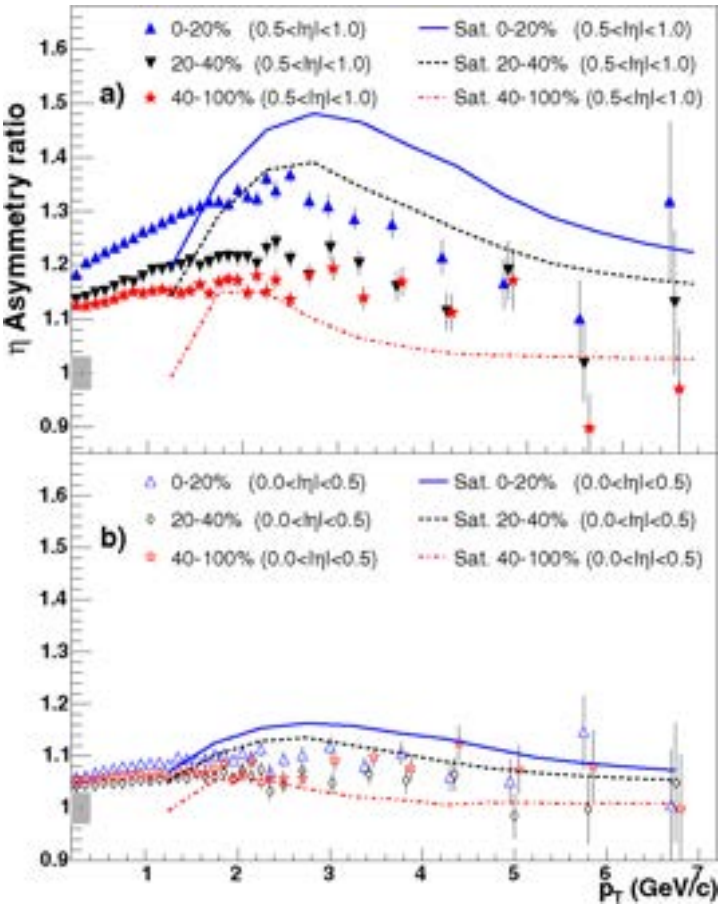

Fig. 33. Comparison of STAR measurements [158] with gluon saturation model calculations [156] for backward (Au side) to forward (d side) charged hadron yield ratios at mid-rapidity in $d+$Au collisions at $\sqrt{s_{NN}} = 200$ GeV. Results are shown as a function of hadron p_T for two different pseudorapidity ranges, (a) $0.5 < |\eta| < 1.0$ and (b) $0.0 < |\eta| < 0.5$, and three different centrality ranges. Centrality is determined experimentally from the measured charged particle multiplicity in the forward Au direction, for $-3.8 < \eta < -2.8$. Figure is taken from Ref. [158].

beam with this gluon field may have their transverse momentum balanced not by a single recoiling parton (and therefore a jet), but rather by a number of relatively soft hadrons with a much more smeared angular correlation than is characteristic of di-jet processes. Such a "mono-jet" signature would not be expected from more conventional sources of shadowing of gluon densities in the Au nucleus [161], which still allow individual quark–gluon, rather than quark–gluon field, scattering. On the other hand, kinematic limits on the accessible p_T values for forward hadrons imply that one is dealing, even in a di-jet framework, with unconventional away-side jets of only a few GeV/c [162]. In this regime, a suitable reference is needed, using $p + p$ or $d + A$ with a sufficiently light nucleus A to place the contributing parton x-range above the anticipated gluon saturation regime. The discriminating power of di-hadron correlations for CGC mono-jets must be demonstrated by modifications in $d +$ Au with respect to this reference.

4.5. Outlook

While large effects have been observed and the phenomenon of jet quenching in dense matter has been firmly established, precision data in a larger-p_T range are needed to fully explore the jet quenching phenomena and their connection to properties of the dense matter. The region $2 < p_T < 6$ GeV/c has significant contributions from non-perturbative processes other than vacuum fragmentation of partons, perhaps revealing novel hadronization mechanisms. Most studies to date of azimuthal anisotropies and correlations of "jets" have by necessity been constrained to this region, with only the inclusive spectra extending to the range where hard scattering is expected to dominate the inclusive yield. High statistics data sets for much higher p_T hadrons are needed to fully exploit azimuthal asymmetries and correlations as measurements of partonic energy loss. Dihadron measurements probing the details of the fragmentation process may be sensitive to the *energy* density, in addition to the gluon density that is probed with the present measurements. Heavy quark suppression is theoretically better controlled, and measurement of it will provide a critical check on the understanding of partonic energy loss. The *differential* measurement of energy loss through measurement of the emerging away-side jet and the recovery of the energy radiated in soft hadrons is still in its initial phase of study. A complete mapping of the modified fragmentation with larger initial jet energy and with a direct photon trigger will crosscheck the energy dependence of energy loss extracted from single inclusive hadron suppression. Experiments at different colliding energies are also useful to map the variation of jet quenching with initial energy density and the lifetime of the dense system.

At the same time as we extend the p_T range for jet quenching studies on the high side, it is crucial also to pursue further (particle-identified) hadron correlation measurements in the soft sector, in order to understand better how jets are modified by interactions with the dense bulk matter. Measurements such as those presented in Figs. 25 and 30 are just beginning to illuminate the processes leading to thermalization of parton energy. The properties of particles that have been substantially degraded, but not completely thermalized, by passage through the bulk may provide particularly fertile ground for exposing possible fundamental modifications (e.g., symmetry violations or restoration) of strong interactions in RHIC collision matter.

5. Some open issues

It should be clear from the detailed discussions of experimental and theoretical results in the preceding sections that some open questions need to be addressed before we can judge the evidence in favor of QGP formation at RHIC to be compelling. In this section we collect a number of such open questions for both experiment and theory. Convincing answers to even a few of these questions might tip the balance in favor of a QGP discovery claim. But even then, it will be important to address the remaining questions to solidify our understanding of the properties of the matter produced in RHIC collisions.

Lattice QCD calculations suggest that a confined state is impossible in bulk, thermodynamically equilibrated matter at the energy densities apparently achieved at RHIC. Indeed, several experimental observations are *consistent* with the creation of deconfined matter.

However, a discovery as important as the observation of a fundamentally new state of matter surely demands proof beyond circumstantial evidence for deconfinement. Can we do better?

One response that has been offered is that the EOS of strongly interacting matter is already known from lattice QCD calculations, so that only the conditions initially attained in heavy-ion collisions, and the degree of thermalization in the matter produced, are open to doubt. Such a view tends to trivialize the QGP search by presuming the answer. Indeed, an important aspect of the original motivation for the experimental program at RHIC was to explore the equation of state of strongly interacting matter under these extreme conditions of energy density. Lattice QCD, in addition to its technical difficulties and attendant numerical uncertainties, attempts to treat bulk, static, thermodynamically equilibrated quark–gluon systems. The relationship of such idealized matter to the finite, rapidly evolving systems produced in relativistic heavy-ion collisions is not a priori clear. One would prefer, then, to take LQCD calculations as guideposts to the transition properties to search for experimentally, but not as unassailable truth. On the other hand, there are sufficient complexities in the theoretical treatment of heavy-ion collisions that one would like to apply all credible constraints in parameterizing the problem. This dichotomy leads to our first question:

- *To what extent should LQCD results be used to constrain the equations of state considered in model treatments of RHIC collisions? How does one allow for independent checks of the applicability of LQCD to the dynamic environment of a RHIC collision?*

Experimentally, to verify the creation of a fundamentally new state of matter at RHIC one would like crosschecks demonstrating that the matter behaves qualitatively *differently* than "normal" (hadronic) matter in a system known or believed to be in a confined state. Although such a demonstration might be straightforward in bulk matter, it becomes an enormous challenge with the limited experimental control one has over thermodynamic variables in heavy-ion collisions. The finite size and lifetime of the matter produced in the early collision stages, coupled with the absence of global thermal equilibrium and of measurements (to date) of local temperature, all work to obscure the hallmark of QGP formation predicted by lattice QCD: a rapid transition around a critical temperature leading to deconfinement and, quite possibly, chiral symmetry restoration (the latter considered here as a sufficient, but not necessary, QGP manifestation). Given these complications, the underlying challenge to theory and experiment is:

- *Can we make a convincing QGP discovery claim without clear evidence of a rapid transition in the behavior of the matter produced? Can we devise probes with sufficient sensitivity to early, local system temperature to facilitate observation of such an onset at RHIC? Can we predict, based on what we now know from SPS and RHIC collisions, at what energies or under what conditions we might produce matter below the critical temperature, and which observables from those collisions should not match smoothly to SPS and RHIC results?*

At the most basic level, it is conceivable that there is no rapid deconfinement transition in nature (or at least in the matter formed fleetingly in heavy-ion collisions), but rather a gradual evolution from dominance of hadronic toward dominance of partonic degrees of freedom. It is not yet clear that we could distinguish such behavior of QCD matter from the blurring of a well-defined QGP transition by the use of tools with insufficient resolution or control.

5.1. What experimental crosschecks can be performed on apparent QGP signatures at RHIC?

Below we briefly discuss some of the key observations that underlie theoretical claims [6–8] that deconfined matter has been produced at RHIC, and ask what crosschecks might be carried out to test this hypothesis.

5.1.1. Jet quenching

As discussed in Section 4, inclusive hadron spectra and two-particle azimuthal correlations at moderate and high p_T clearly demonstrate that jets are suppressed in central RHIC Au + Au collisions, relative to scaled NN collisions. The lack of suppression (indeed, the enhancement, due to the Cronin effect) in d + Au collisions at RHIC provides a critical crosscheck that the quenching is not an initial-state effect. Measurements with respect to the event reaction plane orientation (see Fig. 29) provide another important crosscheck, demonstrating that the magnitude of the suppression depends strongly on the amount of matter traversed. Such jet quenching was first predicted [46] within the framework of parton energy loss in traversing a QGP. However, more recent theoretical work [58] casts doubt that deconfinement of the medium is essential to the phenomenon, or would be manifested clearly in the energy-dependence of quenching. Nonetheless, experimental hints of a possibly interesting energy dependence to quenching phenomena should be pursued as a potential crosscheck on formation of a new state of matter.

Moderate-p_T (up to 4 GeV/c) yields from Pb–Pb collisions at the SPS [163] appear to show an enhancement over a scaled *parameterized* p–p reference spectrum. However, questions raised about the p–p parameterization [164], combined with the unavailability of measurements constraining the initial-state (Cronin) enhancement at these energies, leave open the possibility that even at SPS, jets in central $A + A$ collisions may turn out to be suppressed *relative to expectations*. Indeed, the data in [163] do demonstrate hadron suppression in central relative to semi-peripheral collisions. Also, it is unclear whether the suppression of away-side two-particle correlations out of the reaction plane, observed at RHIC (see Fig. 29), might be of similar origin as the away-side out-of-plane broadening observed at the SPS [103]. These ambiguities are amplified by the limited p_T range covered in SPS measurements, spanning only a region where RHIC results suggest that hard parton scattering and fragmentation may not yet be the dominant contributing hadron production mechanism. These observations lead to the following question:

- *Is there a qualitative change in the yield of high-p_T hadrons in $A + A$ collisions between SPS and RHIC energies? Or does hadron suppression rather evolve smoothly with energy, reflecting a gradual growth in initial gluon density and parton energy*

loss? Is it feasible to make meaningful measurements of hard probes at sufficiently low collision energy to test for the absence or gross reduction of jet quenching in matter believed to be in a hot hadronic (i.e., confined) gas state?

5.1.2. Constituent-quark scaling of yields and anisotropies

The baryon *vs*. meson systematics of R_{CP} (Fig. 15) and the apparent scaling of elliptic flow with the number of constituent quarks (Fig. 20) in the intermediate p_T range strongly suggest collective behavior at a pre-hadronic level, a necessary aspect of QGP formation and thermalization in heavy-ion collisions. Once again, one would like to observe the *absence* of this behavior for systems in which QGP is not formed. High-quality, particle-identified elliptic flow data do not yet exist at SPS (or lower) energies in this p_T region.

- *Should constituent-quark scaling of v_2 in the intermediate p_T sector be broken if a QGP is not formed? If so, is an appropriate statistically meaningful, particle-identified measurement of v_2 at intermediate p_T feasible at $\sqrt{s_{NN}}$ below the QGP formation threshold?*

Alternatively, we could seek to establish the role of constituent quarks more convincingly by additional predictions of the quark coalescence models introduced to characterize this intermediate p_T region. For this purpose it may be helpful to integrate the coalescence models with other (e.g., gluon saturation or hydrodynamics) models that might serve to constrain the anticipated initial conditions and coalescence parameters as a function of centrality or collision energy.

- *Coalescence models have provided a simple ansatz to recognize the possible importance of constituent quark degrees of freedom in the hadronization process in $A + A$ collisions at RHIC, and to suggest that these constituent quarks exhibit collective flow. Once model parameters have been adjusted to account for the observed ratios of yields and elliptic flow strengths for baryons vs. mesons, can integration of key features from other models enhance predictive power? For example, can the centrality-dependence of these ratios, or meson vs. baryon correlations (angular or otherwise) at moderate p_T be predicted?*

5.1.3. Strong elliptic flow in agreement with hydrodynamics

In contrast to the above signatures, which require access to moderate-to-high p_T values, observables in the soft sector have already been extensively explored, even from Bevalac energies. The only soft-sector observable selected as a "pillar" of the QGP claim at RHIC, in Ref. [6], is the strong elliptic flow, whose magnitude, mass and p_T-dependence for mid-central collisions are in reasonable agreement with expectations based on ideal hydrodynamic flow (see Fig. 18). Furthermore, the agreement appears better for an equation of state that includes passage through a phase transition from partonic to hadronic matter.

This success leads to the claim [3,6] that the elliptic flow has finally, in near-central collisions at RHIC energies, reached the ideal hydrodynamic "limit", suggesting creation of equilibrated, low-viscosity matter at an early stage in the collision (when geometric

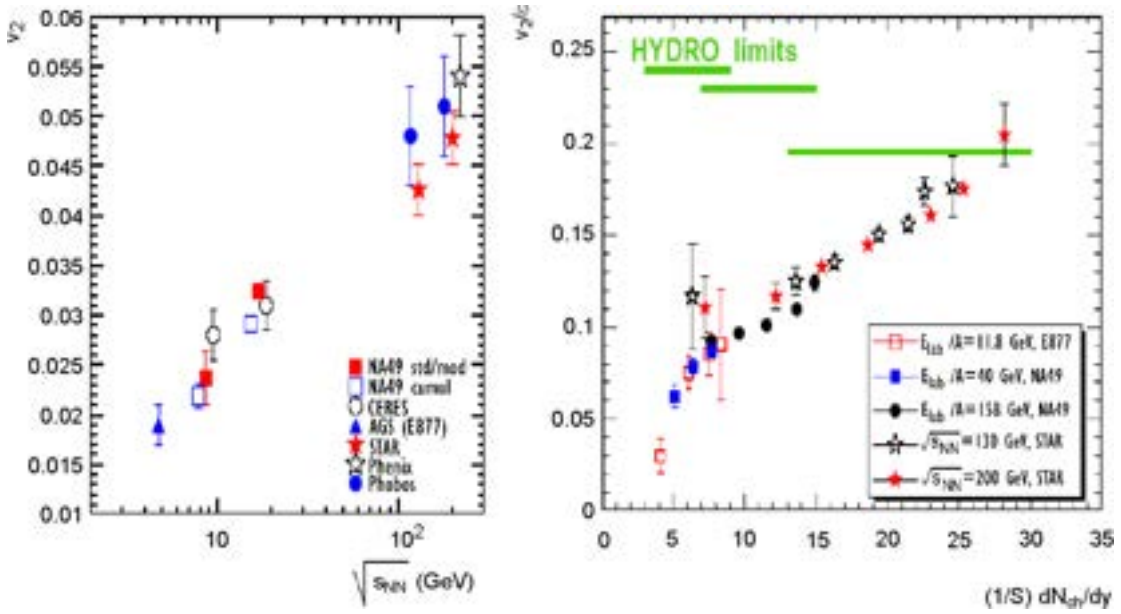

Fig. 34. (a) Energy dependence of elliptic flow measured near mid-rapidity for mid-central collisions ($\sim$ 12–34% of the geometric cross section) of $A \sim 200$ nuclei at the AGS, SPS and RHIC. (b) Mid-rapidity elliptic flow measurements from various energies and centralities combined in a single plot of v_2 divided by relevant initial spatial eccentricity vs. charged-particle rapidity density per unit transverse area in the $A + A$ overlap region. The figures, taken from Ref. [100], highlight the smooth behavior of flow vs. energy and centrality. The rightmost points represent near-central STAR results, where the observed v_2/ϵ ratio becomes consistent with limiting hydrodynamic expectations for an ideal relativistic fluid. The hydrodynamic limits are represented by horizontal lines [100] drawn for AGS, SPS and RHIC energies (from left to right), for one particular choice of EOS that assumes no phase transition in the matter produced.

anisotropy is still large). However, the results from many experiments clearly indicate a smoothly rising $v_2(\sqrt{s_{NN}})$, while the hydrodynamic limit for given initial spatial eccentricity and fixed EOS is falling with increasing energy (see Fig. 34). It is thus unclear from the available data whether we are observing at RHIC the interesting onset of saturation of a simple physical limit particularly relevant to QGP matter, or rather an accidental crossing point of experiment with a necessarily somewhat simplified theory. It is of major significance that ideal hydrodynamics appears to work at RHIC for the first time. This conclusion—and in particular the evidence for an equation of state containing a phase change—would be much strengthened if the hydrodynamic limit were demonstrated to be relevant as well under conditions far removed from those in RHIC measurements to date. Future measurements in central collisions of heavier and highly deformed nuclei (e.g., $U + U$ [3]) possible after a planned upgrade of the ion source for RHIC, or at significantly lower or higher energy (the latter awaiting LHC turn-on) will provide the possibility of additional crosschecks of this important conclusion.

- *Is the ideal hydrodynamic limit for elliptic flow relevant to heavy-ion collisions over a broad range of conditions, within which near-central Au + Au collisions at full RHIC energy represent merely a first "sighting"? Will v_2 at LHC energies surpass the hydrodynamic limit? Is thermalization likely to be sufficiently established in collisions below*

$\sqrt{s_{NN}} \approx 100$ GeV to permit meaningful tests of hydrodynamics? If so, will measurements at lower RHIC energies reveal a non-trivial energy dependence of v_2, such as that predicted in Fig. 7 by ideal hydrodynamics incorporating a phase transition? Can one vary the initial spatial eccentricity of the bulk matter independently of centrality and degree of thermalization, via controlled changes in the relative alignment of deformed colliding nuclei such as uranium?

5.1.4. Dependence of observables on system size

The above questions focused on excitation function measurements, which traditionally have played a crucial role in heavy-ion physics. It is also desirable to explore the appearance and disappearance of possible QGP signatures as a function of system size. To date, system size variations have been examined at RHIC primarily via the centrality dependence of many observables. A number of variables have been observed to change rapidly from the most peripheral to mid-peripheral collisions, and then to saturate for mid-central and central collisions. Examples of this type of behavior include: the strength (I_{AA} in Ref. [71]) and $\Delta\eta$ width (Fig. 25) of near-side di-hadron correlations; the ratio of measured v_2 to the hydrodynamic limit for relevant impact parameter [105]; the strangeness saturation parameter γ_s deduced from statistical model fits to measured hadron yield ratios (inset in Fig. 12) [86]. Do these changes reflect a (QGP) transition with increasing centrality in the nature of the matter first produced, or merely the gradual growth in importance of hadronic initial- and final-state interactions, and in the degree of thermalization achieved, as the number of nucleon participants increases? One's answer to this question may depend on how rapid the variation with centrality appears, but this in turn depends on what measure one uses for centrality, as emphasized in the lower frames of Fig. 25.

As the centrality changes for given colliding nuclei, so, unavoidably, does the initial shape of the overlap region. In order to unravel the influence of different initial conditions on the evolution of the matter formed in heavy-ion collisions, it will be important to measure as well the dependence of observables such as those above on the size of the colliding nuclei.

- *Do RHIC measurements as a function of centrality already contain hints of the onset of QGP formation in relatively peripheral regions? Will future measurements for lighter colliding nuclei permit more definitive delineation of these apparently rapid changes with system size?*

5.2. Do the observed consistencies with QGP formation demand a QGP-based explanation?

Because it is difficult to control the degree of thermalization achieved in heavy-ion collisions, and to measure directly the temperature at which it is initially achieved, it is possible that none of the crosschecks discussed in the preceding subsection for RHIC energies and below may provide definitive experimental resolution concerning QGP formation. In this case, our reliance on the comparison with theory would be significantly increased, and the questions posed below become especially important. Here, we question the *uniqueness* of

a QGP-based explanation. In other words, do the data *demand* a scenario characterized by thermalized, deconfined matter?

5.2.1. Strong elliptic flow

The hydrodynamic overestimate of elliptic flow at energies below RHIC has been attributed either to a failure to achieve complete thermalization in those collisions [3] or to their earlier transition to a viscous hadronic phase [6]. These interpretations suggest that the observed energy-dependence of flow (Fig. 34) is dominated by the complex dynamics of early thermalization and late hadronic interactions. While application of hydrodynamics relies on local thermal equilibrium, it is not obvious that agreement with data after parameter adjustment necessarily proves thermalization. The following question is posed in this light.

- *The unprecedented success of hydrodynamics calculations assuming ideal relativistic fluid behavior in accounting for RHIC elliptic flow results has been interpreted as evidence for both early attainment of local thermal equilibrium and an equation of state with a soft point, characteristic of the predicted phase transition. How do we know that the observed elliptic flow cannot result, alternatively, from a harder EOS coupled with incomplete or late thermalization and/or significant viscosity in the produced matter?*

Even if we *assume* thermalization (and hence the applicability of hydrodynamics), it is clear that a complete evaluation of the "theoretical error bars" has yet to be performed. When parameters are adjusted to reproduce spectra, agreement with v_2 measurements in different centrality bins is typically at the 20–30% level. The continuing systematic discrepancies from HBT results, and from the energy dependence of elliptic flow when simplified freezeout parameterizations are applied, suggest some level of additional ambiguity from the treatment of late-stage hadronic interactions and from possibly faulty assumptions of the usual hydrodynamics calculations (see Section 2.2). When theoretical uncertainties within hydrodynamics are fairly treated, does a convincing signal for an EOS with a soft point survive?

- *The indirect evidence for a phase transition of some sort in the elliptic flow results comes primarily from the sensitivity in hydrodynamics calculations of the magnitude and hadron mass-dependence of v_2 to the EOS. How does the level of this EOS sensitivity compare quantitatively to that of uncertainties in the calculations, gleaned from the range of parameter adjustments, from the observed deviations from the combination of elliptic flow, spectra and HBT correlations, and from the sensitivity to the freezeout treatment and to such normally neglected effects as viscosity and boost non-invariance?*

5.2.2. Jet quenching and high gluon density

The parton energy loss treatments do not directly distinguish passage through confined vs. deconfined systems. Although effects of deconfinement must exist at some level, e.g., on the propagation of radiated soft gluons, their inclusion in the energy loss models might well be quantitatively masked by other uncertainties in the calculations. Evidence of de-

confinement must then be indirect, via comparison of the magnitude of inferred gluon or energy densities early in the collision to those suggested by independent partonic treatments such as gluon saturation models. The actual energy loss inferred from fits to RHIC data, through the rapidly expanding collision matter, is only slightly larger than that indicated through static cold nuclei by fits to semi-inclusive deep inelastic scattering data. The significance of the results is then greatly magnified by the correction to go from the expanding collision matter to an equivalent static system at the time of the initial hard scattering. The quantitative uncertainties listed in the question below will then be similarly magnified. What, then, is a reasonable guess of the range of initial gluon or energy densities that can be accommodated, and how does one demonstrate that those densities can only be reached in a deconfined medium?

- *Does the magnitude of the parton energy loss inferred from RHIC hadron suppression observations **demand** an explanation in terms of traversal through deconfined matter? The answer must take into account quantitative uncertainties in the energy loss treatment arising, for example, from the uncertain applicability of factorization in-medium, from potential differences (other than those due to energy loss) between in-medium and vacuum fragmentation, and from effects of the expanding matter and of energy loss of the partons through cold matter preceding the hard scattering.*

Gluon saturation models set a QCD scale for anticipated gluon densities, that can then be compared to values inferred from parton energy loss treatments, modulo the questions asked above and below. An important question, given that RHIC multiplicity data are used as input to the models (e.g., to fix the proportionality between gluon density and hadron yields) is whether they provide information truly independent from the initial energy density inferred via the simple Bjorken hydrodynamic expansion scenario (Eq. (4)) from measured rapidity densities of transverse energy.

- *If there is a truly universal gluon density saturation scale, determined already from HERA $e-p$ deep inelastic scattering measurements, why cannot RHIC $A+A$ particle multiplicities be predicted a priori without input from RHIC experimental data? Is not the A- (or N_{part}-) dependence of the gluon densities at the relevant Bjorken x-ranges predicted in gluon saturation treatments? Can saturated entrance-channel gluon densities in overlapping cold nuclei be directly compared to the early gluon densities in thermalized hot matter, inferred from parton energy loss treatments of jet quenching?*

6. Overview and outlook

6.1. What have we learned from the first three years of RHIC measurements?

Already in their first three years, all four RHIC experiments have been enormously successful in producing a broad array of high-quality data illuminating the dynamics of heavy-ion collisions in a new regime of very high energy densities. STAR, in particular, has established a number of seminal, striking results highlighted in Sections 3 and 4 of this

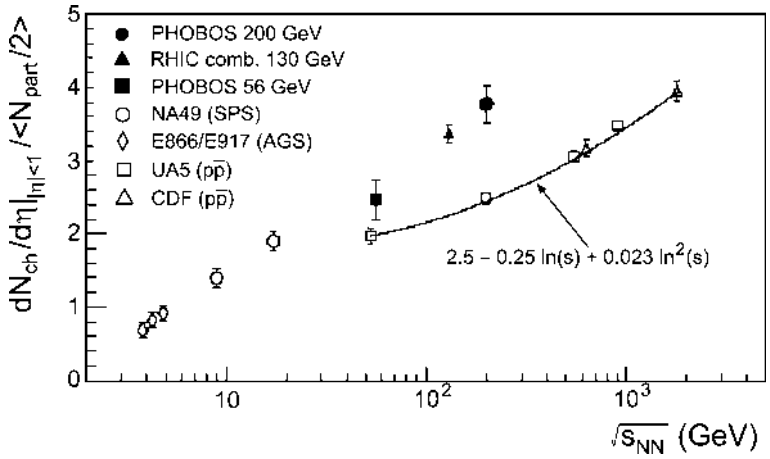

Fig. 35. Measured mid-rapidity charged particle densities, scaled by the calculated number of participant nucleons, for central collisions of $A \sim 200$ nuclei at AGS, SPS and RHIC, plotted as a function of the center-of-mass energy. Results for $\bar{p} + p$ collisions are shown for comparison. Figure from [80].

document. In parallel, there have been significant advances in the theoretical treatment of these collisions. The theory-experiment comparison indicates that central $\mathrm{Au} + \mathrm{Au}$ collisions at RHIC produce a unique form of strongly interacting matter, with some dramatic and surprisingly simple properties. A number of the most striking experimental results have been described to a reasonable quantitative level, and in some cases even predicted beforehand, using theoretical treatments inspired by QCD and based on QGP formation in the early stages of the collisions.

The observed hadron spectra and correlations at RHIC reveal three transverse momentum ranges with distinct behavior: a soft range (p_T 1.5 GeV/c) containing the vast majority of produced hadrons, representing most of the remnants of the bulk collision matter; a hard-scattering range (p_T 6 GeV/c), providing partonic probes of the early collision matter; and an intermediate range (1.5 p_T 6 GeV/c) where hard processes coexist with softer ones. The behavior in each of these ranges is quite different than would be expected from an incoherent sum of independent nucleon–nucleon collisions; for the hard sector, in particular, this is one of the most important new observations at RHIC. Below we summarize the major findings described in earlier sections within each of these three ranges, in each case listing them in approximate decreasing order of what we judge to be their level of robustness with respect to current experimental and theoretical ambiguities. This is not intended necessarily to represent order of importance, as some of the presently model-dependent conclusions are among the strongest arguments in favor of QGP formation.

6.1.1. Soft sector

- The matter produced exhibits *strong collective flow*: most hadrons at low-p_T reflect a communal transverse velocity field resulting from conditions early in the collision, when the matter was clearly expanding rapidly under high, azimuthally anisotropic, pressure gradients and frequent interactions among the constituents. The commonality of the velocity is clearest from the systematic dependence of elliptic flow strength on hadron mass at low-p_T (see Fig. 18), from the common radial flow velocities extracted

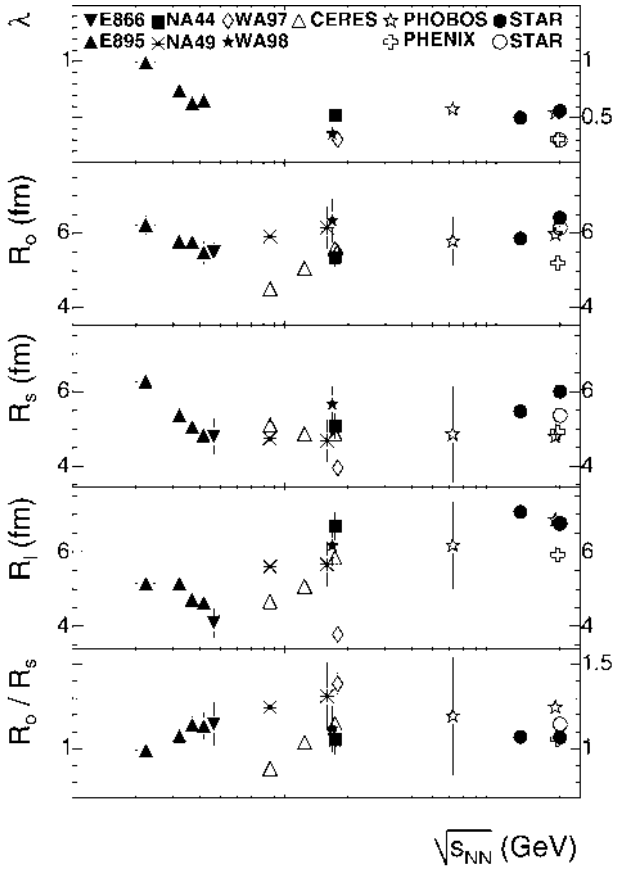

Fig. 36. Energy dependence of HBT parameters extracted from pion pair correlations in central $A + A$ ($A \sim 200$) collisions at mid-rapidity and pair $k_T \approx 0.2$ GeV/c. The data span the AGS, SPS and RHIC. Figure from [166].

by fitting observed spectra (Fig. 14), and from the measurements of HBT and non-identical particle correlations [120]. All of these features fit naturally, at least in a qualitative way, within a hydrodynamic description of the system evolution.

- Most bulk properties measured appear to fall on quite smooth curves with similar results from lower-energy collisions. Examples shown include features of integrated two-hadron p_T correlations (Fig. 24), elliptic flow (Fig. 34), charged particle density (Fig. 35) and emitting source radii inferred from HBT analyses (Fig. 36). Similarly, the centrality-dependences observed at RHIC are generally smooth (but see Fig. 25 for a possible exception). These experimental results contrast with theoretical speculations and predictions made before RHIC start-up, which often [11,30,165] suggested strong energy dependences accompanying the hadron-to-QGP transition. The observed smooth general behavior has been primarily attributed to the formation of matter over a range of initial local conditions, even at a given collision energy or centrality, and to the absence of any direct experimental determination of early temperature. In any case, the results clearly highlight *the difficulty of observing any rapid "smoking-gun" onset of a transition to a new form of matter*.
- Despite the smoothness of the energy and centrality dependences, two important milestones related to the attainment of thermal equilibrium appear to be reached for the first

time in near-central RHIC collisions at or near full energy. The first is that *the yields of different hadron species, **up to and including multi-strange hadrons**, become consistent with a grand canonical statistical distribution* at a chemical freezeout temperature of 163 ± 5 MeV and a baryon chemical potential ≈ 25 MeV (see Fig. 12). This result places an effective lower limit on the temperatures attained if thermal equilibration is reached during the collision stages preceding this freezeout. This lower limit is *essentially equal to the QGP transition temperature predicted by lattice QCD calculations* (see Fig. 1).

- At the same time (i.e., for near-central RHIC collisions) the mass- and p_T-dependence of the observed hadron spectra and of the strong elliptic flow in the soft sector become *consistent, at the* $\pm$20–30*% level, with hydrodynamic expectations for an **ideal** relativistic fluid* formed with an initial eccentricity characteristic of the impact parameter. These hydrodynamic calculations have not yet succeeded in also quantitatively explaining the emitting hadron source size inferred from measured HBT correlations (see Fig. 22). Nonetheless, their overall success suggests that the interactions among constituents in the initial stages of these near-central collisions are characterized by very short mean free paths, leading to *quite rapid ($\tau \quad 1$ fm/c) attainment of at least approximate local thermal equilibrium*. The short mean free path in turn suggests a very dense initial system.
- Based on the rapid attainment of thermal equilibrium, and making the assumption of longitudinal boost-invariant expansion, one can extract [84] a rough lower bound on the initial energy density from measured rapidity densities [81,83] of the total transverse energy (dE_T/dy) produced in the collisions. These estimates suggest that in central Au + Au collisions at RHIC, *matter is formed at an initial energy density well above the critical density* (~ 1.0 GeV/fm^3) predicted by LQCD for a transition to the QGP.
- Measurements of two-hadron angular correlations and of the power spectrum of local charged-particle density fluctuations reveal strong near-side correlations surviving in the soft sector, reminiscent of jet-like behavior in some aspects, but with a strong pseudorapidity broadening introduced by the presence of the collision matter. The observed structure (see Fig. 25) suggests that *soft jet fragments are not fully thermalized with the bulk matter, but nonetheless show the effects of substantial coupling to that matter* in a considerable broadening of the jet "peak" in pseudorapidity difference between two hadrons.
- Hydrodynamics calculations are best able to reproduce RHIC results for hadron spectra and the magnitude and mass-dependence of elliptic flow (Fig. 18) by utilizing *an equation of state incorporating a soft LQCD-inspired phase transition from QGP to hadronic matter*. However, the calculations also exhibit comparable sensitivity to other a priori unknown features, e.g., the details of the hadronic final-state interactions and the time at which thermal equilibrium is first attained. In light of these competing sensitivities, it is not yet clear if the experimental results truly *demand* an EOS with a soft point.

6.1.2. Intermediate sector

- In the intermediate-p_T range, the elliptic flow strength v_2 saturates and we see systematic meson vs. baryon differences (rather than a systematic mass-dependence) in both yield (see Fig. 15) and v_2 value (Fig. 20). In the same region we also observe clear jet-like angular correlation peaks in the near-side azimuthal difference distributions between pairs of hadrons (see Fig. 29). The most natural interpretation for this combination of characteristics is that *the intermediate-p_T yield arises from a mixture of partonic hard-scattering (responsible for the jet-like correlations) and softer processes (responsible for the meson–baryon differences).*
- *The saturated v_2 values appear to scale with the number of constituent (or valence) quarks n in the hadron studied,* i.e., v_2/n vs. p_T/n falls on a common curve for mesons and baryons (see Fig. 20). If this trend persists as the particle-identified intermediate-p_T data are improved in statistical precision for a suitable variety of hadron types, it would provide direct experimental evidence for the relevance of sub-hadronic degrees of freedom in determining flow for hadrons produced at moderate p_T in RHIC collisions.
- Quark recombination models are able to provide a reasonable account of the observed meson and baryon spectra, as well as the v_2 systematics, in the intermediate sector by *a sum of contributions from coalescence of thermalized constituent quarks following an exponential p_T spectrum and from fragmentation of initially hard-scattered partons with a power-law spectrum* [70]. It is not yet clear if the same mixture can also account quantitatively for the azimuthal dihadron correlation (including background under the jet-like peaks) results as a function of p_T. Other models [69,72] mix the above contributions by also invoking recombination of hard-scattered with thermal partons.

6.1.3. Hard sector

- The dominant characteristic of the hard regime is *the strong suppression of hadron yields in central $Au+Au$ collisions,* in comparison to expectations from $p+p$ or peripheral Au + Au collisions, scaled by the number of contributing binary (nucleon–nucleon) collisions (see Fig. 31). Such suppression sets in already in the intermediate sector, but saturates and remains constant as a function of p_T throughout the hard region explored to date. Such suppression was not seen in $d+$Au collisions at RHIC, indicating that it is *a final-state effect associated with the collision matter produced in $Au+Au$*. It is consistent with effects of parton energy loss in traversing dense matter, predicted before the data were available [146,147].
- Azimuthal correlations of moderate- (see Fig. 29) and high-p_T [144] hadrons exhibit clear jet-like peaks on the near side. However, *the anticipated away-side peak associated with dijet production is suppressed* by progressively larger factors as the Au + Au centrality is increased, and for given centrality, as the amount of (azimuthally anisotropic) matter traversed is increased (see Fig. 29). Again, no such suppression is observed in $d+$Au collisions. The suppression of hadron yields and back-to-back correlations firmly establish that *jets are quenched by very strong interactions with the matter produced in central $Au+Au$ collisions*. The jet-like near-side correlations survive presumably because one observes preferentially hard fragments of partons

scattered outward from the surface region of the collision zone. Effects of interaction with the bulk matter are nonetheless still seen on the near side, primarily by the broadened distribution in pseudorapidity of softer correlated fragments (see Fig. 25 and Ref. [145]).

- Many features of the observed suppression of high-p_T hadrons, including the centrality-dependence and the p_T-independence, can be described efficiently by *perturbative QCD calculations incorporating parton energy loss* in a thin, dense medium (see Fig. 31). To reproduce the magnitude of the observed suppression, despite the rapid expansion of the collision matter the partons traverse, these treatments need to assume that *the initial gluon density when the collective expansion begins is more than an order of magnitude greater than that characteristic of cold, confined nuclear matter* [146]. The inferred gluon density is consistent, at a factor ~ 2 level, with the saturated densities needed to account for RHIC particle multiplicity results in gluon saturation models (see Fig. 11).
- The yields of hadrons at moderate-to-high-p_T in central $d + \mathrm{Au}$ collisions exhibit a systematic dependence on pseudorapidity, marked by *substantial suppression, with respect to binary scaling expectations, of products near the deuteron beam direction, in contrast to substantial enhancement of products at mid-rapidity and near the Au beam direction* (see Figs. 32 and 33). This pattern suggests a depletion of gluon densities at low Bjorken x in the colliding Au nucleus, and is *qualitatively consistent with predictions of gluon saturation models*. Measurements to date cannot yet distinguish interactions with a classical gluon field (color glass condensate) from interactions with a more conventionally shadowed density of individual gluons.
- Angular correlations between moderate-p_T and soft hadrons have been used to explore how transverse momentum balance is achieved, in light of jet quenching, opposite a high-p_T hadron in central $\mathrm{Au} + \mathrm{Au}$ collisions. The results show the balancing hadrons to be significantly larger in number, softer (see Fig. 30) and more widely dispersed in angle compared to $p + p$ or peripheral $\mathrm{Au} + \mathrm{Au}$ collisions, with *little remnant of away-side jet-like behavior*. To the extent that hard scattering dominates these correlations at moderate and low-p_T, the results could signal an approach of the away-side parton toward thermal equilibrium with the bulk matter it traverses. As mentioned earlier, progress toward thermalization of jet fragments on the near-side is also suggested by soft-hadron correlations.
- The hard sector was not accessed in SPS experiments, so any possible energy dependence of jet quenching can only be explored via the hadron nuclear modification factor in the intermediate-p_T range. While the results (see Fig. 37) leave open the possibility of a rapid transition [53], one is not expected on the basis of theoretical studies of parton energy loss [58]. Furthermore, serious questions have been raised [164] about the validity of the $p + p$ reference data used to determine the SPS result in the figure.

In summary, the RHIC program has enabled dramatic advances in the study of hot strongly interacting matter, for two basic reasons. With the extended reach in initial energy density, the matter produced in the most central RHIC collisions appears to have attained conditions that considerably simplify its theoretical treatment: essentially ideal fluid expansion, and approximate local thermal equilibrium beyond the LQCD-predicted

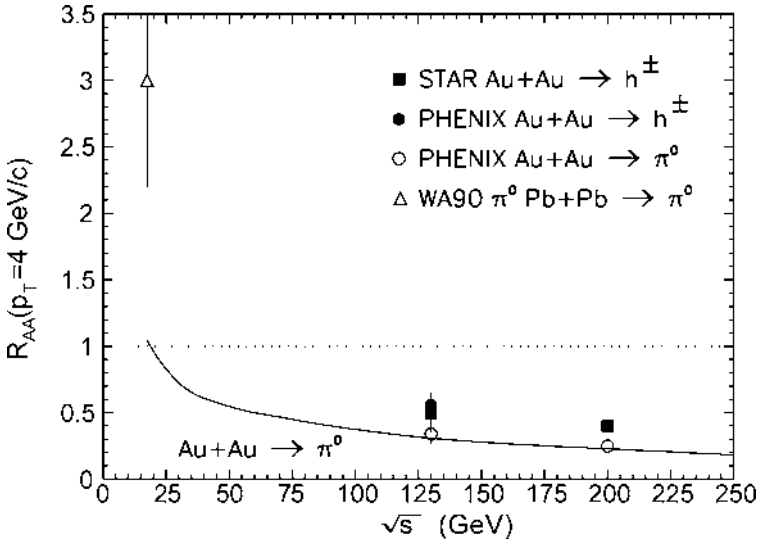

Fig. 37. The nuclear modification factor measured for 4 GeV/c hadrons in central $A + A$ ($A \sim 200$) collisions at SPS and two RHIC energies, showing (Cronin) enhancement at the lower energy and clear jet-quenching suppression at RHIC. The small difference between RHIC charged hadron and identified π^0 results reflects meson vs. baryon differences in this p_T range. The solid curve represents a parton energy loss calculation under simplifying assumptions concerning the energy-dependence, as described in [146].

threshold for QGP formation. With the extended reach in particle momentum, the RHIC experiments have developed probes for behavior that was difficult to access at lower collision energies: jet quenching and apparent constituent quark scaling of elliptic flow. These results indicate, with fairly modest reliance on theory, that RHIC collisions produce highly opaque and dense matter that behaves collectively. The magnitude of the density inferred from parton energy loss treatments, together with the hints of constituent quark collective flow, argue against the effectiveness of a purely hadronic treatment of this unique strongly interacting matter. It appears from the most robust signals to evolve for a significant fraction of its lifetime as a *low-viscosity, pre-hadronic liquid*.

If one takes seriously all of the theoretical successes mentioned above, they suggest the following more detailed overall picture of RHIC collisions: Interactions of very short mean free path within the gluon density saturation regime lead to a rapidly thermalized partonic system at energy densities and temperatures above the LQCD critical values. This thermalized matter expands collectively and cools as an ideal fluid, until the phase transition back to hadronic matter begins, leading to a significant pause in the build-up of elliptic flow. During the phase transition, constituent quarks emerge as the effective degrees of freedom in describing hadron formation at medium p_T out of this initially partonic matter. Initially hard-scattered partons (with lower color interaction cross sections than the bulk partons) traversing this matter lose substantial energy to the medium via gluon radiation, and thereby approach, but do not quite reach, equilibration with the bulk matter. Thus, some evidence of degraded jets survives (e.g., see Fig. 29), depending on the amount of matter traversed. Any claim of QGP discovery based on RHIC results to date requires an assessment of the robustness, internal consistency, quantitative success and predictive power of this emerging picture.

6.2. Are we there yet?

The consistency noted above of many RHIC results with a QGP-based theoretical framework is an important and highly non-trivial statement! Indeed, it is the basis of some claims [6–8] that the quark–gluon plasma has already been discovered at RHIC. However, these claims are associated with QGP definitions [6,7] that do not specifically highlight deconfinement as an essential property to be demonstrated. In our judgment, for reasons mentioned below, and also reflected in the list of open questions provided in Section 5 of this document, it is premature to conclude definitively that the matter produced in central RHIC collisions is a quark–gluon plasma, as this term has been understood by the scientific community for the past 20 years (see Appendix B).

- The RHIC experiments have not yet produced *direct* evidence for deconfinement, or indeed for any clear transition in thermodynamic properties of the matter produced. It may be unreasonable to expect a clear onset of deconfinement in heavy-ion systems as a function of collision energy, because the matter, even if locally thermalized, is presumably formed over a range of initial temperatures at any given collision energy. Thus, in the emerging theoretical picture, the matter produced in heavy-ion collisions at SPS was probably also formed in part above the critical energy density, but over a smaller fraction of the volume and with shorter-lived (or perhaps never attained) thermal equilibrium, in comparison with RHIC collisions. At still lower collision energies, where the critical conditions might never be reached, various aspects of the theoretical framework applied at RHIC become inapplicable, precluding a simple theory-experiment comparison over a range from purely hadronic to allegedly QGP-dominated matter.
- The indirect evidence for a thermodynamic transition and for attainment of local thermal equilibrium in the matter produced at RHIC are intertwined in the hydrodynamics account for observed hadron spectra and elliptic flow results. The uniqueness of the solution involving early thermalization and an EOS with a soft mixed phase is not yet demonstrated. Nor is its robustness against changes in the treatment of the late hadronic stage of the evolution, including the introduction of viscosity and other modifications that might be needed to reduce discrepancies from HBT measurements.
- The indirect evidence for deconfinement rests primarily on the large initial gluon densities inferred from parton energy loss fits to the observed hadron suppression at high-p_T, and on the supposition that such high densities could only be achieved in deconfined matter. The latter supposition has yet to be demonstrated in a compelling theoretical argument. The agreement with initial gluon densities suggested by color glass condensate approaches is encouraging, but is still at a basically qualitative level. The measurements suggest that matter is formed at initial temperatures and energy densities at or above the critical values predicted by LQCD for a deconfinement transition. But they do not establish the detailed relevance of the lattice calculations to the fleeting dynamic matter produced in heavy-ion collisions.
- The role of collectively flowing constituent quarks in hadron formation at intermediate-p_T is not yet well established experimentally. If it becomes so established by subsequent measurements and analyses, this will hint at the existence of a collective,

thermalized partonic stage in the system evolution. However, that hint will fall short of a conclusive QGP demonstration until some interpretational ambiguities are resolved: Is it really *constituent*, rather than *current* (valence) quarks that coalesce? If the former, do the constituent quarks then merely represent the effective degrees of freedom for hadronization of a QGP, or do they indicate an intermediate, pre-hadronic evolutionary stage, after the abundant gluons and current quarks have coalesced and dynamical chiral symmetry breaking has been reintroduced? If there is a distinct constituent quark formation stage, is thermalization achieved before, or only during, that stage?

- The theory remains a patchwork of different treatments applied in succession to each stage of the collision evolution, without yet a clear delineation of the different aspects as distinct limits of one overarching, seamless theory. The theoretical claims of QGP discovery in [8], considered together, rely on five "pillars of wisdom" for RHIC central Au + Au collisions, and each invokes a separate model or theoretical approach for its interpretation:
  (i) statistical model fits to measured hadron yields to infer possible chemical equilibrium across the u, d and s sectors;
  (ii) hydrodynamics calculations of elliptic flow to suggest early thermalization and soft EOS;
  (iii) quark recombination models to highlight the role of thermalized constituent quarks in intermediate-sector v_2 scaling;
  (iv) parton energy loss models to infer an initial gluon density from high-p_T hadron suppression observations;
  (v) gluon saturation model fits to observed hadron multiplicities and yields at large rapidity, to suggest how high-density QCD may predetermine the achieved initial gluon densities.

  Each movement of the theoretical suite has its own assumptions, technical difficulties, adjusted parameters and quantitative uncertainties, and they fit together somewhat uneasily. Until they are assimilated into a more self-consistent whole with only a few overall parameters fitted to existing data, it may be difficult to assess theoretical uncertainties quantitatively or to make non-trivial quantitative predictions whose comparison with future experimental results have the potential to prove the theory wrong.

The bottom line is that in the absence of a direct "smoking gun" signal of deconfinement revealed by experiment alone, a QGP discovery claim must rest on the comparison with a promising, but still not yet mature, theoretical framework. In this circumstance, clear predictive power with quantitative assessments of theoretical uncertainties are necessary for the present appealing picture to survive as a lasting one. The matter produced in RHIC collisions is fascinating and unique. The continuing delineation of its properties will pose critical tests for the theoretical treatment of non-perturbative QCD. But we judge that a QGP discovery claim based on RHIC measurements to date would be premature. We do not propose that a comprehensive theoretical understanding of all observed phenomena must be attained before a discovery claim is warranted, but only that at least some of the serious open questions posed above and in Section 5 be successfully answered.

6.3. What are the critical needs from future experiments?

The above comments make it clear what is needed most urgently from theory. But how can future measurements, analyses and heavy-ion collision facilities bring us to a clearer delineation of the fundamental properties of the unique matter produced, and hopefully to a more definitive conclusion regarding the formation of a quark–gluon plasma? We briefly describe below the goals of some important anticipated programs, separated into short-term and long-term prospects, although the distinction in time scale is not always sharp. In the short term, RHIC measurements should concentrate on verifying and extending its new observations of jet quenching and v_2 scaling; on testing quantitative predictions of theoretical calculations incorporating a QGP transition at lower energies and for different system sizes; on measuring charmed-hadron and charmonium yields and flow to search for other evidence of deconfinement; and on testing more extensive predictions of gluon saturation models for forward hadron production. Some of the relevant data have already been acquired during the highly successful 2004 RHIC run—which has increased the RHIC database by an order of magnitude—and simply await analysis, while other measurements require anticipated near-term upgrades of the detectors. In the longer term, the LHC will become available to provide crucial tests of QGP-based theoretical extrapolations to much higher energies, and to focus on very high-p_T probes of collision matter that is likely to be formed deep into the gluon saturation regime. Over that same period, RHIC should provide the extended integrated luminosities and upgraded detectors needed to undertake statistically challenging measurements to probe directly the initial system temperature, the pattern of production yields among various heavy quarkonium species, the quantitative energy loss of partons traversing the early collision matter, and the fate of strong-interaction symmetries in that matter.

Important short-term goals include the following:

- *Establish v_2 scaling more definitively.* Extend the particle-identified flow measurements for hadrons in the medium-p_T region over a broader-p_T range, a wider variety of hadron species, and as a function of centrality. Does the universal curve of v_2/n vs. p_T/n remain a good description of all the data? How is the scaling interpretation affected by anticipated hard contributions associated with differential jet quenching through spatially anisotropic collision matter? Can the observed di-hadron angular correlations be quantitatively accounted for by a 2-component model attributing hadron production in this region to quark coalescence (with correlations reflecting only the collective expansion) plus fragmentation (with jet-like correlations)? Do hadrons such as ϕ-mesons or Ω-baryons, containing no valence u or d quarks, and hence with quark-exchange contributions to hadronic interaction cross sections suppressed in normal nuclear matter, follow the same flow trends as other hadrons? Do the measured v_2 values for resonances reflect their constituent quark, or rather their hadron, content? These investigations have the potential to establish more clearly that constituent quarks exhibiting collective flow are the relevant degrees of freedom for hadronization at medium p_T.
- *Establish that jet quenching is an indicator of parton, and not hadron, energy loss.* Extend the measurements of hadron energy loss and di-hadron correlations to higher-p_T,

including particle identification in at least some cases. Do the meson–baryon suppression differences seen at lower p_T truly disappear? Does the magnitude of the suppression remain largely independent of p_T, in contrast to expectations for hadron energy loss [53]? Does one begin to see a return of away-side jet behavior, via punch-through of correlated fragments opposite a higher-p_T trigger hadron? Improve the precision of di-hadron correlations with respect to the reaction plane, and extend jet quenching measurements to lighter colliding nuclei, to observe the non-linear dependence on distance traversed, expected for radiating partons [4]. Measure the nuclear modification factors for charmed meson production, to look for the "dead-cone" effect predicted [54] to reduce energy loss for heavy quarks.

- *Extend RHIC Au + Au measurements down toward SPS measurements in energy, to test quantitative predictions of the energy-dependence.* Does the suppression of high-p_T hadron yields persist, and does it follow the gentle energy-dependence predicted in Fig. 37? Do the gluon densities inferred from parton energy loss model fits to hadron yields follow energy-dependent trends expected from gluon saturation models? Does elliptic flow remain in agreement with calculations that couple expansion of an ideal partonic fluid to a late-stage, viscous hadron cascade? Do meson–baryon differences and indications of constituent-quark scaling persist in hadron yields and flow results at intermediate p_T? Do quark coalescence models remain viable, with inferred thermal quark spectra that change sensibly with the (presumably) slowly varying initial system temperatures? The study of the evolution with collision energy of differential measurements such as those in Fig. 25 promises to yield important insight into the dynamical processes which occur during system evolution.
- *Measure charmonium yields and open charm yields and flow, to search for signatures of color screening and partonic collectivity.* Use particle yield ratios for charmed hadrons to determine whether the apparent thermal equilibrium in the early collision matter at RHIC extends even to quarks with mass significantly greater than the anticipated system temperature. From the measured p_T spectra, constrain the relative contributions of coalescence vs. fragmentation contributions to charmed-quark hadron production. Compare D-meson flow to the trends established in the u, d and s sectors, and try to extract the implications for flow contributions from coalescence vs. possibly earlier partonic interaction stages of the collision. Look for the extra suppression of charmonium, compared to open charm, yields expected to arise from the strong color screening in a QGP state (see Fig. 2).
- *Measure angular correlations with far forward high-energy hadrons in $d + Au$ or $p + Au$ collisions.* Search for the mono-jet signature anticipated for quark interactions with a classical (saturated) gluon field, as opposed to di-jets from quark interactions with individual gluons. Correlations among two forward hadrons are anticipated to provide the best sensitivity to the gluon field at sufficiently low Bjorken x to probe the possible saturation regime.

Longer-term prospects, requiring much greater integrated luminosities (as anticipated at RHIC II) or other substantial facility developments, include:

- *Develop thermometers for the early stage of the collisions, when thermal equilibrium is first established.* In order to pin down experimentally where a thermodynamic transition may occur, it is critical to find probes with direct sensitivity to the temperature well before chemical freezeout. Promising candidates include probes with little final-state interaction: direct photons—measured down to low momentum, for example, via γ–γ HBT, which is insensitive to the large π^0 background—and thermal dileptons. The former would require enhanced pair production tracking and the latter the introduction of hadron-blind detectors and techniques.
- *Measure the yields and spectra of various heavy quarkonium species.* Recent LQCD calculations [17] predict the onset of charmonium melting—which can be taken as a signature for deconfinement—at quite different temperatures above T_c for J/ψ vs. ψ'. Similar differences are anticipated for the various Υ states. While interpretation of the yield for any one quarkonium species may be complicated by competition in a QGP state between enhanced heavy quark production rates and screened quark–antiquark interactions, comparison of a measured hierarchy of yields with LQCD expectations would be especially revealing. They would have to be compared to measured yields for open charm and beauty, and to the corresponding quarkonium production rates in $p+p$ and $p+A$ collisions. Clear identification of ψ' and separation of Υ states require upgrades to detector resolution and vertexing capabilities.
- *Quantify parton energy loss by measurement of mid-rapidity jet fragments tagged by a hard direct photon, a heavy-quark hadron, or a far forward energetic hadron.* Such luminosity-hungry coincidence measurements will elucidate the energy loss of light quarks vs. heavy quarks vs. gluons, respectively, through the collision matter. They should thus provide more quantitative sensitivity to the details of parton energy loss calculations.
- *Test quantitative predictions for elliptic flow in $U+U$ collisions.* The large size and deformation of uranium nuclei make this a considerable extrapolation away from RHIC Au + Au conditions, and a significant test for the details of hydrodynamics calculations that are consistent with the Au + Au results [3]. If the relative alignment of the deformation axes of the two uranium nuclei can be experimentally controlled, one would be able to vary initial spatial eccentricity largely independently of centrality and degree of thermalization of the matter.
- *Measure hadron multiplicities, yields, correlations and flow at LHC and GSI energies, and compare to quantitative predictions based on models that work at RHIC.* By fixing parameters and ambiguous features of gluon saturation, hydrodynamics, parton energy loss and quark coalescence models to fit RHIC results, and with guidance from LQCD calculations regarding the evolution of strongly interacting matter with initial temperature and energy density, theorists should make quantitative predictions for these observables at LHC and GSI before the data are collected. The success or failure of those predictions will represent a stringent test of the viability of the QGP-based theoretical framework.
- *Devise tests for the fate of fundamental QCD symmetries in the collision matter formed at RHIC.* If the nature of the QCD vacuum is truly modified above the critical temperature, then chiral and $U_A(1)$ symmetries may be restored, while parity and CP may conceivably be broken [167]. Testing these symmetries in this unusual form of strongly

interacting matter is of great importance, even if we do not have a crisp demonstration beforehand that the matter is fully thermalized and deconfined. Indeed, if evidence were found for a clear change in the degree of adherence to one of the strong interaction symmetries, in comparison with normal nuclear matter, this would likely provide the most compelling "smoking gun" for production of a new form of matter in RHIC collisions. Approaches that have been discussed to date include looking for meson mass shifts in dilepton spectra as a signal of chiral symmetry restoration, and searching for CP violation via $\Lambda - \bar{\Lambda}$ spin correlations or electric dipole distributions of produced charge with respect to the reaction plane [167]. It may be especially interesting to look for evidence among particles emerging opposite an observed high-p_T hadron tag, since the strong suppression of away-side jets argues that the fate of the away-side particles may reflect strong interactions with a maximal amount of early collision matter. These tests will begin in the short term, but may ultimately need the higher statistics available in the longer term to distinguish subtle signals from dominant backgrounds.

6.4. Outlook

The programs we have outlined above for desirable advances in theory and experiment represent a decade's worth of research, not all of which must, or are even expected to, *precede* a discovery announcement for the quark–gluon plasma. We can imagine several possible scenarios leading to a more definitive QGP conclusion. Identification of a single compelling experimental signature is still conceivable, but the most promising prospects are long-term: establishment of a telling pattern of quarkonium suppression vs. species; observation of clear parity or CP violation, or of chiral symmetry restoration, in the collision matter; extraction of a transition signal as a function of measured early temperature. It is also possible that a single theoretical development could largely seal the case: e.g., a compelling argument that gluon densities more than an order of magnitude higher than those in cold nuclear matter really do *demand* deconfinement; or sufficient hydrodynamics refinement to demonstrate that RHIC flow results really do *demand* a soft point in the EOS. Perhaps the most likely path would involve several additional successes in theory-experiment comparisons, leading to a preponderance of evidence that RHIC collisions have produced thermalized, deconfined quark–gluon matter.

In any scenario, however, RHIC has been, and should continue to be, a tremendous success in its broader role as an instrument for discovery of new features of QCD matter under extreme conditions. The properties already delineated, with seminal contributions from STAR, point toward a dense, opaque, non-viscous, pre-hadronic liquid state that was not anticipated before RHIC. Determining whether the quarks and gluons in this matter reach thermal equilibrium with one another before they become confined within hadrons, and eventually whether chiral symmetry is restored, are two among many profound questions one may ask. Further elaboration of the properties of this matter, with eyes open to new unanticipated features, remains a vital research mission, independent of the answer that nature eventually divulges to the more limited question that has been the focus of this document.

Acknowledgements

We thank the RHIC Operations Group and RCF at BNL, and the NERSC Center at LBNL for their support. This work was supported in part by the HENP Divisions of the Office of Science of the US DOE; the US NSF; the BMBF of Germany; IN2P3, RA, RPL, and EMN of France; EPSRC of the United Kingdom; FAPESP of Brazil; the Russian Ministry of Science and Technology; the Ministry of Education and the NNSFC of China; Grant Agency of the Czech Republic, FOM of the Netherlands, DAE, DST, and CSIR of the Government of India; Swiss NSF; the Polish State Committee for Scientific Research; and the STAA of Slovakia.

Appendix A. Charge

This report was prepared for the STAR Collaboration in response to the following charge from the Spokesperson, delivered to a drafting committee on 18 March 2004.

> "Thank you very much for agreeing to help in preparing a draft whitepaper to serve as the starting point for a focused discussion by the STAR Collaboration of the experimental evidence regarding the role of the quark–gluon plasma in RHIC heavy ion collisions."
>
> "The charge to this panel is to make a critical assessment of the presently available evidence to judge whether it warrants a discovery announcement for the QGP, using any and all experimental and theoretical results that address this question. The white paper should pay particular attention to identifying the most crucial features of the QGP that need to be demonstrated experimentally for a compelling claim to be made. It should summarize those data that may already convincingly demonstrate some features, as well as other data that may be suggestive but with possible model-dependence, and still other results that raise questions about a QGP interpretation. If the conclusion is that a discovery announcement is at present premature, the paper should outline critical additional measurements and analyses that would make the case stronger, and the timeline anticipated to produce those new results."
>
> "The white paper should be of sufficient quality and scientific integrity that, after incorporation of collaboration comments, it may be circulated widely within the RHIC and larger physics communities as a statement of STAR's present assessment of the evidence for the QGP."

Appendix B. Definitions of the quark–gluon plasma in nuclear physics planning documents

One's conclusion concerning the state of the evidence in support of quark–gluon plasma formation is certainly influenced by the definition one chooses for the QGP state. Recent

positive claims have been based on definitions different from that chosen in this work (see Section 1), leaning more toward either an operational definition based on actual RHIC measurements [6], or a demonstration that experiments have reached conditions under which lattice QCD calculations predict a QGP state [7]. We have rather chosen to extract what we believe to be the consensus definition built up in the physics community from the past 20 years' worth of planning documents and proposals for RHIC. In this section, we collect relevant quotes concerning the QGP from a number of these documents.

A relativistic heavy-ion collider facility was first established as the highest priority for new construction by the 1983 Nuclear Science Advisory Committee (NSAC) Long Range Plan [168]. In discussing the motivation for such a facility, that document states:

> "Finally, under conditions of very elevated energy density, nuclear matter will exist in a wholly new phase in which there are no nucleons or hadrons composed of quarks in individual bags, but an extended *quark–gluon plasma*, within which the quarks are deconfined and move independently. . . . The production and detection of a quark–gluon plasma in ultra-relativistic heavy ion collisions would not only be a remarkable achievement in itself, but by enabling one to study quantum chromodynamics (QCD) over large distance scales it would enable one to study fundamental aspects of QCD and confinement unattainable in few-hadron experiments. . . . A second, chiral-symmetry restoring, transition is also expected at somewhat higher energy density, or perhaps coincident with the deconfinement transition; such a transition would be heralded by the quarks becoming effectively massless, and low mass pionic excitations no longer appearing in the excitation spectrum."

The high priority of such a collider was confirmed in the 1984–1986 National Academy of Sciences survey of Nuclear Physics [169], which stated:

> "A major scientific imperative for such an accelerator derives from one of the most striking predictions of quantum chromodynamics: that under conditions of sufficiently high temperature and density in nuclear matter, a transition will occur from excited hadronic matter to a quark–gluon plasma, in which the quarks, antiquarks and gluons of which hadrons are composed become 'deconfined' and are able to move about freely. The quark–gluon plasma is believed to have existed in the first few microseconds after the big bang, and it may exist today in the cores of neutron stars, but it has never been observed on Earth. Producing it in the laboratory will thus be a major scientific achievement, bringing together various elements of nuclear physics, particle physics, astrophysics, and cosmology."

The glossary of the above document [169] defined quark–gluon plasma in the following way:

> "An extreme state of matter in which quarks and gluons are deconfined and are free to move about in a much larger volume than that of a single hadron bag. It has never been observed on earth."

In the 1984 proposal for RHIC from Brookhaven National Laboratory [170], the QGP was described as follows:

> "The specific motivation from QCD is the belief that we can assemble macroscopic volumes of nuclear matter at such extreme thermodynamic conditions as to overcome the forces that confine constituents in normal hadrons, creating a new form of matter in an *extended confined plasma of quarks and gluons*."

The 1989 NSAC Long Range Plan [171], in reconfirming the high priority of RHIC, states:

> "The most outstanding prediction based on the theory of the strong interaction, QCD, is that the properties of matter should undergo a profound and fundamental change at an energy density only about one order of magnitude higher than that found in the center of ordinary nuclei. This change is expected to involve a transition from the confined phase of QCD, in which the degrees of freedom are the familiar nucleons and mesons and in which a quark is able to move around only inside its parent nucleon, to a new deconfined phase, called the quark–gluon plasma, in which hadrons dissolve into a plasma of quarks and gluons, which are then free to move over a large volume."

The 1994 NSAC Assessment of Nuclear Science [172] states:

> "When nuclear matter is heated to extremely high temperatures or compressed to very large densities we expect it to respond with a drastic transformation, in which the quarks and gluons, that are normally confined within individual neutrons and protons, are able to move over large distances. A new phase of matter, called quark–gluon plasma (QGP), is formed. At the same time chiral symmetry is restored making particles massless at the scale of quark masses. Quantum chromodynamics (QCD) of massless quarks is chirally (or left–right) symmetric, but in the normal world this symmetry is spontaneously broken giving dynamical masses to quarks and the particles composed of quarks."

The 1996 NSAC Long Range Plan [173] repeats the emphasis on chiral symmetry restoration in addition to deconfinement:

> "At temperatures in excess of T_c nuclear matter is predicted to consist of unconfined, nearly massless quarks and gluons, a state called the *quark–gluon plasma*. The study of deconfinement and chiral symmetry restoration is the primary motivation for the construction of the relativistic heavy ion collider (RHIC) at Brookhaven National Laboratory."

The most recent National Academy of Sciences survey of Nuclear Physics [174] puts it this way:

> "At RHIC such high energy densities will be created that the quarks and gluons are expected to become deconfined across a volume that is large compared to that of a hadron.

> By determining the conditions for deconfinement, experiments at RHIC will play a crucial role in understanding the basic nature of confinement and shed light on how QCD describes the matter of the real world. ... Although the connection between chiral symmetry and quark deconfinement is not well understood at present, chiral symmetry is expected to hold in the quark–gluon plasma."

Finally, the 2004 NuPECC (Nuclear Physics European Collaboration Committee) Long Range Plan for nuclear physics research in Europe [175] states:

> "The focus of the research in the ultra-relativistic energy regime is to study and understand how collective phenomena and macroscopic properties, involving many degrees of freedom, emerge from the microscopic laws of elementary particle-physics. ... The most striking case of a collective bulk phenomenon predicted by QCD is the occurrence of a phase transition to a deconfined chirally symmetric state, the quark gluon plasma (QGP)."

In short, every statement concerning the QGP in planning documents since the conception of RHIC has pointed to deconfinement of quarks and gluons from hadrons as the primary characteristic of the new phase. More recent definitions have tended to include chiral symmetry restoration as well. Based on the above survey, we believe that the definition used in this paper would be very widely accepted within the worldwide physics community as a "minimal" requirement for demonstrating formation of a quark–gluon plasma.

References

[1] P. Jacobs, X.N. Wang, hep-ph/0405125.
[2] D.H. Rischke, Prog. Part. Nucl. Phys. 52 (2004) 197.
[3] P.F. Kolb, U. Heinz, in: R.C. Hwa, X.N. Wang (Eds.), Quark Gluon Plasma 3, World Scientific, Singapore, 2003, nucl-th/0305084.
[4] M. Gyulassy, I. Vitev, X.N. Wang, B.W. Zhang, in: R.C. Hwa, X.N. Wang (Eds.), Quark Gluon Plasma 3, World Scientific, Singapore, 2003, nucl-th/0302077;
R. Baier, D. Schiff, B.G. Zakharov, Annu. Rev. Nucl. Part. Sci. 50 (2000) 37.
[5] B. Tomášik, U.A. Wiedemann, in: R.C. Hwa, X.N. Wang (Eds.), Quark Gluon Plasma 3, World Scientific, Singapore, 2003, hep-ph/0210250.
[6] M. Gyulassy, nucl-th/0403032.
[7] M. Gyulassy, L. McLerran, Nucl. Phys. A 750 (2005) 30.
[8] New discoveries at RHIC: the current case for the strongly interactive QGP, RIKEN-Brookhaven Research Center Scientific Articles, vol. 9, May 2004.
[9] J. Glanz, Like Particles, 2 Houses of Physics Collide, New York Times, 20 January 2004, Section F, page 1;
K. Davidson, Universe-Shaking Discovery, or More Hot Air?, San Francisco Chronicle, 19 January 2004.
[10] G. Brumfiel, What's in a name? Nature, 26 July 2004.
[11] J.W. Harris, B. Müller, Annu. Rev. Nucl. Part. Sci. 46 (1996) 71.
[12] U. Heinz, M. Jacob, nucl-th/0002042.
[13] K.H. Ackermann, et al., Nucl. Instrum. Methods A 499 (2003) 624.
[14] F. Karsch, in: Lecture Notes in Physics, vol. 583, Springer, Berlin, 2002, p. 209.
[15] O. Kaczmarek, F. Karsch, E. Laermann, M. Lütgemeier, Phys. Rev. D 62 (2000) 034021.
[16] T. Matsui, H. Satz, Phys. Lett. B 178 (1986) 416;
F. Karsch, M.T. Mehr, H. Satz, Z. Phys. C 37 (1988) 617.

[17] M. Asakawa, T. Hatsuda, Phys. Rev. Lett. 92 (2004) 012001;
S. Datta, et al., J. Phys. G 30 (2004) S1347.
[18] E. Laermann, O. Philipsen, Annu. Rev. Nucl. Part. Sci. 53 (2003) 163.
[19] Z. Fodor, S.D. Katz, JHEP 0404 (2004) 050.
[20] Z. Fodor, S.D. Katz, Phys. Lett. B 534 (2002) 87;
Z. Fodor, S.D. Katz, JHEP 0203 (2002) 014.
[21] L.D. Landau, Izv. Akad. Nauk, Ser. Fiz. 17 (1953) 51.
[22] E. Shuryak, Prog. Part. Nucl. Phys. 53 (2004) 273.
[23] R. Stock, J. Phys. G 30 (2004) S633.
[24] T. Biro, B. Müller, Phys. Lett. B 578 (2004) 78, and references therein.
[25] R. Hagedorn, Nuovo Cimento Suppl. 3 (1965) 147.
[26] H. Sorge, Phys. Lett. B 402 (1997) 251.
[27] H. Sorge, Phys. Rev. Lett. 82 (1999) 2048.
[28] S.A. Bass, A. Dumitru, Phys. Rev. C 61 (2000) 064909.
[29] D. Teaney, J. Lauret, E. Shuryak, Phys. Rev. Lett. 86 (2001) 4783, nucl-th/0110037.
[30] P.F. Kolb, J. Sollfrank, U. Heinz, Phys. Rev. C 62 (2000) 054909.
[31] H. Sorge, Phys. Rev. C 52 (1995) 3291.
[32] P. Huovinen, P.F. Kolb, U. Heinz, P.V. Ruuskanen, S.A. Voloshin, Phys. Lett. B 503 (2001) 58.
[33] H. van Hecke, H. Sorge, N. Xu, Phys. Rev. Lett. 81 (1998) 5764.
[34] N. Xu, Z. Xu, Nucl. Phys. A 715 (2003) 587c.
[35] D. Teaney, Phys. Rev. C 68 (2003) 034913.
[36] K. Morita, S. Muroya, C. Nonaka, T. Hirano, Phys. Rev. C 66 (2004) 054904, and references therein.
[37] P. Braun-Munzinger, K. Redlich, J. Stachel, in: R.C. Hwa, X.N. Wang (Eds.), Quark Gluon Plasma 3, World Scientific, Singapore, 2003, nucl-th/0304013.
[38] K. Huang, Statistical Mechanics, Wiley, 1988.
[39] E. Fermi, Prog. Theor. Phys. 5 (1950) 570.
[40] E.V. Shuryak, Phys. Lett. B 42 (1972) 357;
J. Rafelski, M. Danos, Phys. Lett. B 97 (1980) 279;
R. Hagedorn, K. Redlich, Z. Phys. C 27 (1985) 541.
[41] P. Braun-Munzinger, J. Stachel, J.P. Wessels, N. Xu, Phys. Lett. B 365 (1996) 1.
[42] V. Koch, Nucl. Phys. A 715 (2003) 108c.
[43] U. Heinz, Nucl. Phys. A 661 (1999) 140c.
[44] A.M. Poskanzer, S.A. Voloshin, Phys. Rev. C 58 (1998) 1671.
[45] G. Torrieri, J. Rafelski, Phys. Lett. B 509 (2001) 239;
Z. Xu, J. Phys. G 30 (2004) S325;
M. Bleicher, H. Stocker, J. Phys. G 30 (2004) S111.
[46] J.D. Bjorken, FERMILAB-PUB-82-59-THY and Erratum (unpublished).
[47] M. Gyulassy, P. Levai, I. Vitev, Nucl. Phys. A 661 (1999) 637;
M. Gyulassy, P. Levai, I. Vitev, Nucl. Phys. B 571 (2000) 197;
M. Gyulassy, P. Levai, I. Vitev, Phys. Rev. Lett. 85 (2000) 5535;
M. Gyulassy, P. Levai, I. Vitev, Nucl. Phys. B 594 (2001) 371.
[48] E. Wang, X.N. Wang, Phys. Rev. Lett. 87 (2001) 142301.
[49] R. Baier, Y.L. Dokshitzer, A.H. Mueller, S. Peigne, D. Schiff, Nucl. Phys. B 483 (1997) 291;
R. Baier, Y.L. Dokshitzer, A.H. Mueller, D. Schiff, Nucl. Phys. B 531 (1998) 403;
R. Baier, Y.L. Dokshitzer, A.H. Mueller, D. Schiff, Phys. Rev. C 60 (1999) 064902;
R. Baier, Y.L. Dokshitzer, A.H. Mueller, D. Schiff, JHEP 0109 (2001) 033.
[50] U.A. Wiedemann, Nucl. Phys. B 588 (2000) 303;
U.A. Wiedemann, Nucl. Phys. A 690 (2001) 731;
C.A. Salgado, U.A. Wiedemann, Phys. Rev. Lett. 89 (2002) 092303;
C.A. Salgado, U.A. Wiedemann, Phys. Rev. D 68 (2003) 014008.
[51] W. Cassing, K. Gallmeister, C. Greiner, Nucl. Phys. A 735 (2004) 277.
[52] G.R. Farrar, H. Liu, L.L. Frankfurt, M.I. Strikman, Phys. Rev. Lett. 61 (1998) 686;
S.J. Brodsky, A.H. Mueller, Phys. Lett. B 206 (1988) 685;
B.K. Jennings, G.A. Miller, Phys. Lett. B 236 (1990) 209;

B.K. Jennings, G.A. Miller, Phys. Rev. D 44 (1991) 692;
B.K. Jennings, G.A. Miller, Phys. Rev. Lett. 69 (1992) 3619;
B.K. Jennings, G.A. Miller, Phys. Lett. B 274 (1992) 442.
[53] X.N. Wang, Phys. Lett. B 579 (2004) 299.
[54] M. Djordjevic, M. Gyulassy, Phys. Lett. B 560 (2003) 37.
[55] A. Airapetian, et al., HERMES Collaboration, Eur. Phys. J. C 20 (2001) 479;
V. Muccifora, HERMES Collaboration, Nucl. Phys. A 715 (2003) 506.
[56] J.M. Moss, et al., hep-ex/0109014.
[57] X.N. Wang, X.F. Guo, Nucl. Phys. A 696 (2001) 788;
B.W. Zhang, X.N. Wang, Nucl. Phys. A 720 (2003) 429.
[58] R. Baier, Nucl. Phys. A 715 (2003) 209c.
[59] J. Breitweg, et al., Eur. Phys. J. C 7 (1999) 609.
[60] A.H. Mueller, Nucl. Phys. B 335 (1990) 115;
A.H. Mueller, Nucl. Phys. B 572 (2002) 227.
[61] L.D. McLerran, R. Venugopalan, Phys. Rev. D 49 (1994) 2233.
[62] L.D. McLerran, hep-ph/0311028.
[63] E. Iancu, R. Venugopalan, in: R.C. Hwa, X.N. Wang (Eds.), Quark Gluon Plasma 3, World Scientific, Singapore, 2003, hep-ph/0303204.
[64] V.N. Gribov, L.N. Lipatov, Sov. J. Nucl. Phys. 15 (1972) 438;
V.N. Gribov, L.N. Lipatov, Sov. J. Nucl. Phys. 15 (1972) 675;
L.N. Lipatov, Sov. J. Nucl. Phys. 20 (1975) 94;
G. Altarelli, G. Parisi, Nucl. Phys. B 126 (1977) 298;
Yu.L. Dokshitzer, Sov. Phys. JETP 46 (1977) 641.
[65] E.A. Kuraev, L.N. Lipatov, V.S. Fadin, Phys. Lett. B 60 (1975) 50;
E.A. Kuraev, L.N. Lipatov, V.S. Fadin, Sov. Phys. JETP 44 (1976) 443;
E.A. Kuraev, L.N. Lipatov, V.S. Fadin, Sov. Phys. JETP 45 (1977) 199;
L.N. Lipatov, Sov. J. Nucl. Phys. 23 (1976) 338;
Ya.Ya. Balitsky, L.N. Lipatov, Sov. J. Nucl. Phys. 28 (1978) 822;
Ya.Ya. Balitsky, L.N. Lipatov, Sov. Phys. JETP Lett. 30 (1979) 355.
[66] D. Kharzeev, M. Nardi, Phys. Lett. B 507 (2001) 121;
D. Kharzeev, E. Levin, Phys. Lett. B 523 (2001) 79.
[67] V.V. Anisovich, V.M. Shekhter, Nucl. Phys. B 55 (1973) 455;
J.D. Bjorken, G.E. Farrar, Phys. Rev. D 9 (1974) 1449;
K.P. Das, R.C. Hwa, Phys. Lett. B 68 (1977) 459;
K.P. Das, R.C. Hwa, Phys. Lett. B 73 (1978) 504, Erratum;
R.G. Roberts, R.C. Hwa, S. Matsuda, J. Phys. G 5 (1979) 1043.
[68] C. Gupt, R.K. Shivpuri, N.S. Verma, A.P. Sharma, Nuovo Cimento A 75 (1983) 408;
T. Ochiai, Prog. Theor. Phys. 75 (1986) 1184;
T.S. Biro, P. Levai, J. Zimanyi, Phys. Lett. B 347 (1995) 6;
T.S. Biro, P. Levai, J. Zimanyi, J. Phys. G 28 (2002) 1561.
[69] S.A. Voloshin, Nucl. Phys. A 715 (2003) 379c;
D. Molnar, S.A. Voloshin, Phys. Rev. Lett. 91 (2003) 092301;
R.J. Fries, B. Müller, C. Nonaka, S.A. Bass, Phys. Rev. Lett. 90 (2003) 202303;
V. Greco, C.M. Ko, P. Levai, Phys. Rev. Lett. 90 (2003) 202302;
Z.W. Lin, C.M. Ko, Phys. Rev. Lett. 89 (2002) 202302;
Z.W. Lin, D. Molnar, Phys. Rev. C 68 (2003) 044901.
[70] B. Müller, nucl-th/0404015.
[71] C. Adler, et al., STAR Collaboration, Phys. Rev. Lett. 90 (2003) 082302.
[72] R.C. Hwa, C.B. Yang, Phys. Rev. C 66 (2002) 025205;
R.C. Hwa, C.B. Yang, Phys. Rev. C 67 (2003) 034902;
R.C. Hwa, C.B. Yang, Phys. Rev. C 70 (2004) 024905.
[73] W. Reisdorf, H.G. Ritter, Annu. Rev. Nucl. Part. Sci. 47 (1997) 663.
[74] J.-Y. Ollitrault, Phys. Rev. D 46 (1992) 229.
[75] X.N. Wang, M. Gyulassy, Phys. Rev. Lett. 86 (2001) 3496.

[76] B.B. Back, et al., PHOBOS Collaboration, Phys. Rev. C 65 (2002) 061901R.
[77] J. Adams, et al., STAR Collaboration, nucl-ex/0311017.
[78] K.J. Eskola, K. Kajantie, P.V. Ruuskanen, K. Tuominen, Nucl. Phys. B 570 (2000) 379.
[79] W. Czyz, L.C. Maximon, Ann. Phys. 52 (1969) 59.
[80] B.B. Back, et al., PHOBOS Collaboration, nucl-ex/0301017.
[81] K. Adcox, et al., PHENIX Collaboration, Phys. Rev. Lett. 87 (2001) 052301.
[82] M.M. Aggarwal, et al., WA98 Collaboration, Eur. Phys. J. C 18 (2001) 651.
[83] C. Adler, et al., STAR Collaboration, Phys. Rev. C 70 (2004) 054907.
[84] J.D. Bjorken, Phys. Rev. D 27 (1983) 140.
[85] J. Adams, et al., STAR Collaboration, Phys. Rev. Lett. 92 (2004) 182301.
[86] O. Barannikova, et al., STAR Collaboration, nucl-ex/0403014.
[87] C. Adler, et al., STAR Collaboration, Phys. Rev. Lett. 89 (2002) 092301;
J. Adams, et al., STAR Collaboration, Phys. Lett. B 595 (2004) 143;
J. Adams, et al., STAR Collaboration, Phys. Rev. C 70 (2004) 041901;
J. Adams, et al., STAR Collaboration, nucl-ex/0406003.
[88] N. Xu, M. Kaneta, Nucl. Phys. A 698 (2002) 306c.
[89] R. Hagedorn, CERN-TH-3918/84.
[90] E. Schnedermann, J. Sollfrank, U. Heinz, Phys. Rev. C 48 (1993) 2462.
[91] P. Braun-Munzinger, J. Stachel, J. Wessels, N. Xu, Phys. Lett. B 344 (1995) 43;
P. Braun-Munzinger, I. Heppe, J. Stachel, Phys. Lett. B 465 (1999) 15.
[92] S.A. Bass, et al., Phys. Rev. C 60 (1999) 021902.
[93] A. Dumitru, S.A. Bass, Phys. Lett. B 460 (1999) 411.
[94] S.S. Adler, et al., PHENIX Collaboration, Phys. Rev. C 69 (2004) 034909.
[95] E. Yamamoto, et al., STAR Collaboration, Nucl. Phys. A 715 (2003) 466c.
[96] K. Schweda, et al., STAR Collaboration, J. Phys. G 30 (2004) S693.
[97] K. Adcox, et al., PHENIX Collaboration, Phys. Rev. Lett. 88 (2002) 242301.
[98] A.M. Poskanzer, S.A. Voloshin, Phys. Rev. C 58 (1998) 1671.
[99] N. Borghini, P.M. Dinh, J.Y. Ollitrault, Phys. Rev. C 64 (2001) 054901.
[100] C. Alt, et al., NA49 Collaboration, Phys. Rev. C 68 (2003) 034903.
[101] C. Adler, et al., STAR Collaboration, Phys. Rev. C 66 (2002) 034904.
[102] A. Tang, et al., STAR Collaboration, AIP Conf. Proc. 698 (2004) 701;
J. Adams, et al., STAR Collaboration, nucl-ex/0409033.
[103] G. Agakichiev, et al., CERES/NA45 Collaboration, Phys. Rev. Lett. 92 (2004) 032301.
[104] J. Adams, et al., STAR Collaboration, Phys. Rev. Lett. 92 (2004) 052302.
[105] C. Adler, et al., STAR Collaboration, Phys. Rev. Lett. 87 (2001) 182301.
[106] P. Huovinen, private communications, 2003.
[107] E. Shuryak, Prog. Part. Nucl. Phys. 53 (2004) 273.
[108] B.B. Back, et al., PHOBOS Collaboration, Phys. Rev. Lett. 89 (2002) 222301.
[109] X. Dong, S. Esumi, P. Sorensen, N. Xu, Z. Xu, Phys. Lett. B 597 (2004) 328.
[110] J. Castillo, et al., STAR Collaboration, J. Phys. G 30 (2004) S1207.
[111] S.S. Adler, et al., PHENIX Collaboration, Phys. Rev. Lett. 91 (2003) 182301.
[112] C. Nonaka, R.J. Fries, S.A. Bass, Phys. Lett. B 583 (2004) 73;
C. Nonaka, et al., Phys. Rev. C 69 (2004) 031902.
[113] For general introduction of two-particle correlation studies, see U.A. Wiedemann, U. Heinz, Phys. Rep. 319 (1999) 145;
B. Jacak, U. Heinz, Annu. Rev. Nucl. Part. Sci. 49 (1999) 529.
[114] G. Bertsch, Nucl. Phys. A 498 (1989) 173c.
[115] D. Rischke, M. Gyulassy, Nucl. Phys. A 597 (1996) 701;
D. Rischke, M. Gyulassy, Nucl. Phys. A 608 (1996) 479.
[116] C. Adler, et al., STAR Collaboration, Phys. Rev. Lett. 87 (2001) 082301;
K. Adcox, et al., PHENIX Collaboration, Phys. Rev. Lett. 88 (2002) 242301.
[117] J. Adams, et al., STAR Collaboration, Phys. Rev. Lett. 92 (2003) 062301.
[118] S. Soff, hep-ph/0202240;
D. Zschiesche, S. Schramm, H. Stocker, W. Greiner, Phys. Rev. C 65 (2001) 064902;
S. Soff, S.A. Bass, A. Dumitru, Phys. Rev. Lett. 86 (2001) 3981.

[119] U. Heinz, hep-ph/0407360.
[120] J. Adams, et al., STAR Collaboration, Phys. Rev. Lett. 91 (2003) 262302.
[121] M. Stephanov, K. Rajagopal, E. Shuryak, Phys. Rev. Lett. 81 (1998) 4816.
[122] S. Voloshin, V. Koch, H.G. Ritter, Phys. Rev. C 60 (1999) 024901.
[123] S. Jeon, V. Koch, Phys. Rev. Lett. 85 (2000) 2076.
[124] M. Asakawa, U. Heinz, B. Müller, Phys. Rev. Lett. 85 (2000) 2072.
[125] S.A. Bass, P. Danielewicz, S. Pratt, Phys. Rev. Lett. 85 (2000) 2689.
[126] Q. Liu, T. Trainor, Phys. Lett. B 567 (2003) 184.
[127] M. Gazdzicki, St. Mrówczyński, Z. Phys. C 54 (1999) 127.
[128] D. Adamava, et al., CERES Collaboration, Nucl. Phys. A 727 (2003) 97.
[129] S.S. Adler, et al., PHENIX Collaboration, Phys. Rev. Lett. 93 (2004) 092301.
[130] G. Westfall, et al., STAR Collaboration, J. Phys. G 30 (2004) S1389.
[131] J. Adams, et al., STAR Collaboration, nucl-ex/0411003;
T.A. Trainor, et al., STAR Collaboration, hep-ph/0406116.
[132] I. Bearden, et al., NA44 Collaboration, Phys. Rev. C 65 (2002) 044903.
[133] J. Adams, et al., STAR Collaboration, Phys. Rev. C 71 (2005) 031901(R).
[134] J. Adams, et al., STAR Collaboration, Phys. Rev. Lett. 90 (2003) 172301.
[135] X.N. Wang, M. Gyulassy, Phys. Rev. D 44 (1991) 3501;
X.N. Wang, M. Gyulassy, Comput. Phys. Commun. 83 (1994) 307.
[136] C. Adler, et al., STAR Collaboration, Phys. Rev. Lett. 89 (2002) 202301.
[137] I. Arsene, et al., BRAHMS Collaboration, Phys. Rev. Lett. 91 (2003) 072305.
[138] S.S. Adler, et al., PHENIX Collaboration, Phys. Rev. Lett. 91 (2003) 072303.
[139] B.B. Back, et al., PHOBOS Collaboration, Phys. Rev. Lett. 91 (2003) 072302.
[140] J. Adams, et al., STAR Collaboration, Phys. Rev. Lett. 91 (2003) 072304.
[141] D. Antreasyan, et al., Phys. Rev. D 19 (1979) 764.
[142] X.N. Wang, Phys. Rep. 280 (1997) 287;
M. Lev, B. Petersson, Z. Phys. C 21 (1987) 155;
T. Ochiai, et al., Prog. Theor. Phys. 75 (1986) 288.
[143] J. Adams, et al., STAR Collaboration, Phys. Rev. Lett. 93 (2004) 252301.
[144] D. Hardtke, et al., STAR Collaboration, Nucl. Phys. A 715 (2003) 272.
[145] F. Wang, et al., STAR Collaboration, J. Phys. G. 30 (2004) S1299;
J. Adams, et al., STAR Collaboration, nucl-ex/0501016.
[146] X.N. Wang, Phys. Lett. B 595 (2004) 165.
[147] I. Vitev, M. Gyulassy, Phys. Rev. Lett. 89 (2002) 252301.
[148] K.J. Eskola, H. Honkanen, C.A. Salgado, U.A. Wiedemann, Nucl. Phys. A 747 (2005) 511.
[149] D. Kharzeev, E. Levin, L. McLerran, Phys. Lett. B 561 (2003) 93.
[150] J. Adams, et al., STAR Collaboration, Phys. Rev. Lett. 91 (2003) 172302.
[151] T. Falter, U. Mosel, Phys. Rev. C 66 (2002) 024608.
[152] K. Gallmeister, C. Greiner, Z. Xu, Phys. Rev. C 67 (2003) 044905.
[153] B.B. Back, et al., PHOBOS Collaboration, Phys. Rev. Lett. 88 (2002) 022302.
[154] I. Arsene, et al., BRAHMS Collaboration, Phys. Rev. Lett. 93 (2004) 242303.
[155] V. Guzey, M. Strikman, W. Vogelsang, Phys. Lett. B 603 (2004) 173.
[156] D. Kharzeev, Y.V. Kovchegov, K. Tuchin, Phys Lett. B 599 (2004) 23.
[157] A.D. Frawley, et al., PHENIX Collaboration, J. Phys. G 30 (2004) S675.
[158] J. Adams, et al., STAR Collaboration, Phys. Rev. C 70 (2004) 064907.
[159] D. Kharzeev, Y.V. Kovchegov, K. Tuchin, Phys. Rev. D 68 (2003) 094013.
[160] D. Kharzeev, E. Levin, L. McLerran, hep-ph/0403271.
[161] R. Vogt, hep-ph/0405060.
[162] A. Ogawa, et al., STAR Collaboration, nucl-ex/0408004.
[163] M.M. Aggarwal, et al., WA98 Collaboration, Phys. Rev. Lett. 81 (1998) 4087;
M.M. Aggarwal, et al., WA98 Collaboration, Phys. Rev. Lett. 84 (2000) 578;
M.M. Aggarwal, et al., WA98 Collaboration, Eur. Phys. J. C 23 (2002) 225.
[164] D. d'Enterria, J. Phys. G 30 (2004) S767.
[165] D.H. Rischke, M. Gyulassy, Nucl. Phys. A 608 (1996) 479.

[166] J. Adams, et al., STAR Collaboration, nucl-ex/0411036.
[167] D. Kharzeev, et al., Phys. Rev. Lett. 81 (1998) 512;
D. Kharzeev, hep-ph/0406125.
[168] A Long Range Plan for Nuclear Science, NSAC Report, 1983.
[169] J. Cerny, et al., Physics Through the 1990s: Nuclear Physics, National Academy Press, Washington, DC, 1986.
[170] RHIC and Quark Matter: Proposal for a relativistic heavy ion collider at Brookhaven National Laboratory, BNL Report 51801, August 1984.
[171] Nuclei, Nucleons, Quarks: Nuclear Science in the 1990's, NSAC Long Range Plan Report, December 1989.
[172] Nuclear Science: Assessment and Promise, NSAC Report, May 1994.
[173] Nuclear Science: A Long Range Plan, NSAC Report, February 1996.
[174] J.P. Schiffer, et al., Nuclear Physics: The Core of Matter, The Fuel of Stars, National Academy Press, Washington, DC, 1999.
[175] M. Harakeh, et al. (Eds.), NuPECC Long Range Plan 2004: Perspectives for Nuclear Physics Research in Europe in the Coming Decade and Beyond, April 2004.

5.1.2 Citations

1. Demir, N; Bass, SA *Shear-Viscosity to Entropy-Density Ratio of a Relativistic Hadron Gas* Physical Review Letters, 102 (17): Art. No. 172302 MAY 1 2009.
2. Nouicer, R; Akiba, Y; Bennett, R ; Boyle, K; Cianciolo, V ; Deshpande, A; Dion, A; Eggleston, M; Enokizono, A; Kaneti, S; Mannel, EJ; Oglvie, C; Pei, H ; Sukhanov, A; Taneja, S; Togawa, M; ***PHENIX-VTX Collaboration*** *Status and Performance of New Silicon Stripixel Detector for the PHENIX Experiment at RHIC: Beta Source, Cosmic-rays and Proton Beam at 120 GeV* Journal of Instrumentation, **4**: Art. No. P04011 APR 2009.
3. Chandra, V; Ranjan, A; Ravishankar, V *On the chromo-electric permittivity and Debye screening in hot QCD* European Physical Journal **A40** (1): 109-117 APR 2009.
4. Mao, YX; Zhou, DC; Xu, CC; Yin, ZB *Study of the photon identification efficiency with ALICE photon spectrometer* Chinese Physics **C32** (7): 543-547 JUL 2008.
5. Dominguez, F; Marquet, C; Wu, B *On multiple scatterings of mesons in hot and cold QCD matter* Nuclear Physics **A823**: 99-119 MAY 15 2009.
6. Fadafan, KB *R-2 curvature-squared corrections on drag force* Journal of High Energy Physics, (12): Art. No. 051 DEC 2008.
7. Zapp, K; Ingelman, G; Rathsman, J; Stachel, J; Wiedemann, UA *A Monte Carlo model for 'jet quenching'* European Physical Journal **C60** (4): 617-632 APR 2009.
8. Bass, SA *Modeling of relativistic heavy-ion collisions with 3+1d hydrodynamic and hybrid models* Acta Physica Polonica **B40** (4): 951-961 APR 2009.
9. Kunihiro, T ; Muller, B ; Ohnishi, A; Schafer, A *Towards a Theory of Entropy Production in the Little and Big Bang* Progress of Theoretical Physics, 121 (3): 555-575 MAR 2009.
10. Xu, MM ; Yu, ML ; Liu, LS *Mechanism of crossover between hadron gas and QGP and the liquid property of sQGP* Nuclear Physics **A820**: 131C-134C APR 1 2009.
11. Lokhtin, IP; Malinina, LV; Petrushanko, SV; Snigirev, AM; Arsene, I; Tywoniuk, K *Heavy ion event generator HYDJET plus plus (HYDrodynamics plus JETs)* Computer Physics Communications, **180** (5): 779-799 MAY 2009.
12. Luo, XF; Shao, M; Li, C ; Chen, HF *Signature of QCD critical point: Anomalous transverse velocity dependence of antiproton-proton ratio* Physics Letters **B673** (4-5): 268-271 MAR 30 2009.
13. York, MA; Moore, GD *Second order hydrodynamic coefficients from kinetic theory* Physical Review **D79** (5): Art. No. 054011 MAR 2009.
14. Fries, RJ ; Muller, B ; Schafer, A *Decoherence and entropy production in relativistic nuclear collisions* Physical Review **C79** (3): Art. No. 034904 MAR 2009.
15. Zborovsky, I *New properties of z-scaling: flavor independence and saturation at low z* International Journal of Modern Physics **A24** (7): 1417-1442 MAR 20 2009.
16. Zschocke, S; Csernai, LP *Pion mass shift and the kinetic freeze-out process* European Physical Journal **A39** (3): 349-363 MAR 2009.
17. Roy, P; Mohanty, B; Balchandran, AP; Bhattacharyya, A; Chaudhuri, AK; Datta, S; Digal, S; Flueret, F; Gupta, S; Jaikumar, P; Lee, SH; Mathur, N; Mishra, A; Mishra, AP; Mishra, H; Mohanty, B; Roy, P; Somia, PS; Srivastava, AM *Working group report: Quark gluon plasma* Pramana-Journal of Physics, **72** (1): 285-294 JAN 2009.
18. Song, J ; Shao, FL; Xie, QB *The influence of net quarks on yields and rapidity spectra of identified hadrons* International Journal of Modern Physics **A24** (6): 1161-1174 MAR 10 2009.
19. Crater, HW; Yoon, JH; Wong, CY *Singularity structures in Coulomb-type potentials in two-body Dirac equations of constraint dynamics* Physical Review **D79** (3): Art. No. 034011 FEB 2009.
20. Springer, T *Sound mode hydrodynamics from bulk scalar fields* Physical Review **D79** (4): Art. No. 046003 FEB 2009.
21. Bass, SA; Gale, C; Majumder, A; Nonaka, C; Qin, GY; Renk, T; Ruppert, J *Systematic comparison of jet energy-loss schemes in a realistic hydrodynamic medium* Physical Review **C79** (2): Art. No. 024901 FEB 2009.

22. Luzum, M; Miller, GA *Elliptic flow from final state interactions in the distorted-wave emission-function model* Physical Review **C79** (2): Art. No. 024902 FEB 2009.
23. Cassing, W *From Kadanoff-Baym dynamics to off-shell parton transport* European Physical Journal-Special Topics, 168: 3-87 FEB 2009.
24. Chaudhuri, AK *Multiplicity, mean p(T), p(T)-spectra and elliptic flow of identified particles in Pb plus Pb collisions at LHC* Physics Letters **B672** (2): 126-131 FEB 16 2009.
25. Okorokov, VA *Azimuthal anisotropy and formation of an extreme state of strongly interacting matter at the relativistic heavy-ion collider (RHIC)* Physics Of Atomic Nuclei, 72 (1): 147-160 JAN 2009.
26. Kokoulina, ES; Kutov, AY; Ryadovikov, VN *High-energy interactions in the region of extreme multiplicities* Physics of Atomic Nuclei, 72 (1): 189-193 JAN 2009.
27. Chandra, V; Ravishankar, V *Viscosity and thermodynamic properties of QGP in relativistic heavy-ion collisions* European Physical Journal **C59** (3): 705-714 FEB 2009.
28. Krieg, D; Bleicher, M *Negative elliptic flow of J/psi's: A qualitative signature for charm collectivity at RHIC* European Physical Journal **A39** (1): 1-4 JAN 2009.
29. Meyer, HB *Density, short-range order, and the quark-gluon plasma* Physical Review **D79** (1): Art. No. 011502 JAN 2009.
30. Oli, S *String Cosmological Models in Five-Dimensional Spacetimes* Chinese Physics Letters, 26 (1): Art. No. 010404 JAN 2009.
31. Wong, CY *Momentum kick model description of the near-side ridge and jet quenching* Physical Review **C78** (6): Art. No. 064905 DEC 2008.
32. Baier, R; Mehtar-Tani, Y *Jet quenching and broadening: The transport coefficient (q)over-cap in an anisotropic plasma* Physical Review **C78** (6): Art. No. 064906 DEC 2008.
33. Klebanov, IR; Maldacena, JM *Solving quantum field theories via curved spacetimes* Physics Today **62** (1): 28-33 JAN 2009.
34. Korotkikh, VL; Lokhtin, IP; Petrushanko, SV; Sarycheva, LI; Snigirev, AM; Eyyubova, GK *Elliptic flow of particles in heavy-ion collisions and possibility of its observation at the LHC energies* Physics of Atomic Nuclei, 71 (12): 2142-2151 DEC 2008.
35. Kopeliovich, BZ ; Rezaeian, AH ; Schmidt, I *Azimuthal asymmetry of pions in pp and pA collisions* Physical Review **D78** (11): Art. No. 114009 DEC 2008.
36. Li, BC; Huang, M *Nonconformality and nonperfectness of fluid near phase transition in lattice QCD* Physical Review **D78** (11): Art. No. 117503 DEC 2008.
37. Wang, MJ; Liu, LS; Wu, YF *Trace initial interaction from final state observable in relativistic heavy ion collisions* Chinese Physics **C33** (1): 36-41 JAN 2009.
38. Adhav, KS; Nimkar, AS; Raut, VB; Thakare, RS *Strange quark matter attached to string cloud in Bianchi type-III space time* Astrophysics and Space Science, 319 (1): 81-84 JAN 2009.
39. Iancu, E *Partons and jets in a strongly-coupled plasma from ADS/CFT* Acta Physica Polonica **B39** (12): 3213-3280 DEC 2008.
40. Torrieri, G; Betz, B; Noronha, J; Gyulassy, M *Mach cones in heavy ion collisions* Acta Physica Polonica **B39** (12): 3281-3307 DEC 2008.
41. Ma, G; Zhang, S; Ma, Y; Cai, X; Chen, J; Zhong, C *Longitudinal broadening of near-side jets due to parton cascade* European Physical Journal **C57** (3): 589-593 OCT 2008.
42. Chen, JW; Huang, M; Li, YH; Nakano, E; Yang, DL *Phase transitions and perfectness of fluids in weakly coupled real scalar field theories* Physics Letters **B670** (1): 18-21 DEC 4 2008.
43. Hubner, K; Karsch, F; Pica, C *Correlation functions of the energy-momentum tensor in SU(2) gauge theory at finite temperature* Physical Review **D78** (9): Art. No. 094501 NOV 2008.
44. Liu, GH; Yan, TZ; Ma, YG; Cai, XZ; Fang, DQ; Shen, WQ; Tian, WD; Wang, HW; Wang, K *Anisotropic flows of nuclear clusters and hard photon in intermediate energy heavy ion collisions* International Journal of Modern Physics E-Nuclear Physics, 17 (9): 1850-1864 OCT 2008.
45. Csanad, M; Csorgo, T; Ster, A; Lorstad, B; Ajitanand, NN; Alexander, JM; Chung, P; Holzmann, WG; Issah, M; Lacey, *Universal scaling of the elliptic flow data at RHIC* European Physical Journal **A38** (3): 363-368 DEC 2008.
46. Krieg, D; Bleicher, M *Decreasing elliptic flow at the CERN Large Hadron Collider: Calculations in a parton recombination approach* Physical Review **C78** (5): Art. No. 054903 NOV 2008.
47. Hauer, M; Begun, VV; Gorenstein, MI *Multiplicity distributions in canonical and microcanonical statistical ensembles* European Physical Journal **C58** (1): 83-110 NOV 2008.

48. Pang, Y *Transverse momentum broadening of heavy quark and gluon energy loss in Sakai-Sugimoto model* Journal of High Energy Physics, (10): Art. No. 041 OCT 2008.
49. Fries, R; Greco, V; Sorensen, P *Coalescence Models for Hadron Formation from Quark-Gluon Plasma* Annual Review of Nuclear and Particle Science, 58: 177-205 2008.
50. Brodsky, SJ; Sickles, A *The baryon anomaly: Evidence for color transparency and direct hadron production at RHIC* Physics Letters **B668** (2): 111-115 OCT 2 2008.
51. Petersen, H; Steinheimer, J; Burau, G; Bleicher, M; Stocker, H *Fully integrated transport approach to heavy ion reactions with an intermediate hydrodynamic stage* Physical Review **C78** (4): Art. No. 044901 OCT 2008.
52. Chiu, CB; Hwa, RC; Yang, CB *Azimuthal anisotropy: Ridges, recombination, and breaking of quark number scaling* Physical Review **C78** (4): Art. No. 044903 OCT 2008.
53. Levy, LAL; Nagle, JL; Rosen, C; Steinberg, P *Quasiparticle degrees of freedom versus the perfect fluid as descriptors of the quark-gluon plasma* Physical Review **C78** (4): Art. No. 044905 OCT 2008.
54. Albacete, JL *Particle multiplicities in nuclear collisions at the LHC from saturation physics* Journal of Physics G-Nuclear And Particle Physics, 35 (12): Art. No. 125110 DEC 2008.
55. Akiba, Y *Experimental Study of Dense Matter at RHIC* Progress of Theoretical Physics Supplement, (174): 88-102 2008.
56. Muller, B *Theoretical Challenges Posed by the Data from RHIC* Progress of Theoretical Physics Supplement, (174): 103-121 2008.
57. Chen, JW *Phase Transitions and the Perfectness of Fluids* Progress of Theoretical Physics Supplement, (174): 145-152 2008.
58. Linnyk, O; Bratkovskaya, EL; Cassing, W Open and hidden charm in proton-nucleus and heavy-ion collisions International Journal of Modern Physics E-Nuclear Physics, 17 (8): 1367-1439 SEP 2008.
59. Troshin, SM; Tyurin, NE *Directed flow as an effect of transient matter rotation in hadron and nucleus collisions* International Journal of Modern Physics E-Nuclear Physics, 17 (8): 1619-1633 SEP 2008,
60. Gavai, RV; Gupta, S; Mukherjee, S *Lattice quantum chromodynamics equation of state: A better differential method* Pramana-Journal of Physics, 71 (3): 487-508 SEP 2008.
61. Moore, GD; Saremi, O *Bulk viscosity and spectral functions in QCD* Journal of High Energy Physics, (9): Art. No. 015 SEP 2008.
62. Luo, XF; Shao, M; Dong, X; Li, C *Nuclear stopping and sideward-flow correlation from 0.35A to 200A GeV* Physical Review **C78** (3): Art. No. 031901 SEP 2008.
63. Akkelin, SV; Hama, Y; Karpenko, IA; Sinyukov, YM *Hydro-kinetic approach to relativistic heavy ion collisions* Physical Review **C78** (3): Art. No. 034906 SEP 2008.
64. Chen, JH; Jin, F; Gangadharan, D; Cai, XZ; Huang, HZ; Ma, YG *Parton distributions at hadronization from bulk dense matter produced in Au plus Au collisions at root sNN=200 GeV* Physical Review **C78** (3): Art. No. 034907 SEP 2008.
65. Fries, RJ; Muller, B; Schafer, A *Stress tensor and bulk viscosity in relativistic nuclear collisions* Physical Review **C78** (3): Art. No. 034913 SEP 2008.
66. Alt, C *et al.* NA49 Collaboration *Energy dependence of multiplicity fluctuations in heavy ion collisions at 20A to 158A GeV* Physical Review **C78** (3): Art. No. 034914 SEP 2008.
67. Luzum, M; Romatschke, P *Conformal relativistic viscous hydrodynamics: Applications to RHIC results at root sNN=200 GeV* Physical Review **C78** (3): Art. No. 034915 SEP 2008.
68. Cassing, W; Bratkovskaya, EL *Parton transport and hadronization from the dynamical quasiparticle point of view* Physical Review **C78** (3): Art. No. 034919 SEP 2008.
69. Filip, P *Elliptic flow in central collisions of deformed nuclei* Physics of Atomic Nuclei, **71** (9): 1609-1618 SEP 2008.
70. Song, HC; Heinz, U *Multiplicity scaling in ideal and viscous hydrodynamics* Physical Review **C78** (2): Art. No. 024902 AUG 2008.
71. Noronha, J; Torrieri, G; Gyulassy, M *Near-zone Navier-Stokes analysis of heavy quark jet quenching in an N=4 super-Yang-Mills plasma* Physical Review **C78** (2): Art. No. 024903 AUG 2008.
72. Ullrich, T *The emerging QCD frontier: the electron-ion collider* Journal of Physics G-Nuclear and Particle Physics, 35 (10): Art. No. 104041 OCT 2008.

73. Noronha, J ; Gyulassy, M ; Torrieri, G *Near zone hydrodynamics of AdS/CFT jet wakes* Journal of Physics G-Nuclear and Particle Physics, 35 (10): Art. No. 104061 OCT 2008.
74. Sahu, PK ; Dash, S ; Mishra, DK ; Phatak, SC *Characterizing jets in heavy-ion collisions by a flow method* Journal of Physics G-Nuclear and Particle Physics, 35 (10): Art. No. 104068 OCT 2008.
75. Averbeck, R *et al.* PHENIX Collaboration *The viscosity to entropy density ratio from PHENIX data on single electron production* Journal of Physics G-Nuclear and Particle Physics, 35 (10): Art. No. 104115 OCT 2008.
76. Hirano, T ; Heinz, U ; Kharzeev, D ; Lacey, R ; Nara, Y *Hadronic dissipative effects on transverse dynamics at RHIC* Journal Of Physics G-Nuclear And Particle Physics, 35 (10): Art. No. 104124 OCT 2008.
77. Bazavov, A ; Berg, BA ; Dumitru, A *Thermalization in SU(3) gauge theory after a deconfining quench* Physical Review **D78** (3): Art. No. 034024 AUG 2008.
78. Liu, H ; Rajagopal, K ; Shi, YM *Robustness and infrared sensitivity of various observables in the application of AdS/CFT to heavy ion collisions* Journal of High Energy Physics, (8): Art. No. 048 AUG 2008.
79. Meyer, HB *Energy-momentum tensor correlators and spectral functions* Journal of High Energy Physics, (8): Art. No. 31 AUG 2008.
80. Grumiller, D ; Romatschke, P *On the collision of two shock waves in AdS(5)* Journal of High Energy Physics, (8): Art. No. 27 AUG 2008.
81. Matsui, T ; Matsuo, M *Quantized meson fields in and out of equilibrium. I: Kinetics of meson condensate and quasi-particle excitations* Nuclear Physics **A809** (3-4): 211-245 SEP 1 2008.
82. Harada, M ; Nemoto, Y *Quasifermion spectrum at finite temperature from coupled Schwinger-Dyson equations for a fermion-boson system* Physical Review **D78** (1): Art. No. 014004 JUL 2008.
83. Dremin, IM ; Eyyubova, GK ; Korotkikh, VL ; Sarycheva, LI *Two-dimensional discrete wavelet analysis of multiparticle event topology in heavy-ion collisions* Journal Of Physics G-Nuclear And Particle Physics, 35 (9): Art. No. 095106 SEP 2008.
84. Huovinen, P *Chemical freeze-out temperature in the hydrodynamical description of Au+Au collisions at root S-NN=200 GeV* European Physical Journal **A37** (1): 121-128 JUL 2008.
85. Giacomelli, G *Hadron-nuclei collisions at high energies* Romanian Reports in Physics, 60 (2): 193-204 2008.
86. Domdey, S ; Ingelman, G ; Pirner, HJ ; Rathsman, J ; Stachel, J ; Zapp, K *QCD evolution of jets in the quark-gluon plasma* Nuclear Physics **A808**: 178-191 AUG 1 2008.
87. Torrieri, G ; Tomasik, B ; Mishustin, I *Freeze-out by bulk viscosity driven instabilities* Acta Physica Polonica **B39** (7): 1733-1744 JUL 2008.
88. Frawley, AD ; Ullrich, T ; Vogt, R *Heavy flavor in heavy-ion collisions at RHIC and RHIC II* Physics Reports-Review Section of Physics Letters, 462 (4-6): 125-175 JUN 2008.
89. David, G ; Rapp, R ; Xu, Z *Electromagnetic probes at RHIC-II* Physics Reports-Review Section of Physics Letters, 462 (4-6): 176-217 JUN 2008.
90. Covlea, V ; Jipa, A ; Besliu, C ; Calin, M ; Esanu, T ; Pavel, V ; Iliescu, B ; Argintaru, D ; Zgura, IS ; Stan, E ; Mitu, C ; Potlog, M ; Cherciu, M ; Sevcenco, A ; Scurtu, A *Some possible analogies in the description of the "classical" plasma and quark-gluon plasma* Journal of Optoelectronics and Advanced Materials, 10 (8): 1958-1963 AUG 2008.
91. Fukutome, T; Iwasaki, M *Effect of soft mode on shear viscosity of quark matter* Progress Of Theoretical Physics, 119 (6): 991-1004 JUN 2008.
92. Kang, ZB ; Qiu, JW *Transverse momentum broadening of vector boson production in high energy nuclear collisions* Physical Review **D77** (11): Art. No. 114027 JUN 2008.
93. Noronha-Hostler, J ; Greiner, C ; Shovkovy, IA *Fast equilibration of hadrons in an expanding fireball* Physical Review Letters, 100 (25): Art. No. 252301 JUN 27 2008.
94. Nakazato, K ; Sumiyoshi, K ; Yamada, S *Astrophysical implications of equation of state for hadron-quark mixed phase: Compact stars and stellar collapses* Source: Physical Review **D77** (10): Art. No. 103006 MAY 2008.
95. Morita, K ; Lee, SH *Critical behavior of charmonia across the phase transition: A QCD sum rule approach* Physical Review **C77** (6): Art. No. 064904 JUN 2008

96. Alt, C *et al.* NA49 Collaboration *Bose-Einstein correlations of pi(-)pi(-) pairs in central Pb+Pb collisions at 20A, 30A, 40A, 80A, and 158A GeV* Physical Review **C77** (6): Art. No. 064908 JUN 2008.
97. Majumder, A ; Fries, RJ ; Muller, B *Photon bremsstrahlung and diffusive broadening of a hard jet* Physical Review **C77** (6): Art. No. 065209 JUN 2008.
98. Chernicoff, M ; Guijosa, A *Acceleration, energy loss and screening in strongly-coupled gauge theories* Journal of High Energy Physics, (6): Art. No. 005 JUN 2008.
99. Li, QF ; Bleicher, M ; Stoker, H *Transport model study of the m(T)-scaling for Lambda, K, and pi HBT-correlations* Physics Letters **B663** (5): 395-399 JUN 5 2008.
100. Fries, RJ Quark and gluon degrees of freedom in high-energy heavy ion collisions Source: NUCLEAR PHYSICS **A805**: 242C-249C JUN 1 2008.
101. Wiedemann, UA *What can be the role of AdS/CFT in the phenomenology of heavy ion collisions?* Nuclear Physics **A805**: 274C-282C JUN 1 2008.
102. Zajc, WA *The fluid nature of quark-gluon plasma* Nuclear Physics **A805**: 283C-294C JUN 1 2008.
103. Cuautle, E ; Paic, G *Radial flow afterburner for event generators and the baryon puzzle* Journal of Physics G-Nuclear And Particle Physics, 35 (7): Art. No. 075103 JUL 2008.
104. Liu, W ; Fries, RJ *Probing nuclear matter with jet conversions* Physical Review **C77** (5): Art. No. 054902 MAY 2008.
105. Majumder, A ; Muller, B *Higher twist jet broadening and classical propagation* Physical Review **C77** (5): Art. No. 054903 MAY 2008.
106. Loganayagam, R *Entropy current in conformal hydrodynamics* Journal of High Energy Physics, (5): Art. No. 087 MAY 2008.
107. Buchel, A *Bulk viscosity of gauge theory plasma at strong coupling* Physics Letters **B663** (3): 286-289 MAY 22 2008.
108. Adhav, KS ; Nimkar, AS ; Dawande, MV *String cloud and domain walls with quark matter in n-dimensional Kaluza-Klein cosmological model* International Journal of Theoretical Physics, 47 (7): 2002-2010 JUL 2008.
109. Tannenbaum, MJ *Heavy ion physics at RHIC* International Journal of Modern Physics E-Nuclear Physics, **17** (5): 771-801 MAY 2008.
110. Gelis, F *Some aspects of ultra-relativistic heavy ion collisions* Acta Physica Polonica **B**: 395-402 Suppl. 2 2008.
111. Chaudhuri, AK *J/psi suppression in the threshold model at RHIC and LHC energy* Journal of Physics G-Nuclear And Particle Physics, **35** (6): Art. No. 065105 JUN 2008.
112. Ejaz, QJ ; Faulkner, T ; Liu, H ; Rajagopal, K *A limiting velocity for quarkonium propagation in a strongly coupled plasma via AdS/CFT* Journal of High Energy Physics, (4): Art. No. 089 APR 2008.
113. Sapeta, S ; Wiedemann, UA *Jet hadrochemistry as a characteristic of jet quenching* European Physical Journal **C55** (2): 293-302 MAY 2008.
114. Abuki, H ; Ciminale, M ; Gatto, R ; Nardulli, G ; Ruggieri, M *Enforced neutrality and color-flavor unlocking in the three-flavor Polyakov-loop Nambu-Jona-Lasinio model* Physical Review **D77** (7): Art. No. 074018 APR 2008.
115. Gubser, SS *Heavy ion collisions and black hole dynamics* International Journal Of Modern Physics **D17** (3-4): 673-678 MAR-APR 2008.
116. Hirano, T ; Heinz, U ; Kharzeev, D ; Lacey, R (Lacey, Roy); Nara, Y *Mass ordering of differential elliptic flow and its violation for phi mesons* Physical Review **C77** (4): Art. No. 044909 APR 2008.
117. Demchik, VI ; Skalozub, VV *The spontaneous generation of magnetic fields at hightemperature in SU(2)-gluodynamics on a lattice* Problems of Atomic Science and Technology, (3): 111-115 Part 1 2007.
118. Zhu, X ; Xu, N; Zhuang, P *Effect of partonic "Wind" on charm quark correlations in high-energy nuclear collisions* Physical Review Letters, **100** (15): Art. No. 152301 APR 18 2008.
119. Trainor, TA *The RHIC azimuth quadrupole: "Perfect liquid" or gluonic radiation?* Modern Physics Letters **A23** (8): 569-589 MAR 14 2008.
120. Pruneau, CA ; Gavin, S ; Voloshin, SA *Transverse radial flow effects on two- and three-particle angular correlations* Nuclear Physics **A802**: 107-121 APR 1 2008.

121. David, G *Recent results on jet energy loss and direct photons at RHIC* European Physical Journal-Special Topics, **155**: 27-36 MAR 2008.
122. Noronha-Hostler, J ; Greiner, C ; Shovkovy, I *Chemical equilibration of baryons in an expanding fireball* European Physical Journal-Special Topics, **155**: 61-66 MAR 2008.
123. Heinz, U ; Kestin, G *Jozso's Legacy: Chemical and kinetic freeze-out in heavy-ion collisions* European Physical Journal-Special Topics, **155**: 75-87 MAR 2008.
124. Petreczky, P *Properties of quark gluon plasma from lattice calculations* European Physical Journal-Special Topics, **155**: 123-130 MAR 2008.
125. Schulze, R ; Bluhm, M ; Kampfer, B *Plasmons, plasminos and Landau damping in a quasiparticle model of the quark-gluon plasma* European Physical Journal-Special Topics, **155**: 177-190 MAR 2008.
126. Armesto, N ; Cunqueiro, L ; Salgado, CA ; Xiang, WC *Medium-evolved fragmentation functions* Journal of High Energy Physics, (2): Art. No. 048 FEB 2008.
127. Mannarelli, M ; Manuel, C *Jet-induced gauge field instabilities in the quark-gluon plasma: A kinetic theory approach* Physical Review **D77** (5): Art. No. 054018 MAR 2008.
128. Wang, YP ; Zhou, DM ; Huang, RD ; Cai, X *Collision geometry and particle production in high energy heavy ion collision experiments* Chinese Physics **C32** (4): 308-328 APR 2008.
129. Liu, QJ ; Zhao, WQ *Elastic parton scattering and nonstatistical event-by-event mean-p(t) fluctuations in Au plus Au collisions at root s(NN)=130 and 200 GeV* Physical Review **C77** (3): Art. No. 034902 MAR 2008.
130. Dusling, K ; Teaney, D *Simulating elliptic flow with viscous hydrodynamics* Physical Review **C77** (3): Art. No. 034905 MAR 2008.
131. Biro, TS ; Urmossy, K ; Barnafoldi, GG *Pion and kaon spectra from distributed mass quark matter* Journal of Physics G-Nuclear And Particle Physics, **35** (4): Art. No. 044012 APR 2008.
132. Stephans, GSF *Exploring the QCD phase diagram with low energy beams at RHIC: critRHIC* Journal of Physics G-Nuclear And Particle Physics, **35** (4): Art. No. 044050 APR 2008.
133. Antinori, F *Strangeness, charm and beauty in quark matter: SQM 2007 experimental overview* Journal of Physics G-Nuclear And Particle Physics, **35** (4): Art. No. 044055 APR 2008.
134. Jin, F ; Ma, YG ; Ma, GL ; Chen, JH ; Zhang, S ; Cai, XZ ; Huang, HZ ; Tian, J ; Zhong, C ; Zuo, JX *Baryon-strangeness correlations in parton/hadron transport model for Au+Au collisions at root s(NN)=200 GeV* Journal of Physics G-Nuclear And Particle Physics, **35** (4): Art. No. 044070 APR 2008.
135. Chen, J *Directed flow of identified particles from Au plus Au collisions at RHIC* Journal of Physics G-Nuclear And Particle Physics, **35** (4): Art. No. 044072 APR 2008.
136. Kitazawa, M ; Kunihiro, T ; Mitsutani, K ; Nemoto, Y *Spectral properties of massless and massive quarks coupled with massive boson at finite temperature* Physical Review **D77** (4): Art. No. 045034 FEB 2008.
137. Benincasa, P ; Buchel, A ; Heller, MP ; Janik, RA *Supergravity description of boost invariant conformal plasma at strong coupling* Physical Review **D77** (4): Art. No. 046006 FEB 2008.
138. Xu, MM ; Yu, ML ; Lianshou, L *Examining the crossover from the hadronic to partonic phase in QCD* Physical Review Letters, **100** (9): Art. No. 092301 MAR 7 2008.
139. Zhang, BW ; Ko, CM (Ko, Che Ming); Liu, W *Thermal charm production in a quark-gluon plasma in Pb-Pb collisions at root S-NN=5.5 TeV* Physical Review **C77** (2): Art. No. 024901 FEB 2008.
140. Pratt, S *Formulating viscous hydrodynamics for large velocity gradients* Physical Review **C77** (2): Art. No. 024910 FEB 2008.
141. Harada, M ; Nemoto, Y ; Yoshimoto, S *Quasi-quark spectrum in the chiral symmetric phase from the Schwinger-Dyson equation* Progress of Theoretical Physics, **119** (1): 117-137 JAN 2008.
142. Caron-Huot, S ; Moore, GD *Heavy quark diffusion in perturbative QCD at next-to-leading order* Physical Review Letters, **100** (5): Art. No. 052301 FEB 8 2008.
143. Min, DP ; Kochelev, N *Glueball-induced partonic energy loss in quark-gluon plasma* Physical Review **C77** (1): Art. No. 014901 JAN 2008.
144. Alver, B *et al.* PHOBOS Collaboration *Importance of correlations and fluctuations on the initial source eccentricity in high-energy nucleus-nucleus collisions* Physical Review **C77** (1): Art. No. 014906 JAN 2008.

145. Conesa, G; Delagrange, H ; Diaz, J; Kharlov, YV ; Schutz, Y *Identification of photon-tagged jets in the ALICE experiment* Nuclear Instruments & Methods in Physics Research Section A-Accelerators Spectrometers Detectors And Associated Equipment, **585** (1-2): 28-39 JAN 21 2008.
146. Hong, B *Response of charged hadrons to a coulomb potential in heavy-ion collisions at the RHIC* Journal of The Korean Physical Society, **52** (2): 221-225 FEB 2008.
147. Iwasaki, M ; Ohnishi, H ; Fukutome, T *Shear viscosity of the quark matter* Journal of Physics G-Nuclear And Particle Physics, **35** (3): Art. No. 035003 MAR 2008.
148. De Cassagnac, RG *What's the matter at RHIC?* International Journal of Modern Physics **A22** (31): 6043-6056 DEC 20 2007.
149. Demchik, VI ; Skalozub, VV *On the spontaneous creation of chromomagnetic fields at high temperature* Physics of Atomic Nuclei, **71** (1): 180-186 JAN 2008.
150. Lindner, M ; Muller, MM *Comparison of Boltzmann kinetics with quantum dynamics for a chiral Yukawa model far from equilibrium* Physical Review **D77** (2): Art. No. 025027 JAN 2008.
151. Muller, B *From quark-gluon plasma to the perfect liquid* Acta Physica Polonica **B38** (12): 3705-3729 DEC 2007.
152. Casalderrey-Solana, J ; Salgado, CA *Introductory lectures on jet quenching in heavy ion collisions* Acta Physica Polonica **B38** (12): 3731-3794 DEC 2007.
153. Jipa, A ; Besliu, C ; Zgura, IS ; Ristea, O ; Ristea, C ; Horbuniev, A ; Arsene, I ; Argintaru, D ; Calin, M ; Esanu, T ; Covlea, V ; Iliescu, B *On a "microscopic Hubble constant" from relativistic nuclear collisions* International Journal of Modern Physics E-Nuclear Physics, **16** (7-8): 1790-1799 AUG-SEP 2007.
154. Zhang, WN ; Ren, YY ; Wong, CY *Pion elliptic flow and hbt interferometry in a granular quark-gluon plasma droplet model* International Journal of Modern Physics E-Nuclear Physics, **16** (7-8): 1832-1838 AUG-SEP 2007.
155. Ristea, C *et al.* BRAHMS Collaborations *Identified particle nuclear modification factors at rapidity 0-3.8 in Au+Au collisions at root(NN)-N-S=200 GeV* International Journal of Modern Physics E-Nuclear Physics, **16** (7-8): 1943-1949 AUG-SEP 2007.
156. Mironov, C ; Castro, M ; Constantin, P ; Kunde, GJ ; Vogt, R *Probing the quark-gluon plasma at the LHC with Z(0)-tagged jets in CMS* International Journal of Modern Physics E-Nuclear Physics, **16** (7-8): 1950-1956 AUG-SEP 2007.
157. Harada, M ; Nemoto, Y ; Yoshimoto, S *Quark spectrum above the critical temperature from Schwinger-Dyson equation* International Journal of Modern Physics E-Nuclear Physics, **16** (7-8): 2282-2288 AUG-SEP 2007.
158. Qin, GY ; Gale, C ; Majumder, A *Electromagnetic radiation from broken symmetries in relativistic nuclear collisions* International Journal of Modern Physics E-Nuclear Physics, **16** (7-8): 2350-2355 AUG-SEP 2007.
159. Hidaka, Y ; Kitazawa, M *Spectrum of soft mode with thermal mass of quarks above critical temperature* International Journal of Modern Physics E-Nuclear Physics, 16 (7-8): 2394-2399 AUG-SEP 2007.
160. Christensen, CH ; Gaardhoje, JJ ; Gulbrandsen, K ; Nielsen, BS; Sogaard, C T*he ALICE forward multiplicity detector* International Journal of Modern Physics E-Nuclear Physics, **16** (7-8): 2432-2437 AUG-SEP 2007.
161. David, G *Electromagnetic probes at RHIC-II* International Journal of Modern Physics E-Nuclear Physics, **16** (7-8): 2549-2554 AUG-SEP 2007.
162. Chen, JW ; Li, YH; Liu, YF ; Nakano, E *QCD viscosity to entropy density ratio in the hadronic phase* Physical Review **D76** (11): Art. No. 114011 DEC 2007.
163. Cotrone, AL ; Pons, JM ; Talavera, P *Notes on a SQCD-like plasma dual and holographic renormalization* Journal of High Energy Physics, (11): Art. No. 034 NOV 2007.
164. Enokizono, A *Observation of non-Gaussian source structure by HBT-imaging analysis* International Journal of Modern Physics E-Nuclear Physics, **16** (10): 3193-3204 NOV 2007.
165. Zhang, WN ; Wong, CY *Explanation of the RHIC HBT puzzle by a granular source of quark-gluon plasma droplets* International Journal of Modern Physics E-Nuclear Physics, **16** (10): 3262-3270 NOV 2007.

166. Alver, B *et al.* PHOBOS Collaboration *Elliptic flow fluctuations in Au+Au collisions at root s(NN)=200 GeV* International Journal of Modern Physics E-Nuclear Physics, **16** (10): 3331-3338 NOV 2007.
167. Du, JX ; Li, N ; Liu, LS *On the relation between the width of charge balance function and hadronization time in relativistic heavy ion collision* International Journal of Modern Physics E-Nuclear Physics, **16** (10): 3355-3362 NOV 2007.
168. Albacete, JL *Particle multiplicities in lead-lead collisions at the CERN Large Hadron Collider from nonlinear evolution with running coupling corrections* Physical Review Letters, **99** (26): Art. No. 262301 DEC 31 2007.
169. Peitzmann, T *Working under pressure - QCD thermodynamics at RHIC* QCD AT WORK 2007, 964: 224-231 2007 Book series title: AIP CONFERENCE PROCEEDINGS.
170. Karsch, F ; Kitazawa, M *Spectral properties of quarks above T-c in quenched lattice QCD* Physics Letters **B658** (1-3): 45-49 DEC 13 2007.
171. Majumder, A ; Nonaka, C ; Bass, SA *Jet modification in three dimensional fluid dynamics at next-to-leading twist* Physical Review **C76** (4): Art. No. 041902 OCT 2007.
172. Luo, XF ; Dong, X ; Shao, M ; Wu, KJ ; Li, C ; Chen, HF ; Xu, HS *Stopping effects in U+U collisions with a beam energy of 520 MeV/nucleon* Physical Review **C76** (4): Art. No. 044902 OCT 2007.
173. Suryanarayana, SV *Virtual photon emission from a quark-gluon plasma* Physical Review **C76** (4): Art. No. 044903 OCT 2007.
174. Brown, DA ; Soltz, R ; Newby, J ; Kisiel, A *Exploring lifetime effects in femtoscopy* Physical Review **C76** (4): Art. No. 044906 OCT 2007.
175. Guptaroy, P ; De, B ; Sau, G ; Biswas, SK ; Bhattacharyya, S *Some aspects of gold-gold collisions at RHIC at root(NN)-N-S=200 GeV and a version of the sequential chain model* International Journal of Modern Physics **A22** (28): 5121-5154 NOV 10 2007.
176. Ducati, MBG ; Goncalves, VP ; Mackedanz, LF *QCD collisional energy loss in an increasingly interacting quark-gluon plasma* International Journal of Modern Physics **A22** (18): 3105-3122 JUL 20 2007.
177. Ko, CM ; Liu, W ; Zhang, BW *Jet flavor conversions in the quark-gluon plasma* Few-Body Systems, 41 (1-2): 63-72 DEC 2007.
178. Nepali, C ; Fai, G ; Keane, D *Selection of special orientations in relativistic collisions of deformed heavy nuclei* Physical Review **C76** (5): Art. No. 051902 NOV 2007.
179. Chandra, V ; Kumar, R ; Ravishankar, V *Hot QCD equations of state and relativistic heavy ion collisions* Physical Review **C76** (5): Art. No. 054909 NOV 2007.
180. Oh, Y ; Ko, CM *Elliptic flow of deuterons in relativistic heavy-ion collisions* Physical Review **C76** (5): Art. No. 054910 NOV 2007.
181. Moore, GD *Next-to-leading order shear viscosity in lambda phi(4) theory* Physical Review **D76** (10): Art. No. 107702 NOV 2007.
182. Mannarelli, M ; Manuel, C *Chromohydrodynamical instabilities induced by relativistic jets* Physical Review **D76** (9): Art. No. 094007 NOV 2007.
183. Kurkela, A *Framework for nonperturbative analysis of a Z(3)-symmetric effective theory of finite temperature QCD* Physical Review **D76** (9): Art. No. 094507 NOV 2007.
184. Horvatic, D ; Klabucar, D ; Radzhabov, AE *eta and eta ' mesons in the Dyson-Schwinger approach at finite temperature* Physical Review **D76** (9): Art. No. 096009 NOV 2007.
185. Mrowczynski, S ; Thoma, MH *What do electromagnetic plasmas tell us about the quark-gluon plasma?* Annual Review of Nuclear and Particle Science, **57**: 61-94 2007.
186. Miller, ML ; Reygers, K ; Sanders, SJ ; Steinberg, P *Glauber modeling in high-energy nuclear collisions* Annual Review of Nuclear and Particle Science, **57**: 205-243 2007.
187. Wang, FQ *Supersonic jets in relativistic heavy-ion collisions* Quark Confinement and the Hadron Spectrum VII, 892: 417-420 2007 Book series title: AIP CONFERENCE PROCEEDINGS Conference. 7th Conference on Quark Confinement and the Hadron Spectrum.
188. Ma, GL ; Zhang, S ; Ma, YG ; Huang, HZ ; Cai, XZ ; Chen, JH ; He, ZJ ; Long, JL ; Shen, WQ ; Shi, XH ; Zuo, JX *Azimuthal correlations of hadrons in a partonic/hadronic transport model* Nuclear Physics Trends, 865: 300-306 2006 Book series title: AIP CONFERENCE PROCEEDINGS Conference. 6th China-Japan Joint Nuclear Physics Symposium.

189. Cuautle, E ; Paic, G *Proton/pion ratios and radial flow in pp and peripheral heavy ion collisions* Particles and Fields, Pt A, 857: 175-178 Part A 2006 Book series title: AIP CONFERENCE PROCEEDINGS Conference. 10th Mexican Workshop on Particles and Fields.
190. Debbe, R *et al.* BRAHMS Collaboration *High rapidity physics with the BRAHMS experiment* Intersections of Particle and Nuclear Physics, 870: 707-711 2006 Book series title: AIP CONFERENCE PROCEEDINGS Conference. 9th Conference on Intersections of Particle and Nuclear Physics.
191. Stachel, J Experimental summary Source: 5th International Conference on Physics and Astrophysics of Quark Gluon Plasma, 50: 293-299 2006 Book series title: JOURNAL OF PHYSICS CONFERENCE SERIES.
192. Qiu, HW *QCD Factorization for heavy quarkonium production at collider energies* Quark Confinement and the Hadron Spectrum VII, 892: 86-92 2007 Book series title: AIP CONFERENCE PROCEEDINGS Conference Title: 7th Conference on Quark Confinement and the Hadron Spectrum.
193. David, G *Electromagnetic probes at RHIC: The present and the future* Quark Confinement and the Hadron Spectrum VII, 892: 380-383 2007 Book series title: AIP CONFERENCE PROCEEDINGS Conference Title: 7th Conference on Quark Confinement and the Hadron Spectrum.
194. Ritter, HG *The role of collective flow in heavy ion collisions* International Journal of Modern Physics E-Nuclear Physics, **16** (3): 677-685 APR 2007.
195. Xu, N *Partonic equation of state in high-energy nuclear collisions* International Journal of Modern Physics E-Nuclear Physics, **16** (3): 715-727 APR 2007.
196. Gyulassy, M *From QED sparks to QCD lightning: (or how I survived W. Greiner's 70th birthday party)* International Journal of Modern Physics E-Nuclear Physics, **16** (3): 787-803 APR 2007.
197. Karsch, F *Hot QCD on the lattice* Progress of Theoretical Physics Supplement, (168): 237-244 2007.
198. Schafer, T *What atomic liquids can teach us about quark liquids* Progress of Theoretical Physics Supplement, (168): 303-311 2007.
199. Blaizot, JP *Weak coupling approaches to the quark-gluon plasma thermodynamics* Progress of Theoretical Physics Supplement, (168): 330-337 2007.
200. Hirano, T *Relativistic hydrodynamics at RHIC and LHC* Progress of Theoretical Physics Supplement, (168): 347-354 2007.
201. Ravagli, L ; Rapp, R *Quark coalescence based on a transport equation* Physics Letters **B655** (3-4): 126-131 NOV 1 2007.
202. Cassing, W *Dynamical quasiparticles properties and effective interactions in the sQGP* Nuclear Physics **A795**: 70-97 NOV 1 2007.
203. Hong, B *Critical evidence for nucleon coalescence in heavy-ion collisions at 400 MeV per nucleon* Journal of the Korean Physical Society, **51** (5): 1640-1644 NOV 2007.
204. Conesa, G ; Delagrange, H ; Diaz, J ; Kharlov, YV ; Schutz, Y *Prompt photon identification in the ALICE experiment: The isolation cut method* Nuclear Instruments & Methods in Physics Research Section A-Accelerators Spectrometers Detectors and Associated Equipment, **580** (3): 1446-1459 OCT 11 2007
205. Accardi, A *Final state interactions and hadron quenching in cold nuclear matter* Physical Review **C76** (3): Art. No. 034902 SEP 2007.
206. d'Enterria, D ; Ballintijn, M ; Bedjidian, M ; Hofman, D ; Kodolova, O ; Loizides, C ; Lokthin, IP ; Lourenco, C ; Mironov, C ; Petrushanko, SV ; Roland, C ; Roland, G ; Sikler, F ; Veres, G *CMS physics technical design report: Addendum on high density QCD with heavy ions* Journal of Physics G-Nuclear And Particle Physics, **34** (11): 2307-2455 NOV 2007.
207. Buchel, A ; Deakin, S ; Kerner, P ; Liu, JT *Thermodynamics of the N=2* strongly coupled plasma* Nuclear Physics **B784** (1-2): 72-102 NOV 12 2007.
208. Li, YQ ; Xu, XM *Cross sections for Meson-meson nonrelsonant reactions* Nuclear Physics **A794** (3-4): 210-230 OCT 15 2007.
209. Bertoldi, G ; Bigazzi, F ; Cotrone, AL ; Edelstein, JD *Holography and unquenched quark-gluon plasmas* Physical Review **D76** (6): Art. No. 065007 SEP 2007.
210. Gubser, SS (; Pufu, SS ; Yarom, A *Energy disturbances due to a moving quark from gauge-string duality* Journal of High Energy Physics, (9): Art. No. 108 SEP 2007.

211. Lacey, RA *Recent results of source function imaging from AGS through CERN SPS to RHIC* Brazilian Journal of Physics, **37** (3A): 893-902 SEP 2007.
212. Ko, CM ; Chen, LW ; Zhang, BW *Heavy-ion collisions at LHC in a multiphase transport model* Brazilian Journal of Physics, **37** (3A): 969-976 SEP 2007.
213. Gavin, S ; Abdel-Aziz, M *Measuring shear viscosity using correlations* Brazilian Journal of Physics, **37** (3A): 1023-1030 SEP 2007.
214. Morita, K *Rapidity dependence of HBT radii based on a hydrodynamical model* Brazilian Journal of Physics, **37** (3A): 1039-1046 SEP 2007.
215. Cassing, W *QCD thermodynamics and confinement from a dynamical quasiparticle point of view* Nuclear Physics **A791** (3-4): 365-381 JUL 15 2007.
216. Berera, A *Large transient states in quantum field theory* Nuclear Physics **A792** (3-4): 306-340 AUG 15 2007.
217. Xu, XM *3-to-3 parton elastic scatterings and early thermalization* High Energy Physics and Nuclear Physics-Chinese Edition, **31** (9): 880-886 SEP 2007.
218. Gubser, SS *Heavy ion collisions and black hole dynamics* General Relativity and Gravitation, **39** (10): 1533-1538 OCT 2007.
219. Wong, CY *Quarkonia and quark drip lines in a quark-gluon plasma* Physical Review **C76** (1): Art. No. 014902 JUL 2007.
220. Zhang, S ; Ma, GL ; Ma, YG ; Cai, XZ ; Chen, JH ; Huang, HZ ; Shen, WQ ; Shi, XH ; Jin, F ; Tian, J ; Zhong, C ; Zuo, JX *Transverse momentum and pseudorapidity dependences of Mach-like correlations for central Au plus Au collisions at root s(NN)=200 GeV* Physical Review **C76** (1): Art. No. 014904 JUL 2007.
221. Miao, H ; Gao, CS ; Zhuang, PF *Hadronization approach for a quark-gluon plasma formed in relativistic heavy ion collisions* Physical Review **C76** (1): Art. No. 014907 JUL 2007.
222. Renk, T ; Ruppert, J *Three-particle azimuthal correlations and Mach shocks* Physical Review **C76** (1): Art. No. 014908 JUL 2007.
223. Torrieri, G *Scaling of v(2) in heavy ion collisions* Physical Review **C76** (2): Art. No. 024903 AUG 2007.
224. Chiu, CB ; Hwa, RC *Particles associated with Omega produced at intermediate p(T)* Physical Review **C76** (2): Art. No. 024904 AUG 2007.
225. Dumitru, A ; Molnar, E ; Nara, Y *Entropy production in high-energy heavy-ion collisions and the correlation of shear viscosity and thermalization time* Physical Review **C76** (2): Art. No. 024910 AUG 2007.
226. Rapp, R *Hot and dense QCD matter and heavy-Ion collisions* Nuclear Instruments & Methods in Physics Research Section B-Beam Interactions With Materials And Atoms, **261** (1-2): 1053-1057 AUG 2007.
227. Xu, N *Partonic equation of state in relativistic heavy ion collisions* Brazilian Journal of Physics, **37** (2C): 773-775 2007.
228. Ko, CM ; Liu, W ; Zhang, BW *Jet conversions in a quark-gluon plasma* Brazilian Journal of Physics, **37** (2C): 855-857 2007.
229. Abuki, H *BCS/BEC crossover in quark matter and evolution of its static and dynamic properties from the atomic unitary gas to color superconductivity* Nuclear Physics **A791** (1-2): 117-164 JUL 1 2007.
230. Shin, GR *Elliptic flow and jet quenching of a parton system after relativistic heavy ion collision* Journal of the Korean Physical Society, 51 (1): 18-23 JUL 2007.
231. Yarom, A *High momentum behavior of a quark wake* Physical Review **D75** (12): Art. No. 125010 JUN 2007.
232. Qin, GY ; Majumder, A ; Gale, C *Photon production from charge-asymmetric hot and dense matter* Physical Review **C75** (6): Art. No. 064909 JUN 2007
233. Andronic, A ; Braun-Munzinger, P ; Redlich, K ; Stachel, J *Statistical hadronization of heavy quarks in ultra-relativistic nucleus-nucleus collisions* Nuclear Physics **A789**: 334-356 JUN 1 2007.
234. Antonov, D ; Domdey, S ; Pirner, HJ *A heavy quark-antiquark pair in hot QCD* Nuclear Physics **A789**: 357-378 JUN 1 2007.
235. Baier, R ; Romatschke, P *Causal viscous hydrodynamics for central heavy-ion collisions* European Physical Journal **C51** (3): 677-687 AUG 2007.

236. Kochelev, N ; Min, DP *Role of glueballs in non-perturbative quark-gluon plasma* Physics Letters **B650** (4): 239-243 JUL 5 2007.
237. Blaizot, JP *Theoretical overview: towards understanding the quark-gluon plasma* Journal of Physics G-Nuclear And Particle Physics, 34 (8): S243-S251 Sp. Iss. SI AUG 2007.
238. Wang, F *In-medium properties of jets* Journal of Physics G-Nuclear And Particle Physics, 34 (8): S337-S344 Sp. Iss. SI AUG 2007.
239. Liu, H *Heavy ion collisions and AdS/CFT* Journal of Physics G-Nuclear And Particle Physics, 34 (8): S361-S368 Sp. Iss. SI AUG 2007.
240. Majumder, A *A comparative study of jet-quenching schemes* Journal of Physics G-Nuclear And Particle Physics, 34 (8): S377-S387 Sp. Iss. SI AUG 2007.
241. Zhuang, PF ; Yan, L ; Xu, N *J/psi continuous regeneration and suppression in quark-gluon plasma* Journal of Physics G-Nuclear And Particle Physics, 34 (8): S487-S494 Sp. Iss. SI AUG 2007.
242. Wiedemann, UA *Opportunities for heavy-ion physics at the large hadron collider LHC* Journal of Physics G-Nuclear And Particle Physics, 34 (8): S503-S509 Sp. Iss. SI AUG 2007.
243. Jacak, BV ; McCumber, MP *The future of quark matter at RHIC* Journal of Physics G-Nuclear And Particle Physics, 34 (8): S543-S550 Sp. Iss. SI AUG 2007.
244. Averbeck, R *Heavy-quark and electromagnetic probes* Journal of Physics G-Nuclear And Particle Physics, 34 (8): S567-S574 Sp. Iss. SI AUG 2007.
245. McLerran, L *Theory summary: Quark matter 2006* Journal of Physics G-Nuclear And Particle Physics, 34 (8): S583-S592 Sp. Iss. SI AUG 2007.
246. Kang, ZB ; Qiu, JW *Nuclear modification to parton distribution functions* Journal Of Physics G-Nuclear And Particle Physics, 34 (8): S607-S610 Sp. Iss. SI AUG 2007.
247. Chaudhuri, AK ; Heinz, U *Effect of jet quenching on hydrodynamical evolution of QGP* Journal of Physics G-Nuclear And Particle Physics, 34 (8): S689-S692 Sp. Iss. SI AUG 2007.
248. Hirano, T ; Heinz, U ; Kharzeev, D ; Lacey, R; Nara, Y *Elliptic flow from a hybrid CGC, full 3D hydro and hadronic cascade model* Journal of Physics G-Nuclear And Particle Physics, 34 (8): S879-S882 Sp. Iss. SI AUG 2007.
249. Arleo, F *Photon-tagged correlations in heavy-ion collisions: kinematic requirements and a case study* Journal of Physics G-Nuclear And Particle Physics, 34 (8): S1037-S1040 Sp. Iss. SI AUG 2007.
250. Wu, YF ; Huang, YP *Two-charge-particle azimuthal correlations and the azimuthal balance function in RQMD and AMPT* Journal of Physics G-Nuclear And Particle Physics, 34 (8): S1113-S1117 Sp. Iss. SI AUG 2007.
251. Megias, E ; Arriola, ER ; Salcedo, LL *Power corrections in the quark-antiquark potential at finite temperature* Physical Review **D75** (10): Art. No. 105019 MAY 2007.
252. Yarom, A *Energy deposited by a quark moving in an N=4 super Yang-Mills plasma* Physical Review **D75** (10): Art. No. 105023 MAY 2007.
253. Liu, W ; Ko, CM ; Zhang, BW *Jet conversions in a quark-gluon plasma* Physical Review **C75** (5): Art. No. 051901 MAY 2007
254. Biedron, B ; Broniowski, W *Rapidity-dependent spectra from a single-freeze-out model of relativistic heavy-ion collisions* Physical Review **C75** (5): Art. No. 054905 MAY 2007.
255. Renk, T ; Eskola, KJ *Prospects of medium tomography using back-to-back hadron correlations* Physical Review **C75** (5): Art. No. 054910 MAY 2007.
256. Accardi, A *Formation time scaling and hadronization in cold nuclear matter* Physics Letters **B649** (5-6): 384-389 JUN 14 2007.
257. Braun-Munzinger, P; Stachel, J *The quest for the quark-gluon plasma* Nature, **448** (7151): 302-309 JUL 19 2007.
258. Baier, R ; Mueller, AH ; Schiff, D *How does transverse (hydrodynamic) flow affect jet-broadening and jet-quenching?* Physics Letters **B649** (2-3): 147-151 MAY 31 2007.
259. Friess, JJ ; Gubser, SS ; Michalogiorgakis, G ; Pufu, SS *Expanding plasmas and quasinormal modes of anti-de Sitter black holes* Journal of High Energy Physics, (4): Art. No. 080 APR 2007.
260. Huot, SC ; Jeon, S ; Moore, GD *Shear viscosity in weakly coupled N=4 super Yang-Mills theory compared to QCD* Physical Review Letters, **98** (17): Art. No. 172303 APR 27 2007.
261. Nakano, E ; Teraguchi, S ; Wen, WY *Drag force, jet quenching, and an AdS/QCD model* Physical Review **D75** (8): Art. No. 085016 APR 2007.

262. Polosa, AD ; Salgado, CA *Jet shapes in opaque media* Physical Review **C75** (4): Art. No. 041901 APR 2007.
263. Chaudhuri, AK *J/psi production in Au+Au and Cu+Cu collisions at root s(NN)=200 GeV and the threshold model* Physical Review **C75** (4): Art. No. 044902 APR 2007.
264. Adil, A ; Gyulassy, M ; Horowitz, W ; Wicks, S C*ollisional energy loss of nonasymptotic jets in a quark-gluon plasma* Physical Review **C75** (4): Art. No. 044906 APR 2007.
265. Liu, H ; Rajagopal, K ; Wiedemann, UA *Wilson loops in heavy ion collisions and their calculation in AdS/CFT* Journal of High Energy Physics, (3): Art. No. 066 MAR 2007.
266. Aktas, C ; Yilmaz, I *Magnetized quark and strange quark matter in the spherical symmetric space-time admitting conformal motion* General Relativity and Gravitation, **39** (6): 849-862 JUN 2007.
267. Zhu, X ; Bleicher, M ; Huang, SL ; Schweda, K ; Stocker, H ; Xu, N ; Zhuang, P *D(D)over-bar correlations as a sensitive probe for thermalization in high energy nuclear collisions* Physics Letters **B647** (5-6): 366-370 APR 19 2007.
268. Chen, JW ; Nakano, E *Shear viscosity to entropy density ratio of QCD below the deconfinement temperature* Physics Letters **B647** (5-6): 371-375 APR 19 2007.
269. Adare, A Afanasiev, S *et al.* PHENIX Collaboration *Scaling properties of azimuthal anisotropy in Au plus Au and Cu plus Cu collisions at root s(NN)=200 GeV* Physical Review Letters, **98** (16): Art. No. 162301 APR 20 2007.
270. Litvinenko, AG *Some results obtained at the relativistic heavy ion collider* Physics of Particles and Nuclei, **38** (2): 204-231 MAR 2007.
271. Ma, GL ; Ma, YG ; Zhang, S ; Cai, XZ ; Chen, JH ; He, ZJ ; Huang, HZ ; Long, JL ; Shen, WQ ; Shi, XH ; Zhong, C ; Zuo, JX *Three-particle correlations from parton cascades in Au plus Au collisions* Physics Letters **B647** (2-3): 122-127 APR 5 2007.
272. Zhang, B *J/psi production from charm coalescence in relativistic heavy ion collisions* Physics Letters **B647** (4): 249-252 APR 12 2007.
273. Blaizot, JP *High temperature phase of QCD* Nuclear Physics **A785** (1-2): 1C-9C MAR 15 2007.
274. Petreczky, P *Lattice QCD at finite temperature* Nuclear Physics **A**, 785 (1-2): 10C-17C MAR 15 2007.
275. Salgado, CA *Jets in heavy ion collisions* Nuclear Physics **A785** (1-2): 85C-92C MAR 15 2007.
276. Drescher, HJ ; Nara, Y *Effects of fluctuations on the initial eccentricity from the color glass condensate in heavy ion collisions* Physical Review **C75** (3): Art. No. 034905 MAR 2007.
277. Mehtar-Tani, Y *Relating the description of gluon production in pA collisions and parton energy loss in AA collisions* Physical Review **C75** (3): Art. No. 034908 MAR 2007.
278. Du, JX ; Li, N ; Liu, LS *Narrowing of the charge balance function and hadronization time in relativistic heavy-ion collisions* Physical Review **C75** (2): Art. No. 021903 FEB 2007.
279. Werner, K *Core-corona separation in ultrarelativistic heavy ion collisions* Physical Review Letters, 98 (15): Art. No. 152301 APR 13 2007 ISSN: 0031-9007.
280. Shao, FL ; Yao, T; Xie, QB *Charged-particle rapidity density in Au plus Au collisions in a quark combination model* Physical Review **C75** (3): Art. No. 034904 MAR 2007 ISSN: 0556-2813.
281. Drescher, HJ ; Nara, Y *Effects of fluctuations on the initial eccentricity from the color glass condensate in heavy ion collisions* Physical Review **C75** (3): Art. No. 034905 MAR 2007 ISSN: 0556-2813.
282. Mehtar-Tani, Y *Relating the description of gluon production in pA collisions and parton energy loss in AA collisions* Physical Review **C75** (3): Art. No. 034908 MAR 2007 ISSN: 0556-2813.
283. Chernicoff, M ; Guijosa, A *Energy loss of gluons, baryons and k-quarks in an N=4SYMplasma* Journal of High Energy Physics, (2): Art. No. 084 FEB 2007 ISSN: 1126-6708.
284. Lacey, RA ; Ajitanand, NN ; Alexander, JM ; Chung, P ; Holzmann, WG ; Issah, M ; Taranenko, A ; Danielewicz, P ; Stocker, H *Has the QCD critical point been signaled by observations at the BNL relativistic heavy ion collider?* Physical Review Letters, 98 (9): Art. No. 092301 MAR 2 2007 ISSN: 0031-9007.
285. Majumder, A *Resolving the plasma profile via differential single inclusive suppression* Physical Review **C75** (2): Art. No. 021901 FEB 2007 ISSN: 0556-2813.
286. Karsch, F *Properties of the quark gluon plasma: A lattice perspective* Nuclear Physics **A783**: 13C-22C FEB 15 2007 ISSN: 0375-9474.

287. Majumder, A *Deciphering the properties of hot and dense matter with hadron-hadron correlations* Nuclear Physics **A783**: 117C-124C FEB 15 2007 ISSN: 0375-9474.
288. Armesto, N *Flow effects on jet profile* Nuclear Physics **A783**: 133C-140C FEB 15 2007 ISSN: 0375-9474.
289. Kovner, A *Particle correlations in saturated QCD matter* Nuclear Physics **A783**: 181C-188C FEB 15 2007 ISSN: 0375-9474.
290. Salgado, CA *Suppression of heavy quarks at RHIC/LHC* Nuclear Physics **A783**: 225C-232C FEB 15 2007 ISSN: 0375-9474.
291. Qiu, JW *Factorization for hadronic heavy quarkonium production* Nuclear Physics **A783**: 309C-316C FEB 15 2007 ISSN: 0375-9474.
292. Accardi, A *Hadronization in cold nuclear matter* Nuclear Physics **A783**: 561C-564C FEB 15 2007 ISSN: 0375-9474.
293. Braun, MA ; Kolevatov, RS ; Vlahovic, B *Two-jet inclusive cross-sections in heavy-ion collisions in the perturbative QCD* Nuclear Physics **A784**: 407-425 MAR 1 2007 ISSN: 0375-9474.
294. Wicks, S ; Horowitz, W ; Djordjevic, M ; Gyulassy, M *Elastic, inelastic, and path length fluctuations in jet tomography* Nuclear Physics **A784**: 426-442 MAR 1 2007 ISSN: 0375-9474.
295. Xu, XM ; Ma, CC ; Chen, AQ ; Weber, HJ *qq(q)over-bar -¿ qq(q)over-bar and qq(q)over-bar -¿ q(qq)over-bar elastic scatterings and thermalization of quark matter and antiquark matter* Physics Letters **B645** (2-3): 146-152 FEB 8 2007 ISSN: 0370-2693.
296. d'Enterria, D *High-energy heavy-ions physics: from RHIC to LHC* Nuclear Physics **A782**: 215C-223C FEB 1 2007 ISSN: 0375-9474.
297. Polosa, AD ; Salgado, CA *Jets in opaque media at RHIC and LHC* Nuclear Physics **A782**: 305C-312C FEB 1 2007 ISSN: 0375-9474.
298. Shin, GR ; Lee, KS I*nitial parton distribution just after heavy-ion collisions* Journal of the Korean Physical Society, 50 (2): 426-432 FEB 2007 ISSN: 0374-4884.
299. Kitazawa, M ; Kunihiro, T ; Nemoto, Y *Novel collective excitations and the quasi-particle picture of quarks coupled with a massive boson at finite temperature* Progress of Theoretical Physics, 117 (1): 103-138 JAN 2007 ISSN: 0033-068X.
300. Fujihara, T ; Inagaki, T ; Kimura, D *Influence of QED corrections on the orientation of chiral symmetry breaking in the NJL model* Progress of Theoretical Physics, 117 (1): 139-160 JAN 2007 ISSN: 0033-068X.
301. Caceres, E ; Guijosa, A *On drag forces and jet quenching in strongly-coupled plasmas* Journal of High Energy Physics, (12): Art. No. 068 DEC 2006 ISSN: 1126-6708.
302. Talavera, P *Drag force in a string model dual to large-N QCD* Journal Of High Energy Physics, (1): Art. No. 086 JAN 2007 ISSN: 1126-6708.
303. Hidaka, Y; Kitazawa, M *Chiral transition and mesonic excitations for quarks with thermal masses* Physical Review **D75**(1): Art. No. 011901 JAN 2007 ISSN: 1550-7998.
304. Ma, CC ; Xu, XM *qq(q)over-bar -¿ qq(q)over-bar reaction in quark-gluon matter* High Energy Physics and Nuclear Physics-Chinese Edition, 31 (2): 162-167 FEB 2007 ISSN: 0254-3052.
305. McLerran, L *Some comments about the high energy limit of QCD* Acta Physica Polonica **B37** (12): 3237-3251 DEC 2006 ISSN: 0587-4254.
306. Gelis, F ; Venugopalan, R T*hree lectures on multi-particle production in the Glasma* Acta Physica Polonica **B37** (12): 3253-3313 DEC 2006 ISSN: 0587-4254.
307. Peshier, A *Rethinking the QCD collisional energy loss* European Physical Journal **C49** (1): 9-12 JAN 2007 ISSN: 1434-6044.
308. Tomasik, B ; Kolomeitsev, EE *Strangeness production time and the K+/pi(+) horn* European Physical Journal **C49** (1): 115-120 JAN 2007 ISSN: 1434-6044.
309. Nouicer, R *Charged particle multiplicities in A+A and p+p collisions in the constituent quarks framework* European Physical Journal **C49** (1): 281-286 JAN 2007 ISSN: 1434-6044.
310. Accardi, A *Space-time evolution of hadronization* European Physical Journal **C49** (1): 347-353 JAN 2007 ISSN: 1434-6044.
311. Pisarski, RD *Effective theory of Wilson lines and deconfinement* Physical Review **D74** (12): Art. No. 121703 DEC 2006 ISSN: 1550-7998.
312. Gubser, SS *Drag force in AdS/CFT* Physical Review **D74** (12): Art. No. 126005 DEC 2006 ISSN: 1550-7998.

313. Ayala, A ; Cuautle, E ; Magnin, J ; Montano, LM *Proton and pion transverse spectra at the BNL Relativistic Heavy Ion Collider from radial flow and finite size effects* Physical Review **C74** (6): Art. No. 064903 DEC 2006 ISSN: 0556-2813.
314. Chiu, CB ; Hwa, RC *Away-side azimuthal distribution in a Markovian parton scattering mode* Physical Review **C74** (6): Art. No. 064909 DEC 2006 ISSN: 0556-2813.
315. Hong, B *Change of the azimuthal asymmetry at high momentum with different parton absorptions in a quark-gluon plasma* Journal of the Korean Physical Society, 49 (6): 2271-2275 DEC 2006 ISSN: 0374-4884.
316. Muller, B ; Nagle, JL *Results from the relativistic heavy ion collider* Annual Review of Nuclear and Particle Science, 56: 93-135 2006 ISSN: 0163-8998.
317. Boyanovsky, D ; de Vega, HJ ; Schwarz, DJ *Phase transitions in the early and present universe* Annual Review of Nuclear and Particle Science, 56: 441-500 2006 ISSN: 0163-8998.
318. Matsuo, T ; Tomino, D ; Wen, WY *Drag force in SYM plasma with B field from AdS/CFT* Journal of High Energy Physics, (10): Art. No. 055 OCT 2006 ISSN: 1126-6708.
319. Ollitrault, JY *Nucleus-nucleus collisions at RHIC: A review* Pramana-Journal of Physics, 67 (5): 899-914 Sp. Iss. SI NOV 2006 ISSN: 0304-4289.
320. Majumder, A ; Muller, B *Baryonic strangeness and related susceptibilities in QCD* Physical Review **C74** (5): Art. No. 054901 NOV 2006 ISSN: 0556-2813.
321. Lappi, T; Venugopalan, R *Universality of the saturation scale and the initial eccentricity in heavy ion collisions* Physical Review **C74** (5): Art. No. 054905 NOV 2006 ISSN: 0556-2813.
322. Torrieri, G *Resonances and fluctuations of strange particles in 200 GeV Au-Au collisions* Journal of Physics **G**-Nuclear and Particle Physics, 32 (12): S195-S203 Sp. Iss. SI DEC 2006 ISSN: 0954-3899.
323. Asakawa, M ; Bass, SA ; Muller, B T*he flavours of the quark-gluon plasma* Journal of Physics **G**-Nuclear and Particle Physics, 32 (12): S411-S419 Sp. Iss. SI DEC 2006 ISSN: 0954-3899.
324. Armesto, N ; Cacciari, M ; Dainese, A ; Salgado, CA ; Wiedemann, UA *Heavy quarks as a test of medium-induced energy loss at RHIC and at the LHC* Journal of Physics **G**-Nuclear and Particle Physics, 32 (12): S421-S427 Sp. Iss. SI DEC 2006 ISSN: 0954-3899.
325. Stephans, GSF *critRHIC: the RHIC low energy program* Journal of Physics **G**-Nuclear and Particle Physics, 32 (12): S447-S453 Sp. Iss. SI DEC 2006 ISSN: 0954-3899.
326. Majumder, A *Deciphering deconfinement in correlations of conserved charges* Journal of Physics **G**-Nuclear and Particle Physics, 32 (12): S473-S478 Sp. Iss. SI DEC 2006 ISSN: 0954-3899.
327. Schuster, T ; Laszlo, A (NA49 Collaboration) *High p(T) spectra of identified particles produced in Pb+Pb collisions at 158 A GeV beam energy* Journal of Physics **G**-Nuclear and Particle Physics, 32 (12): S479-S482 Sp. Iss. SI DEC 2006 ISSN: 0954-3899.
328. Yang, HY (BRAHMS Collaboration) *Strangeness production in p+p and d+Au collisions at RHIC* Journal of Physics **G**-Nuclear and Particle Physics, 32 (12): S491-S494 Sp. Iss. SI DEC 2006 ISSN: 0954-3899.
329. Asakawa, M ; Bass, SA ; Muller, B *Anomalous transport processes in anisotropically expanding Quark-Gluon plasmas* Progress of Theoretical Physics, 116 (4): 725-755 OCT 2006 ISSN: 0033-068X.
330. Mishustin, IN *Possible links between the liquid-gas and deconfinement-hadronization phase transitions* European Physical Journal **A30** (1): 311-316 OCT 2006 ISSN: 1434-6001.
331. Liu, H ; Rajagopal, K ; Wiedemann, UA *Calculating the jet quenching parameter* Physical Review Letters, 97 (18): Art. No. 182301 NOV 3 2006 ISSN: 0031-9007.
332. Iida, H; Doi, T ; Ishii, N; Suganuma, H ; Tsumura, K *Charmonium properties in deconfinement phase in anisotropic lattice QCD* Physical Review **D74** (7): Art. No. 074502 OCT 2006 ISSN: 1550-7998.
333. Casalderrey-Solana, J ; Teaney, D *Heavy quark diffusion in strongly coupled N=4 Yang-Mills theory* Physical Review **D74** (8): Art. No. 085012 OCT 2006 ISSN: 1550-7998.
334. Dai, J ; Nair, VP *Color Skyrmions in the quark-gluon plasma* Physical Review **D74** (8): Art. No. 085014 OCT 2006 ISSN: 1550-7998.
335. Adil, A ; Drescher, HJ; Dumitru, A ; Hayashigaki, A ; Nara, Y *Eccentricity in heavy-ion collisions from color glass condensate initial conditions* Physical Review **C74** (4): Art. No. 044905 OCT 2006 ISSN: 0556-2813.

336. Yu, ML ; Du, JX ; Liu, LS *Effect of an equilibrium phase transition on multiphase transport in relativistic heavy ion collisions* Physical Review **C74** (4): Art. No. 044906 OCT 2006 ISSN: 0556-2813.
337. Chaudhuri, AK *J/psi production in Au plus Au collisions root s(NN) =200 GeV and the nuclear absorption* Physical Review **C74** (4): Art. No. 044907 OCT 2006 ISSN: 0556-2813.
338. Ma, GL ; Zhang, S ; Ma, YG ; Huang, HZ ; Cai, XZ ; Chen, JH ; He, ZJ ; Long, JL ; Shen, WQ ; Shi, XH ; Zuo, JX *Di-hadron azimuthal correlation and Mach-like cone structure in a parton/hadron transport model* Physics Letters **B641** (5): 362-367 OCT 19 2006 ISSN: 0370-2693.
339. Armesto, N *Nuclear shadowing* Journal of Physics **G**-Nuclear And Particle Physics, 32 (11): R367-R393 NOV 2006 ISSN: 0954-3899.
340. Franz, A *Five years of tracking heavy ion collisions at RHIC* Nuclear Instruments & Methods in Physics Research Section A-Accelerators Spectrometers Detectors and Associated Equipment, 566 (1): 54-61 OCT 1 2006 ISSN: 0168-9002.
341. Friess, JJ ; Gubser, SS ; Michalogiorgakis, G *Dissipation from a heavy quark moving through N=4 super-Yang-Mills plasma* Journal of High Energy Physics, (9): Art. No. 072 SEP 2006 ISSN: 1126-6708.
342. Chernicoff, M ; Garcia, JA ; Guijosa, A *The energy of a moving quark-antiquark pair in an N=4 SYM plasma* Journal of High Energy Physics, (9): Art. No. 068 SEP 2006 ISSN: 1126-6708.
343. Baier, R ; Schiff, D *Deciphering the properties of the medium produced in heavy ion collisions at RHIC by a pQCD analysis of quenched large p perpendicular to pi(0) spectra* Journal of High Energy Physics, (9): Art. No. 059 SEP 2006 ISSN: 1126-6708.
344. Armesto, N ; Edelstein, JD ; Mas, J J*et quenching at finite 't Hooft coupling and chemical potential from AdS/CFT* Journal of High Energy Physics, (9): Art. No. 039 SEP 2006 ISSN: 1126-6708.
345. Arleo, F *Hard pion and prompt photon at RHIC, from single to double inclusive production* Journal of High Energy Physics, (9): Art. No. 016 SEP 2006 ISSN: 1126-6708.
346. Cheng, M ; Christ, NH; Datta, S ; van der Heide, J ; Jung, C ; Karsch, F ; Kaczmarek, O ; Laermann, E ; Mawhinney, RD ; Miao, C ; Petreczky, P ; Petrov, K ; Schmidt, C ; Umeda, T *Transition temperature in QCD* Physical Review **D74** (5): Art. No. 054507 SEP 2006 ISSN: 1550-7998.
347. Mukherjee, S *Robustness of baryon-strangeness correlation and related ratios of susceptibilities* Physical Review **D74** (5): Art. No. 054508 SEP 2006 ISSN: 1550-7998.
348. Cunqueiro, L; de Deus, JD ; Pajares, C *Multiplicity associated to high p(T) events and multiplicity fluctuations* Physical Review **C74** (3): Art. No. 034901 SEP 2006 ISSN: 0556-2813.
349. Greene, SV (Greene, S. V.) (PHENIX Coll.) *Highlights from the PHENIX experiment - Part 1* Nuclear Physics **A774**: 93-102 AUG 7 2006 ISSN: 0375-9474.
350. Cole, BA *High p(T) probes of dense matter created in heavy ion collisions at RHIC* Nuclear Physics **A774**: 225-236 AUG 7 2006 ISSN: 0375-9474.
351. Akiba, Y (PHENIX Collaboration) *Probing the properties of dense partonic matter at RHIC* Nuclear Physics **A774**: 403-408 AUG 7 2006 ISSN: 0375-9474.
352. Csanad, M ; Csorgo, T ; Lorstad, B ; Ster, A *Universal scaling of the rapidity dependent elliptic flow and the perfect fluid at RHIC* Nuclear Physics **A774**: 535-538 AUG 7 2006 ISSN: 0375-9474.
353. Adil, A ; Gyulassy, M; Hirano, T *3D jet tomography and the twisted color glass condensate* Nuclear Physics **A774**: 593-596 AUG 7 2006 ISSN: 0375-9474.
354. Djordjevic, M ; Gyulassy, M ; Vogt, R ; Wicks, S *The single electron puzzle at RHIC* Nuclear Physics **A774**: 689-692 AUG 7 2006 ISSN: 0375-9474.
355. Gazdzicki, M ; Gorenstein, M *Transparency, mixing and reflection of initial flows in relativistic nuclear collisions* Physics Letters **B640** (4): 155-161 SEP 14 2006 ISSN: 0370-2693.
356. Nawa, ; Nakano, E ; Yabu, H *Diquark Bose-Einstein condensation* Physical Review **D74** (3): Art. No. 034017 AUG 2006 ISSN: 1550-7998.
357. Romatschke, P ; Venugopalan, R *The unstable glasma* Physical Review **D74** (4): Art. No. 045011 AUG 2006 ISSN: 1550-7998.
358. Renk, T *High p(T) hadrons as probes of the central region of Au-Au collisions at root S-NN=200 GeV* Physical Review **C74** (2): Art. No. 024903 AUG 2006 ISSN: 0556-2813.

359. Zhang, WN ; Ren, YY ; Wong, CY *Analysis of pion elliptic flow and Hanbury-Brown-Twiss interferometry in a granular quark-gluon plasma droplet model* Physical Review **C74** (2): Art. No. 024908 AUG 2006 ISSN: 0556-2813.
360. Moore, GD *Numerical studies of QGP instabilities and implications* European Physical Journal **A29** (1): 53-57 JUL 2006 ISSN: 1434-6001.
361. Tannenbaum, MJ *Recent results in relativistic heavy ion collisions: from 'a new state of matter' to 'the perfect fluid'* Reports On Progress In Physics, 69 (7): 2005-2059 JUL 2006 ISSN: 0034-4885.
362. Hayashigaki, A *Proton and anti-proton production in the forward region of d+Au collisions at RHIC from the color glass* Nuclear Physics **A775** (1-2): 51-68 AUG 21 2006 ISSN: 0375-9474.
363. Yilmaz, I *String cloud and domain walls with quark matter in 5-D Kaluza-Klein cosmological model* General Relativity and Gravitation, 38 (9): 1397-1406 SEP 2006 ISSN: 0001-7701.
364. Chaudhuri, AK ; Heinz, U *Effects of jet quenching on the hydrodynamical evolution of quark-gluon plasma* Physical Review Letters, 97 (6): Art. No. 062301 AUG 11 2006 ISSN: 0031-9007.
365. Paech, K ; Pratt, S *Origins of bulk viscosity in relativistic heavy ion collisions* Physical Review **C74** (1): Art. No. 014901 JUL 2006 ISSN: 0556-2813.
366. Hong, B *Charmed Baryon production from the quark coalescence process in Au+Au collisions at the RHIC* Journal of the Korean Physical Society, 49 (1): 77-81 JUL 2006 ISSN: 0374-4884.
367. Kuhlman, A ; Heinz, U ; Kovchegov, YV *Gluon saturation effects in relativistic U+U collisions* Physics Letters **B638** (2-3): 171-177 JUL 6 2006 ISSN: 0370-2693.
368. Back, BB ; Baker, MD ; Ballintijn, M ; Barton, DS ; Betts, RR ; Bickley, AA ; Bindel, R ; Budzanowski, A ; Busza, W ; Carroll, A ; Chai, Z ; Decowski, MP ; Garcia, E ; Gburek, T ; George, N ; Gulbrandsen, K ; Gushue, S ; Halliwell, C ; Hamblen, J ; Hauer, M; Heintzelman, GA ; Henderson, C ; Hofman, DJ ; Hollis, RS ; Holynnski, R ; Holzman, B ; Iordanova, A ; Johnson, E ; Kane, JL ; Katzy, J ; Khan, N ; Kucewicz, W ; Kulinich, P ; Kuo, CM ; Lin, WT ; Manly, S ; McLeod, D ; Mignerey, AC ; Nouicer, R ; Olszewski, A ; Pak, R ; Park, IC ; Pernegger, H ; Reed, C ; Remsberg, LP ; Reuter, M ; Roland, C ; Roland, G ; Rosenberg, L ; Sagerer, J ; Sarin, P ; Sawicki, P ; Seals, H ; Sedykh, I ; Skulski, W ; Smith, CE ; Stankiewicz, MA ; Steinberg, P ; Stephans, GSF ; Sukhanov, A ; Tang, JL ; Tonjes, MB; Trzupek, A ; Vale, C ; van Nieuwenhuizen, GJ ; Vaurynovich, SS ; Verdier, R ; Veres, GI ; Wenger, E ; Wolfs, FLH ; Wosiek, B ; Wozniak, K ; Wuosmaa, AH ; Wyslouch, B *Energy dependence of directed flow over a wide range of pseudorapidity in Au plus Au collisions at the BNL relativistic heavy ion collider* Physical Review Letters, 97 (1): Art. No. 012301 JUL 7 2006 ISSN: 0031-9007.
369. Asakawa, M; Bass, SA; Muller, B *Anomalous viscosity of an expanding quark-gluon plasma* Physical Review Letters, 96 (25): Art. No. 252301 JUN 30 2006 ISSN: 0031-9007.
370. Lindner, M ; Muller, MM *Comparison of Boltzmann equations with quantum dynamics for scalar fields* Physical Review **D73** (12): Art. No. 125002 JUN 2006 ISSN: 1550-7998.
371. Baier, R; Romatschke, P; Wiedemann, UA *Dissipative hydrodynamics and heavy-ion collisions* Physical Review **C73** (6): Art. No. 064903 JUN 2006 ISSN: 0556-2813.
372. Armesto, N; Cacciari, M; Dainese, A; Salgado, CA; Wiedemann, UA *How sensitive are high-p(T) electron spectra at RHIC to heavy quark energy loss?* Physics Letters **B637** (6): 342-346 JUN 22 2006 ISSN: 0370-2693.
373. Andronic, A; Braun-Munzinger, P; Stachel, J *Hadron production in central nucleus-nucleus collisions at chemical freeze-out* Nuclear Physics **A772** (3-4): 167-199 JUN 26 2006 ISSN: 0375-9474.
374. Zapp, K ; Ingelman, G ; Rathsman, J; Stachel, J *Jet quenching from soft QCD scattering in the quark-gluon plasma* Physics Letters **B637** (3): 179-184 JUN 8 2006 ISSN: 0370-2693.
375. Majumder, A; Wang, XN *Landau-Pomeranchuck-Migdal interference and Cherenkov-like gluon bremsstrahlung in dense matter* Physical Review **C73** (5): Art. No. 051901 MAY 2006 ISSN: 0556-2813.
376. Hong, B; Ji, CR; Min, DP *Light-front wavefunction dependence of quark recombination* Physical Review **C73** (5): Art. No. 054901 MAY 2006 ISSN: 0556-2813.
377. Muller, B; Schafer, A *Decoherence time in high energy heavy ion collisions* Physical Review **C73** (5): Art. No. 054905 MAY 2006 ISSN: 0556-2813.
378. Hirano, T; Heinz, U; Kharzeev, D; Lacey, R; Nara, Y *Hadronic dissipative effects on elliptic flow in ultrarelativistic heavy-ion collisions* Physics Letters **B636** (6): 299-304 MAY 25 2006 ISSN: 0370-2693.

379. Stachel, J *Has the quark-gluon plasma been seen?* International Journal of Modern Physics **A21** (8-9): 1750-1761 APR 10 2006 ISSN: 0217-751X.
380. Klebanov, IR *QCD and string theory* International Journal of Modern Physics **A21** (8-9): 1831-1842 APR 10 2006 ISSN: 0217-751X.
381. Li, YQ; Xu, XM *Cross sections for pi pi ¡-¿ pp and pi pi ¡-¿omega omega reactions* Chinese Physics Letters, 23 (5): 1132-1135 MAY 2006 ISSN: 0256-307X.
382. Adil, A; Gyulassy, M; Hirano, T *3D jet topography of the twisted color glass condensate* Physical Review **D73** (7): Art. No. 074006 APR 2006 ISSN: 1550-7998.
383. Cleymans, J; Oeschler, H; Redlich, K; Wheaton, S C*omparison of chemical freeze-out criteria in heavy-ion collisions* Physical Review **C73** (3): Art. No. 034905 MAR 2006 ISSN: 0556-2813.
384. Nepali, C; Fai, G; Keane, D A*dvantage of U+U over Au+Au collisions at constant beam energy* Physical Review **C73** (3): Art. No. 034911 MAR 2006 ISSN: 0556-2813.
385. Ayala, A; Cuautle, E; Magnin, J; Montano, LM; Raya, A *Finite size effects on pion spectra in relativistic heavy-ion collisions* Physics Letters **B634** (2-3): 200-204 MAR 9 2006 ISSN: 0370-2693.
386. Dumitru, A; Portugal, L; Zschiesche, D *Inhomogeneous freeze-out in relativistic heavy-ion collisions* Physical Review **C73** (2): Art. No. 024902 FEB 2006 ISSN: 0556-2813.
387. Borysova, MS; Sinyukov, YM; Akkelin, SV; Erazmus, B; Karpenko, IA *Hydrodynamic source with continuous emission in Au plus Au collisions at root s=200 GeV* Physical Review **C73** (2): Art. No. 024903 FEB 2006 ISSN: 0556-2813.
388. Bleibel, J; Burau, G; Faessler, A; Fuchs, C *Energy densities and equilibration in heavy ion collisions at root s(NN)=200 GeV with the quark-gluon string model* Nuclear Physics **A767**: 218-232 MAR 6 2006 ISSN: 0375-9474.
389. Romatschke, P; Venugopalan, R *Collective non-Abelian instabilities in a melting color glass condensate* Physical Review Letters, 96 (6): Art. No. 062302 FEB 17 2006 ISSN: 0031-9007.
390. Kitazawa, M; Kunihiro, T; Nemoto, Y *Quark spectrum above but near critical temperature of chiral transition* Physics Letters **B633** (2-3): 269-274 FEB 9 2006 ISSN: 0370-2693.
391. Petreczky, P; Teaney, D *Heavy quark diffusion from the lattice* Physical Review **D73** (1): Art. No. 014508 JAN 2006 ISSN: 1550-7998.
392. Renk, T; Ruppert, J *Mach cones in an evolving medium* Physical Review **C73** (1): Art. No. 011901 JAN 2006 ISSN: 0556-2813.
393. Jeon, S; Shi, LJ; Bleicher, M *Detecting quark gluon plasma with charge transfer fluctuations* Physical Review **C73** (1): Art. No. 014905 JAN 2006 ISSN: 0556-2813.
394. Gelis, F; Kajantie, K; Lappi, T *Chemical thermalization in relativistic heavy ion collisions* Physical Review Letters, 96 (3): Art. No. 032304 JAN 27 2006 ISSN: 0031-9007.
395. Heuser, JM; Muller, WFJ; Senger, P; Muntz, C; Stroth, J (CBM Collaboration) *A high-performance silicon tracker for the Compressed Baryonic Matter experiment at FAIR* Czechoslovak Journal of Physics, 55 (12): 1649-1653 DEC 2005 ISSN: 0011-4626.
396. Nikolaev, NN; Schafer, W; Zakharov, BG *Nonlinear k(perpendicular to) factorization for gluon-gluon dijets produced off nuclear targets* Physical Review **D72** (11): Art. No. 114018 DEC 2005 ISSN: 1550-7998.
397. Back, BB *Consequences of energy conservation in relativistic heavy-ion collisions* Physical Review **C72** (6): Art. No. 064906 DEC 2005 ISSN: 0556-2813.
398. Cleymans, J; Redlich, K; Turko, L *Thermodynamic limit and semi-intensive quantities* Journal Of Physics **G**-Nuclear And Particle Physics, 31 (12): 1421-1435 DEC 2005 ISSN: 0954-3899.
399. Stankus, P *Direct photon production in relativistic heavy-ion collisions* Annual Review of Nuclear And Particle Science, 55: 517-554 2005 ISSN: 0163-8998.
400. Baier, R; Kovner, A; Nardi, M; Wiedemann, UA *Particle correlations in saturated QCD matter* Physical Review **D72** (9): Art. No. 094013 NOV 2005 ISSN: 1550-7998.
401. Shi,L; Jeon, S Charge transfer fluctuations as a signal for quark-gluon plasma Physical Review **C72** (3): Art. No. 034904 SEP 2005 ISSN: 0556-2813.

402. Apanasevich, L; Bacigalupi, J; Baker, W; Begel, M; Blusk, S; Bromberg, C; Chang, P; Choudhary, B; Chung, WH; de Barbaro, L; DeSoi, W; Dlugosz, W; Dunlea, J; Engels, E; Fanourakis, G; Ferbel, T; Ftacnik, J; Garelick, D; Ginther, G; Glaubman, M; Gutierrez, P; Hartman, K; Huston, J; Johnstone, C; Kapoor, V; Kuehler, J; Lirakis, C; Lobkowicz, F; Lukens, P; Mansour, J; Maul, A; Miller, R; Oh, BY; Osborne, G; Pellett, D; Prebys, E; Roser, R; Shepard, P; Shivpuri, R; Skow, D; Slattery, P; Sorrell, L; Striley, D; Toothacker, W; Tripathi, SM; Varelas, N; Weerasundara, D; Whitmore, JJ; Yasuda, T; Yosef, C; Zielinski, M; Zutshi, V (Fermilab E706 Coll.) *Nuclear effects in high-p(T) production of direct photons and neutral mesons* Physical Review **D72** (3): Art. No. 032003 AUG 2005 ISSN: 1550-7998.

403. Back, BB; Baker, MD; Ballintijn, M; Barton, DS; Becker, B; Betts, RR; Bickley, AA; Bindel, R; Budzanowski, A; Busza, W; Carroll, A; Chai, Z; Decowski, MP; Garcia, E; Gburek, T; George, NK; Gulbrandsen, K; Gushue, S; Halliwell, C; Hamblen, J; Harrington, AS; Hauer, A; Heintzelman, GA; Henderson, C; Hofman, DJ; Hollis, RS; Holynski, C; Holzman, B; Iordanova, A; Johnson, E; Kane, JL; Katzy, J; Khan, N; Kucewicz, W; Kulinich, P; Kuo, CM; Lee, JW; Lin, WT; Manly, S; McLeod, D; Mignerey, AC; Nouicer, R; Olszewski, A; Pak, R; Park, IC; Pernegger, H; Reed, C; Remsberg, LP; Reuter, A; Roland, C; Roland, G; Rosenberg, L; Sagerer, J; Sarin, P; Sawicki, P; Seals, H; Sedykh, I; Skulski, W; Smith, CE; Stankiewicz, MA; Steinberg, P; Stephans, GSF; Sukhanov, A; Tang, JL; Tonjes, MB; Trzupek, A; Vale, CM; van Nieuwenhuizen, GJ; Vaurynovich, SS; Verdier, R; Veres, GI; Wenger, E; Wolfs, FLH; Wosiek, B; Wozniak, K; Wuosmaa, AH; Wyslouch, B; Zhang, J (PHOBOS Collaboration) *The PHOBOS perspective on discoveries at RHIC* Nuclear Physics **A757** (1-2): 28-101 AUG 8 2005 ISSN: 0375-9474.

5.1.3 Conference presentations

1. M. Šumbera, *Ultra-relativistic nucleus-nucleus collisions: past, present and future (from CERN to BNL and back)* . Czech-Taiwan workshop on the intermediate and high energy physics, Prague, March 3.-5.2003. Czechoslovak Journal of Physics, Volume 53, Number 8 / August, 2003.

2. M. Šumbera, *Results from STAR.* Invited talk at Atlas overview week, Prague, Czech Republic, 13.-19.9.2003.

3. M. Šumbera,*Heavy Ions and Quark-Gluon Plasma.* Invited talk at 15^{th} Conference of Czech and Slovak physicists, Košice, Slovakia, 11.-14.9. 2005.

4. J. Nemchik, M. Šumbera, *Nuclear Effects in High-p_T Hadron Production at Large x.* Talk at 38th International Symposium on Multiparticle Dynamics ISMD08, September 15-20, 2008 DESY, Hamburg, Germany [244].

5.2 Femtoscopy at RHIC: Selected results

5.2.1 Introductory notes

Progress in understanding the space-time structure of multiparticle production via momentum correlations of two or more particles at small relative momenta [R66] - called nowadays the correlation femtoscopy [R65] - is currently driven by high-statistics data sets accumulated in heavy ion experiments at RHIC and SPS [74, 77, 78, 82, 90, 91, 94, 95, 98, 100, 111, 113, 116, 120, 137, 145, 150, 166, 171, 178, 196, 200, 225], [R65, R66]. In particular, an ambitious program of the STAR collaboration at RHIC exploiting good particle identification has already provided a variety of femtoscopic measurements in different identical and non-identical particle systems (see Table5.1). Let us note that some of these systems were actually measured for the first time [180, 200].

	π^+	π^-	K^+	K^-	K^0_s	p	$\bar{p}$	Λ	$\bar{\Lambda}$	Ξ	$\bar{\Xi}$
$\bar{\Xi}$	[180,200]	[180,200]									
Ξ	[180,200]	[180,200]									
$\bar{\Lambda}$						[178]	[178]				
Λ						[178]	[178]				
$\bar{p}$	[R100]	[R100]	[R100]	[R100]		[R99]	[R99]				
p	[R100]	[R100]	[R100]	[R100]		[R99,R101]					
K^0_s					[196]						
K^-	[150]	[150]		[R101]							
K^+	[150]	[150]	[R101]								
π^-	[166,R99]	[166,200, R97,R98]									
π^+	[166,200, R97,R98]										

Table 5.1: Table of published femtoscopic studies at RHIC for various particle combinations. "Traditional" identical-particle interferometry lies along the lowest diagonal line of cells. Addapted from [R102].

Article reprint

Brazilian Journal of Physics, vol. 37, no. 3A, September, 2007 925

Selected Results on Strong and Coulomb-Induced Correlations from the STAR Experiment

M. Šumbera for the STAR Collaboration
Nuclear Physics Institute, Academy of Sciences of the Czech Republic, 250 68 Řež, Czech Republic

Received on 13 December, 2006

Using recent high-statistics STAR data from Au+Au and Cu+Cu collisions at full RHIC energy I discuss strong and Coulomb-induced final state interaction effects on identical (π π) and non-identical (π Ξ) particle correlations. Analysis of π Ξ correlations reveals the strong and Coulomb-induced FSI effects, allowing for the first time to estimate spatial extension of π and Ξ sources and the average shift between them. Source imaging techniques provide clean separation of details of the source function and are applied to the one-dimensional relative momentum correlation function of identical pions. For low momentum pions, and/or non-central collisions, a large departure from a single-Gaussian shape is observed.

Keywords: Heavy ions; Femtoscopy

I. INTRODUCTION

Progress in understanding the space-time structure of multiparticle production via femtoscopy is currently driven by high-statistics data sets accumulated in heavy ion experiments at RHIC and SPS accelerator [1–4, 10]. In particular, an ambitious program of the STAR collaboration at RHIC exploiting good particle identification has already provided a vast variety of femtoscopic measurements in different identical and non-identical particle systems, some of which were actually measured for the first time [4]. This contribution is a progress report on two currently pursued STAR femtoscopy analyses. Both of them were introduced already at the previous WPCF meeting last year in Kroměříž [2]. The first focuses on non-identical particle correlations in rather exotic meson–baryon system π Ξ [5]. Previous investigations have shown that correlations among these two charged hadrons reveal not only the Coulomb but also strong final state interaction (FSI) effects [11, 12]. The order of magnitude difference in mass, plus ΔB=1/ΔS=2 gap in baryon/ strangeness quantum numbers, makes the π Ξ system an important tool to study the interplay between matter flow on the partonic and hadronic levels. The second analysis exploits particle correlations in a more conventional system of two identical charged pions [6]. Its aim is to understand the geometry of the source. The ultimate and rather ambitious aspiration of this project is to extract pion-pion scattering lengths. This goal will make heavy ion femtoscopic measurements fully competitive to a dedicated particle physics experiments trying to extract this important parameter of the strong interaction [3, 7, 8]. Basic prerequisites for such measurements are good knowledge of correlations due to quantum statistics and Coulomb interactions.

II. STUDYING SPACE-TIME STRUCTURE OF MULTI-STRANGE BARYON SOURCE VIA π Ξ CORRELATIONS

In ultra-relativistic heavy-ion collisions at RHIC, hot and dense strongly interacting matter is created exhibiting properties of de-confined partonic matter [9, 13]. Almost instantaneous equilibration of the produced matter is indicated by recent heavy flavor measurements [9, 14], and represents one of the greatest puzzles coming from RHIC [9]. The early partonic collectivity also shows up in a subsequent evolution of the system leading to strong collective expansion of the bulk matter as demonstrated by large values of observed elliptic flow [9, 13]. These observations are further substantiated by STAR multi–strange baryon measurements showing that Ξ and Ω baryons reveal significant amount of elliptic flow which is comparable to ordinary non–strange baryons [15]. The sizable multi–strange baryon elliptic flow, which obeys constituent quark scaling [16], confirms that a substantial part of the collective motion has indeed developed prior to hadronization. This picture is also corroborated by a more recent STAR analysis of the centrality dependence of hyperon yields carried out within the framework of a thermal model [17]. The observed scaling behavior of strange baryons is consistent with a scenario of hadron formation from constituent quark degrees of freedom through quark recombination provided that the coalescence took place over a volume that is much larger than the one created in any elementary collisions.

These observations fit nicely into ideal hydrodynamic evolution starting from the system of de-confined QCD matter. However, they are also consistent with a more realistic hybrid macroscopic/microscopic transport approach [20] which takes into account the strength of dissipative effects prevalent in the latter hadronic phase of the reaction. The hybrid model calculations indicate that at the top RHIC energy the hadronic phase of the heavy-ion reactions is of significant duration (at least 10 fm/c), making hadronic freeze-out a continuous process, strongly depending on hadron flavor and momenta. In particular, heavy hadrons, which are quite sensitive to radial flow effects, obtain the additional collective push created by resonant (quasi)elastic interactions during that fairly long-lived hadronic rescattering stage [21].

It is clear that questions concerning multi–strange baryon decoupling from the hot and strongly interacting partonic/hadronic system is an interesting one, but also not an easy one to solve. Could this be provided by femtoscopy? What kind of relevant information can be obtained via low-relative-velocity correlations of multi-strange baryons with the other hadrons? Since non-identical particle correlations are sensitive not only to the extent of the source, but also to the average shift in emission time and position among differ-

ent particle species [19], the answer is affirmative. The femtoscopy of non-identical particles was already used to show that the average emission points of pions, kaons and protons produced in heavy-ion collisions at SPS and RHIC are not the same [3, 7, 10, 22, 23]. In a hydrodynamically inspired blast-wave approach [18], the mass ordering of average space-time emission points of different particle species naturally appears due to the transverse expansion of the source. This effect increases with the mass difference of the measured particle pair. Hence, studying correlations in the π Ξ system where the mass difference is very large should provide rather sensitive test of the emission asymmetries introduced by the transverse expansion of the bulk matter.

Moreover, in addition to the Coulomb interaction studied in the π K system, the small relative momentum π Ξ correlations may provide a clear signal of the strong interaction, revealing itself via the Ξ 1530 resonance. Expressing particle momentum in the pair rest frame, $\mathbf{k}$ $\mathbf{p}_\pi$ $\mathbf{p}_\Xi$ via pair invariant mass $M_{\pi\Xi}$ and m_π and m_Ξ

$$k \quad \frac{M_{\pi\Xi}^2 \quad m_\pi \quad m_\Xi \;^{2\,1\,2} M_{\pi\Xi}^2 \quad m_\pi \quad m_\Xi \;^{2\,1\,2}}{2M_{\pi\Xi}} \qquad (1)$$

One expects the Ξ 1530 peak to show up in the correlation function C k at k 150 MeV/c. Due to its rather long lifetime, $\tau_{\Xi\ 1530}$ $22 fm\ c$, the resonance could also be rather sensitive to the π Ξ interaction during the long-lived hadronic phase. This should be investigated by both π Ξ femtoscopy as well as via direct measurements of Ξ 1530 spectra. While the first signal of the Ξ resonance in heavy ion collision was seen in femtoscopy analysis just two years ago [24], the first preliminary STAR measurements concerning the Ξ spectra and their yields were presented only recently at the Quark Matter conference in Shanghai this year [25].

A. Data selection

Though in previous analyses [5, 11, 12, 24] the π Ξ correlations were studied for two different system d+Au and Au+Au and also at two different energies, in this contribution I will concentrate on Au+Au data at $\sqrt{s_{NN}}$ = 200 GeV from RHIC Run IV only. The data were divided into several centrality classes. During the run, the central trigger was used to enhance the fraction of the 10% most central events. Track-level cuts based on dE dx particle identification in the STAR Time Projection Chamber were used. Pion sample momenta p_t were limited to [0.125, 1.] GeV/c. After the dE dx cuts, the upper p_T-limit was 0.8 GeV/c and 0.6 GeV/c at y 0 and y 0 8, respectively. Charged Ξs were reconstructed topologically in the p_t range [0.7, 3.] GeV/c. To increase the total number of analyzed π Ξ pairs in this analysis we have used a wider rapidity cut than in the previous STAR femtoscopy analyses [26]. The cut y 0 8 instead of y 0 5 was employed for both particle species. Total number of extracted Ξ used in this analysis are given in Table I.

TABLE I: **200 GeV Au+Au, Run IV data set**

Centrality	No. of Ξ		No. of Ξ		No. of Ξ	
0 –10%	1084	10^3	595	10^3	489	10^3
10 – 40%	412	10^3	226	10^3	186	10^3
40 – 80%	145	10^3	79	10^3	66	10^3

B. Data analysis and corrections

The event–mixing technique was used to obtain the uncorrelated two-particle distribution in the pair rest frame. To remove spurious correlations of non-femtoscopic origin, the uncorrelated pairs were constructed from events with sufficient proximity in primary vertex position along the beam direction, multiplicity and event plane orientation variables. Pair cuts were used to remove effects of track splitting and merging. The resulting raw correlation function was then corrected for the purity of both particle species. The correction was performed individually for each bin in $\mathbf{k}$ k $cos\theta$ φ of the 3-dimensional (3D) correlation function as described bellow.

C. Pair purity analysis

The pair purity, defined as a fraction of primary π Ξ pairs, was calculated as a product of the particle purities of both particle species. The Ξ purity was obtained from reconstructed Ξ invariant mass plots as a function of transverse momentum. Pion purity was estimated using the parameter $\bar{\lambda}$ of the standard parametrization of the identical π π correlation function. The identical pion measurements were performed with the same pion cuts as those used in the π Ξ analysis. Since the value of the λ parameter is influenced by decays of long-lived resonances as well as by the non-Gaussian shape of the correlation function, the pion purity correction can be a significant source of systematic error.

In order to make contact with the previous STAR identical pion analyses [26] in Fig. 1, we present the k_T–dependence of parameters λ, R_{out}, R_{side} and R_{long} entering the standard out-side-long decomposition of the 3D correlation function C $\mathbf{q}$ 1 λ exp $q_{out}^2 R_{out}^2$ $q_{side}^2 R_{side}^2$ $q_{long}^2 R_{long}^2$. Here, k_T $\mathbf{p}_{1T}$ $\mathbf{p}_{1T}$ 2 is the average transverse momentum of two pions. On the same figure the ratio R_{out} R_{side} is aso plotted. We conclude that the improved cuts used in the present analysis do not change the values of extracted parameters, but due to the increased acceptance in rapidity and transverse momenta of the pions, our analysis covers also region of lower k_T.

We have also studied the influence of electrons on the purity of the pion sample. Exclusion of pions with dE dx within 2σ around the electron band has changed the value of the parameter λ in the k_T interval [0.15, 0.25] GeV/c by 50% at maximum. However, the other parameters characterizing the 3D correlation function of identical pions (the radii R_{out},R_{side},R_{long}) as well as the π Ξ correlation functions re-

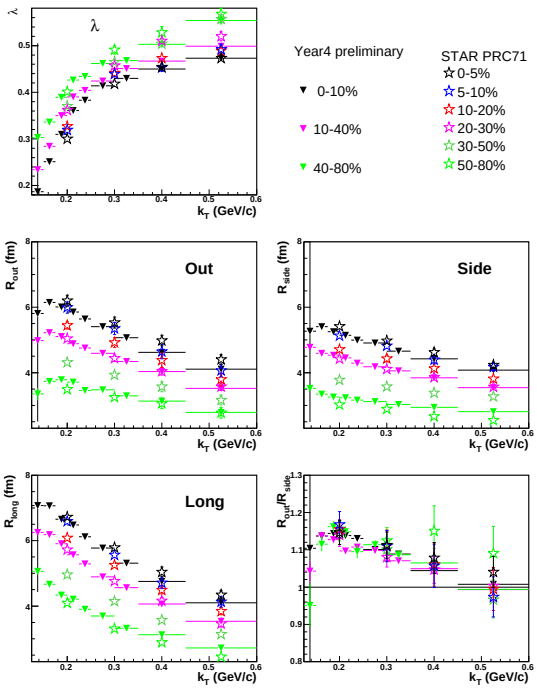

FIG. 1: (Color online) The comparison between parameters of 3D Gaussian fits to the correlation functions of identical charged pions produced in Au+Au collisions at 200 GeV. Previous [26] (open stars) and this analysis (full triangles). Error bars contain only statistical uncertainties.

mained unchanged.

D. Results in 1D source size information

The π Ξ correlation functions $C\ k$ were analyzed in the pair rest frame ($\mathbf{k}$ $\mathbf{p}_\pi$ $\mathbf{p}_\Xi$). The results for unlike sign pairs are presented in Fig. 2.

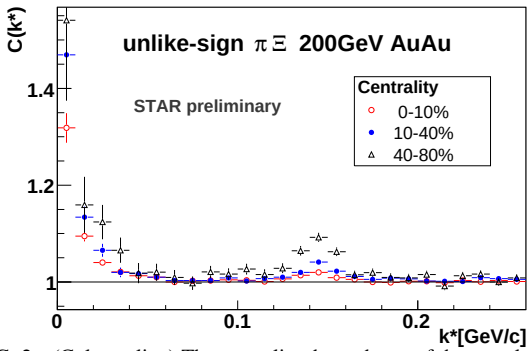

FIG. 2: (Color online) The centrality dependence of the correlation function of the combined sample of unlike-sign π Ξ pairs .

For all centralities, the low k region is dominated by the Coulomb interaction. The strong interaction manifests itself in a peak around k 150 MeV/c corresponding to the Ξ (1530). The peak's centrality dependence clearly shows high sensitivity to the source size. Contrary to the Coulomb region, the correlation function in the resonance region does not suffer from the low statistics and can thus in principle be used to extract sizes of the sources more effectively than in the former case.

E. Results in 3D asymmetry measurement

The information about the shift in average emission points between π and Ξ can be extracted from the angular part of the 3D correlation function C $\mathbf{k}$ $C\ k$ $\cos\theta$ φ .

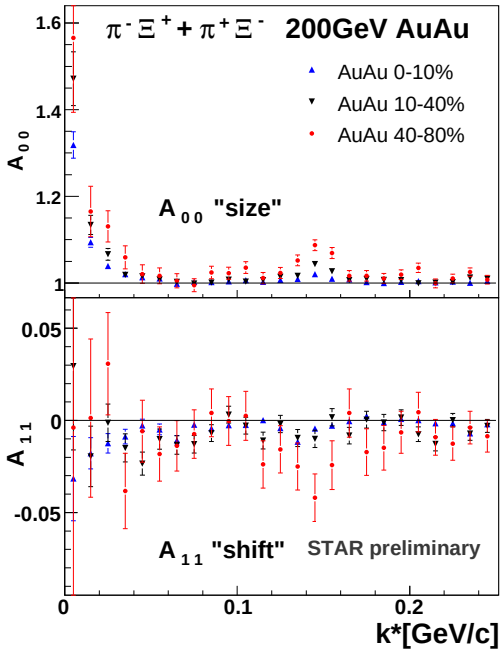

FIG. 3: (Color online) $A_{00}\ k$ and $A_{11}\ k$ coefficients of spherical decomposition for the combined sample of unlike-sign π Ξ pairs from three different centrality bins.

The function is binned in k $\cos\theta$ φ with $\Delta_{\cos\theta}$ $\frac{2}{N_{cos\theta}}$ and Δ_φ $\frac{2\pi}{N_\varphi}$ as the bin sizes in $\cos\theta$ and ϕ, respectively. After its decomposition into spherical harmonics [27],

$$A_{lm}\ k \quad \frac{\Delta_{\cos\theta}\Delta_\varphi}{4\pi} \sum_i^{all\ bins} Y_{lm}\ \theta_i\ \varphi_i\ C\ k\ \cos\theta_i\ \varphi_i \qquad (2)$$

Symmetry further limits the number of relevant components. This is due to the fact that individual coefficients appearing in the above decomposition represent different symmetries of the source. Thus for azimuthally symmetric identical particle source at midrapidity, only A_{lm} with even values of l and m

do not vanish. On the other hand, for non–identical particle correlations the coefficients with odd values of l and m are allowed.

For both cases, the most important coefficient is $A_{00}\ k$ representing the angle-averaged correlation function $C\ k$. The latter is sensitive to the source size only, whereas in the non–identical particle case $A_{11}\ k$ measures a shift of the average emission point in the R_{out} direction.

The decomposition of the correlation function into spherical harmonics was used to study the centrality dependence of asymmetry in emission between pions and Ξs. The results are presented in Fig. 3. The coefficient A_{11} which is non-zero in all centrality bins clearly confirms that the average space-time emission points of pions and Ξ are not the same.

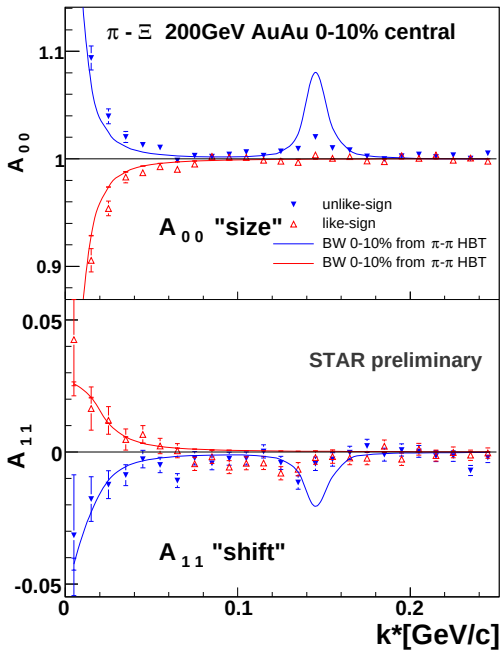

FIG. 4: (Color online) Comparison of $A_{00}\ k$ and $A_{11}\ k$ coefficients of spherical decomposition for combined sample of unlike-sign π Ξ pairs from 10% most central Au+Au collisions with the FSI model predictions.

In Fig. 4 the experimental results for the 10% most central, the highest statistics bin, are compared to a model calculation exploiting strong and Coulomb final state interaction [28].The theoretical correlation function was constructed from the particle emission separation distribution. For this purpose, the momenta of real particles were used. The emission coordinates of both π and Ξ were generated using the blast wave model [18]. This model, encompassing correlation between particle momenta and their space-time coordinates, was used with a single set of parameters for generating emission coordinates of both π and Ξ. These parameters were obtained from experimentally measured pion spectra and π π emission radii. Let us note that using the same set of parameters for the Ξ source as for the pions implicitly assumes significant transverse flow of Ξ. In the Coulomb region, the theoretical correlation function is in qualitative agreement with the data. Moreover, the orientation of the shift and its magnitude agrees with the scenario in which the Ξ participates in the transverse expansion. However, in the region dominated by the strong final state interaction the calculations over predict both the size and the shift coefficients.

F. Extracting the source parameters

For further analysis we have used only the low k region dominated by the Coulomb interaction, excluding thus the region around the Ξ 1530 peak (see Fig. 5).

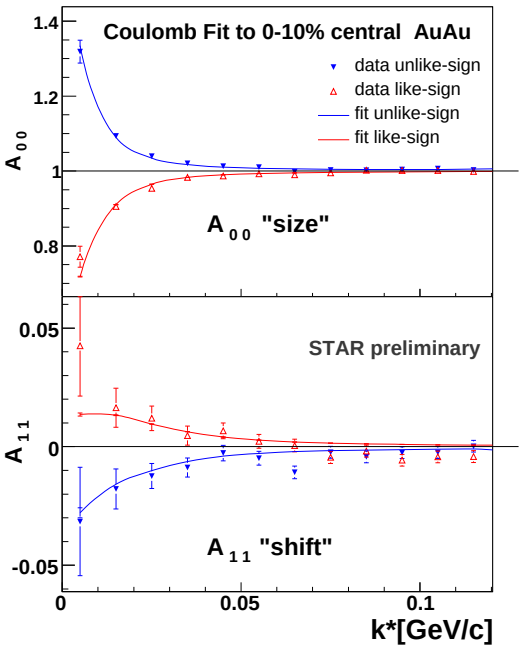

FIG. 5: (Color online) Comparison of $A_{00}\ k$ and $A_{11}\ k$ coefficients from the spherical decomposition of the combined sample of like-sign π Ξ and unlike-sign π Ξ pairs from the 10% most central Au+Au collisions, along with the FSI model predictions.

The theoretical correlation function was calculated using the momentum distribution of pairs extracted from real data. The emission coordinates were randomly generated from the two-parameter source distribution constructed in the following way. For both particle species, the Gaussian shape of their source was assumed with the sources shifted in the R_{out} direction relative to each other. In the pair rest frame this can be expressed via two parameters R and Δ_{out} characterizing the pair separation distribution in Δr . Here, R represents the width of the Gaussian and Δ_{out} represents the shift in the R_{out} direction. Values of the source parameters were then extracted by finding a minimum value of χ^2 between theoretical and real

Brazilian Journal of Physics, vol. 37, no. 3A, September, 2007 929

correlation function. Fitting was done simultaneously for like and unlike–sign correlation functions.

For the most central Au+Au collisions this method yields the first preliminary values of R 6 7 1 0 fm and Δ_{out} 5 6 1 0 fm. The errors are purely statistical. Systematic error studies are under way and their values are expected to be of the order of the statistical ones. In our case a negative value of the shift means that average emission point of Ξ is positioned more to the outside of the whole fire-ball than the average emission point of pion as expected in the Ξ flow scenario.

III. IDENTICAL PION CORRELATIONS

A. Motivation

In ultra–relativistic heavy–ion collisions femtoscopy can also be employed to extract information related to the strong interaction among the particles [3, 10]. In recent STAR analyses the strong FSI was studied via two–K_s^0 interferometry [29] and in proton-lambda correlations [30]. A model that takes the effect of the strong interaction into account has been used to fit the measured correlation functions. In the p $\overline{\Lambda}$ and $\overline{p}$ Λ correlations, which were actually measured for the first time, annihilation channels and/or a negative real part of the spin-averaged scattering length was needed in the FSI calculation to reproduce the measured correlation function.

At the previous WPCF meeting an ambitious proposal to exploit the correlations among identical charged pions to extract pion-pion scattering lengths was made [8]. The potential for such measurements at RHIC, and also later at the LHC stems from the fact that, compared to a dedicated particle physics experiments measuring scattering lengths parameters a_0^0 and a_0^2 like BNL-E865 [31] or Dirac [32], heavy ion experiments provide a much larger number of pion pairs at small relative momenta in a single event plus very large data samples (10^7 10^9 events). The real challenge when studying the strong interaction among identical charged pions then is to beat down all systematical errors pertinent to the ultra–relativistic heavy ion collisions environment. Coulomb interaction, pion purity and geometry of the pion source need to be kept under control. Varying the source size (k_T or centrality) may provide a good handle on this.

In particular, the bias arising from the frequently used Gaussian assumption of the source shape needs to be addressed. Using the high statistics sample of Au+Au events from the STAR experiment at RHIC's highest energy accumulated during the run IV, it was found that for all k_T and centrality bins the Lévy stable source parametrization does not bring an advantage in describing the detailed shape of measured three-dimensional correlation function [6].

The next step in this direction is to exploit the model-independent imaging technique of Brown and Danielewicz [33, 34] and reconstruct the source itself. This is done via inverting Koonin-Pratt equation (see e.g. [1]):

$$C\ q \quad 1 \quad 4\pi \quad K_0\ q\ r\ S\ r\ r^2 dr$$

$$K_0\ q\ r \quad \frac{1}{2} \quad \Phi\ \mathbf{q}\ \mathbf{r}\ ^2 \quad 1\ d\ cos\theta_{\mathbf{q}\ \mathbf{r}}$$

$$q \quad \frac{1}{2} \quad \overline{p_1 \quad p_2\ ^2} \qquad (3)$$

which expresses the 1D correlation function $C\ q$ in terms of the probability $S\ r$ to emit a pair of particles at a separation r in the c.m. frame. $S\ r$ is usually called the source function. All FSI is encoded in the (angle averaged) final state wave function $\Phi\ \mathbf{q}\ \mathbf{r}$ describing the propagation of the pair from a relative separation of $\mathbf{r}$ in the pair c.m. to the detector with relative momentum $\mathbf{q}$. The angle between vectors $\mathbf{q}$ and $\mathbf{r}$ is denoted by $\theta_{\mathbf{q}\ \mathbf{r}}$. The procedure to extract $S\ r$ via inversion of Eq. 3 is given in [34].

B. Testing the inversion procedure

To test reproducibility of he original source function by the imaging procedure we have generated Bose-Einstein (B-E) correlated and Coulomb interacting pion pairs. The momentum spectra of the pions were obtained from the 10% most central Au+Au RQMD generated events at $\overline{s_{NN}}$=200 GeV. The pions coordinates were randomly sampled from an isotropic 3D Gaussian distribution with the radius R=5 fm. The instantaneous emission $\delta\tau$=0 of particles was assumed. Using pion momenta and their coordinates the B-E correlations and Coulomb FSI were introduced using the procedure described in [36]. Results for correlations and source functions are displayed on Fig. 6. In order to compare with the input Gaussian source the extracted source function was fitted with the Gaussian distribution again:

$$g\ r\ R \quad \frac{\lambda}{2\ \overline{\pi} R^{\ 3}} e^{\ \frac{r^2}{4R^2}} \qquad (4)$$

Let us note that the r^2-weighting of $S\ r$ appearing in the normalization condition of the source function:

$$4\pi \int_0^\infty S\ r\ r^2 dr \quad \lambda \qquad (5)$$

makes the normalization constant λ more sensitive to the behavior of $S\ r$ at r R than one would naively expect. Since the latter is determined by the imaging from values of the correlation function $C\ q$ at very small q, fulfilment of the above normalization condition using data with limited statistics in the low q bins may be hard to achieve. This may explain why values of the extracted parameters R and λ from the single-Gaussian fit were found to be smaller than the input ones. While for R the discrepancy is about 4% for λ it is almost 25%.

C. 1D imaging analysis of the pion source from Au+Au and Cu+Cu collisions

The same data set of Au+Au events from Run IV, used in the previously described π Ξ correlation analysis, was also

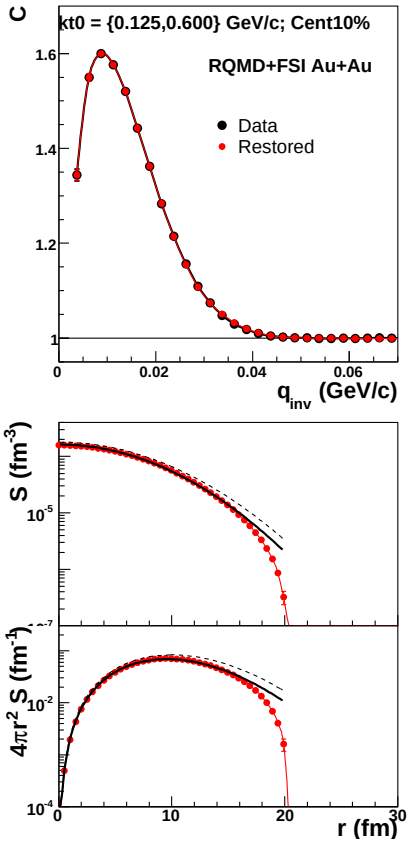

FIG. 6: (Color online) The 1D imaging analysis of an isotropic Gaussian source using pion momentum spectra from RQMD simulating the 10% most central Au+Au collisions at $\sqrt{s_{NN}}$ =200 GeV. Top: original (black filled circles) and restored by imaging technique (red filled circles) correlation function $C\ q$. To guide the eye the data points are connected by a smooth line of the same color. Middle: 1D source function $S\ r$ (red filled circles). The full black line represents the result of a single-Gaussian fit to $S\ r$, dashed line - input Gaussian distribution. Bottom: $4\pi r^2 S\ r$.

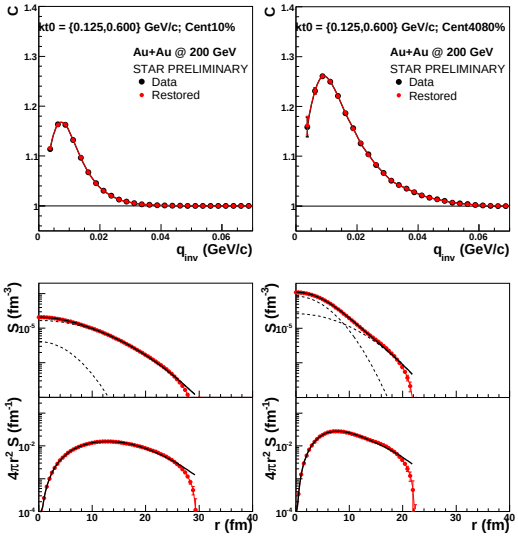

FIG. 7: (Color online) 1D imaging analysis of identical charged pions from Au+Au collisions at $\sqrt{s_{NN}}$ =200 GeV. Results are shown for the 10% most central (the left panel) and for peripheral(centrality 40-80%) collisions (the right panel). Top: the measured correlation function C(q) (black filled circles), restored correlation function from imaging technique (red filled circles). To guide the eye the data points are connected by a smooth line of the same color. Middle: 1D source function $S\ r$ (red filled circles). The full black line represents the result of a double-Gaussian fit to $S\ r$. Two dashed lines show contribution of each of two Gaussians. Bottom: $4\pi r^2 S\ r$: (red filled circles). Full black line represents result of a double-Gaussian fit.

used for the reconstruction of the pion source. The second data set employed in the imaging analysis consists of about 8 million Cu+Cu minimum bias events at $\sqrt{s_{NN}}$=200 GeV accumulated during the Run V. Selected results from 1D imaging analysis of the pion source using centrality selected Au+Au and Cu+Cu events are displayed on Fig. 7 and 8, respectively.

Compared to the model example discussed in the previous paragraph the extracted source functions now develop long tails [35] and cannot thus be described by a single Gaussian distribution. The only exception are the data from the 10% most central Au+Au collisions (Fig. 7.) To account for the observed behavior we use the simplest extension of Eq. 4 and assume that the source function contains contributions from two Gaussians. While the first Gaussian $g\ r\ R_1$ contributing with fraction $1\quad\alpha$ is responsible for the long tails the second one $g\ r\ R_2$ contributing with weight α of width the $R_2\quad R_1$ describes the source function at small r. The double Gaussian distribution:

$$G\ r\ R_1\ R_2\qquad 1\quad\alpha\ g\ r\ R_1\qquad\alpha g\ r\ R_2\quad R_1\qquad R_2 \tag{6}$$

now seems to describe data quite well. Comparing Au+Au to Cu+Cu collisions of the same centrality we conclude that the long tails are more pronounced for the smaller system.

All source functions presented so far were obtained from data integrated over the whole range of average pair transverse momenta k_T= [0.125, 0.600] GeV/c). In the following I will present results showing how much the observed departure from a single Gaussian shape depends on particle transverse momenta.

Such an analysis was performed and is displayed in Figs. 9-11. While for Au+Au collisions the statistics allowed us to use 9 bins in k_T for Cu+Cu we have used only 4 bins. In Fig. 9 the lowest k_T= [0.125, 0.250] GeV/c and the highest k_T= [0.450, 0.600] GeV/c bins from Cu+Cu 10% most central collisions are compared. We see that the long tail present in the lowest k_T bin, which is characterized by the Gaussion with the width $R\quad 7$ fm, completely disappears from the highest k_T bin.

Figures 10 and 11 show the k_T-dependence of the double Gaussian fit parameters for Cu+Cu and Au+Au collisions at three different centralities. We observe that with increasing k_T, the contribution of the second Gaussian is less and less

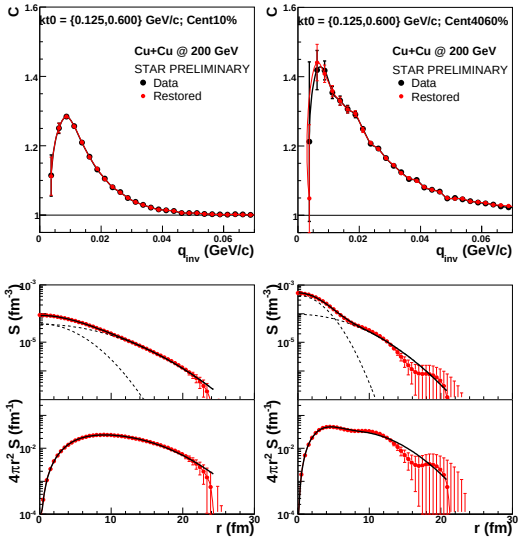

FIG. 8: (Color online) 1D imaging analysis of identical charged pions from Cu+Cu collisions at $\sqrt{s_{NN}}$ =200 GeV. Results are shown for the 10% most central (the left panel) and for peripheral (centrality 40-60%) collisions (the right panel). Top: C(q). Middle: 1D source function $S\ r$. Bottom: $4\pi r^2 S\ r$. Labels are same as on Fig. 7.

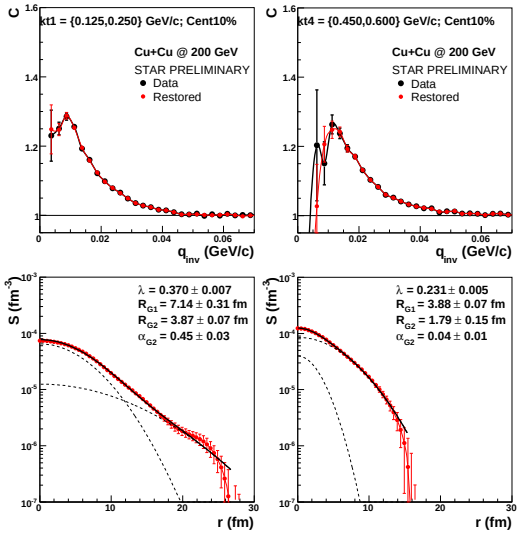

FIG. 9: (Color online) The 1D imaging analysis of identical charged pions from the 10% most central Cu+Cu collisions at $\sqrt{s_{NN}}$=200 GeV. Results are shown for the lowest (the left panel) and for the highest (the right panel) k_T-bin. Top: correlation function C(q). Middle: 1D source function $S\ r$ Bottom: $4\pi r^2 S\ r$. Labels are same as on Fig. 7.

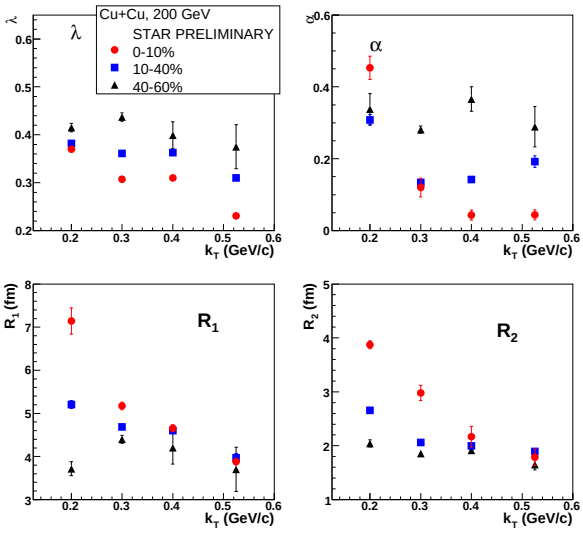

FIG. 10: (Color online) The k_T-dependence of source parameters of identical charged pions from Cu+Cu collisions at $\sqrt{s_{NN}}$=200 GeV taken at three different centralities: 0-10% - full red circles, 10-40% - full blue squares, 40-60% - full black triangles.

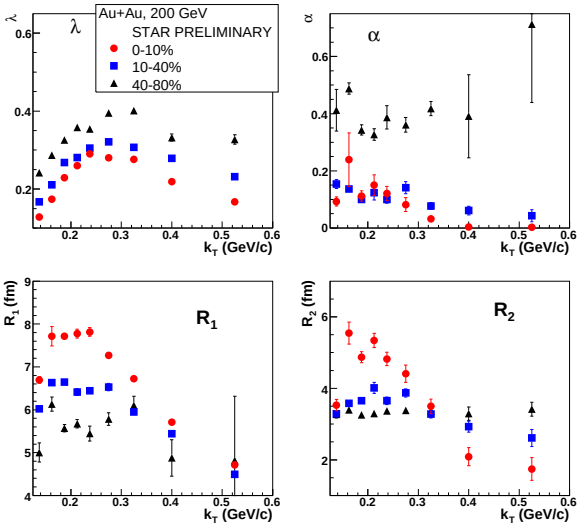

FIG. 11: (Color online) The k_T-dependence of source parameters of identical charged pions from Au+Au collisions at $\sqrt{s_{NN}}$=200 GeV taken at three different centralities: 0-10% - full red circles, 10-40% - full blue squares, 40-80% - full black triangles.

prominent. This behavior is more pronounced in Cu+Cu collisions. Let us note that the long tails observed in the low-k_T bins may then indicate an important role played by the pions from long-lived resonance decays. An interesting observation which may have some relevance to the observed behavior regarding the random walk nature of particle freeze-out in coordinate space was made by T. Csörgő at this meeting [37].

IV. SUMMARY

High-statistics STAR data from Au+Au and Cu+Cu collisions taken at full RHIC energy and three different centralities were used to discuss recent progress in identical (π π) and non-identical (π Ξ) particle femtoscopy. In the π Ξ system the strong and Coulomb-induced FSI effects were observed, making it possible for the first time to estimate the average shift and width between π and Ξ source. The 1D imaging of the identical pion source reveals a significant departure from a single Gaussian shape. The observed long tails, which could be fairly well described by allowing for the second Gaussian, are more pronounced for the sources produced at large impact parameters. The effect is stronger for Cu+Cu than for Au+Au collisions. For all centralities and both colliding systems the highest departure from a single Gaussian shape is observed for sources emitting particle with a small average pair transverse momenta k_T. For the highest analyzed k_T the source is to a good approximation a single Gaussian.

Acknowledgements

This work was supported in part by the IRP AV0Z10480505 and by GACR grants 202/04/0793 and 202/07/0079. The data analysis was performed by Michal Bysterský and Petr Chaloupka as a part of their Ph.D. thesis work. I would like to thank to both of them for important input to my talk. My gratitude goes also to the organizers of this excellent meeting, in particular to Sandra Padula.

[1] M. A. Lisa, S. Pratt, R. Soltz, and U. Wiedemann, Ann. Rev. Nucl. Part. Sci. **55**, 357 (2005) [arXiv:nucl-ex/0505014].
[2] Proc. XXXV Int. Symp. on Multiparticle Dynamics (ISMD 2005), Kroměříž, Czech Republic, August 9-15, 2005 and of the Workshop on Particle Correlations and Femtoscopy (WPCF 2005), Kroměříž, Czech Republic, August 15-17, 2005. Edited by V. Šimák, M. Šumbera, Š. Todorova, B. Tomášik, AIP Conference Proceedings 828 (2006), ISBN 0-7354-0320-1.
[3] R. Lednický, ibid, p. 423 (2006).
[4] M. Lisa, ibid, p. 226 (2006).
[5] P. Chaloupka, ibid, p. 610 (2006).
[6] M. Bysterský, ibid, p. 205 (2006) [arXiv:nucl-ex/0511053].
[7] R. Lednický, Proc. CIPPQG'01, Palaiseau, France, arXiv:nucl-th/0112011; Phys. Atom. Nucl. **67**, 72 (2004).
[8] M. Bysterský and F. Retiere: "Measuring scattering length at STAR," unpublished talk at WPCF 2005. Available at http://www.particle.cz/conferences/wpcf2005/talks/retiere.ppt.
[9] Proc. 18th Int. Conf. on Ultra-Relativistic Nucleus-Nucleus Collisions, Budapest, Hungary, 4-9 August, 2005, edited by T. Csörgő, G. Dávid, and P. Lévai, Nucl. Phys. A **774** (2006).
[10] R. Lednický, ibid, p. 189 (2006).
[11] P. Chaloupka, ibid, p. 603 (2006).
[12] P. Chaloupka, Proc. SQM 2006 Int. Conf on Strangeness in Quark Matter, University of California Los Angeles, March 26-31, 2006, edited by K. Barish, H. Z. Huang, J. Kapusta, G. Odyniec, J. Rafelski, and C. A. Whitten Jr., J. Phys. G **32**, S537 (2006).
[13] J. Adams *et al.* [STAR Collaboration], Nucl. Phys. A **757**, 102 (2005).
[14] B. I. Abelev *et al.* [STAR Collaboration], arXiv:nucl-ex/0607012.
[15] J. Adams *et al.* [STAR Collaboration], Phys. Rev. Lett. **95**, 122301 (2005).
[16] D. Molnar and S. A. Voloshin, Phys. Rev. Lett. **91**, 092301 (2003), R. J. Fries, B. Muller, C. Nonaka, and S. A. Bass, Phys. Rev. Lett. **90**, 202303 (2003).
[17] J. Adams *et al.* [STAR Collaboration], arXiv:nucl-ex/0606014.
[18] F. Retiere and M. A. Lisa, Phys. Rev. C **70**, 044907 (2004).
[19] R. Lednicky, V. L. Lyuboshits, B. Erazmus, and D. Nouais, Phys. Lett. B **373**, 3034 (1996).
[20] C. Nonaka and S. A. Bass, Phys. Rev. C **75**, 014902 (2007).
[21] U. W. Heinz, J. Phys. G **31**, S717 (2005).
[22] C. Blume *et al.* [NA49 Collaboration], Nucl. Phys. A **715**, 55 (2003).
[23] J. Adams *et al.* [STAR Collaboration], Phys. Rev. Lett. **91**, 262302 (2003).
[24] P. Chaloupka [STAR Collaboration], Nucl. Phys. A **749**, 283 (2005).
[25] R. Witt, talk at 19th Int. Conf. on Ultra–Relativistic Nucleus–Nucleus Collisions, Shanghai, China, November 14-20, 2006, arXiv:nucl-ex/0701063.
[26] J. Adams *et al.* [STAR Collaboration], Phys. Rev. C **71**, 044906 (2005).
[27] Z. Chajecki, T. D. Gutierrez, M. A. Lisa, and M. Lopez-Noriega [the STAR Collaboration], arXiv:nucl-ex/0505009.
[28] S. Pratt and S. Petriconi, Phys. Rev. C **68**, 054901 (2003).
[29] B. I. Abelev [STAR Collaboration], Phys. Rev. C **74**, 054902 (2006); S. Bekele and R. Lednicky, "Neutral Kaon Correlations in $\sqrt{s_{NN}}$ 200 GeV Au+Au collisions at RHIC", Proc. WPCF 2006.
[30] J. Adams *et al.* [STAR Collaboration], arXiv:nucl-ex/0511003.
[31] S. Pislak *et al.* [BNL-E865 Collaboration], Phys. Rev. Lett. **87**, 221801 (2001).
[32] B. Adeva *et al.* [DIRAC Collaboration], Phys. Lett. B **619**, 50 (2005).
[33] D. A. Brown and P. Danielewicz, Phys. Lett. B **398**, 252 (1997).
[34] D. A. Brown and P. Danielewicz, Phys. Rev. C **57**, 2474 (1998).
[35] S. S. Adler *et al.* [PHENIX Collaboration], arXiv:nucl-ex/0605032.
[36] R. Lednický and V.L. Lyuboshitz, Yad. Fiz. **35**, 1316 (1982) [Sov. J. Nucl. Phys. **35**, 770 (1982)]. Fortran program provided by R. Lednický.
[37] M. Csanad, T. Csörgő, and M. Nagy, arXiv:hep-ph/0702032.

5.2.3 Conference presentations

1. M. Šumbera,$\pi - \Xi$ *Correlations at RHIC*. Invited talk at 47^{th} WORKSHOP OF THE INFN ELOISATRON PROJECT "Physics of Hadronic Interactions at LHC with Nucleons and Nuclei and Phase Transition Physics" THE 1st PHYSICS ALICE WEEK, Erice, Italy, 4.-10.12. 2005.

2. M. Šumbera, *Selected results on Strong and Coulomb-induced correlations from STAR experiment*. Invited talk at II Workshop on Particle Correlations and Femtoscopy - WPCF 2006. *SãoPaulo*, Brasil, 9. -11.9.2006.

3. M. Šumbera, *Femtoscopy with exotic species*. Invited talk at III Workshop on Particle Correlations and Femtoscopy - WPCF 2007. Santa Rosa, California, 1.-3.8.2007.

5.2.4 Further developments

In [245] predictions of hydrodynamics-parametrized statistical hadronization model HYDJET++ were compared with the above $\pi-\Xi$ femtoscopic data. It was demonstrate how decay of resonances and collective flow affect shift between the average freeze-out space-time points of Ξ and π. To determine influence of the freeze-out on this shift different freeze-out scenaria were studied: single freeze-out at $T_{th} = T_{ch} = 165$ MeV; thermal freeze-out at $T_{th} = 100$ MeV and combined scenario when Ξ and $\Xi^*(1530)$ are emitted at chemical freeze-out while all other particles are emitted at the thermal freeze-out. Results of performed analysis sems to indicate that the best description of transverse momentum spectra and space-time differences is achieved within the combined scenario. The theoretical analysis is still in progress [246].

5.3 Experiment ALICE

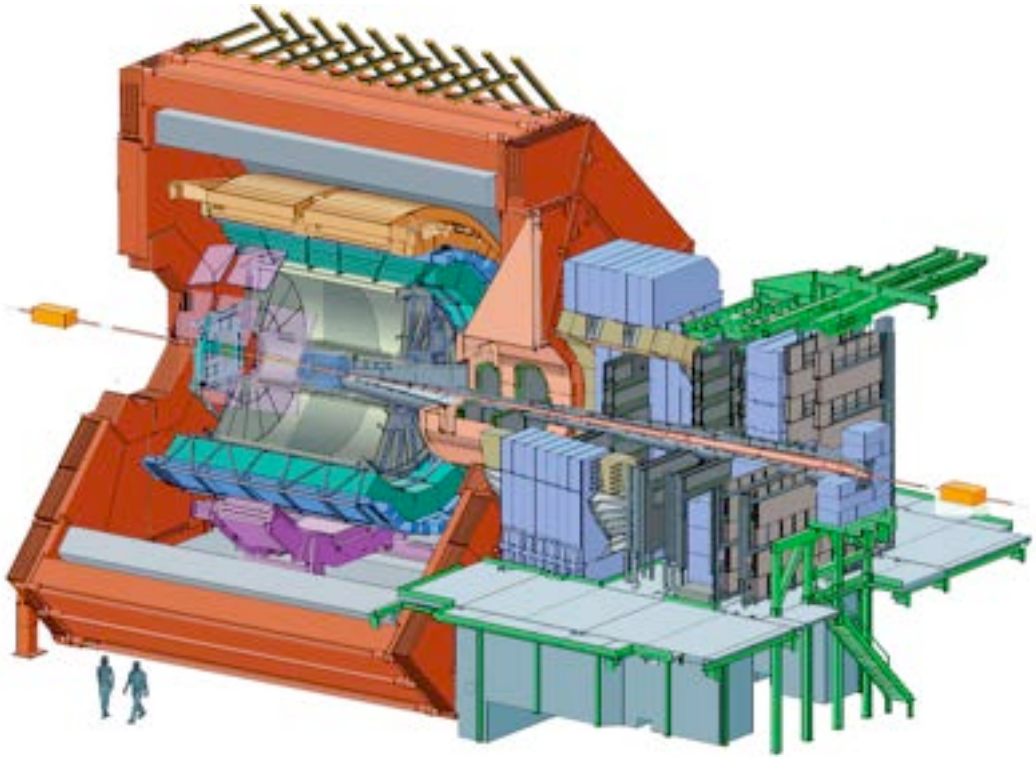

Figure 5.2: Cutaway side view of the **A** **L**arge **I**on **C**ollider **E**xperiment (ALICE) detector [238]. The Inner Tracker System (ITS), a large volume TPC, electromagnetic calorimeters EMCal and PHOS surrounded by the time-of- flight and transition radiation detectors (TOF and TRD) are all embeded into solenoidal L3 magnet (outer diameter 16m) with a uniform magnetic field of maximum value 0.5 T. The forward muon arm (right) exploiting a large dipole magnet with a 3 Tm field is placed outside the L3 magnet.

5.3.1 Introductory notes

ALICE is a dedicated heavy-ion experiment to exploit the unique physics potential of nucleus-nucleus interactions at Large Hadron Collider (LHC) at CERN. Its aim is to study the physics of strongly interacting matter at extreme energy densities, where the formation of a new phase of matter, the quark-gluon plasma, is expected. First discussion of This more than a decade old article represents one of the first reviews of ultra-relativistic heavy ion program at Large Hadron Collider (LHC). It is based in part on the material contained in "Letter of Intent for A Large Ion Collider Experiment" [227] published just one year earlier. Later on, in 1995, " A L I C E Technical Proposal for A Large Ion Collider Experiment at the CERN LHC" was published [229] and was followed by various Technical Design Reports of its different sub-systems (see e.g. [232], [233], [234]). Current status of ALICE physics capabilities is described in two volume "Alice: Physics Performance Report" [236]. Recent description of the ALICE detector can be found in [238].

The ALICE detector was ready for the first LHC beams by the end of 2007. However at the time of writing this thesis even the proton beams have not arrived yet. According to the original scenario [228] the accelerator had to be be build as a 2-stage project. The first stage consists of particle collider with an energy of 10 TeV ready to start in 2004. By 2008 the accelerator was planned to be upgraded by adding additional magnets to reach the final c.m.s. energy 14 TeV. Since then the LHC design and also its time schedule went through the several modifications [236] but as of now (summer 2009) it appears that the first p+p collisions will take place this fall. Due to the superconducting magnet malfunctioning the energy will be not 14 TeV but 7 TeV.

Article reprint

EXPERIMENT ALICE*)

M. ŠUMBERA

Nuclear Physics Institute, ASCR, 250 68 Řež, Czech Republic

Received 16 March 1995

An overview of A Large Ion Collider Experiment (ALICE) at the Large Hadron Collider (LHC) at CERN is given. After a brief description of the LHC serving as an accelerator of the heavy ions physical goals of the ALICE are discussed. Later range from "standart" Quark Gluon Plasma physics through the large cross section pp physics to the physics which can be done with two intensive beams of nearly real photons. The review is completed by discussion of the main detector components.

Contents

1 Introduction

Statistical QCD predicts that, at sufficiently high energy density, there will be a transition from a normal color-confined phase of hadronic matter to a plasma of deconfined quarks and gluons. The same transition which in the early universe took place in the inverse direction some 10^{-5}s after the Big Bang and which might play a role still today in the core of collapsing neutron stars. The experimental programs at the future heavy ion (AA) colliders, the BNL Relativistic Heavy Ion Collider (RHIC) and the CERN Large Hadron Collider (LHC), which will come into operation around the turn of the century, will provide for the first time the opportunity to study nuclear matter under such extreme energy density and very high temperatures.

At the RHIC two independent rings with 3.45 T superconducting magnets located in the existing 3.8 km tunnel of the earlier abandoned ISABELLE/CBA

*) Invited lecture given at the International School-Workshop "Relativistic Heavy-Ion Physics", Prague (Czech Republic), 19–23 September 1994.

project will allow collisions between different nuclei, including protons, at a top energy of $(250 \times Z/A)$ GeV/n, i.e. up to a c.m.s. energy of 500 GeV for p+p and 200 GeV for Au+Au. 9 T superconducting magnets of the LHC, which will be located in the 27 km long LEP tunnel, will provide a maximum energy of $(7 \times Z/A)$ TeV/n, i.e. a c.m.s. energy of 14 TeV for p+p and 5.5 TeV/n for Pb+Pb. The RHIC being a dedicated collider machine for ultra-relativistic AA collisions have six interaction regions available for experiments, out of which four have been assigned for the initial set of experiments - two with large detectors (STAR and PHENIX) and two smaller ones (PHOBOS and BRAHMS). On the LHC only one dedicated heavy ion detector (ALICE) is foreseen. Later it is supposed to share its running time with dedicated pp detectors (ATLAS, CMS) which are optimized for physics differing by several orders of magnitude in event rate, multiplicity and p_t. Since planned experiments at the RHIC are described in the other lecture of this school [1] in the following I will confine myself to discussion of the LHC experiment ALICE only. However, when appropriate I will use parameters of the RHIC machine for comparison.

2 The LHC as a heavy ion accelerator

The crucial quantity entering the design of every collider experiment is the available luminosity L:

$$L = f\gamma \frac{N^2 k}{4\pi\epsilon\beta^*}\,, \tag{1}$$

where f is the revolution frequency, γ is the Lorentz factor of the beam, ϵ is the emittance, β^* is the betatron function at the collision point, k is a number of bunches and N is a number of particles per bunch. Since the event rate for a certain process is given by its cross section times the luminosity, the possibility of studying rare phenomena depends on the maximum luminosity accessible. At the same time the rate of background processes, which in general have large cross sections, will increase L, reaching at some point the maximum event rate that the experiment can handle.

These effects limit the luminosity half-life via the loss of ions in the bunch. The decay rate λ_T is given by the formula:

$$\lambda_T = -\frac{1}{N}\frac{\mathrm{d}N}{\mathrm{d}t} = \frac{N_{IR} L \sigma_T}{kN} \tag{2}$$

in which N_{IR} is the number of interaction regions and σ_T is the total cross section for the electromagnetic effects. Substitution for L from (1) into the last equation yields

$$\lambda_T \propto N\sigma_T\,. \tag{3}$$

The maximum number N of ions per bunch then follows from the requirement of the luminosity half-life and from the value of σ_T.

2.1 Electromagnetic excitation in ultra-relativistic heavy ion collisions

Discussing constraints imposed by the machine on the experiment with heavy ions, it may come first as a surprise to see that at LHC these background processes are no more due to the strong interactions — with a characteristic dependence of the nuclear interaction cross section on a number of nucleons $A_{\mathrm{I,II}}$ in colliding nuclei I and II

$$\sigma_{\mathrm{R}} = \pi r_0^2 (A_{\mathrm{I}}^{1/3} + A_{\mathrm{II}}^{1/3} - \delta)^2 \quad \text{with} \quad r_0 \approx 1.35\,(\mathrm{fm}) \quad \text{and} \quad \delta \approx 1.1 \tag{4}$$

— but are solely due to the coherent action of all charges in a nucleus. A classical description of this phenomenon dates back to Fermi [5], Weizsäcker [6] and Williams [7] and is known as a method of equivalent photons or Weizsäcker-Williams approximation (WWA). It is based on the equivalence between the perturbative action of the field of fast moving charged particle and flux of electromagnetic radiation, or more properly, momentum of the radiation represented as a spectral decomposition into virtual photons. This equivalence is true as far as the effects caused by different spectral components add up incoherently, i.e., perturbation caused by the fields is small enough.

The solution for the time-dependent electromagnetic fields mutually seen by the two ions can be found, for example, in the textbook on 'Classical Electrodynamics' [8]. The longitudinal ($\|$) and transversal ($\perp$) field components, induced by a heavy ion I passing a target II at distance b and with velocity β are given by formula:

$$\begin{aligned} E_{\|}(t) &= \frac{-Z_{\mathrm{I}} e \gamma \beta t}{(b^2 + \gamma^2 \beta^2 t^2)^{3/2}}\,, \\ \vec{E}_{\perp}(t) &= \frac{Z_{\mathrm{I}} e \gamma \vec{b}}{(b^2 + \gamma^2 \beta^2 t^2)^{3/2}}\,, \\ B_{\|}(t) &= 0; \quad \vec{B}_{\perp}(t) = \vec{\beta} \times \vec{E}_{\perp}\,. \end{aligned} \tag{5}$$

Let us note that for $\gamma \gg 1$ these fields act on a very short time scale of order $\Delta t \approx b/\gamma c$. During this time fields $\vec{E}_{\perp}(t)$ and $B_{\perp}(t)$ are *equivalent* to linearly polarized pulse $P_{\|}$ of radiation incident on a target in the beam direction. Thus according to the equivalent photon method, the strong and rapidly time varying field of the point charge Z_{I} is seen by a passing charge as a flux of virtual (nearly real) photons with intensity

$$I(\omega, b) = \frac{c}{4\pi} |\vec{E}(\omega) \times \vec{B}(\omega)| \approx \frac{c}{2\pi} |E_{\perp}(\omega)|^2 \sim Z_{\mathrm{I}}^2\,, \tag{6}$$

where $\vec{E}(\omega)$, $\vec{B}(\omega)$ and $E_{\perp}(\omega)$ are fourier components of the fields $\vec{E}$, $\vec{B}$ and $E_{\perp}$. The energy spectrum of these photons falls as $\propto 1/E_{\gamma}$ up to a maximum energy

$$E_{\gamma}^{\max} = \hbar \gamma c / b_{\min}\,. \tag{7}$$

The interaction between colliding nuclei becomes dominantly electromagnetic for impact parameters b exceeding the size of the radii of colliding nuclei

$$b > b_{\min} = R_{\mathrm{I}} + R_{\mathrm{II}} \approx \sqrt{\sigma_{\mathrm{R}}/\pi}\,. \tag{8}$$

Returning back to the case of heavy ions at the LHC let us note that the most important background electromagnetic processes here are the creation of e^+e^- pairs with subsequent e^- atomic shell capture (ec) and electromagnetic dissociation (ed) of the ion due to the field of another one passing close to it. At the LHC energies $\sigma_{ec} = 106(Z/82)^7$ barns and $\sigma_{ed} = 180(Z/82)^{10/3}$ barns [9]. The coherence shows up in a very strong dependence on the charge Z of the ions. For the Pb ions where electromagnetic processes are dominant limiting factor on the luminosity one gets in total $\sigma_{ec}+\sigma_{ed} \approx 300$ barns which is well above value $\sigma_R^{Pb+Pb} \approx 6$ barns calculated from equation 4. The corresponding maximum number N is 9.4×10^7 ions/bunch.

3 Physics with ALICE

Being the only one dedicated AA detector foreseen at the LHC, ALICE — A Large Ion Collider Experiment [2] — is designed to be a general-purpose experiment, aiming at a comprehensive study of hadrons, electrons, and photons produced in the collisions of heavy nuclei, up to the highest particle multiplicities anticipated at the LHC. In addition to the program with heavy ions ALICE's physics agenda includes also a study of photon-photon reactions and a number of large cross-section pp processes not accessible to the dedicated pp experiments.

3.1 Heavy ion collisions

The aim of heavy ion physics programme will be the study of strongly interacting matter at extreme energy densities. Contrary to the RHIC various different approaches to search for the QGP must be integrated into a design of a single heavy ion experiment at the LHC. On the other hand the energies available at the LHC will provide a significantly *better* environment for QGP studies than at lower energies. Table 1 from [11] which is based on a survey of a large amount of models and predictions gives a summary of some of the relevant parameters for central Pb+Pb collisions. One can see that the system created in nuclear collisions at the LHC will be *hotter, bigger and longer-lived.*

As a consequence of the high multiplicities achieved in central nucleus-nucleus collisions (see Table 1) many important quantities characterizing highly excited matter will be available on *event-by-event* basis. Let us note that at today's heavy ion accelerators (SPS or AGS) one can measure only the *ensemble average* of many individual events with similar initial conditions (e.g. similar impact parameter). However, *different* scenaria of hadronic to QGP phase transition may lead to nearly identical *average* values of observables but will generally differ in their *fluctuations* around this average. Let us give some examples.

- Slope parameter T_0 extracted from the transverse momentum distributions of pions and kaons in individual events will make it possible to characterize separate events by their 'temperature'. Events with extremely high temperature which are predicted [14] to result from deflagration of QGP will be easily identified.

Table 1. Comparison between SPS, RHIC and LHC predictions for central Pb+Pb collisions: $\mathrm{d}N/\mathrm{d}y$ — charged particle multiplicity; ϵ — energy density (assuming $\tau_0 = 1$ in all cases); V_f — final volume at freeze-out; τ_0 — formation (thermalization) time; τ_c — time spend in QGP phase. For a number of these parameters, the average *relative increase* compared to the SPS is shown in a separate row (i.e., SPS numbers are one by definition).

	$\sqrt{s}$ (GeV/u)	$\frac{\mathrm{d}N}{\mathrm{d}y}$	ϵ (GeV/fm^3)	V_f (fm^3)	τ_0 (fm/c)	τ_c (fm/c)	$\frac{\tau_c}{\tau_0}$
SPS	17	500–800	1.7–2.7	$\approx 10^3$	≥ 1?	≤ 1?	
			1	**1**		**1**	**1**
RHIC	200	700–2000	2.3–6.8	$\approx 7 \times 10^3$	≤ 1?	1.5–4	
			2	**7**		**3**	**5**
LHC	5500	3000–8000	8.0–27	$\approx 2 \times 10^4$	≤ 0.2?	4–11	
			7	**20**		**7**	$\geq$ **30**

- A measurement of K/π ratio provides information on relative concentration of strange and nonstrange quarks. Events with extremely large K/π ratio will be good candidates for the formation of QGP where enhanced strangeness production results from chemical equilibrium of quarks and gluons.
- Correlations between identical bosons will allow to determine source parameters and thus provide information on event freeze-out geometry and its expansion dynamics.
- Fluctuations in particle ratios, energy density, entropy density and flow of different particle species as a function of transverse momentum, rapidity and azimuthal angle. These fluctuations may result from the process of hadronization of a QGP [15].

3.2 Large cross section pp and pA physics

Soft and semi-hard pp and pA collisions at the LHC besides serving as a comparison data for a heavy ion program represent an interesting subject in itself. Let us note that particles produced in these collisions will spread more or less uniformly over a kinematic range of some 20 units of pseudorapidity, from $-10 < \eta < 10$. In order to exploit the physics potential of this region fully, it is important to extend ALICE coverage over this entire kinematic range. Physics agenda of such *a full acceptance detector* is vast, and largely orthogonal to that of the planned major pp detectors which focus on rare, high p_t processes. It consists of study of the following subjects:

- Measurement of elastic scattering and total cross-section.
- Study of soft diffraction (Pomeron exchange) including single and double diffraction.

- Measurement of the rapidity distributions of heavy flavours, jets and gauge bosons in diffractive events. In the scenario where the Pomeron is regarded as a real particle this will make it possible to determine its gluon and quark structure functions.

- Measurement of the inclusive distribution of forward reaction products and studies of leading particles. Some strange phenomena, seen in cosmic rays, may find a natural explanation if the energy flow in the far-forward region is better understood.

- Study of meson-meson and meson-nucleon interactions via leading particle tags.

- Study of the fractal nature of QCD phase space and the onset of color-coherence effects via analysis of multi-jet global patterns and of jets-within-jets.

- Pattern analysis, including the search for disoriented chiral condensate and related phenomena, and other correlation studies of multi-particle production.

As an example let us discuss in more detail study of states containing *rapidity gaps* since they already encompass a wide range of phenomena. Rapidity gaps, namely regions of rapidity containing no final-state particles, are expected to occur between jets when a color-singlet is exchanged between the interacting hard partons. The exchange of γ, $W^{\pm}$, Z^0 and QCD Pomeron is expected to give event such topology. Typical representatives of this class are so-called *diffractive tags*, such as a single far-forward proton, or an inelastic, low-p_t, high-mass beam-fragment system, or a beam-fragment system containing a tagging jet, which define exchange of soft, semi-soft, and hard Pomerons, respectively [16]. Typical color-octet jet events (single gluon or quark exchange) have usually particles between jets, but even in these events rapidity gaps can be enforced by carefully tagging leading particles. *Leading particle tags* such as Δ, neutron, or unfragmented ion will create *non-Pomeron rapidity gaps*, within which occur *meson-meson*, *meson-photon*, etc. collisions at the TeV scale in the c.m.s.. Clearly the detector which wants to measure such exotic processes should have the capability not only of crisply defining these tags, which typically occur for $|\eta| > 6$, but also to observe the collision products at smaller η.

To summarize. In contrast to ATLAS and CMS experiments, ALICE will be able to study *complete range of non-perturbative and semi-perturbative QCD processes.*

3.3 Two photon physics

As already discussed in Section 2 fast moving nuclei are surrounded by a strong electromagnetic field, which can be seen as a pulse of real photons according to Weizsäcker-Williams method of equivalent photons. Intense heavy ion beams which will be available at the LHC represent a prolific source of such photons. Since their cut-off energy is inversely proportional to the ion radius (see Eq. 7), resulting

maximum invariant mass M of intermediate object X which can be produced via $\gamma\gamma \rightarrow$ X collision is 80, 170 and above 500 GeV for Pb, Ca and protons. Different decay channels of such intermediate objects into fermion-antifermion pairs X $\rightarrow$ $f\bar{f}$ or charged boson pairs X $\rightarrow$ b^+b^- can be studied and reasonable statistics accumulated at high invariant masses $M_{\gamma\gamma}$ well above the reach of LEP 200. In addition to this photoproduction physics, similar to what is done at HERA, can be performed at much larger c.m.s. energies.

Cross section for particle production in heavy ion collisions via two photon fusion $\gamma\gamma \rightarrow$ X can be calculated using Weizsäcker-Williams method:

$$\sigma^{\mathrm{WW}}_{\mathrm{A_I A_{II}} \rightarrow \mathrm{A_I A_{II}} \mathrm{X}} = \int \mathrm{d}\omega_{\mathrm{I}} \int \mathrm{d}\omega_{\mathrm{II}} n_{\mathrm{I}}(\omega_{\mathrm{I}}) n_{\mathrm{II}}(\omega_{\mathrm{II}}) \sigma_{\gamma\gamma \rightarrow \mathrm{X}}(\omega_{\mathrm{I}}, \omega_{\mathrm{II}}) \,. \tag{9}$$

Here $n_i(\omega_i)$, $i = \mathrm{I}, \mathrm{II}$ is the number of equivalent photons of energy ω_i for nucleus A_i and $\sigma_{\gamma\gamma \rightarrow \mathrm{X}}(\omega_{\mathrm{I}}, \omega_{\mathrm{II}})$ is the cross section of elementary sub-process $\gamma\gamma \rightarrow$ X. The equivalent photon number $n(\omega)$ can be expressed in terms of elastic nuclear charge form factor F_{A} of the nucleus A moving with Lorentz factor $E/m_{\mathrm{A}} = \gamma$ as

$$n(\omega) = \frac{2Z^2\alpha}{\pi\omega} \int_{\omega/\gamma}^{\infty} \mathrm{d}k \frac{k^2 - (\omega/\gamma)^2}{k^3} (F_{\mathrm{A}}(k^2))^2 \,. \tag{10}$$

Modern parton language formulation for expression (9) uses instead of energies of the photons fractions $x_i = \omega_i/E$ and interprets a number of equivalent photons $n(\omega)$ as a photon distribution function $f_{\gamma/\mathrm{Z}}(x)$. The result remains the same but allows extension of the calculations to the other processes. For example, if one of the photon distribution functions is replaced by the gluon distribution, function $f_{\mathrm{g/A}}(x)$ cross section for photon-gluon fusion $\gamma\mathrm{g} \rightarrow$ X process can be calculated. Let us note that photon-gluon collisions allow the study of the gluon distributions in ions and, in the case of proton beams, one may also envisage photon-Pomeron interactions.

Returning back to the two photon processes one can see after substitution of (10) into (9) that $\sigma^{\mathrm{AA}}_{\gamma\gamma}$ increases with the fourth power of the ion charge. On the other hand, as already discussed in Section 2, the cross-sections for electron capture $\sigma_{\mathrm{ec}} \propto Z^7$ and electromagnetic dissociation $\sigma_{\mathrm{ed}} \propto Z^{10/3}$ scale with Z even more dramatically. This results in reduction of the beam lifetime and hence of the luminosities to max. $10^{27}(10^{31})$ $\mathrm{cm}^{-2}\mathrm{s}^{-1}$ for Pb (Ca) ion beams. As a consequence, the highest two photon luminosities can be achieved neither with protons nor with Pb ions but with Ca beams.

The large statistics which can be obtained with Ca ions enable extensive studies of $C = +1$ states and multiquark states even with low branching ratios into photons. As an example, 10000 η_b's can be produced in a 10^6 s run with Ca ions. The quark content of some exotic final states b created via $\gamma\gamma \rightarrow \mathrm{m^+m^-}$ like '*multiquark mesons*' ($\mathrm{qq\bar{q}\bar{q}}$) can be analyzed since their coupling is similarly to the case of initial state heavy ions proportional to the fourth power of their charge.

Let us note that the cross section (9) for two photon fusion has to be understood as a total cross section in the impact parameter space of two colliding nuclei. However, since strong interactions which take place at $b \leq b_{\mathrm{min}}$ could mask

a clean experimental signal of the electromagnetic process cut-off in impact parameter $b > b_{\min}$ must be introduced. Impact parameter dependent extension of equivalent photon method was developed in [17]. Calculations for the scalar standard model Higgs-boson production via process $\gamma\gamma \rightarrow$H show that the cross section is reduced only by factor ≈ 2 when discarding collisions with $b \lesssim b_{\min}$.

On the experimental side implementation of such trigger veto on nuclear processes will allow ALICE to study the production of intermediate-mass Higgs and supersymmetric particles in a much cleaner environment compared to deep inelastic pp collisions which will be measured by ATLAS and CMS. It is quite probable that decays of Higgs boson into beauty particles from reaction $\gamma\gamma \rightarrow$ H $\rightarrow$ b$\bar{\text{b}}$ may be observable. However, in view of the limited statistics and the beauty background, detailed studies are required before any conclusions about the detectability of new heavy particles can be drawn.

As can be seen from the above list, physics agenda of $\gamma\gamma$ collisions is not less attractive than the QGP physics itself. However, before its full integration into the detector design further studies should be carried out in areas as the positive trigger for low invariant mass and the trigger veto against hadronic interactions. Physics of such 'silent events' which can be produced in heavy ion collisions at the LHC will be rewarding one.

4 Detector

Physics goals outlined in the previous section define design criteria and constrains which must be fulfilled by the detector. The most stringent one is the ability to analyze complex patterns in individual events. The ALICE detector should provide an opportunity to isolate and study interesting classes of events via their global pattern structure in phase space thus making it extremely versatile in the types of physics that it can tackle.

4.1 Central part

This part of the detector is devoted to physics at mid-rapidity, i.e. the region of minimum number of baryons and maximum energy density. The existence of this region is a unique feature of the LHC not shared by the lower energy machines like RHIC or SPS. Another important feature of heavy ion collisions at the LHC is the existence of a wide spectrum of observables which can be measured on *event-by-event* basis.

In general, the sensitivity for all single event observables is proportional to the number of detected particles and therefore to the geometrical acceptance. On the other hand the rapidity region relevant to *single event studies* is in general smaller than the total width of the central region (4–5 units). This follows from the fact that the rapid longitudinal expansion will separate the total reaction volume created in nuclear collision into 'sub-volumes' at different rapidities, which are not in a thermal contact. Therefore the acceptance of the central part of ALICE ($(90 \pm 45)^\circ$, i.e., $|\eta| < 0.9$ over the full azimuth) has been chosen such that a sensitive *event-by-event*

analysis can be carried out at the highest particle densities expected for Pb+Pb collisions (see Table 2).

The central part which is embedded in a large magnet with a weak solenoidal field (0.2 T) consists (from inside out) of an inner tracking system (ITS) with five layers of high-resolution tracking detectors (1 silicon pixel + 4 silicon drift detectors), a cylindrical time projection chamber (TPC), a particle identification array (TOF or RICH detectors), and a single-arm electromagnetic calorimeter PHOS.

Table 2. Comparison of typical values of particle densities per square centimeter between SPS (as compiled from several heavy ion experiments) and ALICE.

Detector	Si-drift	Si-pixel	TPC	PHOS	RICH	TOF
SPS	$\approx$ 10–20	$\approx$ 5–10	$\approx$ 0.05–1.0	$\approx$ 0.1–0.3	$\approx 25 \times 10^{-4}$	occupancy $\approx$ 15%
ALICE	$\approx$ 1–5	$\approx$ 20	$\approx$ 0.1	$\approx$ 0.3	$\approx 50 \times 10^{4}$	occupancy $\approx$ 10%

This part of detector which is very similar to the STAR detector at RHIC [1,10] is optimized for the measurement of the momenta and identification of particles of low p_t, i.e. from a few tens of MeV to a few GeV, which constitute the bulk of particle production. However, it is designed to handle an order higher multiplicities than STAR (its granularity must be sufficient to track 16000 particles with good efficiency). Nevertheless, the situation will be in some respect even better than at the SPS Pb+Pb ongoing experiments (see Table 2). First, at the LHC particles though more numerous than at the SPS are scattered not into a relatively narrow forward cone characteristic for fixed target experiments but into the full solid angle of 4π. Second, the distance of the ALICE detectors from vertex has been chosen such that even if the narrow jets of particles will be produced in hard scattering of partons the particle density should be less or comparable to SPS experiments. Hence, better separation of the individual particles is possible.

4.2 Forward extensions

Most of the physics topics itemized in Subsections 3.2 and 3.3 are inaccessible without extending ALICE into forward and far-forward region. Let us note that especially far-forward region ($|\eta| > 6$) is very difficult to access experimentally since it corresponds to very high momentum particles emerging at few mrad in angle. The demands on the detector architecture for doing this are therefore high and will be defined by the physics priorities as time evolves. In the time of writing this contribution most of this 'non-QGP' programme is still in a preparatory state. What is, however, important even now is that the magnetic architecture of the forward detector, which affects the machine lattice, and the far-forward Roman-pot tracking system, which must be inserted within the final-focus system of machine elements, deserves the highest priority. The reason for this is the recent (16^{th} December 1994) approval of the LHC, which sets the dead line for its opening to 2004 and hence

also for early finalization of the machine. Let us now briefly describe design of this part of ALICE.

The free space in the two forward arms allows an extension from the central pseudorapidity region $|\eta| < 1.5$ almost continuously into the forward and far-forward region. To match the acceptance of the central solenoidal magnet a dipole magnet with an aperture of about $\pm 15°$ will be placed as close as possible to the endplates of the solenoid. The momentum resolution will be sufficient to resolve the resonances in the Υ family, i.e. less than 1% over most of the kinematic region.

A second dipole magnet with a stronger field (around 1.5 T), will be placed further upstream. It will deflect far-forward particles out of the beam. The highest energetic particles will then pass the forward quadrupoles and the dipole magnet D1 which separates the beams.

Several hundred meters further upstream precise position detectors will measure diffractive as well as elastic scattered protons. Extrapolation to $t = 0$ can then be used for a luminosity independent determination of the total cross-section via the optical theorem.

One of the two forward arms will be optimized for muon detection in heavy ion runs. To cope with the large particle density leading to many decay muons in the low p_t range, a dense absorber is foreseen close to the interaction point and a careful shielding of the beams. Muons will be well measured and identified in the pseudorapidity interval $2 < |\eta| < 4$. The absorber design will be determined by the ability to separate J/ψ from ψ' and to reduce the background to an acceptable level. For proton runs the muons will be identified with absorbers placed behind the track measurement. Thus the tracking architecture will be identical in the two forward arms.

The impact parameter of the collision will be determined by measuring the total energy of non-interacting nucleons with three different Zero-Degree Calorimeters (ZDC). Neutron, proton and negative particle's ZDC will be located about 29 m downstream of the the LHC dipole magnet D1. Later it will provide separation between the neutron and proton spectators and the beam remnants ($Z/A \approx 0.4$). Two identical sets of such calorimeters will be placed on both sides of the interaction point.

The ZDC between the separated beams, will be complemented by electromagnetic calorimeters, with emphasis on high spatial shower resolution. The electromagnetic calorimetry will cover the complete pseudorapidity region $|\eta| > 1.5$.

5 Conclusion

Few months after this school a long awaited news came from CERN. On 16$^{\text{th}}$ December 1994 CERN Council agreed to approve construction of the LHC. According to its decision an accelerator should be build as a 2-stage project. First stage being a particle collider with an energy of 10 TeV must be ready to start the research programme on top quark, charge parity violations and heavy ion physics in 2004. By 2008 the accelerator will be upgraded by adding additional magnets to reach the final c.m.s. energy 14 TeV. From now on, more than nine years before

the startup of the LHC, the design work on the detectors is gaining on speed. The heavy ion community is looking with great excitement to the coming years, when a major step in our understanding of strong interactions is expected to occur.

References

[1] Plasil F.: Czech. J. Phys. *45* (1995) xxx (this Proceedings).

[2] Letter of Intent for A Large Ion Collider Experiment at the CERN Large Hadron Collider, CERN/LHCC/93-16, March 1993.

[3] The ALICE Collaboration: ALICE/93-33, Internal Note/GEN, November 1993.

[4] The ALICE Collaboration: CERN/LHCC/94-15, March 1994.

[5] Fermi E.: Z. Physik *29* (1924) 315.

[6] Weizsäcker C.: Z. Physik *88* (1934) 612.

[7] Williams E.J.: Proc. Roy. Soc. A *139* (1933) 163.

[8] Jackson J.D.: Classical Electrodynamics, Wiley, New York, 1975.

[9] Giubellino P.: *in* Proceedings of a NATO Advanced Study Institute on Particle Production in Highly Excited Matter (Ed. H. H. Gutbrod and J. Rafelski). NATO ASI Series, Series B: Physics, Vol. 303, Plenum Press, New York, 1993, p. 175.

[10] Harris J. W.: *ibid*, p. 89.

[11] Schukraft J.: Invited talk at the 5th Int. Conf. on Nucleus-Nucleus Collisions, Taormina, Italy, 1994. Preprint CERN-PPE/94-139, 1994.

[12] Grabiak M. et al.: J. Phys. G *15* (1989) L25.

[13] Papageorgiu E.: Phys. Rev. D *40* (1989) 92; Nucl. Phys. A *498* (1989) 593c.

[14] Shuryak E.V. and Zhirov O.V.: Phys. Lett. B *89* (1980) 253; *171* (1986) 99.

[15] Van Hove L.: Z. Phys. C *27* (1985) 135.

[16] Eggert K. and Morsch A.: Nucl. Instrum. Methods A *351* (1994) 174.

[17] Rau J. et al: J. Phys. G *16* (1990) 211.

5.3.3 Further developments

Recent review of electromagnetic processes expected at LHC can be found in [**R81, R82**]. Corresponding maximum number N obtained in [228] 9.4×10^7 ions/bunch is very close to more recent estimate [236] 7×10^7 ions/bunch reflecting change in the number of interacting regions from 2 to 3.

Experiment ALICE at LHC at CERN (Fig.5.2) will study heavy-ion collisions at a $\sqrt{s_{NN}} = 5.5$ TeV. Almost a factor 30 higher than at RHIC. The expectation from 1994 on the most important parameters characterizing matter produced in central Pb+Pb collisions at LHC and their comparison to SPS and RHIC are summarized in Table 1. Note that at that time no results on ultra-relativistic collisions of heavy systems were available. That's why the values in Table 1 are based on the models or on the p+p/light ion extrapolations only.

In contrast to that the Table 5.2 is based on the extrapolations [236, R1, R64] from the SPS [63, 78, 90, 94] and the RHIC [171] measurements to the LHC. The final volume at freeze-out was estimated as $\mathrm{V_f} = R_{long} \cdot R_{side} \cdot R_{out}$ using the already mentioned linear dependence of the radii on $(dN_{ch}/d\eta)^{1/3}$. The energy density was estimated from the relation

$$\epsilon(\tau_0 = \frac{1}{\pi R^2} \frac{1}{\tau_0} \frac{dE_T}{dy} \tag{5.1}$$

due to Bjorken [R68] which may serve as a conservative upper limit. Here the initially produced collision volume is approximated by a cylinder of length $dz = \tau_0 dy$ and the transverse radius $R \propto A^{1/3}$.

A part of the differences between the values of both tables is due to unexpectedly rapid thermalization of the super-dense matter created at RHIC. That matter was found to be strongly and not weakly interacting and its explosive character produces too small freeze-out volumes and much smaller number of final state hadrons than originally conceived.

	$\sqrt{s}$ (GeV/u)	$\frac{dN}{dy}$	ϵ (GeV/fm^3)	V_f (fm^3)	τ_0 (fm/c)	τ_c (fm/c)	$\frac{\tau_c}{\tau_0}$
SPS	17	500–800	1.7–2.7 **1**	$\approx 10^3$ **1**	≥ 1?	≤ 1? **1**	**1**
RHIC	200	700–2000	2.3–6.8 **2**	$\approx 7 \times 10^3$ **7**	≤ 1?	1.5–4 **3**	**5**
LHC	5500	3000–8000	8.0–27 **7**	$\approx 2 \times 10^4$ **20**	≤ 0.2?	4–11 **7**	**≥ 30**

Table 1. (from [228]): Comparison between SPS, RHIC and LHC predictions for central Pb+Pb collisions: dN/dy – charged particle multiplicity; ϵ – energy density (assuming $\tau_0 = 1$ in all cases); V_f – final volume at freeze-out; τ_0 – formation (thermalization) time; τ_c – time spend in QGP phase. For a number of these parameters, the average relative increase compared to the SPS is shown in bold in a separate row (i.e., SPS numbers are **1** by definition).

Another important difference between the tables is due to a change of a paradigm. Nowadays the nuclear collisions at LHC are expected to be driven by parton-parton or even classical fields scaterrings [R29] rather than by the nucleon and string degrees of freedom. The bulk of multiparticle production at LHC will be from partons with

	$\sqrt{s}$ (GeV/u)	$\frac{dN}{dy}$	ϵ (GeV/fm^3)	V_f (fm^3)	τ_0 (fm/c)	τ_c (fm/c)	$\frac{\tau_c}{\tau_0}$
SPS	17	380±20	3 ± 0.6	≈150	≥ 1?	≤ 1?	
			1	**1**		**1**	**1**
RHIC	200	650±50	6 ± 1	≈200	≤ 0.1	≈3	
			2	**4/3**		**3**	**30**
LHC	5500	1100 - 2200	8 - 10	≈400	≤ 0.01?	4 - 11	
			2.5	**3**		**7**	**≥ 30**

Table 5.2: Comparison between measurements (SPS, RHIC) and LHC predictions for central Pb+Pb collisions. The legend is the same as in Table 1.

momentum fractions $x \leq 10^{-3}$ [236]. Partons with these very small x values interact coherently with several partons in the other nucleus. It thus is very unlikely that the pQCD collinear factorization approach resulting in a convolution of probabilities will suffice for describing multiparticle production at the LHC [R64]. One way to understand the properties of the nuclear wave function at small x is to realize that at sufficiently small x, the parton distributions saturate. This happens when the density of partons is such that they overlap in the transverse plane, their repulsive interactions are sufficiently strong to limit further growth to be at most logarithmic [R63]. The large parton density per unit transverse area provides a scale, the saturation scale Q_s^2. The estimate for the LHC $Q_s^2 = 2 - 3$ GeV$^2 \gg \Lambda_{QCD}$ i.e. $\alpha_S \ll 1$ shows that even though the physics of small-x partons is non-perturbative, it can be studied with weak coupling [R29].

Existence of this semi-hard regime was predicted already in 1984 [R63] but it took about the next 15 years to get accustomed to it. Nowadays the situation is very different. There are even attempts to interpret the forward suppression observed in d+Au collisions at RHIC invoking the saturation picture [R29] even though more standard explanation is at hand [242].

Chapter 6

Conclusions

The program to study high-density nuclear matter was formulated a long time ago [R10–R12]. At about that time new phase of QCD matter – deconfined and chirally symmetric QGP – was predicted [R16, R17]. Over the last 30 years the author of this thesis had a privilege to participate in a wide international effort to search for the new states of high-density strongly interacting matter at JINR Synchrophasotron [8], GSI SIS [43]- [52], [50], CERN SPS [63]- [59], [78]- [67], BNL RHIC [166, 171, 180, 200] and at CERN LHC [228, 236, 238] accelerators.

On the road toward this 'Holly Grail' of contemporary nuclear physics several interesting phenomena were encountered. The squeeze-out of neutral pions [43, 46] and general scaling laws of subthreshold particle production [43,48,49,52] at SIS. The superdense highly non-trivial medium [90] exhibiting the thermal features [63] accompanied by a large particle flow effects [90] at SPS. The other phenomena, like the hypothetical disoriented chiral condensate, remained hidden beyond the observation limits [59].

Even in simpler hadron-hadron system the multiparticle production at high energies provides mixed and sometime puzzling signals hidden behind non-perturbative hadronization drapery. It is thus gratifying to learn that some general and robust phenomenological regularities governing its asymptotic behavior can be established [30, 33, 40].

First, essentially circumstantial evidence about the QGP, came from the CERN SPS experiments. The result [R51] was based on combination of several observed signals (strangeness enhancement, J/ψ suppression, dilepton [90,97,110] and direct photon [80] production) each of them also allowing for a non-QGP explanation.

Soon after the CERN QGP announcement the RHIC machine started to deliver its new results. The following three years have witnessed a plethora of interesting, sometimes even unexpected, results [171]. The first RHIC data have confirmed that the magnitude of observed collective phenomena is consistent with equation of state expected from the QGP. Hadronic degrees of freedom are unable to account for the early formation of significant pressure leading to explosive collective behavior [R6]. The non-trivial properties of the matter created at RHIC were also found in the region where according to standard wisdom pQCD calculations should be valid: large deficit of high-pt hadrons (the jet quenching), large (and approximately p_T-independent) azimuthal asymmetry and baryon/meson ratio much larger than in the usual jet fragmentation.

The QCD matter found at RHIC thus exhibits so far unobserved behavior. Very high density, strongly interacting partonic matter (made of constituent quarks) is

formed, reaching thermal equilibrium very early in the collision [171]. Surprisingly enough, the superdense matter does not behave as the ideal gas of free quarks and gluons that was searched for during previous decades but as a perfect fluid of very low viscosity [R6, R21, R31].

In the meantime the new analyses [112,117] of the old SPS data rediscovered some of the RHIC most prominent findings at the lower energies. It remains to be seen whether the same kind of matter awaits us also at the LHC or ideal gas QGP will finally show up there or, what is most likely, some surprises will happen [228, 236, R2, R21].

Chapter 7

Author's published papers and other references

7.1 Author's publications

Author's publications

[1] **"Inelastic Interactions of Protons With Photoemulsion Nuclei At 4.5-Gev/C"**
B. P. Bannik *et al.*
Czech. J. Phys. B **31**, 490 (1981) SPIRES entry

[2] **"Nuclear Interactions Of 4.5-Gev/C Protons In Emulsion And The Cascade Evaporation Model"**
V. I. Bubnov *et al.*
Z. Phys. A **302**, 133 (1981) SPIRES entry

[3] **"Inelastic Interactions Of 4.5-Gev/C Protons With Emulsion Nuclei Not Accompanied By Relativistic Charged Particles"**
M. Sumbera and S. Vokal
Acta Phys. Slov. **32**, 265 (1982) SPIRES entry

[4] **"Inelastic Interactions Of Protons With (Co) And (Ag Br) Nuclei At 4.5-Gev/C"**
V. I. Bubnov *et al.* [ALMA ATA-BUCHAREST-KOSICE-LENINGRAD-MOSCOW- ULAN BATOR COLLABORATION Collaboration] SPIRES entry
Alma Ata Inst. High Energy Phys. Acad. Sci. - 81-11 (REC.FEB.82) 16p

[5] **"Backward Particle Production By Protons And C-12 Nuclei In Emulsion At Momenta Of 4.5-Gev/C/A"**
A. Abdel-salam, M. Sumbera and S. Vokal
JINR-E1-82-509(1982) SPIRES entry

Submitted to Int. Conf. on Nucleus-Nucleus Collisions, East Lansing, Michigan, Sep 26 - Oct 1, 1982

[6] **"Inelastic Interactions Of Protons And Alpha Particles With Nuclei At 4.5-Gev/C Per Nucleon With Fast Hadron Backward Emission"**
S. Vokal, R. Togoo, J. Tucek, G. S. Shabratova and M. Shumbera
JINR-1-83-652() SPIRES entry (Submitted to Z. Phys. A)

[7] **"Central Nuclear Collisions Of He And C With Ag And Br At 4.5-Agev Momentum"**
A. Abdel-salam *et al.* [Bucharest-Dubna-Leningrad-Ulan Bator Collaboration]
JINR-P1-83-577(1983) SPIRES entry

[8] **"Inelastic Interactions Of Protons And Alphas With Nuclei At A Momentum Of 4.5-Gev/C Per Nucleon Accompanied By Fast Hadron Backward Emission"**
G. S. Shabratova, M. Sumbera, R. Togoo, J. Tucek and S. Vokal
Z. Phys. A **318**, 75 (1984) SPIRES entry

[9] **"Angular Spectra of Secondary Particles In Interactions Of Protons And Carbon Nuclei With Photoemulsion Nuclei At P (0) = 4.5-Gev/C/A (In Russian)"**
S. Vokal and M. Šumbera
Yad. Fiz. **39**, 1474 (1984) SPIRES entry

[10] **"The Total Disintegration Of Lead Nuclei By C-12 Nuclei At A Momentum Of 4.5-Gev/C Per Nucleus"**
S. Vokal, M. Karabova, A. Mukhtorov, R. Togoo, K. D. Tolstov, J. Tucek and M. Shumbera
JINR-P1-84-552(1984) SPIRES entry

[11] **"Investigation Of Multiple Particle Cumulative Production In 4 Pi Geometry. (In Russian)"**
S. A. Averichev *et al.* SPIRES entry
Dubna Jinr - 85-512 (85,REC.DEC.) 15p

[12] **"MULTIPLICITIES AND A NUCLEI IN THE PHOTOEMULSION AT 4.1A-GeV/c"**
N. P. Andreeva *et al.*
Sov. J. Nucl. Phys. **45**, 78 (1987) [Yad. Fiz. **45**, 123 (1987)] SPIRES entry

[13] **"THE SPHERE: A DETECTOR SYSTEM FOR THE STUDY OF MULTIPLE PARTICLE CUMULATIVE PRODUCTION IN 4 PI GEOMETRY"**
M. Sumbera SPIRES entry
*IN *HIRSCHEGG 1987, PROCEEDINGS, GROSS PROPERTIES OF NUCLEI AND NUCLEAR EXCITATIONS*, 290-293.*

[14] **"PARTICULARITIES OF Ne-22 NUCLEI INELASTIC INTERACTIONS WITH EMULSION AT 4.1-A/GeV/c"**
A. El-Naghy *et al.*
JINR-E1-87-472(1987) SPIRES entry
Submitted to Int. Conf. on Ultrarelativistic Nucleus-Nucleus Collisions, Quark Matter '87, Schloss Nordkirchen, West Germany

[15] **"Fragmentation of Ne-22 in Emulsion at 4.1-a/GeV/c"**
A. El-Naghy *et al.*
J. Phys. G **14**, 1125 (1988) SPIRES entry

[16] **"Observation Of Particle Collective Flux In The Collisions Of 4.1-A-Gev/C Ne-22 With Ag, Br Emulsion Nuclei"**
B. P. Bannik *et al.*
Z. Phys. A **329**, 341 (1988) SPIRES entry

[17] **"Some Peculiarities Of Sideward Flow Of Particles In Ne-22 Collisions With Emulsion Nuclei At 4.1 A-Gev/C"**
B. P. Bannik *et al.*
J. Phys. G **14**, 949 (1988) SPIRES entry

[18] **"EXPERIMENTAL STUDY OF NUCLEAR FLOW IN NE-22 + (AG, BR) INELASTIC INTERACTIONS AT 4.1-A/GEV/C"**
N. P. Andreeva *et al.*
Acta Phys. Slov. **38**, 65 (1988) SPIRES entry

[19] **"Transverse Momenta Of Alpha Fragments From Interactions Of Ne-22 With Emulsion Nuclei At A Momentum Of 4.1-A/Gev/C"**
N. P. Andreeva *et al.*
JETP Lett. **47**, 23 (1988) [Pisma Zh. Eksp. Teor. Fiz. **47**, 20 (1988)] SPIRES entry

[20] **"THE STUDY OF TOTAL DISINTEGRATION OF LEAD NUCLEI WITH Mg-24 NUCLEI AT 4.5-a/GeV/c"**
S. A. Krasnov *et al.* [Dubna-Cairo-Kosice-Rez Collaboration]
JINR-P1-88-389(1988) SPIRES entry (Submitted to Acta Phys. Slovaca)

[21] **"Search for collective effects in Ne-22 + (Ag, Br) and Mg-24 + Pb central collisions at 3.3-A/GeV and 3.6-A/GeV"**
G. S. Shabratova, M. Sumbera and S. Vokal SPIRES entry
*In *Hirschegg 1989, Proceedings, Gross properties of nuclei and nuclear excitations* 34-38*

[22] **"INELASTIC INTERACTIONS OF SILICON NUCLEI WITH NUCLEAR EMULSION AT 4.5-A/GeV/c"**
B. U. Ameeva *et al.*
Sov. J. Nucl. Phys. **51**, 669 (1990) [Yad. Fiz. **51**, 1047 (1990)] SPIRES entry

[23] **"An Experiment to search cumulative muon pairs with low invariant mass"**
S. V. Afanasev *et al.* [SPHERE Collaboration] SPIRES entry
Dubna JINR - 7(46)-90 (90/11,rec.Feb.91) 6-18.C

[24] **"Observation Of Cumulative Muon Pairs With Low Invariant Mass"**
M. Sumbera *et al.* SPIRES entry
Prepared for 19th International Workshop on Gross Properties of Nuclei and Nuclear Excitations, Hirschegg, Austria, 21-26 Jan 1991

[25] **"An Experiment on the A-dependence of the cross-section for relativistic deuteron fragmentation into cumulative pions"**
S. V. Afanasev *et al.* [SPHERE Collaboration] SPIRES entry
Dubna JINR - 5(51)-91 (92/01,rec.Mar.) 5-13.C

[26] **"Observation of cumulative muon pairs with low invariant mass"**
S. V. Afanasev *et al.* SPIRES entry
Prepared for 10th International Seminar on High-energy Physics Problems, Dubna, USSR, 24-29 Sep 1990

[27] **"Characteristics Of The Total Disintegration Of Ag And Br Nuclei By Ne-22 And Si-28 Nuclei With Momentum In The Range 4.1-A/Gev/C To 4.5-A/Gev/C. Alma Ata-Bucharest-Cracow-Dubna-Dushanbe-Erevan-Gatchina-Kosice-Moscow Rez-St. Peters"**
N. P. Andreeva *et al.*
Sov. J. Nucl. Phys. **55**, 569 (1992) [Yad. Fiz. **55**, 1010 (1992)] SPIRES entry

[28] **"Study of charged multiplicity in cumulative pion production"**
S. V. Afanasev *et al.* SPIRES entry
Dubna JINR - 1(58)-93 (93/02,rec.Apr.) 21-26.C

[29] **"The Relativistic projectile nuclei fragmentation and A-dependence of nucleon Fermi momenta. (In Russian)"**
B. U. Ameeva *et al.* [Alma Ata-Bucharest-Dubna-Dushanbe-Erevan- Kosice-St Petersburg- and Moscow-R] SPIRES entry
Dubna JINR - 5(68)-94 (94/12,rec.Mar.95) 43-50

[30] **"Energy Independent Number Of Clusters And Multiplicity Distribution At Collider And Beyond"**
V. Simak and M. Sumbera
Czech. J. Phys. B **36**, 1267 (1986) SPIRES entry

[31] **"SUPERCLUSTERS IN MULTIPLICITY DISTRIBUTIONS?"**
V. Simak, M. Sumbera and I. Zborovsky SPIRES entry
*In *Kazimierz 1986, Proceedings, Elementary particle physics* 67-74. (see Conference Index)*

[32] **"ENTROPY IN THE MULTIPARTICLE PRODUCTION"**
V. Simak, M. Sumbera and I. Zborovsky
Print-88-0065 (PRAGUE)(1987) SPIRES entry
Contributed to 18th Int. Symp. on Multiparticle Dynamics, Tashkent, USSR, Sep 8-12, 1987

[33] **"ENTROPY IN MULTIPARTICLE PRODUCTION AND ULTIMATE MULTIPLICITY SCALING"**
V. Simak, M. Sumbera and I. Zborovsky
Phys. Lett. B **206**, 159 (1988) SPIRES entry

[34] **"Entropy Scaling: Evolution Of Parton Showers Or (Thermo)Dynamics?"**
V. Simak, M. Sumbera and I. Zborovsky SPIRES entry
*In *Bechyne 1988, Proceedings, Hadron interactions* 387-393. (see HIGH ENERGY PHYSICS INDEX 29 (1991) No. 15578)*

[35] **"Entropy Of The Multiplicity Distributions"**
V. Simak, M. Sumbera and I. Zborovsky
FZU-CSAV-1987-8 SPIRES entry
*In *Uppsala 1987, Proceedings, High energy physics, vol. 1* 476-480.*

[36] **"Multiplicities in high-energy p anti-p interactions"**
V. Simak, N. Sumbera and I. Zborovsky SPIRES entry
*In *Kazimierz 1989, Proceedings, Frontiers in particle physics* 582-588*

[37] **"Entropy scaling and multifractal analysis of multiplicity distributions"**
V. Simak, M. Sumbera and I. Zborovsky SPIRES entry
*In *Smolenice 1989, Proceedings, Hadron structure '89* 342-349*

[38] **"Entropy Scaling At High-Energy P Anti-P Interactions"**
M. Sumbera, I. Zborovsky and V. Simak SPIRES entry
*In *Bechyne 1989, High energy experiments and methods* 201-206*

[39] **"Entropy, dimensions and other multifractal characteristics of multiplicity distributions"**
V. Simak, M. Pachr, M. Sumbera and I. Zborovsky SPIRES entry
Prepared for International Workshop on Local Equilibrium in Strong Interaction Physics - LESIP IV: Correlations and Multiparticle, Marburg, W.Germany, 14-16 May 1990

[40] **"Entropy, dimensions and other multifractal characteristics of multiplicity distributions"**
M. Pachr, M. Sumbera, I. Zborovsky and V. Simak
Mod. Phys. Lett. A **7**, 2333 (1992) SPIRES entry

[41] **"Entropy scaling: Evolution of parton showers or (thermo)dynamics?"**
V. Simak, M. Sumbera and I. Zborovsky SPIRES entry
Prepared for 19th International Symposium on Multiparticle Dynamics: New Data and Theoretical Trends, Arles, France, 13-17 Jun 1988

[42] **"Entropy and multifractal analysis of multiplicity distributions from p p simulated events up to LHC energies"**
M. K. Suleymanov, M. Sumbera and I. Zborovsky
arXiv:hep-ph/0304206 SPIRES entry

[43] **"Neutral pion production in heavy ion collisions at SIS energies"**
M. Sumbera, H. Lohner, A. E. Raschke, L. B. Venema and H. W. Wilschut
KVI-973(1993) SPIRES entry
Talk presented at the XXI. International Workshop on Gross Properties of Nuclei and Nuclear Excitations, Hirschegg, Austria, January 18-22, 1993

[44] **"Investigation of reabsorption effects in subthreshold pi0 production"**
R. Holzmann *et al.* [TAPS Collaboration]
GSI-93-25(1993) SPIRES entry
Contribution to 2nd European Workshop on Nuclear Physics, Megeve, France, Mar 29 - Apr 2, 1993

[45] **"Azimuthal Asymmetry Of Neutral Pion Emission In Au + Au Reactions At 1-Gev/U"**
L. B. Venema *et al.*
KVI-983(1993) SPIRES entry (Submitted to Phys.Rev.Lett.)

[46] **"Azimuthal asymmetry of neutral pion emission in Au+Au reactions at 1 GeV/nucleon"**
L. B. Venema *et al.*
Phys. Rev. Lett. **71**, 835 (1993) SPIRES entry

[47] **"Flow effects in Bi + Pb collisions at 1-GeV/u"**
A. Kugler, V. Wagner, M. Pachr, M. Sumbera, S. Hlavac and R. S. Simon
Acta Phys. Polon. B **25**, 691 (1994) SPIRES entry
Talk presented at 23rd Mazurian Lakes Summer School on Nuclear Physics: Frontier Topics in Nuclear, Astronuclear and Astroparticle Physics, Piaski, Poland, 18-28 Aug 1993

[48] **"Mass dependence of pi0 production in heavy ion collisions at 1-A/GeV"**

O. Schwalb *et al.*
Phys. Lett. B **321**, 20 (1994) SPIRES entry

[49] **"Transverse momentum distributions of eta mesons in near threshold relativistic heavy ion reactions"**
F. D. Berg *et al.*
Phys. Rev. Lett. **72**, 977 (1994) SPIRES entry

[50] **"Emission of nucleons and light fragments relative to the reaction plane in Bi + Pb collisions at 1-GeV/u"**
A. Kugler *et al.*
Phys. Lett. B **335**, 319 (1994) SPIRES entry

[51] **"Response of TAPS to monochromatic photons with energies between 45-MeV and 790-MeV"**
A. R. Gabler *et al.*
Nucl. Instrum. Meth. A **346**, 168 (1994) SPIRES entry

[52] **"Neutron emission in $Bi + Pb$ collisions at $1GeV/u$"**
M. Pachr, M. Sumbera, A. Kugler, V. Wagner, s. Hlavac and R. S. Simon
Czech. J. Phys. **45**, 663 (1995) [Acta Phys. Slov. **44**, 35 (1994)] SPIRES entry
Prepared for International School / Workshop for Young Physicists: Relativistic Heavy Ion Physics, Prague, Czech Republic, 19-23 Sep 1994

[53] **"Mass dependence in the flow of light fragments emitted from the expanding collision zone"**
A. Kugler, R. Pleskac, V. Wagner, M. Pachr, M. Sumbera, R. S. Simon and S. Hlavac SPIRES entry
*In *Hirschegg 1994, Proceedings, Multifragmentation* 125-129*

[54] **"Detection of relativistic neutrons by BaF-2 scintillators"**
V. Wagner *et al.*
Nucl. Instrum. Meth. A **394**, 332 (1997) SPIRES entry

[55] **"Photon and neutral meson production in 158-A-GeV Pb-208 + Pb collisions"**
T. Peitzmann *et al.* [WA98 Collaboration]
Nucl. Phys. A **610**, 200C (1996) SPIRES entry
Prepared for 12th International Conference on Ultra-Relativistic Nucleus-Nucleus Collisions (Quark Matter 96), Heidelberg, Germany, 20- 24 May 1996

[56] **"First evidence of directed flow at 158-A-GeV Pb + Pb collisions in WA98 experiment"**
M. M. Aggarwal *et al.* [WA98 Collaboration]
Prog. Theor. Phys. Suppl. **129**, 179 (1997) SPIRES entry
Prepared for International School on the Physics of Quark Gluon Plasma, Hiroshima, Japan, 3-6 Jun 1997

[57] **"Recent results from CERN-WA98"**
M. M. Aggarwal *et al.* [WA98 Collaboration] SPIRES entry
Prepared for 13th Winter Workshop on Nuclear Dynamics, Key Marathon, Florida, 1-8 Feb 1997

[58] **"Search for disoriented chiral condensates: An Experimental perspective"**
T. K. Nayak *et al.* [WA98 Collaboration]
VECC-NEX-97005(1997) SPIRES entry

Talk given at 3rd International Conference on Physics and Astrophysics of Quark Gluon Plasma (ICPAQGP 97), Jaipur, India, 17-21 Mar 1997

[59] **"Search for disoriented chiral condensates in 158-A-GeV Pb + Pb collisions"**
M. M. Aggarwal *et al.* [WA98 Collaboration]
Phys. Lett. B **420**, 169 (1998) [arXiv:hep-ex/9710015] SPIRES entry

[60] **"Present status and future of DCC analysis"**
T. K. Nayak *et al.* [WA98 Collaboration]
Nucl. Phys. A **638**, 249C (1998) [arXiv:hep-ex/9802019] SPIRES entry
Talk given at 13th International Conference on Ultrarelativistic Nucleus-Nucleus Collisions (Quark Matter 97), Tsukuba, Japan, 1-5 Dec 1997

[61] **"Recent results on Pb + Pb collisions at 158-A-GeV from the WA98 experiment at CERN"**
M. M. Aggarwal *et al.* [WA98 Collaboration]
Nucl. Phys. A **638**, 147 (1998) SPIRES entry
Given at 13th International Conference on Ultrarelativistic Nucleus-Nucleus Collisions (Quark Matter 97), Tsukuba, Japan, 1-5 Dec 1997

[62] **"Collective flow in 158-A-GeV Pb + Pb collisions"**
M. M. Aggarwal *et al.* [WA98 Collaboration]
Nucl. Phys. A **638**, 459 (1998) SPIRES entry
Given at 13th International Conference on Ultrarelativistic Nucleus-Nucleus Collisions (Quark Matter 97), Tsukuba, Japan, 1-5 Dec 1997

[63] **"Centrality dependence of neutral pion production in 158-A-GeV Pb-208 + Pb-208 collisions"**
M. M. Aggarwal *et al.* [WA98 Collaboration]
Phys. Rev. Lett. **81**, 4087 (1998) [Erratum-ibid. **84**, 578 (2000)] [arXiv:nucl-ex/9806004] SPIRES entry

[64] **"Wavelet analysis in search for the disoriented chiral condensate"**
H. Lohner *et al.* [WA98 Collaboration] SPIRES entry
Prepared for UIC Summer Workshop on Particle Distributions in Hadronic and Nuclear Collisions, Chicago, Illinois, 11-13 Jun 1998

[65] **"Searching for DCCs with the WA98 experiment at CERN"**
P. A. Steinberg *et al.* [WA98 Collaboration] SPIRES entry
Prepared for UIC Summer Workshop on Particle Distributions in Hadronic and Nuclear Collisions, Chicago, Illinois, 11-13 Jun 1998

[66] **"Directed flow in 158-A-GeV Pb-208 + Pb-208 collisions"**
M. M. Aggarwal *et al.* [WA98 Collaboration]
arXiv:nucl-ex/9807004 SPIRES entry (Submitted to Phys.Rev.Lett.)

[67] **"Elliptic emission of K+ and pi+ in 158-A-GeV Pb + Pb collisions"**
M. M. Aggarwal *et al.* [WA98 Collaboration and WA98 Collaboration]
Phys. Lett. B **469**, 30 (1999) SPIRES entry

[68] **"Elliptic emission of K+ in 158-A-GeV Pb + Pb collisions"**
M. M. Aggarwal *et al.* [WA98 Collaboration]
Nucl. Phys. A **661**, 464 (1999) SPIRES entry
Prepared for 14th International Conference on Ultrarelativistic Nucleus-Nucleus Collisions (QM 99), Torino, Italy, 10-15 May 1999

[69] **"First results from the CERES radial TPC"**
G. Agakishiev *et al.* [CERES Collaboration]
Nucl. Phys. A **661**, 673 (1999) SPIRES entry
Prepared for 14th International Conference on Ultrarelativistic Nucleus-Nucleus Collisions (QM 99), Torino, Italy, 10-15 May 1999

[70] **"Freeze-out parameters in central 158-A-GeV Pb-208 + Pb-208 collisions"**
M. M. Aggarwal *et al.* [WA98 Collaboration]
Phys. Rev. Lett. **83**, 926 (1999) [arXiv:nucl-ex/9901009] SPIRES entry

[71] **"Systematics of inclusive photon production in 158-A-GeV Pb induced reactions on Ni, Nb, and Pb targets"**
M. M. Aggarwal *et al.* [WA98 Collaboration]
Phys. Lett. B **458**, 422 (1999) [arXiv:nucl-ex/9903006] SPIRES entry

[72] **"Collective flow in Pb + Pb collisions at the CERN-SPS"**
S. Nishimura *et al.* [WA98 Collaboration]
CNS-REP-21(1999) SPIRES entry
Talk given at 15th Winter Workshop on Nuclear Dynamics, Park City, UT, 9-16 Jan 1999

[73] **"Recent results from the WA98 experiment"**
T. Peitzmann *et al.* [WA98 Collaboration]
Nucl. Phys. A **661**, 191 (1999) SPIRES entry
To be published in the proceedings of 14th International Conference on Ultrarelativistic Nucleus-Nucleus Collisions (QM 99), Torino, Italy, 10-15 May 1999

[74] **"Two Particle Correlations In 158-A-Gev Collisions"**
M. M. Aggarwal *et al.* [WA98 Collaboration]
Nucl. Phys. A **661**, 427 (1999) SPIRES entry
To be published in the proceedings of 14th International Conference on Ultrarelativistic Nucleus-Nucleus Collisions (QM 99), Torino, Italy, 10-15 May 1999

[75] **"Search for disoriented chiral condensates in 158-A-GeV Pb + Pb collisions"**
T. K. Nayak *et al.* [WA98 Collaboration]
Nucl. Phys. A **663**, 745 (2000) [arXiv:nucl-ex/9909018] SPIRES entry
Talk given at 15th International Conference on Particles and Nuclei (PANIC 99), Uppsala, Sweden, 10-16 Jun 1999

[76] **"Delta++ production in 158-A-GeV Pb-208 + Pb-208 interactions at the CERN SPS"**
M. M. Aggarwal *et al.* [WA98 Collaboration]
Phys. Lett. B **477**, 37 (2000) SPIRES entry

[77] **"Collective flow and HBT in Pb + Pb collisions at the CERN-SPS"**
M. M. Aggarwal *et al.* [WA98 Collaboration]
Nucl. Phys. A **663**, 729 (2000) SPIRES entry
Prepared for 15th International Conference on Particles and Nuclei (PANIC 99), Uppsala, Sweden, 10-16 Jun 1999

[78] **"Central Pb + Pb collisions at 158-A-GeV/c studied by pi- pi- interferometry"**
M. M. Aggarwal *et al.* [WA98 Collaboration]
Eur. Phys. J. C **16**, 445 (2000) [arXiv:hep-ex/0003009] SPIRES entry

[79] **"Direct photon production in 158-A-GeV Pb-208 + Pb-208 collisions"**
M. M. Aggarwal *et al.* [WA98 Collaboration]
arXiv:nucl-ex/0006007 SPIRES entry (Submitted to Phys.Rev.C)

[80] **"Observation of direct photons in central 158-A-GeV Pb-208 + Pb-208 collisions"**
M. M. Aggarwal *et al.* [WA98 Collaboration]
Phys. Rev. Lett. **85**, 3595 (2000) [arXiv:nucl-ex/0006008] SPIRES entry

[81] **"Scaling of particle and transverse energy production in 208-Pb + 208-Pb collisions at 158-A-GeV"**
M. M. Aggarwal *et al.* [WA98 Collaboration]
Eur. Phys. J. C **18**, 651 (2001) [arXiv:nucl-ex/0008004] SPIRES entry

[82] **"Three pion interferometry results from central Pb + Pb collisions at 158-A-GeV/c"**
M. M. Aggarwal *et al.* [WA98 Collaboration]
Phys. Rev. Lett. **85**, 2895 (2000) [arXiv:hep-ex/0008018] SPIRES entry

[83] **"Localized charged-neutral fluctuations in 158-A-GeV Pb + Pb collisions"**
M. M. Aggarwal *et al.* [WA98 Collaboration]
Phys. Rev. C **64**, 011901 (2001) [arXiv:nucl-ex/0012004] SPIRES entry

[84] **"Multiplicity distributions and charged-neutral fluctuations"**
T. K. Nayak *et al.* [WA98 Collaboration]
Pramana **57**, 285 (2001) [arXiv:nucl-ex/0103007] SPIRES entry
To appear in the proceedings of International Symposium on Nuclear Physics (ISNP2K), Trombay, Mumbai, India, 18-22 Dec 2000

[85] **"Transverse mass distributions of neutral pions from Pb-208 induced reactions at 158-A-GeV"**
M. M. Aggarwal *et al.* [WA98 Collaboration]
Eur. Phys. J. C **23**, 225 (2002) [arXiv:nucl-ex/0108006] SPIRES entry

[86] **"Multiplicity distributions and charged neutral fluctuations"**
T. K. Nayak *et al.* [WA98 Collaboration]
arXiv:nucl-ex/0108026
VECC-CONF-INPC-01(2001) SPIRES entry
Prepared for International Nuclear Physics Conference (INPC 2001): Nuclear Physics and the 21st Century, Berkeley, California, 30 Jul - 3 Aug 2001

[87] **"Event-by-event fluctuations in particle multiplicities and transverse energy produced in 158-A-GeV Pb + Pb collisions"**
M. M. Aggarwal *et al.* [WA98 Collaboration]
Phys. Rev. C **65**, 054912 (2002) [arXiv:nucl-ex/0108029] SPIRES entry

[88] **"New results on Pb Au collisions at 40-A-GeV from the CERES/NA45 experiment"**
K. Filimonov *et al.* [CERES/NA45 Collaboration]
arXiv:nucl-ex/0109017 SPIRES entry
Talk given at International Nuclear Physics Conference (INPC 2001): Nuclear Physics and the 21st Century, Berkeley, California, 30 Jul - 3 Aug 2001

[89] **"Direct photons in WA98"**
M. M. Aggarwal *et al.*
Nucl. Phys. A **698**, 135 (2002) SPIRES entry

Prepared for 15th International Conference on Ultrarelativistic Nucleus-Nucleus Collisions (QM2001), Stony Brook, New York, 15-20 Jan 2001

[90] **"New results from CERES"**
D. Adamova *et al.* [CERES Collaboration]
Nucl. Phys. A **698**, 253 (2002) SPIRES entry
Prepared for 15th International Conference on Ultrarelativistic Nucleus-Nucleus Collisions (QM2001), Stony Brook, New York, 15-20 Jan 2001

[91] **"One-, two- and three-particle distributions from central Pb + Pb collisions at 158-A-GeV/c"**
L. Rosselet *et al.* [WA98 Collaboration]
Nucl. Phys. A **698**, 647 (2002) SPIRES entry
Prepared for 15th International Conference on Ultrarelativistic Nucleus-Nucleus Collisions (QM2001), Stony Brook, New York, 15-20 Jan 2001

[92] **"Lambda production in 40-A-GeV/c Pb Au collisions"**
W. Schmitz *et al.* [CERES Collaboration]
J. Phys. G **28**, 1861 (2002) [arXiv:nucl-ex/0201002] SPIRES entry
Contributed to 6th International Conference on Strange Quarks in Matter: 2001: A Flavorspace Odyssey (SQM2001), Frankfurt, Germany, 25- 29 Sep 2001

[93] **"Centrality dependence of charged-neutral particle fluctuations in 158-A-GeV Pb-208 + Pb-208 collisions"**
M. M. Aggarwal *et al.* [WA98 Collaboration]
Phys. Rev. C **67**, 044901 (2003) [arXiv:nucl-ex/0206017] SPIRES entry

[94] **"Beam energy and centrality dependence of two-pion Bose-Einstein correlations at SPS energies"**
D. Adamova *et al.* [CERES collaboration]
Nucl. Phys. A **714**, 124 (2003) [arXiv:nucl-ex/0207005] SPIRES entry

[95] **"Universal pion freeze-out in heavy-ion collisions"**
D. Adamova *et al.* [CERES Collaboration]
Phys. Rev. Lett. **90**, 022301 (2003) [arXiv:nucl-ex/0207008] SPIRES entry

[96] **"Particle density fluctuations"**
B. Mohanty *et al.*
Nucl. Phys. A **715**, 339 (2003) [arXiv:nucl-ex/0208019] SPIRES entry
Presented at 16th International Conference on Ultrarelativistic Nucleus-Nucleus Collisions, Quark Matter 2002 (QM 2002), Nantes, France, 18-24 Jul 2002

[97] **"Enhanced production of low-mass electron pairs in 40-A-GeV Pb Au collisions at the CERN SPS"**
D. Adamova *et al.* [CERES/NA45 Collaboration]
Phys. Rev. Lett. **91**, 042301 (2003) [arXiv:nucl-ex/0209024] SPIRES entry

[98] **"One-, two-, and three-particle distributions from 158A GeV/c central Pb+Pb collisions"**
M. M. Aggarwal *et al.* [WA98 Collaboration]
Phys. Rev. C **67**, 014906 (2003) [arXiv:nucl-ex/0210002] SPIRES entry

[99] **"Study of electron pair and hadron production with In and Pb beams at the CERN SPS. (Addendum 2 to proposal SPSC-P-P280)"**
D. Adamova *et al.* [CERES Collaboration]
CERN-SPSC-2002-033(2002) SPIRES entry

[100] **"Interferometry of direct photons in central Pb-208 + Pb-208 collisions at 158-A-GeV"**
M. M. Aggarwal *et al.* [WA98 Collaboration]
Phys. Rev. Lett. **93**, 022301 (2004) [arXiv:nucl-ex/0310022] SPIRES entry

[101] **"Latest results from CERES/NA45"**
J. P. Wessels *et al.* [CERES/NA45 Collaboration]
Nucl. Phys. A **715**, 262 (2003) [arXiv:nucl-ex/0212015] SPIRES entry
Contributed to 16th International Conference on Ultrarelativistic Nucleus-Nucleus Collisions: Quark Matter 2002 (QM 2002), Nantes, France, 18-24 Jul 2002

[102] **"Photon Flow In 158-A-Gev Pb + Pb Collisions"**
S. Nikolaev *et al.* [WA98 Collaboration]
Nucl. Phys. A **715**, 579 (2003) SPIRES entry
Prepared for 16th International Conference on Ultrarelativistic Nucleus-Nucleus Collisions: Quark Matter 2002 (QM 2002), Nantes, France, 18-24 Jul 2002

[103] **"Event-by-event fluctuations of the mean transverse momentum in 40-A-GeV/c, 80-A-GeV/c, and 158-A-GeV/c Pb - Au collisions"**
D. Adamova *et al.* [CERES Collaboration]
Nucl. Phys. A **727**, 97 (2003) [arXiv:nucl-ex/0305002] SPIRES entry

[104] **"Azimuthal anisotropy of photon and charged particle emission in Pb-208 + Pb-208 collisions at 158-A-GeV/c"**
M. M. Aggarwal *et al.* [WA98 Collaboration]
Eur. Phys. J. C **41**, 287 (2005) [arXiv:nucl-ex/0406022] SPIRES entry

[105] **"Event-by-event fluctuations at SPS"**
H. Appelshauser *et al.* [CERES Collaboration]
Nucl. Phys. A **752**, 394 (2005) [arXiv:nucl-ex/0409022] SPIRES entry
To appear in the proceedings of International Nuclear Physics Conferences (INPC 2004), Goteborg, Sweden, 27 Jun - 2 Jul 2004

[106] **"Centrality and transverse momentum dependence of collective flow in 158-A-GeV Pb + Pb collisions measured via inclusive photons"**
M. M. Aggarwal *et al.* [WA98 Collaboration]
Nucl. Phys. A **762**, 129 (2005) [arXiv:nucl-ex/0410045] SPIRES entry

[107] **"Latest Results on e^+e^- Pair Production in Ceres"**
D. Adamova *et al.* [CERES Collaboration]
Nucl. Phys. A **749**, 160 (2005) SPIRES entry
Prepared for 18th Nuclear Physics Division Conference: Phase Transitions in Strongly Interacting Matter, Prague, Czech Republic, 23-29 Aug 2004

[108] **"Leptonic and charged kaon decay modes of the Phi meson measured in heavy-ion collisions at the CERN SPS"**
D. Adamova *et al.* [CERES Collaboration]
Phys. Rev. Lett. **96**, 152301 (2006) [arXiv:nucl-ex/0512007] SPIRES entry

[109] **"Pion freeze-out time in Pb + Pb collisions at 158-A-GeV/c studied via pi-/pi+ and K-/K+ ratios"**
M. M. Aggarwal *et al.* [WA98 Collaboration]
arXiv:nucl-ex/0607018 SPIRES entry

[110] **"Modification of the rho meson detected by low-mass electron-positron pairs in central Pb-Au collisions at 158 A GeV/c"**

D. Adamova *et al.*
Phys. Lett. B **666**, 425 (2008) [arXiv:nucl-ex/0611022] SPIRES entry

[111] **"Azimuthal HBT and transverse momentum fluctuations from CERES"**
D. Miskowiec *et al.* [CERES Collaboration]
PoS C **POD07**, 065 (2007) SPIRES entry

[112] **"Suppression of High-pT Neutral Pions in Central Pb+Pb Collisions at $\sqrt{s_{NN}}$ = 17.3 GeV"**
M. M. Aggarwal *et al.* [WA98 Collaboration]
Phys. Rev. Lett. **100**, 242301 (2008) [arXiv:0708.2630 [nucl-ex]] SPIRES entry

[113] **"Source radii at target rapidity from two-proton and two-deuteron correlations in central Pb+Pb collisions at 158 A GeV"**
M. M. Aggarwal *et al.* [WA98 Collaboration]
arXiv:0709.2477 [nucl-ex] SPIRES entry

[114] **"Dilepton measurements with CERES"**
A. Marin *et al.* [CERES Collaboration]
PoS C **POD07**, 034 (2007) [arXiv:0802.2679 [nucl-ex]] SPIRES entry
To appear in the proceedings of 4th International Workshop on Critical Point and Onset Deconfinement, Darmstadt, Germany, 9-13 Jul 2007

[115] **"Scale-dependence of transverse momentum correlations in Pb-Au collisions at 158A GeV/c"**
D. Adamova *et al.* [CERES Collaboration]
Nucl. Phys. A **811**, 179 (2008) [arXiv:0803.2407 [nucl-ex]] SPIRES entry

[116] **"Azimuthal dependence of pion source radii in Pb+Au collisions at 158 A GeV"**
D. Adamova *et al.* [CERES Collaboration]
arXiv:0805.2484 [nucl-ex] SPIRES entry

[117] **Modification of jet-like correlations in Pb-Au collisions at 158A GeV/c**
D. Adamová, ..., M. Šumbera *et al.* (CERES Collaboration), , Phys. Lett. B **678**, 259 (2009).

[118] **"Multiplicity distribution and spectra of negatively charged hadrons in Au + Au collisions at s(NN)**(1/2) = 130-GeV"**
C. Adler *et al.* [STAR Collaboration]
Phys. Rev. Lett. **87**, 112303 (2001) [arXiv:nucl-ex/0106004] SPIRES entry

[119] **"Identified particle elliptic flow in Au + Au collisions at s(NN)**(1/2) = 130-GeV"**
C. Adler *et al.* [STAR Collaboration]
Phys. Rev. Lett. **87**, 182301 (2001) [arXiv:nucl-ex/0107003] SPIRES entry

[120] **"Pion interferometry of s(NN)**(1/2) = 130-GeV Au + Au collisions at RHIC"**
C. Adler *et al.* [STAR Collaboration]
Phys. Rev. Lett. **87**, 082301 (2001) [arXiv:nucl-ex/0107008] SPIRES entry

[121] **"Antideuteron and anti-helium-3 production in s(NN)**(1/2) = 130-GeV Au + Au collisions"**
C. Adler *et al.* [STAR Collaboration]
Phys. Rev. Lett. **87**, 262301 (2001) [Erratum-ibid. **87**, 279902 (2001)] [arXiv:nucl-ex/0108022] SPIRES entry

[122] **"Measurement of inclusive antiprotons from Au + Au collisions at s(NN)**(1/2) = 130-GeV"**
C. Adler *et al.* [STAR Collaboration]
Phys. Rev. Lett. **87**, 262302 (2001) [arXiv:nucl-ex/0110009] SPIRES entry

[123] **"Strangeness in Au + Au collisions at s(NN)**(1/2) = 130-GeV observed with the STAR detector"**
L. S. Barnby *et al.* [STAR Collaboration]
J. Phys. G **28**, 1535 (2002) SPIRES entry
Prepared for 6th International Conference on Strange Quarks in Matter: 2001: A Flavorspace Odyssey (SQM2001), Frankfurt, Germany, 24-29 Sep 2001

[124] **"Mid-rapidity Lambda and Antilambda production in Au + Au collisions at s(NN)**(1/2) = 130-GeV"**
C. Adler *et al.* [STAR Collaboration]
Phys. Rev. Lett. **89**, 092301 (2002) [arXiv:nucl-ex/0203016] SPIRES entry

[125] **"Midrapidity phi production in Au+Au collisions at sNN =130 GeV"**
C. Adler *et al.* [STAR Collaboration]
Phys. Rev. C **65**, 041901 (2002) SPIRES entry

[126] **"STAR detector overview"**
K. H. Ackermann *et al.* [STAR Collaboration]
Nucl. Instrum. Meth. A **499**, 624 (2003) SPIRES entry

[127] **"Azimuthal anisotropy of K^0_S and Lambda + anti-Lambda production at mid-rapidity from Au + Au collisions at $\sqrt{s_{NN}}$ = 130 GeV"**
C. Adler *et al.* [STAR Collaboration]
Phys. Rev. Lett. **89**, 132301 (2002) [arXiv:hep-ex/0205072] SPIRES entry

[128] **"K*(892)0 production in relativistic heavy ion collisions at S(NN)**(1/2) = 130-GeV"**
C. Adler *et al.* [STAR Collaboration]
Phys. Rev. C **66**, 061901 (2002) [arXiv:nucl-ex/0205015] SPIRES entry

[129] **"Elliptic flow from two- and four-particle correlations in Au + Au collisions at s(NN)**(1/2) = 130-GeV"**
C. Adler *et al.* [STAR Collaboration]
Phys. Rev. C **66**, 034904 (2002) [arXiv:nucl-ex/0206001] SPIRES entry

[130] **"Coherent ρ^0 production in ultra-peripheral heavy ion collisions"**
C. Adler *et al.* [STAR Collaboration]
Phys. Rev. Lett. **89**, 272302 (2002) [arXiv:nucl-ex/0206004] SPIRES entry

[131] **"Azimuthal anisotropy and correlations in the hard scattering regime at RHIC"**
C. Adler *et al.* [STAR Collaboration]
Phys. Rev. Lett. **90**, 032301 (2003) [arXiv:nucl-ex/0206006] SPIRES entry

[132] **"Kaon production and kaon to pion ratio in Au + Au collisions at s(NN)**(1/2) = 130-GeV"**
C. Adler *et al.* [STAR Collaboration]
Phys. Lett. B **595**, 143 (2004) [arXiv:nucl-ex/0206008] SPIRES entry

[133] **"Centrality dependence of high p_T hadron suppression in Au+Au collisions at $\sqrt{s}_{NN}$ = 130-GeV"**
C. Adler *et al.* [STAR Collaboration]
Phys. Rev. Lett. **89**, 202301 (2002) [arXiv:nucl-ex/0206011] SPIRES entry

[134] **"Disappearance of back-to-back high p_T hadron correlations in central Au+Au collisions at $\sqrt{s_{NN}}$ = 200-GeV"**
C. Adler *et al.* [STAR Collaboration]
Phys. Rev. Lett. **90**, 082302 (2003) [arXiv:nucl-ex/0210033] SPIRES entry

[135] **"Strange anti-particle to particle ratios at mid-rapidity in s(NN)**(1/2) = 130-GeV Au + Au collisions"**
J. Adams *et al.* [STAR Collaboration]
Phys. Lett. B **567**, 167 (2003) [arXiv:nucl-ex/0211024] SPIRES entry

[136] **"Azimuthal anisotropy at RHIC: The first and fourth harmonics"**
J. Adams *et al.* [STAR Collaboration]
Phys. Rev. Lett. **92**, 062301 (2004) [arXiv:nucl-ex/0310029] SPIRES entry

[137] **"Azimuthally sensitive HBT in Au + Au collisions at s(NN)**(1/2) = 200-GeV"**
J. Adams *et al.* [STAR Collaboration]
Phys. Rev. Lett. **93**, 012301 (2004) [arXiv:nucl-ex/0312009] SPIRES entry

[138] J. Adams *et al.* [STAR Collaboration], Phys. Rev. Lett. **92**, 052302 (2004) [arXiv:nucl-ex/0306007].

[139] **"An update from STAR - using strangeness to probe relativistic heavy ion collisions"**
H. Caines *et al.* [STAR Collaboration]
J. Phys. G **30**, S61 (2004) SPIRES entry
Prepared for 7th International Conference on Strangeness in Quark Matter (SQM 2003), Atlantic Beach, North Carolina, 12-17 Mar 2003

[140] **"Photon and neutral pion production in Au + Au collisions at s(NN)**(1/2) = 130-GeV"**
J. Adams *et al.* [STAR Collaboration]
Phys. Rev. C **70**, 044902 (2004) [arXiv:nucl-ex/0401008] SPIRES entry

[141] **"Production of e+ e- pairs accompanied by nuclear dissociation in ultra-peripheral heavy ion collision"**
J. Adams *et al.* [STAR Collaboration]
Phys. Rev. C **70**, 031902 (2004) [arXiv:nucl-ex/0404012] SPIRES entry

[142] **"Narrowing of the balance function with centrality in Au + Au collisions s(NN)**(1/2) = 130-GeV"**
J. Adams *et al.* [STAR Collaboration]
Phys. Rev. Lett. **90**, 172301 (2003) [arXiv:nucl-ex/0301014] SPIRES entry

[143] **"Transverse momentum and collision energy dependence of high p(T) hadron suppression in Au + Au collisions at ultrarelativistic energies"**
J. Adams *et al.* [STAR Collaboration]
Phys. Rev. Lett. **91**, 172302 (2003) [arXiv:nucl-ex/0305015] SPIRES entry

[144] **"Evidence from d + Au measurements for final-state suppression of high p(T) hadrons in Au + Au collisions at RHIC"**
J. Adams *et al.* [STAR Collaboration]
Phys. Rev. Lett. **91**, 072304 (2003) [arXiv:nucl-ex/0306024] SPIRES entry

[145] **"Three-pion HBT correlations in relativistic heavy-ion collisions from the STAR experiment"**
J. Adams *et al.* [STAR Collaboration]
Phys. Rev. Lett. **91**, 262301 (2003) [arXiv:nucl-ex/0306028] SPIRES entry

[146] **"Rapidity and centrality dependence of proton and anti-proton production from Au-197 + Au-197 collisions at s(NN)**(1/2) = 130-GeV"**
J. Adams *et al.* [STAR Collaboration]
Phys. Rev. C **70**, 041901 (2004) [arXiv:nucl-ex/0306029] SPIRES entry

[147] **"Multiplicity fluctuations in Au + Au collisions at s(NN)**(1/2) = 130-GeV"**
J. Adams *et al.* [STAR Collaboration]
Phys. Rev. C **68**, 044905 (2003) [arXiv:nucl-ex/0307007] SPIRES entry

[148] **"rho0 production and possible modification in Au + Au and p + p collisions at s(NN)**(1/2) = 200-GeV"**
J. Adams *et al.* [STAR Collaboration]
Phys. Rev. Lett. **92**, 092301 (2004) [arXiv:nucl-ex/0307023] SPIRES entry

[149] **"Multi-strange baryon production in Au Au collisions at s(NN)**(1/2) = 130-GeV"**
J. Adams *et al.* [STAR Collaboration]
Phys. Rev. Lett. **92**, 182301 (2004) [arXiv:nucl-ex/0307024] SPIRES entry

[150] **"Pion kaon correlations in Au + Au collisions at s(NN)**(1/2) = 130-GeV"**
J. Adams *et al.* [STAR Collaboration]
Phys. Rev. Lett. **91**, 262302 (2003) [arXiv:nucl-ex/0307025] SPIRES entry

[151] **"Event-by-event fluctuations in Au Au collisions at s(NN)**(1/2) = 130-GeV"**
J. Adams *et al.* [STAR Collaboration]
Phys. Rev. C **71**, 064906 (2005) [arXiv:nucl-ex/0308033] SPIRES entry

[152] **"Pion, kaon, proton and anti-proton transverse momentum distributions from p + p and d + Au collisions at s(NN)**1/2 = 200-GeV"**
J. Adams *et al.* [STAR Collaboration]
Phys. Lett. B **616**, 8 (2005) [arXiv:nucl-ex/0309012] SPIRES entry

[153] **"Identified particle distributions in p p and Au + Au collisions at s**(1/2) = 200-GeV"**
J. Adams *et al.* [STAR Collaboration]
Phys. Rev. Lett. **92**, 112301 (2004) [arXiv:nucl-ex/0310004] SPIRES entry

[154] J. Adams *et al.* [STAR Collaboration], Phys. Rev. Lett. **92**, 171801 (2004)

[155] **"Centrality and pseudorapidity dependence of charged hadron production at intermediate p_T in Au + Au collisions at $\sqrt{s_{NN}}$ = 130-GeV"**
J. Adams *et al.* [STAR Collaboration]
Phys. Rev. C **70**, 044901 (2004) [arXiv:nucl-ex/0404020] SPIRES entry

[156] **"Phi meson production in Au + Au and p + p collisions at s**(1/2) = 200-GeV"**
J. Adams *et al.* [STAR Collaboration]
Phys. Lett. B **612**, 181 (2005) [arXiv:nucl-ex/0406003] SPIRES entry

[157] **"Hadronization geometry and charge-dependent number autocorrelations on axial momentum space in Au Au collisions at s(NN)**(1/2) = 130-GeV"**
J. Adams *et al.* [STAR Collaboration]
Phys. Lett. B **634**, 347 (2006) [arXiv:nucl-ex/0406035] SPIRES entry

[158] **"Transverse-momentum dependent modification of dynamic texture in central Au + Au collisions at s(NN)**(1/2) = 200-GeV"**
J. Adams *et al.* [STAR Collaboration]
Phys. Rev. C **71**, 031901 (2005) [arXiv:nucl-ex/0407001] SPIRES entry

[159] **"Measurements of transverse energy distributions in Au + Au collisions at s(NN)**(1/2) = 200-GeV"**
J. Adams *et al.* [STAR Collaboration]
Phys. Rev. C **70**, 054907 (2004) [arXiv:nucl-ex/0407003] SPIRES entry

[160] **"Open charm yields in d + Au collisions at s(NN)**(1/2) = 200-GeV"**
J. Adams *et al.* [STAR Collaboration]
Phys. Rev. Lett. **94**, 062301 (2005) [arXiv:nucl-ex/0407006] SPIRES entry

[161] **"Azimuthal anisotropy and correlations at large transverse momenta in p + p and Au + Au collisions at s(NN)**(1/2) = 200-GeV"**
J. Adams *et al.* [STAR Collaboration]
Phys. Rev. Lett. **93**, 252301 (2004) [arXiv:nucl-ex/0407007] SPIRES entry

[162] **"Transverse momentum correlations and minijet dissipation in Au Au collisions at s(NN)**(1/2) = 130-GeV"**
J. Adams *et al.* [STAR Collaboration]
J. Phys. G **34**, 799 (2007) [arXiv:nucl-ex/0408012] SPIRES entry

[163] **"Pseudorapidity asymmetry and centrality dependence of charged hadron spectra in d + Au collisions at s(NN)**(1/2) = 200-GeV"**
J. Adams *et al.* [STAR Collaboration]
Phys. Rev. C **70**, 064907 (2004) [arXiv:nucl-ex/0408016] SPIRES entry

[164] **"Azimuthal anisotropy in Au + Au collisions at s(NN)**(1/2) = 200-GeV"**
J. Adams *et al.* [STAR Collaboration]
Phys. Rev. C **72**, 014904 (2005) [arXiv:nucl-ex/0409033] SPIRES entry

[165] **"Minijet deformation and charge-independent angular correlations on momentum subspace (eta, phi) in Au-Au collisions at s(NN)**(1/2) = 130-GeV"**
J. Adams *et al.* [STAR Collaboration]
Phys. Rev. C **73**, 064907 (2006) [arXiv:nucl-ex/0411003] SPIRES entry

[166] **"Pion interferometry in Au + Au collisions at s(NN)**(1/2) = 200-GeV"**
J. Adams *et al.* [STAR Collaboration]
Phys. Rev. C **71**, 044906 (2005) [arXiv:nucl-ex/0411036] SPIRES entry

[167] **"K*(892) resonance production in Au + Au and p + p collisions at s(NN)**(1/2) = 200-GeV at STAR"**
J. Adams *et al.* [STAR Collaboration]
Phys. Rev. C **71**, 064902 (2005) [arXiv:nucl-ex/0412019] SPIRES entry

[168] **"Open Charm Production From D + Au Collisions In Star"**
M. Calderon de la Barca Sanchez *et al.* [STAR Collaboration]
Eur. Phys. J. C **43**, 187 (2005) SPIRES entry
Prepared for International Conference on Hard and Electromagnetic Probes of High Energy Nuclear Collisions (HP 2004), Ericeira, Portugal, 4-10 Nov 2004

[169] **"Charm Production In The Star Experiment At Rhic"**
A. A. P. Suaide *et al.* [STAR Collaboration]

Eur. Phys. J. C **43**, 193 (2005) SPIRES entry
Prepared for International Conference on Hard and Electromagnetic Probes of High Energy Nuclear Collisions (HP 2004), Ericeira, Portugal, 4-10 Nov 2004

[170] **"Recent High-P(T) Results From Star"**
C. A. Gagliardi *et al.* [STAR Collaboration]
Eur. Phys. J. C **43**, 263 (2005) SPIRES entry
Prepared for International Conference on Hard and Electromagnetic Probes of High Energy Nuclear Collisions (HP 2004), Ericeira, Portugal, 4-10 Nov 2004

[171] **"Experimental and theoretical challenges in the search for the quark gluon plasma: The STAR collaboration's critical assessment of the evidence from RHIC collisions"**
J. Adams *et al.* [STAR Collaboration]
Nucl. Phys. A **757**, 102 (2005) [arXiv:nucl-ex/0501009] SPIRES entry

[172] **"Distributions of charged hadrons associated with high transverse momentum particles in p p and Au + Au collisions at s(NN)**(1/2) = 200-GeV"**
J. Adams *et al.* [STAR Collaboration]
Phys. Rev. Lett. **95**, 152301 (2005) [arXiv:nucl-ex/0501016] SPIRES entry

[173] **"Multiplicity and pseudorapidity distributions of photons in Au + Au collisions at s(NN)**(1/2) = 62.4-GeV"**
J. Adams *et al.* [STAR Collaboration]
Phys. Rev. Lett. **95**, 062301 (2005) [arXiv:nucl-ex/0502008] SPIRES entry

[174] **"Multi-strange baryon elliptic flow in Au + Au collisions at s(NN)**(1/2) = 200-GeV"**
J. Adams *et al.* [STAR Collaboration]
Phys. Rev. Lett. **95**, 122301 (2005) [arXiv:nucl-ex/0504022] SPIRES entry

[175] **"Incident energy dependence of p(t) correlations at RHIC"**
J. Adams *et al.* [STAR Collaboration]
Phys. Rev. C **72**, 044902 (2005) [arXiv:nucl-ex/0504031] SPIRES entry

[176] **"Transverse-momentum p(t) correlations on (eta,Phi) from mean-p(t) fluctuations in Au - Au collisions at s(NN)**(1/2) = 200-GeV"**
J. Adams *et al.* [STAR Collaboration]
J. Phys. G **32**, L37 (2006) [arXiv:nucl-ex/0509030] SPIRES entry

[177] **"Directed flow in Au + Au collisions at s(NN)**(1/2) = 62-GeV"**
J. Adams *et al.* [STAR Collaboration]
Phys. Rev. C **73**, 034903 (2006) [arXiv:nucl-ex/0510053] SPIRES entry

[178] **"Proton Lambda correlations in central Au + Au collisions at s(NN)**(1/2) = 200-GeV"**
J. Adams *et al.* [STAR Collaboration]
Phys. Rev. C **74**, 064906 (2006) [arXiv:nucl-ex/0511003] SPIRES entry

[179] **"Multiplicity and pseudorapidity distributions of charged particles and photons at forward pseudorapidity in Au + Au collisions at s(NN)**(1/2) = 62.4-GeV"**
J. Adams *et al.* [STAR Collaboration]
Phys. Rev. C **73**, 034906 (2006) [arXiv:nucl-ex/0511026] SPIRES entry

[180] P. Chaloupka , ..., M. Šumbera *et al.* (STAR Collaboration), Non-identical particle correlations at $\sqrt{s_{NN}} = 62$GeV and 200 GeV at STAR, Nucl. Phys. A **774** (2006) 603.

[181] **"Strangelet search at RHIC"**
B. I. Abelev *et al.* [STAR Collaboration]
Phys. Rev. C **76**, 011901 (2007) [arXiv:nucl-ex/0511047] SPIRES entry

[182] **"Measurement of charm flow with the STAR heavy flavour tracker"**
Z. Xu *et al.*
J. Phys. G **32**, S571 (2006) SPIRES entry
Prepared for International Conference on Strangeness in Quark Matter (SQM2006), Los Angeles, California, 26-31 Mar 2006

[183] **"Identified hadron spectra at large transverse momentum in p + p and d + Au collisions at s(NN)**(1/2) = 200-GeV"**
J. Adams *et al.* [STAR Collaboration]
Phys. Lett. B **637**, 161 (2006) [arXiv:nucl-ex/0601033] SPIRES entry

[184] **"Measurements of identified particles at intermediate transverse momentum in the STAR experiment from Au + Au collisions at s(NN)**(1/2) = 200-GeV"**
J. Adams *et al.* [STAR Collaborations and STAR-RICH Collaborations]
arXiv:nucl-ex/0601042 SPIRES entry (Submitted to Phys.Rev.C)

[185] **"Forward neutral pion production in p+p and d+Au collisions at s(NN)**(1/2) = 200-GeV"**
J. Adams *et al.* [STAR Collaboration]
Phys. Rev. Lett. **97**, 152302 (2006) [arXiv:nucl-ex/0602011] SPIRES entry

[186] **"A heavy flavor tracker for STAR"**
Z. Xu *et al.*
LBNL-PUB-5509 SPIRES entry

[187] **"Direct observation of dijets in central Au + Au collisions at s(NN)**(1/2) = 200-GeV"**
J. Adams *et al.* [STAR Collaboration]
Phys. Rev. Lett. **97**, 162301 (2006) [arXiv:nucl-ex/0604018] SPIRES entry

[188] **"Strange baryon resonance production in s(NN)**(1/2) = 200-GeV p + p and Au + Au collisions"**
J. Adams *et al.* [STAR Collaboration]
Phys. Rev. Lett. **97**, 132301 (2006) [arXiv:nucl-ex/0604019] SPIRES entry

[189] **"The Energy dependence of p_t angular correlations inferred from mean-p(t) fluctuation scale dependence in heavy ion collisions at the SPS and RHIC"**
J. Adams *et al.* [STAR Collaboration]
J. Phys. G **33**, 451 (2007) [arXiv:nucl-ex/0605021] SPIRES entry

[190] **"Identified baryon and meson distributions at large transverse momenta from Au + Au collisions at s(NN)**(1/2) = 200-GeV"**
B. I. Abelev *et al.* [STAR Collaboration]
Phys. Rev. Lett. **97**, 152301 (2006) [arXiv:nucl-ex/0606003] SPIRES entry

[191] **"Scaling Properties of Hyperon Production in Au+Au Collisions at $\sqrt{(}s_{NN}) =$ 200 GeV"**
J. Adams *et al.* [STAR Collaboration]
Phys. Rev. Lett. **98**, 062301 (2007) [arXiv:nucl-ex/0606014] SPIRES entry

[192] **"The Multiplicity dependence of inclusive p_t spectra from pp collisions at $\sqrt{s} =$ 200-GeV"**

J. Adams *et al.* [STAR Collaboration]
Phys. Rev. D **74**, 032006 (2006) [arXiv:nucl-ex/0606028] SPIRES entry

[193] **"Delta(phi) Delta(eta) correlations in central Au + Au collisions at s(NN)**(1/2) = 200-GeV"**
J. Adams *et al.* [Star Collaboration]
Phys. Rev. C **75**, 034901 (2007) [arXiv:nucl-ex/0607003] SPIRES entry

[194] **"Transverse momentum and centrality dependence of high-pt non-photonic electron suppression in Au+Au collisions at $\sqrt{s_{NN}}$ = 200 GeV"**
B. I. Abelev *et al.* [STAR Collaboration]
Phys. Rev. Lett. **98**, 192301 (2007) [arXiv:nucl-ex/0607012] SPIRES entry

[195] **"Strange particle production in p + p collisions at s**(1/2) = 200-GeV"**
B. I. Abelev *et al.* [STAR Collaboration]
Phys. Rev. C **75**, 064901 (2007) [arXiv:nucl-ex/0607033] SPIRES entry

[196] **"Neutral kaon interferometry in Au + Au collisions at s(NN)**(1/2) = 200-GeV"**
B. I. Abelev *et al.* [STAR Collaboration]
Phys. Rev. C **74**, 054902 (2006) [arXiv:nucl-ex/0608012] SPIRES entry

[197] **"Longitudinal double-spin asymmetry and cross section for inclusive jet production in polarized proton collisions at s**(1/2) = 200-GeV"**
B. I. Abelev *et al.* [STAR Collaboration]
Phys. Rev. Lett. **97**, 252001 (2006) [arXiv:hep-ex/0608030] SPIRES entry

[198] **"Rapidity and species dependence of particle production at large transverse momentum for d + Au collisions at s(NN)**(1/2) = 200-GeV"**
B. I. Abelev *et al.* [STAR Collaboration]
Phys. Rev. C **76**, 054903 (2007) [arXiv:nucl-ex/0609021] SPIRES entry

[199] **"Mass, quark-number, and s(NN)**(1/2) dependence of the second and fourth flow harmonics in ultra-relativistic nucleus nucleus collisions"**
B. I. Abelev *et al.* [the STAR Collaboration]
Phys. Rev. C **75**, 054906 (2007) [arXiv:nucl-ex/0701010] SPIRES entry

[200] **"Selected results on strong and Coulomb-induced correlations from the STAR experiment"**
M. Sumbera [STAR Collaboration]
Braz. J. Phys. **37**, 925 (2007) [arXiv:nucl-ex/0702015] SPIRES entry

[201] **"Charged particle distributions and nuclear modification at high rapidities in d+Au collisions at $\sqrt{s_{NN}}$ = 200 GeV"**
B. I. Abelev *et al.* [STAR Collaboration]
arXiv:nucl-ex/0703016 SPIRES entry (Submitted to Phys.Lett.B)

[202] **"Partonic flow and Phi-meson production in Au + Au collisions at s(NN)**(1/2) = 200-GeV"**
B. I. Abelev *et al.* [STAR Collaboration]
Phys. Rev. Lett. **99**, 112301 (2007) [arXiv:nucl-ex/0703033] SPIRES entry

[203] **"Energy dependence of $\pi^{\pm}$, p and $\bar{p}$ transverse momentum spectrafor Au+Au collisions at $\sqrt{s_{\rm NN}}$ = 62.4 and 200 GeV"**
B. I. Abelev *et al.* [STAR Collaboration]
Phys. Lett. B **655**, 104 (2007) [arXiv:nucl-ex/0703040] SPIRES entry

[204] **"Global polarization measurement in Au+Au collisions"**
B. I. Abelev *et al.* [STAR Collaboration]
Phys. Rev. C **76**, 024915 (2007) [arXiv:0705.1691 [nucl-ex]] SPIRES entry

[205] **"Enhanced strange baryon production in Au+Au collisions compared to p+p at sqrts = 200 GeV"**
B. I. Abelev *et al.* [STAR Collaboration]
Phys. Rev. C **77**, 044908 (2008) [arXiv:0705.2511 [nucl-ex]] SPIRES entry

[206] **"Measurement of Transverse Single-Spin Asymmetries for Di-Jet Production in Proton-Proton Collisions at $\sqrt{s} = 200$ GeV"**
B. I. Abelev *et al.* [STAR Collaboration]
Phys. Rev. Lett. **99**, 142003 (2007) [arXiv:0705.4629 [hep-ex]] SPIRES entry

[207] **"Forward Λ Production and Nuclear Stopping Power in d + Au Collisions at $\sqrt{s_{NN}} = 200$ GeV"**
B. I. Abelev *et al.* [STAR Collaboration]
Phys. Rev. C **76**, 064904 (2007) [arXiv:0706.0472 [nucl-ex]] SPIRES entry

[208] **"Longitudinal double-spin asymmetry for inclusive jet production in p+p collisions at $\sqrt(s) = 200GeV$"**
B. I. Abelev *et al.* [STAR Collaboration]
Phys. Rev. Lett. **100**, 232003 (2008) [arXiv:0710.2048 [hep-ex]] SPIRES entry

[209] **"ρ^0 Photoproduction in Ultra-Peripheral Relativistic Heavy Ion Collisions with STAR"**
B. I. Abelev *et al.* [STAR Collaboration]
Phys. Rev. C **77**, 034910 (2008) [arXiv:0712.3320 [nucl-ex]] SPIRES entry

[210] **"Hadronic resonance production in d+Au collisions at $\sqrt{s_{NN}} = 200$ GeV at RHIC"**
B. I. Abelev *et al.* [STAR Collaboration]
Phys. Rev. C **78**, 044906 (2008) [arXiv:0801.0450 [nucl-ex]] SPIRES entry

[211] **"Spin alignment measurements of the $K^{*0}(892)$ and $\phi(1020)$ vector mesons in heavy ion collisions at $\sqrt{s}_{NN} = 200$ GeV"**
B. I. Abelev *et al.* [STAR Collaboration]
Phys. Rev. C **77**, 061902 (2008) [arXiv:0801.1729 [nucl-ex]] SPIRES entry

[212] **"Forward Neutral Pion Transverse Single Spin Asymmetries in p+p Collisions at $\sqrt{s} = 200GeV$"**
B. I. Abelev *et al.* [STAR Collaboration]
Phys. Rev. Lett. **101**, 222001 (2008) [arXiv:0801.2990 [hep-ex]] SPIRES entry

[213] **"Centrality dependence of charged hadron and strange hadron elliptic flow from $\sqrt(s_{NN}) = 200$ GeV Au+Au collisions"**
B. I. Abelev *et al.* [STAR Collaboration]
Phys. Rev. C **77**, 054901 (2008) [arXiv:0801.3466 [nucl-ex]] SPIRES entry

[214] **"Charmed hadron production at low transverse momentum in Au+Au collisions at RHIC"**
B. I. Abelev *et al.* [STAR Collaboration]
arXiv:0805.0364 [nucl-ex] SPIRES entry

[215] **"Indications of Conical Emission of Charged Hadrons at RHIC"**
B. I. Abelev *et al.* [STAR Collaboration]
Phys. Rev. Lett. **102**, 052302 (2009) [arXiv:0805.0622 [nucl-ex]] SPIRES entry

[216] **"Charge Independent(CI) and Charge Dependent(CD) correlations vs. Centrality from $\Delta\phi\Delta\eta$ Charged Pairs in Minimum Bias Au + Au Collisions at 200 Gev"**
B. I. Abelev *et al.* [STAR Collaboration]
arXiv:0806.0513 [nucl-ex] SPIRES entry (Submitted to Phys.Rev.C)

[217] **"System-size independence of directed flow at the Relativistic Heavy-Ion Collider"**
B. I. Abelev *et al.* [STAR Collaboration]
Phys. Rev. Lett. **101**, 252301 (2008) [arXiv:0807.1518 [nucl-ex]] SPIRES entry

[218] **"Beam-Energy and System-Size Dependence of Dynamical Net Charge Fluctuations"**
B. I. Abelev *et al.* [STAR Collaboration]
Phys. Rev. C **79**, 024906 (2009) [arXiv:0807.3269 [nucl-ex]] SPIRES entry

[219] **"Systematic Measurements of Identified Particle Spectra in pp, d^+ Au and Au+Au Collisions from STAR"**
B. I. Abelev *et al.* [STAR Collaboration]
Phys. Rev. C **79**, 034909 (2009) [arXiv:0808.2041 [nucl-ex]] SPIRES entry

[220] **"Measurements of ϕ meson production in relativistic heavy-ion collisions at RHIC"**
B. I. Abelev *et al.* [STAR Collaboration]
arXiv:0809.4737 [nucl-ex] SPIRES entry

[221] **"Energy and system size dependence of ϕ meson production in Cu+Cu and Au+Au collisions"**
B. I. Abelev *et al.* [STAR Collaboration]
Phys. Lett. B **673**, 183 (2009) [arXiv:0810.4979 [nucl-ex]] SPIRES entry

[222] **"Observation of Two-source Interference in the Photoproduction Reaction $AuAu \to AuAu\rho^0$"**
B. I. Abelev *et al.* [STAR Collaboration]
Phys. Rev. Lett. **102**, 112301 (2009) [arXiv:0812.1063 [nucl-ex]] SPIRES entry

[223] **"Measurement of D* Mesons in Jets from p+p Collisions at sqrts = 200 GeV"**
B. I. Abelev *et al.* [STAR Collaboration]
Phys. Rev. D **79**, 112006 (2009) [arXiv:0901.0740 [hep-ex]] SPIRES entry

[224] **"K/pi Fluctuations at Relativistic Energies"**
B. I. Abelev *et al.* [STAR Collaboration]
arXiv:0901.1795 [nucl-ex] SPIRES entry

[225] **"Pion Interferometry in Au+Au and Cu+Cu Collisions at RHIC"**
B. I. Abelev *et al.* [STAR Collaboration]
arXiv:0903.1296 [nucl-ex] SPIRES entry (Submitted to Phys.Rev.C)

[226] **"J/psi production at high transverse momentum in p+p and Cu+Cu collisions at $\sqrt{s_{NN}}$ = 200 GeV**
B. I. Abelev *et al.* [STAR Collaboration]
arXiv:0904.0439 [nucl-ex] SPIRES entry

[227] **"Letter of Intent for A Large Ion Collider Experiment"**
N. Antoniou *et al.* [ALICE Collaboration]
CERN-LHCC-93-16(1993) SPIRES entry

[228] **"Experiment ALICE"**
M. Sumbera
Czech. J. Phys. **45**, 579 (1995) SPIRES entry
Prepared for International School / Workshop for Young Physicists: Relativistic Heavy Ion Physics, Prague, Czech Republic, 19-23 Sep 1994

[229] **"ALICE: Technical proposal for a large ion collider experiment at the CERN LHC "**
CERN-LHCC-P-3

[230] **"The forward muon spectrometer of ALICE"**
S. Beole *et al.* [ALICE Collaboration]
CERN-LHCC-96-32(1996) SPIRES entry

[231] **"Physics of ultra-relativistic heavy-ion collisions: Recent results and future perspectives. Proceedings, International School-Workshop for Young Physicists in Relativistic Heavy-Ion Physics, RHIP'97, Prague, Czech Republic, Septem"**
M. Sumbera SPIRES entry
Prepared for International School - Workshop for Young Physicists: Physics of Ultra-relativistic Heavy Ion Collisions: Recent Results and Future Perspectives (RHIP 97), Prague, Czech Republic, 1-5 Sep 1997

[232] **"ALICE technical design report: Detector for high momentum PID"**
S. Beole *et al.* [ALICE Collaboration]
CERN-LHCC-98-19(1998) SPIRES entry

[233] **"ALICE technical design report: Photon multiplicity detector (PMD)"**
G. Dellacasa *et al.* [ALICE Collaboration]
CERN-LHCC-99-32(1999) SPIRES entry

[234] **"ALICE technical design report of the inner tracking system (ITS)"**
G. Dellacasa *et al.* [ALICE Collaboration],
CERN-LHCC-99-12.

[235] **"ALICE: Addendum to the technical design report of the time of flight system (TOF)"**
P. Cortese *et al.* [ALICE Collaboration]
CERN-LHCC-2002-016(2002) SPIRES entry

[236] F. Carminati *et al.* (ALICE Collaboration), ALICE: Physics performance report, volumes I and II, J. Phys. G **30** (2004) 1517.
J. Phys. G: Nucl. Part. Phys. 32 (2006) 12952040.

[237] **"ALICE electromagnetic calorimeter technical design report"**
P. Cortese *et al.* [ALICE Collaboration]
CERN-LHCC-2008-014(2008) SPIRES entry

[238] **"The Alice Experiment at the CERN LHC"**
K. Aamodt *et al.* [ALICE Collaboration]
JINST **0803**, S08002 (2008) [JINST **3**, S08002 (2008)] SPIRES entry

[239] M. Šumbera, 1996, unpublished.

[240] **"Critical Behavior Of The Characteristics Of Hadron Nucleus And Nucleus Nucleus Interactions Depending On The Centrality Degree Of Collisions"**
M. K. Suleimanov, M. Sumbera, A. S. Vodopianov and I. Zborovsky

AIP Conf. Proc. **603**, 389 (2001) SPIRES entry
Prepared for 8th Meeting on Mesons and Light Nuclei, Prague, Czech Republic, 2-6 Jul 2001

[241] **"Status and Promise of Particle Interferometry in Heavy-Ion Collisions"**
S. Bekele *et al.*
arXiv:0706.0537 [nucl-ex] SPIRES entry
Presented at 2nd Workshop on Particle Correlation and Femtoscopy (WPCF 2006), Sao Paulo, Brazil, 9-11 Sep 2006

[242] **"Nuclear suppression at large forward rapidities in d-Au collisions at relativistic and ultrarelativistic energies"**
J. Nemchik, V. Petracek, I. K. Potashnikova and M. Sumbera
Phys. Rev. C **78**, 025213 (2008) [arXiv:0805.4267 [hep-ph]] SPIRES entry

[243] **"Parton Rescatterings in Large-x Nuclear Suppression at RHIC"**
J. Nemchik and M. Sumbera
arXiv:0811.3837 [hep-ph] SPIRES entry
Talk given at 38th International Symposium on Multiparticle Dynamics ISMD08, Hamburg, Germany, 15-20 Sep 2008 and talk given at 19th International Baldin Seminar on High Energy Physics Problems: Relativistic Nuclear Physics and Quantum Chromodynamics (ISHEPP 2008), Dubna, Russia, 29 Sep - 4 Oct 2008

[244] **"Proceedings of the 38th International Symposium on Multiparticle Dynamics (ISMD08)"**
J. Bartels *et al.*
arXiv:0902.0377 [hep-ph]
DESY-PROC-2009-01(2009) SPIRES entry

[245] **"Pi Xi Correlations: Model Comparison And Xi*(1530) Puzzle"**
P. Chaloupka, M. Sumbera and L. V. Malinina,
Acta Phys. Polon. B **40** (2009) 1185.

[246] **"$\pi^{\pm}\Xi^{\mp}$ Correlations and the $\Xi^{*}(1530)$ Puzzle"**
B. O. Kerbikov, R. Lednicky, L. V. Malinina, P. Chaloupka and M. Sumbera
arXiv:0907.0617 [nucl-th] SPIRES entry

7.2 Other references

The other references

[R1] R. Stock, *Nucleus-Nucleus Collisions and the QCD Matter Phase Diagram*, in Landolt-Börnstein - Group I Elementary Particles, Nuclei and Atoms, Vol.**21**A, Chapter 7, Springer Berlin Heidelberg,2009. arXiv:0807.1610 [nucl-ex].

[R2] D. G. d'Enterria *et al.*, (CMS Collaboration), J. Phys. G **34** (2007) 2307.

[R3] H. Stöcker and W. Greiner, Phys. Rept. **137** (1986) 277.
[R4] J. Y. Ollitrault, Phys. Rev. D **46** (1992) 229.
[R5] J. Pišút, N. Pišútová and P. Závada, Z. Phys. C **67**, 467 (1995).
[R6] U. W. Heinz, arXiv:0901.4355 [nucl-th].
[R7] W. Heisenberg, Z. Phys. 113(1939)61, 126(1940)569, 133(1952)65, Nature 164(1949).
[R8] E. Fermi, Prog. Theor. Phys. 5 (1950) 570.
[R8] L. D. Landau, Izv. Akad. Nauk Ser. Fiz. **17** (1953) 51.
[R9] W. Kittel, E. A. De Wolf, *Soft multihadron dynamics*. Hackensack, USA: World Scientific (2005) 652 p.
[R10] G. F. Chapline, M. H. Johnson, E. Teller and M. S. Weiss, Phys. Rev. D **8** (1973) 4302.
[R11] W. Scheid, H. Muller and W. Greiner, Phys. Rev. Lett. **32** (1974) 741.
[R12] M. I. Sobel, H. A. Bethe, P. J. Siemens, J. P. Bondorf, Nucl. Phys. A **251** (1975) 502.
[R13] T. D. Lee and G. C. Wick, Phys. Rev. D **9** (1974) 2291.
[R14] D. J. Gross and F. Wilczek, Phys. Rev. Lett. **30** (1973) 1343.
[R15] H. D. Politzer, Phys. Rev. Lett. **30** (1973) 1346.
[R16] J. C. Collins and M. J. Perry, Phys. Rev. Lett. **34**, 1353 (1975).
[R17] N. Cabibbo and G. Parisi, Phys. Lett. B **59** (1975) 67.
[R18] E. V. Shuryak, Sov. Phys. JETP **47**, 212 (1978) [Zh. Eksp. Teor. Fiz. **74**, 408 (1978)].
[R19] K. Huang and S. Weinberg, Phys. Rev. Lett. **25** (1970) 895.
[R20] R. Stock, Phys. Rept. **135** (1986) 259.
[R21] E. Shuryak, Prog. Part. Nucl. Phys. **62** (2009)48.
[R22] M. Chaplin, Water Structure and Science, http://www.lsbu.ac.uk/water/phase.html.
[R23] D. Boyanovsky, H. J. de Vega, D. J. Schwarz, Ann. Rev. Nucl. Part. Sci. **56**, 441 (2006).
[R24] S. Weinberg, *Cosmology*, Oxford, UK: Oxford Univ. Pr. (2008) 593 p.
[R25] K. Kajantie *et al.*, Phys. Rev. Lett. **77**, 2887 (1996).
[R26] Y. Aoki, G. Endrodi, Z. Fodor, S. D. Katz and K. K. Szabo, Nature **443**, 675 (2006).
[R27] M. Cheng *et al.*, Phys. Rev. D **77**, 014511 (2008).
[R28] D. Rischke, Prog. Part. Nucl. Phys. **52** (2004)197.
[R29] L. McLerran and R. D. Pisarski, Nucl. Phys. A **796**, 83 (2007).
[R30] M. Buballa, Phys. Rept. **407** (2005) 205.
[R31] M. Gyulassy and L. McLerran, Nucl. Phys. A **750** (2005) 30.
[R32] S. Ichimaru, Rev. Mod. Phys. **54**, 1017 (1982).
[R33] M. H. Thoma, J. Phys. G **31**, L7 (2005),
[R34] J. Aichelin, Phys. Rept. **202** (1991) 233.
[R35] S. A. Bass *et al.*, Prog. Part. Nucl. Phys. **41**, 255 (1998).
[R36] K. Werner, Phys. Rept. **232** (1993) 87.
[R37] J. J. Griffin and K. K. Kan, Rev. Mod. Phys. **48** (1976) 467.
[R38] B.R. Laughlin, Int. J. Mod. Phys. A **18** (2003) 831.
[R39] I. M. Dremin and J. W. Gary, Phys. Rept. **349**, 301 (2001).
[R40] W. Feller, *Introduction to Probability Theory and its Applications*, Vol. I., Wiley 1971.
[R41] A. Giovannini, L. Van Hove, Z. Phys. C 30 (1986) 391.
[R42] I. Zborovský, Z. Phys. C **63** (1994) 257.
[R43] T. D. Lee, Phys. Rev. D **6** (1972) 3617.
[R44] I. Szapudi, A. S. Szalay, Astr. J. **408** (1993) 43.
[R45] UA5 collab., Phys. Rept. **154**, 247 (1987).
[R46] A. A. Baldin, JINR Rapid Comm. No.3[54]-92, Phys. Atom. Nucl. **56**, 385 (1993).
[R47] V. S. Stavinsky, Proc. 9^{th} ISHEPP, Vol. 1., JINR, D1, 2-88-6652, Dubna 1988, p.190.
[R48] G. Odyniec *et al.*, Proc. 8th. High Energy Heavy Ion Study, Berkeley, 1987.
[R49] S. Backović *et al.*, JINR Rapid Communications. No.2[53]-92,(1992)56.

[R50] G. I. Barenblat, *Scaling, Self-similarity, and Intermediate Asymptotics*, Cambridge Univiversity Press (1996) 386 p.
[R51] U. W. Heinz and M. Jacob, arXiv:nucl-th/0002042.
[R52] B. Mohanty and J. Serreau, Phys. Rept. **414** (2005) 263.
[R53] H. A. Gustafsson *et al.*, Phys. Rev. Lett. **52** (1984) 1590.
[R54] H. H. Gutbrod *et al.*, Phys. Lett. B **216** (1989) 267.
[R55] M. Demoulins *et al.*, Phys. Lett. B **241**, 476 (1990).
[R56] D. Brill *et al.*, Phys. Rev. Lett. **71** (1993) 336.
[R57] T. Alexopoulos *et al.*, (E735 Collaboratio), Phys. Lett. B **435** (1998) 453.
[R58] J. Feder, *Fractals*, Plenum Press,New York and London 1988.
[R59] B. Z. Kopeliovich *et al.* Phys. Rev. Lett. **88** (2002) 232303.
[R60] J. W. Cronin *et al.* Phys. Rev. D **11** (1975) 3105.
[R61] L. Van Hove, Phys. Lett. B **118**, 138 (1982).
[R62] E. Schnedermann, J. Sollfrank and U. W. Heinz, Phys. Rev. C **48** (1993) 2462.
[R63] L. V. Gribov, E. M. Levin and M. G. Ryskin, Phys. Rept. **100** (1983) 1.
[R64] N. Borghini and U. A. Wiedemann, J. Phys. G **35** (2008) 023001.
[R65] R. Lednicky, Nucl. Phys. A **774** (2006) 189.
[R66] M. A. Lisa *et al.*, Ann. Rev. Nucl. Part. Sci. **55** (2005) 357.
[R67] D. H. Rischke and M. Gyulassy, Nucl. Phys. A **608** (1996) 479.
[R68] J. D. Bjorken, Phys. Rev. D **27** (1983) 140.
[R69] J. D. Walecka, *Theoretical nuclear and subnuclear physics*. Second Edition. Imperial College Press and Word Scientific Publishing Co. Pte. Ltd. 2004.
[R70] J. Letessier and J. Rafelski, *Hadrons and quark - gluon plasma*, Camb. Monogr. Part. Phys. Nucl. Phys. Cosmol. **18**, 1 (2002).
[R71] K. Yagi, T. Hatsuda and Y. Miake, *Quark-Gluon Plasma: From Big Bang To Little Bang*, Camb. Monogr. Part. Phys. Nucl. Phys. Cosmol. **23**, 1 (2005).
[R72] R. Hagedorn, *How We Got To QCD Matter From The Hadron Side By Trial And Error*. In Proc. Int. Conf.on Ultra-Relativistic Nucleus-Nucleus Collisions, 4th, Helsinki, Finland, Jun 17-21, 1984. Edited by K. Kajantie. Springer-Verlag, Lect. Notes Phys. **221**, 53 (1985). Scanned Version (KEK Library)
[R73] R. M. Weiner, Int. J. Mod. Phys. E **15** (2006) 37.
[R74] H. G. Ritter, *The Role of Collective Flow in Heavy Ion Collisions*, Int. J. Mod. Phys.E **16**,(2007) 677.
[R75] R. Stock, *Relativistic nucleus nucleus collisions: From the BEVALAC to RHIC* J. Phys. G **30**, S633 (2004).
[R76] K.G. Wilson, Cornell Report No. CLNS-131/1970 reprinted in:Proc. Fourteenth Scottisch Universities Summer School Conf. (1973), eds. R.L. Crawford and R. Jen- nings (Academic Press, New York 1974);
R.P. Feynman in: Proc. Int. Conf. Neutrino 72 (Baltonfured, 1972), eds. A. Frenkel and G. Marx (Budapest, 1973).
[R77] *Quark-Gluon Plasma: Theoretical Foundations* An annotated reprint collection; Edited by J. Kapusta, B. Muller and J. Rafelski. ISBN: 0-444-51110-5 , 836 pages , 2003.
[R78] J. Letessier,J. Rafelski, *Hadrons and QuarkGluon Plasma*; Cambridge University Press ISBN: 0-521-38536-9, 413 pages, 2002.
[R79] A. Giovannini and R. Ugoccioni, Phys. Lett. B **558**, 59 (2003) [arXiv:hep-ph/0301173].
[R80] E. Andersen *et al.* [NA36 Collaboration], Phys. Lett. B **516**, 249 (2001) [arXiv:hep-ex/0011091].
[R81] K. Hencken *et al.*, Phys. Rept. **458**, 1 (2008) [arXiv:0706.3356 [nucl-ex]].
[R82] G. Baur, K. Hencken and D. Trautmann, Phys. Rept. **453**, 1 (2007) [arXiv:0706.0654 [nucl-th]].
[R83] D. E. Miller, Phys. Rept. **443**, 55 (2007) [arXiv:hep-ph/0608234].
[R84] S. Hegyi, Phys. Lett. B **327**, 171 (1994) [arXiv:hep-ph/9403245].

[R85] A. Adare *et al.* [PHENIX Collaboration], Phys. Rev. C **78** (2008) 044902 [arXiv:0805.1521 [nucl-ex]].
[R86] A. Bershadskii, Physica A **253**, 23 (1998).
[R87] A. Breakstone *et. al.,* Phys. Rev. D **30**, 528 (1984).
[R88] R.E. Ansorge *et. al.,* UA5 Collaboration, Z. Phys. C **43** *Particles and Fields*, 357 (1989).
[R89] UA5 collab., Phys. Rep. **154**, 247 (1987).
[R90] DELPHI collab., Z. Phys. C **52***Particles and Fields*, 271 (1991).
[R91] A.V. Bautin, Physics-Uspekhi **38**, 609 (1995) (English translation, AIP, New York).
[R92] D. Ghosh *et al.,* Phys. Rev. C **65**, 067902 (2002).
[R93] F. Takagi, Phys. Rev. Lett. **72**, 32 (1994).
[R94] R. Arnaldi *et al.* [NA60 Collaboration], Phys. Rev. Lett. **96**, 162302 (2006)
[R95] R. Arnaldi *et al.* [NA60 Collaboration], Phys. Rev. Lett. **100**, 022302 (2008)
[R96] R. Arnaldi *et al.* [NA60 Collaboration], Phys. Rev. Lett. **102**, 222301 (2009)
[R97] [PHENIX Collaboration] S. S. Adler, et al., Phys. Rev. Lett. **93**, 152302 (2004).
[R98] [PHOBOS Collaboration] B. B. Back, et al. (2004), Phys. Rev. C **73**, 031901 (2006).
[R99] H. P. Gos, Eur. Phys. J. C **49**, 75 (2007).
[R100] A. Kisiel, AIP Conf. Proc. **828**, 603 (2006).
[R101] M. Heffner [PHENIX Collaboration], J. Phys. G **30**, S1043 (2004).
[R102] M. Lisa, AIP Conf. Proc. **828**, 226 (2006)